

**TRACE ELEMENTS IN COAL FROM COLLINSVILLE, BOWEN
BASIN, AUSTRALIA – IN-GROUND MODE OF OCCURRENCE
AND BEHAVIOUR DURING UTILISATION.**

**Robert John Boyd
B.Sc., M.Sc.(hons) (Geol); Dip Environmental Science.**

**A Thesis Submitted to The School of Earth Sciences for the Degree of
Doctor of Philosophy in Geology.**

**James Cook University.
Townsville, Queensland
Australia.**

September 2004

STATEMENT OF ACCESS

I, the undersigned, author of this work, understand that James Cook University will make this thesis available for use within the University Library and, via the Australian Digital Theses network, for use elsewhere.

I understand that, as an unpublished work, a thesis has significant protection under the Copyright Act and;

I do not wish to place any further restriction on access to this work.

Or

I wish this work to be embargoed until : *Permission from the sponsors is gained*

Or

I wish the following restrictions to be placed on this work :

Signature _____

12/4/05
Date

ELECTRONIC COPY

I, the undersigned, the author of this work, declare that the electronic copy of this thesis provided to the James Cook University Library, is an accurate copy of the print thesis submitted, within the limits of the technology available.

Signature

Date

29/4/05.

STATEMENT OF SOURCES

DECLARATION

I declare that this thesis is my own work and has not been submitted in any form for another degree or diploma at any university or other institution of tertiary education. Information derived from the published or unpublished work of others has been acknowledged in the text and a list of references is given.

Signature

12/4/05.
Date

Abstract.

Analysis of samples gathered during delineation of a coal resource is becoming increasingly sophisticated as various organisations attempt to predict and understand the technological behaviour of the mined product. Analysis to determine the concentration of trace elements in coal is becoming more prevalent, and not just merely for academic curiosity. Increased environmental awareness has impelled the need to consider potential negative impacts on the ecosystem caused by liberation of trace elements from coal during utilisation.

The aims of this thesis are to: 1) Determine the concentration of trace elements in coal seams mined to supply the Collinsville pulverised fuel combustion plant at the Collinsville open cut, Northern Bowen Basin, Australia; 2) Determine the mineralogy and, using graphical relationships, the likely mode of occurrence of trace elements in the sampled pits; 3) Determine the mode of occurrence of trace elements in the pulverised fuel of the Collinsville power plant using the USGS sequential leaching method, and contrast the results with the same analysis for an unrelated fuel from another coal fired power utility (Mitsui Mining's Omutu City plant, Kyushu, Japan); 4) Examine the partitioning behaviour of trace elements in the Collinsville power utility, and contrast the results with the partitioning behaviour of trace elements in the Mitsui combustion utility to assess the influence of trace element mode of occurrence on partitioning behaviour; 5) Examine the mobility of trace elements from solid ash waste from the Collinsville power utility, and compare with the mobility of trace elements from the Mitsui power utility solid waste to assess the influence of mode of occurrence on the leachability of trace elements and; 6) Determine the partitioning behaviour of trace elements in carbonisation of Bowen seam coal at the Bowen coke works and compare with the partitioning behaviour of the same elements in combustion.

Lithotype logging of coal exposed in the highwalls of the Blake Central, Blake West and Bowen No.2 pits was undertaken. Of particular note was the presence of dull heat affected coal toward the roof of the Blake Central pit seam, toward the floor of the

Bowen No.2 pit seam, and the presence of bed-parallel intrusions within the seam in the Blake West pit. In the Blake West pit seam, the intrusion caused thermal alteration of the coal to coke over a 60cm zone immediately adjacent to the intrusion with a further 1.10-1.25m zone of dull heat altered coal beyond the coked zone. In the Blake Central, 4.5m of dull heat-affected coal occurred near the roof of the seam. In the Bowen No.2 pit, 1.2m of heat-affected coal occurred near the floor of the seam. Beyond the heat affected zone, lithotype logging of the Blake seams noted a number of rock partings, but no convincing dulling upward cycles due to progressive drying of the mire, noted in other studies of Permian coal, were found. No partings were found in the Bowen seam and only one convincing dulling upward cycles was logged. In part the absence of dulling upward cycles is due to heat alteration of the coal, but the numerous influxes of sediment laden water into the Blake seam mire also acted to terminate any significant dulling upward cycles by raising both nutrient levels and the water table.

Following lithotype logging, channel sampling of the pits resulted in a total of 76 samples, 25 from the Blake Central pit, 36 from the Blake West pit and 15 from the Bowen No.2 pit. The channel sampling intervals were determined approximately by coal lithotype interval, with some amalgamations to restrict sample numbers. The channel samples were analysed for proximate analysis, coal petrography and vitrinite reflectance (selected samples) and for major and trace elements using XRF and INAA.

The lithotype logs, proximate analysis data and coal petrography were integrated to infer the depositional environment of the Blake and Bowen seams. The generally high ash yield, common stone bands, low sulphur content of the coal and rare pyrite in the Blake seam suggests the depositional environment was a Class 3 topotelmitic peat with a variable water table. The moderate ash yield, the absence of common stone bands, sulphur contents of ~2% and the moderate pyrite content of the coal in the Bowen seam suggests the depositional environment was a Class 2 topotelmitic peat with a high water table.

The igneous intrusions have caused extensive alteration of vitrinite to semi-coke, a general decrease in the volatile matter content and an increase in the vitrinite reflectance [Ro(max)] toward the intrusion.

Mineralogy was calculated from major and trace elements using normative analysis, calibrated by XRD analysis of low temperature ash from selected samples. The mineralogy of the Blake seam samples is dominated by kaolinite, with subordinate quartz, illite, feldspar, and siderite, and minor concentrations of pyrite, gorceixite, goyazite and anatase. The mineralogy of the Bowen seam samples is dominated by kaolinite, with subordinate quartz, illite and pyrite, and minor concentrations of siderite, gorceixite, goyazite and anatase/ rutile/ iron oxides.

The concentration of trace elements in the channel samples was determined by INAA and XRF. The INAA and XRF concentrations of iron and uranium show a reasonable statistical relationship suggesting the two analysis methods are consistent with each other. The concentration of trace elements in the Blake and Bowen seams is generally low compared to world average ranges for coal and to crustal averages. Only gold, copper, hafnium, thorium and ytterbium were found to be above the world coal average range in the Blake seam. Only gold and copper were found to be above world coal average range in the Bowen seam coal.

Trace element mode of occurrence was inferred using graphical relationships between normative mineral and trace element concentrations. In the Blake seam, arsenic, possibly chromium, copper, mercury, nickel and lead were inferred to be associated with pyrite. Bromine, cobalt, selenium, and zinc appeared to be organically bound. Cerium, caesium, europium, lanthanum, rubidium, and scandium showed a graphical relationship with illite. However, cerium, europium, lanthanum and scandium, along with hafnium, lutetium, neodymium, samarium, terbium, thorium, uranium and vanadium also showed a graphical relationship with gorceixite or gorceixite plus goyazite. It was inferred the latter group of elements are associated with monazite or zircon. In addition to the REE phosphate mode of occurrence, some rare earth elements also showed an affinity for

kaolinite. Thorium and uranium were also inferred to be associated with feldspars. Antimony, tantalum and ytterbium were found to be dominantly associated with kaolinite.

In the Bowen seam, arsenic, cobalt, possibly chromium, copper, mercury, molybdenum, nickel, lead, antimony, selenium and zinc showed a graphical relationship with pyrite. The elements cerium, hafnium, neodymium, rubidium, samarium, tantalum, thorium, uranium and tungsten all showed significant graphical relationships with the anatase/ rutile/ FeO grouping of minerals. It is inferred that the relationship is due to the presence of monazite, zircon, xenotime, REE phosphates, tungstates or other trace minerals, the distribution of which mirrors the distribution of the anatase/ rutile/ FeO grouping. Uranium and thorium were inferred to be associated with REE phosphates and zircon respectively, plus illite. The elements bromine, europium, lanthanum, terbium and vanadium were inferred to be associated with illite. A mixed illite/ heavy mineral suite mode of occurrence is inferred for samarium, tantalum, thorium and uranium. The elements caesium, lutetium, scandium, and ytterbium were inferred to be associated with kaolinite.

The effect of igneous intrusions on the concentration of a number of minerals and trace elements was also examined. The presence of semi-coke or an inferred distance of heat alteration was used to distinguish heat affected and unaffected samples. Depletion or enrichment of minerals and elements was inferred using ply thickness weighted average concentration figures for altered and unaltered samples and trends of concentration change toward the intrusion. Some consistent changes in the concentration of trace elements and minerals were found across all three pits sampled. The minerals siderite and pyrite are depleted in the heat affected zone, but goyazite is enriched, particularly toward the margins of the heat affected zone. The elements bromine and strontium (the latter mirroring the goyazite trend) are concentrated in the heat affected zone. The elements cobalt, mercury, manganese (mirroring the pyrite trend), nickel and possibly arsenic and zinc are depleted in heat affected samples from all three pits sampled. The inconsistent behaviour of some other trace elements (molybdenum, chromium and

possibly selenium) in response to the igneous intrusion appears to be the result of different modes of occurrence of trace elements between pits.

Samples of pulverised fuel were collected from the Collinsville and Japanese (Mitsui) pulverised fuel utilities. The concentration of major and trace elements was determined by INAA, XRF and (for the Collinsville sample) ICP-MS & ICP-AES. INAA analysis suggests gold, cerium, cobalt, europium, hafnium, lanthanum, lutetium, molybdenum, neodymium, scandium, selenium, samarium, strontium, tantalum, thorium, tungsten and ytterbium are at the upper end or above the world average concentration range in the Collinsville pulverized fuel. Only gold, hafnium and thorium are at the upper end or above the world coal concentration range in the Japanese pulverized fuel.

Sequential leaching of the pulverised fuels was undertaken according to the USGS protocol. The sequential leach data was interpreted to infer trace element mode of occurrence in the pulverised fuel. A number of significant differences in the mode of occurrence of antimony, arsenic, chromium, cobalt, nickel, selenium, uranium and zinc were found between the two combustion plants studied. The element vanadium had almost identical modes of occurrence in fuel from both plants studied.

A comparison of trace element mode of occurrence determined for the Collinsville power utility pulverised fuel by sequential leaching with mode of occurrence determined for the in-ground feed coals using graphical methods showed a reasonable level of agreement. It is concluded that the use of two methods of determining mode of occurrence provides better definition of mineral type in some cases. For example a siderite mode of occurrence could be determined using graphical relationship whereas the sequential leach data gave only a carbonate mode of occurrence. Further, the sequential leach data solved the problem of parallel graphical relationships. For example, galena was determined to be the mode of occurrence of lead from the sequential leach data, whereas graphical relationships indicated a pyrite mode of occurrence because of the relationship with sulphur.

Combustion of coal occurs in three phases, namely devolatilisation, combustion of the volatile matter, and combustion of the residual char. Mineral matter may be excluded from the residual char particles due to desegregation and separation in the milling process, or included within the char particle. During combustion, trace elements partition between the bottom ash, the fly ash, and flue gas (lost up the stack). The concentration of trace elements in ash samples from the Collinsville and Mitsui power utilities was determined by INAA and XRF. The partitioning behaviour of the trace elements is examined by calculating relative enrichment values for the trace elements. Generally the partitioning behaviour and classification of trace elements in this study matched those found in previous published studies for a given element.

The relative enrichment trends of elements exhibiting significant differences in mode of occurrence between the two combustion plants sampled (ie antimony, arsenic, chromium, cobalt, nickel, selenium, uranium and zinc plus vanadium) were examined to determine the control of mode of occurrence on the partitioning behaviour. It is hypothesised that the relative volatility of a particular element in combustion reflects the temperature at which the host mineral or the organic matter thermally decomposes. Thus organically bound elements should be more volatile than pyrite associated elements, which should be more volatile than carbonate associated elements, which should be substantially more volatile than silicate associated elements. Other factors that may influence partitioning behaviour such as the major element chemistry of the ash, plant design and operating conditions, and temperature variations within the combustion chamber were discounted as significantly influencing relative enrichment differences for the two combustion plants studied. It is concluded that element mode of occurrence has a strong influence on the relative volatility of a given element, and that comparison of sequential leach results from two pulverised fuel utilities has the potential allow prediction of the relative volatility of trace elements in combustion. Some complications may arise due to exclusion of some mineral grains and localised variations in the oxidation state within the combustion zone.

Solid combustion wastes (fly ash and bottom ash) are commonly disposed of in landfill and impoundment facilities. Unless the landfill is impermeable to water, disposal of solid

wastes in such fashion allows interaction with the hydrogeological system and could lead to detrimental environmental impacts. Leaching of indicative “total waste” composites made up by blending fly ash and bottom ash samples from each power utility in an 80/20 proportion was undertaken using the TCLP protocol. The concentration of trace elements in the leachates was compared to recreational water and drinkwater guideline values. The concentration of barium, manganese, and selenium in the Collinsville leachate exceeds both the recreational and drinkwater guideline concentrations. The concentration of nickel in the Collinsville leachate was found to exceed the recommended drinkwater concentration, but is below recreational water guideline value. The concentration of boron and selenium in the Mitsui leachate was found to exceed both the recreational and drinkwater guideline values. The concentration of barium in the Mitsui leachate was found to exceed the drinkwater standard. The concentration of an element in the ash sample was found to be a poor indicator of the mobility of the element.

Elements that showed substantial differences in mode of occurrence in the pulverised fuel (ie antimony, arsenic, chromium, cobalt, nickel, selenium, uranium and zinc plus vanadium) were examined to assess the influence of mode of occurrence on the leachability of the element from solid combustion waste. It is concluded that, where the difference in element mobility between the two composite ash samples is significant, mode of occurrence does exert some control on the proportion of a trace element in the ash that can be mobilised by the TCLP protocol. In particular, trace elements present in coal associated with silicates appear substantially unavailable for mobilisation by the TCLP protocol.

The concentration of trace elements in samples of feed coal, coke and breeze from the Bowen coke works was determined by INAA and XRF. A new index (the CRE index) was developed to characterise the enrichment or depletion of trace elements in the coke and breeze. Coke is classified as enriched (Class 1), neither enriched nor depleted (Class 2), depleted (Class 3) or highly depleted (Class 4). Breeze was classified as enriched (denoted “e”), neither enriched nor depleted (denoted “a”) and depleted (denoted “d”).

Comparison of the partitioning behaviour of trace elements in combustion and carbonisation was undertaken by comparing the RE and CRE data. It is concluded that all but the most volatile elements (sulphur, selenium, arsenic and tungsten) are substantially retained in the coke. The substantial retention of trace elements in coke is likely due to the lower temperature at which carbonisation occurs compared to pulverised fuel combustion temperatures. The behaviour of trace elements in the breeze is similar to their behaviour in combustion, being controlled by mode of occurrence and element volatility. Trace elements associated with pyrite are generally enriched in the breeze, excepting highly volatile elements such as sulphur, selenium and arsenic, which appear to substantially volatilise. Silicate associated elements and those elements associated with heavy minerals are also generally non-volatile excepting tungsten that is depleted in the coke and breeze.

The concentration of trace elements in the pit channel samples and in the pulverised fuel sample suggest the elements barium, selenium, mercury, thorium, copper, manganese, nickel and vanadium warrant further investigation in Collinsville pit and combustion wastes. The data suggests the elements thorium, boron, selenium and barium warrant further investigation in the Japanese combustion plant. Further work to verify that relative differences in mode of occurrence inferred from USGS sequential leaching are useful as indicators of trace element volatility and leachability is recommended.

The environmentally significant trace elements cobalt, molybdenum, antimony, strontium, zinc and possibly arsenic and chromium are enriched in the breeze samples from the Bowen coke works. Leaching studies to determine the proportion and concentration of trace elements in the leachate upon disposal of the waste is worth consideration. Further studies to characterise trace element partitioning during carbonisation in a slot oven are recommended.

Acknowledgements.

I would like to thank the following people for their assistance with this PhD.

My supervisor Dr Peter Crosdale, who organised research grants and a scholarship at James Cook University, provided accommodation to the entire family for our first two weeks in Townsville, provided training in the petrography of Australian coals, introduced me to all the right people (and a few of the wrong ones at wine club) and then watched bemused as we all moved back to New Zealand ten months later to resume full time employment. Dr Crosdale also undertook a thorough and useful review of manuscript drafts. Thank you for your technical advice, encouragement and forbearance. I did eventually finish the thesis!

Mr Ray Slater (then Resource Management Superintendent at the Collinsville coal mine) for his considerable help and advice, the benefit of his expertise on the Collinsville operations, organising access to the mine to undertake sampling, and organising the saving of splits of the Bowen coke works train samples. Thank you also to Theiss mining contractors, Collinsville for covering the cost of the proximate analysis of the pit channel samples.

Mr Ian Borthwick for providing access to the Collinsville power utility and gathering samples of pulverised fuel, bottom ash and fly ashes.

Mr Oki Nishioka for organising the gathering of coal and ash samples at Mitsui Mining's Omutu City pulverised coal combustion utility in Kyushu, Japan.

Mr John Laidlaw for allowing access to the Bowen coke works and for gathering samples of coke and breeze over several months.

Messrs Hugh McMillan and Trevor Daly of SGS Ngakawau, New Zealand for undertaking low temperature ashing and sulphur analysis of numerous samples.

Dr Jane Newman for agreeing to train me (once again!) in the measurement of vitrinite reflectance and coal petrography point counting. Also for the encouragement that a PhD could be completed part time and some inspirational discussions on coal science over a lot of years. Mr Colin Nunweek is thanked for mounting the petrographic samples under Dr Newman's supervision.

Thanks to the Geology Department, University of Canterbury, New Zealand for providing access to use the petrographic microscope. Particular thanks to Dr Kerry Swanson, who always seemed to have an appropriate sized "bit of wire" to carry out the odd technical fix.

Dr Nigel Newman of CRL Energy for undertaking low temperature ashing and organising XRD analysis of selected samples, and for some useful observations on the results.

Thanks to the United States Geological Survey, particularly Dr Bob Finkelman and Dr Curtis Palmer for undertaking sequential leaching analysis of the Collinsville pulverised fuel as part of the world Coal Quality Database programme; also for supplying a number of useful papers and some helpful correspondence. Also particular thanks to Dr Palmer who assisted with the preparation and explanation of the chondrite normalised plots.

Dr Zhongsheng Li, for setting up and running the sequential leaching of the Japanese pulverised fuel sample at Canterbury University, Christchurch, New Zealand.

Particular thanks to Solid Energy New Zealand, especially Mr Barry Bragg, for organising substantial funding to cover the XRF analytical costs over the latter stages of this project and providing an extra week of leave a year for the past three years.

Thanks to Dr Doug Lewis who inspired a enthusiasm for research and technical reading, and Mr Frank Taylor who gave me my first coal job and instilled a sense of the value of practical geology. Thanks also to my “room mate” at Solid Energy Jonny McNee for the laughs.

My parents, David and Anne, who taught me the value working to achieve a goal, and have continuing to be there for advice, encouragement and the occasional meal and accommodation for studies in Christchurch.

And finally to my wife Fran, who packed up the household to move to Australia so I could quit work and go back to uni, and then packed it up to move back again so I could go back to work and study as well!!; who watched family finances disappear into the analytical bills black hole and assorted text books; who understood when I disappeared night after night into the study and worked at weekends instead of doing the garden; who listened to my inane ravings, and who remained lovingly supportive. Also to my children Erica and Michelle, who have had to be content with short hours (and temper) from their father for the last five years. I could not have done it without you and I cannot thank you enough. I love you all.

Table of Contents.

	Page
Statement of Access	i
Abstract	ii
Acknowledgements	x
List of Figures	xix
List of Tables	xxviii
List of Appendices	xxxii
Statement of Sources	xxxiii

Chapter 1 Literature Review.

	Page
1.0. Chapter Resume	1
1.1. Introduction	1
1.2. Trace Elements of Environmental Interest	8
1.3. Geological Aspects of Trace Elements in Coal	10
1.3.1. Concentration of Trace Elements in Coal	10
1.3.1.1. Definitions	10
1.3.1.2. Comparison of Trace Element Concentrations	10
1.3.2. Mode of Occurrence	13
1.3.2.1. Introduction	13
1.3.2.2. Methods of Determining Modes of Occurrence	14
1.3.3. Controls on Trace Element Occurrence in Coal	19
1.3.3.1. Sediment Provenance	19
1.3.3.2. Depositional Environment	21
1.3.3.3. Fixation of Elements by Plants and Plant Debris	24
1.3.3.4. Coal Rank	26
1.3.3.5. Geochemical Nature of Groundwater and Country Rocks	27

1.3.3.6.	Summary – Geological Aspects of Trace Elements in Coal	28
1.4.	Trace Elements in Coal Combustion	30
1.4.1.	Introduction	30
1.4.2.	Definitions	30
1.4.3.	Partitioning of Trace Elements in Combustion	32
1.4.4.	Controls on Trace Element Partitioning in Combustion	36
1.4.4.1.	Elemental Volatility	36
1.4.4.2.	Mode of Occurrence	37
1.4.4.3.	Collection Point and Characteristics of the Ash.	38
1.4.4.4.	Combustion Regime	40
1.4.5.	The Environmental Importance of Fly Ash	41
1.4.6.	Fly Ash Leaching	42
1.4.7.	Case Studies	44
1.4.8.	Conclusions – Coal Combustion Aspects of Trace Elements	47

Chapter 2 Study Aims and Methods.

2.0.	Project Design	48
2.1.	Aims	48
2.2.	Methods	49
2.3.	Analytical Methods	50
2.3.1.	Instrumental Neutron Activation Analysis (INAA)	53
2.3.2.	X-Ray Fluorescence (XRF)	58
2.3.3.	Inductively Coupled Mass Spectrometry (ICP-MS)	63
2.3.4.	Miscellaneous	63
2.3.5.	X-Ray Diffraction (XRD)	64
2.3.6.	Coal Petrography and Vitrinite Reflectance Analysis	63
2.3.7.	Leaching Methods	65
2.4.	Comparison of INAA and XRF Analytical Results	66

2.5.	Concluding Remarks	67
------	--------------------	----

Chapter 3 Collinsville Opencut: Coal Characterisation, Trace Element Concentration and Mode of Occurrence.

3.0.	Chapter Resume	69
3.1.	Samples	69
3.2.	Coal Characteristics	77
3.2.1.	The Blake Seam	77
3.2.2.	The Bowen Seam	92
3.2.3.	Mineral Matter from Normative Analysis	98
3.2.3.1.1.	Blake Central and Blake West Normative Analysis	99
3.2.3.1.2.	Bowen No.2 Normative Analysis	118
3.2.3.1.3.	Tabulated Normative Mineral Assemblages	126
3.3.	Trace Element Concentration and Mode of Occurrence	131
3.3.1.	Trace Elements in the Blake Seam	131
3.3.1.1.	Concentration of Trace Elements in the Blake Seam	131
3.3.1.2.	Mode of Occurrence of Trace Elements in the Blake Seam	134
3.3.2.	Trace Elements in the Bowen Seam	143
3.3.2.1.	Concentration of Trace Elements in the Bowen Seam	143
3.3.2.2.	Mode of Occurrence of Trace Elements in the Bowen Seam	145
3.3.3.	Concluding Remarks on Inference of Mode of Occurrence Inferences Using Graphical Relationships.	150
3.4.	The Effect of Igneous Intrusions on the Concentration of Trace Elements in the Blake and Bowen Seam Samples.	152

3.4.1.	Trends of Enrichment and Depletion of Trace Elements at Collinsville	152
3.4.2.	Comparison of the Influence of Intrusions on Trace Elements at Collinsville with Other Examples	162
3.5.	Chapter Summary	168

Chapter 4 Trace Element Concentration and Mode of Occurrence in Selected Pulverised Fuel Combustion Plant Samples.

4.0.	Chapter Resume	170
4.1.	Sample Description	170
4.2.	Sample Analysis	174
4.3.	Analysis Results	177
4.4.	Mode of Occurrence from Sequential Leach Data	180
4.5.	Mode of Occurrence for Other Elements Analysed for Individual Coals	197
4.6.	Significant Differences in the Mode of Occurrence Between the Collinsville and Japanese Pulverised Fuel Samples	207
4.7.	Chapter Summary	211

Chapter 5 Trace Element Partitioning Behaviour in Pulverised Fuel Combustion.

5.0.	Chapter Resume	213
5.1.	Sample Description	213
5.2.	Factors Other than Mode of Occurrence Affecting Partitioning Behaviour	217
5.3.	Partitioning Behaviour	218
5.4.	Comparison of Partitioning Behaviour	247
5.5.	Chapter Summary	252

Chapter 6 Trace Element Partitioning Behaviour in Carbonisation.

6.0.	Chapter Resume	254
6.1.	Samples	254
6.2.	Analysis Results	255
	6.2.1. Coal Quality	255
	6.2.2. Trace Element Partitioning Behaviour	256
	6.2.3. Grouping of Elements by Partitioning Behaviour in Carbonisation	290
6.3.	Comparison of Coke Breeze and Soil Element Concentrations	293
6.4.	Chapter Summary	295

Chapter 7 Leachability of Trace elements from Solid Waste from Pulverised Fuel Combustion.

7.0.	Chapter Resume	296
7.1.	Samples	296
7.2.	Results	297
	7.2.1. Concentration of Trace Elements in Combustion Wastes and Soils	297
	7.2.2. Concentration of Trace Elements in TCLP Leachates Compared to Water Quality Guidelines	298
	7.2.3. Proportion of Trace Elements in Solid Waste Mobilised by the TCLP Protocol	302
7.3.	Discussion	307
7.4.	Chapter Summary	309

Chapter 8 Synthesis.

8.0.	Chapter Resume	310
8.1.	Assessment of Trace Element Mode of Occurrence – Comparison of Graphical and Statistical Results	310
8.2.	The Control of Mode of Occurrence on Trace Element Partitioning and Leachability	315
8.2.1.	The Control of Mode of Occurrence on Trace Element Partitioning	315
8.2.2.	The Control of Mode of Occurrence on Trace Element Leachability	327
8.3.	Comparison of the Partitioning Behaviour of Trace Elements in Combustion and Carbonisation	330
8.3.	Chapter Summary	337

Chapter 9 Conclusions and Further Work.

9.0.	Pit Sample Data	340
9.0.1.	Depositional Environment of the Blake and Bowen Seams.	340
9.0.2.	Concentration and Mode of Occurrence of Trace Elements in the Blake and Bowen Seams	340
9.0.3.	The Effect of Igneous Intrusions on the Coal and on the Concentration of Trace Elements.	344
9.1.	Combustion Sample Data	345
9.1.1.	The Control of Mode of Occurrence on Trace Element Partitioning Behaviour in Combustion and Carbonisation	345
9.1.2.	The Control of Mode of Occurrence on Trace Element Mobility from Carbonisation Waste Material	348

9.2. The Control of Mode of Occurrence on Trace Element Partitioning Behaviour in Carbonisation.	349
9.4. Further Work	351
References Cited	355

List of Figures.

Chapter 1.

Figure 1.1.	General Representation of the Effects of Increases of Concentration of a Trace Element	6
Figure 1.2.	Classification of Elements by Their Behaviour During Combustion and Gasification	33
Figure 1.3.	The Relationship Between Particle Deposition in Lungs and Particle Diameter	43

Chapter 2.

Figure 2.1.	Sample BC6.37-6.55 vs Repeat 1	57
Figure 2.2.	Sample BO2.60-2.90 vs Repeat 2	57
Figure 2.3.	Sample Train 213 vs Repeat 3	57
Figure 2.4.	Sample U3 Fly Ash vs Repeat 4	58
Figure 2.5.	Comparison of Ash Percent, Proximate and 400°C Ashing Methods	61
Figure 2.6.	Schematic Diagram Showing the Principal Components of an ICP-MS Instrument	62
Figure 2.7.	Iron by INAA vs Iron by XRF	66
Figure 2.8.	Uranium by INAA vs Uranium by XRF	67

Chapter 3.

Figure 3.1.	Location of Collinsville Coalmine	70
Figure 3.2.	Stratigraphic Column for the Collinsville Coal Measures.	71
Figure 3.3.	Relative Location of the Pits Sampled for this Study	74

Figure 3.4.	In-Pit Bench in the Blake Central pit, Blake Seam	75
Figure 3.5.	Coal Degeneration in the Highwall of the Blake Central Pit, Blake Seam, Following Exposure to the Weather	75
Figure 3.6.	Bed-Parallel Igneous Intrusions in the Blake West Pit, Blake Seam	76
Figure 3.7.	Close-up of Igneous Intrusions in the Blake West Pit, Blake Seam	76
Figure 3.8.	Strip Log of Pit Samples from the Blake Central Pit	80
Figure 3.9.	Blake Central Pit Inertinite vs Volatile Matter	82
Figure 3.10.	Blake Central Distance from Roof of Seam (m) vs Volatile Matter (daf)	82
Figure 3.11.	Semi-coke in the Bowen Seam Coal, Bowen No.2 Pit	83
Figure 3.12.	Strip Log of Pit Samples from the Blake West Pit	86
Figure 3.13.	Blake West Pit Inertinite vs Volatile Matter	90
Figure 3.14.	Blake West Distance from Roof of Seam (m) vs Volatile Matter (daf)	90
Figure 3.15.	Strip Log of Pit Samples from the Bowen No.2 Pit	95
Figure 3.16.	Bowen No.2 Pit Inertinite vs Volatile Matter	96
Figure 3.17.	Bowen No.2 Distance from Roof of Seam (m) vs Volatile Matter (daf)	97
Figure 3.18.	Sodium vs Potassium, Blake Central Samples	101
Figure 3.19.	Sodium vs Potassium, Blake Central Samples Excluding One High Potassium Figure	101
Figure 3.20.	Sodium vs Potassium, Blake West Samples	102
Figure 3.21.	Phosphorous vs Barium, Blake Central Samples	105
Figure 3.22.	Phosphorous vs Barium, Blake West Samples	106
Figure 3.23.	Residual Phosphorous vs strontium, Blake Central Samples	106
Figure 3.24.	Residual Phosphorous vs strontium, Blake West Samples	107
Figure 3.25.	Iron vs Manganese, Blake Central Samples	112
Figure 3.26.	Iron vs Manganese, Blake West Samples	113

Figure 3.27.	Residual Iron Left After Siderite Calculation vs Sulphur, Blake Central Samples	114
Figure 3.28.	Residual Iron Left After Siderite Calculation vs Sulphur, Blake West Samples	115
Figure 3.29.	Ash vs Residual Sulphur Left After Pyrite Calculation, Blake Central Samples	115
Figure 3.30.	Ash vs Residual Sulphur Left After Pyrite Calculation, Blake West Samples	116
Figure 3.31.	Iron vs Magnesium, Blake Central Samples	117
Figure 3.32.	Iron vs Magnesium, Blake West Samples	117
Figure 3.33.	Iron vs Total Sulphur, Bowen No.2 Samples	122
Figure 3.34.	Ash vs Total Sulphur, Bowen No.2 Samples	122
Figure 3.35.	Residual Iron vs Manganese, Bowen No.2 Samples	124
Figure 3.36.	Residual Iron vs Magnesium, Bowen No.2 Samples	124
Figure 3.37.	Residual Iron vs Titanium, Bowen No.2 Samples	125
Figure 3.38.	Hafnium vs Uranium, Blake Central	138
Figure 3.39.	Hafnium vs Uranium, Blake West	139
Figure 3.40.	Thorium vs Uranium, Blake Central	139
Figure 3.41.	Thorium vs Uranium, Blake West	139
Figure 3.42.	Ash vs Tungsten, Blake Central	141
Figure 3.43.	Ash vs Tungsten, Blake West	141
Figure 3.44.	Chondrite and Ash normalised REE concentration, Blake Central.	142
Figure 3.45.	Chondrite and Ash normalised REE concentration, Blake West.	143
Figure 3.44.	Hafnium vs Uranium, Bowen No.2	149
Figure 3.47.	Thorium vs Uranium, Bowen No.2	149
Figure 3.48.	Chondrite and Ash normalised REE concentration, Bowen No.2.	150
Figure 3.49.	Strip Log Showing Vertical Changes in Minerals and Trace Elements in the Blake Central Pit Seam	157
Figure 3.50.	Strip Log Showing Vertical Changes in Minerals and Trace Elements in the Blake West Pit Seam	158

Figure 3.51.	Strip Log Showing Vertical Changes in Minerals and Trace Elements in the Bowen No.2 Pit Seam	159
--------------	--	-----

Chapter 4.

Figure 4.1.	Schematic of the Collinsville Coal Fired Power Plant	172
Figure 4.2.	Schematic of the Mitsui Mining Coal Fired Power Plant	173
Figure 4.3.	Positions for Isokinetic Sampling	174
Figure 4.4.	INAA/ XRF Results vs the USGS Results for Collinsville Pulverised Fuel	176
Figure 4.5.	INAA/ XRF Results vs MW-ICP-MS Results for Japanese Pulverised Fuel	177
Figure 4.6.	Proportions of Antimony Leached	183
Figure 4.7.	Proportions of Arsenic Leached	185
Figure 4.8.	Proportions of Barium Leached	186
Figure 4.9.	Proportions of Beryllium Leached	187
Figure 4.10.	Proportions of Boron Leached	188
Figure 4.11.	Proportions of Chromium Leached	189
Figure 4.12.	Proportions of Cobalt Leached	190
Figure 4.13.	Proportions of Copper Leached	191
Figure 4.14.	Proportions of Lead Leached	191
Figure 4.15.	Proportions of Manganese Leached	192
Figure 4.16.	Proportions of Nickel Leached	193
Figure 4.17.	Proportions of Selenium Leached	194
Figure 4.18.	Proportions of Tin Leached	195
Figure 4.19.	Proportions of Uranium Leached	195
Figure 4.20.	Proportions of Vanadium Leached	196
Figure 4.21.	Proportions of Zinc Leached	197
Figure 4.22.	Proportions of Cadmium and Molybdenum Leached	198
Figure 4.23.	Proportions of Rare Earth Elements Leached	199

Figure 4.24.	Proportions of Aluminium, Bromine & Phosphorous Leached	200
Figure 4.25.	Proportions of Row 4 Transition Metals Leached	201
Figure 4.26.	Proportions of Heavy Metals Leached	203
Figure 4.27.	Proportions of Group I and II Elements Leached	205

Chapter 5.

Figure 5.1.	The Collinsville Coal Fired Power Station	214
Figure 5.2.	Relative Enrichment of Silicon	221
Figure 5.3.	Relative Enrichment of Aluminium	221
Figure 5.4.	Relative Enrichment of Iron	222
Figure 5.5.	Relative Enrichment of Magnesium	223
Figure 5.6.	Relative Enrichment of Sodium	223
Figure 5.7.	Relative Enrichment of Titanium	225
Figure 5.8.	Relative Enrichment of Manganese	225
Figure 5.9.	Relative Enrichment of Phosphorous	225
Figure 5.10.	Relative Enrichment of Sulphur	226
Figure 5.11.	Relative Enrichment of Gold	227
Figure 5.12.	Relative Enrichment of Arsenic	227
Figure 5.13.	Relative Enrichment of Boron	228
Figure 5.14.	Relative Enrichment of Barium	229
Figure 5.15.	Relative Enrichment of Cobalt	229
Figure 5.16.	Relative Enrichment of Chromium	230
Figure 5.17.	Relative Enrichment of Copper	231
Figure 5.18.	Relative Enrichment of Caesium	231
Figure 5.19.	Relative Enrichment of Mercury	232
Figure 5.20.	Relative Enrichment of Molybdenum	233
Figure 5.21.	Relative Enrichment of Nickel	233
Figure 5.22.	Relative Enrichment of Lead	234
Figure 5.23.	Relative Enrichment of Rubidium	235

Figure 5.24.	Relative Enrichment of Antimony	235
Figure 5.25.	Relative Enrichment of Selenium	236
Figure 5.26.	Relative Enrichment of Tin	237
Figure 5.27.	Relative Enrichment of Thorium	238
Figure 5.28.	Relative Enrichment of Uranium	238
Figure 5.29.	Relative Enrichment of Vanadium	239
Figure 5.30.	Relative Enrichment of Tungsten	240
Figure 5.31.	Relative Enrichment of Zinc	240
Figure 5.32.	Relative Enrichment of Cerium	241
Figure 5.33.	Relative Enrichment of Europium	242
Figure 5.34.	Relative Enrichment of Hafnium	242
Figure 5.35.	Relative Enrichment of Iridium	243
Figure 5.36.	Relative Enrichment of Lanthanum	243
Figure 5.37.	Relative Enrichment of Lutetium	244
Figure 5.38.	Relative Enrichment of Neodymium	244
Figure 5.39.	Relative Enrichment of Scandium	245
Figure 5.40.	Relative Enrichment of Samarium	245
Figure 5.41.	Relative Enrichment of Strontium	246
Figure 5.42.	Relative Enrichment of Tantalum	246
Figure 5.43.	Relative Enrichment of Terbium	247
Figure 5.44.	Relative Enrichment of Ytterbium	247

Chapter 5.

Figure 6.1.	Bowen Coke Works	255
Figure 6.2.	Quality Parameters of Coal Delivered to the Bowen Coke Works During Time of Sampling	256
Figure 6.3.	Concentration of Silicon in Feed Coal and Coke with Time	258
Figure 6.4.	Silicon CRE for Coke and Breeze with Time	258
Figure 6.5.	Concentration of Aluminium in Feed Coal and Coke with Time	259

Figure 6.6.	Aluminium CRE for Coke and Breeze with Time	259
Figure 6.7.	Concentration of Iron in Feed Coal and Coke with Time	260
Figure 6.8.	Iron CRE for Coke and Breeze with Time	260
Figure 6.9.	Concentration of Sodium in Feed Coal and Coke with Time	261
Figure 6.10.	Sodium CRE for Coke and Breeze with Time	261
Figure 6.11.	Concentration of Titanium in Feed Coal and Coke with Time	262
Figure 6.12.	Titanium CRE for Coke and Breeze with Time	262
Figure 6.13.	Concentration of Manganese in Feed Coal and Coke with Time	263
Figure 6.14.	Manganese CRE for Coke and Breeze with Time	263
Figure 6.15.	Concentration of Phosphorous in Feed Coal and Coke with Time	264
Figure 6.16.	Phosphorous CRE for Coke and Breeze with Time	264
Figure 6.17.	Concentration of Sulphur in Feed Coal and Coke with Time	265
Figure 6.18.	Sulphur CRE for Coke and Breeze with Time	265
Figure 6.19.	Concentration of Gold in Feed Coal and Coke with Time	266
Figure 6.20.	Gold CRE for Coke and Breeze with Time	266
Figure 6.21.	Concentration of Arsenic in Feed Coal and Coke with Time	267
Figure 6.22.	Arsenic CRE for Coke and Breeze with Time	267
Figure 6.23.	Concentration of Barium in Feed Coal and Coke with Time	268
Figure 6.24.	Barium CRE for Coke and Breeze with Time	268
Figure 6.25.	Concentration of Bromine in Feed Coal and Coke with Time	269
Figure 6.26.	Bromine CRE for Coke and Breeze with Time	269
Figure 6.27.	Concentration of Cobalt in Feed Coal and Coke with Time	270
Figure 6.28.	Cobalt CRE for Coke and Breeze with Time	270
Figure 6.29.	Concentration of Chromium in Feed Coal and Coke with Time	271
Figure 6.30.	Chromium CRE for Coke and Breeze with Time	271
Figure 6.31.	Concentration of Caesium in Feed Coal and Coke with Time	272
Figure 6.32.	Caesium CRE for Coke and Breeze with Time	272
Figure 6.33.	Concentration of Hafnium in Feed Coal and Coke with Time	273
Figure 6.34.	Hafnium CRE for Coke and Breeze with Time	273
Figure 6.35.	Concentration of Molybdenum in Feed Coal and Coke with Time	274
Figure 6.36.	Concentration of Nickel in Feed Coal and Coke with Time	275

Figure 6.37.	Concentration of Rubidium in Feed Coal and Coke with Time	276
Figure 6.38.	Concentration of Antimony in Feed Coal and Coke with Time	276
Figure 6.39.	Antimony CRE for Coke and Breeze with Time	277
Figure 6.40.	Concentration of Selenium in Feed Coal and Coke with Time	277
Figure 6.41.	Selenium CRE for Coke and Breeze with Time	278
Figure 6.42.	Concentration of Strontium in Feed Coal and Coke with Time	278
Figure 6.43.	Strontium CRE for Coke and Breeze with Time	279
Figure 6.44.	Concentration of Thorium in Feed Coal and Coke with Time	279
Figure 6.45.	Thorium CRE for Coke and Breeze with Time	280
Figure 6.46.	Concentration of Uranium in Feed Coal and Coke with Time	280
Figure 6.47.	Uranium CRE for Coke and Breeze with Time	281
Figure 6.48.	Concentration of Tungsten in Feed Coal and Coke with Time	281
Figure 6.49.	Tungsten CRE for Coke and Breeze with Time	282
Figure 6.50.	Concentration of Zinc in Feed Coal and Coke with Time	282
Figure 6.51.	Zinc CRE for Coke and Breeze with Time	283
Figure 6.52.	Concentration of Cerium in Feed Coal and Coke with Time	283
Figure 6.53.	Concentration of Europium in Feed Coal and Coke with Time	284
Figure 6.54.	Concentration of Lanthanum in Feed Coal and Coke with Time	284
Figure 6.55.	Concentration of Lutetium in Feed Coal and Coke with Time	284
Figure 6.56.	Concentration of Neodymium in Feed Coal and Coke with Time	285
Figure 6.57.	Concentration of Scandium in Feed Coal and Coke with Time	285
Figure 6.58.	Concentration of Samarium in Feed Coal and Coke with Time	285
Figure 6.59.	Concentration of Tantalum in Feed Coal and Coke with Time	286
Figure 6.60.	Concentration of Terbium in Feed Coal and Coke with Time	286
Figure 6.61.	Concentration of Ytterbium in Feed Coal and Coke with Time	286
Figure 6.62.	Cerium CRE for Coke and Breeze with Time	287
Figure 6.63.	Europium CRE for Coke and Breeze with Time	287
Figure 6.64.	Lanthanum CRE for Coke and Breeze with Time	288
Figure 6.65.	Lutecium CRE for Coke and Breeze with Time	288
Figure 6.66.	Neodymium CRE for Coke and Breeze with Time	288
Figure 6.67.	Scandium CRE for Coke and Breeze with Time	289

Figure 6.68.	Samarium CRE for Coke and Breeze with Time	289
Figure 6.69.	Tantalum CRE for Coke and Breeze with Time	289
Figure 6.70.	Terbium CRE for Coke and Breeze with Time	290
Figure 6.71.	Ytterbium CRE for Coke and Breeze with Time	290

Chapter 9.

Figure 9.1.	Collinsville Coalmine Pit Sample Summary.	342
Figure 9.2.	Coal Utilisation Summary Diagram - Combustion.	347
Figure 9.3.	Coal Utilisation Summary Diagram – Combustion & Carbonisation.	350

List of Tables.

Chapter 1.

Table 1.1.	Coal Ash Chemistry and Slagging/ Fouling Characteristics	5
Table 1.2.	Trace Elements of Environmental Interest	9
Table 1.3.	Content of Environmentally Significant Trace Elements in World Coals	12
Table 1.4.	Likely Trace Element Mode of Occurrence from Literature Scores	14
Table 1.5.	Percentage of Coal Ash from Various Combustion Configurations	32
Table 1.6.	Element Partitioning Class Comparison	34
Table 1.7.	Distribution of Elements Among Bottom Ash, Fly Ash and Flue Gas	35

Chapter 2.

Table 2.1.	Analytical Methods used in this Study	52
Table 2.2.	INAA Element Detection Limits	54
Table 2.3.	Repeat Analysis by INAA	56
Table 2.4.	Comparison of Ash Percent, Proximate and 400°C Ashing Methods	61

Chapter 3.

Table 3.1.	Interpretation of Depositional Environment from Coal Characteristics	91
------------	---	----

Table 3.2.	Residual Phosphorous in Blake Central Samples following Normative Calculations.	108
Table 3.3.	Residual Phosphorous in Blake West Samples following Normative Calculations.	109
Table 3.4.	Residual Phosphorous in Bowen No.2 Samples following Normative Calculations.	120
Table 3.5.	Normative Mineral Assemblage (ppm) – Blake Central Samples	127
Table 3.6.	Normative Mineral Assemblage (ppm) – Blake West Samples	128
Table 3.7.	Normative Mineral Assemblage (ppm) – Bowen No.2 Samples	129
Table 3.8.	Comparison of XRD and Normative Mineral Assemblages	130
Table 3.9.	Concentration of Trace Elements in the Blake Seam Compared to World Coal and Crustal Averages	133
Table 3.10.	Mode of Occurrence of Trace Elements in the Blake Seam	136
Table 3.11.	Concentration of Trace Elements in the Bowen Seam Compared to World Coal and Crustal Averages	144
Table 3.12.	Mode of Occurrence of Trace Elements in the Bowen Seam	146
Table 3.13.	Weighted Average Trace Element Concentration in Heat Affected and Unaffected Samples	154

Chapter 4.

Table 4.1.	Analysis Results for Collinsville and Japanese Pulverised Fuel Samples by Analysis Method	178
Table 4.2.	Raw Sequential Leaching Results	180
Table 4.3.	Tabulated Mode of Occurrence from Interpretation of Sequential Leach Data.	206
Table 4.4.	The Proportion of Each Trace Element Leached by Each Reagent and the Absolute Differences between Results for the Two Fuel Samples	208

Chapter 5.

Table 5.1.	Elemental Concentrations of Major and Trace Elements in Combustion Plant Solid Waste Streams.	216
Table 5.2.	Major Element Oxides in Ash	218
Table 5.3.	Trace Element Classification into 3 Classes Based on their Behaviour During Combustion in the Boiler and Ducts with their Relative Enrichment Factors (RE)	219
Table 5.4.	Partitioning Class of Elements in Collinsville, Mitsui and Literature Example Combustion Plants	252

Chapter 6.

Table 6.1.	Classification of Elements by Partitioning Behaviour in Carbonisation.	290
Table 6.2.	Classification of Element Partitioning Behaviour in Carbonisation	293
Table 6.3.	Trace Element Concentration in Bowen Plant Coke Breeze and World Average Soils	294

Chapter 7.

Table 7.1.	Trace Element Concentration in Ash and Bottom Ash	301
Table 7.2.	Water Quality Guideline Values and TCLP Concentrations	302
Table 7.3.	Analysis of Water from Observation Bores and Duck Pond Adjacent to Collinsville Power Plant Ash Dams	302
Table 7.4.	Calculated Proportions of Element Mobilised by the TCLP Protocol	307

Chapter 8.

Table 8.1.	Comparison of Mode of Occurrence from Graphical and Sequential Leaching Methods	311
Table 8.2.	Significant Differences in Mode of Occurrence Related to Volatility and Leachability	323
Table 8.3.	Trace Element Mode of Occurrence and Partitioning Behaviour in Combustion and Carbonisation	332
Table 8.4.	Absolute Difference Between Breeze CRE Figures	337

List of Appendices.

Appendix 1. Health Effects of Trace Elements	381
Appendix 2. Mode of Occurrence of Trace Elements in Coal	397
Appendix 3. Maceral and $RO_{(max)}$ Analysis Results	429
Appendix 4. Proximate and Elemental Analysis Results for Collinsville Channel Samples	435
Appendix 5. XRD Analysis of Low Temperature Ash	445
Appendix 6. Graphs to Determine Mode of Occurrence of Trace Elements in Blake Central, Blake West and Bowen No.2 Pits	448
Appendix 7. Proximate and Elemental Analysis Results for Bowen Coke Works Samples	494

Chapter 1.

Literature Review.

1.0. Chapter Resume.

Chapter 1 comprises a short introduction to trace elements in coal and coal utilisation, presenting a review of pertinent published literature and outlining the major reasons for the surge of interest in this topic. The chapter covers a number of different aspects, including health effects, concentration, mode of occurrence and geological aspects of trace elements in coal, as well as the behaviour of trace elements in combustion and leachability of fly-ash.

1.1. Introduction.

In a competitive marketing environment (Knapp, 1999), detailed knowledge of coal quality may be a deciding factor in marketing success. Information on the concentration of key trace elements in a prospective coal may be required by the purchaser to better manage increasingly strict environmental impact requirements and for price bargaining. Studies of trace elements in coal are, therefore, impelled by both financial and environmental concerns.

At present, the majority of coal mined is combusted for electricity generation or carbonised to produce metallurgical coke. Liquefaction and gasification of coal, although historically important, are currently of minor importance (although this could change). The suitability of a coal for use in the major utilisations can be divided into limitations governed by the organic, and the inorganic, constituents of the coal.

The elements carbon, hydrogen, nitrogen, oxygen and sulphur are generally considered to make up the organic fraction of the coal, although this is not always valid (Daniels and Altaner, 1993). The industrial properties of the organic fraction of coal are controlled by coal rank and coal type. Coal rank is the degree of coalification (ie the degree of physical and chemical change) the degraded plant material has undergone along a continuum from the peat stage to the meta-anthracite stage. The degree of coalification depends mainly on the maximum temperature surrounding

rocks have attained and the period for which it is maintained, and pressure, which may retard chemical reactions but promotes physical changes (such as loss of porosity and alignment of structural units).

However, the organic chemistry of individual coals of the same rank may be radically different, these differences being due to coal type. Coal type is determined, in the “classical” sense, by the proportions of the various macerals in the coal (ie the proportion of inertinite, vitrinite and liptinite, and by implication, sub-macerals thereof). The chemistry of each maceral group differs from the others. Liptinite is less aromatic than vitrinite, containing a higher proportion of aliphatic groups and correspondingly higher hydrogen (Teichmüller et al., 1998). Inertinite is more aromatic than vitrinite, containing more carbon but with very low hydrogen contents (Teichmüller et al., 1998). The chemistry of vitrinite is intermediate between chemistry of the liptinite and the inertinite groups. Variations in the proportions of the maceral groups in different coals would clearly result in very different chemical properties. For example, some Australian coals (eg Blair Athol, some Lithgow seams, Coorabin) are relatively low in vitrinite and high in inertinite and, consequently, are considered sub-hydrous (low in hydrogen) (Suggate, 1998).

A second type-controlled variation in coal chemistry may be caused by variation in the chemistry sub-macerals, particularly the vitrinite sub-macerals. Telocollinite (now called collotelinite) (International Committee for Coal and Organic Petrology, 1998) and telinite are woody vitrinite sub-macerals exhibiting a slightly higher reflectance than desmocollinite (now called collodetrinite) (International Committee for Coal and Organic Petrology, 1998) which may contain fine lipoid (liptinitic) inclusions.

A third type-controlled variation in coal chemistry is caused by variations in the chemistry of a single sub-maceral (eg telocollinite/ telovitrinite) (Newman, 1985; Newman, 1991; Newman et al., 1991). In such cases it is thought that the vitrinite absorbs hydrogen or hydrogen-rich substances. Coal type may be a reflection of the depositional environment of the precursor peat, but the relationships are complex.

Rank and type determine which utilisation process is most suitable for a particular coal. For example, coking coals are generally required to have moderate to high thermoplasticity, high Free Swelling Index (FSI) figures (~5 plus) and, ideally, a Coke Strength after Reaction (CSR) between 57 & 75. These properties are mostly governed by rank, prime coking coals having a vitrinite reflectance of between $R_o(\max)$ 1.2% & 1.4% (ACIRL, 1996; Diessel, 1998), but coal type (Quick, 1992; Rentel, 1987), and inorganic content and composition (see below) also exert a strong influence. Steaming coal requirements are broader and depend in part on plant design and operating conditions. However, good thermal coals are generally of lower rank, such coals being easier to ignite and giving greater flame stability due to the higher volatile matter content. Further, low rank coals have a higher rate of char burnout due to the less ordered carbon structure of the coal (Diessel, 1998) and greater porosity that allows easier ingress of combustive gasses. Coal rank also exerts some control on the grindability (HGI) of a thermal coal (Diessel, 1998; Hower and Parekh, 1991).

The inorganic constituents of the coal may limit utilization by negatively impacting on the industrial process or plant, and/ or by production of environmental pollutants in gases or from solid wastes. Ash constituents and some element information will often be required before a customer commits to buying a given coal. In general the elemental analyses requested are a reflection of utilization impact concerns. For example, the ratio of acidic to basic constituents in the coal ash will influence the fusion temperature of the ash (AFT) (Couch, 1994; Gray, 1987; Moore and Fergusson, 1997; Vuthaluru, 1999). A number of indexes have been devised to assess the impact of the acidic/ basic ratio on combustion processes, eg slagging index, fouling index (Table 1.1.). “High” concentrations of chlorine, fluorine, and vanadium in the feed coal may cause corrosion of the combustion equipment (Caswell et al., 1984; Liu et al., 2000; Shearer et al., 1997; Spears and Zheng, 1999). High vanadium coals may cause agglomeration in fluidised bed combustion boilers (Anthony and Jia, 2000). In carbonisation, basic elements can catalyse reduction reactions in the blast furnace, increasing coke consumption and production of breeze, and reducing coke strength and porosity (Coin, 1995; Diessel, 1998; Gunn, 1988). A 1% increase in the concentration of sulphur is thought to increase the coke consumption rate by as much as 32 kg per net ton of hot metal (Zimmerman, 1979) and greatly increase the production of slag. Phosphorous in coking coals also contributes to the slag, but most

will eventually end up in the product steel (Ward et al., 1996) making it brittle (Dennis, 1963; Moore and Moore, 1999). Boron in coking coal also ends up in the steel and causes brittleness (Swaine, 1990).

Inorganic constituents may also have an adverse effect on the environment (ignoring possible greenhouse effects caused by CO₂ from combustion of the organic matter). Increasing attention is now being given to the potential environmental impact of trace elements released by coal utilization. It has long been known that sulphur from coal combustion can cause acid rain (Bouska and Pesek, 1999). Similarly chlorine and fluorine in coal can also cause acidic emissions. A number of studies have shown that trace elements from coal combustion and combustion residues increase the concentration of toxic elements in the biosphere, in some cases resulting in negative health impacts on plants, animals and humans, (Agrawal et al., 1993; Bencko and Symon, 1977a; Bencko and Symon, 1977b; Clark et al., 1999; Finkelman, 1993; Gupta, 1999; Gutenmann and Bache, 1976; Huggins et al., 1999; Klusek et al., 1993; Knott et al., 1985; Panov et al., 1999; Swaine, 1989; Swaine, 1990; Swaine and Goodarzi, 1995; Wadge and Hutton, 1986; Zheng et al., 1999). Trace elements may be detrimental if intake or exposure is present at concentrations less than or greater than the optimum range (Swaine and Goodarzi, 1995) (Figure 1.1.) for a given organism, toxicity depending also on speciation (Huggins et al., 1999), organism tolerance (Bowen, 1966), and element antagonism or synergism (Kizilshtein and Kholodkov, 1999; Swaine, 1995; Wood, 1974) (Appendix 1). The concern is that the release of trace elements from coal utilization will result in elemental concentrations exceeding the toxicity threshold of some plants and animals (including humans).

Table 1.1. Coal Ash Chemistry and Slagging/ Fouling Characteristics.

THIS TABLE HAS BEEN REMOVED DUE TO
COPYRIGHT RESTRICTIONS

Source: Leonard, J.W. (1991)

THIS IMAGE HAS BEEN REMOVED DUE TO COPYRIGHT RESTRICTIONS

Figure 1.1. General Representation of the Effects of Increases of Concentration of a Trace Element. Source Swaine & Goodarzi (1995).

The widespread availability of large coal resources, coupled with decreasing opportunities to dam rivers for hydroelectric power generation, and the social unacceptability of nuclear power, suggest that coal consumption, for energy generation at least, will increase for some decades to come, particularly in developing countries (eg China, India) (Fyfe, 1999). Some coals mined in these developing countries are notable for a higher than “average” concentration of environmentally hazardous trace elements, eg Chinese coals, see Table 1.3., (Ren et al., 1999). Japanese power companies are now formulating standards as to the maximum allowable concentration of trace elements in supplied coal (Nishioka, Mitsui Mining; pers com, 1999).

Although the impact of some trace elements on animal and plant health is currently the prime impetus for studying trace elements in coal, there are other potential reasons for interest. Depending on concentration and distribution, trace elements may also be a source of economic by-products (Seredin, 1996), of use in prospecting for ore deposits, for soil amelioration, and for seam correlation purposes (Finkelman, 1993).

The use of trace element data in characterizing coals already mined is of little use for the prediction of future environmental impacts because the inhomogeneity, even within a seam, of elemental contents precludes meaningful extrapolation to new seams and mining blocks (see below). Therefore, trace element studies will need to be ongoing with mine development and coal use to adequately monitor element concentrations in the current product.

1.2. Trace Elements of Environmental Interest in Coal.

Trace elements are only of environmental concern if there is some recognisable impact on the health and well being of the ecosystem. However it is recognised that the impact of some trace elements may not be clinically detectable, or make take years or decades to become apparent. It should be noted that “health impact” is not anthropocentric in nature, and any negative impact on any part of the biosphere is generally viewed as undesirable by local, regional and national authorities as well as by the public. Any emphasis on human health impacts in this document are, therefore, merely a reflection of the literature reviewed.

It is notable that many of the trace elements listed as potentially environmentally deleterious if they are concentrated to toxic levels by coal utilisation are essential in low concentrations for the growth and well being of plants and animals. There is potential for trace elements from coal combustion waste to provide environmentally useful by-products if managed properly. For example, there is some potential to use fly-ash as a soil ameliorant to add essential elements to deficient soils (Finkelman, 1993), although studies need to be undertaken to ensure that the acid conditions of the soil will not release toxic cations from the fly-ash (Jones, 1995).

Four groups of environmentally significant elements are recognised (Swaine and Goodarzi, 1995; Zhang et al., 2004) (Table 1.2.). Group I elements are known to be hazardous in some circumstances, although the concentration of these elements is known to be low in most coals. Group IIA includes the elements B, Mn and Mo, which should be taken into consideration in leachates from wastes or during mine reclamation, and chlorine, which can cause acid emissions. Group IIB elements are unlikely to cause problems, although the radioactive elements U and Th should clearly be kept to a minimum. Group III elements are not expected to cause problems in the concentrations given for most coals.

Table 1.2. Trace Elements of Environmental Interest. From Swaine & Goodarzi (1995).

I	IIA	IIB	III
As	B	Be	Ba
Cd	Cl	Cu	Co
Cr	F	P	Sb
Hg	Mn	Th	Sn
Se	Mo	U	Tl
	Ni	V	
	Pb	Zn	

The health impacts of the environmentally significant trace elements listed in Table 1.2. are detailed in Appendix 1 along with comments about the essentiality, toxic effects and any synergistic or antagonistic interactions a particular element might have.

Predicting the toxicity of an element in the biosphere is not a simple matter of presence, or indeed of elemental concentration. An organism's diet, source of exposure, synergistic and antagonistic element interactions, elemental speciation, and tolerance variations between species all play an important role in determining any adverse effects caused by element absorption. Further, some poisons such as lead are cumulative so environmental and health impacts may not be immediately apparent. Hazard and risk assessment requires that even hazards perceived as having a low probability but with potentially significant impact be considered. Because the potential impacts are hard to predict or quantify for the reasons given above, caution is needed when assessing the environmental impact of elements released by coal utilization.

1.3. Geological Aspects of Trace Elements in Coal.

1.3.1. Concentration of Trace Elements in Coal.

1.3.1.1. Definitions.

Trace elements are defined as being present in concentrations up to 1000 ppm (0.1 %) dry basis in most coals (Lindahl and Finkelman, 1986; Swaine, 1990). Other authors suggest the upper concentration for an element to be classed as trace is 200 ppm (Mukhopadhyay et al., 1998).

In some cases elements usually considered as “trace” in coal are present in very high concentrations, eg arsenic present at 32,000 ppm and fluorine at 3600 ppm in Chinese coals (Ren et al., 1999); chlorine at 9100 ppm (Swaine, 1995) or 10,000 ppm (Valkovic, 1983a) in UK coals. Elements present in such concentrations could hardly be considered trace for the coal concerned. Knowledge of the concentration of trace elements in a coal can be important when comparing coals for purchase if such high levels might cause undue environmental impacts or be detrimental in utilisation.

A trace element is defined here as an element present in most coals in concentrations less than 1000ppm.

1.3.1.2. Comparison of Trace Element Concentrations.

For most coals, the concentration of trace elements is no higher than that of soils and shales (Swaine, 1989; Swaine, 1990) (exceptions being selenium, germanium, molybdenum and lead), and lower in many trace elements than some fertilizers. Swaine (1995) states that “coals with unusually high contents of trace elements must not be forgotten because these are the ones that may give problems during mining and usage” (Swaine, 1989; Swaine, 1990; Swaine, 1995). While the concentration of trace elements in most coals may be similar to soils and shales, the combustion of coal concentrates some elements in solid waste fractions (which must be disposed of) and emits others to the atmosphere as a point source over a long period of time. Some elements such as lead may accumulate in the environment over time, so the long-term impacts of using a particular coal may not be immediately apparent.

Average values of trace element concentration can be difficult to use as a basis for comparing coals due to the inhomogeneity elemental distribution, even within a single seam (Swaine, 1995). Inhomogeneity is caused by the complex geochemical controls on trace element concentration and distribution, namely “intake of trace element during plant growth, enrichment during plant decay, sedimentation and diagenesis, burial and coalification, and subsequent late-stage mineralization” (Mukhopadhyay et al., 1998). A number of trace elements have been shown to have a log frequency distribution so a geometric mean may be more useful when comparing coals (Bouska and Pesek, 1999; Swaine, 1995; White et al., 1989). The concentration range of trace elements in coal mined from New South Wales and Queensland mines is generally similar over time, so useful comparisons may be made between data sets showing a concentration range (Swaine, 1995). Table 1.3. shows the range of trace element contents published for a number of world coals by country.

Another method for comparing the trace element contents of coals is to use an independent ‘yard stick’. Comparison of “Clarke Values” (average concentration of the element in the earths crust), eg (Taylor, 1964), with coal elemental analysis results indicate the enrichment or depletion of a given element compared to the earths crust (Faure, 1991; Skinner and Porter, 1987); examples include (Beaton et al., 1991), (Casagrande and Erchull, 1977), (Eskenazy, 1982), (Goodarzi, 1987b) and (Goodarzi, 1988). Rare earth elements may be converted to a chondrite normalised basis in order to assess enrichment or depletion of the element; examples include (Birk and White, 1991), (Eskenazy, 1987) and (Seredin, 1996).

Table 1.3. - Content of Environmentally Significant Trace Elements in World Coals.

THIS TABLE HAS BEEN REMOVED DUE TO COPYRIGHT RESTRICTIONS

(1) Zubovic et al (1980); (2) Clark and Swaine (1962), Swaine (1977);
(3) mostly from Goodarzi and co-workers; (4) several (cited by Swaine, 1990)
(5) Ren et al. (1999); ^aDale and Lavrencic (1993)

Table based on Swaine (1995).

Because the concentration and redistribution of elements occurs during industrial utilization processes, some workers, e.g. (Toole-O'Neil et al., 1999) have suggested that it may be of practical benefit to compare coals on an equal energy basis. The logic behind this suggestion is that, for example, while a prospective lignite fuel may contain a lower concentration of elements of concern than an alternative bituminous coal, the additional coal consumed to provide the same quantity of energy could result in a greater total volume of deleterious elements being released to the environment. (NB Low rank coals may also have more elements loosely bound to the organic coal structure as cations, which may be more readily released to the atmosphere during combustion).

1.3.2. Mode of Occurrence.

1.3.2.1. Introduction.

The mode of occurrence of a trace element in coal is important in anticipating the behaviour of the element during coal cleaning, combustion, and weathering and leaching of coal and utilisation waste products (Finkelman, 1993; Finkelman, 1995; Mukhopadhyay et al., 1996; Mukhopadhyay et al., 1999; Querol et al., 1995). The use of a coal with a low concentration of a particular trace element could still result in a detrimental environmental impact if the mode of occurrence allows the element to be readily released during utilisation.

A large number of papers provide mode of occurrence data for coals from around the world (Appendix 2, Table 1.4.), providing a good survey of the most common and, therefore, most likely modes of occurrence for an element. Appendix 2 lists the elements of environmental interest from Table 1.2., and scores the modes based on the number of papers in which that mode was encountered (a full description of the scoring method can be found in Appendix 2). Table 1.4. is a summary of the mode of occurrence score results. The mode of occurrence scores provide an additional aid to the interpretation of new analytical results in this study.

Table 1.4., Likely Trace Element Mode of Occurrence from Literature Scores.

Element	Organic	Inorganic	Sulphide	Clays	Carbonate	Others
Antimony	13	41	36			10
Arsenic	15	14	69	1		1
Barium	21	19		21	35	4
Beryllium	75			25		
Boron	81					19
Cadmium			32			68
Chlorine	61					39
Chromium	22	28		30		20
Cobalt	33	19	23	14	6	5
Copper	22	20	38	13		7
Lead	5	13	65			17
Manganese	18	19	10		37	16
Mercury		8	78			14
Molybdenum	34	6	49			11
Nickel	23	11	36			31
Phosphorous	6					94
Selenium	25	7	43			24
Thallium			83			17
Thorium	1	40				59
Tin	9	30	33			28
Uranium	39	32		22		7
Vanadium	30	25		35		10
Zinc	7	16	35			42

1.3.2.2. Methods of Determining Modes of Occurrence.

A number of methods to determine or indicate trace element mode of occurrence in coal are described in the literature. No individual method is flawless, so several complementary methods should be used wherever possible to provide a robust mode of occurrence assessment. While some modes of occurrence are more frequently encountered for an element, many have several potential occurrence modes (Table 1.4.). One apparent fact is that a large number of trace elements of environmental concern are either dominantly or sometimes hosted by pyrite; ie, fourteen out of the twenty four trace elements of environmental concern listed in Goodarzi and Swaine (1995); see also (Finkelman, 1979; Spears et al., 1999). The concentration and mode of occurrence of an element in coal depends on a complex set of geological interactions between the “intake of trace elements during plant growth, enrichment during plant decay, sedimentation and diagenesis, burial and coalification, and late-stage mineralization” (Mukhopadhyay et al., 1998). Such a complex set of

circumstances is seldom identical between different locations, so it is no surprise that, as for elemental concentrations, the mode of occurrence varies on a worldwide scale for most elements. Such complexity means that coal deposits need to be studied on a case-by-case basis.

Determination of trace element mode of occurrence in coal has been undertaken in a variety of ways. To follow is a short review of some common methods.

SEM-EDX.

A scanning electron microscope equipped with an energy dispersive X-ray detector (SEM-EDX) has been used by some workers to locate and analyse accessory minerals in coal. Therefore, SEM-EDX directly determines the organic and/ or inorganic phase containing the trace element, and the concentration of the trace element in the host.

Advantages over other methods include:

- 1) The accessory mineral matter can be observed and analysed in situ (Finkelman, 1978). Liberation of accessory minerals from coal by ashing, even low temperature radio frequency ashing, may alter the mineral matter composition and form to a greater or lesser degree (Doolan et al., 1985; Finkelman et al., 1984; Mitchell and Gluskoter, 1976; O'Gorman and Walker, 1971). Further, ashing may result in the loss of some volatile trace elements. Only in-situ direct determination using a method such as SEM-EDX avoids alteration issues caused by ashing.
- 2) The textural features of the mineral matter can be observed and some interpretation made regarding the origin of the grain, ie detrital, authigenic or extra-terrestrial in origin (Finkelman and Stanton, 1978).

SEM-EDX has been used by a number of researchers, eg (Beaton et al., 1991; Finkelman, 1980; Mukhopadhyay et al., 1996; Palmer and Filby, 1984; Van Der Flier-Keller and Fyfe, 1986), or in combination with other techniques, eg (Vickridge et al., 1990). Similar techniques include ion microprobe analysis (Finkelman et al., 1984) and nuclear microprobe (Vickridge et al., 1990).

Disadvantages in the use of SEM-EDX are that it is not a bulk analysis technique, it is time consuming, and it is labour intensive. Because of these disadvantages, other methods are frequently used for more general studies.

Float-Sink.

The float-sink method assumes that elements concentrated in the float fraction are organically bound and elements concentrated in the sink fraction are inorganically bound. The density fractions may be further analysed to determine the mode of occurrence more specifically by:

- 1) Sequential extraction of the mineral phases (Feng and Hong, 1999; Miller and Given, 1986)
- 2) XRD or SEM analysis (Mukhopadhyay et al., 1996; Querol et al., 1995; Seredin, 1996; Spears and Martinez-Tarazona, 1993).
- 3) By graphing trace elements against major elements related to mineral matter species by normative analysis (Newman, 1988; Ward, 1980).
- 4) By statistical analysis (Querol et al., 2001a).

A further variant is the analysis of the float-sink data for various size fractions of a low temperature radio frequency ash with integration of mineral matter information from XRD and SEM analysis to deduce mode of occurrence (Palmer and Filby, 1984).

The major flaw in the float sink method is that small grains may be rafted up with the lightest density fraction (Finkelman, 1980). The effect of poor liberation makes some elements appear to be organically associated when in fact they are present within fine mineral grains. Problems of mineral alteration in radio frequency ashing (Finkelman et al., 1984) and detection limits for XRD (~0.1 %) (Lewis and McConchie, 1994) may limit the approach of Palmer and Filby (1984).

Statistical/ Graphical.

Graphical relationships between trace element concentration and the ash (or 1/ ash) yield for a series of samples (eg from plies in a channel sample) can be used to infer the organic or inorganic affinity of the element. An element is considered organically bound if it maintains almost the same level or decreases with increasing ash yield, but it is considered inorganically bound if its concentration in coal increases with increasing ash yield. If elements are determined on an in-ash basis, then inorganically bound elements would maintain a horizontal trend line, and organically bound elements decrease in proportion to ash yield. (NB there is a problem with loss of

volatile elements such as mercury during ashing). A large number of authors use the graphical approach, eg (Beaton et al., 1991; Dilles and Hill, 1984; Eskenazy, 1982; Eskenazy, 1987; Eskenazy et al., 1994; Goodarzi, 1987b; Goodarzi, 1987c; Goodarzi and Van Der Flier-Keller, 1988; Grieve and Goodarzi, 1993; Hower and Bland, 1989; Szilágyi, 1971), or 1/ash (Newman et al., 1997).

A more refined graphical method involves graphing the concentration of a mineral or an element representative of a mineral (eg K for illite) in coal against the concentration of the trace elements of interest, eg (Dewison, 1989; Gayer et al., 1999; Mukhopadhyay et al., 1996; Spears and Zheng, 1999; Van Der Flier-Keller and Fyfe, 1986; Ward et al., 1999). Computer programmes are now available to carry out normative analysis with operator input to define the most likely minerals present in a deposit (Ward and Taylor, 1996). Graphical methods using elemental indicators of specific minerals or normative mineralogical concentrations provide a more informative indication of mode of occurrence, however knowledge of the mineral matter is a prerequisite. The second method has been used in conjunction with the float-sink technique to provide better indications of mode of occurrence in separation experiments.

The shortcoming of the graphical technique is that analysis of trace element mode of occurrence is not direct (cf SEM-EDX). Not all graphical relationships necessarily point to a common mineral host. A positive correlation coefficient could simply point to a common source for graphically related elements rather than a common mode of occurrence (Finkelman, 1980; Finkelman, 1993). One example of how this error could arise is documented for vanadium, which was originally organically bound (substituting for magnesium in chlorophyll) (Riley and Saxby, 1986), but was remobilised and became associated with clay minerals during diagenesis (Patterson et al., 1986). Potentially vanadium could show a good inverse correlation with ash yield (indicating an organic association), but the element is actually associated with clay minerals. A second potential source of error could result from the redistribution of elements at low ranks by aquifer water. Mobile elements could end up with a spatial relationship with unrelated detrital material (Brockway et al., 1991). One final problem is that low ash in a sample does not necessarily indicate that the elements are

associated with the organic fraction; the elements could equally be present as microscopic mineral grains, as noted for the float-sink method.

Petrographic Relationships.

The trace elements content of vitrinite concentrates has been analysed and compared to whole coal concentrates. A plot of the ratio of the two is used to indicate organic and inorganic affinity (Ghosh et al., 1987; Lyons et al., 1989). The method assumes that the vitrinite fraction represents the original 'organic' composition of the coal and the whole coal is influenced by detrital and authigenic processes (eg by mineralization of inertinite). The major flaws in this method are that permeation of trace element transporting groundwaters may not necessarily be limited to non-vitrinite fractions of the coal, and different plant parts may concentrate different elements (Casagrande and Erchull, 1976).

Sequential Leaching.

Sequential leaching selectively mobilises elements from 'specific' mineral fractions by the use of mineral-specific acids, thus indicating mode of occurrence. Ammonium acetate ($\text{CH}_3\text{COONH}_4$) is used to mobilize loosely bound ions that may be organically associated or ions absorbed on clays; hydrochloric acid (HCl) to mobilise elements bound into carbonates or monosulphides such as chalcopyrite, sphalerite and galena; hydrofluoric acid (HF) to mobilize elements bound into silicates (quartz and clay minerals); and nitric acid (HNO_3) to mobilise elements in disulphides (pyrite) (Feng and Hong, 1999; Finkelman et al., 1990; Laban and Atkin, 1999; Miller and Given, 1987; Palmer et al., 1999; Palmer et al., 1998). Knowledge of the mineral matter in the coal is also useful for providing a robust interpretation, therefore XRD and/ or SEM analysis of the samples may be required.

Although not a direct technique, sequential leaching seems to provide a reasonable 'bulk' indication of the mode of occurrence and the proportions of an element in each mode for multi-mode elements. The method requires support analysis of XRD to determine the mineralogy of the sample, and XRF/ ICP/ INAA or some other elemental analysis technique to analyse the leachate. Leaching studies may also be undertaken in conjunction with float sink experiments.

Sequential leaching has some shortcomings (Querol et al., 1998). There are some indications that ammonium acetate may attack calcite. Further, ashing of coal residues may yield 0.3% ash, indicating incomplete digestion of the inorganic constituents, probably in part due to shielding of some digestible inorganics by the organic matter (Willett et al., 2003). Some minerals (eg phosphates and sulphates) may be dissolved by several of the acids (Laban and Atkin, 1999). Finally, all of the reagents are dangerous, particularly hydrofluoric acid.

A fuller description of techniques used to indicate or determine the mode of occurrence of trace elements in coal is contained in Finkelman (1980).

1.3.3. Controls on Trace Element Occurrence in Coal.

A number of geological, hydrological and biological controls dictate the concentration, mode of occurrence and distribution of trace elements in coal. The relative importance of these factors varies according to the history of the deposit and the stage of coalification (Goodarzi, 1995a). The controls on trace elements in coal are:

- During early stages of coal formation:
 1. Provenance of the sediments entering the depositional basin.
 2. Depositional environment of the mire.
 3. Ability of plants, plant debris and bacteria to fix elements.
- During coalification stages:
 1. Changes in rank.
 2. The geochemical nature of groundwater and country rocks.

1.3.3.1. Sediment Provenance.

Rocks outcropping in the source area exert a strong influence on the concentration and mode of occurrence of trace elements supplied to a peat mire. The contribution of detrital material to trace element content and mode of occurrence is particularly important for coals with ash yields exceeding 8% (Finkelman, 1993). Given the influence of the source rocks, it is perhaps surprising that relatively few papers deal in detail with the effect of source rock on coal quality (cf depositional environment controls, for example).

A number of Chinese coals have been classified on the basis of the geological and geochemical controls on the contained trace elements (Ren et al., 1999). They suggest that source rock exerts the dominant influence on coals laid down in small fault-controlled basins where the sedimentation rate is rapid and the basin fills quickly (Brownfield et al., 1995; Ren et al., 1999). In such cases, elements present in high concentrations in the source rocks will be found in high concentrations in the coal.

Specific examples of source rock chemistry being responsible for anomalous trace element concentrations include tungsten (Eskenazy, 1982); copper, lead, and zinc from mineralised zones in the hinterland (Mukhopadhyay et al., 1998); and manganese rich source rocks supplying streams and hydrothermal waters (Robbins et al., 1990). Perhaps more convincing evidence of the importance of provenance is reported where lateral variations in trace element concentration in coal can be spatially related to the sediment source. High sulphur and arsenic zones were found in the North Bohemian Basin coal adjacent to sediment-supplying mountain ranges (Bouska and Pesek, 1999). The concentration patterns of some trace elements in samples from the Bullmoose mine (Canada) were examined using GIS and related to provenance controls (Van Der Flier-Keller and Bartier, 1993).

Examples relating a specific source rock type to trace element content and/or mode of occurrence include association with volcanoclastics or ash fall debris (Goodarzi and Van Der Flier-Keller, 1988; Goodarzi and Van Der Flier-Keller, 1989; Jiménez et al., 1999; Ren et al., 1999; Seredin, 1996). Cr-spinels are noted as a particularly important mode of occurrence for chromium in areas where ultramafic source rocks have contributed debris to the coal (Kolker and Finkelman, 1998). High chromium in coal has also been related to chromium-bearing minerals eroded from nearby ophiolite and serpentinite bodies (Brownfield et al., 1995).

Elevated concentrations of chlorine, sodium, calcium, and possibly barium in the coal from the St. Rose and Chimney Corner coalfields (Cape Breton, Canada) were caused by mobilisation of these elements from gypsum, anhydrite, carbonates, halite, and potash salt formations brought into contact with the coal by faulting (Beaton et al., 1993).

Clay minerals are a commonly cited mode of occurrence for a number of trace elements. Fixation of rare earth elements (Birk and White, 1991), uranium (Zodrow et al., 1987), and boron (Spears, 1965) into clay minerals in the source area has been found to cause enrichment of these elements in the receiving coal. The presence of boron fixed into clay minerals in the source area has some implications for the use of boron as a palaeosalinity indicator.

Modern day variations in the selenium content of tributaries of the Orinoco River are caused by alkaline weathering of shale outcrops with high selenium contents, demonstrating the influence of provenance on the chemistry of the depositional basin (Yee et al., 1987).

It should be noted that the geochemistry of trace elements in a coal might not be a direct reflection of the geochemistry of the source area. Trace element distribution in sediments is also controlled by clast size fractionation and transport distance (Cullers, 1994; Dominik and Stanley, 1993; Duke, 1985). It is well known that the relative proportions of different clast types in a bedload changes downstream depending on the mechanical and chemical stability of the clasts (Bradley, 1970). Climatic conditions in the source area may also influence the proportions of trace elements delivered to a peat by preferentially weathering certain minerals (Mann and Cavaroc, 1973). For example, a light rare earth element anomaly found in coals of the Sydney Basin, Nova Scotia (associated with detrital illite and quartz) is due to preferential removal of these elements from feldspars in the source area (Birk and White, 1991).

A further complexity is that some elements may be re-mobilised from the detrital minerals (Finkelman, 1993; Spears and Martinez-Tarazona, 1993; Ward et al., 1996) making inferences of source rock influence on trace element concentration difficult in some cases.

1.3.3.2. Depositional Environment.

It has long been recognised that some aspects of coal quality and elemental composition are controlled by the depositional environment, importantly the sulphur content of coal (Bustin and Lowe, 1987; Querol et al., 1999b; Teichmüller et al., 1998). Marine-influenced coals often show increased sulphur content and an

increased proportion of pyritic sulphur to total sulphur content (Casagrande et al., 1977). Given that pyrite is a common mode of occurrence for several elements of environmental interest (eg antimony, arsenic, cobalt, mercury, molybdenum, selenium) or may allow substitution of the Fe ion for a number of others, it is no surprise that coals deposited in a marine influenced environment show increased concentrations of some elements of concern (Gayer et al., 1999; Hower et al., 1996; Ren et al., 1999; Spears et al., 1999).

The concentration of boron in coals and sediments is commonly used as an indicator of palaeosalinity (Boggs, 1987; Bohor and Gluskoter, 1973; Bouska, 1981; Goodarzi and Swaine, 1994; Goodarzi and Van Der Flier-Keller, 1989; Mukhopadhyay et al., 1998). Coals with concentrations of boron up to 50ppm are considered fresh water influenced; coals with a concentration of 50-110ppm are considered as influence by mildly brackish water; coals with a concentration of greater than 110ppm boron are considered as brackish water influenced (Goodarzi, 1995a; Teichmüller et al., 1998). Boron concentration has also been used in combination with other trace elements to infer depositional environment, eg boron/ beryllium ratio (Dominik and Stanley, 1993); plots of B versus Cr, Na, S & U (Goodarzi, 1987b); plots of B versus S, and B versus Br/Cl ratio (Goodarzi, 1988); and B vs Cr (Goodarzi and Van Der Flier-Keller, 1988).

There is considerable discussion in the literature on the use boron as an indicator of depositional environment. Some authors recommend using only the boron bound in illite to indicate palaeoenvironmental conditions (Bohor and Gluskoter, 1973), reasoning that boron is extracted from water mainly by fine-grained argillaceous sediments, with illite (the main host) firmly fixing the boron in the mineral matrix. However, misinterpretation of palaeoenvironment may arise if the boron is fixed into illite prior to release from the source area (Bohor and Gluskoter, 1973; Spears, 1965). Correction for the boron in illite can be made (Curtis, 1964), but this adjustment may fail to rectify the problem of anomalous data sets where the element concentration does not concur with sedimentological evidence (Couch, 1971). Such problems may result from preferential binding of soluble organic matter to the illite where dissolved organic matter in the water is high (Curtis, 1964). An antipathetic relationship has been found to exist between boron and organic carbon (Eagar, 1962). The boron

content in the water would then be a reflection of the geochemical equilibrium with organic matter rather than by the degree of incorporation into clay minerals.

Further errors could result where tourmaline was a major mode of occurrence for boron, or where element depletion during diagenesis occurred (Eskenazy et al., 1994). Eskenazy et al. (1994) found “the mean content of boron could hardly be regarded as a definitive indicator of salinity”, and Eagar (1962) concluded “factors other than the salinity of the waters in which these sediments accumulated have influenced their boron contents”.

Van der Flier Keller and Bartier (1993) found the distribution of chlorine in the coal they studied was related to the direction in which the palaeoshoreline lay.

More complicated geochemical schemes involving several elements have been used to indicate the depositional environment of sediments and coals. Marine influenced coals were found to contain higher concentrations of Zn, Fe, pyritic sulphur, sulphate sulphur and possibly Ca; whereas fluviially influenced coals were higher in Cu, Cr, Ti, K, Si, and Al (Bailey, 1981). Depositional environment has been deduced using boron (higher in marine influenced coals), gallium (higher in fresh water influence sediments), and rubidium (Degens et al., 1958). A study of B, Cr, Cu, Ga, Ni, and V concentrations in marine and non-marine sediments concluded good differentiation of paleoenvironment could be made on the basis of B and V alone (Boggs, 1987; Potter et al., 1963).

Differences in the elemental contents of marine-influenced versus freshwater-influenced coals are the most commonly cited examples of depositional controls. However, other examples of the impact of depositional environment include studies that show enrichment of Ti, Zr, Y, and Nb (Dewison, 1989); and enrichment of Zr and Nb (Spears and Martinez-Tarazona, 1993) in coal were caused by volcanic ash falls. Studies of vertical variations in Mn, Zn, Cu, Ni, Co, Sr, and Ca in the Pond Creek coal bed concluded these variations reflected changes in pH at the time of deposition (Hower and Bland, 1989). The chemical conditions within the swamp may also influence the distribution of trace elements by re-mobilisation, eg lead (Urban et al., 1990); phosphorous (Rao and Walsh, 1997; Ward et al., 1996); calcium, magnesium,

and sodium (Brockway et al., 1991); and iron (Spears and Martinez-Tarazona, 1993). Re-mobilisation has important implications on the use of graphical relationships to interpret element mode of occurrence (see Section 1.3.2.2.).

Particle settling in areas of reduced current flow at the margins of mires may also control the distribution of trace elements (McCarthy et al., 1989). It should be noted that this effect might also result from adsorption of ions into humic acid (Section 1.3.3.3.) or the flocculation of clay minerals (Staub and Cohen, 1978) at the margins of the mire.

The topography of the peat mire may also exert some control on trace element distribution in the coal since the concentration of inorganic elements decreases with peat accumulation in an ombrogenous mire because the peat surface is above most floods (Cameron et al., 1989). Thus the concentration of major and trace elements increase from the top of the peat to the base of the peat.

In summary, while the depositional environment of a peat undoubtedly exerts a major influence on the trace element content of the resultant coal seam, the range of geochemical schemes used to indicate environment suggests similar environments may have markedly different geochemical signatures. Mire chemistry and hydrodynamics may act to modify the element distribution and mode of occurrence. It must be concluded that the control of depositional environment on trace element chemistry is as variable as the control exerted by provenance.

1.3.3.3. Fixation of Elements by Plants and Plant Debris.

Plants have been found to concentrate certain major elements (eg Ca, Na, Mg) relative to the associated water and peat (Casagrande and Erchull, 1977), with particular species preferentially taking up certain metals compared with other plant species. Casagrande and Erchull (1977) also found that within one plant, different anatomical parts may have different concentrations of some elements, which casts doubt on the validity of using of vitrinite concentrates to indicate the original plant trace element input; eg (Ghosh et al., 1987; Lyons et al., 1989). The logical implication of plant specific geochemical makeup is that different communities forming peat in different locations within a swamp may result in peats with a spatially variable geochemical

signature. For example, high proportions of silicon, iron, potassium, phosphorous, calcium, and magnesium were contributed directly from plant matter in a swamp system in the Okavango delta (McCarthy et al., 1989).

Casagrande and Erchull (1977) also noted that some trace metals such as chromium, copper, iron, and lead were present at higher concentrations in the peat than in the plants, and there is a tendency for coals world wide to be enriched in heavy rare earth elements relative to light rare earth elements (Eskenazy, 1987; Eskenazy, 1999; Seredin, 1996) due to the greater ability of HREE's to form organic complexes. Experimental work found that heavy rare earth element sorption to xylain was pH and time dependant (Eskenazy, 1999). Maximum sorption was found at the range pH 3-5, and equilibrium was reached in 5-7 days.

Humic acids from humification processes were able to concentrate uranium at an enrichment factor of 10,000:1 from very dilute solutions in natural waters (Szalay, 1964). Enrichment factors for thorium, rare earth elements, and zirconium are higher than for uranium, but enrichment of these elements is constrained by their solubility in natural waters and their mobility at pH 4-7 (Szalay, 1964). Vanadium is also fixed by the cation exchange properties of humic acid, and had a geochemical enrichment factor of "at least 50,000:1" (Szalay and Szilágyi, 1967).

The elements Ge, V, Be, Ti, Ga, B, Ni, Cr, Co, Y, Mo, Cu, Sn, La, and Zn may form organic substances such as organo-metallic complexes of the chelate type according to citations in Bouska (1981). The metal is probably attached to nitrogen, a bond that is firmer than that of complexes in which the metal is bound to oxygen. The pH of the environment is an important factor in this process, but the formation of chelates is also governed by the ionic potential of the metal (Bouska, 1981; Zubovic et al., 1961). Metals with a higher ionic potential have a higher capacity to bind to the organic matter in the coal (and visa versa). The stability of the chelate helps determine whether the element remains in the coal during initial coalification.

Microbial activity may also play an important role in mediating fixation and precipitation of some elements in coal (Robbins et al., 1990).

It is clear from field studies and laboratory experiments that plants and humic acids from humification of plant debris may fix trace elements, possibly controlling the distribution of trace elements between maceral and sub-maceral groups, and spatially within a mire. Fixation of some elements may be mediated by microbial activity. Thus biological processes and humification products may exert an influence on trace element content and distribution within a resultant coal seam.

1.3.3.4. Coal Rank.

A number of authors have suggested that, with increasing rank, the concentration of certain trace elements changes eg (Goodarzi, 1988; Goodarzi, 1995a; Goodarzi et al., 1985; Goodarzi and Van Der Flier-Keller, 1988; Lindahl and Finkelman, 1986; Vassilev et al., 2000a). It is generally accepted that some elements, eg Ca, Mg, Na, B, Ba, Sr (Lindahl and Finkelman, 1986); B, Be, Ge, Sb (Teichmüller et al., 1998), may be associated with organic functional groups (eg carboxyl groups) (Section 1.3.3.3.) in coal. The association of ions with functional groups is a particular feature of low rank coals, where a sizable fraction of the inorganic matter may be chemically bound to the organic fraction of the coal (Brockway et al., 1991; Miller and Given, 1986; Miller and Given, 1987). With increasing rank, these functional groups are lost from coal (Teichmüller et al., 1998) and it is thought that the associated trace elements may be concurrently expelled.

Data for U.S. coals with ranks ranging from lignite to anthracite showed a decrease in Ca, Mg, Na, B, Ba, and Sr coincident with increasing rank (Lindahl and Finkelman, 1986). Decreasing concentrations of arsenic and sulphur were associated with increasing rank and were related to concurrent porosity loss (Goodarzi and Van Der Flier-Keller, 1988). Chlorine concentration was found to increase with increasing rank, but then decrease to low levels by the anthracite stage, possibly reflecting changes in porosity (Vassilev et al., 2000a).

Recently, the idea that boron concentration decreases with rank has been reviewed and it was concluded that there is no evidence for boron concentration decreasing with increasing rank (or a very complex relationship), at least for the coals used in the studies (Eskenazy et al., 1994; Goodarzi and Swaine, 1994). A lack of correlation between trace element chemistry of vitrinite concentrates and rank, age, and floral

composition of the coals has also been observed (Lyons et al., 1989). However, graphical information for arsenic, copper, chromium, manganese, molybdenum, and vanadium shows an apparent decrease in elemental concentration coincident with increasing rank (Goodarzi, 1995a).

It appears that there is some evidence for a decrease in the concentration of certain elements that are organically associated at low ranks. However, the inhomogeneity of elemental distribution and concentration related to variations in provenance, depositional environment, plant factors, hydrology, and other controls appear to make conclusive proof difficult to obtain.

1.3.3.5. Geochemical Nature of Groundwater and Country Rocks.

Hydrogeological influences have been invoked to explain features of trace element enrichment and distribution. Anomalously high concentrations of Na, Ba, B, and Ca in a seam deposited in a freshwater environment were suggested to result from circulating groundwaters (Beaton et al., 1991). In Victorian Brown coals (Australia), where Ca, Mg, and a considerable proportion of Na are organically bound, the concentration of these elements at the top of the seam was explained by transport in groundwaters and deposition due to evaporative losses at the upper surface of the peat (Brockway et al., 1991). Enrichment of germanium, molybdenum, and uranium in the upper sections of seams studied in the West Shandong mining district of China have been attributed to diagenetic infiltration fluids enriched in these elements (Querol et al., 1999b). The No. 9 seam in Pingshuo mine in the Shanxi Province of China has higher than average concentrations of Ca, Mn, Ba, Sr, Zn, and Cd due to the formation of epigenetic carbonates from groundwaters influenced by carbonate rich country rocks (Ren et al., 1999). Manganese may be delivered to peat by manganese-bearing groundwaters (Robbins et al., 1990). Observed concentration and patterns of concentration of rare earth elements in Eastern Russian coals are caused by the delivery of these elements by groundwaters (Seredin, 1996).

Late-stage import of ions for authigenic mineral formation is also found in some coals. Cleat or vein infilling by sphalerite (Gluskoter and Lindahl, 1973; Hatch et al., 1976) or pyrite (Hower et al., 1996) is clearly due to circulation of ion-bearing

groundwaters. Both these minerals have been found to allow the substitution of additional environmentally detrimental elements within their lattice.

The composition of the country rocks is the over-riding control on the composition of ions in groundwater. Studies of sediments show the composition of groundwater may evolve with time and burial (Bonham, 1980; Curtis et al., 1986), and depends on the composition of the sediments in the groundwater zone. There is, therefore, the possibility that the trace elements delivered to a seam by groundwaters may change with burial and time. For example, epigenetic pyrite may contain more arsenic than syngenetic pyrite (Finkelman, 1982; Hower et al., 1996).

1.3.3.6. Summary - Geological Aspects of Trace Elements in Coal.

The elements present in “trace” concentrations in coal are location specific, with individual seams or basins potentially falling within a specific range of concentrations. A comparison of elemental concentration is of interest when choosing a coal with the least environmental impact for the proposed use. Comparisons based on ranges of values and both arithmetic and geometric means are seen as being more useful than arithmetic average figures alone. For combustion purposes, comparison on an equal energy basis appears to be a useful method of comparing feed coals during environmental impact studies. Enrichment or depletion of elements compared to crustal or chondrite values may be of academic interest.

The most apparent feature of the geological controls on trace elements in coal is variability. The influences on element delivery to a coal bed (ie sediment provenance, depositional environment, the ability of plant, plant debris and bacteria to fix elements, and the geochemical nature of groundwater) all affect the elements supplied, and vary both spatially and temporally. Rank changes might act to modify the trace element assemblage during burial. The complexity of geological controls is particularly apparent for depositional environment factors, where no flawless geochemical indicator of depositional environment has been found to date.

It is a logical conclusion that the mode of occurrence and concentration of an element within coals will also vary as discussed in Sections 1.3.1 and 1.3.2., reflecting the inhomogeneity of element supply controls. It appears that some broad consistency of

mode of occurrence and range of element values can be related to depositional environment, but these generalisations are fallible. Generalisations should be treated with caution, and continued analysis and monitoring will be required to ensure an understanding of the concentration and element distribution within a mining block.

1.4. Trace Elements in Coal Combustion.

1.4.1. Introduction.

Trace elements exiting a coal combustion plant will be partitioned between three phases; namely bottom-ash, fly-ash and vapour. Vapour and some fraction of the finest fly-ash are emitted to the atmosphere. The percentage of the fine fly-ash emitted depends on the efficiency of the particulate control systems and the presence or absence of flue-gas scrubbing devices. In most modern power plants, more than 99% of fine particulates are removed by control devices such as electrostatic precipitators or fabric filters, and scrubbers may also remove some fraction of arsenic, boron, mercury, selenium, bromine, sulphur, chlorine, fluorine, and iodine present as components of flue gas (Clarke, 1995). The fate of elements that escape the control devices is beyond the scope of this research. However, models of plume behaviour and dispersion (Carras, 1995; Querol et al., 1999a), and data on the deposition of elements (Godbeer and Swaine, 1995) and fly-ash (Agrawal et al., 1993) from the atmosphere are available. Further discussion in this review will be restricted mainly to fly-ash and bottom-ash.

1.4.2. Definitions.

Bottom-ash generally consists of coarse ash particles greater than 100 μm (Meij, 1995). Bottom-ash is granular and similar in texture to concrete sand. Slag (which may be removed along with the bottom-ash) is shiny black granular material that is very hard and abrasive (Keefer, 1993). Bottom-ash is dominantly made up of inorganic matter but some unburnt carbon may also be present.

Fly-ash is more complicated in origin and form. Fly-ash is generally comprises fine ash particles of less than 100 μm size (Meij, 1995), varying in size down to 0.01 μm , with most particles ranging from 10-20 μm (Diessel, 1998) collected at various points downstream of the combustion chamber. Fly-ash is composed of inorganic elements, [dominantly present as quartz, glass, mullite, non magnetic iron oxides and magnetic spinel (Hulett et al., 1980; Jones, 1995; Sokol et al., 2002), with some substitution of other minor elements (Jones, 1995; Mukhopadhyay et al., 1996)], and perhaps minor unburnt carbon (Maroto-Valer et al., 2001) (although modern power plants usually achieve greater than 99% burnout).

Fly-ash may occur in a number of forms, classification depending on the thickness of the particle walls and number of vesicles. Hollow glassy fly-ash particles are termed cenospheres (Fishman et al., 1999). Cenospheres with smaller spheres inside are termed pleuroospheres (Fishman et al., 1999). Hollow iron rich particles may be termed ferrospheres (Fishman et al., 1999). In addition, char in varying forms may also be present (Bailey et al., 1990). The large surface area to volume ratio of the fly-ash particles, increasing as particle size decreases, is an important factor in the capture of some volatile trace elements from the flue-gas by fly-ash.

The form of fly-ash is, in part, a function of the mineral precursors in the coal. The two main groups of minerals in coal, adventitious and inherent, tend to differ in particle size and follow different pathways during combustion. The particle size of an adventitious mineral is more commonly larger than the milling size and can be present as extraneous or excluded grains in the feedstock, or may be rejected from the mill (generally <1% of the original feed; Hower, pers comm. 2005). These mineral separates may melt, decompose or fragment depending on their composition. Minerals with a low ash fusion temperature coagulate as slag on the boiler surface (or report to the bottom-ash) unless melting is accompanied by expansion, in which case a buoyant cenosphere may form.

Inherent minerals are usually present as small grains and remain encapsulated within the crushed coal particles. These minerals are termed included minerals. In non-swelling coals, the char particles burn progressively inward and the molten mineral droplets eventually coalesce to form a single particle, proportional in size to the ash content of the original coal particle (coalescence model). Alternative models suggest no coalescence takes place but each inorganic particle remains discrete. Probably the truth contains elements of both models in varying proportions (Seggiani et al., 2000). In swelling coal particles, char cenospheres are formed which disintegrate on combustion resulting in fragmented inorganic contents.

Fly-ash, particularly in pulverised coal combustion plants, makes up a large or dominant proportion of solid wastes (Table 1.5.). Fly-ash is the dominant host of

many environmentally sensitive trace elements following combustion and may pose a significant environmental hazard.

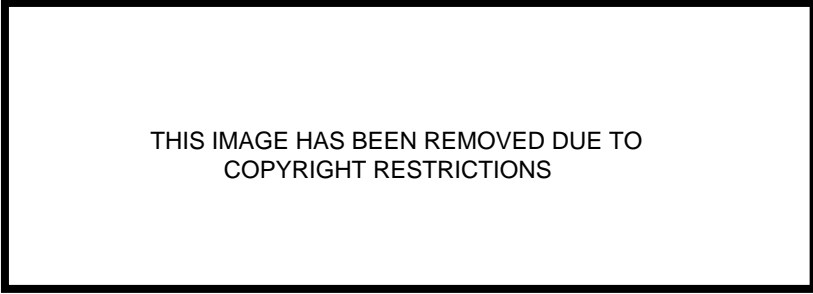
Furnace	Bottom-ash %	Boiler Slag %	Fly-ash %
Stoker fired, travelling	100	-	-
Stoker fired, spreader	-	45-85	15-55
Cyclone fired	-	80-85	15-20
Pulverised coal, wet bottom	50	-	50
Pulverised coal, dry bottom	20-25	-	75-80

1.4.3. Partitioning of Trace Elements in Combustion.

Inorganic elements have been divided into three classes based on their partitioning behaviour in combustion processes (Figure 1.2.; Table 1.6) (Clarke, 1995; Meij, 1995; Valkovic, 1983b).

Class I elements do not vaporise and are readily incorporated into the slag. These elements form a melt, which contributes to both fly-ash and slag. The elements involved are partitioned approximately equally between the slag and inlet fly-ash with no apparent tendency to concentrate in the outlet fly-ash (Meij, 1995).

Class II elements are volatilised, and later condense on and become adsorbed onto the fly-ash. Because the slag is quickly removed, Class II elements are not incorporated into or condense on the bottom-ash. Thus the Class II elements become concentrated in the inlet fly-ash compared to the slag, and in the outlet fly-ash compared to the inlet fly-ash. Meij (1995) further subdivides Class II elements, depending on the degree of volatility. The difference between Classes I and IIc is not always distinct, varying between “test series”. Further comment on the distinctions between the Class II subdivisions are not given by Meij (1995).



THIS IMAGE HAS BEEN REMOVED DUE TO
COPYRIGHT RESTRICTIONS

Figure 1.2. Classification of Elements by their Behaviour during Combustion and Gasification. (from Clarke, 1995)

Class III elements have a low dew point and tend not to condense anywhere within the power plant. If no flue-gas desulphurisation installations are present, virtually all of the Class III elements remain completely in the gas phase and are emitted to the atmosphere. [NB Fifty percent of fluorine may be removed as HF where scrubbers are fitted, with only the less toxic SiF₄ emitted (Valkovic, 1983b)]. However it has been found that up to ~10% of mercury in coal may remain in furnace ash (Billings and Matson, 1972) and some proportion may be captured by the fly-ash (Maroto-Valer et al., 2001; Sakulpitakphon et al., 2004; Sakulpitakphon et al., 2000). The capture of a highly volatile element such as mercury by the fly-ash (see also Section 1.4.4.3.) illustrates the difficulty in providing an absolute partitioning behaviour classification for any particular element.

Table 1.6. shows some variations in element classification, suggesting some behaviour differences between different coals and test series (also suggested by

Figure 1.2.). A number of factors may control the partitioning of elements, potentially causing variations in the classification of elements.

Average figures for the partitioning of a number of elements are presented in Table 1.7.

Table 1.6. Element Partitioning Class Comparison.

Element Class Assignment - Meij (1995) and Valkovic (1983b).		
Element	Meij (1995)	Valkovic (1983b)
Aluminium	I	I
Antimony	-	II
Arsenic	II a	II
Barium	II c	I
Beryllium	II b	-
Boron	III	-
Bromine	III	III
Cadmium	II a	II
Caesium	I	I
Calcium	I	I
Carbon	III	-
Cerium	I	I
Chlorine	III	III
Chromium	II c	I
Cobalt	II b	I
Copper	II b	II
Europium	I	I
Fluorine	III	-
Gallium	-	II
Germanium	II a	-
Hafnium	I	I
Iodine	III	-
Iron	I	I
Lanthanum	I	I
Lead	II a	II
Magnesium	I	I
Manganese	II c	I
Mercury	III	III
Molybdenum	II a	II (?)
Nickel	II b	I (?)
Nitrogen	III	-
Phosphorous	II b	-
Potassium	I	I
Rubidium	II c	I
Samarium	I	I
Scandium	I	I

Selenium	III	II
Silicon	I	I
Sodium	II c	I
Strontium	I / II c	I
Sulphur	II a / III	-
Tantalum	-	I
Thallium	II a	-
Thorium	I	I
Titanium	I	I
Tungsten	II b	-
Uranium	II b	I
Vanadium	II b	I
Zinc	II a	II

Table 1.7 Distribution of Elements Among Bottom-ash, Fly-ash and Flue Gas.

(from Valkovic, 1983b)

Element (% of total in plant)	Bottom-ash (22.2%)	Fly-ash (77.1%)	Flue Gas (0.7%)
Aluminium	20.5	78.8	0.7
Antimony	2.7	93.4	3.9
Arsenic	0.8	99.1	0.005
Barium	16.0	83.9	0.009
Beryllium	16.9	81.0	2.0
Boron	12.1	83.2	4.7
Cadmium	15.7	80.5	3.8
Calcium	18.5	80.7	0.8
Chlorine	16.0	3.8	80.2
Chromium	13.9	73.7	12.4
Cobalt	15.6	82.9	1.5
Copper	12.7	86.5	0.8
Fluorine	1.1	91.3	7.6
Iron	27.9	71.3	0.8
Lead	10.3	82.2	7.5
Magnesium	17.2	82	0.8
Manganese	17.3	81.5	1.2
Mercury	2.1	0.0	97.9
Molybdenum	12.8	77.8	9.4
Nickel	13.6	68.2	18.2
Selenium	1.4	60.9	27.7
Silver	3.2	95.5	1.3
Sulphur	3.4	8.8	87.8
Titanium	21.1	78.3	0.6
Uranium	18.0	80.6	1.5
Vanadium	15.3	82.3	2.4
Zinc	29.4	68.0	2.6

1.4.4. Controls on Trace Element Partitioning in Combustion.

Partitioning of elements in combustion processes is complex and related to at least four variables, namely elemental and oxide volatility, mode of occurrence (inorganic particle size and mineral association), collection point and characteristics of the ash, and combustion regime.

1.4.4.1. Elemental Volatility.

The prime control on element partitioning is the volatility of the element in the combustion process (Gayer et al., 1999; Meij, 1995; Valkovic, 1983b); Tables 1.6 & 1.7. The vaporisation sequence of the volatile elements also varies according to whether the element is in an elemental or oxidised state (Valkovic, 1983b), so the temperature and oxidation potential of the furnace is important in determining enrichment or depletion of elements in ash types. The relative order of volatilities for trace elements is (Valkovic, 1983b):

For elements in oxides, sulphates, carbonates, silicates and phosphates:

As \approx Hg > Cd > Pb \approx Bi \approx Tl > Ag \approx Zn > Cu \approx Ga > Sn > Li \approx Na \approx K \approx Rb \approx Cs

For elements in the elemental state, the order is:

Hg > As > Cd > Zn > Sb \geq Bi > Tl > Mn > Ag \approx Sn \approx Cu > Ga \approx Ge

For sulphides the relative order of volatility is:

As \approx Hg > Sn \approx Ge \geq Cd > Sb \approx Pb \geq Bi > Zn \approx Tl > Cu > Fe \approx Co \approx Ni \approx Mn \approx Ag

Species boiling or sublimating below or at 1550°C during coal combustion include:

As, As₂O₃, AsS₃; Ba; Bi; Ca; Cd, CdO, CdS; Cr(CO)₆, CrCl₃, CrS; K; Mg; Ni(CO)₄; PbCl₂, PbO; Rb; Se, SeO₂, SeO₃; Sb, SbS₃, SbO₃; SnS; Sr; Tl, Tl₂O, Tl₂O₃; Zn, ZnS

It is apparent from these lists that the volatility of the elements and elemental oxides is closely related to the partitioning classes of elements in combustion given in Tables 1.6. and Figure 1.2.

Following on from the initial volatilisation of trace elements in the combustion chamber, partitioning behaviour will then depend on the temperature at which the off-

gases fall below the dew point a particular element (Mastalerz et al., 2004; Sakulpitakphon et al., 2004; Sakulpitakphon et al., 2000). Thus, for example, mercury concentration will increase in the fly-ash downstream as the temperature cools and allow the element to condense on the fine ash particles (Sakulpitakphon et al., 2000).

1.4.4.2. Mode of Occurrence.

The mode of occurrence of a trace element in the coal is another influence on the partitioning behaviour of the element in combustion (Finkelman, 1982; Finkelman, 1994; Kolker and Finkelman, 1998; Vassilev et al., 2000b; Willett et al., 2003). Trace element affinity plays a strong role in determining the element behaviour during combustion (Querol et al., 1995), with sulphide or organic affinities being oxidised during coal combustion and consequently showing volatile behaviour. The element behaviour reflected either the temperature rise accompanying oxidation, or reactions with Cl, F, Na, or S compounds inducing volatility in some elements such as As, Se, and Cd. Oxidation of pyrite to iron sulphate and sulphuric acid is known to be highly exothermic (Moore and Moore, 1999). Vassilev et al (2000) suggested “chlorine and bromine with a high volatile behaviour show a tendency for concentration in the easily decomposing phases in coal” (eg in particular, organics, chlorides, moisture, combined water and exchangeable cations).

Up to 90% of selenium and bromine and some nickel volatilised during ashing experiments was interpreted as evidence of (and due to) the organic association of these elements (Finkelman et al., 1990). Other ashing experiments found boron was retained at 815°C, with variable losses at higher temperatures (Doolan et al., 1985) (cf literature they cited that suggest a significant loss of boron occurs at 370°C). They suggested that the common organic affinity of boron could be an explanation for the high emissions noted in the literature for this otherwise refractory element. They concluded the variation in the volatility of boron found in their study reflected the control of the “chemical forms of the element present in the individual coals, and possibly the oxidative conditions during the preparation of the ash residues”.

Mineral-laden regions in a coal might be at a lower temperature during coal combustion than the mineral-poor regions, which has a clear implication for elemental

volatility and partitioning (Thompson and Argent, 1999). Valković (1983b) cited studies that found the partitioning of trace elements was related to the particle size of the host minerals in the coal. This relationship between particle size and partitioning behaviour could be related to the furnace temperature anisotropy outlined by Thompson et al. (1999).

Valković (1983b) succinctly summarised the control of mode of occurrence when he wrote enrichment of elements in specific ash species “was dependant on the volatility of the elements at both combustion and lower temperatures, and the volatility was in turn determined by the vapour pressure of the chemical species in which the element existed at a specific temperature”. He further suggested that the “division into depleted and enriched elements appears to be roughly independent of the operating characteristics of the combustion facilities, but is mainly determined by the geochemical and physiochemical properties of the elements”. Possibly the latter comment overstates the case (given the strong dependence of the classes of volatility/temperature relationships), but it does emphasise the importance of mode of occurrence on element partitioning.

1.4.4.3. Collection Point and Characteristics of the Ash.

The point in the combustion plant at which the ash was collected may also influence the partitioning behaviour of trace elements. The temperature of flue gas decreases downstream from the combustion chamber (~1300°C) to the final fly-ash collection point, eg temperatures in the fly-ash ESP have been found to be in the range of 40-80°C (Fernandez-Turiel et al., 2004). The flue gas temperature progressively falls below the dew point of volatile trace elements, which then condense on the entrained fly-ash particles (Senior et al., 2000). Thus fly-ash collected at different points downstream will have different proportions of condensed volatile trace elements. The type of ash collection device may also have an influence on partitioning behaviour. For example, collection in a cooler baghouse system results in particles having a relatively higher concentration of mercury compared to particles collected in an ESP system (Sakulpitakphon et al., 2000) (possibly also reflecting the longer residence time of particles in baghouses compared to ESP systems; Hower, pers comm., 2005).

The size consist of fly-ash also influences the partitioning behaviour of trace elements in the combustion plant. In general, fine sized fly-ash particles will have a higher concentration of volatile trace elements due to the larger surface area of the fine particles (Galbreath et al., 2000; Helble, 2000; Linton et al., 1976; Seames and Wendt, 2000; Senior et al., 2000; Senior et al., 2000), with a number of authors also noting the importance of fly-ash composition on this process.

The bulk chemistry of the coal and coal ash (Yan et al., 1999) may also influence partitioning behaviour. The proportion of mercury emitted is reduced in instances where coal that also contains a high chlorine content is burnt because HgCl_2 (formed by reaction of HCl with some of the mercury) has a lower volatility than elemental Hg (Liu et al., 2001; Meij, 1995; Senior et al., 2000; Zeng et al., 2004). Correlation between the concentration of unburnt carbon and the concentration of mercury in ash has also been noted (Hassett and Eylands, 1999; Mardon and Hower, 2004; Sakulpitakphon et al., 2000; Wu et al., 2000), with carbon form also having an influence (Hower and Masterlerz, 2001). Carbon and lime were found to promote vaporisation of lead and zinc, but scavenged arsenic (Wang and Tomita, 2003). Calcium oxide from the thermal decomposition of zeolites during combustion sorbs arsenic, boron, and sulphur (Querol et al., 1997b). Formation of aluminosilicate matrices rich in calcium during combustion was found to be responsible for capture and retention of boron (Clemens et al., 2000). However, titanium, present in high concentrations in one of the samples, competed for the calcium and imposed a secondary control on boron partitioning. Arsenic, antimony, and chromium, predicted to be volatile and vaporise, were found to be considerably less volatile than expected due to reactions with constituents in the bulk ash at combustion temperatures (Senior et al., 2000).

A series of sorbents (zeolites, kaolinite, montmorillonite, coals enriched in kaolinite and calcite, and lime and portlandite) were tested to assess the ability of these minerals to capture and sterilise trace elements during municipal waste combustion (Vassilev et al., 1999). It was found that kaolinite, montmorillonite, or coals enriched in these minerals are particularly efficient in capturing a range of elements (Vassilev et al., 1999). These minerals are commonly present in coal.

Pilot scale combustion studies found that, given a long residence time in the furnace and temperatures in excess of 950-1000°C, arsenic volatility is reduced by the formation of calcium arsenates and inclusion of arsenic into developing calcium and aluminosilicate matrices (Clemens et al., 1999). Selenium is captured by calcium to form calcium selenates (in similar fashion to the capture of sulphur by calcium), and boron was found to have a particular affinity for incorporation into silicate matrices. The silicate matrices are formed by the reaction of disordered and reactive silica and alumina phases (from the breakdown of kaolinite) with calcium oxide at temperatures above 950°C. Shorter residence time and lower temperatures in the furnace did not allow sufficient time for the silicate matrix to develop and capture boron (Clemens et al., 1999). Calcite breakdown occurs at lower temperatures, so the capture of arsenic, selenium, and sulphur is still observed at reduced temperatures, but boron capture is not. These experiments apply to underfed-stoker or fluidised-bed combustion regimes and are probably not applicable to pulverised-fuel combustion plants where residence time is very short; milliseconds according to Diessel (Diessel, 1998). Further, no comment was made on the mode of occurrence of the elements in the coal prior to combustion. However, calcium complexing has been found to exert a strong control of the partitioning behaviour of arsenic, selenium, and cadmium in tests simulating commercial (pulverised fuel?) furnace conditions (Seames and Wendt, 2000).

1.4.4.4. Combustion Regime.

The combustion regime also influences the emission of trace elements (Miller et al., 2002; Steenari et al., 1999). Fluidised bed combustion residues result from sulphation reactions and by-products of these reactions, and tend to leach calcium and sulphur to the environment (Armesto and Merino, 1999). In contrast, residues from pulverised-coal combustion are basically the inorganic fraction of the coal with proportions influenced by the operating conditions and element volatility (Section 1.4.4.1.), and leach only elements from the mineral matter. Only fluorine and manganese were found to mobilise in a fluidised-bed combustion plant; whereas fluorine, mercury, and selenium mobilise in a pulverised coal combustion plant; and beryllium, fluorine, mercury, and selenium mobilise in a cyclone combustion plant (Demir et al., 2001). They concluded that the mobilities of the 15 trace elements investigated were lower in the FBC plant than in the other types of plant tested (Demir et al., 2001). The conversion to low-NO_x emitting combustion systems resulted in a near doubling of

the unburnt carbon in the ash (Hower et al., 1999), although some reduction of unburnt carbon is possible with engineering modifications.

1.4.5. The Environmental Importance of Fly-ash.

While atmospheric pollution is of concern, the trace elements in fly-ash are of particular concern to geoscientists because of the geochemical interactions implicit in landfill type fly-ash disposal options. Further, of the twenty-four trace elements of environmental concern, the following elements are dominantly concentrated in the ash: Class I - Thorium; Class I or II – barium, chromium, cobalt, manganese, vanadium, uranium; Class II – antimony, arsenic, beryllium, cadmium, copper, lead, molybdenum, nickel, phosphorous, thallium, zinc; Class II or III – boron, selenium. Only boron, chlorine, fluorine and mercury (ie the Class III elements) are not concentrated in ash, although the classification of boron is not certain. Thus a large number of the elements of environmental concern in coal are, or can be, concentrated in fly-ash or bottom-ash by combustion. Importantly, of the elements partitioned to the ash, all the environmentally sensitive elements except thorium occur in some proportion (often a high proportion) in the fly-ash (see Table 1.7.). Table 1.5. shows the relative proportions of different ash types from various power plants. Up to 75-80% of ash refuse from a pulverised-fuel power station occurs as fly-ash (Murarka et al., 1993; Valkovic, 1983b). Fly-ash is, therefore, the dominant host of trace elements of environmental concern in terms of numbers of elements and element proportions, and often comprises the largest proportion of the solid waste from a coal-fired power plant.

Trace elements hosted by fly-ash particles tend to be present as thin (~0.1 μm), enriched coatings adsorbed to the outside of the fly-ash particle (Fishman et al., 1999; Linton et al., 1976; Valkovic, 1983b). These coatings may also be enriched in sulphur from the reaction of condensed sulphuric acid aerosols and the glassy matrix (Fishman et al., 1999). (NB It has been suggested that ashes are at equilibrium with the combustion conditions rather than a transient state, so segregation of the trace elements at the surface of a particle is due to freezing out during the growth of mullite crystals (Hulett et al., 1980)). In fluidised bed combustion, virtually no melting occurs but trace elements still occur as crystalline compounds on the surface of fly-ash particles (Steenari et al., 1999). However, Cr, Pb, and Cd can substitute for Al in

mullite crystals (Ramesh and Kozinski, 2001), although in this case the trace elements would be environmentally unavailable.

The smaller the fly-ash particle, the greater the weight percent of trace elements due to the greater surface area to volume ratios of the fine particles (Valkovic, 1983b). One implication of this factor is that highly efficient particulate emission control devices are a necessity to control trace element emissions. Unfortunately, even with efficient particle collection devices in place, the very finest particles that may escape the collection devices are also the most toxic, and are readily inhaled into the lungs of organisms (Figure 1.3.). The second implication is that fine particles of fly-ash present a large surface area of readily desorbed trace-element laden coating to the environment.

1.4.6. Fly-ash Leaching.

A number of potential options exist for disposing or using fly-ash, including cement (pozzolonic admixture), dumping at sea, stockpiling as embankments, replacement for sea sand or machine sand in concretes and mortars, light-weight aggregate, aerated concrete, flowable fill in building basements, a pigment replacing TiO_2 or talc in paint, backfilling and sealing stoppings in underground coal mines, as a sanitary landfill cover, in sludge fixation and stabilisation, as a soil ameliorant, and as a sorbant in conjunction with lime in flue-gas desulphurisation (Foner et al., 1999; Héquet et al., 2001; Keefer, 1993; Shi and Xu, 2001; Swaine, 1990; Valkovic, 1983b). Several of these disposal options implicitly involve the interaction of the fly-ash particles with weathering and hydrological processes, leading to some new research into ways of sterilising fly-ash, for example by making it into glass (Sheng et al., 2003). However, leaching of fly-ash following disposal is a major environmental concern given the quantity of material involved. For example in the US alone ~100 MT of fly-ash per year is produced (Finkelman, 2000).

The mobilisation of trace elements into solution is primarily a function of pH (given constant Eh) (Jones, 1995). In general, fly-ash leachate is alkaline in nature, however mobilisation of the sulphur and trace element-rich coating on the fly-ash may result in an initial leachate that is slightly acidic. Further, recarbonation (absorbtion of CO_2 from the atmosphere) by alkaline leachates can reduce the overall pH of the leachate

to approximately pH 8 (Jones, 1995). Fly-ash amended with manure results in reduced pH (by the generation of CO₂) and increased the extractable K, Na, Zn, and Mn (Schwab, 1993). Notwithstanding other controls, oxyanions (arsenic, boron, molybdenum, selenium) are most mobile at a pH of about 9 - 11, and cations (cadmium, copper, lead, nickel and zinc) are mobile at pH 4 to 7.

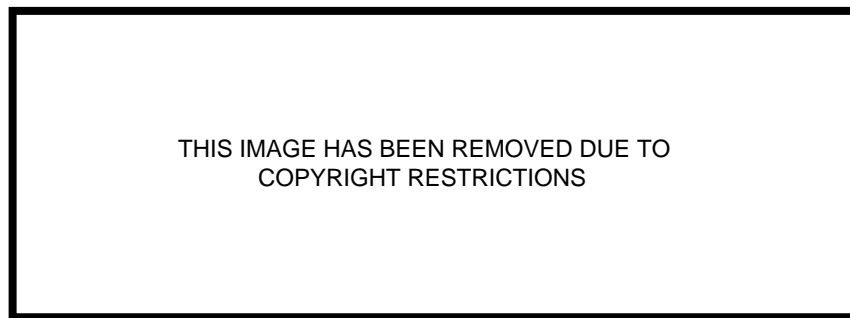


Figure 1.3. The Relationship between Particle Deposition in Lungs and Particle Diameter. (from Valkovic, 1983b)

A number of other factors also influence the elements present in solution (Jones, 1995). Fly-ash leached using solutions ranging through slightly acidic; neutral and slightly alkaline; and slightly reducing and slightly oxidising solutions (using samples of ten-year old and fresh fly-ash) showed that the highest concentration of Cd, Ni, Cr, and As is released by the reducing solution, and that elements are still released from ten-year old fly-ash (Sandhu et al., 1993). Given the low microbial activity in fly-ash

and the low concentration of bioavailable organic carbon, it is probably unlikely that conditions would become sufficiently reducing to affect iron and sulphur solubilities (the most likely elements to be reduced) (Jones, 1995). However, Sandhu et al (1993) found increased levels of organic matter in older fly-ash near the surface. Further, other studies have shown that fly-ash may require amendment by an organic substance, such as manure, to enable plant growth (Schwab, 1993). The last two studies suggest that the redox conditions of the fly-ash may evolve over time and change the chemistry of the leachate, and also by implication, element speciation. The speciation of some elements is important. Although the arsenate oxyanion is the most stable under oxidising conditions, at lower redox conditions arsenate may be reduced to the more mobile and more toxic arsenite anion. The arsenite anion is thought to be the most common phase present in leachates (Jones, 1995).

Elements present within the geochemically more inert substrate of the fly-ash are released according to the rate at which the substrate is dissolved whilst elements adsorbed as coatings on the outside of the fly-ash particles are readily mobilised without having to dissolve the substrate fly-ash particle. As discussed for redox potential, this mechanism may cause the composition of the leachate to vary over time (Jones, 1995). Where trace elements are locked into the crystal structure of mullite, they may be environmentally unavailable (Ramesh and Kozinski, 2001).

The formation of secondary minerals may also have a profound influence on the elements found in solution. Co-precipitation of selenite with CaCO_3 controls the concentration of that anion in solution under mildly alkaline conditions (Jones, 1995). Under strongly reducing conditions, insoluble As_2S_3 (orpiment) may form and be incorporated into pyrrhotite or pyrite if sufficient Fe^{2+} is available (Jones, 1995). Precipitation of $\text{Ca}_3(\text{AsO}_4)_2 \cdot 6\text{H}_2\text{O}$ and $\text{Ca}_2\text{V}_2\text{O}_7$ has been found to occur as a result of a high concentration of calcium in solution (Querol et al., 2001b). Occlusion or adsorption of molybdenum onto or into newly formed oxides of iron can reduce molybdenum mobility in some circumstances (Keefer et al., 1993).

1.4.7. Case Studies.

A number of leaching studies on fly-ash waste have investigated the remobilisation of trace elements of environmental concern (Fernández-Turiel et al., 1994; Fishman et

al., 1999; Jones, 1995; Knott et al., 1985; Sandhu et al., 1993; Schwab, 1993; Steenari et al., 1999; Teixeira et al., 1999).

Clark et al. (1999) examined the potential for coal combustion products to be used as a soil ameliorant in acidic soils. Fly-ash was found to be high in boron compared to fluidised-bed combustion or flue-gas desulphurisation wastes. Boron is of particular concern because the oxidised form, expected as a result of combustion (depending on the element's mode of occurrence in coal, operating temperature and residence time) (Clarke and Sloss, 1992), is readily leached and the element has a narrow necessity range. Boron was found to accumulate in maize and toxicity was suspected (Clark et al., 1999). It was suggested continued loading would probably lead to increasing problems. However, it was concluded that maize growth was generally enhanced by the addition of the coal combustion wastes; (Clark et al., 1999; Menon et al., 1993). It was also found that, of the two plant species used to test element uptake from manure and soil amended fly-ash (soybean and sorghum), soybean plants were particularly susceptible to boron toxicity (Schwab, 1993). The data of Schwab suggests that plants exhibit variable tolerance to boron, presenting a further complication to assessment of environmental impact.

Clark et al (1999) noted increased pH decreased the availability of boron to plants; a vital point because most fly-ash is alkaline in nature (Jones, 1995). However, this factor would seem to imply that placement of alkaline fly-ash into an acidic environment could increase boron availability. Another potential problem in the use of fly-ash as a soil amendment is that fly-ash is often poor in nitrogen and phosphorous, elements essential for plant growth (Agrawal et al., 1993).

Fly-ash leaching experiments have found the extractable fraction of elements under natural conditions ranged from 1.5-56.4% of the total concentration in fly-ash, with cadmium, cobalt, copper, and zinc having the highest extractable fractions (Fernández-Turiel et al., 1994). [NB Bulk analysis can provide a poor measure of the actual concentrations of many toxic elements that are present as coatings on the particle, and therefore in direct contact with the environment (Linton et al., 1976)]. Fernández-Turiel et al. (1994) found that cobalt, nickel, lead, and zinc are mainly associated with surface oxide-bound and iron oxide-bound fractions, which control

the extractability. Other leaching studies found that, of the elements studied (cadmium, nickel, chromium, and arsenic), nickel was the most mobile and cadmium the least mobile (Sandhu et al., 1993).

Selenium has been studied by a number of authors because it has “an especially narrow interval of necessity ... between the levels of insufficiency and excess” (Herring, 1990). Cases of selenium contamination of lake water by fly-ash have been documented (Brown, 1990; Klusek et al., 1993). High selenium contents (>200 ppm dry weight) in sweet white clover grown on fly-ash and increased selenium concentrations in guinea pigs fed the clover have also been documented (Gutenmann and Bache, 1976). Cabbage grown on the fly-ash also showed increased levels of selenium (3.7 ppm compared to 0.05 ppm in the control group). Carrots, millet, onions, potatoes, and tomatoes also all showed higher concentrations of Se (up to 1 ppm) compared to the control groups (0.02 ppm) (Gutenmann and Bache, 1976; Wadge and Hutton, 1986).

Selenium was found to be concentrated in a wide variety of plants growing on an ash landfill, however flue-gas desulphurisation waste (containing CaSO_3 , which readily oxidises to gypsum CaSO_4) acted to reduce selenium uptake because of the antagonistic relationship between sulphur and selenium in plants (Weinstein et al., 1993). The uptake of selenium was also found to be species dependent (Weinstein et al., 1993).

The toxic concentration of an element varies according to the tolerance of the plant species and environmental factors such as pH, which dictates the solubility of the element and its availability to the plants (Knott et al., 1985) (see Appendix 1.). Gutenmann and Bache (1976) suggested that oxidation of selenium in fly-ash to a higher valence, more soluble form may be responsible for the mobility and availability of selenium. [NB Selenate is the most oxidised form of selenium, the most soluble and the most toxic; selenite and elemental selenium are less toxic and mobile (Herring, 1990)].

A series of experiments found that 90% of soluble salts were removed with the first extraction, mobilisation levelling off by the third extraction (Menon et al., 1993).

Their data suggests that the release of elements from a given volume of fly-ash will decrease with time, assuming other geochemical influences do not exert an influence (see Section 1.4.6.).

Depending on the concentration of trace elements and their mode of occurrence (eg adsorbed to the fly-ash), the quantities of waste concerned, and the geochemical conditions of the disposal site, there is some potential to release trace elements to the environment causing unwanted environmental degradation. The chemistry of fly-ash leaching is complex, with the leaching of elements and uptake by plants dependant on pH, Eh, secondary mineral precipitation, antagonistic mineral relationships, and time.

1.4.8. Conclusions – Coal Combustion Aspects of Trace Elements.

Trace elements of environmental concern are classified according to their partitioning behaviour in combustion, which is a reflection of the volatility of the elements, the element's mode of occurrence in the coal, collection point and characteristics of the ash, and combustion regime. Fly-ash makes up the bulk of solid combustion waste from many power stations, hosts the dominant number and proportion of the environmentally sensitive trace elements, and holds many trace elements as a thin, adsorbed coating on the particle that is readily available for mobilisation. Many of the fly-ash disposal options result in contact between the natural geochemical system and the fly-ash particles. A large number of studies show that fly-ash can cause deleterious impacts on the biosphere. For these reasons, fly-ash is potentially a hazardous by product of coal combustion in terms of trace element impacts on the environment. However, with proper management and care it may also be possible make use of the fly-ash.

Chapter 2.

Study Aims and Methods

2.0. Project Design.

2.1. Aims.

Trace elements in coal are of interest for a number of reasons, but currently the prime impetus for study is concern about the negative environmental impact some elements can have on the biosphere. The concentration, mode of occurrence and distribution of trace elements in coal is spatially highly variable, even over short distances, due to the complex source(s) of elements in coal, making assessment of these factors an ongoing requirement if a product coal is to be characterised ahead of delivery to a customer.

Combustion processes act to concentrate inorganic elements in coal and partition the elements between vapour, fly-ash and bottom-ash phases. Of these three phases, fly-ash is dominant both volumetrically compared to the other waste streams and in terms of the number and proportion of trace elements partitioned to it during combustion. Negative environmental impacts have been found in some cases where fly-ash is disposed without consideration for remobilisation of trace elements into the biosphere. However, the chemistry of trace element leaching from fly-ash is complex and difficult to predict.

The prime focus of research in this project is the Collinsville coal opencast mine situated at Collinsville in the Northern Bowen Basin, Queensland, Australia. At the time of sampling, coal from the Blake and Bowen seams was mined and delivered to the Collinsville pulverised fuel combustion plant for steam raising, and coal from the Bowen seam was railed to the Bowen coke works for carbonisation. No detailed data on the concentration and mode of occurrence of trace elements in the Collinsville coal were available. Further, no data on the partitioning behaviour of trace elements in the Collinsville coal during combustion and carbonisation was available.

The literature search uncovered no data comparing the partitioning behaviour across two (or more) combustion plants for one element with different modes of occurrence

in the feed coal. Further, no data was found comparing the leachability of an element from fly-ash from two (or more) different combustion plants being fed coal containing the element in different modes of occurrence. Also, no data was found describing the partitioning of trace elements in carbonisation.

Given that Collinsville coal is utilised in combustion and carbonisation, research into the coal and utilisation of the coal from Collinsville provided a good opportunity to fill a number of perceived gaps in the current state of knowledge of trace elements, both locally and on a broad scale. The aims of this project are:

1. To determine the concentration and mode of occurrence of trace elements in the Collinsville mine coal. The impact of igneous intrusions on trace element concentration is also assessed.
2. To gather samples from the Collinsville coal-fired power plant and determine trace element mode of occurrence and element partitioning behaviour. Samples were also gathered from a Japanese coal-fired power plant and trace element mode of occurrence and partitioning behaviour determined using the same methods used for the Collinsville samples. The Japanese power plant was sampled in an attempt to ensure the mode of occurrence of trace elements was different to the Collinsville coal. The two sets of combustion samples were compared to assess the effect of mode of occurrence differences on partitioning behaviour. Further, ash samples were composited and leached using the TCLP protocol to determine and compare the effect of mode of occurrence on the leachability of trace elements
3. To gather samples from the Bowen coke works to determine the partitioning behaviour of trace elements in carbonisation.

2.2. Methods.

The Collinsville opencast coalmine operates in the northern Bowen Basin and mined around 3 MT a year at the time of sampling. Ply-by-ply channel samples, divided according to lithotype (see Section 3.1 for further details), were gathered from three opencast pits at the Collinsville coal mine using a geological pick and analysed using INAA, XRF, and XRD (selected samples only). The results are interpreted using normative analysis to determine mineral assemblages. Graphical relationships

between normative analysis mineralogy and trace element concentration are used to infer trace element mode of occurrence. Channel samples that are heat affected are recognised by the presence of semi-coke in petrographic samples or by inferred distance of heating. The ply-thickness weighted-average trace element concentrations of heat affected and unaffected samples, and trends in concentration with distance from the intrusion were used to determine the impact of igneous intrusions on trace element concentration.

A sample of pulverised fuel being fed into combustion unit 3, bottom-ash, ash from three locations within the unit 3 combustion chamber and fly-ash was gathered from the Collinsville coal-fired power utility (see Section 4.1. for further details). The pulverised fuel sample was sequentially leached according to the USGS methodology and the results interpreted to infer mode of occurrence. The relative enrichment factor was calculated for the ash samples to determine the partitioning behaviour for a number of major and trace elements. A composite sample comprising 80% fly-ash and 20% bottom-ash was made up and subjected to the TCLP leaching protocol. A sample of pulverised fuel, bottom-ash, ash from the combustion chamber outlet and from the fly-ash bin was gathered from a Japanese coal fired power utility. The Japanese sample set was analysed using the same methodology applied to the Collinsville sample set. The results are compared to determine the influence of trace element effect mode of occurrence on element partitioning behaviour and the mobility of trace elements from the solid wastes.

Samples of feed coal, coke, and quench tower washings (coke breeze) were gathered from the Bowen coke works. A new index (the coke relative enrichment factor) is used to assess the partitioning behaviour of trace elements in carbonisation. The partitioning behaviour of trace elements in combustion and carbonisation of the Collinsville coal is compared.

2.3. Analytical Methods.

Table 2.1. shows the analytical methods used to determine element concentration in this study. INAA was chosen as the principal analytical technique for this thesis because the method requires little sample preparation (reducing the likelihood of loss of volatile elements or contamination), provided a reasonable “bulk” analysis (cf

SEM-EDX, for example), was readily available via a commercial laboratory and was reasonably priced. An analytical method to determine Si, Al, Mg, Ti, Mn, P, S, Cu, Pb, & V was then sought. Laser ablation ICP-MS was examined and trailed but the results showed no comparison with the INAA results. It was assumed the differences were caused by ablation of a single surface of a pressed powder pellet being unrepresentative of the bulk analysis. Eventually standard XRF analysis of a fused disc was used to determine Si, Al, Mg, Ti, and P concentration, with iron determined for comparison with the INAA results. XRF of pressed-powder pellets was used to determine Cu, Pb, and V concentration, with uranium analysed for comparison with the INAA results. In hindsight all the major elements, in particular K and Ca, should have been determined by XRF of a fused disc, however the difficulties with the low INAA detection limit for Ca and K in whole coal were not appreciated prior to initiation of normative calculations to determine mineralogy, and by then no sample remained for further analysis, even if finance had been available to undertake this re-analysis (see also Section 2.5; Chapter 3).

Table 2.1. Analytical Methods used in this Study.

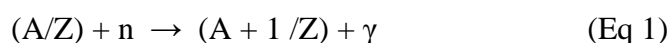
Element	INAA	XRF	ICP-MS	ICP-AES	ICP-OES	LECO SC32
Silicon		X		X		
Aluminium		X		X		
Iron	X	X		X		
Calcium	X			X		
Magnesium		X		X		
Sodium	X			X		
Potassium	X			X		
Titanium		X				
Manganese		X	X	X	X	
Phosphorous		X		X		
Sulphur						X
Gold	X					
Silver	X					
Arsenic	X		X	X	X	
Barium	X		X	X	X	
Boron			X	X	X	
Bromine	X					
Cadmium			X			
Cerium	X					
Cobalt	X		X		X	
Chromium	X		X	X	X	
Caesium	X		X			
Copper		X (PP)	X	X	X	
Europium	X					
Hafnium	X					
Lithium				X		
Mercury	X					
Iridium	X					
Lanthanum	X					
Lutetium	X			X		
Molybdenum	X		X			
Neodymium	X					
Nickel	X		X	X	X	
Lead	X	X (PP)	X		X	
Rubidium	X		X			
Antimony	X		X		X	
Scandium	X			X		
Selenium	X		X		X	
Samarium	X					
Strontium	X			X		
Tantalum	X					
Tin			X			
Terbium	X					
Thorium	X			X		
Uranium	X	X (PP)	X			
Vanadium		X (PP)	X	X	X	
Tungsten	X					
Yttrium				X		
Ytterbium	X					
Zinc	X		X	X	X	
Zirconium				X		

PP = Pressed Powder analysis; other XRF all fused disc.

2.3.1. Instrumental Neutron Activation Analysis (INAA).

The concentration of gold, silver, arsenic, barium, bromine, calcium, cobalt, chromium, caesium, iron, hafnium, mercury, iridium, potassium, molybdenum, sodium, nickel, rubidium, antimony, scandium, selenium, strontium, tantalum, thorium, uranium, tungsten, zinc, lanthanum, cerium, neodymium, samarium, europium, terbium, ytterbium, and lutetium was analysed in solid samples using INAA. Samples were analysed by Actlabs, an international group of commercial laboratories with extensive experience with INAA analysis. Table 2.2. shows the detection limits stated in the Actlabs 1999 fee schedule. ACTLABS state analysis is undertaken to ISO protocols Guide 25 standard, with laboratories taking part in “international round-robins and routine ACTLABS Group comparisons” (ACTLABS 1999 Fee Schedule). Although a standard reference material was not run for comparison, it is considered that ACTLABS quality assurance methods were sufficient.

INAA is a “well tried method suitable for whole coal and related materials” (Swaine, 1990). Analysis involves thermal neutron irradiation of small encapsulated samples (~1gm) (Nadkarni, 1980), followed by instrumental measurement of the emission of radioactive isotopes formed by the various elements. When an element of atomic number Z and atomic weight A is placed in a flux of neutrons, there is a defined chance that the element will capture a neutron, thus yielding a new isotope of the same element but with a mass one unit heavier (Equation 1); (Valkovic, 1983b).



In many cases the newly formed nucleide is radioactive, therefore the emitted radiation can be used to determine the presence of that radioactive nucleide. The emission of radioactive species by neutron capture is given by the activation equation (Equation 2); (Valkovic, 1983b).

$$A_o = N\sigma\phi (1-e^{-[0.693t_i/T_{1/2}]}) \quad (\text{Eq 2})$$

Where A_0 = disintegration rate of induced radionuclide at end of radiation
 N = atoms of element irradiated
 ϕ = neutron or particle flux
 σ = cross section of element
 t_i = irradiation time
 $T_{1/2}$ = half life of induced radionuclide

Equation 2 shows that the disintegration rate of an induced radionuclide (and, therefore, the sensitivity of INAA analysis) is a function of the amount of the element of interest in the sample, the flux, and the cross section.

The advantage of INAA for trace element analysis is that it is a multi element technique (in the case of this study, providing 35 elements) requiring minimal sample preparation and small sample size. The lack of significant sample preparation reduces the risk of contamination. Because the samples do not require ashing to improve sensitivity, INAA can be used to analyse for volatile elements such as mercury and arsenic without risking losses during sample preparation. Studies comparing trace element analysis using several different methods have found INAA to be a high precision technique (Palmer and Klizas, 2001).

Table 2.2. INAA Element Detection Limits.

Element	Detection Limit	Element	Detection Limit
Gold	0.1 ppb	Rubidium	1 ppm
Silver	0.2 ppm	Antimony	0.005 ppm
Arsenic	0.01 ppm	Scandium	0.01 ppm
Barium	5 ppm	Selenium	0.1 ppm
Bromine	0.01 ppm	Strontium	10 ppm
Calcium	0.01 %	Tantalum	0.05 ppm
Cobalt	0.1 ppm	Thorium	0.1 ppm
Chromium	0.3 ppm	Uranium	0.01 ppm
Caesium	0.05 ppm	Tungsten	0.05 ppm
Iron	0.005 %	Lanthanum	0.01 ppm
Hafnium	0.05 ppm	Cerium	0.1 ppm
Mercury	0.05 ppm	Neodymium	0.3 ppm
Iridium	0.1 ppb	Samarium	0.001 ppm
Potassium	0.01 %	Europium	0.05 ppm
Molybdenum	0.05 ppm	Terbium	0.1 ppm
Sodium	1 ppm	Ytterbium	0.005 ppm
Nickel	2 ppm	Lutetium	0.001 ppm

An additional split from each of four randomly chosen samples was tested to determine repeatability of the INAA analyses. Graphs of elemental concentration are shown in Figures 2.1., 2.2., 2.3., and 2.4. Figures 2.1., 2.2., and 2.3. graph repeat analyses for coals, but exclude iron, an element present in considerably higher concentrations than the trace elements shown, inclusion of which would obscure the relationships at lower concentrations. Figure 2.4. shows repeat analysis figures for a fly-ash from Unit 3 of the Collinsville coal fired power plant, therefore iron is included because the concentration of the other elements have been increased due to the loss of the carbonaceous coal material. The graphed figures exclude samples where one or both of the analyses for the two repeats are below the limit of detection (Table 2.3. shows all data). Figures 2.1., 2.2., 2.3., and 2.4. show a strong correlation coefficient between the two data sets. However, if the relationships were perfect, the equation for the trend line would be $Y = X$. In Figure 2.1., the equation is $Y = 0.7330X + 2.8549$, suggesting the repeat figures are generally less than the original figures. The equations for the trend lines in Figures 2.2., 2.3. and 2.4. are $Y = 1.1429X - 0.7597$; $Y = 1.0367X + 1.0082$; and $Y = 0.8818X + 3.4822$ respectively. The latter three repeat samples show a relationship closer to the expected one to one relationship. Given the inhomogeneity of coal (and fly-ash?), some differences between splits are to be expected. It is considered from the repeat samples that INAA generally shows reasonably good repeatability.

Table 2.3. Repeat Analysis by INAA.

	BC 6.37-6.55	Repeat 1	BO 2.60-2.90	Repeat 2	Coal Train No.213	Repeat 3	Collinsville Power U3 Fly-ash	Repeat 4
Fe (PPM)	11900	12400	7720	7950	1620	1680	25300	25500
Na (PPM)	523.00	479.00	157.00	136.00	101	74	807	681
K (PPM)	2500.00	<500	900.00	<500	<500	<500	2500	<500
Au (PPB)	<0.2	3	0.5	<0.2	1.5	1.2	<2.1	2.3
As (PPM)	0.65	0.52	0.62	0.59	0.59	0.75	5	3.2
Ba (PPM)	140	93	130	150	230	250	1900	1700
Br (PPM)	6.1	5.6	7.2	7.9	4.5	5.5	3.9	5.1
Ce (PPM)	81	72	26	24	34	37	180	170
Co (PPM)	10	12	1.8	2.2	8.5	9.1	20	20
Cr (PPM)	23	24	33	34	23	26	58	65
Cs (PPM)	0.72	0.85	0.4	0.58	0.27	0.33	3	3.1
Eu (PPM)	1.2	1.13	0.4	0.4	0.65	0.63	2.81	2.86
Hf (PPM)	5.4	5.7	4	4.4	3.2	3.6	18	19
Hg (PPM)	0.42	<0.05	<0.05	<0.05	<0.05	0.16	<0.05	<0.05
Ir (PPM)	<0.1	<0.2	<0.2	<0.2	<0.1	<0.1	<0.1	<0.2
La (PPM)	43	39	10	8.9	18	19	100	99
Lu (PPM)	0.746	0.746	0.209	0.213	0.251	0.254	1.87	1.83
Mo (PPM)	<0.05	9.7	0.98	3.2	1.3	1.2	<0.05	<0.05
Nd (PPM)	37	23	8.4	7	15	12	85	76
Ni (PPM)	64	<2	24	<2	<2	27	<5	<5
Rb (PPM)	9	11	<1	4	<1	3	12	15
Sb (PPM)	0.54	0.51	0.16	0.15	0.2	0.25	1.8	1.9
Sc (PPM)	12	14	8.9	9.1	6.9	7.8	27	30
Se (PPM)	3.2	3.1	1.5	1.5	1.5	2	6.4	5.3
Sm (PPM)	6.3	5.7	1.8	1.4	2.2	2.1	15	14
Sr (PPM)	<10	<10	79	<10	140	120	860	700
Ta (PPM)	0.67	0.63	0.49	0.45	0.46	0.45	2.1	2.1
Tb (PPM)	1.4	1.4	0.3	0.3	0.4	0.5	3	3.1
Th (PPM)	12	12	9.2	9.2	7.7	7.4	37	34
U (PPM)	3.3	2.8	1.8	1.9	1.1	1.2	7.5	7.4
W (PPM)	3	3.3	3.5	3.6	2.8	2.8	4.5	9.5
Yb (PPM)	4.82	4.96	1.41	1.44	1.66	1.69	11.2	12.2
Zn (PPM)	40	53	18	18	62	78	210	240

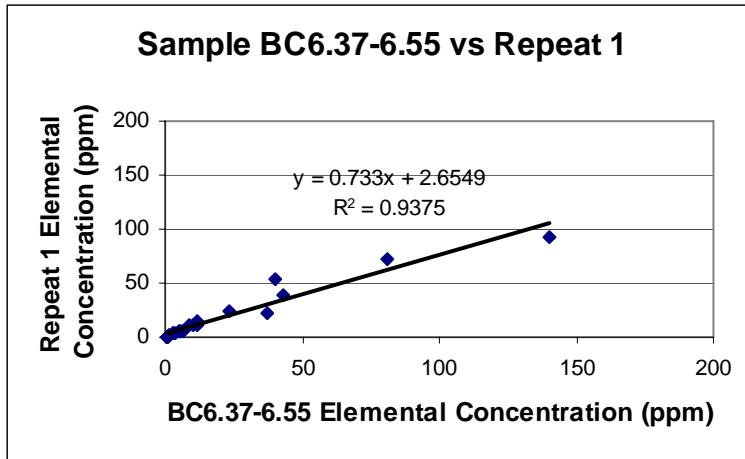


Figure 2.1. Sample BC6.37-6.55 vs Repeat 1

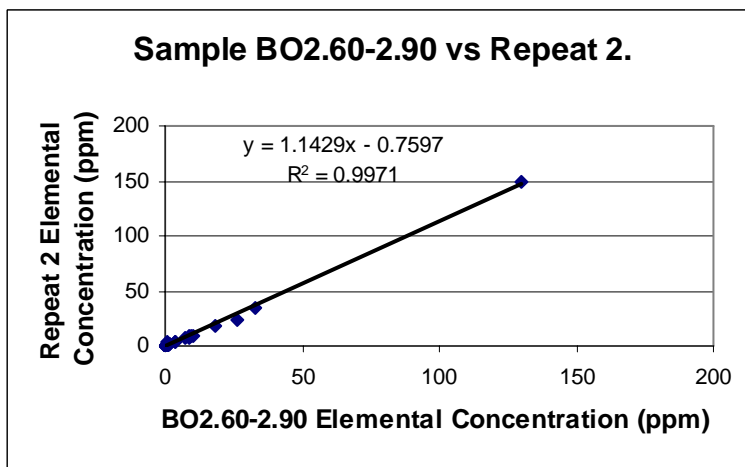


Figure 2.2. Sample BO2.60-2.90 vs Repeat 2

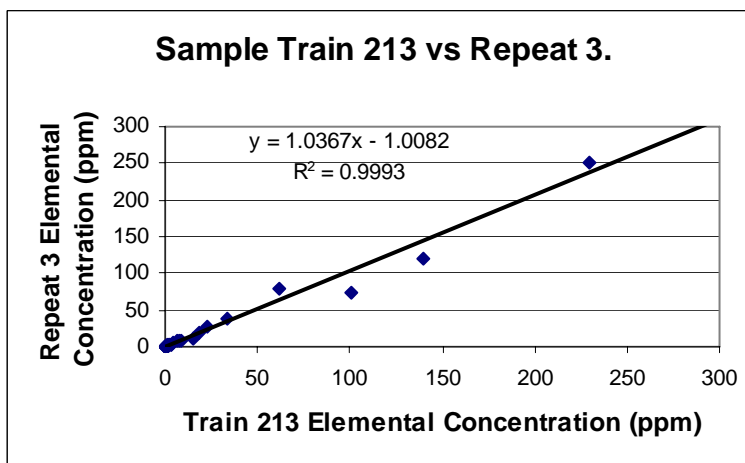


Figure 2.3. Sample Train 213 vs Repeat 3

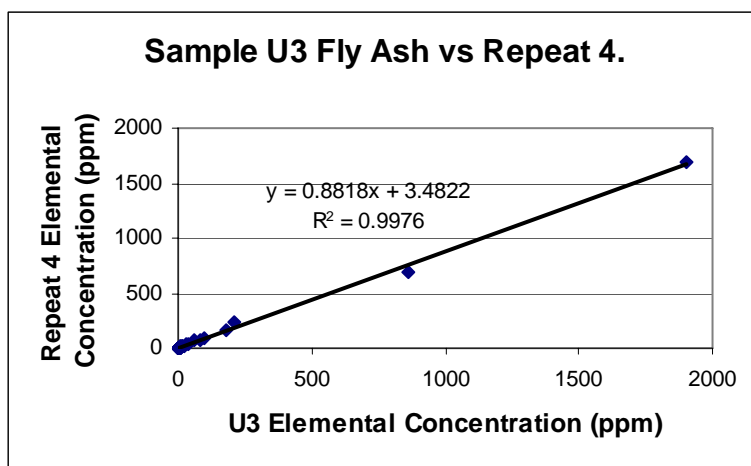


Figure 2.4. Sample U3 Fly-ash vs Repeat 4

However, from Table 2.3, there are differences in the concentration of potassium, nickel and molybdenum for some repeat samples. Such differences are clearly cause for some concern, particularly for potassium, which is used as an index element to calculate illite in Chapter 3. It is advised that all calculations involving potassium, nickel and molybdenum be treated with caution since no further aliquots of the study samples remain to check the validity of the analytical figures.

2.3.2. X-Ray Fluorescence (XRF).

The “major” elements silicon, aluminium, iron, manganese, magnesium, titanium and phosphorous were analysed by X Ray fluorescence (XRF) of borate fusion glass discs prepared from 400°C ash. The elements copper, lead, uranium, and vanadium were analysed by XRF of pressed powder pellets prepared from 400°C ash. The coal was ashed for reasons outlined below. The USGS ashes at a temperature of 525°C (Evans et al., 2001), and recommend slow stepping up of the temperature gradually to 300°C in 1 hour, and to 500°C in 2 hours. Ashing is continued for 2 hours, along with intermittent stirring to ensure all carbonaceous material is removed (Palmer 2001, pers comm.). Ashing was undertaken by SGS Ngakawau Laboratory at a maximum temperature of 400°C. XRF analysis of the 400°C ash samples was undertaken by SpectroChem Analytical Limited, Wellington, New Zealand. The detection limits stated by Spectrochem for the major elements is 100ppm, and for the trace elements is 1ppm. However, XRF analysis was undertaken on 400°C ash so major and trace elements present at considerably lower concentrations in whole coal are detected.

X-Ray fluorescence is a good technique for determining the bulk elemental chemistry of a specimen, usually presented to the instrument as either a fused glass disc or a pressed powder pellet. The technique has been applied for the analysis of both major and trace elements in coal (Ayala et al., 1994; Dewison and Kanaris-Sotiriou, 1986; Johnson et al., 1989; Swaine, 1990). The detection limit is indicated to be of the order of 10ppm or less (Lewis and McConchie, 1994; Potts, 1987). XRF is commonly used to analyse for elements from fluorine to uranium, but more modern equipment can now analyse elements with atomic numbers as low as boron (Ness, 1998). The technique, therefore, has the potential to analyse coals for a wide range of elements from trace to major quantities.

Conceptually the theory of XRF is relatively simple and is based on the observation of Moseley (1913, cited in Potts, 1987) who noted that the wavelength of an x-ray emission was directly related to the atomic number of an element. What Moseley had observed was the result of energy arising from the transition of electrons between orbital shells in an atom. An atom is made up of a nucleus (comprising protons and neutrons) surrounded by a number of electrons that occupy a series of discrete orbital shells; each orbital shell also has a discrete energy. These energy shells are designated K, L, M, N, O etc (using Siegbahn notation) with increasing distance from the nucleus. (NB, the K shell is monoenergetic but subsequent shells out from the nucleus are actually made up of increasing numbers of sub-shells. For a given element, the positive charge of the nucleus (imparted by the protons) is balanced by the number of negatively charged orbital electrons. The strength with which the electrons are held in place depends on the proximity of the orbital shell to the nucleus. This energy is measured by the ionisation potential; the higher the ionisation potential the more stable the electron. K shell orbitals have the largest (negative) ionization potential.

When an atom is bombarded with sufficient energy, an electron may be dislodged from its orbital shell; ie the ionisation potential of the given electron is exceeded. Loss of an electron will leave the atom in an unstable state, and in order to regain stability, an electron from shell further out from the nucleus will move in to fill the vacancy. For example, if an electron from the K-shell was lost during bombardment, an electron from the L or M shell will move in to refill the vacancy. In order to

undertake this transition, the electron must lose some energy. The lost energy is given off as an X Ray. The overall factor controlling the potential energy of the electrons in each orbital shell is the magnitude of the positive charge of the nucleus, hence the observed correlation between the atomic number and the X-ray emission.

X ray fluorescence analysis suffers from a number of interferences and matrix effects. These may be dealt with by using suitable standards, modifying samples to reduce the effect (eg by making fusion discs), or by using mathematical corrections. A full discussion on inter-element interferences and matrix effects is not included here. Suffice to say that XRF analysis of whole coal for trace elements has been undertaken in the past with some success (Mills and Turner, 1980; Smith, 1999), however the USGS concluded that “X Ray whole-coal procedures were classed as low precision procedures” (Palmer and Klizas, 2001). Evans et al (2001) note the problem with XRF analysis of whole coals is due to the very light coal matrix and the scarcity of reliable coal standards. In order to provide high-precision determinations of the trace elements copper, lead, uranium, and vanadium, coal samples were ashed at 400°C to ensure trace elements were not lost due to volatilisation. The USGS found that X-Ray analysis of low temperature (525°C) coal ash provided results with a high precision (Evans et al., 2001; Palmer and Klizas, 2001). However, ashing of a sample by any method makes the applicability of XRF for analysis of highly volatile elements such as mercury impossible.

Copper, lead, uranium, and vanadium in this study were analysed by XRF on pressed powder pellets of low temperature ash. The XRF concentrations have been recalculated to whole coal basis using the ash percent determined by proximate analysis for each sample. Note, the ash determined by standard proximate analysis and the 400°C ashing procedure was found to be essentially the same; see Table 4. and Figure 2.5.

Table 2.4. Comparison of Ash Percent, Proximate and 400°C Ashing Methods.

Sample Number	Standard Proximate Analysis Ash%	Low Temperature (400°C) Ash%
BO0.72-1.07	11.7	12.3
BC2.00-2.50	14.8	8
BC5.39-5.49	34.3	33.4
BC6.23-6.35	28.9	30.3
Coal Train 208	12.2	12
Coal Train 211	11.3	11.2
Coal Train 216	12.5	12.4
Coal Train 218	10.8	10.7

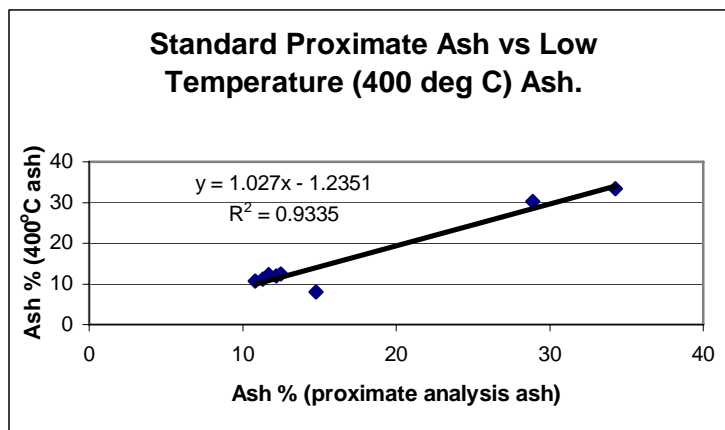


Figure 2.5. Comparison of Ash Percent, Proximate and 400°C Ashing Methods.

2.3.3. Inductively-Coupled Plasma Mass Spectrometry (ICP-MS).

Inductively-Coupled Plasma Mass Spectrometry (ICP-MS) was used to analyse for the elements manganese, arsenic, boron, barium, beryllium, cadmium, cobalt, chromium, copper, molybdenum, nickel, lead, antimony, selenium, tin, uranium, vanadium, and zinc for the Japanese pulverised fuel sample, and leachates thereof. Analysis was undertaken at Agriquality, Wellington, New Zealand. Also the USGS analysed for some trace elements in the Collinsville coal using ICP-MS at the USGS laboratory. A fuller description of the elements analysed for using ICP-MS and the comparability of the results with the Actlabs INAA results for the combustion samples can be found in Chapter 4. Tin and uranium in the TCLP leachate testing (Chapter 7) were also analysed by ICP-MS.

Analysis by ICP-MS requires that the sample be in solution. Clearly this is a disadvantage when analysing solid samples such as coal. In the case of the Japanese

coal sample, the solid material had to be dissolved (using a HF/ HCl/ HNO₃ mixture) whilst heated by a microwave oven. Some risk of losing volatile elements is apparent, although the comparisons with the INAA results in Chapter 4 suggest the methods are generally comparable. The solution is then “aspirated in an argon stream through high energy radio-frequency coils to form a plasma with a temperature of about 10,000°K” (Lewis and McConchie, 1994) (see Figure 2.1.3.a.). The ions in the plasma are analysed using a quadropole mass spectrometer.

The advantages of ICP-MS are that it can analyse for multiple elements at the same time and has very low detection limits. The disadvantage is the requirement for solid samples to be in solution. Microwave digest preparation to dissolve solid samples runs the risk of loss of volatile elements and adds expense to the analysis. The USGS considers ICP-MS to be a high precision procedure (Palmer and Klizas, 2001).

Figure 2.6. Schematic Diagram Showing the Principal Components of an ICP-MS Instrument.



Reproduced from Figure 9-13 of Lewis & McConchie (1994) Analytical Sedimentology.

2.3.4. Miscellaneous.

Sulphur in coal was analysed using a LECO SC32 sulphur analyser at SGS Laboratories, Ngakawau, New Zealand. LECO is a standard piece of equipment for undertaking sulphur analysis and no further explanation is given here.

Most of the elements in the TCLP leachates (Chapter 7) were analysed by ICP-OES (Optic Emission Spectrometry). The method depends on the “measurement of emission of atoms which have been energised to boost their valence electrons above their normal stable levels” (Swaine, 1990). Several methods of atomic excitation are noted by Swaine (1990), including inductively-coupled plasma excitation. The TCLP leachates were already in solution, and so required no further preparation. Analysis by ICP-OES was undertaken at Cawthron Laboratories, Nelson, New Zealand. ICP-OES has also been used in the past for analysis of trace elements in coal ash (Rivoldini and Cara, 1992), but as for ICP-MS, digestion of the ash to get the sample into solution was required.

2.3.5. X-Ray Diffraction (XRD).

X-Ray Diffraction (XRD) analysis of the Low Temperature Ash Oxygen Plasma (LTA-OP) of selected Blake and Bowen seam samples from the Collinsville open cut mine was undertaken to determine the mineral assemblage in the coal, and thereby calibrate the normative analysis. XRD analysis was undertaken at the University of Canterbury, New Zealand under the supervision of Dr Nigel Newman (CRL Energy Ltd).

The low-temperature ash was prepared using a two-chambered LTA304(2) plasma asher. Preparation of the low-temperature ash was undertaken by CRL Energy, Christchurch, New Zealand. The oxidation is believed to have proceeded to 90% completion at temperatures not exceeding 150°C by radio-frequency plasma oxidation (Newman, NA; pers comm. 2003). Because plasma oxidation occurs at such low temperatures, the thermal alteration of mineral matter is thought to be minimal, although some changes have been found to occur (Finkelman et al., 1984).

XRD analysis is a standard analytical technique used by geologists for the identification of mineral matter. Most XRD systems consist of an X-Ray source, a

goniometer to hold and rotate the sample, and an X-Ray detection and processing system (Lewis and McConchie, 1994). The technique relies on the fact X-Rays are diffracted by the atomic layers in crystals. Because each mineral has a distinct atomic layer spacing (called d spacing), and the diffraction of the X-Rays is a function of this spacing, measurements of the diffraction pattern can be used to identify the mineral species. Samples for powder diffraction must be finely ground (<5µm). Minerals with good X-Ray reflectivity can be detected down to ~0.1% (Lewis and McConchie, 1994). XRD will not detect non-crystalline species.

Generally minerals are determined from the readout using computer search-match programmes, but care is required because some improbable identifications may be provided by the computer (Lewis and McConchie, 1994). The computer programme can also provide an estimate of the proportions of the different mineral species in the sample using the relative intensity of the 100% peak of each mineral. Canterbury University Geology Department used the programme “TRACES” to identify and estimate the proportions of mineral species present in XRD samples for this study. Lewis & McConchie (1994) note there are considerable difficulties in achieving accurate determinations of mineral proportions, eg mass absorption effects, difficulties with preferred orientations of some minerals, crystalline sizes etc. Dr Newman provided a number of comments on the “TRACES” data (see Section 3.2.3.3. for specifics).

2.3.6. Coal Petrography and Vitrinite Reflectance Analysis.

Maceral point counts and reflectance measurements were undertaken on a Zeiss UMSP50 incident light microscope at the Department of Geology, Canterbury University, Christchurch, New Zealand by the author. Point counts were undertaken using an automatic point count stage. Each sample was split into two sub-samples and a polished block made of each split. Sample preparation was undertaken by Mr Colin Nunweek and Mr Nick Moore under supervision of Dr Jane Newman. At least 250 counts were made on each polished block (ie 500 counts per sample) to provide a precise determination of maceral proportions. Identification of macerals was determined to standard criteria (International Committee for Coal and Organic Petrology (ICCP), 2001; International Committee for Coal and Organic Petrology, 1998; Teichmüller et al., 1998). Point counting was undertaken using standard

methods (ISO - International Standard ISO 7404-3, 1994a). Independent maceral point counting of two samples by Dr Peter Crosdale found good repeatability for the maceral groups (Crosdale, pers comm. 2002).

Vitrinite reflectance measurement was undertaken on the same microscope equipment by the author. Wherever sufficient vitrinite was present, 50 measurements were made on each split (ie 100 measurements per sample). Measurement was undertaken to standard specifications (ISO - International Standard ISO 7404-5, 1994b). Calibration of the instrument was undertaken using sapphire [Ro(max) 0.6%], YAG [Ro(max) 0.915%] and glass [Ro(max) 1.02%] standards. The calibration of the equipment was checked after each polished block, or during measurement of a block if the measurements appeared anomalous. In general, the microscope equipment proved stable, changes in reflectance measurements during analysis of a polished block usually being traced to dirt in the refractive oil.

2.3.7. Leaching Methods.

The USGS sequential leaching method, used for indicating the mode of occurrence of trace elements in coal, has been outlined in Section 1.3.2.2.

The TCLP protocol was used to produce an extraction fluid to determine the concentration and proportion of antimony, arsenic, barium, boron, chromium, cobalt, copper, lead, manganese, nickel, selenium, vanadium, and zinc that could be mobilised from a 20% bottom-ash/ 80% fly-ash composite sample for the two power stations studied. The TCLP protocol requires a sample of at least 100 grams. The solid sample material is leached for 18 \pm 2 hours in an agitator vessel capable of rotating the sample end over end at 30 \pm 2 rpm. Extraction fluids are made up using reagent water (defined as “water in which an interferant is not observed at or above the method’s detection limit of the analyte(s) of interest”) as a dilutant. Extraction fluid #1 is made up by adding 5.7 mL of glacial CH₃CH₂OOH to 500 mL of reagent water, then adding 64.3 mL of 1N NaOH and diluting to a volume of 1 litre. Extraction fluid #2 is made up by adding 5.7 mL of glacial CH₃CH₂OOH to 500 mL of reagent water to a volume of 1 litre. The choice of extraction fluid depends on the alkalinity of the solid waste material. The agitated slurry is then filtered through a borosilicate glass fibre filter with an effective pore size of 0.6 to 0.8 μ m. In addition,

when evaluating metals (ie this study), the filters must be washed with 1N nitric acid followed by three consecutive rinses with deionised water. If the original sample contained no liquid phase, the filtered liquid material is defined as the final TCLP extract.

The TCLP extract was analysed using ICP-OES (Section 2.3.4.).

2.4. Comparison of INAA and XRF Analytical Results.

A discussion of the reproducibility of some analytical results using INAA and ICP-MS is included in Chapter 4. ICP-MS was only used on some selected combustion plant samples relating to the combustion plant samples. Collinsville channel samples, combustion plant samples from Collinsville and Japan, and coke samples from the Bowen coke works were all analysed by INAA and XRF. Iron was analysed by both INAA and fusion bead XRF; uranium by both INAA and pressed powder pellet XRF. Figures 2.2a. and 2.2b. show the relationship between iron from INAA and XRF and uranium from INAA and XRF respectively. The relationship between analysed iron values from INAA and XRF is generally excellent, although there are three notable exceptions, probably due to analytical errors or inhomogeneity between sample splits. The relationship between uranium analysed by INAA and uranium analysed by XRF is also strong, although the scatter is considerably greater than for iron. It is concluded that the reproducibility of iron and uranium for INAA and XRF is acceptable, and inferred that the two data sets are comparable.

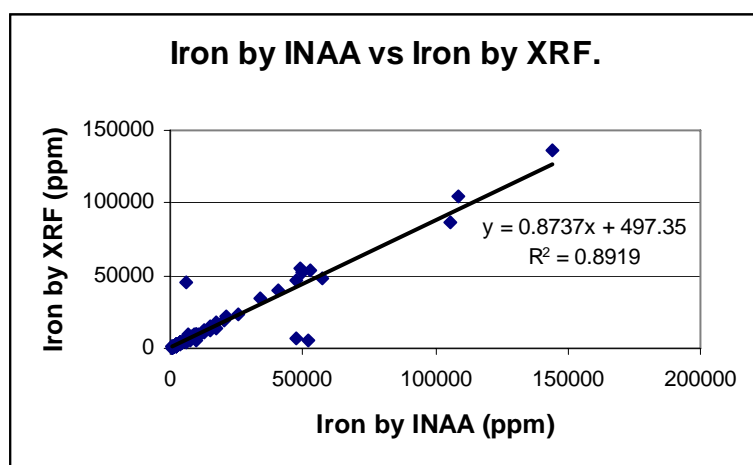


Figure 2.7. Iron by INAA vs Iron by XRF

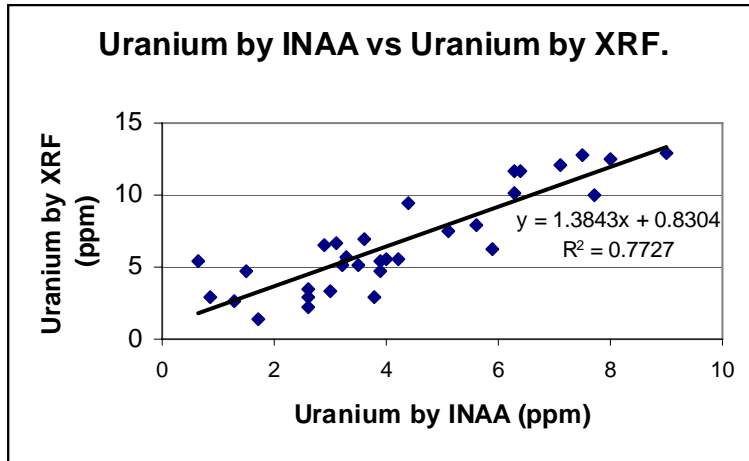


Figure 2.8. Uranium by INAA vs Uranium by XRF

2.5. Concluding Remarks.

One of the major issues in undertaking elemental analysis of a large number samples is gaining high quality data at a reasonable price. The two methods chosen (INAA and XRF) appeared to provide good quality, comparable data at a reasonable price. However, given the issues involving the poor repeatability of potassium and the general lack of potassium and calcium figures (see Chapter 3), it is concluded that in future studies, all the major elements including those already provided by INAA, should be analysed by XRF on a fusion bead.

Second, it should also be noted that the ACTLABS INAA data is used in preference to the pressed powder or fused disc data for the normative and partitioning behaviour calculations in order to use an internally consistent data set (NB this assumes any errors involving the INAA data set are systematic). Although this approach has the weakness that the data can be criticised regarding the reliability of any specific figure, as a whole the inferences using the data are still considered valid. Thus, even if application of another analytical technique might give elemental concentrations at variance with the INAA figures, the consistent use of the INAA figures to calculate, for example, classification of the partitioning behaviour of an element in combustion would still make the classification valid.

Third, sufficient sample for XRF analysis of low temperature ash pressed powder pellets was only available for a limited number of samples. Therefore, analysis figures for copper, lead, and vanadium are limited. It is recommended that future

studies take larger quantities of sample if pressed powder pellet XRF analysis is to be undertaken. Further, it is considered advisable that the researcher decides on the methods of analysis prior to sampling to ensure a sufficient quantity of each sample is gathered.

Chapter 3.

Collinsville Opencut: Coal Characterisation, Trace Element Concentration and Mode of Occurrence.

3.0. Chapter Resume.

The analysis results for ply-by-ply channel samples from the Blake and Bowen seams in the Collinsville Coal mining operation, Collinsville, Bowen Basin, Australia, are presented in this chapter. The Blake West, Blake Central (mining Blake seam coal), and Bowen No.2 (mining Bowen seam coal) open-cut pits were sampled. These three pits produced the feed coal for the Collinsville coal-fired power station at the time of sampling.

Lithotype logs, proximate analysis, maceral point count analysis, and measurement of vitrinite reflectance [Ro(max)] are used to characterise the coal and infer the depositional environment for the three pits sampled. Major and trace element analyses characterise the elemental concentrations in the channel samples. Mineralogy is deduced using normative calculations aided by XRD analysis of low-temperature ash from selected samples. Trace element mode of occurrence is deduced using graphical methods. The effect of igneous intrusions on the coal and on the concentration of trace elements within the three pits is discussed.

3.1. Samples.

Channel samples were gathered from the Collinsville opencast coalmine in the northern Bowen Basin (Figure 3.1.) on the 12th and 13th September, 1999. At the time of sampling, the Collinsville coalmine was a joint venture operation comprising 75% Mt Isa Mining (MIM) and 25% Itochu Coal Resources Australia. Theiss Contractors operated the mine on behalf of the owners. Production for the 1999/2000 year was slightly in excess of 3 MT.

The Collinsville coalmine extracts coal from the Collinsville Coal Measures, which are “informally divided into the upper and lower sequences separated by the marine Glendoo Sandstone Member” (Martini and Johnson, 1987; Woolfe et al., 1996) (Figure 3.2). The Murray, Garrick, and Peace seams occur above the Glendoo

Sandstone; and the Scott, Denison, Potts, Little Bowen, Bowen, and Blake seams occur below the Glendoo Sandstone (stated in descending stratigraphic order).

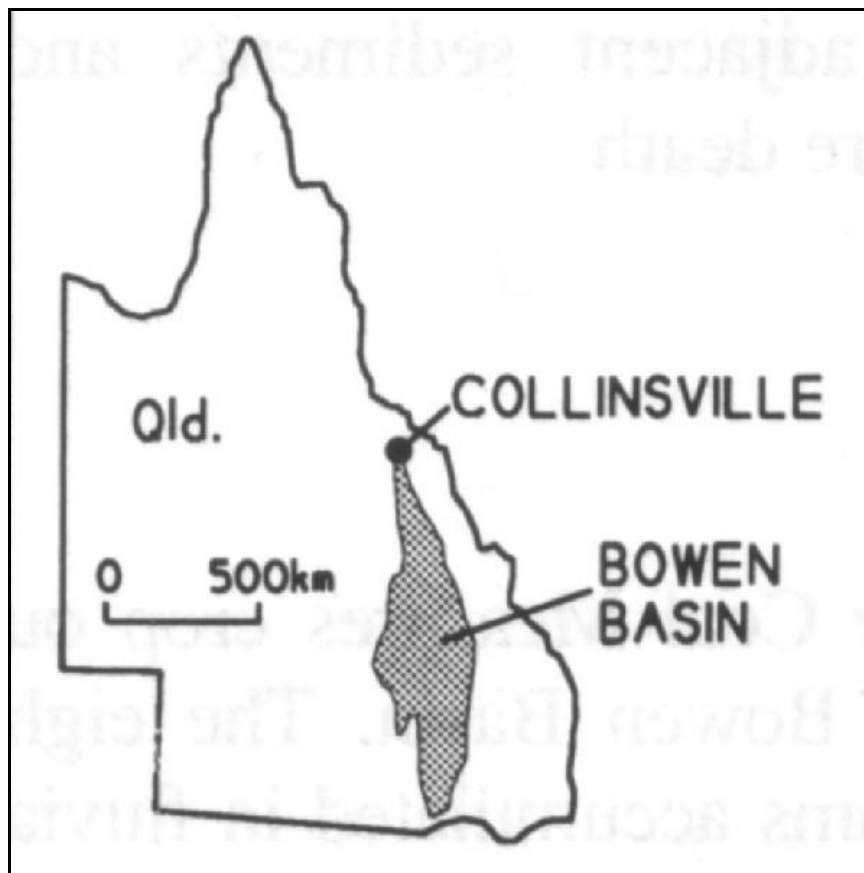


Figure 3.1. Location of Collinsville Coalmine. Source: Woolf et al, (1996)

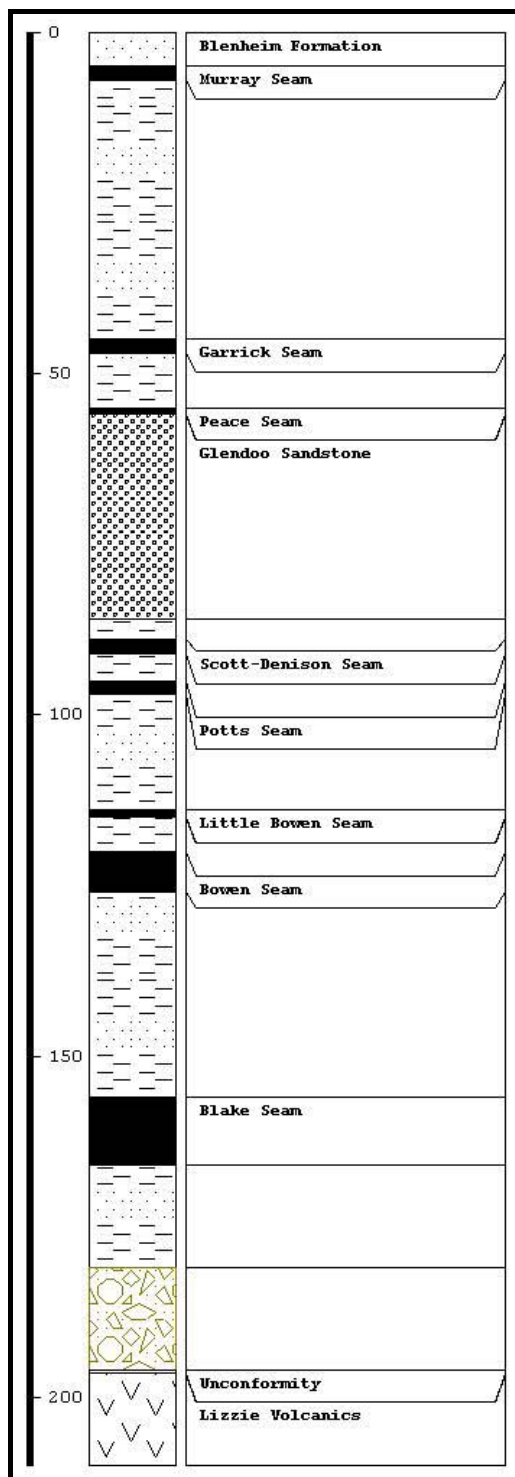


Figure 3.2. Stratigraphic Column for the Collinsville Coal Measures.
 Compiled from Gunn, (1988); Martini & Johnson (1987); and Woolf et al. (1996)

The Blake West, Blake Central, and Bowen No.2 pits (Figure 3.3.) were channel sampled. At the time of sampling, the Collinsville power station was fuelled with coal from the three sampled pits at a nominal blend of 70% Blake Seam/ 30% Bowen Seam.

The coal lithotypes exposed in each pit were logged using standard criteria (Australian Standard 2916-1986, 1986). Sampling was undertaken to reflect lithotype boundaries, although some amalgamation of lithotypes was required to limit sample numbers. A total of 76 samples were gathered from the three pits, 25 from the Blake Central pit (“BC” samples), 36 from the Blake West pit (“BW” and “BWB” samples) and 15 from the Bowen No.2 pit (“BO” samples). The numbering of samples generally reflects the distance down from the true roof of the seam. However, the Blake Seam in the Blake Central and Blake West pits was too thick to be readily sampled at a single locality, ie as a single channel from roof to floor. The full seam was sampled in the Blake Central pit by sampling the top half of the seam in the main highwall, and the bottom half from an in-pit bench shown in Figure 3.4.. Continuous sample numbering was possible in the Blake Central pit because individual lithotypes could be traced along the highwall and no divergence from the true roof of the seam was apparent.

The seam in the Blake West pit was sampled by moving along the highwall, taking advantage of the seam roof rising away from the bench, and in-pit benches, to sample stratigraphically lower intervals. Some complications were encountered in the Blake West pit because the lithotypes within the seam diverged from the true roof along the highwall. Therefore, within the Blake West (BW) group of samples, the sample numbers jump from 0.93m to 1.20m below true roof as sampling moved along the highwall, although the lithotypes are contiguous.

The thinner Bowen No.2 pit seam was sampled as a single channel at one location.

Degradation of the coal due to exposure to weather made sampling difficult in some places (eg the lower section of the seam in both the Blake West and Blake Central pits, the latter shown in Figure 3.5.). Every effort was made to avoid the degraded areas, eg by sampling the in-pit bench in the Blake Central pit. However degraded coal was unavoidable in the Blake West pit, hence the bottom part of the seam is logged as undifferentiated (Figure 3.12.) and sampled in nominal 0.5m ply intervals.

An additional complication in the Blake West pit was the presence of bed-parallel igneous intrusions within the seam, shown in Figures 3.6. and 3.7.. An aureole of columnar jointed natural coke was found immediately adjacent to the intrusive body (Figure 3.7.), and the coal adjacent to the coke had been heat affected to the point that no lithotype distinction was possible (ie all the coal appeared dull). The intrusive body was entirely altered to white clay, presumably kaolinite(?). Because of these complications, samples from the Blake West pit are divided into a “BW” set (samples from above the intrusion) and a “BWB” set (samples from beneath the intrusion). In the strip logs presented later in Chapter 3, the Blake West sample depths are corrected and a ‘composite’ strip log is presented for this pit (Figure 3.12.).

Heat-affected coal was also apparent at the top section of the seam in the Blake Central pit and the bottom section of the Bowen No.2 seam (the intrusion apparently being located in the roof or floor rocks respectively). Again, lithotype distinction in the heat-affected sections of the Blake Central and Bowen No.2 seams was impossible, and the coal was logged as DD. The coal in the upper part of the Blake Central seam was sampled at a nominal 0.5m ply interval, and the bottom part of the Bowen No.2 pit divided into two plies of 0.6m thickness.

Proximate analysis was undertaken for all channel samples by SGS Collinsville laboratory. A split was returned to the author, split using cone and quartering, and despatched for analysis by INAA and XRF for trace and major element concentration. Where sufficient sample was available, petrographic splits for each sample were returned to the author by SGS Collinsville. Two-resin mounted crushed-grain blocks were prepared from each petrographic sample by Mr Colin Nunweek, and were analysed by the author. Petrographic and reflectance analysis was undertaken on each polished block to ensure repeatability. The petrographic and reflectance analysis figures are the average of the two sample blocks.

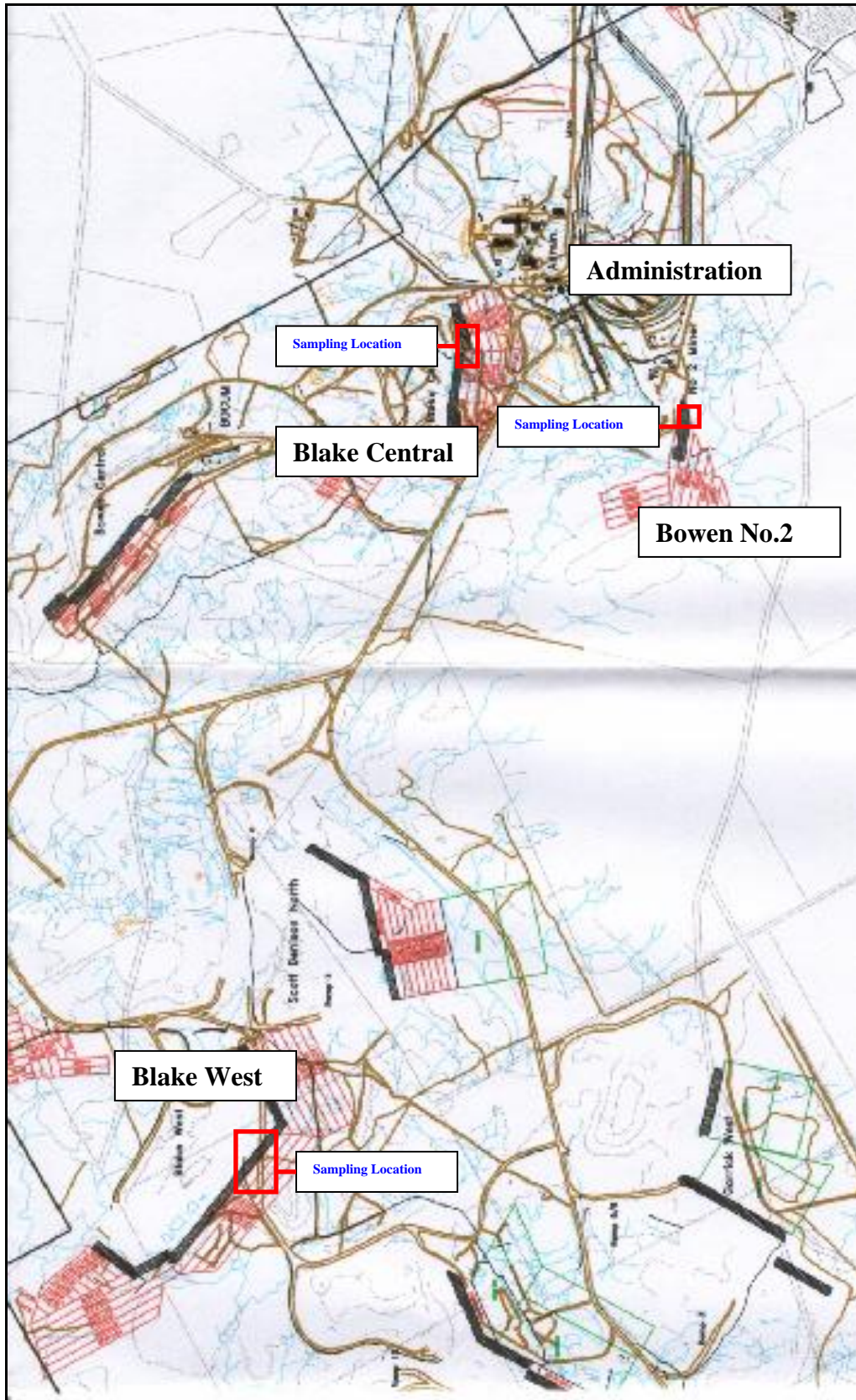


Figure 3.3. Relative location of the pits sampled for this study.



Figure 3.4. In-pit bench in the Blake Central pit, Blake Seam.



Figure 3.5. Coal degradation in the highwall of Blake Central pit, Blake Seam following exposure to the weather.



Figure 3.6. Bed-parallel igneous intrusions in the Blake West pit, Blake Seam.



Figure 3.7. Close-up of igneous intrusions in Blake West pit, Blake Seam. Note the aureole of columnar jointed coke immediately adjacent to the intrusion. Intrusive body diameter 2m.

3.2. Coal Characteristics.

Maceral point count and reflectance analysis results for each pit are presented in Appendix 3. Proximate and elemental analysis data for each pit are presented in Appendix 4. Strip logs for the Blake Central, Blake West, and Bowen No.2 pits were compiled using the Rockware computer programme Logplot and are presented in Figures 3.8., 3.12. and 3.15. respectively. The composite logs show the graphical lithotype log, the lithotype name and the sample number of that lithotype, Ro(max), volatile matter (dry ash free basis), fixed carbon, vitrinite, inertinite, and semi-coke contents. Note, not all samples have a corresponding maceral and Ro(max) analysis because of a lack of sample material in some instances. Analysis of Ro(max) is further restricted to maceral samples which did not show alteration of vitrinite to semi-coke. A liptinite column is not plotted because this maceral was rarely noted, probably in part due to the convergence of liptinite and vitrinite reflectance at about the rank of the Collinsville coal (Teichmüller et al., 1998).

3.2.1. The Blake Seam.

Blake Central Open Cut.

With reference to Figure 3.8., the lower section of the Blake Seam in the Blake Central pit (~4.2m from the roof downward) is notable for the presence of several thin partings of carbonaceous or highly carbonaceous mudstone. Working from the base of the seam upward, these partings may be preceded by bright-banded (BB) or bright (Br) lithotypes, probably due to an influx of nutrients into the mire culminating in the incursion responsible for depositing the mudstone band. In some cases (samples BC 5.98-6.11 & BC6.23-6.35), the coal above the mudstone bands is dull with minor bright bands (DM lithotype). Generally, the DM lithotype corresponds with increased inertinite contents (dominantly structured inertinite such as fusinite and semifusinite) (Figure 3.8.), indicating autochthonous oxidation of the accumulating plant material (Diessel, 1992). DM bands above mudstone partings are interpreted as being due to an ongoing supply of oxygenated water to the mire following deposition of the mudstone layer. No dulling-upward cycles are recognised in the basal 1m of the Blake Central pit seam, probably due to the intermittent influxes of sediment-laden water, nourishing and saturating the mire.

Above the DM band logged at 5.98 to 6.11m, a thicker coal sequence appears to dull upward (ie from the BB lithotype at 5.49 to 5.98m to a DM band at 5.39 to 5.49m), however, the BB lithotype at 5.11 to 5.39 again precedes sediment incursions with an accompanying bright band in the interval between 5.00 and 5.11m down from the roof. A second possible dulling upward cycle is present in the interval 4.55 to 5.00 (BB) succeeded by 4.22 to 4.55m (DM), but the cycle is interrupted by another sediment incursion. The mudstone logged at 4.18 to 4.22m essentially marks the end of useful lithotype logging in the Blake Central pit, with only Br and DM lithotypes logged between ~3 and 4m, but above 3m only DM or DD lithotypes logged due to the progressively greater influence of thermal alteration. The increasing contact metamorphism in the seam is shown by the increase in vitrinite reflectance up-section (Figure 3.8.), sample 4.00-4.13 showing a mean maximum reflectance of $R_o(\max)$ 1.39% (vitrinite in samples closer to the roof of the seam being completely altered to semi-coke).

The intermittent incursion of sediment into the Blake Central mire has resulted in a seam with moderate (10.0% adb) to high (70.4% adb, mudstone parting) ash yield plys, with a ply-thickness weighted average of 24.1% (adb). Palaeozoic coals often show “dulling-upward” cycles, thought to be caused by increased amounts of inertinite due to increased degradation and oxidation of the peat (Croisdale, 1995). However, it appears that the numerous sediment incursions into the Blake Seam in the Blake Central pit prevented the development of significant dulling-upward cycles.

Maceral analysis of the Blake Central pit samples suggests the Blake Seam coal is high in inertinite (samples ranging from 25.4% to 91.6%, ply-thickness weighted average 56.2%), and low in vitrinite (ranging from 7.4% to 70.0%, ply-thickness weighted average 30.2%) (Appendix 3). Vitrinite reflectance averages ~1.25% for the Blake Central pit, but there is a notable increase in reflectance up-section toward the samples where vitrinite has been altered to semi-coke. Limited analysis suggests an average $R_o(\max)$ of ~1.2% for coal unaffected by heat in the Blake West pit. Samples containing semi-coke (Figure 3.11.) are considered to be significantly heat affected. Some subtle heat alteration may well occur beneath the samples containing semi-coke.

The volatile matter (daf basis) content of the Blake Seam in the Blake Central pit varies in response to coal type and also to the degree of thermal alteration, ie proximity to the overlying igneous intrusion. Figure 3.8. shows volatile matter (daf) varies approximately inversely to the proportion of inertinite, as found previously in other studies (Diessel, 1992; Suggate, 1998). Figure 3.9. demonstrates a relatively poor relationship between inertinite (mineral matter and rock fragment free) and volatile matter (daf) for the Blake Central petrographic samples (samples shown as a pink squares are considered on the basis of petrographic evidence as heat affected).

The volatile matter (daf) content in the Blake Central seam decreases in a reasonably regular fashion toward the top of the seam in response to thermal alteration (Figure 3.8.). (NB Very high volatile matter figures for the mudstone partings should be ignored because a high proportion of the volatile matter in these samples is contributed by thermal decomposition of the mineral matter, an error exaggerated by calculating to a dry ash free basis. In particular, any carbonates present would contribute a high proportion of volatile matter in some samples). Figure 3.10. shows volatile matter (daf) with distance from the seam roof. Points shown in pink in Figure 3.10. are considered significantly heat affected on the basis of petrographic evidence (ie presence of semi-coke). The trend of change shown by the pink squares suggests thermal alteration extends ~5.5m down into the coal from the roof of the seam. Vitritinite reflectance also increases upward from about the same position within the seam (Figure 3.8.) (Appendix 3). The petrographic evidence and reflectance data suggests thermal alteration extends at least to BC5.39-5.49 (ie ~5.5m down from the roof contact). Unfortunately a clear distinction between heat affected and unaffected samples on the basis of volatile matter (daf) could not be proposed. In part the lack of a discernable volatile matter (daf) cutoff is due to the subtle decay in thermal alteration over distance. However, the volatile matter content also partly reflects contributions from thermal decay of mineral matter, which varies with ash yield and mineral matter type. Therefore, the presence of semi-coke is used as an indicator of heat-affected samples.

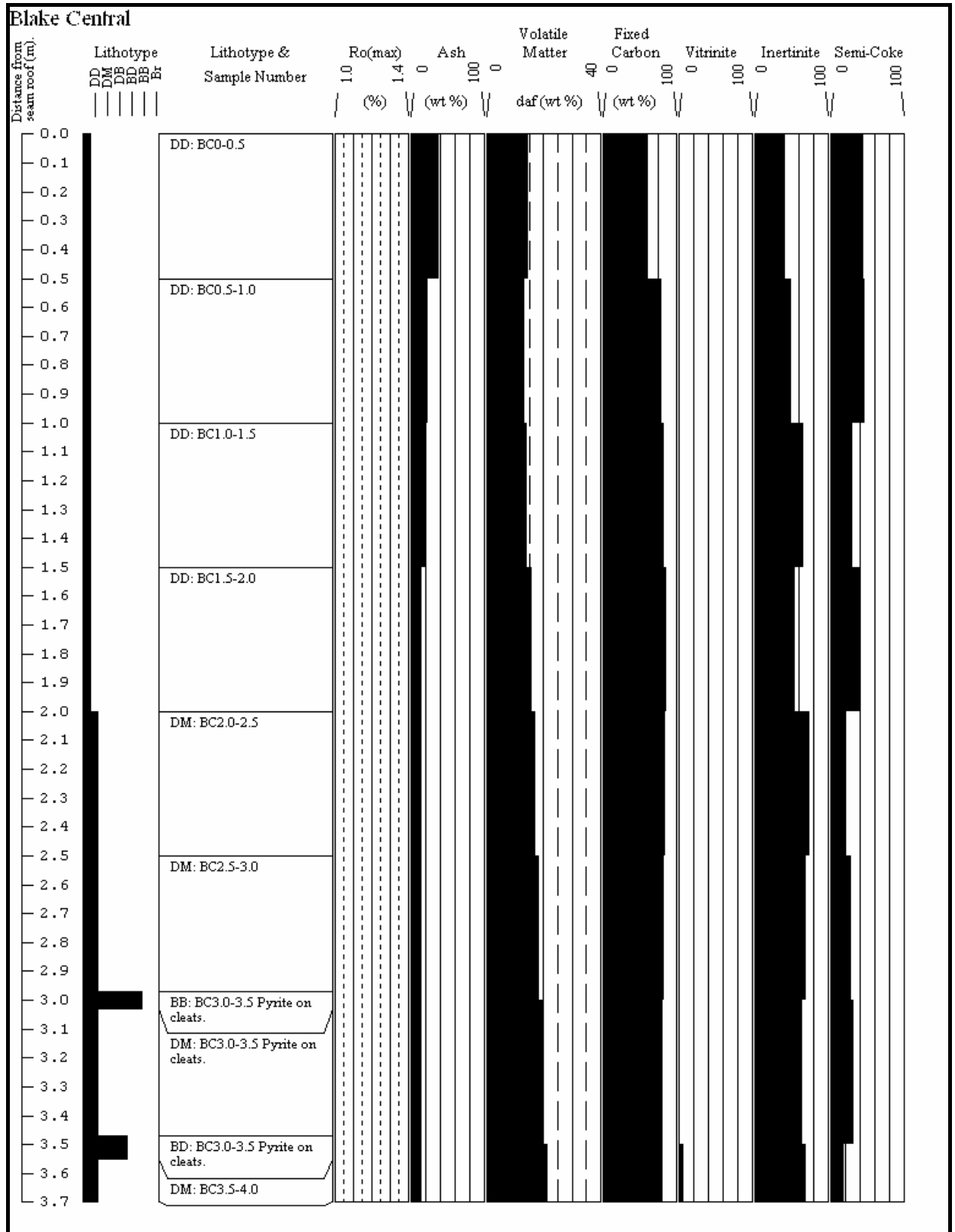


Figure 3.8. Strip log of pit samples from the Blake Central pit.

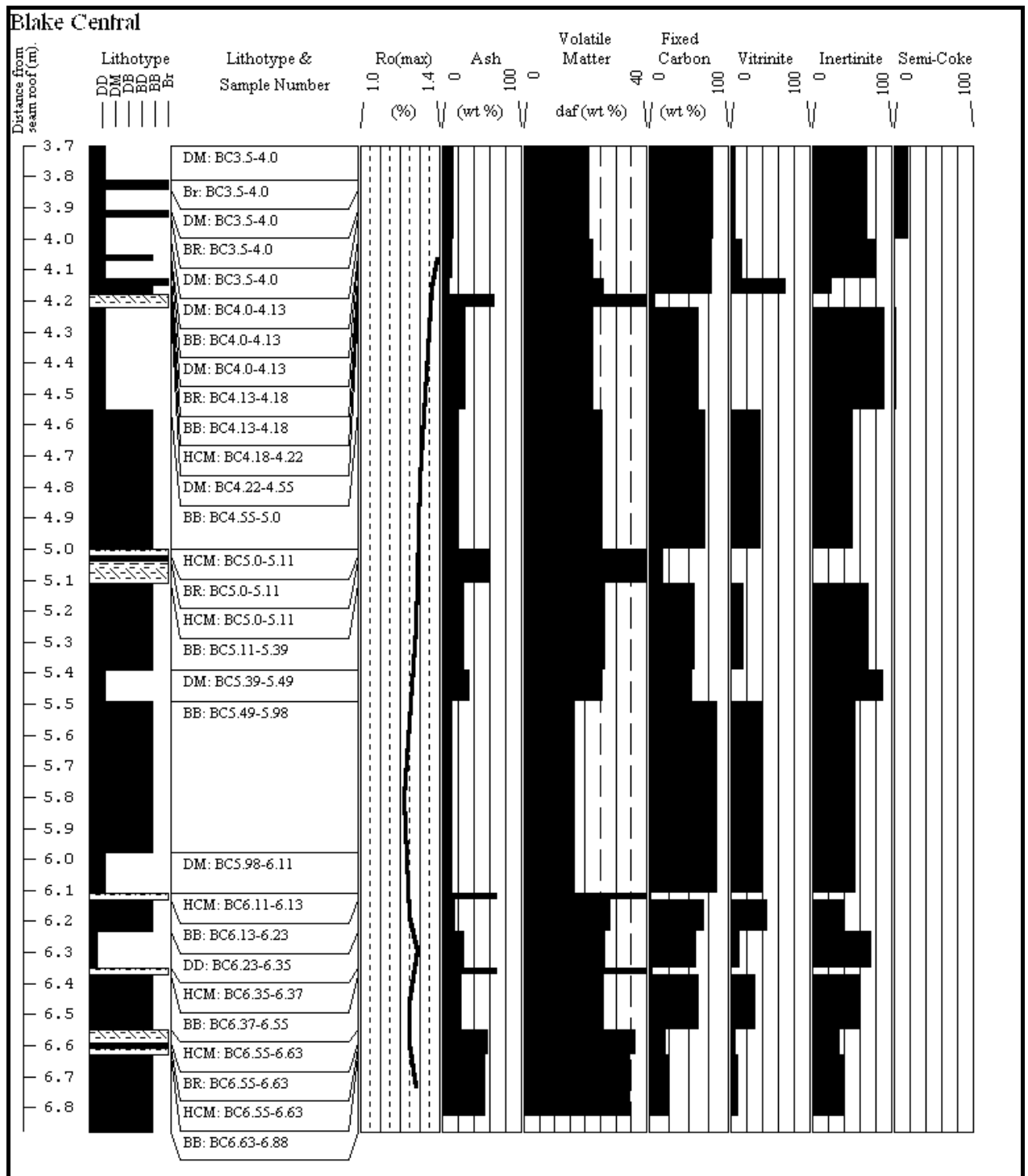


Figure 3.8. Strip log of pit samples from the Blake Central pit (cont).

<u>Key</u>	
DD	= Dull Coal
DM	= Dull with minor bright bands
DB	= Dull with common Bright Bands
BD	= Interbedded Dull and Bright coal
BB	= Bright coal with Dull Bands
Br	= Bright Coal
Fus	= Fusain
HAC	= High Ash Coal
HCM	= Highly Carbonaceous Mudstone
CM	= Carbonaceous Mudstone
MS	= Mudstone

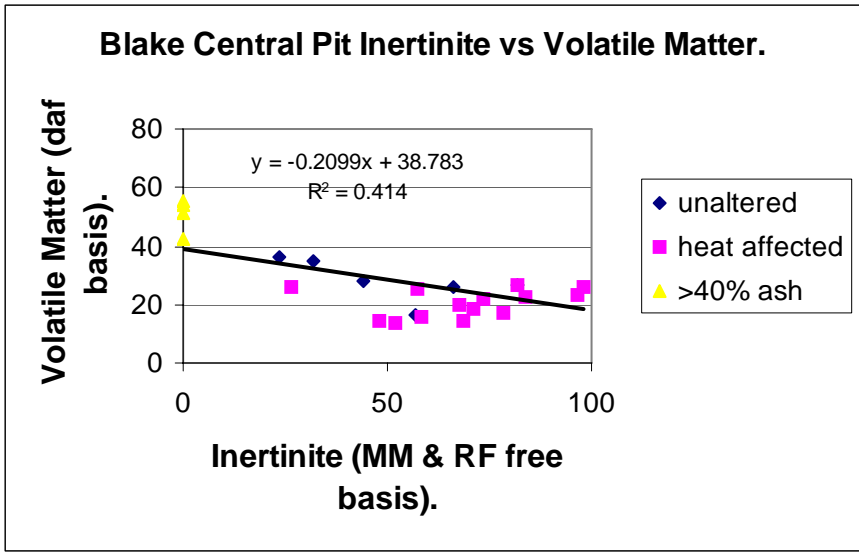


Figure 3.9. Blake Central Pit Inertinite vs Volatile Matter

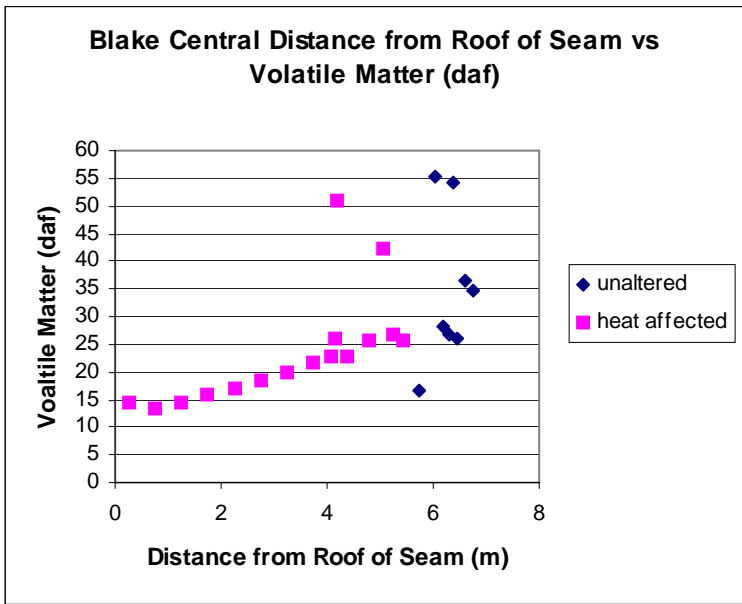


Figure 3.10. Blake Central Distance from Roof of Seam (m) vs Volatile Matter (daf)



Figure 3.11. Semi-coke in Bowen Seam coal, Bowen No.2. Pit.
Sample Number BO3.61-4.21. Field of view 50 μm wide. Polarised light.

Blake West Open Cut.

The seam in the Blake West pit (Figure 3.12.) is divided into three sections as follows: coal above the igneous intrusion; coal between the intrusion and a thick (0.74m) mudstone parting 11m from the roof; and coal below the parting. The coal interval above the intrusion for which lithotype logging was possible appears to brighten upward, before culminating in trio of dull lithotypes (DM, DD, and DM) immediately beneath the true roof, possibly indicating a sudden mire death (ie no nutrient bearing water influencing the mire prior to cessation of peat deposition) following oxidation of the upper layers of peat.

Adjacent to the intrusion, lithotype logging of the coal was not possible, the coal being heat affected and logged as a DD lithotype for 1.1m before grading downward into a 0.60m thick coked aureole. Beneath the intrusion, the same pattern emerges with a 0.65m thick coked aureole grading downward into a 1.25m DD layer of heat affected coal.

Lithotype logging suggests the central portion of the Blake West seam beneath the macroscopically recognisable heat affected zone is essentially bright banded (BB),

probably due to intermittent incursions of sediment (six partings in all ranging in thickness from 2cm to 8cm) with associated supply of nutrients to the mire. Unlike the Blake Central seam, the mudstone units are not succeeded by a dull lithotype, possibly indicating the incursions were short-lived events with little lasting effect on the water chemistry of the mire. Dull horizons (DB) only occur in three places in the central section of the seam, in all three cases within a thicker (greater than 0.5m) uninterrupted horizon of coal.

The central section of the Blake West seam is also notable for the presence of two fusain bands, the thicker of the two (sample number BWB 2.78-3.04) being 16cm thick. In both cases the fusain band is associated with BB lithotypes. The 16cm thick band immediately underlies a 6cm mudstone parting. One possible explanation is that these fusain bands represent fire splays (Diessel, 1992), with the sediment incursion resulting from the lowered peat topography. If the fusain bands had been the result of progressive drying out of the mire, an association with other dull lithotypes would be expected.

The bottom section of the Blake West pit seam is undifferentiated because exposure to weathering prevented lithotype logging of the face. Therefore, no deductions regarding cycles of deposition are possible. The undifferentiated portion of the seam was sampled in 0.5m ply intervals.

The intermittent incursion of sediment into the Blake West mire has resulted in a seam with a low (6.6% adb) to high (75.2% adb, mudstone parting) ash yield (ply-thickness weighted average 23.2% adb) (figures exclude the intrusive body but include coke and heat-affected samples).

Maceral analysis of the central part of the Blake West seam pit samples confirms the Blake Central analysis results, with inertinite ranging from 33.2% to 84.3% (ply-thickness weighted average 62.8%); and vitrinite ranging from 10.1% to 56.2% (ply-thickness weighted average 28.0%). (NB Maceral analysis results ignore heat-affected samples).

No maceral analyses are available for the upper section of the seam, and the relationship between inertinite (mineral matter and rock fragment free) and volatile matter (daf) (Figure 3.13.) for the mid-seam section of the Blake West pit for which corresponding petrographic samples were available is not discernable.

Picking heat-affected samples is more complicated in the Blake West seam. Petrographic evidence for the central part of the seam suggests heat alteration (presence of incipient semi coke) extends down to sample BWB4.28-4.40 (ie 4.40m down from the floor of the intrusion) (Figure 3.12; Appendix 3). However, no petrographic samples were available for the upper part of the seam. Other research has shown the thickness of the heat altered zone is almost identical above and below a sill (Khorasani et al., 1990). Given the section of coal above the intrusion is only 2.88m thick, it is considered likely that the entire upper section of the seam overlying the sill is heat affected.

Figure 3.14. shows volatile matter (daf) with distance from the seam roof. Points shown in pink in Figure 3.14. are considered heat affected on the basis of the presence of semi coke or because they fall within the likely zone of heat alteration above the sill. As for the Blake Central samples, a clear distinction between heat-affected and unaffected samples on the basis of volatile matter (daf) could not be proposed. The intervals logged as baked (DD lithotype) and coked are significantly lower in volatile matter (daf) than the interval for which lithotype logging was possible. However, samples showing some incipient semi-coke do not show substantially reduced volatile matter (daf). As for the Blake Central seam, the lack of a discernable volatile matter (daf) cutoff is in part due to the subtle decay in thermal alteration over distance and in part due to volatile matter contributed from thermal decay of mineral matter. The presence of semi-coke is used as an indicator of heat alteration, as outlined for the Blake Central seam. Where petrographic evidence is lacking, it is inferred that the zone of alteration above the sill will be the same thickness as the zone of alteration below the sill, ie will include the entire section of the seam above the intrusive body.

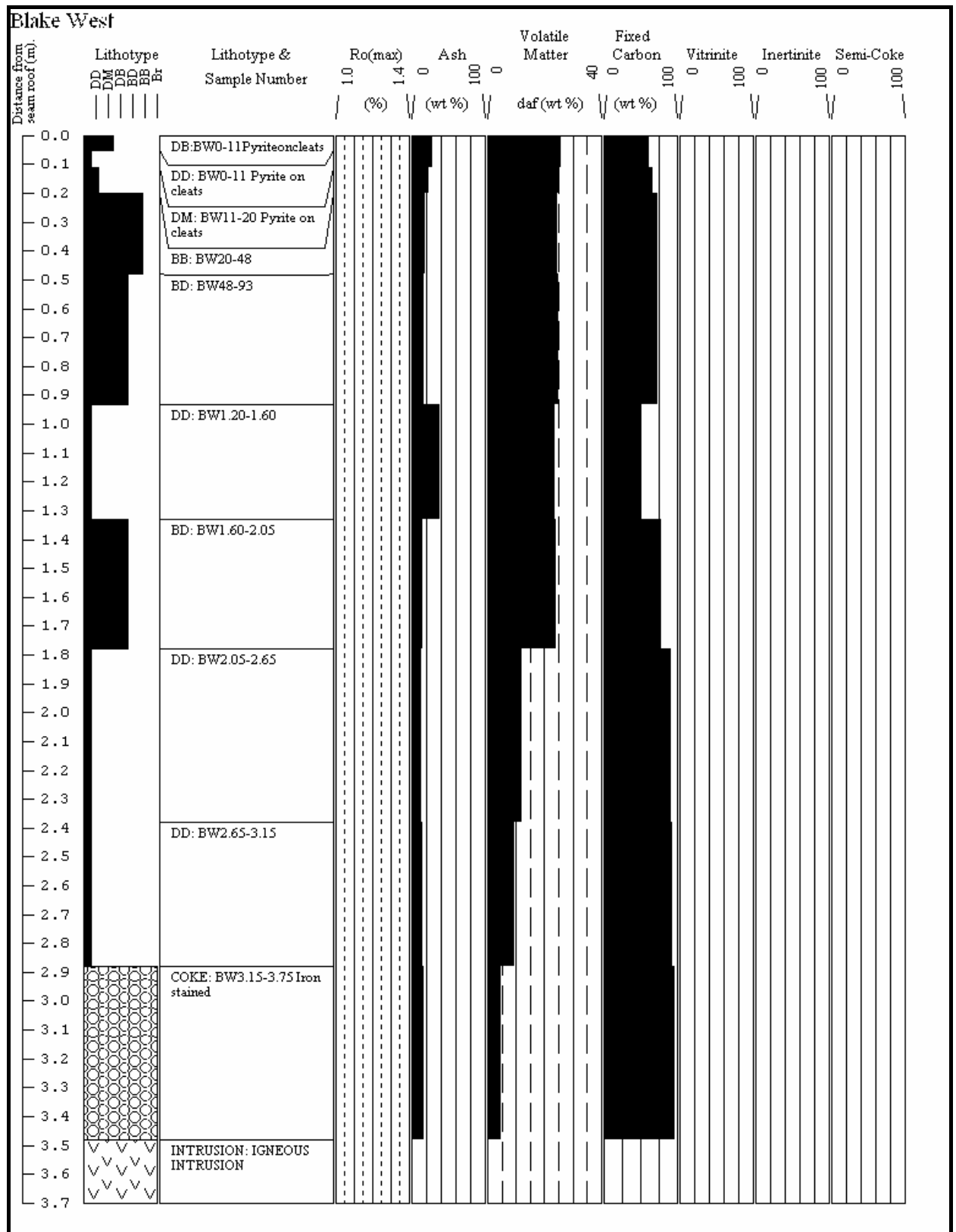


Figure 3.12. Strip log of pit samples from the Blake West pit.

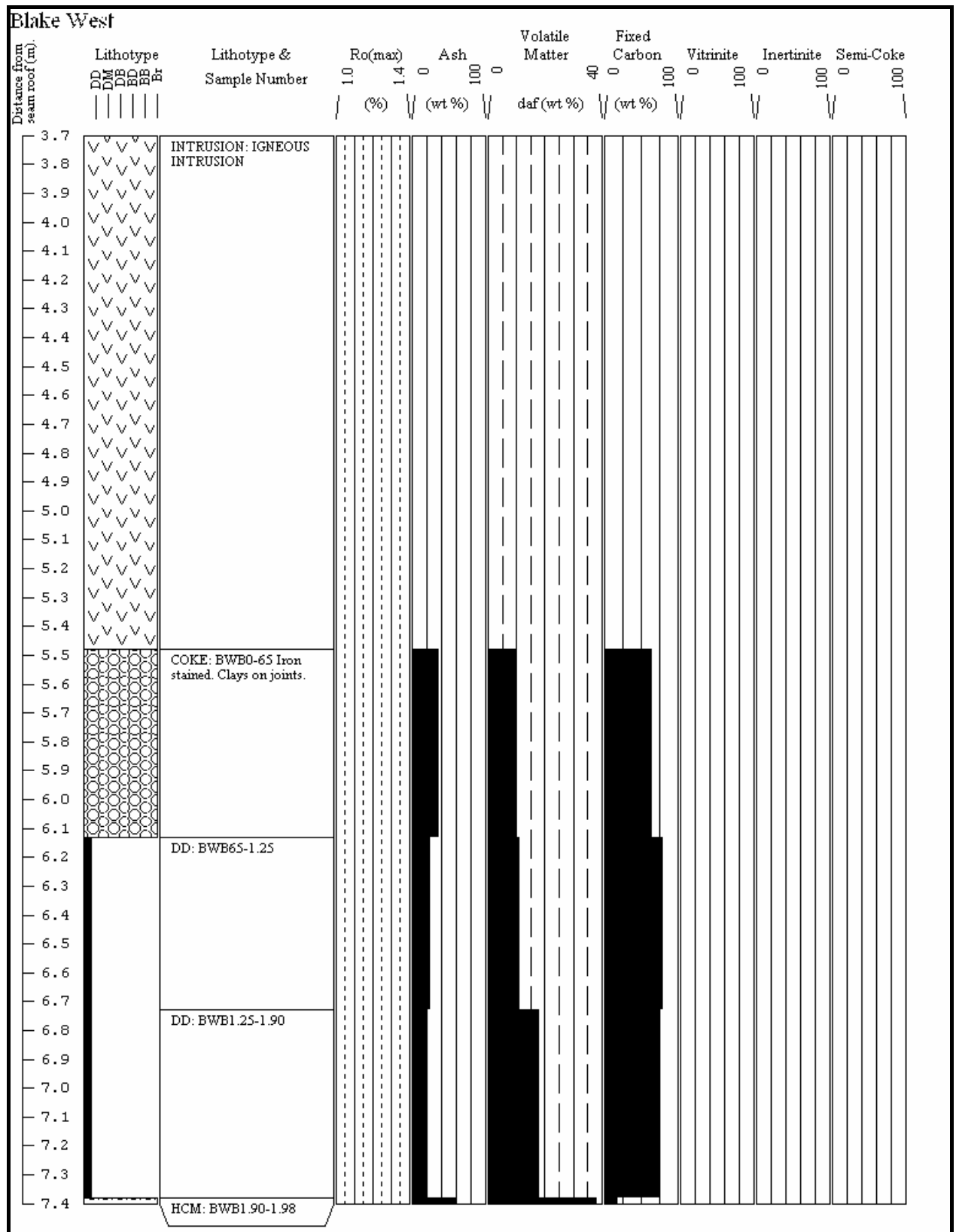


Figure 3.12. Strip log of pit samples from the Blake West pit (cont).

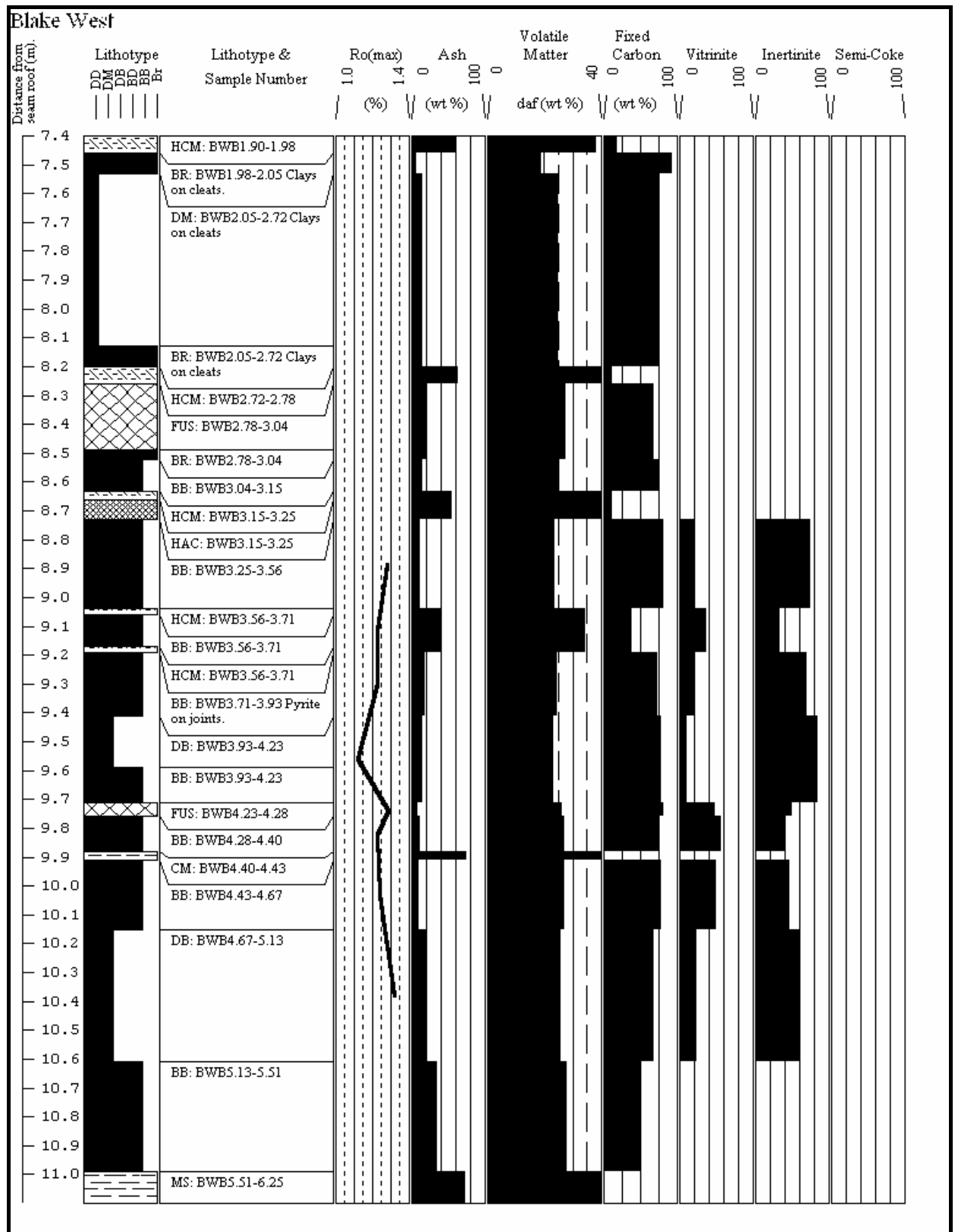


Figure 3.12. Strip log of pit samples from the Blake West pit (cont).

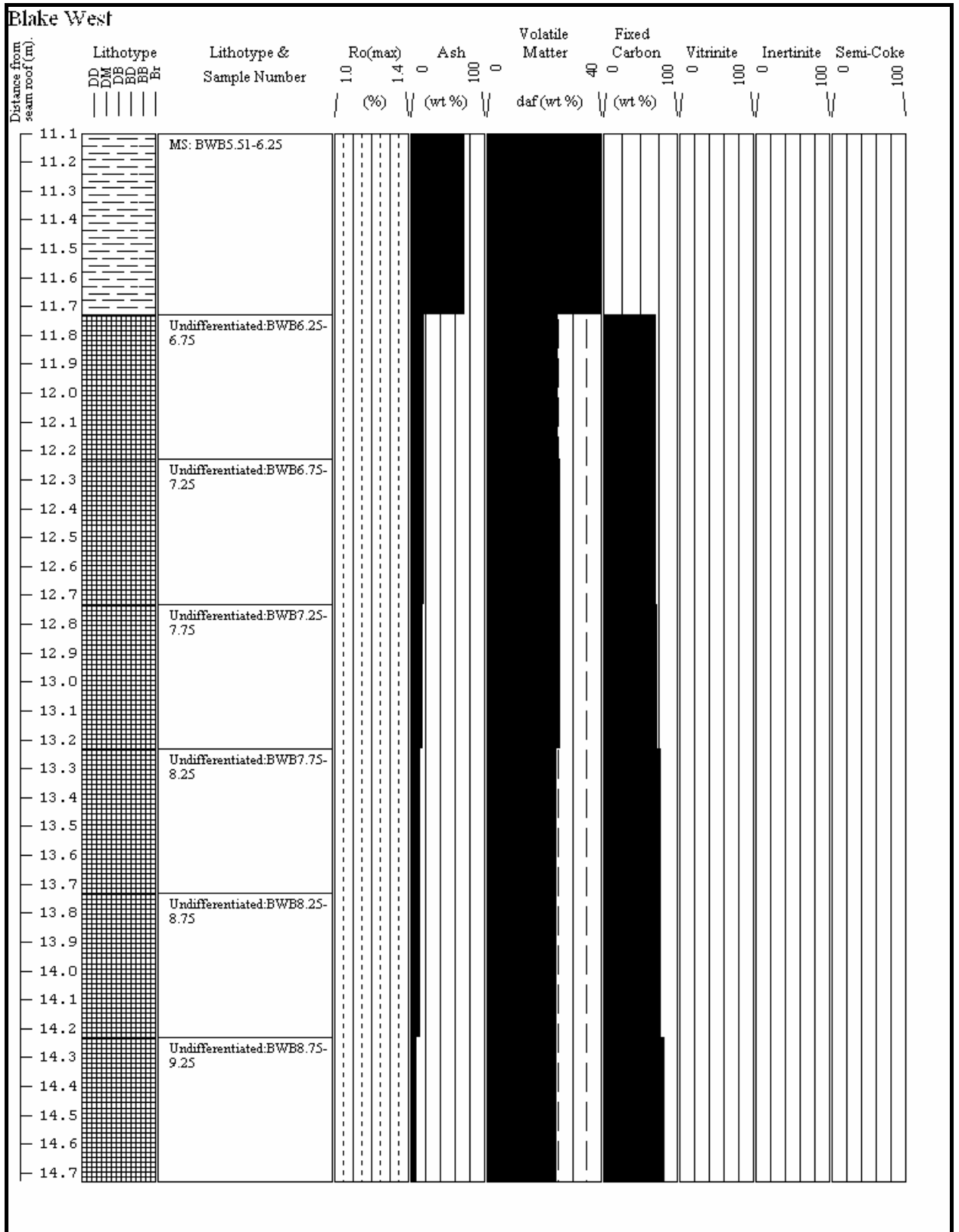


Figure 3.12. Strip log of pit samples from the Blake West pit (cont).

Key	=	
DD	=	Dull Coal
DM	=	Dull with minor bright bands
DB	=	Dull with common Bright Bands
BD	=	Interbedded Dull and Bright coal
BB	=	Bright coal with Dull Bands
Br	=	Bright Coal
Fus	=	Fusain
HAC	=	High Ash Coal
HCM	=	Highly Carbonaceous Mudstone
CM	=	Carbonaceous Mudstone
MS	=	Mudstone

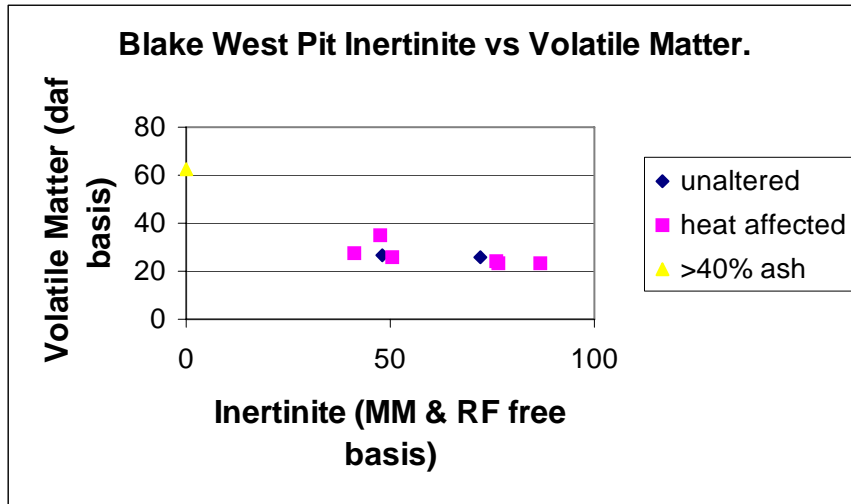


Figure 3.13. Blake West Pit Inertinite vs Volatile Matter

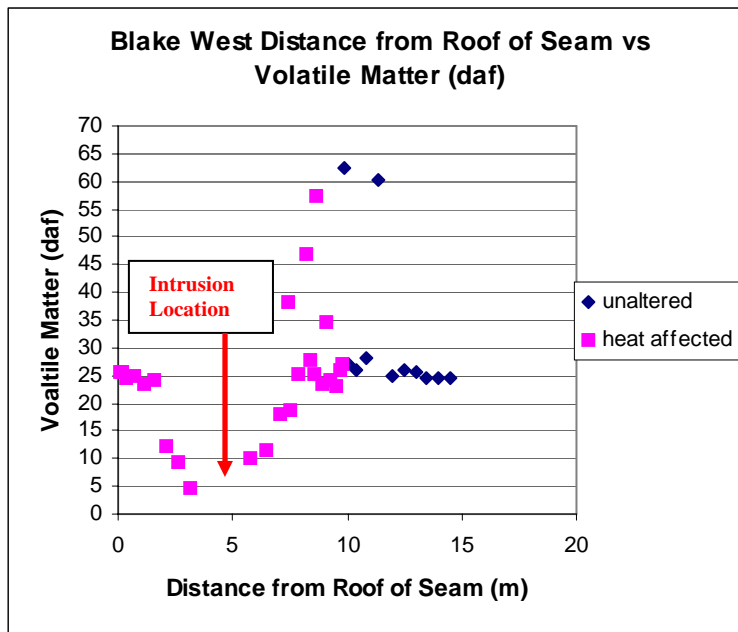


Figure 3.14. Blake West Distance from Roof of Seam (m) vs Volatile Matter (daf)

Blake Seam Depositional Environment.

With reference to Table 3.1., the generally high ash yield of the Blake Seam coal from both pits (Appendix 4), common stone bands, low sulphur content of the coal (Appendix 4) (ply thickness weighted average sulphur 0.24% for Blake West (limited analyses, see below) and 0.60% for Blake Central) and rare pyrite (Section 3.2.3.1.) suggest a Class 3 topotelmitic peat with a variable water table. The paucity of dull-coal lithotypes (other than those caused by thermal alteration) suggests a moderate nutrient supply and few drying episodes (as discussed above). Previous sedimentology studies have interpreted a fluvial depositional environment for the Blake Seam (Martini and Johnson, 1987), a view supported by the analysis of the coal characteristics and lithotypes.

Table 3.1. Interpretation of Depositional Environment from Coal Characteristics.

THIS TABLE HAS BEEN REMOVED DUE TO COPYRIGHT RESTRICTIONS

3.2.2. The Bowen Seam.

Bowen No.2 Open Cut.

Figure 3.15. shows a strip log for the Bowen seam in the Bowen No.2 pit. Lithotype logging of the lower 3.06m section of the 4.21m Bowen No.2 seam appears to indicate a brightening upward cycle. However, this apparent lithotype variation is almost certainly caused by thermal alteration rather than original depositional factors. The lower 1.2m of the Bowen No.2 seam was logged as a DD lithotype, the dull nature apparently caused by thermal alteration.

The DD lithotype is succeeded (upward) by a DM lithotype, interrupted in two places by fusain bands (samples BO2.45-2.60 and BO2.91-3.01). The DM lithotype is in turn succeeded by a DB lithotype (sample number BO1.15-1.85). The upper section of the Bowen No.2 seam is dominated by dull (DM & DB) lithotypes. There is an apparent dulling-upward lithotype sequence starting at sample number BO72-1.07 (Br) up to sample number BO37-72, with a band of fusain (sample BO34-37) at the top. Above this apparent dulling sequence, there is an apparent brightening-upward sequence over the final 0.34m of the seam prior to true roof. The brightening-upward sequence may reflect increasing sediment supply prior to mire death, the increased brightness being paralleled by an increasing ash yield. Woolf et al., (1996) suggest rising sea level and inundation by saline water caused the cessation of the Bowen seam peat accumulation.

Only four of the seven samples available for maceral analysis were not heat affected (vitrinite altered to semi-coke; Appendix 3). On the basis of the limited unaltered samples, inertinite content ranges from 51.4% to 80.2%, with a ply thickness weighted average of 64.9%, and vitrinite content ranges from 16.2% to 41.2%, with a ply-thickness weighted average of 30.2%. It appears from this analysis that the inertinite content of the Bowen seam is marginally higher than that of the Blake seam, however the basal 2–3m section of the Bowen seam is known to be relatively vitrinite-rich and was mined selectively in the Bowen central pit for carbonisation at the time of sampling (Slater, pers comm. 1999). Vitrinite reflectance averages $R_o(\max)$ 1.10%, suggesting the Bowen seam is lower rank than the Blake seam (the Bowen seam overlies the Blake seam by ~35-40m (Martini and Johnson, 1987).

However, the three samples available for reflectance analysis suggest a rapid reflectance increase downward within the seam, probably due to heat alteration caused by the presence of an igneous intrusion somewhere within the floor rock of the Bowen No.2 pit.

Maceral analysis of sample BO1.15-1.85 found an absence of semi-coke. The next sample (stratigraphically descending order) available for petrographic analysis was BO2.45-2.60, a fusain band that contained significant semi-coke. It is, therefore, considered that samples up to and including BO1.85-2.45 are heat affected (ie up to 2.3m from the floor of the seam).

Figure 3.16. shows inertinite (rock fragment and mineral matter free) versus volatile matter (daf). Figure 3.16. suggests volatile matter is in part controlled by inertinite content (as for the Blake seam data sets), whereas heat affected samples are reduced to a lower volatile matter content but still show the effect of coal type. The offset in volatile matter figures (rather than completed disorganisation of the trend) could suggest that the intrusive body has had a smaller effect on the Bowen data set. Unfortunately, the difference in volatile matter between BO1.15-1.85 and BO2.45-2.60 shows the lower sample has only 0.3% less volatile matter (daf), despite maceral data to suggest one sample is significantly heat affected.

Figure 3.17. shows volatile matter (daf) with distance from the seam roof. Points shown in pink in Figure 3.17. are considered heat affected (ie presence of semi-coke), with vitrinite reflectance also increasing downward from about the same position within the seam (Figure 3.15.) (Appendix 3). As for the Blake Seam samples, a clear distinction between heat affected and unaffected samples on the basis of volatile matter (daf) could not be proposed. As noted for the Blake Central samples, the lack of a discernable volatile matter (daf) cutoff is in part due to the subtle decay in thermal alteration over distance. Volatile matter content from thermal decay of mineral matter is probably also an issue, although the ash yield from the Bowen No.2 seam samples is generally lower than the Blake Seam samples.

The Bowen No.2 seam mire was not subjected to any sediment incursions (as evidenced by the lack of partings), and the ash yield of the coal is lower than most of

the Blake seam samples analysed (ranging from 6.2% to 33.4%; ply-thickness weighted average 12.89%). The sulphur content in the Bowen seam is higher than in the Blake seam, the ply-thickness weighted average being 1.79%, but sulphur is enriched toward the top of the seam suggesting this element percolated down from above; also noted by Woolf et al., (1996).

Bowen Seam Depositional Environment.

With reference to Table 3.1., the moderate ash yield of the Bowen seam coal (Appendix 4), the absence of common stone bands, sulphur contents of ~2%, and the moderate pyrite content of the coal (Section 3.2.2.2.) suggest a Class 2 topotelmitic peat with a high water table. However, the presence of at least one recognisable dulling upward cycle (others potentially being obscured by thermal alteration) and the presence of a number of fusain bands (not associated with sediment incursions) suggest several drying episodes could have occurred. Previous sedimentology studies have interpreted a fluvial paralic depositional environment for the Bowen seam (Martini and Johnson, 1987; Woolfe et al., 1996). Martini & Johnson (1987) also note the lower ash content of the Bowen seam (compared to the Blake seam), giving the “indication of a raised peatland”. Lithotype logging, the presence of fusain bands, and the vitrinite rich nature of the lower section of the seam with increased inertinite in upper seam intervals would support the interpretation of a raised peat with intermittent cycles of drying and oxidation.

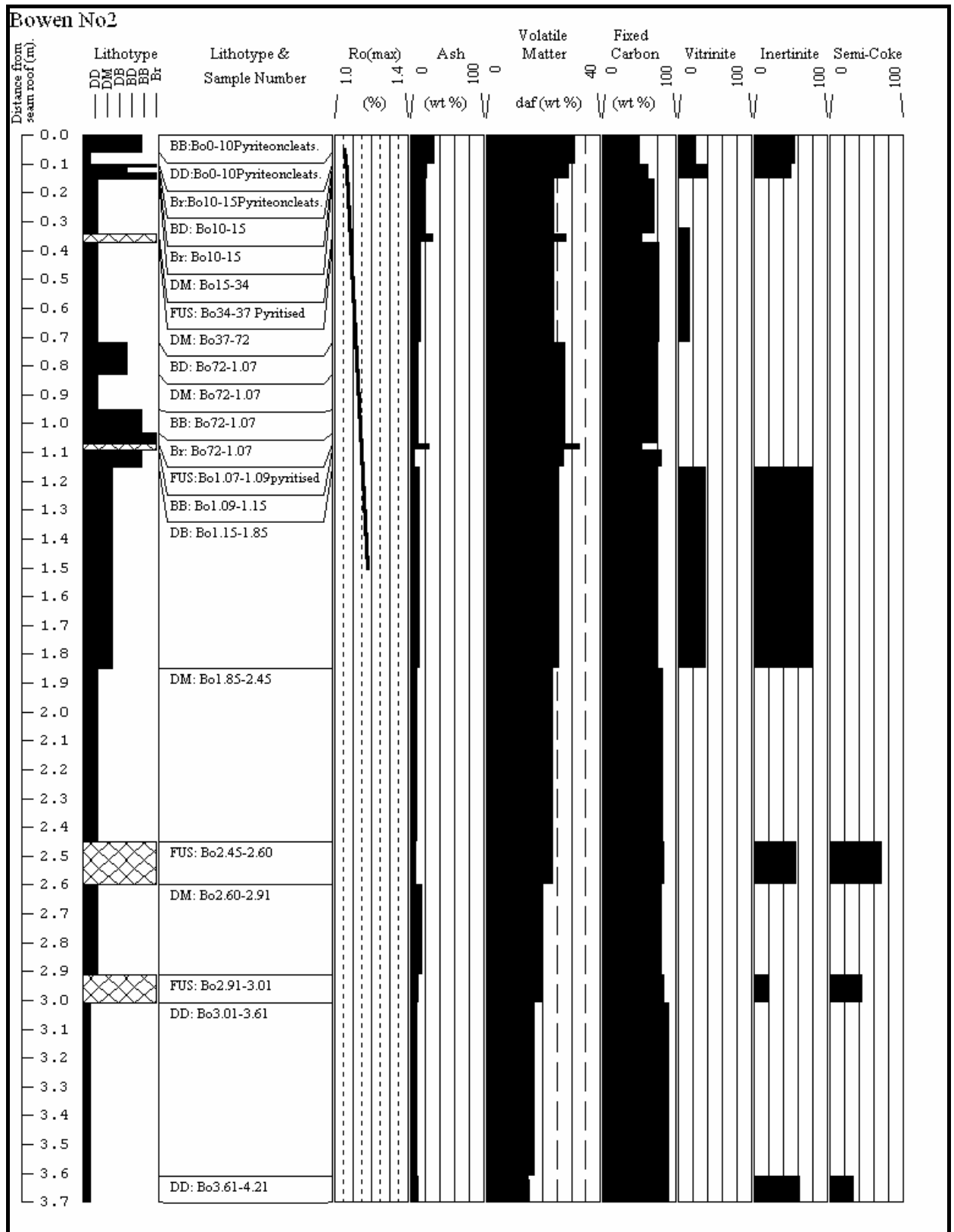


Figure 3.15. Strip log of pit samples from the Bowen No.2 pit.

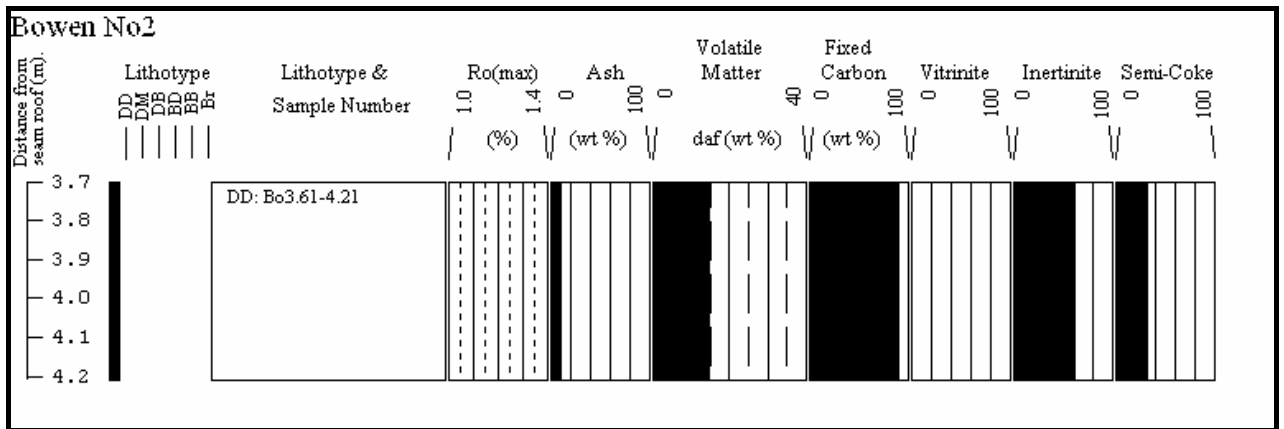


Figure 3.15. Strip log of pit samples from the Bowen No.2 pit. (cont).

- Key**
- DD = Dull Coal
 - DM = Dull with minor bright bands
 - DB = Dull with common Bright Bands
 - BD = Interbedded Dull and Bright coal
 - BB = Bright coal with Dull Bands
 - Br = Bright Coal
 - Fus = Fusain
 - HAC = High Ash Coal
 - HCM = Highly Carbonaceous Mudstone
 - CM = Carbonaceous Mudstone
 - MS = Mudstone

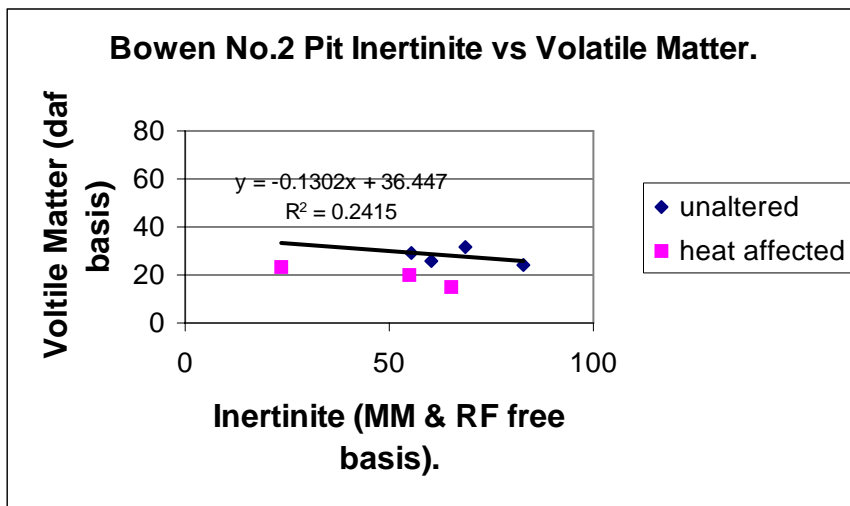


Figure 3.16. Bowen No.2 Pit Inertinite vs Volatile Matter

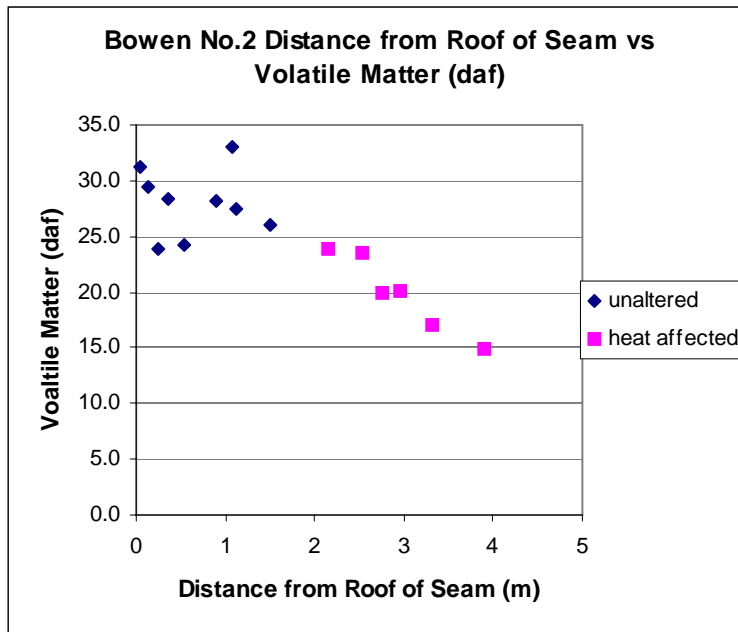


Figure 3.17. Bowen No.2 Distance from Roof of Seam (m) vs Volatile Matter (daf).

3.2.3. Mineral Matter from Normative Analysis.

Normative analysis attempts to calculate mineral matter from major element concentrations using the stoichiometric formulae of minerals suspected or known to be present in the coal (Cohen and Ward, 1991; Newman, 1988; Ward, 2002). Ideally the normative mineral assemblage is calibrated using some direct measurement of the mineral matter assemblage in the coal, eg XRD analysis of low temperature ash (Newman, 1988). Selected major elements may be used as a “proxy” for a particular mineral (eg potassium for illite), and plotted against the trace element of interest to search for graphical relationships and infer mode of occurrence (Dewison and Kanaris-Sotiriou, 1986; Gayer et al., 1999; Mukhopadhyay et al., 1996; Spears and Zheng, 1999; Van Der Flier-Keller and Fyfe, 1986; Ward et al., 1999). A problem arises when using a selected major element as a “stand in” for mineral concentration if that element is partitioned between several mineral species (eg Fe is commonly present in siderite and pyrite; aluminium may be present in illite, kaolinite, goyazite, goyazite and feldspars in the samples analysed in this study). Calculation of a normative mineralogical assemblage has been undertaken for each of the Blake and Bowen seam pits in an attempt to provide a better indication of the mineral matter present in each ply sample (cf using a single major element) for use in determining trace element mode of occurrence using graphical relationships.

The results of proximate and elemental analysis of the Blake seam channel samples are presented in Appendix 4. Sulphur was measured on the 400°C ash prepared for XRF analysis (rather than whole coal) for most Blake West samples (shown as S.O.A.; ie sulphur on ash). Attempts to relate the concentration of sulphur in ash to the concentration of sulphur in whole coal proved fruitless for these Blake West samples, and no sample remained to allow analysis of sulphur on whole coal. All the sulphur in ash figures were discarded and are not considered further in this study.

The results of XRD analysis of LTA-OP from selected Blake Central, Blake West and Bowen No.2 pit samples are presented in Appendix 5.

3.2.3.1. Blake Central and Blake West Normative Analysis.

Analysis of selected samples from the Blake West and Blake Central pits by X-Ray diffraction of low temperature ash (Appendix 5) indicate a mineral assemblage dominated by kaolinite and (to a lesser degree) quartz. In addition, variable amounts of siderite, illite, pyrite, marcasite, feldspar, gorxeite/ Al phosphate and anatase were found in one or more samples.

Feldspar.

A trace of feldspar was indicated by XRD of low temperature ash from two samples from the Blake Central pit. Figure 3.17 shows a relatively poor relationship between sodium and potassium. The relationship is improved slightly when one high potassium value is excluded (Figure 3.19.) (best fit line equation $Y = 6.9672X - 721.41$; correlation coefficient 0.3356). A cross plot of Blake West samples (Figure 3.20.) also shows a weak relationship between sodium and potassium. Exclusion of two outlier points (one high potassium, one low potassium) gave a much stronger graphical relationship (equation $Y = 7.0352X - 207.43$) with a correlation coefficient of 0.6926. No graphical relationship between either potassium and sodium or calcium could be found, therefore, it is concluded that alkali feldspar $[(Na/K)AlSi_3O_8]$ is the dominant feldspar group present in the Blake Seam samples.

It is notable that the statistical correlation equations derived from Figures 3.19. and 3.20. (using the Blake West relationship outlined above that excludes the high and low potassium points) show a similar slope to the trend lines, even though the intersection point with the Y axis is not the same. The XRD analyses suggest potassium is more dominantly present within illite, implying the alkali feldspars trend toward an albite type composition. It is worth noting that previous studies of sandstone composition found plagioclase feldspar dominates in south-eastern and central areas of the Bowen Basin (Baker et al., 1993). Therefore, a statistical relationship that had the same slope as the defined cross plot relationships (use $7.00X$), but which lay below all analysed potassium values, was sought to indicate the proportion of potassium to be assigned to feldspars. The lowest concentration of the potassium values in the Blake Central plot (sodium 390ppm, potassium 800ppm) was used to indicate a suitable Y axis intersect value. The calculated potassium for the low concentration Blake Central sample is 1996ppm. The difference between the

analysed and the actual result is 1196ppm, therefore a Y intersect of 1200 is used in the calculation of potassium (Equation 1)

$$\text{Equation 1} \quad \text{Potassium (ppm)} = \text{Sodium (ppm)} \times 7.00 - 1200$$

Feldspar [(Na/K)AlSi₃O₈] concentration is calculated using sodium as an index element to calculate the concentration of potassium in the mineral using Equation 1. The Equation 1 calculation of potassium applies unless the analysed potassium is below the limit of detection, or if the calculated potassium figure was greater than the analysed potassium figure, or if the calculated potassium values are negative, in which case potassium is assumed to equal zero. The calculation of potassium concentration using the concentration of sodium as the index element, the above caveats withstanding, is used in order to preferentially partition potassium into illite, ie it assumes potassium does not substitute for sodium in the feldspar lattice to a consistent degree. The concentration of aluminium, silicon, and oxygen in feldspars is calculated using Equations 2, 3 and 4.

$$\text{Equation 2} \quad \text{Feldspar aluminium} = (\text{feldspar Na} \times 1.17) + (\text{feldspar K} \times 0.69)$$

$$\text{Equation 3} \quad \text{Feldspar silicon} = (\text{feldspar Na} \times 3.67) + (\text{feldspar K} \times 2.16)$$

$$\text{Equation 4} \quad \text{Feldspar oxygen} = (\text{feldspar Na} \times 5.57) + (\text{feldspar K} \times 3.27)$$

The total concentration of feldspar (ppm) in the sample is calculated by summing the concentration of feldspar sodium, feldspar potassium, feldspar aluminium, feldspar silicon, and feldspar oxygen.

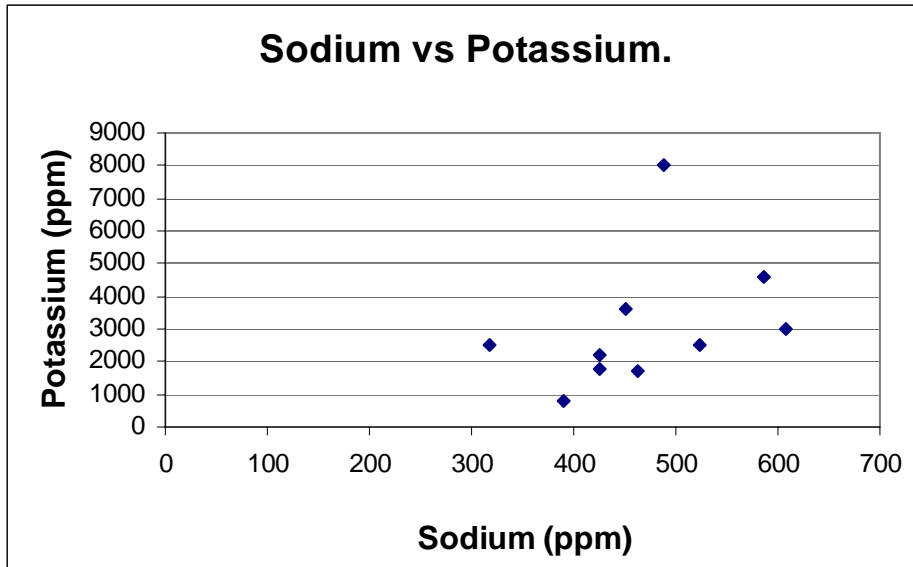


Figure 3.18. Sodium vs potassium, Blake Central samples.

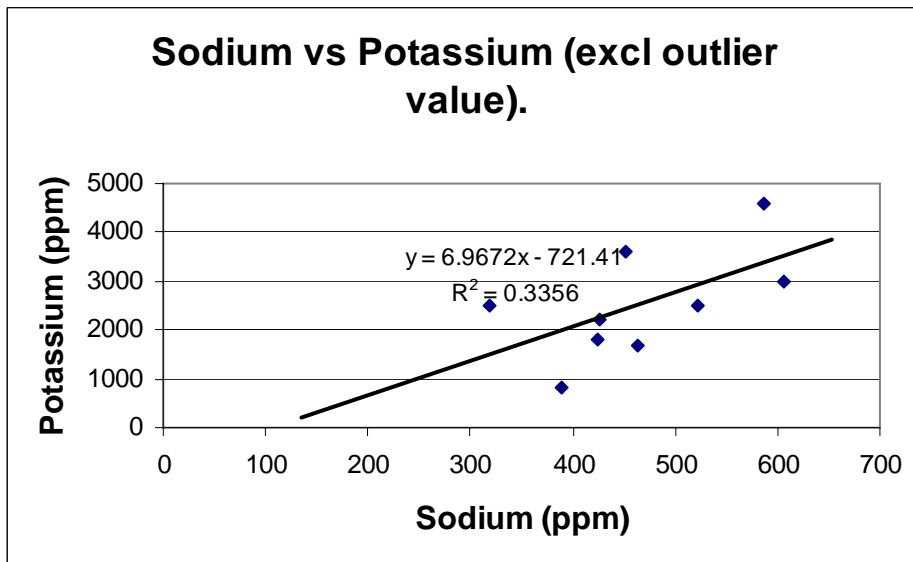


Figure 3.19. Sodium vs potassium, Blake Central samples excluding one high potassium figure.

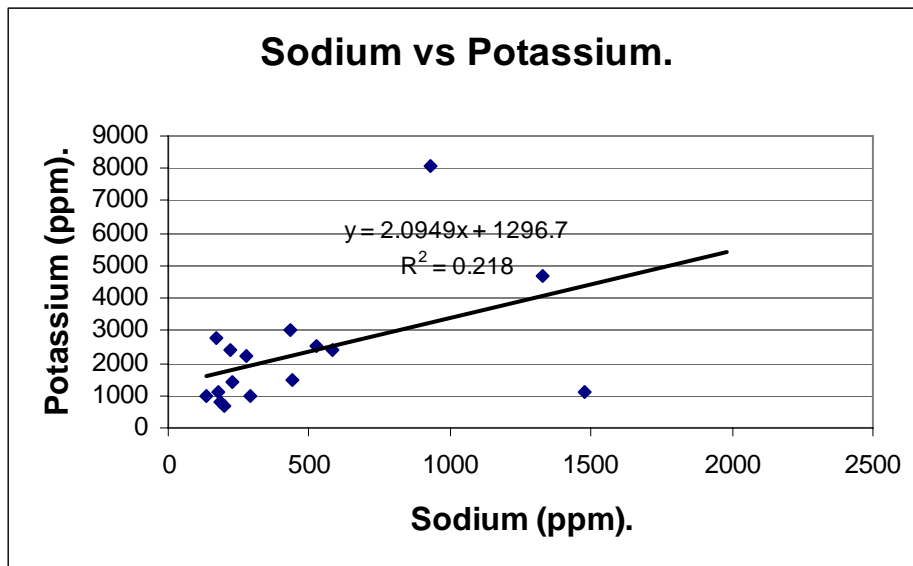


Figure 3.20. Sodium vs potassium, Blake West samples.

NB, Regression used in calculations excludes the high potassium and low potassium points (see text).

Illite.

Trace amounts of illite were found in three Blake West LTA-OP samples analysed by XRD (Appendix 5), with a further sample containing 15% illite (estimated using “TRACES”). Two of the three Blake Central LTA-OP samples analysed by XRD contained 10% illite, the third sample contained 25% illite. Potassium was used as the index element in the calculation of illite, although this strategy is severely limited by the lack of potassium analyses from INAA analysis. The concentration of potassium in illite was calculated by subtracting the feldspar potassium from the total sample potassium concentration. The formula $K_1Al_4(Si_{6.5}Al_{1.5}O_{20}).OH_4$ was used for illite. This formula assumes that illite is degraded by transport and has not been reordered during subsequent burial, and that no well-ordered authigenic illite is present. The assumption of a degraded illite is considered valid given the positive relationship with ash yield (indicating the mineral is substantially detrital in origin), and that previous studies have suggested Bowen Basin sediments were derived from stable cratonic or volcanic arc sources (Baker et al., 1993). Fine grained illite/ muscovite shed into a stable cratonic setting would be particularly susceptible to physiochemical attack in the weathering environment.

The concentration of aluminium, silicon, oxygen and water was calculated using Equations 5, 6, 7 & 8.

Equation 5 Illite aluminium = (illite K x 3.45)

Equation 6 Illite silicon = (illite K x 5.02)

Equation 7 Illite oxygen = (illite K x 8.18)

Equation 7 Illite water of hydration = (illite K x 0.409) + (illite K x 0.102)

The total concentration of illite (ppm) in the sample is calculated by summing the concentrations of illite potassium, illite aluminium, illite silicon, illite oxygen, and water of hydration.

As noted above, calculation of the concentration of illite is severely limited by the lack of potassium figures from INAA analysis. Further, the repeatability of the available potassium analyses appears poor (Section 2.3.1.). Therefore, the normative concentration figures for illite should be treated with caution.

Gorceixite & Goyazite.

Initial attempts at normative mineral calculations moved next to calculating kaolinite using the remaining aluminium, and then quartz using the remaining silicon.

However, this initial calculation attempt resulted in a large number of negative quartz figures, a very unlikely circumstance given XRD analysis results showed quartz is present in most samples. Re-checking of the XRD analysis results found 10% of a “Ba-Al phosphate hydroxide” (CRL Energy Lab report, 16/06/2003) in one of the Blake West samples (BWB4.23-4.28). Further, cross plots for phosphorous and barium found a poor (Blake Central, Figure 3.21.) to moderate (Blake West, Figure 3.22.) graphical relationship between the two elements for Blake Seam samples.

The chemical formulae for gorceixite used in this calculation is

$\text{BaAl}_3(\text{PO}_4)_2(\text{OH})_5 \cdot \text{H}_2\text{O}$ (Ward, 2002). Barium was used as the index element in the

calculation of gorceixite. The weights of aluminium, phosphorous, oxygen, hydrogen, and water were calculated using Equations 8, 9, 10, 11 & 12.

Equation 8 Gorceixite aluminium = (gorceixite Ba x 0.583)

Equation 9 Gorceixite phosphorous = (gorceixite Ba x 0.451)

Equation 10 Gorceixite oxygen = (gorceixite Ba x 1.515)

Equation 11 Gorceixite hydrogen = (gorceixite Ba x 0.036)

Equation 12 Gorceixite water = (gorceixite Ba x 0.0146) + (gorceixite Ba x 0.1165)

The total concentration of gorceixite (ppm) in the sample was calculated by summing the concentrations of gorceixite barium, gorceixite aluminium, gorceixite phosphorous, gorceixite oxygen, gorceixite hydrogen, and water.

The concentration of residual phosphorous (ppm) was calculated by subtracting the phosphorous concentration calculated to be present as gorceixite from the total phosphorous concentration in the sample. The residual phosphorous left after calculation of gorceixite was plotted against strontium concentration. A moderate relationship was found to exist between the residual phosphorous and strontium for both the Blake Central and Blake West pit samples (Figures 3.23. & 3.24.). Such a relationship indicates the presence of goyazite $[\text{SrAl}_3(\text{PO}_4)_2(\text{OH})_5 \cdot \text{H}_2\text{O}]$, and would be one reason why the relationship between barium and phosphorous shown in Figures 3.21. and 3.22. is not stronger.

The concentration of goyazite was calculated using strontium as the index element. The weights of aluminium, phosphorous, oxygen, hydrogen, and water were calculated using Equations 13, 14, 15, 16 & 17.

Equation 13 Goyazite aluminium = (goyazite Sr x 0.924)

Equation 14 Goyazite phosphorous = (goyazite Sr x 0.707)

Equation 15 Goyazite oxygen = (goyazite Sr x 2.374)

Equation 16 Goyazite hydrogen = (goyazite Sr x 0.057)

Equation 17 Goyazite water = (goyazite Sr x 0.0228) + (goyazite Sr x
0.1826)

The total concentration of goyazite (ppm) in the sample was calculated by summing the concentrations of goyazite barium, goyazite aluminium, goyazite phosphorous, goyazite oxygen, goyazite hydrogen, and water.

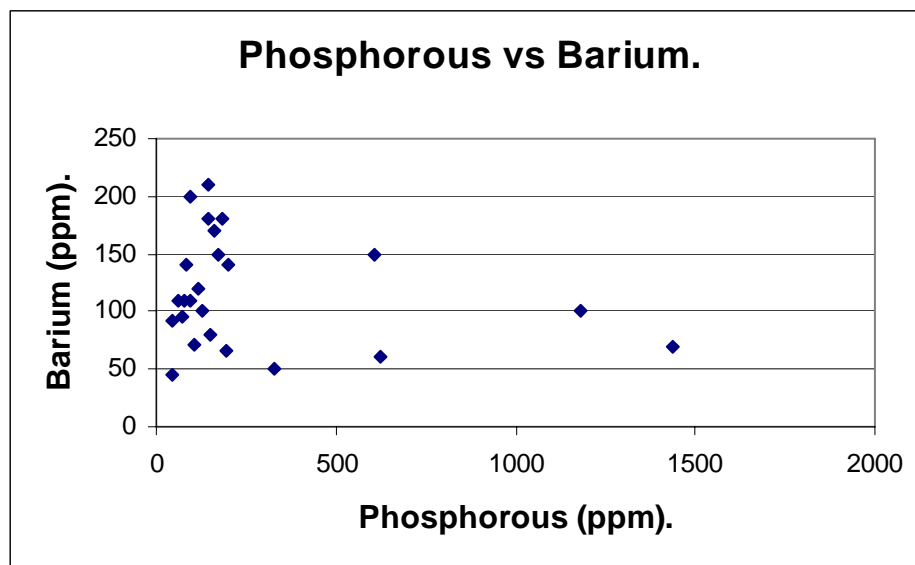


Figure 3.21. Phosphorous vs barium, Blake Central samples.

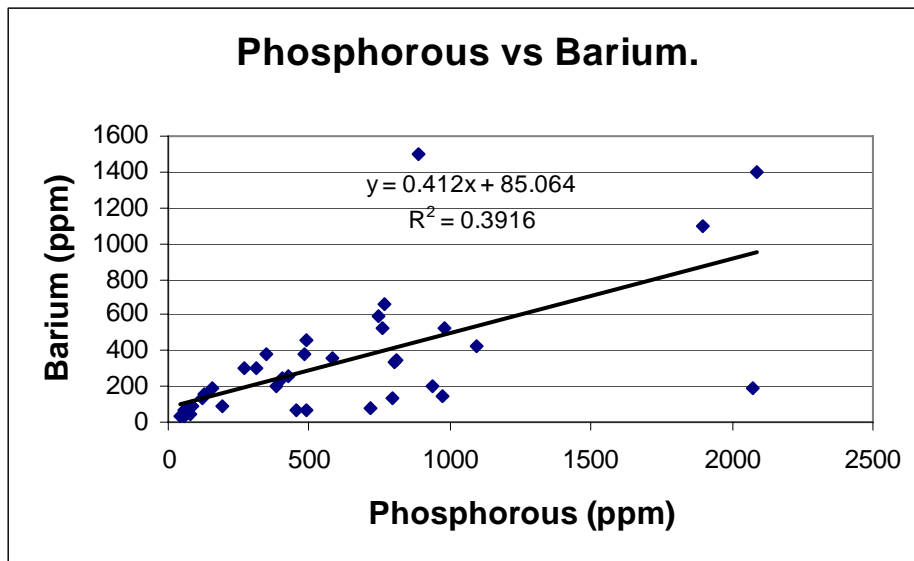


Figure 3.22. Phosphorous vs barium, Blake West samples.

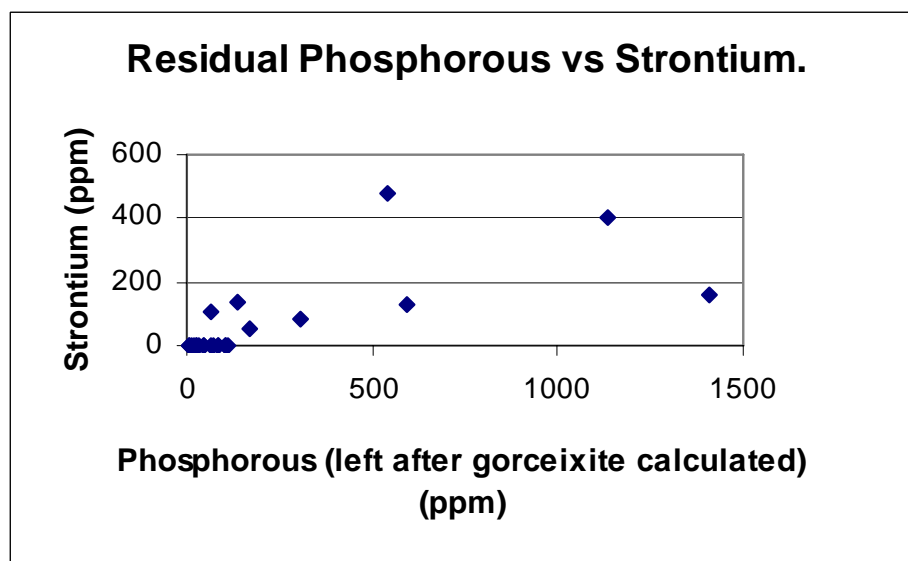


Figure 3.23. Residual phosphorous vs strontium, Blake Central samples.

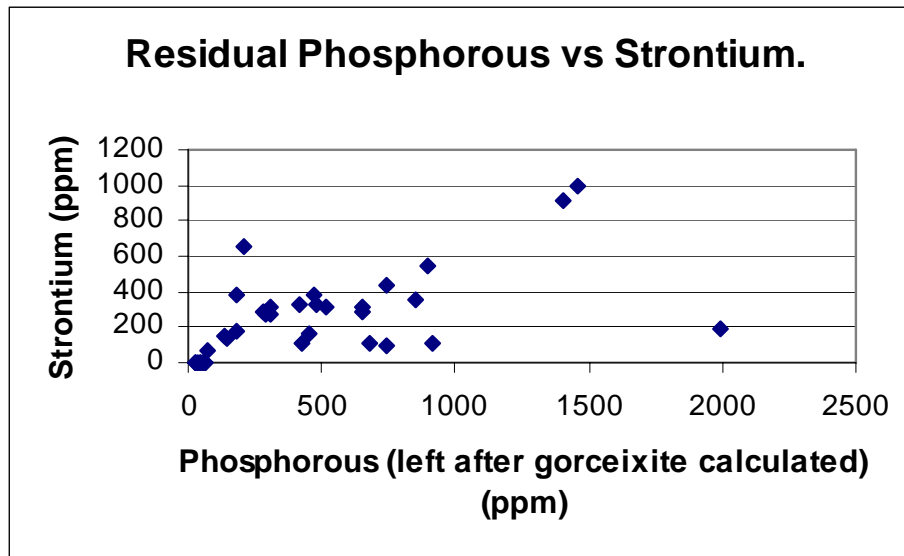


Figure 3.24. Residual phosphorous vs strontium, Blake West samples.

A residual concentration of phosphorous remained following subtraction of gorceixite and goyacite phosphorous for almost all the Blake seam samples (Tables 3.2. and 3.3.). While the absolute value of the residuals is generally not high, as a proportion of the total phosphorous in the sample, the amount is sometimes very high (+80% in a few cases). No other phosphorous minerals other than gorceixite and goyacite were indicated by the XRD analysis. Further, cross-plots of calcium versus residual phosphorous, aluminium versus residual phosphorous, and cerium plus lanthanum plus thorium plus neodymium versus residual phosphorous found no strong graphical relationships to support the presence of apatite, crandallite or monazite. It is apparent that one or (more likely) several unrecognised modes of occurrence for phosphorous exist in the Blake seam coal. However these modes cannot be determined from the present data set. Negative values of phosphorous residuals (indicating overcalculation of gorceixite and goyacite using Ba and Sr and index elements) are rare and are not considered significant.

Table 3.2 Residual Phosphorous in Blake Central Samples following Normative Calculations.

Sample Number	Residual (ppm)	Residual (% of Total P in Sample)
BC 0.00-0.50	6	7
BC 0.50-1.00	12	20
BC 1.00-1.50	4	8
BC 1.50-2.00	26	56
BC 2.00-2.50	246	74
BC 2.50-3.00	502	81
BC 3.00-3.50	129	66
BC 3.50-4.00	1295	90
BC 4.00-4.13	851	72
BC 4.13-4.18	-14	
BC 4.18-4.22	85	65
BC 4.22-4.55	102	56
BC 4.55-5.00	199	33
BC 5.00-5.11	41	20
BC 5.11-5.39	103	60
BC 5.39-5.49	83	52
BC 5.49-6.11	73	70
BC 6.11-6.13	27	35
BC 6.13-6.23	44	47
BC 6.23-6.35	30	41
BC 6.35-6.37	114	76
BC 6.37-6.55	21	25
BC 6.55-6.63	65	45
BC 6.63-6.88	48	34

Table 3.3. Residual Phosphorous in Blake West Samples following Normative Calculations.

Sample Number	Residual (ppm)	Residual (% of Total P in Sample)
BW 0.00-0.11	34	52
BW 0.11-0.20	42	51
BW 0.20-0.48	43	76
BW 0.48-0.93	24	58
BW 1.20-1.60	26	45
BW 1.60-2.05	56	72
BW 2.05-2.65	344	70
BW 2.65-3.15	56	29
BW 3.15-3.75	-88	0
BWB 0.00-0.65	751	36
BWB 0.65-1.25	438	45
BWB 1.25-1.90	295	39
BWB 1.90-1.98	30	11
BWB 1.98-2.05	446	55
BWB 2.05-2.72	249	33
BWB 2.72-2.78	24	16
BWB 2.78-3.04	118	25
BWB 3.04-3.15	201	26
BWB 3.15-3.25	59	45
BWB 3.25-3.56	-247	0
BWB 3.56-3.71	50	14
BWB 3.71-3.93	80	16
BWB 3.93-4.23	186	32
BWB 4.23-4.28	759	40
BWB 4.28-4.40	99	25
BWB 4.40-4.43	63	52
BWB 4.43-4.67	83	19
BWB 4.67-5.13	511	47
BWB 5.13-5.51	431	53
BWB 5.51-6.25	95	25
BWB 6.25-6.75	601	64
BWB 6.75-7.25	1857	89
BWB 7.25-7.75	835	86
BWB 7.75-8.25	670	84
BWB 8.25-8.75	602	84
BWB 8.75-9.25	347	76

Kaolinite.

The XRD analysis of all Blake seam samples from both the Blake Central and Blake West pits show a high concentration of kaolinite (Appendix 5). All remaining aluminium left after calculation of feldspars, illite, gorceixite, and goyazite was assigned to kaolinite $[Al_4(Si_4O_{10})OH_8]$. Aluminium was used as the index element in the calculation of kaolinite. The weight of silicon, oxygen, and water was calculated using equations 18, 19 and 20.

Equation 18 $\text{Kaolinite silicon} = (\text{kaolinite Al} \times 1.04)$

Equation 19 $\text{Kaolinite oxygen} = (\text{kaolinite Al} \times 1.48)$

Equation 20 $\text{Kaolinite water of hydration} = (\text{kaolinite Al} \times 0.148) +$
 $(\text{kaolinite Al} \times 0.074)$

The total concentration of kaolinite (ppm) in the sample was calculated by summing the concentrations of kaolinite aluminium, kaolinite silicon, kaolinite oxygen, and water of hydration. It is acknowledged that kaolinite will thermally decompose at $\sim 300^{\circ}\text{C}$. However it is assumed that the silicon and aluminium will not mobilise, and the only significant concentration error will be due to the loss of water from the structure of the mineral.

Quartz.

All residual silicon left after calculation of feldspar, illite, and kaolinite was assigned to quartz. Silicon was used as the index element, and oxygen was calculated using Equation 21.

Equation 21 $\text{Quartz oxygen} = (\text{quartz Si} \times 1.14)$

The total concentration of quartz (ppm) in the sample was calculated by summing the concentrations of quartz silicon and quartz oxygen.

At this point in the calculations a further problem became apparent. The residual silicon was calculated by subtracting the concentration of silicon used in feldspar, illite, and kaolinite from the total sample silicon concentration. It was found that some residual silicon values were negative. In the case of the Blake West samples, the negative value ranged to a maximum of minus 7069ppm (minus 0.7 weight percent), and averaged approximately minus 3000ppm. Only one negative value (minus 387.4ppm) was found for the Blake Central samples. The negative values were restricted to samples that contained potassium at concentrations below the detection limit of INAA (500ppm). It is concluded that the lack of a potassium value resulted in under estimation of the concentration of feldspar and (in particular) illite in

the sample. The under estimation of illite in turn resulted in excess aluminium being available for the calculation of kaolinite, which in turn consumed excess silicon (aluminium being the index element in the calculation of kaolinite). It is concluded that feldspar and (in particular) illite are under estimated, kaolinite over estimated and quartz underestimated in samples in which potassium is present in concentrations below the detection limit of INAA (see Appendix 4). It is further concluded that potassium would have been better analysed using the standard XRF analysis of ash.

Siderite.

The XRD analysis of the Blake Central LTA-OP samples (Appendix 5) suggested trace quantities of siderite may be present, while sample BWB4.23-4.28 from the Blake West pit contained an estimated 55% siderite in LTA-OP. The presence of carbonates was also noted in the polished petrographic samples, often infilling telinite cell lumens (Appendix 3). Cross plots of manganese versus iron found a very strong graphical relationship between these elements in both the Blake Central (Figure 3.25.) and Blake West (Figure 3.26.) samples. Exclusion of one (potentially misleading) sample from Blake West pit that contained very high concentrations of both iron and manganese still gave a strong linear relationship with an equation of $Y = 0.0135X - 16.656$, and for which the correlation coefficient remained very high (0.7973). The statistical relationship between iron and manganese for Blake West samples excluding the very high concentration sample has the same slope (0.0135X) as the slope of the linear relationship for the Blake Central samples.

In order to take account of the fact that some iron may be present within the Blake seam samples as pyrite, manganese was used as the index element in the calculation of siderite. As noted above, the graphical relationship between iron and manganese is very similar for the Blake Central and Blake West pits if the very high siderite concentration sample in the Blake West pit is excluded. The slope of the statistical relationship was taken as 0.0135, and the Y axis intersect point as 17.75 [ie the average of 16.66 (Blake West) and 18.84 (Blake Central)]. The statistical relationship defined for the Blake West samples was re-arranged to calculate iron (Equation 22), unless the total iron concentration was less than the calculated iron concentration, in which case the total iron concentration was used. A siderite Fe concentration of 1314.82ppm was calculated where manganese was below the limit of detection of

INAA (ie assumed to be zero). Note, the use of manganese as the index element for siderite imposes an artificial lower limit on the calculated concentration of siderite.

The concentration of carbon and oxygen required for siderite were calculated using iron and manganese as index elements as outlined in Equations 22 & 23.

Equation 22 Siderite carbon = (siderite Fe x 0.215) + (siderite Mn x 0.219)

Equation 23 Siderite oxygen = (siderite Fe x 0.859) + (siderite Mn x 0.874)

The total concentration of siderite (ppm) in the sample was calculated by summing the concentrations of siderite iron, siderite manganese, siderite carbon and siderite oxygen.

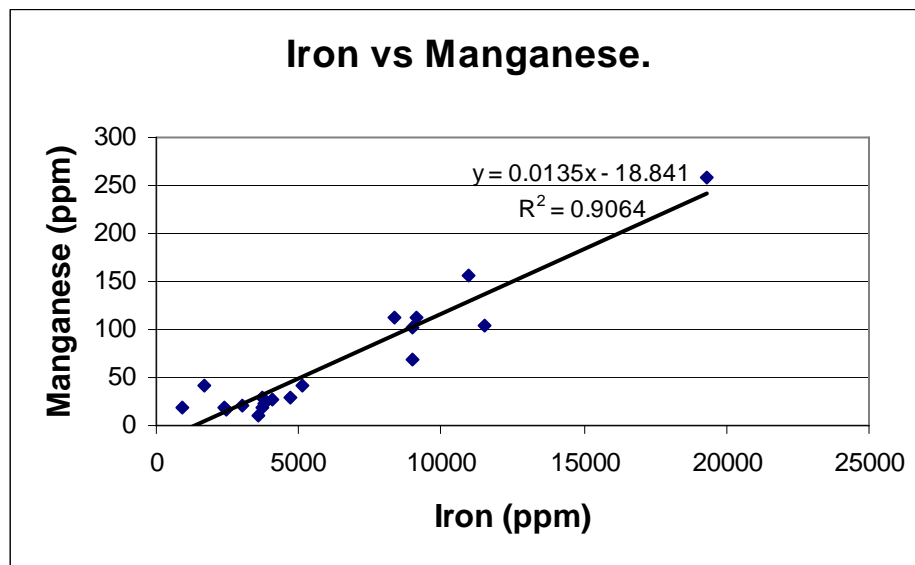


Figure 3.25. Iron versus manganese, Blake Central samples.

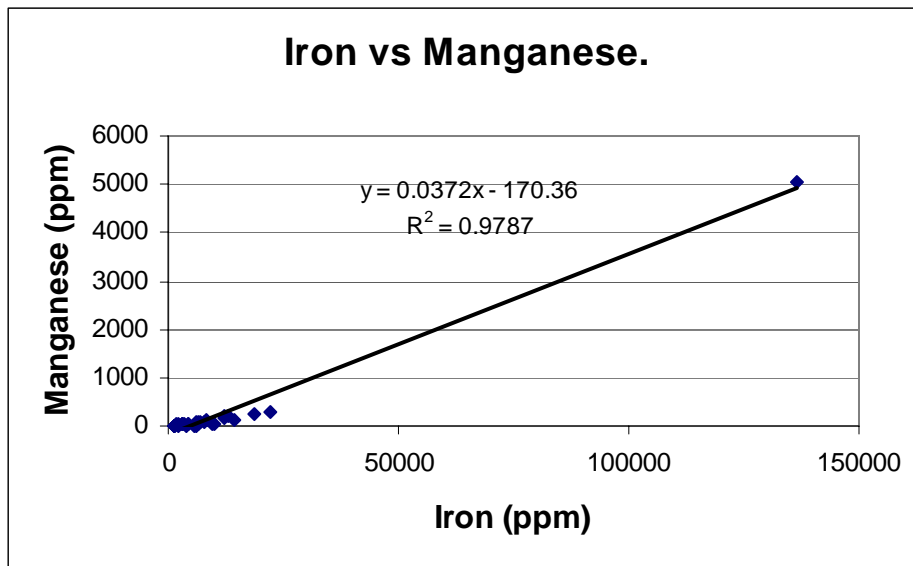


Figure 3.26. Iron versus manganese, Blake West samples.

NB, Regression used in calculations excludes high iron and manganese outlier (see text).

Pyrite.

The XRD analysis (Appendix 5) of the Blake Central and Blake West seam samples indicated a trace of pyrite (FeS_2) could be present in some samples (CRL Energy Lab report, 16/06/2003). In addition, minor pyrite occurring as fracture infills was noted in a number of the petrographic samples (Appendix 3), and the presence of pyrite on cleat was also noted in some hand specimens (Figures 3.8. and 3.12.). Cross plots of the residual iron remaining after calculation of siderite against total sulphur found a moderate relationship existed for some samples in the Blake Central pit (with some scatter) (Figure 3.27.). The Blake West cross plot of residual iron against total sulphur is strong but is based on less data because it excludes the sulphur values measured on the 400°C ash (Figure 3.28.).

The residual iron concentration remaining after siderite calculation was used as the index element in the calculation of pyrite. The required weight of sulphur required was determined using Equation 24.

$$\text{Equation 24} \quad \text{Pyrite sulphur} = (\text{pyrite Fe} \times 1.148)$$

The total concentration of pyrite (ppm) in the sample was calculated by summing the concentrations of pyrite iron and pyrite sulphur.

Cross plots of residual sulphur against ash (Figures 3.29. and Figure 3.30.) suggest any remaining sulphur left after calculation of pyrite is organically bound (as would be expected), with scatter possibly due to the presence of other minor undetected sulphide minerals.

It is acknowledged that forms of sulphur data on each ply would have made calculation of pyrite figures redundant, and may have provided a cleared picture of mineral matter concentrations and mode of occurrence inferences. Unfortunately form of sulphur analysis was beyond the budget available for this study.

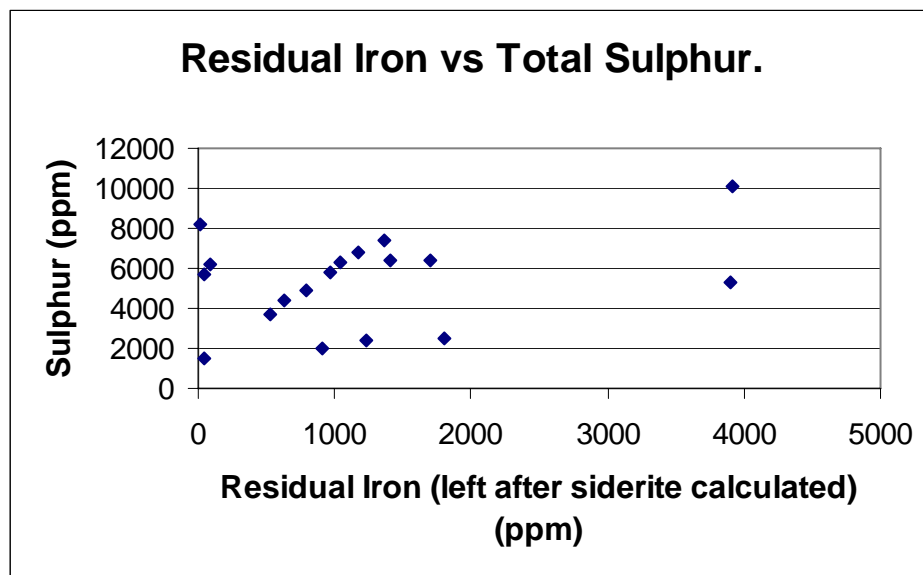


Figure 3.27. Residual iron left after siderite calculation vs sulphur, Blake Central samples.

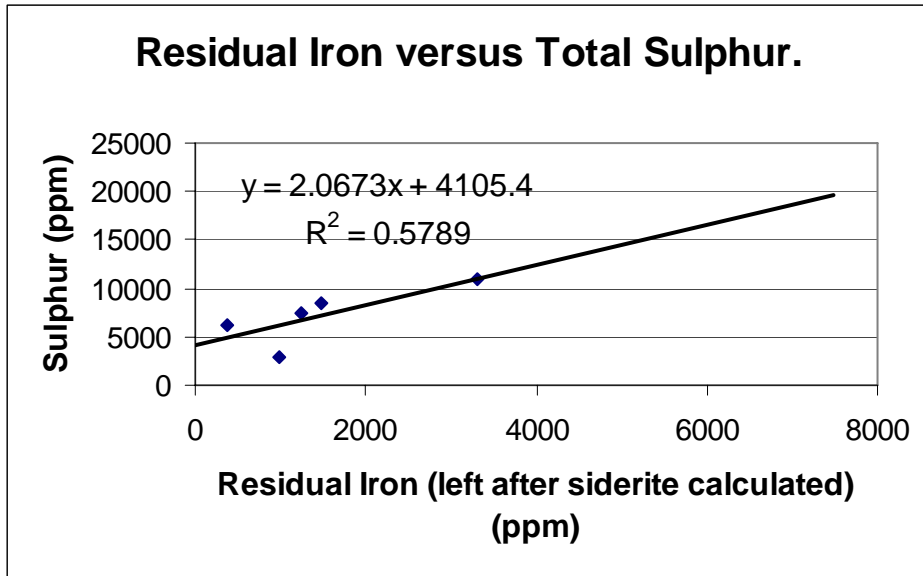


Figure 3.28. Residual iron left after siderite calculation vs sulphur, Blake West samples.

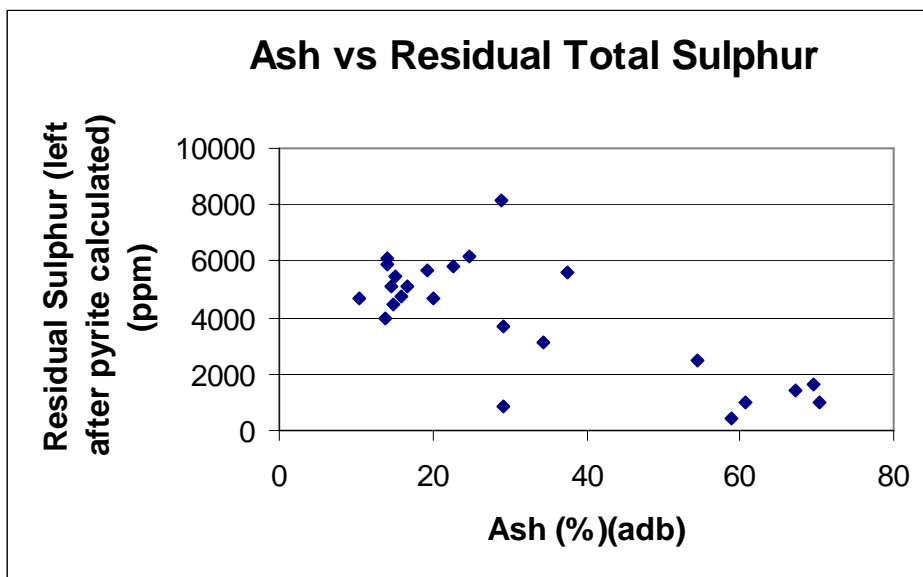


Figure 3.29. Ash vs residual sulphur left after pyrite calculation, Blake Central samples.

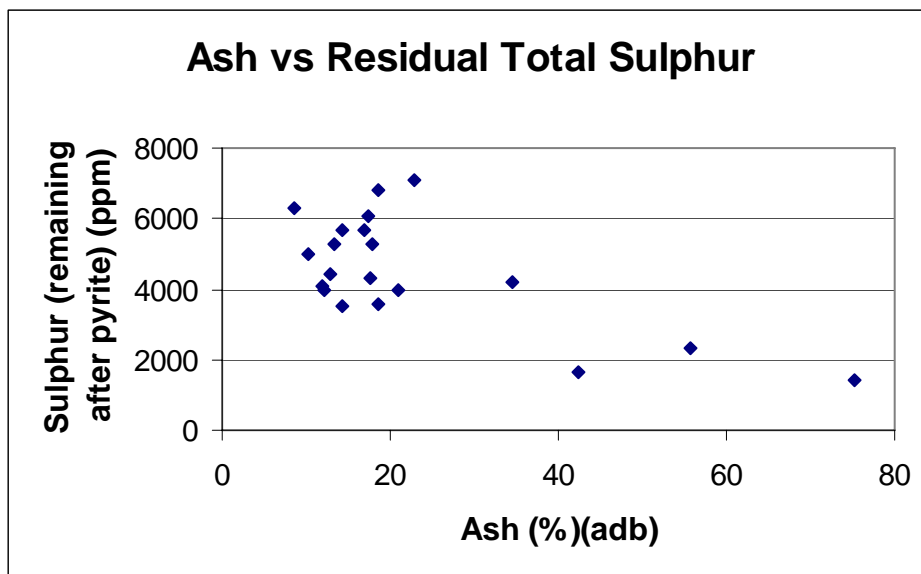


Figure 3.30. Ash vs residual sulphur left after pyrite calculation, Blake West samples.

Anatase.

The XRD analysis of one of the Blake Central samples analysed by XRD (BC 4.00-4.13) indicated the presence of anatase (TiO_2). Sample BC6.63-6.88 was notable for the presence of green-reflecting acicular crystals that could be rutile (which has the same formula as anatase). In the apparent absence of any other titanium minerals, all titanium is assigned to anatase. The requisite weight of oxygen to form this mineral is calculated using Equation 25.

$$\text{Equation 25} \quad \text{Anatase oxygen} = (\text{anatase Ti} \times 0.668)$$

The total concentration of anatase (ppm) in the sample was calculated by summing the concentrations of anatase titanium and anatase oxygen.

Unassigned Major Elements.

In spite of the numerous analyses of magnesium, no graphical correlation could be found between this major element and any other major element. Further, XRD analysis failed to detect any magnesium-bearing mineral, with the possible exception of feldspar. However, the lack of correlation between magnesium and either sodium or potassium suggested the element is not bound into feldspar. Cross plots of ash versus magnesium for the Blake Central (Figure 3.31.) and Blake West (Figure 3.32.) channel sample analyses suggest magnesium is associated with ash rather than with

the organic fraction of the coal. Further inferences on the mode of occurrence of magnesium are drawn in Section 3.3.1.2.

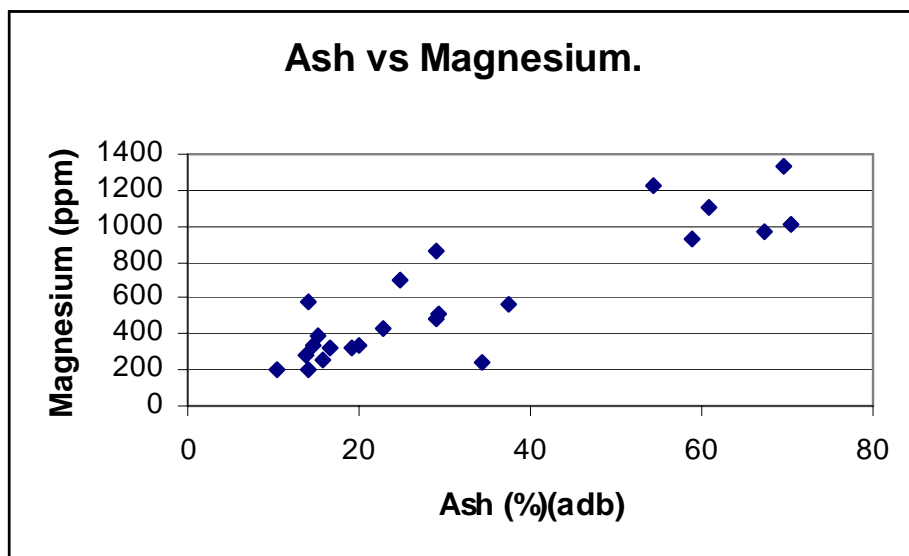


Figure 3.31. Ash vs magnesium, Blake Central samples.

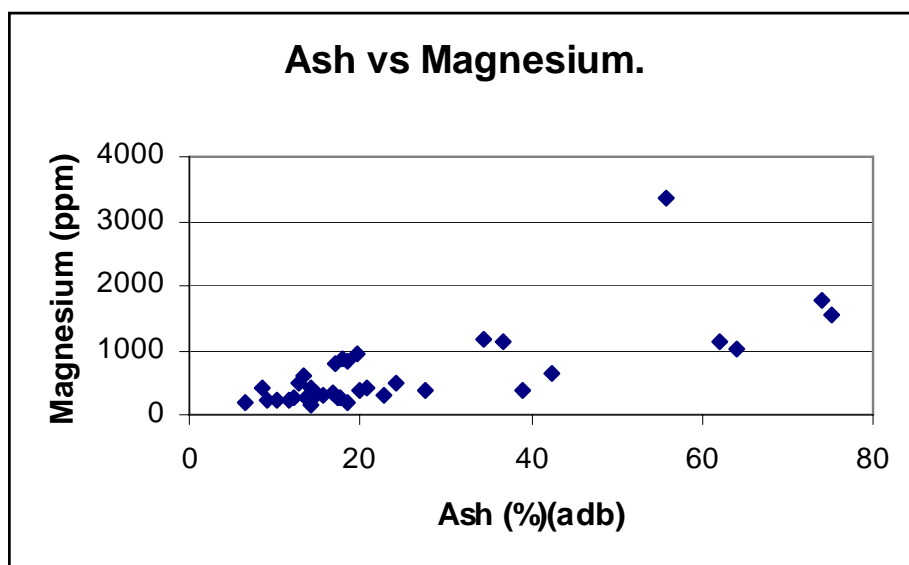


Figure 3.32. Ash vs magnesium, Blake West samples.

A mode of occurrence for calcium could not be determined. Few samples contained calcium at a concentration above the limit of detection of INAA (300ppm). Among the Blake Central samples, only BC5.11-5.39 contained calcium above the INAA detection limit (2700ppm). Among the Blake West samples, four samples contained calcium at a concentration above the INAA detection limit: BWB 3.93-4.23 (3800ppm); BWB 4.23-4.28 (3200ppm); BWB 6.75-7.25 (2500); and BWB7.25-7.75 (2200ppm). It is perhaps notable that the BWB samples containing calcium in

appreciable concentrations are in discrete groups of two samples. Possibly the distribution of calcium within the seam indicates calcium is present as distinct nodules of calcite and, therefore, shows no correlation with any other major element.

3.2.3.2. Bowen No.2 Normative Analysis.

The results of proximate and elemental analysis of the Bowen No.2 pits seam channel samples are presented in Appendix 4. The results of XRD analysis of low temperature ash from selected Bowen No.2 pits samples are presented in Appendix 5. No feldspar was detected in the XRD analysis of the Bowen No.2 samples, and no correlation is apparent between sodium, potassium and magnesium. It is, therefore, assumed that feldspar is absent from the Bowen No.2 samples or is present in very minute quantities.

Illite.

A trace of illite was found in one of the Bowen No.2 samples analysed by XRD. It has been assumed that all potassium is bound into illite. Potassium was used as the index element in the calculation of illite, and the same mineral formula used as in Section 3.2.3.1.. One sample (BO0.34-0.37) contained potassium in very high concentrations (26000ppm). Such a high value appears at odds with the other Bowen No.2 samples. Further, this sample was analysed by XRD and no illite was detected. It is assumed that a transposition error occurred at the time the original results were reported, and the figure is adjusted to 2600ppm (a figure in better agreement with other figures). The figure was not excluded entirely in order to minimise over-estimation of kaolinite, as has occurred for the Blake Seams.

The concentration of aluminium, silicon, oxygen, and water was calculated using Equations 5, 6, 7 & 8. The total concentration of illite (ppm) in the sample is calculated by summing the concentrations of illite potassium, illite aluminium, illite silicon, illite oxygen, and water of hydration.

As noted above for the Blake seam calculations, calculation of the concentration of illite in the Bowen seam is severely limited by the lack of potassium figures from INAA analysis. Further, the repeatability of the available potassium analyses appears

poor (Section 2.3.1.). Therefore, the normative concentration figures for illite should be treated with caution.

Gorceixite & Goyazite.

No Bowen seam XRD analysis results indicated the presence of gorceixite or goyazite, and the graphical relationship between Ba and Sr is poor (possibly due to the generally low concentration of strontium in the coal, many samples containing strontium at concentrations below the limit of detection for INAA). Both barium and strontium are present in the Bowen seam at lower concentrations than the Blake Central samples, and substantially lower concentrations than the Blake West samples. However, it is assumed that these minerals are the mode of occurrence for Ba and Sr as for the Blake seam samples.

The concentration of gorceixite is calculated for Bowen seam samples using barium as the index element, and goyazite is calculated using strontium as the index element, as for the Blake seams (Section 3.2.3.1.). The weights of aluminium, phosphorous, oxygen, hydrogen, and water in gorceixite were calculated using Equations 8, 9, 10, 11 & 12. The weights of aluminium, phosphorous, oxygen, hydrogen and water in goyazite were calculated using Equations 13, 14, 15, 16 & 17. The total weight of gorceixite (ppm) in the sample was calculated by summing the concentrations of gorceixite barium, gorceixite aluminium, gorceixite phosphorous, gorceixite oxygen, gorceixite hydrogen, and water. The total concentration of goyazite (ppm) in the sample was calculated by summing the concentrations of goyazite barium, goyazite aluminium, goyazite phosphorous, goyazite oxygen, goyazite hydrogen, and water.

As for the Blake seam samples, a residual concentration of phosphorous remained following subtraction of gorceixite and goyazite phosphorous for almost all the Bowen seam samples (Tables 3.4.). Again, the absolute value of the residuals is generally small, but as a proportion of the total phosphorous in the sample is, the amount is sometimes very high (+80% in a several instances). The presence of gorceixite and goyazite in the Bowen seam coal is speculative, and cross-plots of calcium versus residual phosphorous, aluminium versus residual phosphorous, and cerium plus lanthanum plus thorium plus neodymium versus residual phosphorous found no strong graphical relationships to support the presence of apatite, crandallite

or monazite. As for the Blake seam coal, it is apparent that one or (more likely) several unrecognised modes of occurrence for phosphorous exist in the Bowen seam coal, but these modes cannot be determined from the present data set. Negative values of phosphorous residuals (indicating overcalculation of gorceixite and goyazite using Ba and Sr and index elements) are rare and are not considered significant.

Table 3.4. Residual Phosphorous in Blake West Samples following Normative Calculations.

Sample Number	Residual (ppm)	Residual (% of Total P in Sample)
BO 0.00-0.10	-354	
BO 0.10-0.15	39	44
BO 0.15-0.34	-24	
BO 0.34-0.37	-6	
BO 0.37-0.72	20	44
BO 0.72-1.07	-1	
BO 1.07-1.09	-23	
BO 1.09-1.15	-5	
BO 1.15-1.85	21	44
BO 1.85-2.45	513	86
BO 2.45-2.60	2302	88
BO 2.60-2.90	-28	
BO 2.90-3.01	341	86
BO 3.01-3.61	352	62
BO 3.61-4.21	287	64

Kaolinite.

The XRD analysis of all the Bowen No.2 samples indicated a significant concentration of kaolinite was present in most samples. All remaining aluminium left after calculation of illite, gorceixite, and goyazite was assigned to kaolinite $[Al_4(Si_4O_{10})OH_8]$. Aluminium was used as the index element in the calculation of kaolinite. The weight of silicon, oxygen, and water was calculated using equations 18, 19 and 20. The total concentration of kaolinite (ppm) in the sample was calculated by summing the concentrations of kaolinite aluminium, kaolinite silicon, kaolinite oxygen, and water of hydration.

Quartz.

All residual silicon left after calculation of feldspar, illite and kaolinite was assigned to quartz. Silicon was used as the index element, and oxygen was calculated using

Equation 21. The total concentration of quartz (ppm) in the sample was calculated by summing the concentrations of quartz silicon and quartz oxygen.

Five of the Bowen No.2 samples were found to contain potassium at a concentration below the INAA detection limit (500ppm). However, no negative silicon values were apparent, possibly because the actual feldspar and illite concentration is lower in the Bowen seam so the error in over calculation of kaolinite is less apparent.

Nonetheless, it is still considered that the kaolinite concentration for these five samples is probably over-estimated and the concentration of quartz underestimated.

Pyrite.

The XRD analysis of the Bowen No.2 seam samples indicated pyrite (FeS_2) was present or likely to be present in two samples (Appendix 5). Pyrite framboids were also noted in petrographic sample BO0-10 (Appendix 3), and in hand specimens (often associated with fusain bands) (Figure 3.15.). A cross plot of iron against total sulphur in the Bowen No.2 seam samples shows a very strong relationship (Figure 3.33.), suggesting most of the iron is present as pyrite. However, the trend line intersects the X (sulphur) axis at 8928.8ppm, suggesting ~8930ppm sulphur is present as a different mode of occurrence. A cross plot of ash versus total sulphur (Figure 3.34.) suggests total sulphur decreases rapidly as ash decreases, with the trend levelling out at a concentration of ~10,000ppm sulphur in low ash samples. Accordingly, it is assumed that organic sulphur makes up between 8930 and 10,000ppm in the Bowen No.2 samples, an average figure of 9464 being subtracted prior to calculation of the concentration of pyrite (although it is acknowledged that this average figure will overestimate organic sulphur in high ash samples). The need to attempt to remove the organic sulphur from the pyrite calculation will be further explained with regard to the siderite calculations below.

Sulphur was used as the index element in the calculation of pyrite. The required weight of sulphur required was determined using Equation 26.

Equation 26 Pyrite iron = (pyrite S x 0.8708)

The total concentration of pyrite (ppm) in the sample was calculated by summing the concentrations of pyrite iron and pyrite sulphur.

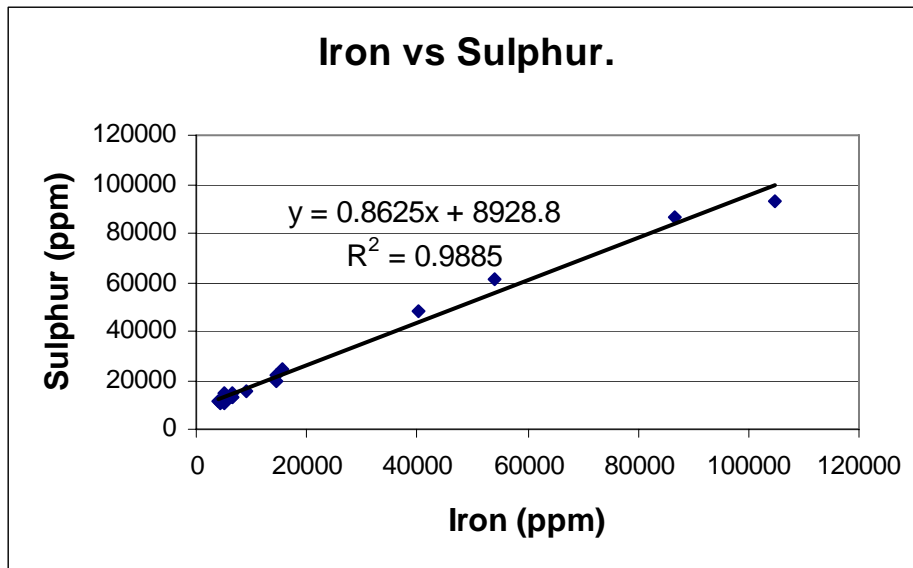


Figure 3.33. Iron vs total sulphur, Bowen No.2 seam samples.

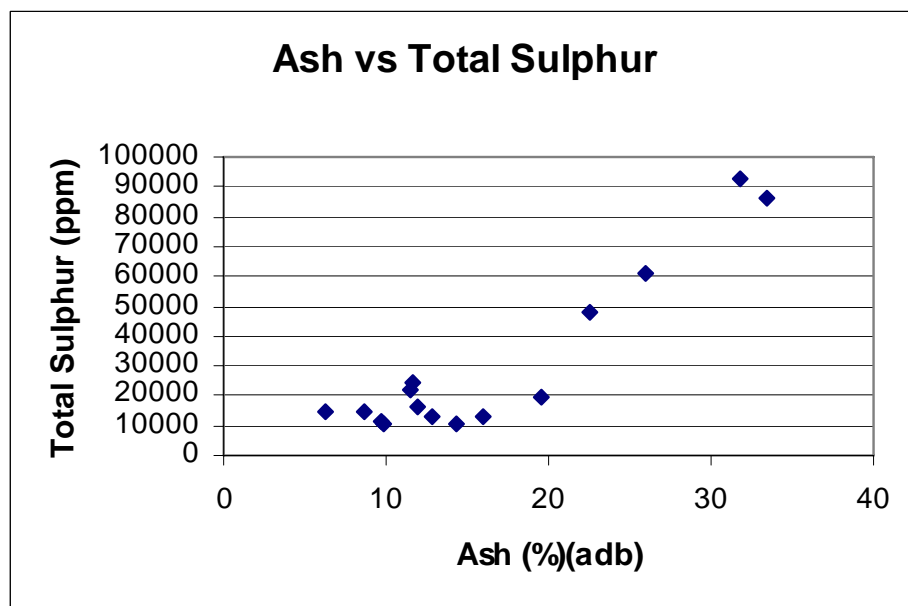


Figure 3.34. Ash vs total sulphur, Bowen No.2 seam samples.

Siderite.

Siderite was not detected in the XRD analysis of the Bowen No.2 LTA-OP samples. However, cross plots of manganese versus iron and magnesium versus iron indicated some, albeit poor, graphical relationships, suggesting siderite could be present in trace

quantities. Using total sulphur, minus the estimated organic sulphur figure of 9464, as the index element to calculate pyrite resulted in some residual iron remaining after calculation of pyritic iron (cf using Fe as the index element for pyrite, in which case the sulphur requirement would have exceeded the total sulphur figure in a number of instances). Cross plots of residual iron versus manganese and residual iron versus magnesium are presented in Figures 3.35. and 3.36. respectively. These two figures show a good relationship between the residual iron left after pyrite calculation and manganese and magnesium, indicating some substitution of the latter two elements in the siderite crystal lattice. The formulae for the linear relationships shown in Figures 3.35. and 3.36. were rearranged to solve for iron, so that manganese and magnesium acted as the index elements to calculate the total iron present as siderite. The rearranged formula to calculate iron from manganese and magnesium are shown in Equations 27 & 28 respectively, unless the concentration of manganese or magnesium is below the limit of detection for XRF, in which case the residual iron figure is used. The two iron concentrations calculated using Equations 27 and 28 are then averaged to give a final siderite iron figure. If the final siderite iron concentration is greater than the residual iron figure then the residual iron figure is used; ie all the residual iron is assumed to be present as siderite.

The concentration of carbon and oxygen required for siderite were calculated using iron, manganese, and magnesium as index elements as outlined in Equations 29 & 30.

$$\text{Equation 27} \quad \text{Siderite iron from manganese} = (\text{Mn} - 10.55) / 0.0042$$

$$\text{Equation 28} \quad \text{Siderite iron from magnesium} = (\text{Mg} - 168.79) / 0.0228$$

$$\text{Equation 29} \quad \text{Siderite carbon} = (\text{siderite Fe} \times 0.215) + (\text{siderite Mn} \times 0.219) + \text{siderite Mg} \times 0.494$$

$$\text{Equation 30} \quad \text{Siderite oxygen} = (\text{siderite Fe} \times 0.859) + (\text{siderite Mn} \times 0.874) + (\text{siderite Mg} \times 1.974)$$

The total concentration of siderite (ppm) in the sample was calculated by summing the concentrations of siderite iron, siderite manganese, siderite magnesium, siderite carbon, and siderite oxygen.

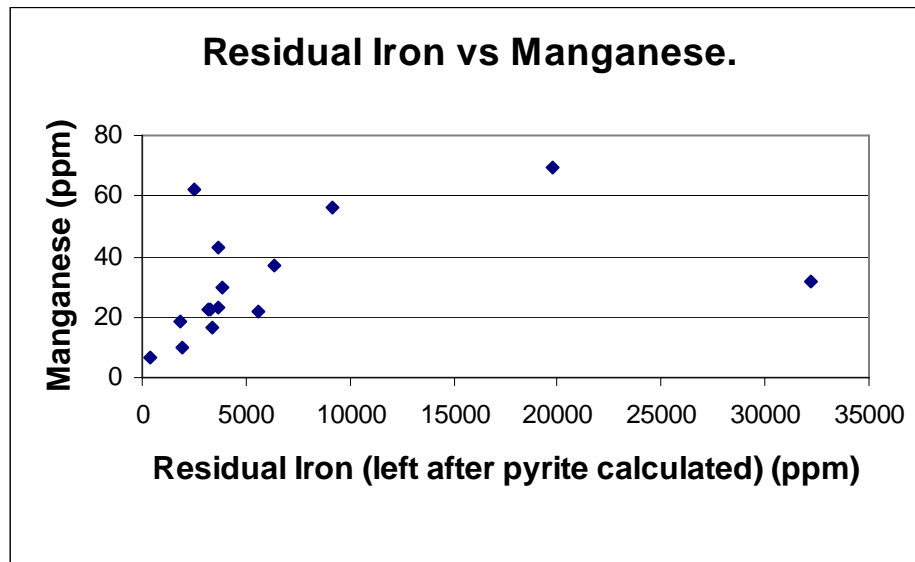
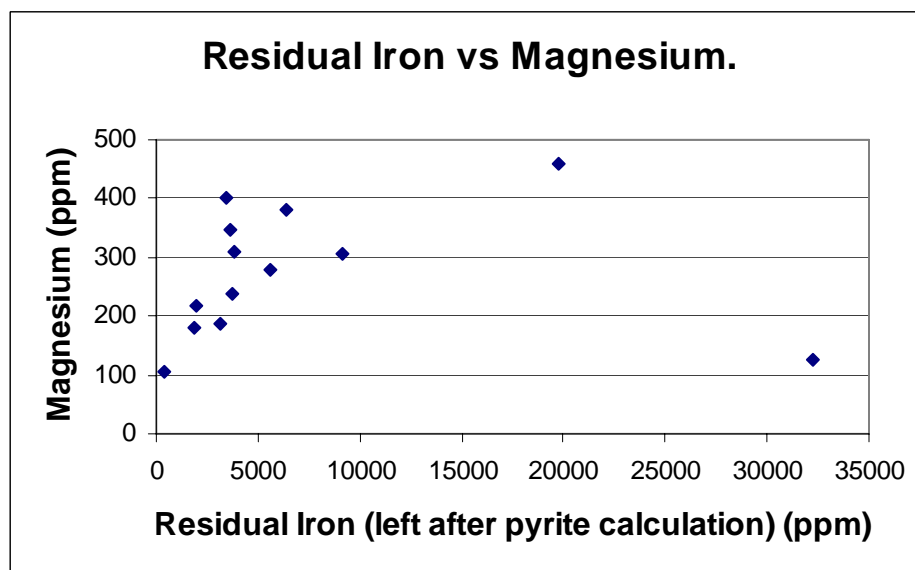


Figure 3.35. Residual iron vs manganese, Bowen No.2 seam samples.



3.36. Residual iron vs magnesium, Bowen No.2 seam samples.

Anatase/ Rutile.

There is no XRD evidence for the presence of anatase. However, there is a moderate relationship between the residual iron concentration remaining after pyrite and siderite iron have been removed (Figure 3.37.), suggesting the presence of rutile (ie TiO_2 with some FeO substitution in the crystal lattice). Some of the residual iron figures appear

higher than would be expected if Fe were substituting for Ti in rutile (Deer et al., 1989), possibly indicating the presence of another iron-bearing phase, or underestimation of pyrite and/ or siderite (ie errors in the normative calculation), or analytical errors. However, it is assumed that the remaining iron is present in rutile or as iron oxide (FeO). The requisite weight of oxygen to form anatase or rutile using titanium as the index element is calculated using Equation 25. The oxygen required to make rutile or iron oxide is calculated using Equation 31.

$$\text{Equation 31} \quad \text{Rutile/ FeO oxygen} = (\text{rutile/ FeO Fe} \times 0.286)$$

The total concentration of anatase/ rutile/ FeO (ppm) in the sample was calculated by summing the concentrations of anatase/ rutile titanium, rutile/ FeO iron and anatase/ rutile/ FeO oxygen.

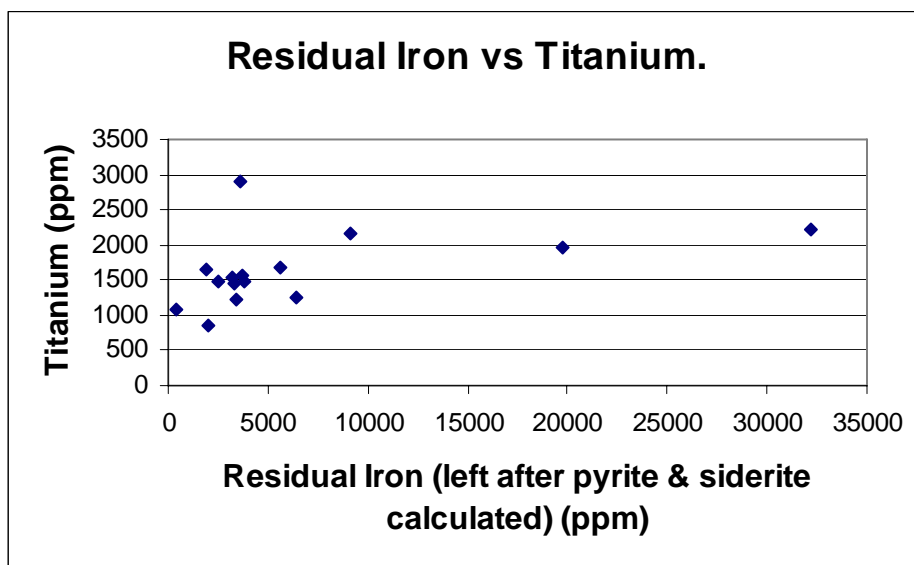


Figure 3.37. Residual iron vs titanium, Bowen No.2 seam samples.

Unassigned Major Elements.

No mode of occurrence for sodium in the Bowen No.2 seam was determined in the normative analysis. Sodium is, however, present in much lower concentrations than in the Blake seam samples (maximum concentration in Bowen No.2 seam samples is 480ppm), so the effect of the issue on calculation of mineral proportions is considered minor. Further inferences on the mode of occurrence of sodium are drawn in Section 3.3.1.2. below.

3.2.3.3. Tabulated Normative Mineral Assemblages.

Tables 3.5., 3.6. and 3.7. present the normative mineral assemblages for the Blake Central, Blake West, and Bowen No.2 seams respectively. Table 3.8. provides a comparison between the normative mineralogy, re-calculated to percent in coal LT-OPA using percent ash determined by standard proximate analysis, and the XRD mineralogy in actual LT-OPA. A number of samples show good agreement, however many samples show major differences in the proportions of quartz and kaolinite. These differences do not appear to be attributable to the problem caused by some samples having a potassium concentration below the detection limit of INAA because the difference between the XRD and normative results for some samples with potassium results is higher than for some samples without potassium results. Possibly one reason for this is the apparent poor repeatability of potassium analysed by INAA, reinforcing the need for caution in the use of and confidence in data involving this element. However, Dr Newman notes for samples BC6.63-6.83, BO0-10 & BO3.61-4.21 (all of which show significantly higher quartz in the XRD than the normative) that quartz is over-estimated by the "TRACES" programme. Further, the "TRACES" programme automatically calculates the recognised minerals to equal 100%, which does not take account of minor mineral groups such as illite and siderite in BC0-50; illite and siderite in BC3.50-4.00; feldspar in BC6.55-6.63; and illite in BO1.15-1.85, all of which are noted as possibly present by Dr Newman, but missed by "TRACES".

The data presented in Table 3.8. for pyrite, siderite, and phosphates suggests the normative analysis figures are generally closer to the XRD analysis figures. One exception is BO0-10, in which the XRD found no pyrite, but which has a normative figure of 14.2% pyrite. Pyrite was noted both in hand specimen (see Figure 3.15.) and in the polished block petrographic sample (Appendix 3) for this sample. Further, in comments accompanying the XRD results, Dr Newman note "unassigned peaks mid-chart are almost certainly pyrite". It appears that the "TRACES" programme has provide a poor quantitative assessment of the pyrite present in this sample.

A further source of error could be introduced in splitting the coal samples for analysis. It should be remembered that the INAA, XRF, and XRD samples are all splits of the original channel sample. Coal is well known to be a heterogeneous substance. Therefore, it is possible small differences in mineralogical content between sample

splits resulted in the observed differences between XRD and XRF mineral assemblages.

It is concluded from the comparisons presented in Table 3.8. that the XRD analysis has correctly determined some of the major mineral groups present in the Collinsville channel samples, with good agreement between the XRD mineral proportions as indicated by “TRACES” and the normative calculation in a number of cases.

However a number of problems and potential sources of error have been identified. It is concluded that proportions of various minerals in the coal calculated by the normative analysis should be treated as indicative. Further, it is concluded that determination of major elements by XRF on fused discs, and the use of float/sink fractionation of the LTA-OP ash followed by quantitative Rietveld-based analysis of the XRD results could have solved some of the issues outlined above.

Table 3.5.

Normative Mineral Assemblage (ppm) - Blake Central Samples									
Sample Number	Quartz	Kaolinite	Illite	Feldspar	Siderite	Pyrite	Gorceixite	Goyazite	Anatase
BC 0.00-0.50	176608	97091	30710	27410	13388	8407	743	0	11470
BC 0.50-1.00	90431	97725	0	7462	7272	2928	409	0	5800
BC 1.00-1.50	84732	83395	0	3491	6896	2066	342	0	4433
BC 1.50-2.00	64692	69548	0	2944	5489	3031	167	0	3306
BC 2.00-2.50	54699	66063	0	5534	4448	3644	190	458	3311
BC 2.50-3.00	35804	52993	30874	5283	6150	2249	223	685	3077
BC 3.00-3.50	36272	81998	0	7051	9067	2533	245	284	3851
BC 3.50-4.00	20953	77658	0	4245	19482	0	256	843	2800
BC 4.00-4.13	5496	101248	0	2065	5921	1710	372	2107	1889
BC 4.13-4.18	685	86033	0	2077	1369	0	446	579	2427
BC 4.18-4.22	0	579189	0	4085	2727	97	372	0	5437
BC 4.22-4.55	36429	209477	0	2293	7223	1367	669	0	6982
BC 4.55-5.00	7541	151206	0	2499	5212	92	557	2528	2868
BC 5.00-5.11	17656	492976	14529	4450	2727	2653	520	737	9544
BC 5.11-5.39	26201	189977	7591	17549	18875	8386	557	0	3480
BC 5.39-5.49	81596	205847	0	1940	18739	1135	632	0	6539
BC 5.49-6.11	20305	97926	0	1529	5703	192	264	0	2834
BC 6.11-6.13	3660	586108	454	17487	2727	1944	409	0	6781
BC 6.13-6.23	20886	118213	0	3423	1760	0	409	0	3023
BC 6.23-6.35	48222	145565	26769	10934	43043	17	353	0	2591
BC 6.35-6.37	36423	519075	54483	6926	3158	0	297	0	1800
BC 6.37-6.55	41599	139126	708	23490	25010	0	520	0	2946
BC 6.55-6.63	85700	380841	29839	19080	2727	3878	669	0	10459
BC 6.63-6.88	92076	260247	105043	21346	18756	0	780	0	9413

Table 3.6.

Normative Mineral Assemblage (ppm) - Blake West Samples									
Sample Number	Quartz	Kaolinite	Illite	Feldspar	Siderite	Pyrite	Gorceixite	Goyazite	Anatase
BW 0.00-0.11	91177	94788	50851	1940	6735	14775	260	0	5628
BW 0.11-0.20	80222	114146	0	1689	5212	7116	331	0	4422
BW 0.20-0.48	81943	63352	18161	1552	4758	3156	111	0	3368
BW 0.48-0.93	77766	56986	19269	2297	2727	2675	145	0	2940
BW 1.20-1.60	270934	80120	9081	3706	2727	2267	260	0	7788
BW 1.60-2.05	44938	78656	0	1734	2727	806	182	0	3411
BW 2.05-2.65	36887	76869	0	2716	4004	0	264	843	3096
BW 2.65-3.15	20600	96586	0	3412	6204	14222	342	685	3334
BW 3.15-3.75	6875	60904	0	4290	4877	16073	1115	2002	2240
BWB 0.00-0.65	0	210383	50415	48541	7705	6009	5203	5267	7437
BWB 0.65-1.25	0	201628	0	5831	5526	0	1970	2265	4309
BWB 1.25-1.90	0	162573	0	3275	2252	0	1970	1686	3596
BWB 1.90-1.98	0	532574	0	6629	3624	0	1115	790	8370
BWB 1.98-2.05	0	17695	37285	4992	2665	0	1263	1528	3362
BWB 2.05-2.72	0	102891	18234	5421	5265	0	2192	1738	3841
BWB 2.72-2.78	0	504330	27242	5043	2727	11	706	337	7654
BWB 2.78-3.04	0	121568	0	17686	44800	0	1412	1422	1918
BWB 3.04-3.15	0	106866	12549	2910	6040	0	2453	2002	2327
BWB 3.15-3.25	0	298975	0	13692	309249	0	595	0	879
BWB 3.25-3.56	41896	52601	0	1963	3350	0	5574	3424	1775
BWB 3.56-3.71	0	353995	2960	9280	2727	2116	1412	948	6801
BWB 3.71-3.93	836	143537	0	1860	3137	0	1709	1528	4985
BWB 3.93-4.23	1284	100266	0	2236	16952	0	1338	1738	4210
BWB 4.23-4.28	0	32857	0	5579	36000	0	4088	4793	1426
BWB 4.28-4.40	0	65460	26152	8606	11996	0	929	1422	5154
BWB 4.40-4.43	0	583497	43586	6652	15727	0	483	0	11683
BWB 4.43-4.67	71	74043	0	4245	6326	0	966	1686	3598
BWB 4.67-5.13	0	140611	21230	17977	7124	0	1598	2897	5474
BWB 5.13-5.51	546	240459	454	23612	27191	0	1301	1633	16214
BWB 5.51-6.25	203	480191	85357	15175	23752	13068	743	1475	19787
BWB 6.25-6.75	8640	119686	0	3959	31345	0	743	1844	6459
BWB 6.75-7.25	0	96319	19977	16887	26497	0	706	1001	3554
BWB 7.25-7.75	0	110143	0	22592	17824	0	520	579	3545
BWB 7.75-8.25	0	82785	0	20880	9621	0	483	516	3101
BWB 8.25-8.75	4101	83142	0	9094	14112	0	282	579	2741
BWB 8.75-9.25	13976	50943	0	3571	6960	3268	245	579	2136

Table 3.7.

Sample Number	Normative Mineral Assemblage (ppm) - Bowen No.2 Samples							Anatase/ Rutile/ FeO
	Quartz	Kaolinite	Illite	Siderite	Pyrite	Gorceixite	Goyazite	
BO 0.00-0.10	34631	81970	67196	29594	143558	3344	0	5086
BO 0.10-0.15	26788	100560	18161	14619	72467	409	0	2066
BO 0.15-0.34	53489	50015	58115	8749	18962	557	0	3338
BO 0.34-0.37	65620	38365	47219	39167	156092	308	0	7597
BO 0.37-0.72	50204	23073	56299	7154	2686	204	0	2824
BO 0.72-1.07	29739	45604	9081	5293	27755	175	0	2449
BO 1.07-1.09	43628	106944	9081	18707	96226	520	0	3803
BO 1.09-1.15	16792	13254	19977	1148	10357	212	0	1782
BO 1.15-1.85	44149	62268	0	4482	6989	216	0	2954
BO 1.85-2.45	33291	46495	0	6363	2312	134	527	2472
BO 2.45-2.60	8894	41114	0	4846	9796	557	1738	1438
BO 2.60-2.90	55296	61726	16345	8838	6428	483	416	4855
BO 2.90-3.01	26719	60923	0	8463	12040	446	0	2029
BO 3.01-3.61	22695	54242	0	3058	4183	260	1370	2972
BO 3.61-4.21	17563	26814	38138	9087	23078	334	895	2461

Table 3.8. Comparison of XRD and Normative Mineral Assemblages

Blake Central				
	Quartz		Kaolinite	
	XRD	Normative	XRD	Normative
BC 0 – 50	33.8	17.7	3.8	9.7
BC 3.50 – 4.00	9.2	2.1	5.0	7.8
B 4.00 - 4.13	0.0	0.5	11.6	10.1
BC 4.18 – 4.22	0.0	0.0	67.2	57.9
BC 6.55 – 6.63	41.2	8.6	17.6	38.1
BC 6.63 – 6.83	27.3	9.2	10.9	26.0

Blake West				
	Quartz		Kaolinite	
	XRD	Normative	XRD	Normative
BWB3.56-3.71	0	0	38.2	9.7
BWB4.23-4.28	0	0	0.9	3.3
BWB4.43-4.67	0	0	7.7	7.4
	Siderite		Phosphates	
	XRD	Normative	XRD	Normative
BWB4.23-4.28	4.7	3.6	0.9	1.0

Bowen No.2				
	Quartz		Kaolinite	
	XRD	Normative	XRD	Normative
BO0-10	26.7	3.5	6.7	8.2
BO37-72	12.2	5.0	2.2	2.3
BO1.15-1.85	11.0	4.1	1.9	6.2
BO3.61-4.21	4.6	1.8	1.7	2.7
	Pyrite			
	XRD	Normative		
BO0-10	0	14.2		
BO3.61-4.21	1.2	2.2		

NB Minerals Given as a Percent of LT-OPA Ash.

3.3. Trace Element Concentration and Mode of Occurrence.

The concentration of trace elements in the channel samples was determined by INAA, except for copper, lead, and vanadium, which were determined by XRF analysis of pressed powder pellets prepared from 400°C ash (Section 2.3.2.) and calculated to whole-coal basis. It was found some elements were below the limit of detection, so these samples could not be used as a guide to elemental concentration or to determine the mode of occurrence of the trace elements. INAA analysis found silver and iridium were present at concentrations below the limit of detection in all the channel samples, so these elements are not considered further in this study. Further, only a few samples had enough material remaining after INAA and major element analysis to allow determination of copper, lead, and vanadium, so indications of trace element concentration and mode of occurrence for these elements are of low confidence.

3.3.1. Trace Elements in the Blake Seam.

3.3.1.1. Concentration of Trace Elements in the Blake Seam.

The channel ply-thickness weighted-average concentration of trace elements in the Blake Central and Blake West pit seams are tabulated in Table 3.9. As noted above, copper, lead, and vanadium values are only available for a few samples, so the weighted averages figures should be viewed with caution. In addition, some plies contained trace element concentrations below the limit of detection of INAA, so the weighted average figures only relate to the plies containing a detectable concentration of the element. Where a large number of plies contain a given element below the detection limit concentration, the weighted average figure may be substantially biased upward.

The cautions outlined above notwithstanding, the concentration of trace elements in the Blake Seam has been rated “Average” or “Above Average”, depending on whether the trace element concentration lies within or above the world coal average concentration range (Swaine, 1990). In the case of the Blake Central pit seam, gold, hafnium, thorium, and ytterbium lie above the average range of world coal range of elemental concentrations. In the case of the Blake West pit seam, the elements gold, copper, hafnium, and thorium lie above the average range world coal range of elemental concentrations. Of the elements found to be present in concentrations at the

high end of the world range, only copper and thorium are considered as potentially environmentally hazardous. Previous studies have also found Bowen Basin coals are generally low in potentially environmentally hazardous trace elements (Riley and Dale, 2000).

A comparison with the crustal elemental concentration average figures (“Clarke Values”) is also shown in Table 3.9. This sort of comparison has been undertaken in a number of previous studies, as outlined in Section 1.3.1.2. Of the elements analysed for this study, gold and selenium are highly enriched, mercury is enriched, and hafnium, thorium, uranium, and tungsten are slightly enriched in both the Blake Central and Blake West pit seams by comparison with the crustal average concentrations. In addition, molybdenum, lead, and antimony are enriched in the Blake West coal.

Table 3.9. Concentration of Trace Elements in the Blake Seam Compared to World Coal and Crustal Averages (ppm).

Element	World Coal Average	Crustal Average	Blake Central Wtd Ave Conc	vs world coal	vs crustal concentration	Blake West Wtd Ave Conc	vs world coal	vs crustal concentration
Gold	0.01	0.002	1.02	Above Average	510.0	1.04	Above Average	520.0
Arsenic	0.5 - 80	2	0.6	Average	0.3	1.31	Average	0.7
Barium	20 - 1000	380	106.56	Average	0.3	329.5	Average	0.9
Bromine	0.5 - 90	4	6.36	Average	1.6	11.24	Average	2.8
Cerium	2 - 70	83	65.96	Average	0.8	54.87	Average	0.7
Cobalt	0.5 - 30	28	4.59	Average	0.2	5.8	Average	0.2
Chromium	0.5 - 60	96	28.77	Average	0.3	38.31	Average	0.4
Caesium	0.3 - 5	1.6	0.94	Average	0.6	1.29	Average	0.8
Copper	0.5 - 50	58	45.15	Average	0.8	61.12	Above Average	1.1
Europium	0.1 - 2	2.2	0.84	Average	0.4	0.78	Average	0.4
Hafnium	0.4 - 5	4	6.14	Above Average	1.5	6.39	Above Average	1.6
Mercury	0.02 - 1	0.02	0.22	Average	11.0	0.13	Average	6.5
Lanthanum	1 - 40	50	35.23	Average	0.7	31.75	Average	0.6
Lutetium	0.03 - 1	0.8	0.52	Average	0.7	0.37	Average	0.5
Manganese	5 - 300	1000	49.37	Average	0.0	109.75	Average	0.1
Molybdenum	0.1 - 10	1.2	1.77	Average	1.5	1.49	Average	1.2
Neodymium	3 - 30	44	26.68	Average	0.6	20.39	Average	0.5
Nickel	0.5 - 50	72	33.17	Average	0.5	20.7	Average	0.3
Lead	2 - 80	10	25.51	Average	2.6	20.58	Average	2.1
Rubidium	2 - 50	70	11.26	Average	0.2	5.91	Average	0.1
Antimony	0.05 - 10	0.2	0.58	Average	2.9	0.45	Average	2.3
Scandium	1 - 10	22	8.75	Average	0.4	8.94	Average	0.4
Selenium	0.5 - 10 ?	0.05	2.55	Average	51.0	2.15	Average	43.0
Samarium	0.5 - 6	7.7	4.63	Average	0.6	3.96	Average	0.5
Strontium	15 - 500	450	184.09	Average	0.4	311.75	Average	0.7
Tantalum	0.1 - 1	2.4	0.71	Average	0.3	0.87	Average	0.4
Terbium	0.5 - 4	1	0.9	Average	0.9	0.75	Average	0.8
Thorium	0.5 - 10	5.8	13.9	Above Average	2.4	12.59	Above Average	2.2
Uranium	0.5 - 10	1.6	2.68	Average	1.7	2.36	Average	1.5
Vanadium	2 - 100	170	53.33	Average	0.3	69.64	Average	0.4
Tungsten	0.5 - 5	1	3.45	Average	3.5	2.73	Average	2.7
Ytterbium	0.3 - 3	3.4	3.4	Above Average	1.0	2.67	Average	0.8
Zinc	5 - 300	82	28.09	Average	0.3	41.18	Average	0.5

Average = within the “average” range or trace element concentrations for coal (Swaine, 1990) Above Average = above the “average” range of trace element concentrations for coal (above average figures shown in bold). Crustal Averages from Skinner & Porter (1987)

3.3.1.2. Mode of Occurrence of Trace Elements in the Blake Seam.

The mode of occurrence of the analysed trace elements in the Blake Central and Blake West pits is shown in Table 3.10. Trace element mode of occurrence has been inferred by graphing the concentration of the mineral (from the normative analysis outlined above) against the concentration of the trace element of interest. The graphs for each trace element are presented in Appendix 6, Part 1. (NB Numbers such as A61E denote Appendix 6, Part 1, Graph E). Samples considered to have been heat affected (Section 3.2.1.) are shown in red.

A number of other researchers have used the graphical approach to deduce trace element mode of occurrence (Section 1.3.2.2.), although usually a particular major element is used as a proxy for a particular mineral (eg potassium for illite). However, the normative calculations above show potassium may be present within feldspars or illite in the Collinsville coals. It was hoped that a more precise assessment of the mode of occurrence for a given element could be provided using the present approach. In some cases, two minerals showed a positive graphical relationship, in which case two modes of occurrence are stated. Minerals shown in brackets in Table 3.9. show a positive relationship with the trace element in question, but further inferences are required (as outlined below).

A rating of the strength of the correlation coefficient between the mineral and the trace element is also given in Table 3.10. The rating varies from P (poor), through I (indication); M (moderate); to G (good). Some scatter is apparent in all the graphical relationships (Appendix 6). The scatter may be caused by: 1) Analytical errors in the major element and/ or trace element analyses; 2) Differences in the concentrations of major and trace elements between splits of the original channel sample; 3) Errors in the normative analysis calculations (see Section 3.2.3.1.); 4) Mixed modes of occurrence for an element; 5) Variable degrees of association or replacement with a mineral (ie the same mineral may contain different concentrations of a particular trace element between samples). In some cases, the exclusion of some data points would result in a much strong correlation coefficient. A red line is hand drawn on to some plots in Appendix 6 (indicated by * in Table 3.10.) to indicate a line of visual “best fit” to the general trend of the points.

A moderate relationship was noted between magnesium and kaolinite for both the Blake Central and Blake West pit samples (Appendix 6, Section A61A). As noted in Section 3.2.3.1., magnesium was unable to be assigned to any normative mineral in the channel samples, although it was inferred that magnesium was likely to be inorganically bound. Three explanations for the graphical relationship between kaolinite and magnesium can be given. First, magnesium is associated with an unknown mineral, the concentration of which parallels the concentration of kaolinite. Second, magnesium substituted for aluminium in the kaolinite lattice. Substitution of magnesium into the kaolinite lattice is generally thought to be negligible (Deer et al., 1989). However, the relationship of kaolinite with magnesium shown in Appendix 6 would only require around 0.2% substitution of magnesium. Third, magnesium could be present as ions held in exchange positions within or attached to the clay minerals. The second or third explanations are preferred given the lack of a relationship between magnesium and any other element, however definitive proof is not available.

Table 3.10. Most Likely Mode of Occurrence of Trace Elements in the Blake Seam.

Element	Blake Central		Blake West	
		rating		rating
Magnesium	Kaolinite	M	Kaolinite	M
Sodium				
Gold			(Anatase)	I
Arsenic	Pyrite	P	Pyrite	M
Bromine	Organic	G	Organic	M
Cerium	Illite/ Gorceixite	M/M	Gorceixite	I*
Cobalt	Organic	G	Organic	G
Chromium	Pyrite	I*	Pyrite	I
Caesium	Illite	M/M	Illite	I
Copper	Pyrite	I*	Pyrite	M
Europium	Illite/ Gorceixite	M/M	Gorceixite	I*
Hafnium	Kaolinite/ Gorceixite	M/I	Gorceixite	P*
Mercury	Pyrite	P	Pyrite	P*
Lanthanum	Illite/(Kaolinite/ Gorceixite?)	I/I	Gorceixite	I*
Lutecium	Kaolinite/ Gorceixite	M/M	Kaolinite/Gorc+Goy	P/P
Molybdenum	Mixed Inorganic/ Organic	M	Inorganic	M
Neodymium	Kaolinite/ Gorceixite	G/M	Gorceixite+Goyazite	I*
Nickel	Pyrite	P*	Pyrite	P*
Lead	Pyrite	P	Pyrite	P*
Rubidium	Illite	M	Kaolinite/ Illite	P*/I
Antimony	Kaolinite	P	Kaolinite	I
Scandium	Gorceixite	G	Illite	I
Selenium	Organic	I	Organic	G
Samarium	Gorceixite (Kaolinite?)	M	Gorceixite+Goyazite	M
Tantalum	Kaolinite	G	Kaolinite	M
Terbium	Gorceixite	M	Kaolinite/ Gorceixite	P/M
Thorium	Feldspars/ Phosphates	P*/M	Anatase/ Gorc+Goy	P/I
Uranium	Feldspars/ Phosphates	P*/I	Anatase/ Gorc+Goy	P/P
Vanadium	Pyrite/ (Gorceixite?)	M/G	Pyrite/ (Gorceixite?)	P*P
Tungsten	(Anatase)	M	(Anatase)	P*
Ytterbium	Kaolinite/ (Organic?)	G	Kaolinite/ (Organic?)	P
Zinc	Organic/ Pyrite	I/G	Inorganic/(mixed?)	P

P = Poor relationship ($R^2 < 0.2$), I = Indications of a relationship ($R^2 0.2 - 0.4$), M = Moderate Relationship ($R^2 0.4 - 0.7$); G = Good relationship ($R^2 > 0.7$). * = visual best fit line ignoring some outlier data points. ? = Few data points.

No graphical relationship with any mineral could be found for gold in the Blake Central samples, but an indication of a relationship between gold and anatase was noted for the Blake West samples (Appendix 6, Section A61AE). It is likely that this relationship is due to a parallel relationship between anatase (or a “heavy mineral” suite) and gold rather than a direct association. It is inferred that gold is present as the native element.

The following elements show some graphical relationship with pyrite: arsenic (A61B) (poor to moderate), chromium (A61F) (indications only), copper (A61H) (indication to moderate), mercury (A61K) (poor), nickel (A61P) (poor), and lead (A61Q) (poor). A pyrite mode of occurrence has been noted for all these elements in previous studies, except for chromium (see Appendix 2). It is suggested that the source of iron and chromium into the mire was the same and resulted in a misleading graphical association. It is more likely on the basis of the data in Appendix 2 that chromium is associated with silicate minerals, chromites or the organic fraction of the coal. Zinc in the Blake Central pit also appears to show some (mixed) affinity for pyrite (A61AD), a mode of occurrence noted in previous work (Appendix 2). However, it should be noted that sphalerite is a much more commonly cited mode of occurrence for zinc. The poor relationships between some elements and pyrite could be caused by mixed element affinities, variable trace element concentrations in different phases of pyrite mineralisation, or errors in the normative concentration of pyrite.

The elements bromine (A61C) (good to moderate), cobalt (A61E) (good), selenium (A61U) (indications to good), and zinc (A61AD) (indications to poor) (in the Blake Central pit) show a negative relationship with ash, indicating an organic mode of occurrence. An organic mode of occurrence has been noted for these elements in previous studies (Appendix 2). However, again it should be noted that zinc is more likely to be associated with sphalerite. Remobilisation of zinc could easily have resulted in a misleading graphical relationship. Further, the relationships are complicated by the apparent enrichment of bromine and selenium, and the loss of cobalt from heat affected samples (see also Section 3.4.).

The trace elements cerium (A61D) (moderate, Blake Central only), caesium (A61G) (moderate to indication), europium (A61I) (moderate, Blake Central only), lanthanum (A61L) (indication, Blake Central only), rubidium (A61R) (indication to moderate), and scandium (A61T) (indication, Blake West only) show a graphical relationship with illite. Swaine (1990) notes illite as a possible mode of occurrence for all these elements.

However, cerium (moderate), europium (moderate), lanthanum (indication) and scandium (good, Blake Central); along with hafnium (A61J) (poor to indication),

lutetium (A61M) (poor to moderate), neodymium (A61O) (moderate to indication), samarium (A61V) (moderate), terbium (A61X) (moderate), thorium (A61Y) (indication to moderate), uranium (A61Z) (poor to indication) and vanadium (A61AA) (poor to good) also show an affinity with gorceixite or gorceixite plus goyazite. Ward (2002) suggests the phosphate monazite may contain varying proportions of cerium, lanthanum, thorium and neodymium. A strong graphical relationship between hafnium and uranium exists for both the Blake Central and Blake West data sets (Figures 3.38. and 3.39.). The mineral zircon always contains some hafnium (Deer et al., 1989), and zircon (along with REE phosphates) is commonly cited as modes of occurrence for uranium. In addition, there is a strong graphical relationship between thorium and uranium (Figures 3.40. and 3.41.). The interpretation of these graphical relationships is that, while a proportion of the phosphorous is present as gorceixite and goyazite (as outlined in Section 3.2.3.1.), a significant proportion of rare earth and radionucleide elements are associated with an undetected REE phosphate/ zircon heavy mineral suite (as also indicated by the significant residual phosphorous remaining after calculation of gorceixite and goyazite; Tables 3.2. and 3.3.).

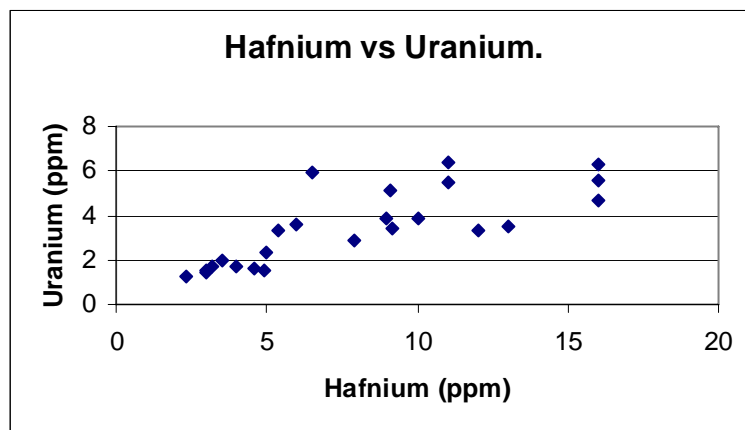


Figure 3.38. Hafnium vs uranium, Blake Central.

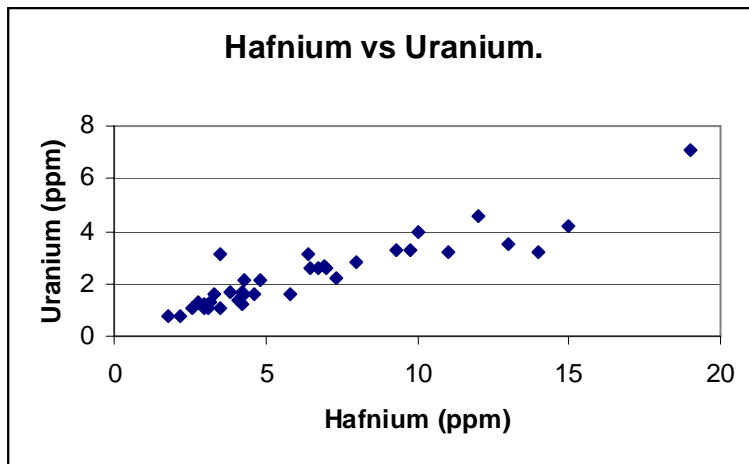


Figure 3.39. Hafnium vs uranium, Blake West.

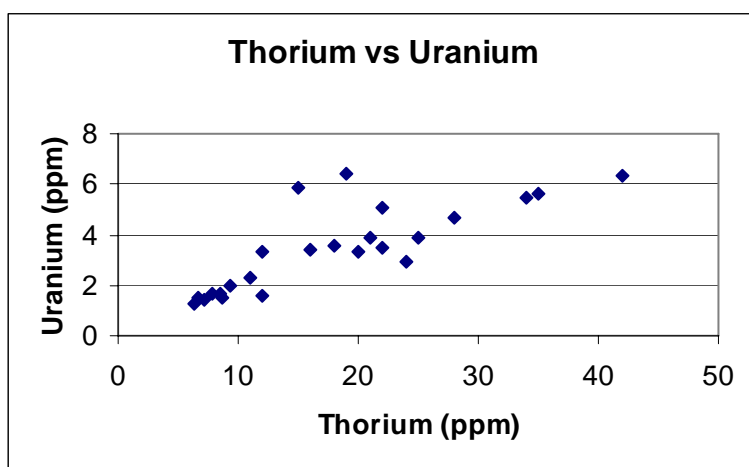


Figure 3.40. Thorium vs uranium, Blake Central.

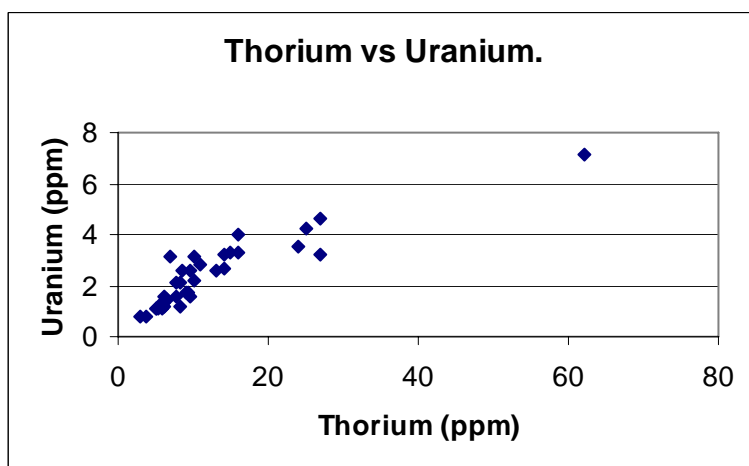


Figure 3.41. Thorium vs uranium, Blake West.

In addition to the REE phosphate mode of occurrence, several rare earth elements show an affinity for kaolinite as follows: lutetium in the Blake Central and Blake West samples, and hafnium, lanthanum, neodymium, and samarium in the Blake

Central samples. In a number of cases these relationships are fitted using a polynomial relationship to make allowance for the non-linear nature of the trend. The non-linear trend is considered to be an artifact of under-estimation of kaolinite due to the lack of potassium figures from INAA analysis of some samples.

Thorium and uranium show some association with feldspars (in addition to the heavy mineral association outlined above) in the Blake Central samples. The relationship is poor, but two distinct visual trends can be seen in the plots, one relating to feldspar concentration, the other probably indicating at least one other mode of occurrence for these two elements (as outlined above). None of the extensive literature on mode of occurrence notes feldspars as a mode of occurrence for thorium, and only one paper inferred feldspars as a mode of occurrence for uranium (Querol et al., 1995). One possible explanation is that the feldspars are distributed in a similar fashion to the heavy mineral suite. For example, feldspars have been found to be far more prevalent in fine grain sizes, even in apparently very compositionally mature sandstones (Odom et al., 1976). If feldspars are mirroring the distribution of a particular heavy mineral, the graphical relationship is simply an artefact of a sedimentary association.

The trace elements antimony (A61S) (poor to indication), tantalum (A61W) (moderate to good), and ytterbium (A61AC) (poor to good) were found to be associated with kaolinite in both sample sets. Swaine (1990) notes clays as a possible mode of occurrence for all these elements (see also Appendix 2). As note above, the parabolic form to some of these graphical relationships is considered to be the result of over-estimation of kaolinite in the normative analysis, as outlined in Section 3.2.3.1..

No definitive mode of occurrence for molybdenum could be deduced for either of the two sample sets. A graph of molybdenum versus ash (see Appendix 6, Section A61N) (moderate relationship) for the Blake Central samples showed evidence for a mixed organic/ inorganic mode of occurrence (heat affected samples appear to show higher concentrations of molybdenum, but a poor inverse relationship with ash). The same graph for the Blake West sample set gives a moderate relationship indicating an inorganic mode of occurrence.

Tungsten was found to be associated with anatase for both Blake seam sample sets (poor to moderate relationships). It appears unlikely that tungsten substitutes directly into the anatase mineral lattice. Swaine (1990) notes a dominant organic association for tungsten; also (Bouska, 1981). However, mineral associations for this element have been found: lead tungstates (Finkelman, 1980), oxides (Finkelman, 1993), clay minerals (Li, 2002), insoluble tungstates (Palmer et al., 1999), illite/ kaolinite (Palmer and Lyons, 1996), aluminosilicates (Querol et al., 1998), and undetected acid resistant oxides or associated clay minerals (Willett et al., 2003). Graphs of tungsten versus ash show some positive relationship (visual best fit lines ignoring some points shown in red), inferring an inorganic association (Figures 3.42. and 3.43.). However, given the lack of a graphical relationship with any of the aluminosilicate minerals, and the poor to moderate relationship with anatase, it is inferred that tungsten is present as tungstates associated with the heavy mineral (anatase, REE phosphates, zircon) suite.

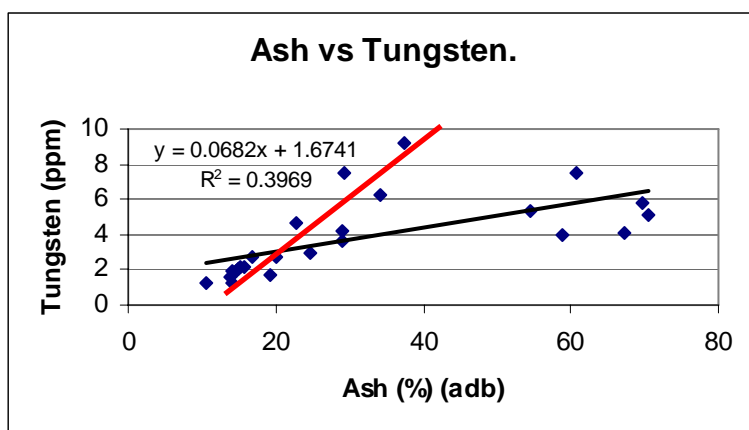


Figure 3.42. Ash vs tungsten, Blake Central.

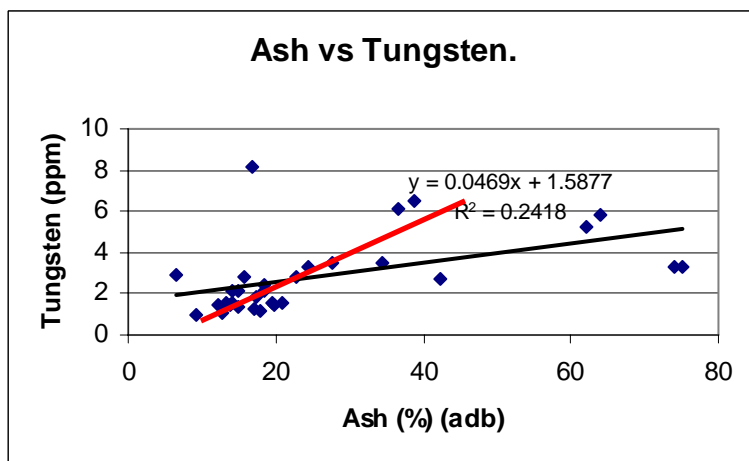


Figure 3.43. Ash vs tungsten, Blake West.

As noted above, a graphical relationship was found between vanadium and gorceixite in both data sets. Vanadium also appears to show some graphical relationship with pyrite in both data sets. Neither phosphates nor pyrite are known modes of occurrence for vanadium (Appendix 2), so interpretation of the graphical relationships is vexatious.

Many of the graphical relationships for the rare earth elements are of low confidence (poor to indications). The rare earth element concentrations were chondrite normalised, and then normalised to the average ash content for each ash range (Figures 3.44. and 3.45.). Both figures 3.44. and 3.45. show a general trend of decreasing concentrations of rare earth elements with increasing ash on an average ash normalised basis. The chondrite and ash normalised plots suggest that at least some fraction of the rare earth elements may be associated with the organic fraction of the coal. However, a similar trend could also occur if one particular mineral in the ash were increasing in proportion to the other minerals as the ash increased, or if low-REE authigenic minerals were partly responsible for the increasing ash content, in which case the REE's are simply being "diluted" by the ash.

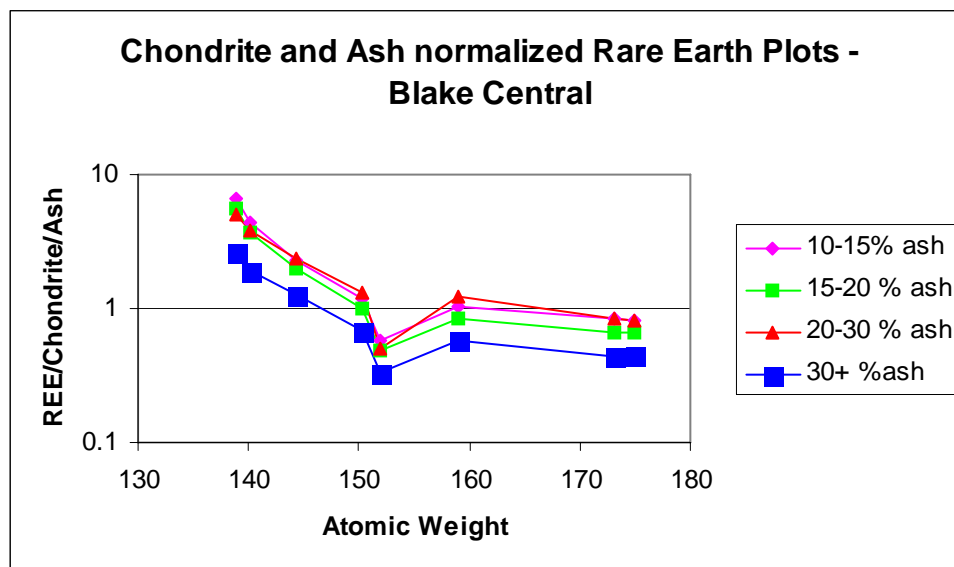


Figure 3.44. Chondrite and Ash normalised REE concentration, Blake Central.

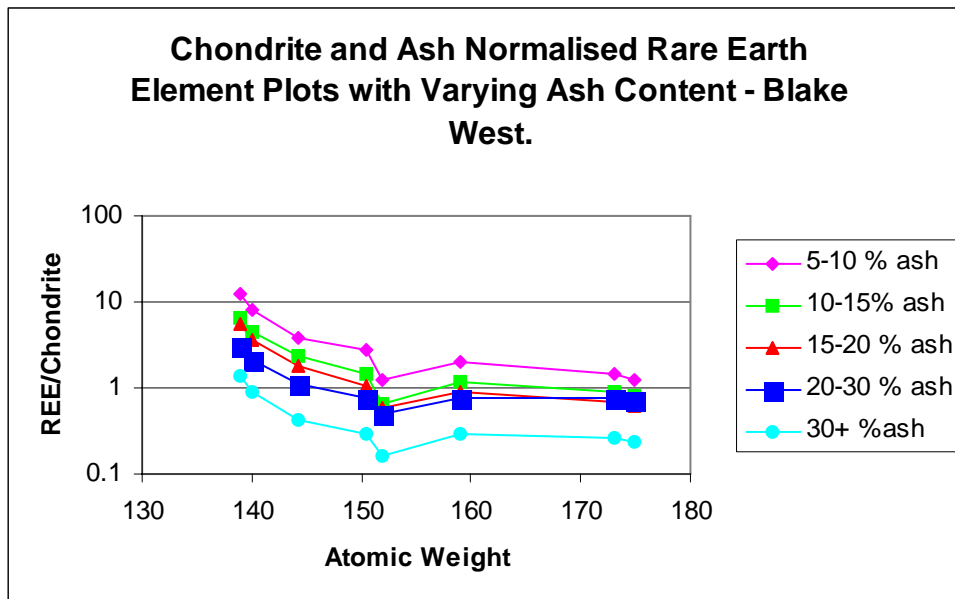


Figure 3.45. Chondrite and Ash normalised REE concentration, Blake West.

3.3.2. Trace Elements in the Bowen Seam.

3.3.2.1. Concentration of Trace Elements in the Bowen No.2 Seam.

The channel ply-thickness weighted average concentrations of trace elements in the Bowen No.2 pit seam are tabulated in Table 3.11. The same cautions as noted for the Blake Seam calculations apply to the Bowen No.2 seam data. That is, copper, lead, and vanadium values are only available for a few samples, so the weighted average figures should be viewed with caution. Further, some plies contained trace element concentrations below the limit of detection of INAA, so the weighted average figures only relate to the plies containing a detectable concentration of the element. Where a large number of plies contain a given element below the detection limit concentration, the weighted average figure is biased upward.

As for the Blake Seam data set, the concentration of trace elements in the Bowen Seam has been rated “Average” or “Above Average”, depending on whether the trace element concentration lies within or above the world coal average concentration range (Swaine, 1990). Only gold and copper lie above the average world coal range, and only copper is considered as potentially environmentally hazardous. Previous studies

have also found Bowen Basin coals are generally low in potentially environmentally hazardous trace elements (Riley and Dale, 2000).

A comparison with the crustal elemental concentration average figures (“Clarke Values”) are also shown in Table 3.11. Of all the elements analysed, gold and selenium are highly enriched, mercury is enriched, and lead and tungsten are slightly enriched by comparison with the crustal averages. The elements gold, mercury, selenium, and tungsten were also enriched in the Blake seam data sets.

Table 3.11. Concentration of Trace Elements in the Bowen No.2 Seam Compared to World Coal and Crustal Averages (ppm).

Element	World Coal Average	Crustal Average	Bowen No.2 Wtd Ave Conc	vs world coal	vs crustal concentration
Gold	0.01	0.002	0.61	Above Average	305.0
Arsenic	0.5 - 80	2	1.56	Average	0.8
Barium	20 - 1000	380	95.32	Average	0.3
Bromine	0.5 - 90	4	6	Average	1.5
Cerium	2 - 70	83	26.79	Average	0.3
Cobalt	0.5 - 30	28	2.06	Average	0.1
Chromium	0.5 - 60	96	26.68	Average	0.3
Caesium	0.3 - 5	1.6	0.23	Average	0.1
Copper	0.5 - 50	58	51.84	Above Average	0.9
Europium	0.1 - 2	2.2	0.36	Average	0.2
Hafnium	0.4 - 5	4	2.47	Average	0.6
Mercury	0.02 - 1	0.02	0.33	Average	16.5
Lanthanum	1 - 40	50	13.89	Average	0.3
Lutetium	0.03 - 1	0.8	0.18	Average	0.2
Manganese	5 - 300	1000	28.28	Average	0.0
Molybdenum	0.1 - 10	1.2	1.1	Average	0.9
Neodymium	3 - 30	44	8.14	Average	0.2
Nickel	0.5 - 50	72	18.99	Average	0.3
Lead	2 - 80	10	12.69	Average	1.3
Rubidium	2 - 50	70	7.18	Average	0.1
Antimony	0.05 - 10	0.2	0.16	Average	0.8
Scandium	1 - 10	22	4.95	Average	0.2
Selenium	0.5 - 10 ?	0.05	1.84	Average	36.8
Samarium	0.5 - 6	7.7	1.5	Average	0.2
Strontium	15 - 500	450	173.87	Average	0.4
Tantalum	0.1 - 1	2.4	0.29	Average	0.1
Terbium	0.5 - 4	1	0.28	Average	0.3
Thorium	0.5 - 10	5.8	5.73	Average	1.0
Uranium	0.5 - 10	1.6	1.16	Average	0.7
Vanadium	2 - 100	170	78.01	Average	0.5
Tungsten	0.5 - 5	1	2.02	Average	2.0
Ytterbium	0.3 - 3	3.4	1.21	Average	0.4
Zinc	5 - 300	82	15.75	Average	0.2

Average = within the “average” range or trace element concentrations for coal (Swaine, 1990) Above Average = above the “average” range of trace element concentrations for coal (above average figures shown in bold). Crustal Averages from Skinner & Porter (1987).

3.3.2.2. Mode of Occurrence of Trace Elements in the Bowen Seam.

The mode of occurrence of the analysed trace elements in the Bowen No.2 pit seam is shown in Table 3.12. As for the Blake seam data sets, trace element mode of occurrence has been inferred by graphing the concentration of the mineral (from the normative analysis outlined above) against the concentration of the trace element of interest. The graphs for each trace element are presented in Appendix 6, Part 2. (NB numbers such as A62C denote Appendix 6, Part 2, Graph C). Again, a rating based on the correlation coefficient of the relationship between the mineral and the trace element is also given in Table 3.12., varying from P (poor); through I (indication); M (moderate); to G (good).

A poor relationship, with a better visual relationship if some points are ignored, was noted between sodium and kaolinite in the Bowen No.2 data set (A62A). Normative analysis of the Bowen No.2 seam failed to determine any mineral containing sodium (Section 3.2.3.2.). There are two possible explanations for the apparant graphical relationship between sodium and kaolinite shown in A62A. First, as for magnesium in the Blake seam data sets, sodium is substituting for aluminium in the kaolinite lattice. The kaolinite graphical relationship suggests the substitution would amount to around 0.2% substitution of sodium. Second, sodium may be present as ions held in exchange positions within or attached to the clay minerals. The same cautions apply for the interpretation sodium is associated with kaolinite as apply for the interpretation that magnesium substitutes for aluminium in kaolinite in the Blake seam data sets above.

An indication of a relationship between gold and the anatase/ rutile/ FeO grouping (A62B) was found for the Bowen No.2 data set. As for the Blake seam samples, it is considered most likely the relationship is due to a parallel relationship between a “heavy mineral” suite and gold rather than a direct association. It is inferred that gold is present as the native element.

Table 3.12. Most Likely Mode of Occurrence of Trace Elements in the Bowen Seam.

Element	Bowen No.2	rating
Magnesium		
Sodium	Kaolinite	P*
Gold	(Anatase/ Rutile/ FeO)	I
Arsenic	Pyrite	M*
Bromine	Illite	M
Cerium	(Anatase/ Rutile/ FeO)	I
Cobalt	Pyrite	M
Chromium	Pyrite	M
Caesium	Kaolinite	M
Copper	Pyrite	G?
Europium	Gorc+Goy/ Illite	P*/I
Hafnium	(Anatase/ Rutile/ FeO)	I*
Mercury	Pyrite	G
Lanthanum	Illite	I
Lutecium	Kaolinite	P
Molybdenum	Pyrite	M
Neodymium	(Anatase/ Rutile/ FeO)	P
Nickel	Pyrite	G?
Lead	Pyrite	G?
Rubidium	(Anatase/ Rutile/ FeO)	M
Antimony	Pyrite	I*
Scandium	Kaolinite	I
Selenium	Pyrite	I
Samarium	Illite/ (Anatase/ Rutile/ FeO)	M/I
Tantalum	Illite/ (Anatase/ Rutile/ FeO)	P/I
Terbium	Illite	I
Thorium	Illite/ (Anatase/ Rutile/ FeO)	I/P*
Uranium	Illite/ (Anatase/ Rutile/ FeO)	P/I*
Vanadium	Illite/ Pyrite	G?/G?
Tungsten	(Anatase/ Rutile/ FeO)	M*
Ytterbium	Kaolinite	P
Zinc	Pyrite	M

P = Poor relationship ($R^2 < 0.2$), I = Indications of a relationship ($R^2 0.2 - 0.4$), M = Moderate Relationship ($R^2 0.4 - 0.7$); G = Good relationship ($R^2 > 0.7$). * = visual best fit line ignoring some outlier data points. ? = Few data points.

The following elements show a graphical relationship with pyrite: arsenic (A62C) (moderate), cobalt (A62F) (moderate), chromium (A62G) (moderate), copper (A62I) (good), mercury (A62L) (good), molybdenum (A62O) (moderate), nickel (A62Q) (good), lead (A62R) (good), antimony (A62T) (indication), selenium (A62V) (indication), and zinc (A62AE) (moderate). A pyrite mode of occurrence has been

noted for all these elements in previous studies except chromium (see Appendix 2). These results are based on moderate to good graphical relationships, and suggest a very high proportion of the elements considered to be potentially environmentally significant are associated with pyrite in the Bowen No.2 seam. There is good potential for the concentration of environmentally significant elements to be reduced if the Bowen coal were to be washed to remove pyrite prior to combustion. As for the Blake seam samples, it is noted that a pyrite mode of occurrence for chromium appears unlikely (Appendix 2). Again, it is suggested that the source of iron and chromium into the mire was the same and resulted in a misleading graphical association. From Appendix 2, it appears more likely that chromium is associated with silicate minerals, chromites or the organic fraction of the coal. Further, Appendix 2 indicates that sphalerite is a more likely mode of occurrence for zinc.

The elements cerium (A62E) (indication), hafnium (A62K) (indication), neodymium (A62P) (poor), rubidium (A62S) (moderate), samarium (A62W) (indication), tantalum (A62X) (indication), thorium (A62Z) (poor), uranium (A62AA) (indication), and tungsten (A62AC) (moderate) all showed some graphical relationship with the anatase/ rutile/ FeO grouping of minerals. It is inferred that the relationship is due to the presence of monazite, zircon, xenotime, REE phosphates, tungstates, or other accessory minerals, the distribution of which mirrors the distribution of the anatase/ rutile/ FeO grouping.

As for the Blake seam samples, a reasonable relationship between hafnium (used here as an indicator of zircon) and uranium was found (Figure 3.46.). Further, a relationship between thorium and uranium was also found (Figure 3.47.), and this relationship is interpreted to indicate the presence of trace amounts of REE phosphates containing neodymium, samarium, some of the tantalum and some of the thorium. However, a graphical relationship between cerium plus lanthanum plus thorium plus neodymium (elements generally found in REE phosphates) and the phosphorous remaining after calculation of gorceixite and goyazite was not found. Possibly the lack of a graphical relationship between cerium plus lanthanum plus thorium plus neodymium and phosphorous is due to the mixed mode of occurrence for thorium and uranium, indicated by graphical relationships between illite and

thorium (A62Z), illite and uranium (A62AA), and illite being the dominant mode of occurrence for lanthanum (A62M).

Previous work suggests rubidium is generally bound into illite or kaolinite (Swaine, 1990), so the graphical relationship between this element and the anatase/ rutile/ FeO grouping is surprising. The graphical relationship between rubidium and the anatase/ rutile/ FeO grouping is moderate, but is based on only five data points because rubidium was present at concentrations below the detection limit of INAA in most of the Bowen seam samples. The graphical relationship between rubidium and anatase/ rutile/ FeO is considered suspect, and probably indicates a physical rather than a chemical association.

Tungsten is inferred to be present in tungstates.

Graphical relationships indicate an illite mode of occurrence for bromine (A62D) (moderate), europium (A62J) (indication), lanthanum (A62M) (indication), terbium (A62Y) (indication), and vanadium (A62AB) (good). A mixed illite/ heavy mineral suite mode of occurrence is inferred for samarium, tantalum, thorium and uranium. An illite mode of occurrence for bromine is unusual, the element generally being organically bound (Swaine, 1990), however the relationship appears robust (ignoring the bromine enriched heat-affected samples). Illite has been noted as a mode of occurrence for europium, lanthanum, and terbium in previous work (Swaine, 1990). A graphical relationship between europium and gorceixite plus goyazite may also indicate some phosphate affinity for this element. Graphical relationships suggest some thorium and uranium may also be associated with illite.

The trace elements caesium (A62H), lutetium (A62N), scandium (A62U), and ytterbium (A62AD) appear to be associated with kaolinite based on their graphical relationships with this mineral. All these elements have been found to be associated with clay minerals in the past (Swaine, 1990).

Graphical relationships exist between vanadium and both illite and pyrite (A62AB). Illite has been noted as a mode of occurrence for vanadium in the past (see Appendix 2), but pyrite has not. On the basis of previous work, the relationship with illite is

considered a more likely mode of occurrence for vanadium, but given the relationship is based on only three data points, the conclusion must be considered provisional.

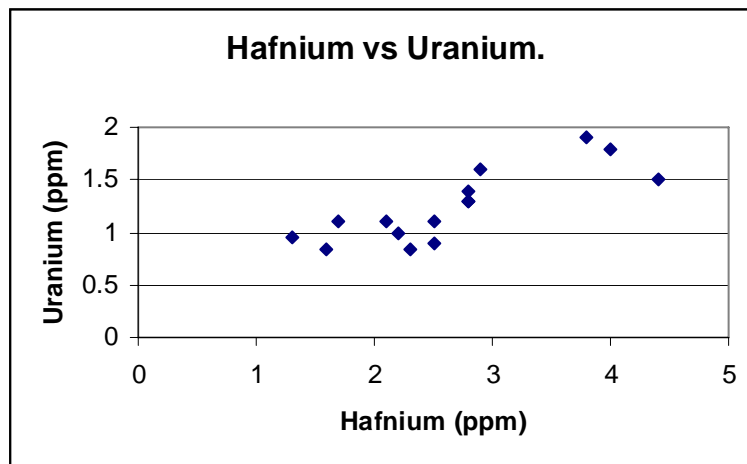


Figure 3.46. Hafnium vs uranium, Bowen No.2.

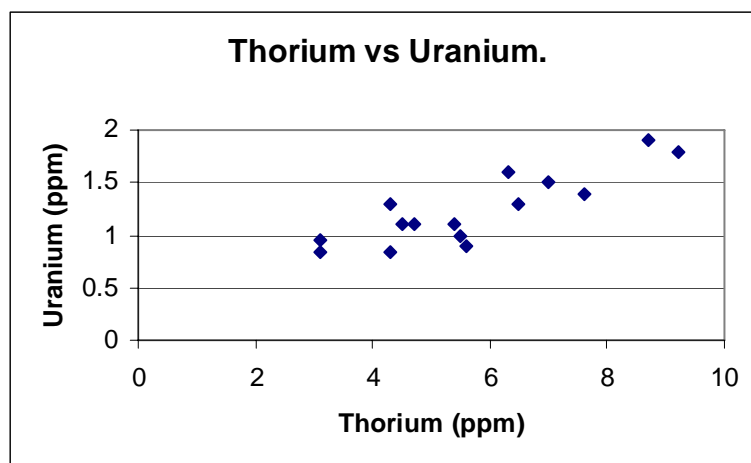


Figure 3.47. Thorium vs uranium, Bowen No.2.

Many of the graphical relationships for the rare earth elements are of low confidence (poor to indication). The rare earth element concentrations were chondrite normalised, and then normalised to the average ash content for each ash range (Figures 3.48.). Figure 3.48. shows a general trend of decreasing concentrations of rare earth elements with increasing ash on an average ash normalised basis. The chondrite and ash normalised plots suggest that at least some fraction of the rare earth elements is associated with the organic fraction of the coal. However, a similar trend could also occur if one particular mineral in the ash were increasing in proportion to the other minerals as the ash increased, or if low-REE authigenic minerals were partly responsible for the increasing ash content, in which case the REE's are simply being

“diluted” by the ash. Addition of authigenic minerals (pyrite and, to a lesser degree, siderite) is proportionately of more importance in the lower-ash Bowen No.2 pit samples, and could, therefore, be partially responsible for changes in the chondrite and ash normalised REE plot with increasing ash.

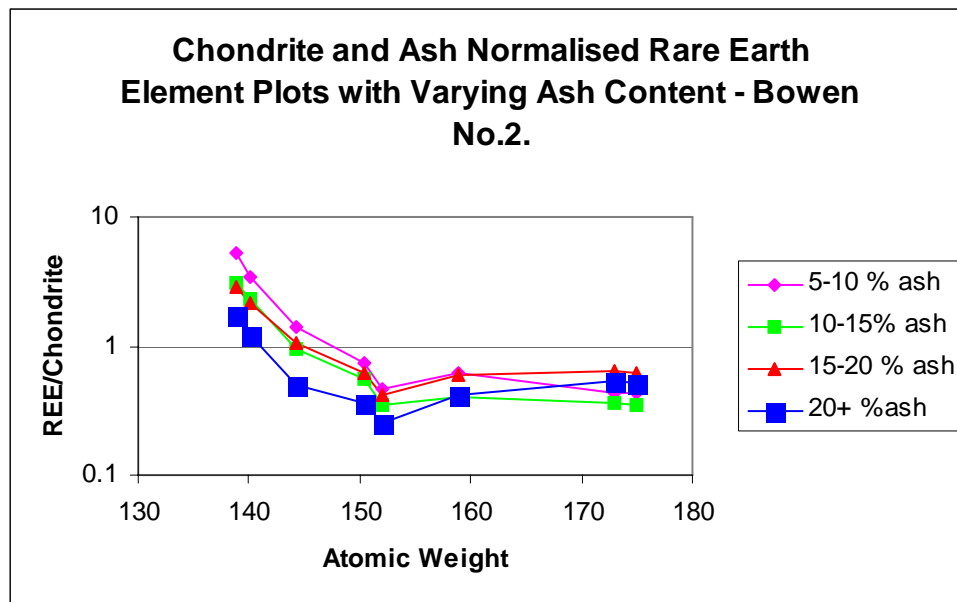


Figure 3.48. Chondrite and Ash normalised REE concentration, Bowen No.2.

3.3.3. Concluding Remarks on Inference of Mode of Occurrence Inferences Using Graphical Relationships.

As noted at the start of Section 3.3.1.1., some scatter is apparent in all the graphical relationships used to infer mode of occurrence in this study. As stated in Section 3.3.1.1., the scatter may be caused by: 1) Analytical errors in the major element and/or trace element analyses; 2) Differences in the concentrations of major and trace elements between splits of the original channel sample; 3) Errors in the normative analysis calculations (see Section 3.2.3.1.); 4) Mixed modes of occurrence for an element; 5) Variable degrees of association or replacement with a mineral (ie the same mineral may contain different concentrations of a particular trace element between samples). In some cases a visual best-fit line ignoring some apparently outlying data supports the mode of occurrence inferences. However, it is recognised that graphical determination of mode of occurrence has a number of shortcomings, as outlined in Section 1.3.2.2. Even where a good relationship has been found between a mineral and a particular trace element, it is possible that the

relationship is physical and not chemical (eg inferences regarding chromium and pyrite association). The mode of occurrence determined using sequential leach analysis of the same coal is compared with the graphical determinations in Section 8.1. to assess the shortcomings of the individual methods.

3.4. The Effect of Igneous Intrusions on the Concentration of Trace Elements in the Blake and Bowen Seam Samples.

3.4.1. Trends in Enrichment and Depletion of Trace Elements at Collinsville.

In order to provide an initial assessment of changes in trace element concentration caused by igneous intrusions, ply thickness weighted average trace element concentrations were calculated separately for heat-affected and unaffected samples. The presence or absence of semi-coke in petrographic samples, and distance from the intrusion where petrographic samples were not available (see Sections 3.2.1. and 3.2.2.) is used to distinguish between heat affected and unaffected samples. Weighted average trace element concentrations, along with the percent difference between the affected and unaffected samples for each seam, are presented in Table 3.13.

Complete loss of volatile matter alone could result in apparent enrichment of a particular element by 20-30% if that element remained in the carbonised coal. Therefore, a cutoff figure of at least plus 50% concentration difference is used in this study to indicate significant enrichment. A cutoff figure of at least minus 40% concentration difference is used in this study to indicate significant depletion of a particular element. Using these criteria, the figures in Table 3.13. provide a first-pass assessment of the changes to trace element concentration caused by the igneous intrusion, as follows:

- Heat-affected samples from the Blake Central pit are enriched in gold, bromine, and strontium; and depleted in cobalt, caesium, europium, lutetium, manganese, neodymium, nickel, terbium, ytterbium; and perhaps depleted in antimony (-36%), samarium (-39%), vanadium (-36%) (few samples) and zinc (-38%). Given that many of the depleted elements exhibit more depletion than mercury (a highly volatile element), and the intrusion does not even contact the seam (cf the Blake West samples), the indications of element depletion must be considered suspect in a number of cases. In particular elements such as the rare earth elements that are considered refractory in pulverised fuel combustion, would not be expected to show significant depletion. Further, ash yield appears to be reduced by 24% in heat affected samples. It would be

expected that ash yield would be higher in heat-affected samples due to loss of volatile matter.

- Heat-affected samples from the Blake West pit are enriched in barium, bromine, copper, antimony, selenium, strontium, thorium, tungsten, ytterbium; and perhaps enriched in gold (38%), lutetium (45%) and molybdenum (45%); and depleted in cobalt, chromium, caesium, and vanadium (few samples). The Blake West pit was notable at time of sampling for the presence of bed parallel igneous intrusions within the coal (see Section 3.1 and Figures 3.5. & 3.6.). Data on the Blake West pit samples is, therefore, the best indicator of the effect of igneous intrusions on the Collinsville coal.
- Heat affected samples from the Bowen No.2 pit are enriched in bromine and strontium; and depleted in gold, arsenic, europium, mercury, lutetium, nickel, ytterbium, and zinc.

Given some of the puzzling changes indicated by the weighted average figures, further analysis of the data was warranted. Figures 3.10., 3.14. and 3.17. indicate that the volatile matter (daf) content decreases in a general fashion toward the igneous intrusion, although a cutoff figure for heat-affected and unaffected samples could not be proposed. Strip logs of the concentration of selected trace elements were prepared using the Rockware programme Logplot. The plots were examined for trends of change with respect to the location of the intrusion, ie toward the roof of the seam in the Blake Central pit, toward the intrusive body within the seam in the Blake West pit, and toward the floor in the Bowen No.2 pit.

Table 3.13. Weighted Average Trace Element Concentration in Heat Affected & Unaffected Samples.

Element	Blake Central			Blake West			Bowen No.2		
	Unaffected	Heat Affected	% Difference	Unaffected	Heat Affected	% Difference	Unaffected	Heat Affected	% Difference
Ash % (adb)	28.39	21.67	-24	26.09	21.09	-19	15.23	11.04	-28
Gold	0.59	1.17	98	1.09	1.50	38	0.79	0.49	-38
Arsenic	0.83	0.57	-31	1.30	1.31	1	2.17	1.07	-51
Barium	116.78	103.97	-11	195.07	406.38	108	112.98	81.48	-28
Bromine	4.55	6.81	50	7.12	13.60	91	4.32	7.31	69
Cerium	85.63	60.98	-29	50.86	57.16	12	26.70	26.86	1
Cobalt	9.75	3.28	-66	8.80	4.09	-54	2.25	1.91	-15
Chromium	22.81	30.28	33	57.73	27.20	-53	31.29	23.07	-26
Caesium	1.62	0.77	-52	1.72	1.04	-40	0.23	0.22	-4
Copper	45.51	44.92	-1	36.89	74.79	103	51.84		
Europium	1.31	0.72	-45	0.84	0.75	-11	10.39	0.34	-97
Hafnium	7.14	5.88	-18	5.41	6.95	28	2.48	2.47	0
Mercury	0.24	0.21	-13	0.14	0.12	-14	0.48	0.21	-56
Lanthanum	43.93	33.03	-25	29.60	32.97	11	14.08	13.74	-2
Lutetium	0.85	0.43	-49	0.29	0.42	45	0.23	0.14	-39
Manganese	79.05	42.13	-47	110.64	109.14	-1	32.86	24.69	-25
Molybdenum	1.74	1.78	2	1.18	1.71	45	1.23	1.00	-19
Neodymium	41.15	23.02	-44	18.32	21.58	18	8.44	7.90	-6
Nickel	39.35	22.69	-42	24.43	17.73	-27	30.00	16.67	-44
Lead	27.94	23.62	-15	22.52	19.49	-13	12.69		
Rubidium	21.63	8.19	-62	5.69	6.14	8	7.18		
Antimony	0.81	0.52	-36	0.28	0.55	96	0.16	0.17	6
Scandium	11.07	8.17	-26	11.33	7.57	-33	4.93	4.97	1
Selenium	3.16	2.40	-24	1.73	2.40	39	1.89	1.80	-5
Samarium	6.70	4.10	-39	3.36	4.31	28	1.58	1.44	-9
Strontium	<10	184.09		236.27	366.88	55	<10	173.87	
Tantalum	0.80	0.69	-14	0.74	0.94	27	0.29	0.30	3
Terbium	1.31	0.79	-40	0.65	0.81	25	0.32	0.25	-22
Thorium	15.21	13.56	-11	8.23	15.08	83	5.69	5.76	1
Uranium	2.80	2.64	-6	1.91	2.62	37	1.15	1.16	1
Vanadium	68.54	43.80	-36	161.76	17.71	-89	78.01		
Tungsten	3.08	3.54	15	1.93	3.20	66	2.13	1.93	-9
Ytterbium	5.50	2.87	-48	2.10	3.00	43	1.56	0.94	-40
Zinc	40.01	24.77	-38	42.09	40.66	-3	21.50	11.23	-48

Blake Central Pit.

Figure 3.49. shows the vertical variation of ash yield and the concentration of selected minerals and trace elements within the Blake Central pit seam. The Blake Central strip log shows ash is less variable over the heat-affected zone, with an increase in ash yield near the roof of the seam. Variations in the concentration of kaolinite and, (to a lesser degree, siderite appear to be the primary controls on ash yield. The rare earth elements lutetium, neodymium, and ytterbium have a partial kaolinite mode of occurrence in the Blake Central seam (3.3.2.2.), and the elements caesium and europium are at least partially associated with illite. It seems unlikely that heating by the igneous intrusions would have resulted in expulsion of mineral matter causing the appreciable decrease in ash yield observed. It is considered more likely that the upper part of the Blake Central seam contained lower ash coal prior to the emplacement of the intrusion. The general lack of non-coal partings over the upper section of the Blake Central seam (Figure 3.49.) suggests the mire became increasingly emergent above channel influence during latter stages of deposition. If the latter is true, it appears most likely that the decreased concentrations of caesium, europium, lutetium, neodymium, samarium and ytterbium noted in Table 3.12. are related more to depositional variations than to heat affects.

Siderite concentration appears to increase away from the intrusion, except for a high concentration zone at the roof of the seam (in parallel with changes in the concentration of manganese, the index element for this mineral).

The concentration of pyrite is uniformly low in the Blake Central coal, apart from small localised concentrations near the roof and at a few isolated horizons toward the base of the seam. The concentration of pyrite at the roof of the seam does not appear to be consistent with heating by igneous intrusions, but could be the result of late stage mineralisation by hydrothermal fluids.

The concentration of goyazite appears to increase away from the intrusion to a maximum on the edge of the heat-affected zone, and then drop to very low concentrations in unaffected coal. The concentration of strontium parallels the goyazite behaviour because strontium acts as the index element for this mineral.

The concentration of arsenic appears to increase away from the intrusion, apart from a high concentration at the roof of the seam related to an increased concentration of pyrite at this location.

The concentration of bromine, chromium, and molybdenum appear to generally increase toward the igneous intrusion. Further, the plot of ash versus molybdenum presented in Appendix 6 also suggests heat affected samples are more concentrated in molybdenum than the unaffected samples (A61N).

The concentration of cobalt, mercury, nickel, antimony, and zinc appear to increase away from the intrusion. The behaviour of selenium is inconclusive.

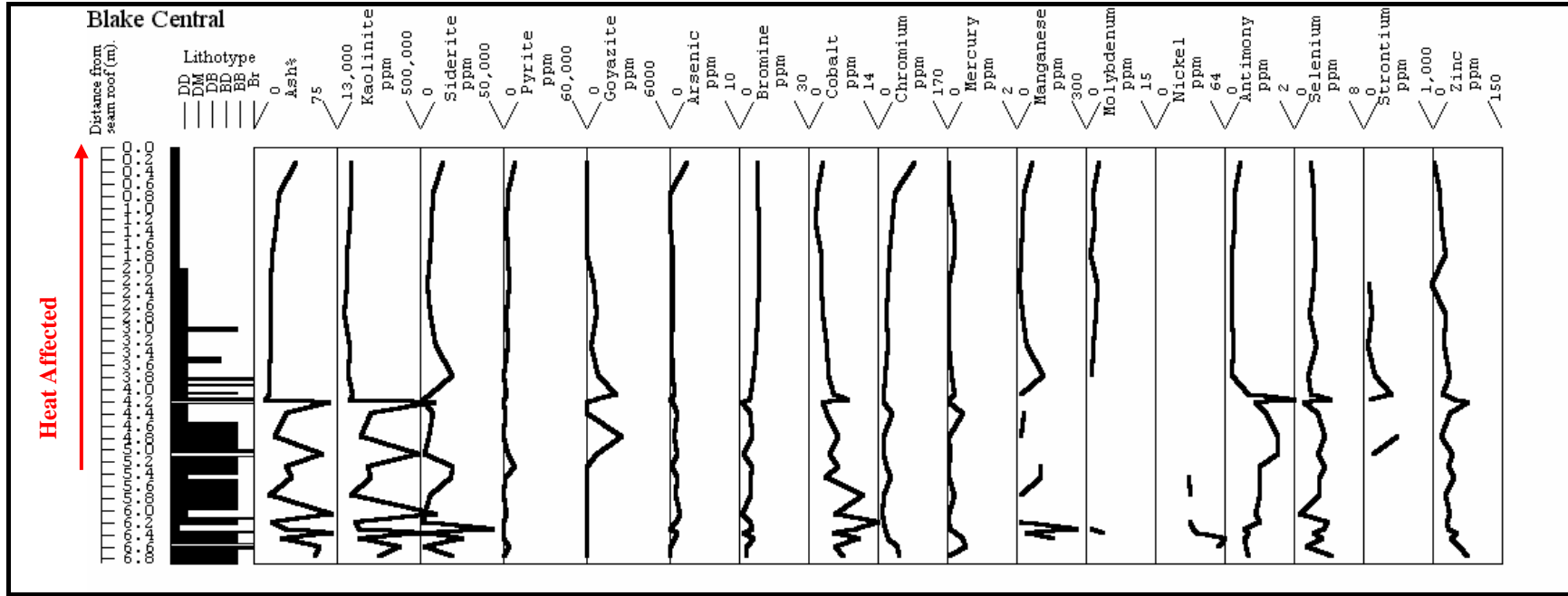


Figure 3.49. Strip Log Showing Vertical Changes in Minerals and Trace Elements in the Blake Central pit seam.

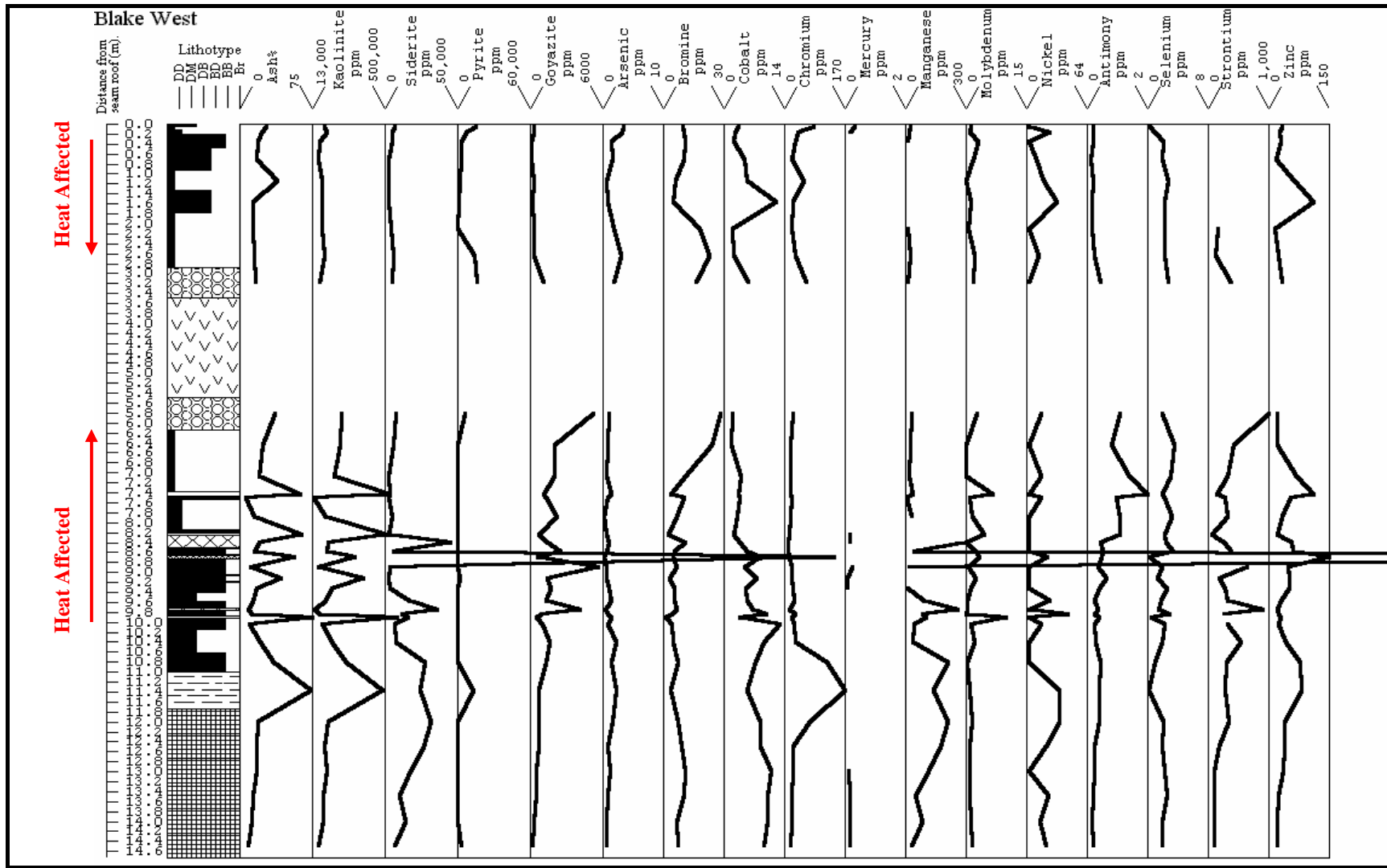


Figure 3.50. Strip Log Showing Vertical Changes in Minerals and Trace Elements in the Blake West pit seam.

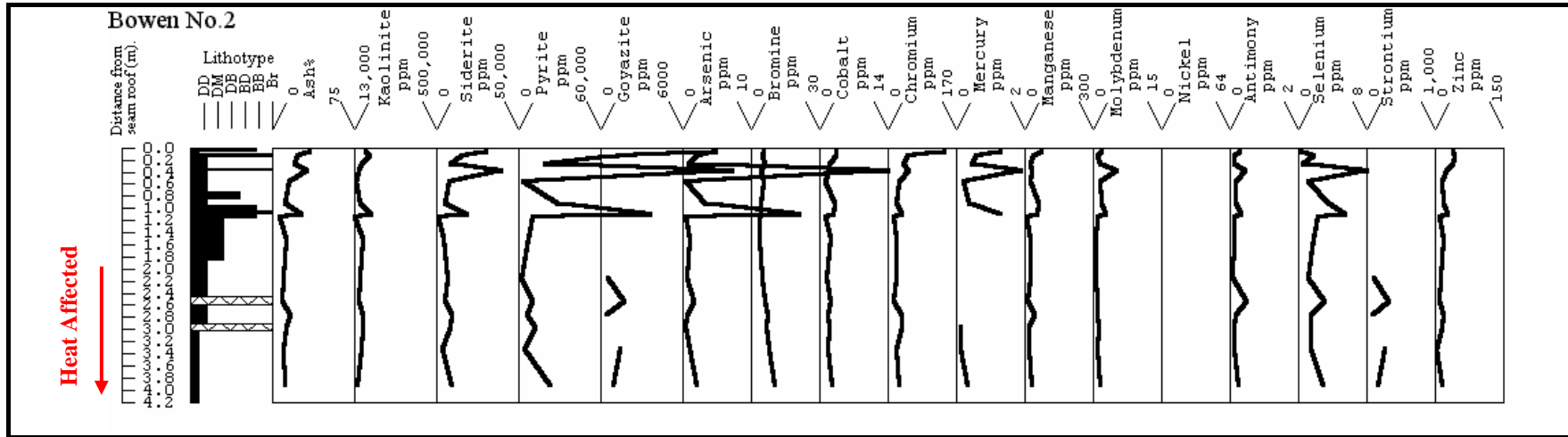


Figure 3.51. Strip Log Showing Vertical Changes in Minerals and Trace Elements in the Bowen No.2 pit seam.

Blake West Pit.

Figure 3.50. shows the vertical variation ash yield and the concentration of selected minerals and trace elements within the Blake West pit seam. The Blake West strip log shows high ash yields (and concentrations of kaolinite) do not generally occur within the heat affected zone (ie the entire upper section of the seam). Again this is ascribed to depositional factors rather than the emplacement of the intrusion. As noted for the Blake Central pit samples, the upper part of the Blake seam, particularly above the intrusive body, in the Blake West pit is free of partings. The lack of partings is attributed to deposition in more emergent mire during latter stages of peat accumulation. However, the difference in ash between the heat-affected and unaffected coal is less significant in the Blake West pit because some small ash partings were present in the heat-affected zone below the intrusion (Figure 3.50.), the altered igneous body being located within the seam itself in the Blake West pit (cf the Blake Central pit).

Siderite is generally present at higher concentrations away from the intrusion (in parallel with changes in the concentration of manganese, the index element for this mineral). However, one zone containing a very high concentration of siderite (as a nodule?) toward the lower margin of the heat-altered zone masks the general trend.

Pyrite is present at low concentrations throughout the Blake West seam, apart from increases at the roof of the seam, close to the intrusive body, and associated with the parting near the base of the seam. The distribution of pyrite concentrations is suggestive of secondary emplacement by hydrothermal solutions along significant lithological contacts. Such a “nuggety” distribution of pyrite may perturb the concentration trends and mask the influence of the igneous intrusion.

Goyazite concentration increases toward the margins of the intrusion (in parallel with changes in the concentration of strontium, the index element for this mineral).

The elements bromine, antimony and selenium show a strong trend of increasing concentration toward the intrusion. Chromium concentration also appears to be increasing toward the intrusion, but the trend is less clear, being partially confused by

variations in ash (as shown by the high concentration of chromium in the mudstone parting toward the base of the seam).

The elements cobalt, mercury, and nickel generally appear more concentrated away from the heat-affected zone, however localised concentrations associated with increased pyrite content (see above) obscure this trend. Molybdenum and zinc may also be more concentrated away from the heat-affected zone, but the trend is perturbed by variations related to ash yield.

Bowen No.2 Pit.

Figure 3.51. shows the vertical variation of ash yield and the concentration of selected minerals and trace elements within the Bowen No.2 pit seam. In the Bowen No.2 strip log, the low ash yield in the heat-affected part of the seam is thought to be due to decreased concentrations of siderite and pyrite (although a high pyrite concentration is present at the base of the seam). High concentrations of siderite and pyrite toward the roof of the seam are attributed to a combination of mineralisation by downward percolating groundwaters during early burial and the thermal decomposition of these minerals by heating at the base of the seam.

Goyazite/ strontium concentration increases downward into the heat-affected zone.

The concentration of arsenic, chromium, mercury, antimony, selenium, and zinc all mirror the behaviour of pyrite and decrease downward toward the floor of the seam (NB concerns regarding the pyrite mode of occurrence for chromium). The concentration of cobalt also shows a marginal increase away from the heat-affected zone. Undoubtedly, the downward decrease in the concentration of these elements is at least partly due the thermal affects of the igneous intrusion in the floor of the seam, but in part could also be due to downward diffusion of pyrite and associated trace elements during deposition of overlying marine sediments.

The element bromine shows a strong trend of increasing concentration into the heat-affected zone.

A trend for nickel could not be plotted because insufficient samples contained this element at concentrations above the detection limit of INAA. The behaviour of molybdenum is inconclusive.

3.4.2. Comparison of the Influence of Intrusions on Trace Elements at Collinsville with Other Examples.

The effect of igneous intrusions on the trace element concentration in coal elsewhere have been documented (Finkelman et al., 1998; Goodarzi, 1995b; Querol et al., 1997a).

Finkelman et al. (1998) studied the effect of a dike on a bituminous coal from Pitkin County, Colorado. They found elements such as fluorine, chlorine, mercury, and selenium were not depleted in coke or heat-affected coal, and attributed this to secondary enrichment following initial expulsion of these volatile elements. High concentrations of calcium, magnesium, iron, manganese, strontium, and CO₂ in the coked region were attributed to reactions with CO and CO₂, generated by initial coking of the coal, and migrating fluids from the intrusion to produce carbonates. Comparatively high concentrations of silver, mercury, copper, zinc, and iron were thought to be a consequence of precipitation of pyrite. The detailed ply-by-ply analysis described in Finkelman et al. (1998) was not attempted here because the ply sampling in the coked zone is considered too coarse.

Goodarzi (1995b) described a previous study by Goodarzi & Cameron (1990) on the influence of a dike on Canadian(?) coals. Goodarzi (1995) divides elements into three groups based on their behaviour upon heating. The first group for elements (example given is chlorine) undergo an apparent progressive depletion toward the dike from unaltered coal to altered coal. The second group of elements, including barium, bromine, chromium, vanadium, and zinc, show a sudden increase in concentration toward the outer edge of the heat-affected zone, and then decrease erratically toward the contact with unaltered coal. The behaviour of the second group of elements is ascribed to adsorption in the coke zone by coke and clay minerals. The third group of elements, including arsenic, molybdenum, sulphur, and antimony, appear little affected until a sudden increase is noted close to the contact. This distribution of elements is ascribed to an association with sulphides, such as pyrite, which break

down at temperatures encountered any closer to the intrusion. Goodarzi found “almost all elements except arsenic and zinc” were concentrated in the coke (manganese highly enriched, thorium very highly enriched).

Querol et al (1997) detailed the results of a study of heat-affected Fuxin coal from the Liaoning Province, China. The coal was heat affected by both dikes and sills. The authors found that only manganese was clearly enriched in coal influenced by the intrusion. The intrusion was not a major source of elemental mobilisation, but did induce major changes in major and trace element affinities. The changes in elemental affinity were thought to be a consequence of the mobilisation of organic, sulphide and carbonate associated elements.

The literature search revealed no consistent change in trace element concentration as a result of igneous intrusions. In this study, some consistent changes were noted between pits at Collinsville as follows:

- Pyrite is present in low concentrations in the Blake seam samples, with localised enrichment zones at the roof and floor of the seam, at the margins of the intrusion in the Blake West pit, and associated with a mudstone parting in the Blake West pit. Because the Blake seam was deposited in a non-marine environment and would likely have contained little pyrite to begin with, it is not possible to definitively ascribe the low concentration of pyrite in heat-affected samples to thermal alteration. Rather, the observed distribution of pyrite appears at least partially due to late stage deposition of this mineral at the margins of the seam and intrusive body. A late-stage deposition of pyrite from hydrothermal fluids is supported by the observation that the mineral generally occurs as a fracture infill in Blake seam petrographic samples. Pyrite in the Bowen No.2 pit seam is present in lower concentrations in heat-affected samples, although enrichment of pyrite at the roof and floor of the seam may indicate some late-stage deposition of this mineral. Further, downward enrichment from overlying marine deposited units cannot be discounted as an origin for the observed enrichment trend in the Bowen coal. Querol et al (1997) and Goodarzi (1995) both note that pyrite mobilisation occurred in heat-affected samples. Mobilisation of pyrite by thermal alteration

is not conclusively proven here, although it appears likely for the Bowen No.2 seam.

- Siderite is present at lower concentrations in heat-affected samples from all the sampled pits, although as with pyrite, some localised concentrations of this mineral may occur at the roof and floor of the seam, and may have also be due to late stage mineralisation. Manganese is depleted in heat-affected samples from all three pits, mirroring the decreased concentration of siderite in heat-affected samples. However, a localised zone containing a very high concentration of siderite and manganese within the heat-affected zone has obscured the trend in the Blake West pit samples. Carbonates are known to thermally dissociate at comparatively low temperatures (~400°C) (Dubrawski and Warne, 1987) (370 – 530°C) (Maes et al., 2000). Therefore, relatively little heating could have liberated this element from the siderite crystal lattice, allowing migration out of the heat-affected coal. Querol et al (1997) note manganese as the only element definitively depleted in heat-affected samples in their study. Finkelman et al (1998) found high manganese concentrations in heat-affected samples associated with high concentrations of carbonates. It is concluded that manganese and, therefore, siderite are depleted in heat-affected coal. However, some enrichment of siderite and manganese appears to have occurred at and immediately below the heat affected coal in the Blake West pit seam.
- Goyazite shows a marked trend of increasing concentration toward the intrusion in the Blake West and Bowen No.2 seam samples, and is increased at the edge of the heat affected zone in the Blake Central samples. Strontium obviously mirrors the distribution of goyazite (strontium being the index element used to calculate goyazite concentration in the normative calculations). The concentration of strontium is universally low (generally below the limit of detection) in samples unaffected by heat. Further, both barium and strontium are present in the Bowen seam at low concentrations, in the Blake Central samples at intermediate concentrations, and in the Blake West samples at high concentrations, approximately mirroring the degree of heat alteration experienced in each pit. Finkelman et al (1998) also found strontium to be enriched in heat-altered zones close to igneous intrusions.

Goodarzi (1995) observed a very similar behaviour in heat-affected Canadian coals. It is concluded that strontium-bearing goyazite is enriched at the margins of the heat-affected zone.

- Bromine is substantially enriched in the heat-affected samples from all the seams, in particular the Blake West pit seam, where the intrusion is located within the seam itself (see Figures 3.46., 3.47. & 3.48.; also Appendix 6, Figures A61C and A62D). It is curious that such a highly volatile element should be enriched in heat-affected coal. However, enrichment of this element in heat-affected samples cannot be simply the result of concentration by devolatilisation of the coal (enrichment exceeds 50% in all samples; Table 3.13.). The behaviour of bromine in the Blake and Bowen seam pits is similar to the behaviour outlined by Goodarzi (1995). Goodarzi (1995) stated the behaviour was “possibly due to mobilisation and migration” of bromine in fluids “into porous coke..” “..which acted as a trap for mobilised elements”. However, in this study there is no consistent evidence for bromine depletion in heat-altered coke at the margins of the intrusions (Figures 3.47.) and the element is enriched right through to the contact with the roof (Figure 3.46.) and floor (Figure 3.48.) of the seam. Therefore, it is inferred that bromine was enriched by hydrothermal fluids associated with the intrusion and trapped in the coke and heat-affected coal.
- Cobalt is substantially depleted in heat-altered samples from both the Blake Central and Blake West, and appears slightly depleted in heat-altered samples from the Bowen No.2 pit. Cobalt is organically bound in the Blake seam samples, and associated with pyrite in the Bowen seam samples. Possibly the different mode of occurrence of cobalt could be the cause of the variable depletion, with pyrite perhaps marginally less susceptible to mild thermal alteration than the organic fraction of the coal.
- Chromium appears to increase in concentration toward the intrusion in the Blake Central and Blake West pits (although the trend is partially obscured by ash variations in the Blake West pit. Chromium in the Bowen No.2 pit increases away from the intrusion, possibly due to the association of this element with pyrite in the Bowen seam (although this association may not be chemical). It is concluded the behaviour of chromium in response to thermal

alteration is determined to some degree by the mode of occurrence of the element.

- Mercury is depleted in heat-affected samples from all three pits. Mercury is probably associated with pyrite in all three pits, and the degree of depletion is related to the concentration of pyrite in the coal (being most marked in the pyrite-rich Bowen No.2 pit seam). Finkelman et al (1998) found that mercury was not depleted in heat-affected samples due to secondary enrichment by the intrusion. Secondary enrichment of mercury may have occurred in zones where pyrite is enriched, however this may not be directly attributable to the igneous intrusions.
- Molybdenum is enriched in the heat-affected Blake seam samples. Molybdenum has a mixed organic/ inorganic mode of occurrence in the Blake Central pit, and an inorganic mode of occurrence in the Blake West pit. Molybdenum is depleted in heat-affected samples from the Bowen No.2 pit. Molybdenum is associated with pyrite in the Bowen No.2 pit seam. As for chromium, it is suggested that differences in the behaviour of molybdenum with respect to the igneous intrusion are due to the different mode of occurrence of this element.
- Nickel appears to be depleted in heat-affected samples from all the sampled pits. Note, however, that nickel does not plot in the Bowen No.2 pit strip log due to insufficient samples being above the detection limit, possibly but not demonstrably due to the intrusion-controlled depletion of this element.
- Zinc is depleted in heat-affected samples from the Blake Central and Bowen No.2 pits. An apparent association of zinc with some high ash bands within heat-affected zone in the Blake West pit makes determination of the effect of the igneous intrusion on the distribution of zinc difficult for the Blake West samples. The mode of occurrence for zinc is uncertain or obscure between pits. The Blake Central zinc appears to be organically bound or associated with pyrite. Zinc in the Blake West pit appears to show a mixed inorganic/ organic affinity. The Bowen seam samples suggest zinc is associated with pyrite in the Bowen No.2 pit. The organic/ pyrite bound Blake Central and pyrite associated Bowen No.2 samples show the greatest depletion, whereas the mixed organic/ inorganic Blake West samples exhibit the least depletion

(in spite of the high degree of thermal alteration in the Blake West pit). The apparent lesser degree of depletion in the Blake West pit could be due to the association of zinc with a less volatile mineral phase such as a clay mineral, or capture by a less volatile mineral phase following heat-induced mobilisation. Goodarzi (1995) noted that zinc was one of the few elements not enriched in coke in their study area.

Less consistent trends were observed for the following elements:

- The concentration of arsenic appears to increase away from the intrusion in the Blake Central pit, however a trend of concentration change was not observed for the Blake West pit.
- A trend of change was not observed for selenium in the Blake Central pit. However, selenium concentration appears to increase toward the intrusion in the Blake West pit. A secondary enrichment would be consistent with the inferences of selenium behaviour made by Finkelman et al (1998).
- Antimony appears to increase in concentration away from the intrusion in the Blake Central pit, and toward the intrusion in the Blake West pit.
- The concentration of arsenic, selenium, and antimony are depleted in heat-affected samples from the Bowen No.2 pit. It is concluded the depletion of these elements is due to loss of pyrite from heat-affected samples from the Bowen No.2 pit.

It concluded that the concentration trends of bromine, cobalt, and strontium are most definitively controlled by proximity to igneous intrusions. It is probable that the proximity of igneous intrusions also exerts an underlying control on the distribution of arsenic, mercury, manganese, and nickel, although late-stage deposition of localised concentrations of siderite and pyrite has obscured concentration trends for trace elements associated with these phases. In addition zinc appears to be generally depleted in heat affected samples.

3.5. Chapter Summary.

Ply-by-ply channel samples from the Blake seam (Blake Central and Blake West pits) and the Bowen seam (Bowen No.2 seam) have been characterised using proximate analysis, maceral analysis, and measurement of vitrinite reflectance. All the Collinsville coal has been found to be inertinite rich. The Blake seam coal averages around $Ro(max) \sim 1.20\%$ (Blake Central) to $Ro(max) \sim 1.30\%$ (Blake West). The Bowen seam is lower reflectance, averaging $\sim Ro(max) 1.10\%$. Lithotype variation and the frequency of partings have been used to infer a fluvial depositional environment for the Blake seam, and a fluvial paralic depositional environment for the Bowen seam. The presence or absence of semi-coke has been used to indicate significant heat alteration of the coal. Where petrographic samples were unavailable, it is assumed heat alteration extends approximately as far above the intrusion as it does below the intrusion in the Blake West pit.

Analysis of the ply samples by XRF, INAA, and LECO SC32 (for sulphur) was undertaken. Normative analysis was used to calculate the mineral assemblage of the samples. Mineral matter in the Blake seam includes alkali feldspar, illite, kaolinite, quartz, goyazite, gorceixite, siderite, pyrite, and anatase. Mineral matter in the Bowen No.2 pit seam includes illite, kaolinite, quartz, goyazite, gorceixite, siderite, pyrite, and anatase/ rutile. In addition, a heavy mineral suite including zircon is indicated from hafnium/ uranium relationships. Normative analysis results were calibrated using XRD analysis of oxygen plasma low temperature ash (OP-LTA) for selected samples.

Elemental analysis showed the concentration of most trace elements is within the range exhibited by coals from other locations. However, the Blake seam channel samples contained higher than average concentrations of gold, copper, hafnium, thorium, and possibly ytterbium; and the Bowen No.2 seam channel samples contained higher than average concentrations of gold and copper.

Trace element mode of occurrence was inferred using graphical relationships with normative mineral matter concentrations. A summary table showing the mode of

occurrence for the trace elements analysed are presented in Table 3.7. (Blake Central and Blake West seam samples) and Table 3.9. (Bowen No.2 seam samples).

The impact of igneous intrusions on the concentration of trace elements in the coal was assessed using weighted average concentrations for heat-affected and unaffected zones within the seam and from trends of concentration change inferred from strip logs. The impact of igneous intrusions was found to show few consistencies between data sets (as also noted in other literature examples). However, the concentration of bromine, cobalt, and strontium are controlled by the proximity to the igneous intrusion. Arsenic, mercury, manganese, nickel, and zinc also show an underlying concentration change related to proximity to igneous intrusions.

Chapter 4.

Trace Element Concentration and Mode of Occurrence in Selected Pulverised Fuel Combustion Plant Samples.

4.0. Chapter Resume.

Pulverised fuel samples were collected from Australian and Japanese coal fired power plants, and were analysed for a range of trace and major elements by INAA and XRF. In addition, the samples were subjected to the USGS sequential-leaching procedure to infer the mode of occurrence of a number of trace elements in the coal.

4.1. Sample Description.

Pulverised fuel samples were gathered from two pulverised fuel combustion plants, as follows:

- The Collinsville Power Station, Collinsville, Northern Queensland, Australia. The Collinsville power station at time of sampling burnt a blend comprising 70% Blake Seam coal and 30% Bowen Seam coal. The coal was mined from the Blake West, Blake Central, and Bowen No.2 pits at the Collinsville Opencast mine to meet a specification of ~20% (adb) ash. A schematic of the Collinsville power station with sampling points is shown in Figure 4.1.
- The Mitsui Coal Mining power plant, Omutu City, Kyushu, Japan. The Mitsui Coal Mining plant at the time of sampling burnt a blend of coal from Indonesia, China, and low-grade high-ash domestic coal, with some Russian coal from time to time at a blended ash specification of ~12% (adb). A schematic of the Mitsui power station with sampling points is shown in Figure 4.2.

The samples were deliberately gathered from two disparate power plants in order to maximise the chance of sampling two feed coals with some significant differences in trace element mode of occurrence. The aim is to examine the control mode of occurrence exerts on the partitioning behaviour of a trace element in combustion (Section 8.2.).

Sampling of the pulverised fuel at the Collinsville combustion plant was undertaken by Ian Borthwick (plant manager), observed by the author, using an isokinetic sampling probe. The fuel in-feed pipe to the Number 3 burner was sampled. The probe was positioned and the stream of pulverised fuel sampled approximately according to the 12 point sampling procedure (Figure 4.3.). Sampling at the Japanese Mitsui power station was undertaken by plant personnel and was not observed by the author. The sampling method employed at the Mitsui power station is uncertain.

Proximate analysis and major and trace element analysis results of the pulverised fuel samples are presented in Table 4.1.

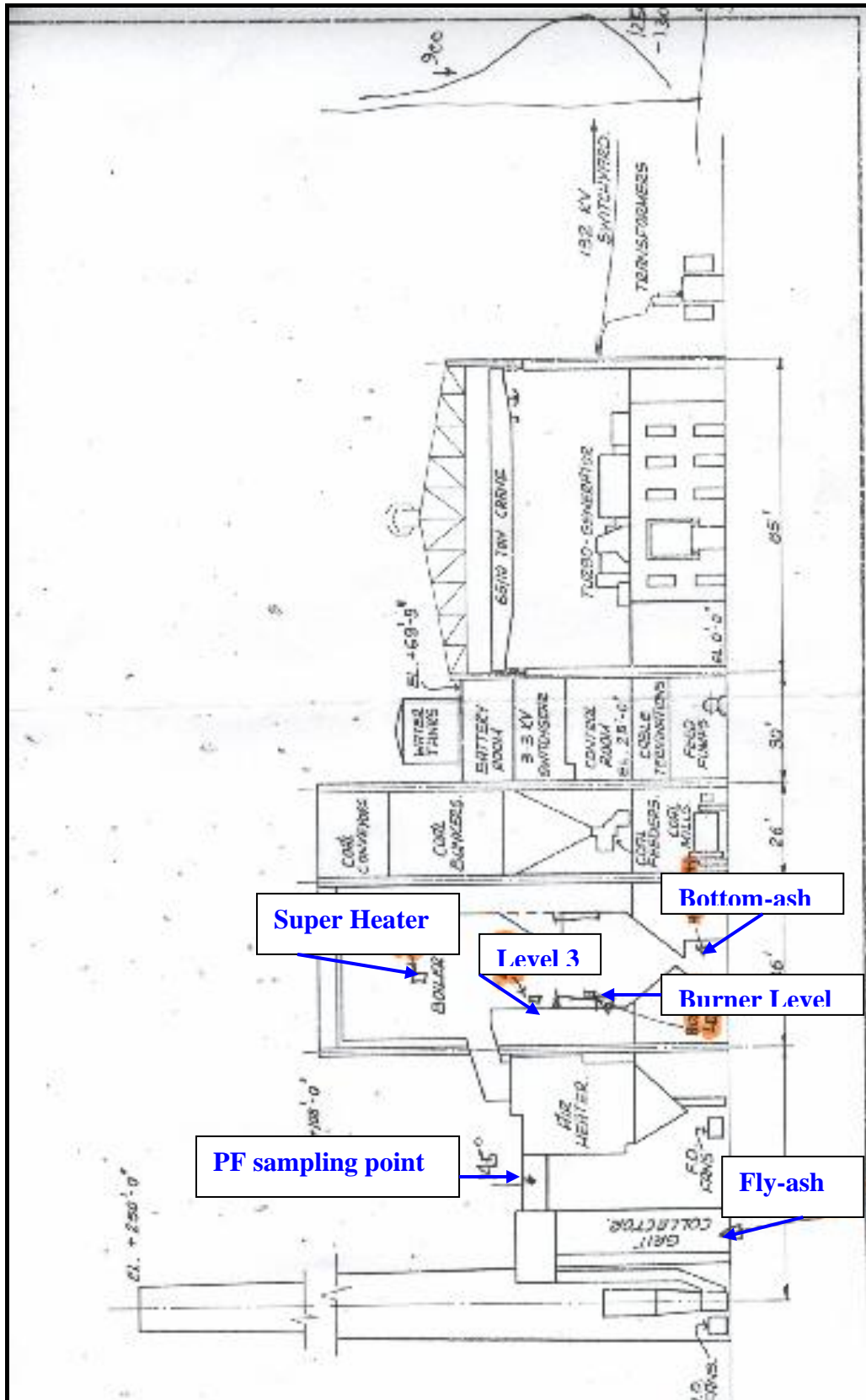


Figure 4.1., Schematic of the Collinsville coal fired power plant showing sampling points.

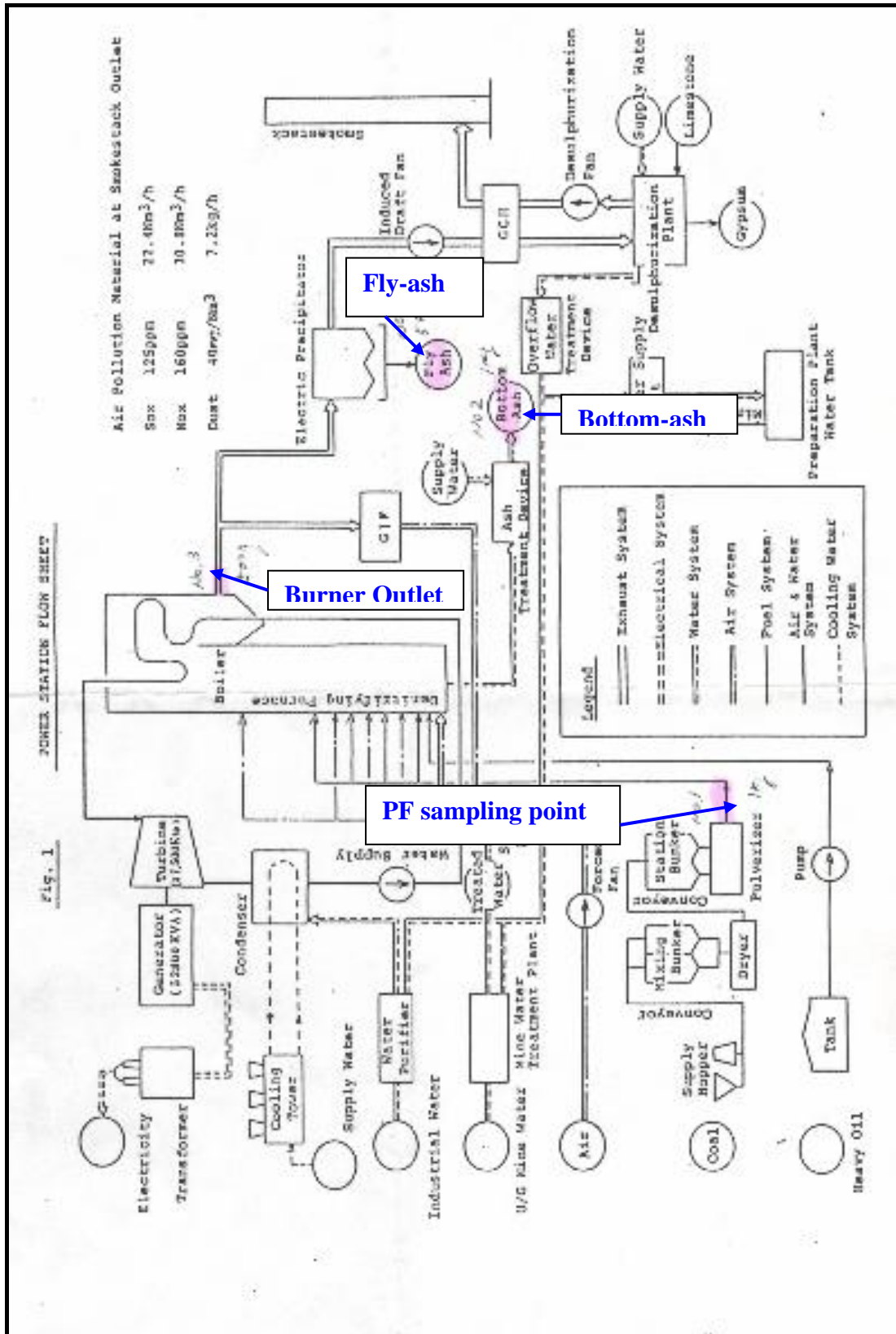


Figure 4.2., Schematic of the Mitsui Mining combustion plant showing sampling points.



THIS IMAGE HAS BEEN REMOVED DUE TO
COPYRIGHT RESTRICTIONS

Figure 4.3., Positions for Isokinetic Sampling.

Source: (Sloss and Gardner, 1995)

4.2. Sample Analysis.

The sample of Collinsville pulverised fuel was split by cone and quartering, and a representative sub-sample sent to Actlabs, Perth, Australia, for analysis by INAA. A further split was dispatched to SGS Ngakawau, New Zealand, for sulphur analysis as well as low-temperature (400°C) ashing. The low-temperature (400°C) ash was then on-sent for analysis for major elements using XRF at Spectrachem laboratories Wellington, New Zealand. The remainder of the sample was despatched to the USGS laboratory at Reston, Virginia, U.S.A. for analysis for a range of trace elements and sequential leach testing (details of the USGS sequential leaching procedure can be found in Section 1.3.2.2.).

A graph of the INAA/ XRF results versus the USGS results (Figure 4.4.) shows a positive relationship, although there are a number of differences in the results for some elements. Where two methods of analysis were employed by the USGS, and one method was INAA, the INAA result is used in preference to the results of the other method. Some of the variability can be ascribed to different detection limits between the two laboratories for a particular element (eg Actlabs INAA has a detection limit of 30ppm for Ni, whereas the USGS INAA and ICP-AES combination analysis was able to measure nickel content below 30ppm). In general the scatter in the data suggests the inter-laboratory variability between the two data sets is quite high. One particularly notable example of this variability is the analysis results for calcium, the Actlabs INAA result being 100,000ppm, the USGS result 470ppm. By converting the major elements to oxide concentrations and summing the results, a reasonable agreement between the USGS oxide-ash yield (22%) and the determined ash yield (21.2%) was found. However, the oxide ash yield for the INAA results was found to be 34.65% (even excluding the anomalously high INAA iron figure). Use of the USGS calcium figure in place of the INAA calcium figure gave an oxide-ash yield of 20.7%, a figure in much better agreement with the determined ash yield of 21.2%. Further, the good agreement with the determined ash yield figure once the INAA calcium is removed and replaced with the USGS number suggests the other INAA and XRF major element figures have a reasonable precision, in spite of the inter-laboratory data scatter indicated by Figure 4.4.. The INAA calcium figure is ignored in favour of the USGS calcium figure for the rest of this project. Note, the INAA figure for iron in the Collinsville pulverised fuel sample appears to be a typographical error, and the XRF and USGS figure of 7400ppm is used hereafter.

Overall the inter-laboratory differences shown in Table 4.2. suggest the INAA figures are high by comparison with the USGS data. Because INAA figures are available for all the fly-ash samples (Chapter 5), the INAA figures are used in preference to the USGS figures (as outlined in Section 2.5.) under the assumption that errors in analysis are consistent within the INAA data set. The USGS data is used only for determination of mode of occurrence using the sequential leaching protocol and will, therefore, not bias calculation of partitioning behaviour in Chapter 5.

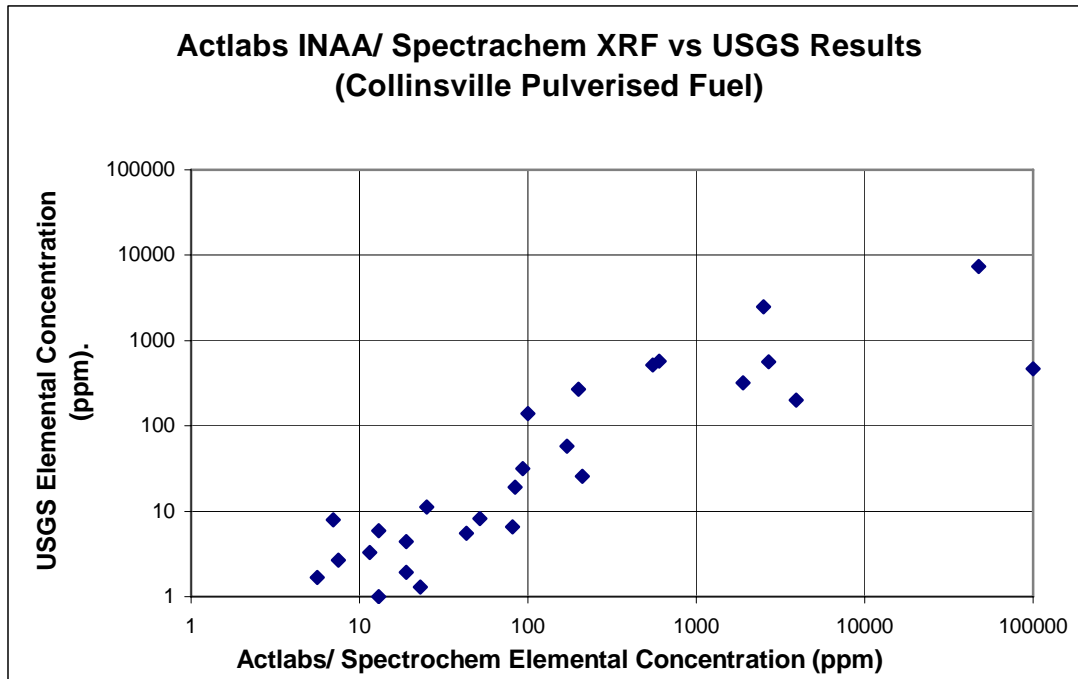


Figure 4.4., INAA/ XRF results vs the USGS results for Collinsville pulverised fuel.

The sample of Japanese pulverised fuel was split by cone and quartering, and a representative sample was sent to Actlabs, Perth, Australia for analysis by INAA. A further split was despatched to SGS Ngakawau, New Zealand for sulphur analysis and low temperature (400°C) ashing. Again, the low-temperature (400°C) ash was then on-sent for analysis for major elements using XRF at Spectrachem laboratories, Wellington, New Zealand. The remainder of the original coal sample was despatched to a laboratory set up by CRL Energy at Canterbury University, Christchurch, New Zealand for sequential leach testing using the USGS methodology. The leachates produced by the sequential leaching procedure were analysed using Microwave-ICP-MS at Agriquality, Wellington, New Zealand.

A graph of the INAA/ XRF results versus the Agriquality microwave inductively coupled plasma mass spectrometry (MW-ICP-MS) results (Figure 4.5.) shows a good positive relationship. The scatter in the Japanese data set is less than the scatter in the Collinsville data set suggesting the interlaboratory analysis variability is smaller. However, if a trend line were fitted to the data in Figure 4.5., the data would still not approach unity, and indicates the MW-ICP-MS generally underestimates the concentrations of the elements analysed compared to the XRF and INAA results. If Figure 4.5. is taken to indicate a systematic error, two possible reasons can be

forwarded; 1) the microwave digestion of the sample prior to ICP analysis did not completely dissolve the sample; 2) the ICP-MS is not properly calibrated.

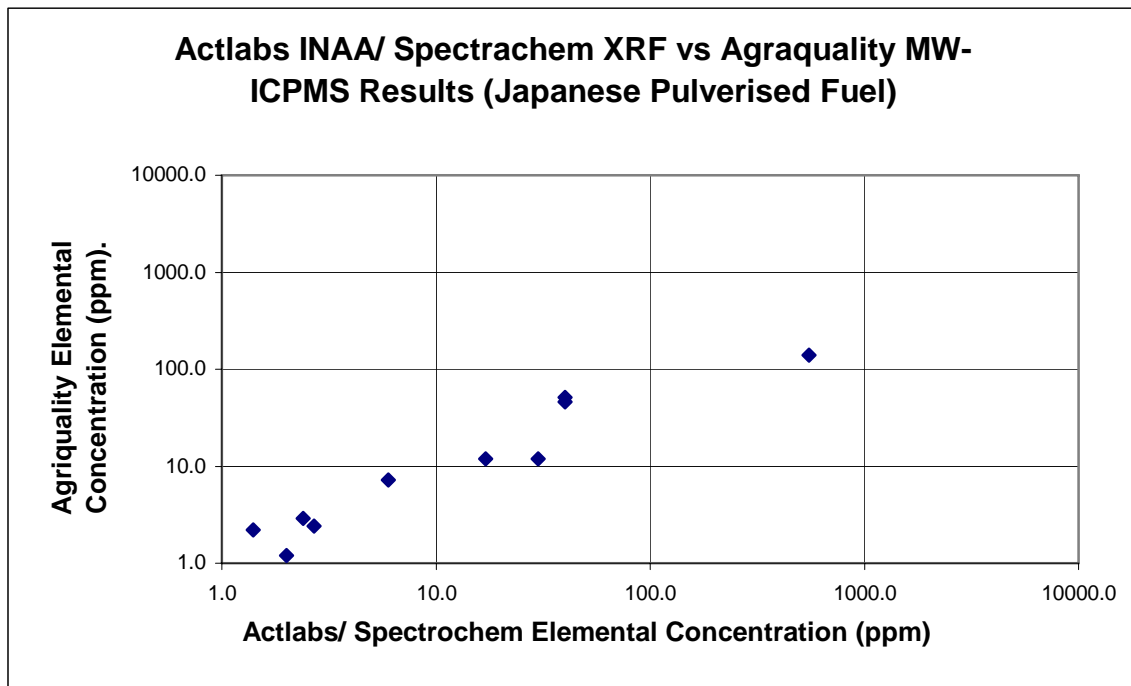


Figure 4.5., INAA/ XRF results vs MW-ICP-MS results for Japanese pulverised fuel.

4.3. Analysis Results.

Table 4.1. presents the analysed concentration of major and trace elements in the Collinsville and Japanese pulverized fuel samples and the respective world coal average concentration ranges as estimated in Swaine (1990). INAA analysis suggests gold, cerium, cobalt, europium, hafnium, lanthanum, lutetium, molybdenum, neodymium, scandium, selenium, samarium, strontium, tantalum, thorium, tungsten and ytterbium are at the upper end or above the world average concentration range in the Collinsville pulverized fuel. Only gold, hafnium, and thorium are at the upper end or above the world coal concentration range in the Japanese pulverized fuel. All other elements are present at concentrations comfortably within their respective world ranges.

Table 4.1., Analysis Results for Collinsville and Japanese Pulverized Fuel Samples by Analysis Method.

	Collinsville Power Pulverised Fuel INAA	Collinsville Power Pulverised Fuel USGS	USGS METHOD	Mitsui Power Plant Pulverised Fuel INAA	Mitsui Power Plant Pulverised Fuel MW-ICP-MS	World Coal Ranges (Swaine, 1990)
Analysis - Air Dried Basis						
Total Moisture						
Moisture% ISO 5068-1983	1.1			3.7		
Ash% ISO 1171-1981	21.2			12.5		
Volatile Matter% ISO 562-1981	17.0			36.5		
Fixed Carbon %	60.7			47.3		
Major Elements						
Si (PPM)		60000.0	AES	20900.0		
Al (PPM)		39000.0	AES	16800.0		
Fe (PPM) (INAA)	47400	7400	INAA/AES	7550		
Fe (PPM) (XRF)	7400			5800		
Ca (PPM)	100000	470	AES	<0.03		
Mg (PPM)		270	AES	1000		
Na (PPM)	3910	200	INAA/AES	193		
K (PPM)	<2700	560	INAA/AES	<0.05		
Ti (PPM)				1200.0		10 - 2000
Mn (PPM)		140	AES	40	51	5 - 300
P (PPM)		570.0	AES	600.0		10 - 3000
S (%)	0.48			0.78		

Table 4.1., Analysis Results for Collinsville and Japanese Pulverized Fuel Samples by Analysis Method (continued).

	Collinsville Power Pulverised Fuel INAA	Collinsville Power Pulverised Fuel USGS	USGS METHOD	Mitsui Power Plant Pulverised Fuel INAA	Mitsui Power Plant Pulverised Fuel MW-ICP-MS	World Coal Ranges (Swaine, 1990)
Trace Elements (PPM in Whole Coal)						
Au (PPB)	51.6			1.8		0.01
Ag (PPM)	<0.3			<0.3		0.02 - 2
As (PPM)	23	1.3	INAA/AES	1.4	2.2	0.5 - 80
B (PPM)		9.7	AES		72	5 - 400
Ba (PPM)	550	520	INAA/AES	550	140	20 - 1000
Be (PPM)		1.5	AES		0.88	0.1 - 15
Br (PPM)	7	7.96	INAA	6		0.5 - 90
Cd (PPM)		0.07	AES		0.09	0.1 - 3
Ce (PPM)	170	57.6	INAA	57		2 - 70
Co (PPM)	43	5.5	MS	6	7.2	0.5 - 30
Cr (PPM)	84	19	INAA/AES	17	12	0.5 - 60
Cu (PPM)		18	AES		18	0.5 - 50
Cs (PPM)	2.2	0.96	INAA/AES	0.93		0.3 - 5
Eu (PPM)	3.94	0.74	INAA	0.81		0.1 - 2
Hf (PPM)	19	4.38	INAA	5.7		0.4 - 5
Hg (PPM)	-0.5	0.07	VAA	-0.05		0.02 - 1
Ir (PPM)	-0.1			-0.1		
La (PPM)	93	31.3	INAA	33		1 - 40
Li (PPM)		37	INAA/AES			1 - 80
Lu (PPM)	2.08	0.42	INAA	0.566		0.03 - 1
Mo (PPM)	13	1	AES	2.7	2.4	0.1 - 10
Nd (PPM)	81	6.61	INAA	24		3 - 30
Ni (PPM)	<30	36	INAA/AES	30	12	0.5 - 50
Pb (PPM)		19	MS		7.2	2 - 80
Rb (PPM)	<5	5.7	INAA/MS	4		2 - 50
Sb (PPM)	2.6	0.45	INAA/MS	0.45	0.4	0.05 - 10
Sc (PPM)	52	8.17	INAA/AES	8.9		1 - 10
Se (PPM)	19	1.92	INAA/HG	2.4	2.9	0.5 - 10 ?
Sm (PPM)	13	5.9	INAA	5		0.5 - 6
Sn (PPM)		4.5	MS		1.6	1 - 10
Sr (PPM)	1900	320	INAA/AES	280		15 - 500
Ta (PPM)	2.1			0.81		0.1 - 1
Tb (PPM)	2.7	0.81	INAA	0.9		0.5 - 4
Th (PPM)	25	11.2	INAA/AES	11		0.5 - 10
Tl (PPM)		0.3	MS			0.2 - 1
U (PPM) (INAA)	7.5	2.66	INAA/MS	2	1.2	0.5 - 10
U (PPM) (XRF)		26	AES		45	2 - 100
V (PPM)	5.6	1.68	INAA	2.5		0.5 - 5
W (PPM)		6.1	AES			2 - 50
Y (PPM)	11.5	3.3	INAA	3.67		0.3 - 3
Yb (PPM)	210	25.5	INAA/AES	40	46	5 - 300
Zn (PPM)		144	AES			5 - 200

4.4. Mode of Occurrence from Sequential Leach Data.

Table 4.2. presents the raw sequential leach data. The figures in Table 4.2. are determined using the USGS sequential leaching protocol (see Section 1.3.2.2. for further explanation). The percentages in Table 4.2. are calculated from the concentration of that element in each leachate as a percentage of the concentration of the element in the pulverised fuel sample. The sequential leach data is interpreted using Figures 4.6. to 4.27 with accompanying explanations below.

Table 4.2. Raw Sequential Leaching Results

Element	Collinsville pf	Japanese pf	Element	Collinsville pf	Japanese pf
Al	% Extracted	% Extracted	La	% Extracted	% Extracted
AmAc	0		AmAc	0	
HCl	0		HCl	0	
HF	90		HF	10	
HNO3	0		HNO3	70	
Fe	% Extracted	% Extracted	Li	% Extracted	% Extracted
AmAc	0		AmAc	0	
HCl	75		HCl	0	
HF	10		HF	90	
HNO3	15		HNO3	0	
Ca	% Extracted	% Extracted	Lu	% Extracted	% Extracted
AmAc	25		AmAc	5	
HCl	60		HCl	0	
HF	15		HF	10	
HNO3	0		HNO3	35	
Mg	% Extracted	% Extracted	Mo	% Extracted	% Extracted
AmAc	20		AmAc		25
HCl	45		HCl		7
HF	25		HF		50
HNO3	0		HNO3		0
Na	% Extracted	% Extracted	Ni	% Extracted	% Extracted
AmAc	30		AmAc	15	0
HCl	10		HCl	10	44
HF	55		HF	40	
HNO3	0		HNO3	5	3
K	% Extracted	% Extracted	Pb	% Extracted	% Extracted
AmAc	5		AmAc	0	0
HCl	5		HCl	40	93
HF	90		HF	10	15
HNO3	0		HNO3	15	22
Ti	% Extracted	% Extracted	Rb	% Extracted	% Extracted
AmAc	0		AmAc	5	
HCl	0		HCl	5	
HF	70		HF	90	
HNO3	0		HNO3	0	
Mn	% Extracted	% Extracted	Sb	% Extracted	% Extracted
AmAc	5	10	AmAc	0	2
HCl	90	144	HCl	20	25
HF	0	14	HF	10	17
HNO3	0	6	HNO3	15	0

Table 4.2. Continued

Element	Collinsville pf	Japanese pf	Element	Collinsville pf	Japanese pf
P	% Extracted	% Extracted	Sc	% Extracted	% Extracted
AmAc	0		AmAc	0	
HCl	15		HCl	15	
HF	75		HF	40	
HNO3	10		HNO3	0	
As	% Extracted	% Extracted	Se	% Extracted	% Extracted
AmAc	0	6	AmAc	0	0
HCl	30	0	HCl	0	0
HF	40	64	HF	0	0
HNO3	10	14	HNO3	40	0
B	% Extracted	% Extracted	Sm	% Extracted	% Extracted
AmAc	10	20	AmAc	0	
HCl	20	27	HCl	5	
HF		0	HF	10	
HNO3	60	77	HNO3	70	
Ba	% Extracted	% Extracted	Sn	% Extracted	% Extracted
AmAc	0	8	AmAc	15	0
HCl	10	61	HCl	5	0
HF	65	72	HF	70	0
HNO3	20	12	HNO3	10	0
Be	% Extracted	% Extracted	Sr	% Extracted	% Extracted
AmAc	10	5	AmAc	0	
HCl	30	5	HCl	5	
HF	65	140	HF	80	
HNO3	15	11	HNO3	5	
Br	% Extracted	% Extracted	Ta	% Extracted	% Extracted
AmAc	0		AmAc	0	
HCl	0		HCl	0	
HF	15		HF	30	
HNO3	10		HNO3	5	
Cd	% Extracted	% Extracted	Tb	% Extracted	% Extracted
AmAc		0	AmAc	0	
HCl		116	HCl	10	
HF		86	HF	10	
HNO3		0	HNO3	55	
Ce	% Extracted	% Extracted	Th	% Extracted	% Extracted
AmAc	0		AmAc	0	
HCl	0		HCl	5	
HF	10		HF	10	
HNO3	70		HNO3	55	
Co	% Extracted	% Extracted	Tl	% Extracted	% Extracted
AmAc	15	5	AmAc	0	
HCl	10	29	HCl	0	
HF	20	14	HF	50	
HNO3	10	0	HNO3	15	

Table 4.2. Continued

Element	Collinsville pf	Japanese pf	Element	Collinsville pf	Japanese pf
Cr	% Extracted	% Extracted	U	% Extracted	% Extracted
AmAc	0	0	AmAc	0	0
HCl	5	16	HCl	5	10
HF	45	54	HF	35	47
HNO3	5	3	HNO3	30	8
Cs	% Extracted	% Extracted	V	% Extracted	% Extracted
AmAc	25		AmAc	0	0
HCl	15		HCl	0	0
HF	55		HF	65	66
HNO3	0		HNO3	0	0
Cu	% Extracted	% Extracted	W	% Extracted	% Extracted
AmAc	0	9	AmAc	0	
HCl	5	66	HCl	5	
HF	20	45	HF	50	
HNO3	25	13	HNO3	5	
Eu	% Extracted	% Extracted	Y	% Extracted	% Extracted
AmAc	0		AmAc	5	
HCl	5		HCl	35	
HF	10		HF	30	
HNO3	70		HNO3	10	
Hf	% Extracted	% Extracted	Yb	% Extracted	% Extracted
AmAc	0		AmAc	5	
HCl	0		HCl	0	
HF	45		HF	10	
HNO3	0		HNO3	35	
Hg	% Extracted	% Extracted	Zn	% Extracted	% Extracted
AmAc	30		AmAc	5	3
HCl	0		HCl	70	70
HF	5		HF	5	20
HNO3	20		HNO3	10	4
			Zr	% Extracted	% Extracted
			AmAc	0	
			HCl	0	
			HF	30	
			HNO3	0	

Antimony.

Figure 4.6. shows the proportions of antimony mobilised by the reagents employed. Sequential leaching of the Collinsville coal sample suggests multiple modes of occurrence for antimony in the coal. The nitric acid and hydrochloric acid soluble fractions are ascribed to pyrite and HCl leachable sulphides respectively (Palmer et al., 1998). The proportion of antimony mobilised by hydrofluoric acid is inferred to indicate some proportion of this element is associated with aluminosilicates. In addition, a large proportion of antimony in the Collinsville sample was not mobilised by the sequential leaching procedure (~55%), indicating either an organic mode of occurrence or shielding of inorganic mineral grains from dissolution by the organic matter (Willett et al., 2003). An organic mode of occurrence for antimony is one of the less common modes for this element (see Appendix 2).

The sequential leaching results for the Japanese pulverised fuel sample also suggest multiple modes of occurrence for antimony. The hydrochloric acid soluble proportion of antimony is again attributed to HCl soluble sulphides. Antimony mobilised by hydrofluoric acid is taken to imply a proportion of this element is associated with aluminosilicates. As noted for the Collinsville coal sample, a large proportion (~56%) of antimony in the Mitsui sample was not mobilised by any of the reagents. The unmobilised fraction of antimony in the Japanese coal is again considered to indicate either an organic mode of occurrence or shielding of inorganic mineral grains from dissolution by the organic matter.

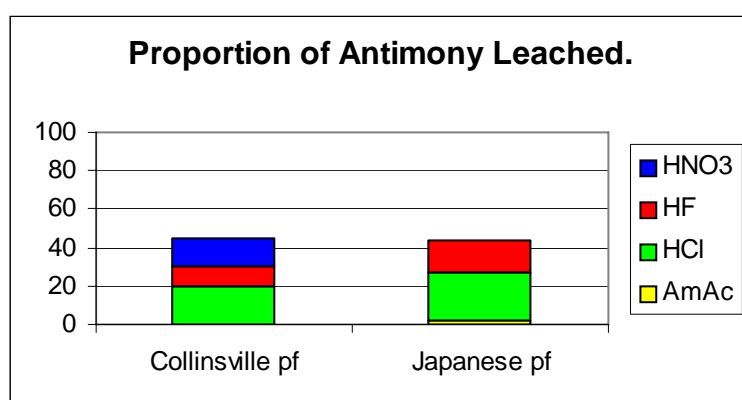


Figure 4.6., Proportions of Antimony Leached.

Arsenic

Figure 4.7. shows the proportions of arsenic mobilised by the reagents employed. The obvious result of sequential leach testing of samples from the Collinsville and Japanese Power utilities is the comparatively minor proportion of arsenic leached by nitric acid (10% and 14% respectively). Appendix 2 shows that the most frequently cited mode of occurrence in the literature for arsenic is the sulphide/ pyrite mode. Therefore, it was expected that most of the arsenic in the two tested samples would be leached by nitric acid.

A high proportion of arsenic in both samples was not leached during testing (20% for the Collinsville sample, 16% for the Japanese sample). Arsenic not mobilised by the leaching is interpreted to indicate an association with the organic fraction of the coal (Palmer et al., 1999; Palmer et al., 1998), or shielding of sulphide grains from dissolution by the organic matter (Willett et al., 2003). An organic mode of occurrence for arsenic has been previously noted in the literature search (see Appendix 2).

The proportion of arsenic leached from the Collinsville sample by hydrochloric acid is high (30%). Previous work (Kolker et al., 2000; Palmer et al., 1999; Palmer et al., 1998) ascribed the arsenic leached by hydrochloric acid to the presence of arsenates (AsO_4^{3-}). Palmer et al (1999) state “arsenate is generally considered to form by oxidation of arsenic-bearing pyrite”. Gypsum was noted during sample collection in several of the Collinsville Coal pits, suggesting pyrite oxidation could have occurred, and providing some support to the inference that the hydrochloric acid leached arsenic is present as arsenates. A further 40% of the arsenic in the Collinsville pulverised fuel sample was leached by hydrofluoric acid. Elements leached by hydrofluoric acid are interpreted to be associated with aluminosilicates, a relatively unusual mode of occurrence for arsenic (see Appendix 2). A possible alternative interpretation is that the hydrofluoric acid was able to extract some organically bound As from the matrix of the coal.

A minor proportion (6%) of arsenic in the Japanese power utility sample was leached by ammonium acetate, indicating an organic association for some of the arsenic in this coal. If the unleached fraction is also interpreted as being organically associated, the

total proportion of organic arsenic is indicated to be 22%. A very large proportion of the arsenic in the Japanese utility sample is leached by hydrofluoric acid (64%). The arsenic mobilised by hydrofluoric acid is interpreted as being associated with aluminosilicates.

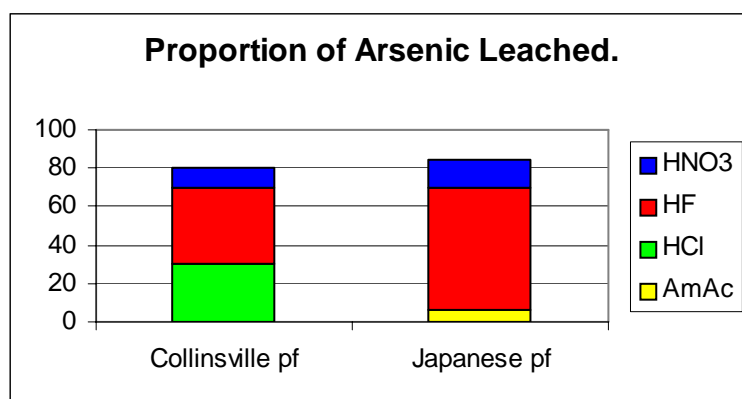


Figure 4.7., Proportions of Arsenic Leached.

Barium.

Figure 4.8. shows the proportions of barium mobilised by the reagents employed. The leaching behaviour of barium is marginally different for the two coal samples sequentially leached. The dominant proportion of soluble barium in the Collinsville sample was mobilised by hydrofluoric acid, indicating an association with aluminosilicates. The aluminosilicate mode of occurrence is commonly noted in the literature (see Appendix 2). A further significant proportion of barium was also mobilised by nitric acid. The nitric acid soluble proportion of the barium is inferred to be present in the coal as barite.

The mass balance for the Japanese sample is poor, with apparently more barium leached than was originally present in the coal. The discrepancy is attributed to analytical error. Nonetheless, the Japanese sample shows sub-equal proportions of barite are mobilised by hydrofluoric and hydrochloric acids. The proportion of barite mobilised by hydrofluoric is inferred to be present in the coal associated with aluminosilicates. The barium mobilised by hydrochloric acid is attributed to dissolution of barite.

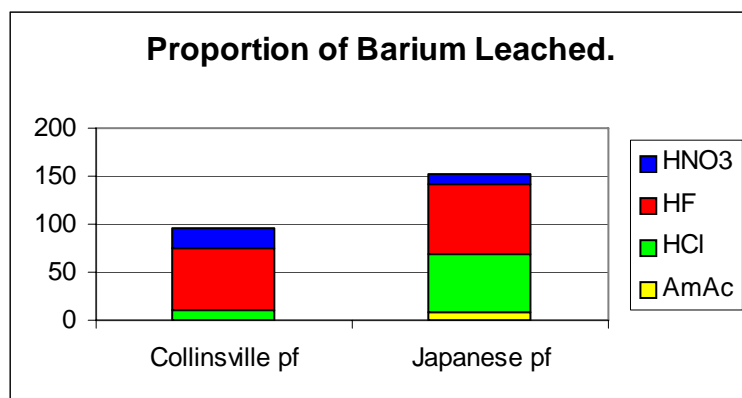


Figure 4.8., Proportions of Barium Leached.

Beryllium.

Figure 4.9. shows the proportions of beryllium mobilised by the reagents employed. The percentage of beryllium leached from the coal exceeds 100% for both the Collinsville and Japanese power utility samples. Some authors suggest that beryllium can be difficult to analyse due to its atomic weight and/ or low abundance (Finkelman, 1980; Palmer et al., 1999) (although the Be content of both these coal samples is high to moderate compared to world coal values). The poor mass balance achieved in the sequential leaching experiments for beryllium is ascribed to analytical errors.

The largest proportion of beryllium is leached from both coal samples by hydrofluoric acid, indicating an association with aluminosilicates (Palmer et al., 1999; Palmer et al., 1998). Finkelman (1980) suggests the aluminosilicate mode of occurrence is uncommon compared to the organic mode. Possibly some beryllium has been liberated from the organic fraction of the coal by hydrofluoric acid, but the mass balances shown would require virtually all the organic Be to be mobilised (ie dissolve all the organic material) which seems an unlikely circumstance.

The Collinsville sample also shows some minor beryllium is leached by ammonium acetate, hydrochloric acid and nitric acid. A common organic association has been noted for beryllium in the literature (see Appendix 2). Potentially some organically bound Be is leached from the coal by the other reagents, or else (in the case of the Be leached by $\text{CH}_3\text{COONH}_4$ and HCL) a minor proportion of the silicate bound Be is mobilised.

The Japanese utility sample showed very small proportions of Be are leached by reagents other than HF. Again this is inferred to be due to a minor organic mode of occurrence or (in the case of the Be leached by $\text{CH}_3\text{COONH}_4$ and HCL) due to mobilisation of a small proportion of the silicate bound beryllium.

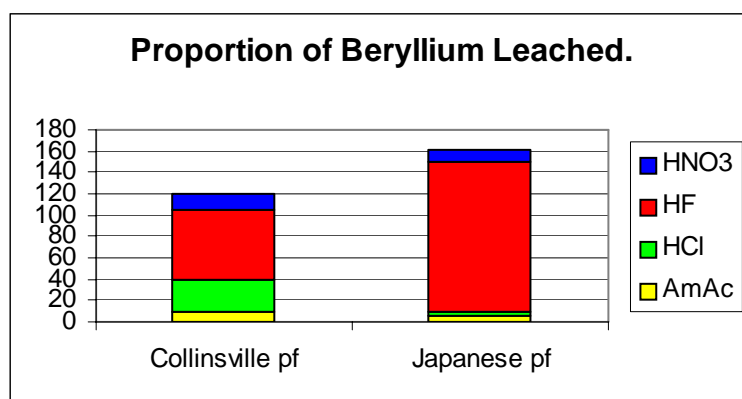


Figure 4.9., Proportions of Beryllium Leached.

Boron.

Figure 4.10. shows the proportions of boron mobilised by the reagents employed. Interpretation of the sequential leach results for boron is difficult because the results are not consistent with known modes of occurrence for this element in coal, and no literature studies discuss the interpretation of sequential leach data for this element. Both the Collinsville and Japanese power utility samples show a large proportion of boron is mobilised by nitric acid, a situation noted by other researchers (Palmer, pers comm. 2002). No literature has been found documenting a pyrite mode of occurrence for boron (Appendix 2). A possible alternative interpretation of the nitric acid mobilised boron is that the reagent is attacking the organic matrix of the coal. Some data suggests that HNO_3 only reacts with pyrite above a certain HNO_3 concentration, and suggests the acid is “consumed preferentially, and to a certain extent” by the organic fraction of the coal (Steel and Patrick, 2001). If the nitric acid is attacking the organic fraction of the coal, then the inference would be that most of the boron is organically bound in the two pulverised fuel samples. Perhaps the relatively minor fraction of boron leached by HCl and ammonium acetate is also due to exchangeable B in the organic matrix, eg as organometallic complexes (Ward, 2002).

Conversely, the total boron leached is in excess of 80% in both cases. Generally organic modes of occurrence are inferred where the mobilised proportion of the

element is low (Palmer et al., 1999; Palmer et al., 1998). An organic mode of occurrence inferred from high nitric acid mobilisation of boron would appear to be at odds with other work, unless boron is weakly bound or bound differently to other organically bound elements.

No boron was leached by HF, which apparently eliminates illite as the mode of occurrence for B, although it should also be noted that BF_3 is very volatile (boiling point -99°C) and would evaporate at room temperature) (Palmer, pers comm. 2002).

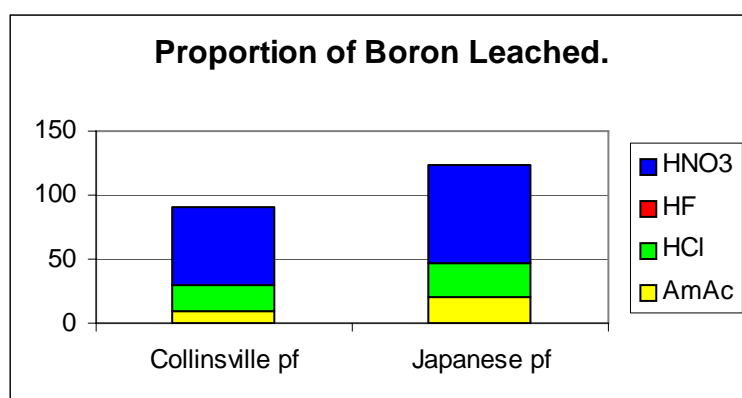


Figure 4.10., Proportions of Boron Leached.

Chromium.

Figure 4.11. shows the proportions of chromium mobilised by the leaching process. Both the Collinsville and the Japanese power station samples show a high proportion of chromium is leached by hydrofluoric acid, indicating a substantial proportion of this element is associated with silicate minerals. Both pulverised fuel samples also show a substantial proportion of the chromium is not mobilised using the leaching procedure, indicating a significant organic mode of occurrence for this element (Willett et al., 2003) (or else the presence of insoluble chromite minerals, cf Palmer, et al. 1999). Both the aluminosilicate and organic modes of occurrence have been found in previous research (Huggins et al., 2000; Palmer et al., 1999; Palmer et al., 1998); see also Appendix 2. In addition, some chromium was leached by nitric acid, suggesting a very minor proportion of chromium may be present associated with pyrite (Huggins et al., 2000). Note the principal mode of occurrence indicated for chromium using the graphical methods was pyrite (Section 3.3.1.), although there was concern that this was due to a physical rather than a chemical relationship. Another minor proportion of chromium in both samples was also leached by hydrochloric acid;

in the case of the Japanese sample this proportion is significant. Palmer, et al. (1998) tentatively infer the HCl mobilised chromium is present in the coal as oxyhydroxides.

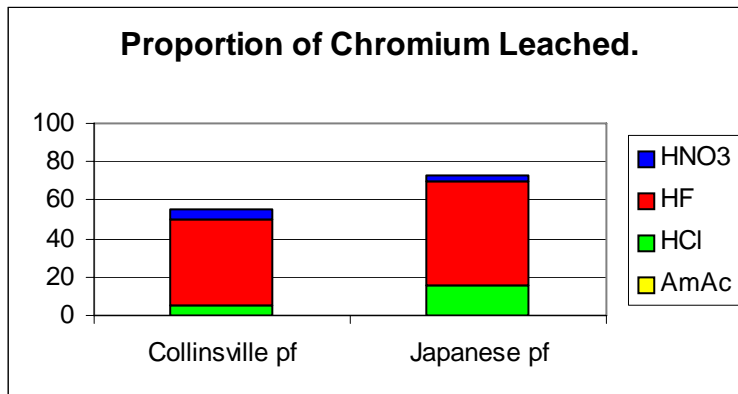


Figure 4.11., Proportions of Chromium Leached.

Cobalt.

Figure 4.12. shows the proportions of cobalt mobilised by the reagents employed. The leaching behaviour of cobalt is very different for the two samples subjected to sequential leach testing. In the case of the Collinsville pulverised fuel sample, sub-equal proportions of cobalt were leached by each of the reagents, a characteristic previously noted by Palmer, et al. (1998). The cobalt leached by ammonium acetate may be present associated with the organic fraction of the coal. A large proportion of the cobalt in the coal sample was not mobilised by any reagent, indicating an organic association of cobalt also occurs in the Collinsville coal sample. The cobalt leached by hydrochloric, hydrofluoric and nitric acid are attributed to carbonate or monosulphide, silicate, and pyrite modes of occurrence respectively (Appendix 2).

The Japanese pulverised fuel sample shows a very large proportion is not mobilised by any reagent, with a further minor proportion of cobalt being mobilised by ammonium acetate. The unmobilised and ammonium acetate mobilised cobalt fractions are interpreted to be associated with the organic fraction of the coal. A relatively large proportion of the cobalt is mobilised by hydrochloric acid, indicating a carbonate or monosulphide mode of occurrence. A further fraction of cobalt is mobilised by hydrofluoric acid indicating some cobalt is associated with silicate minerals.

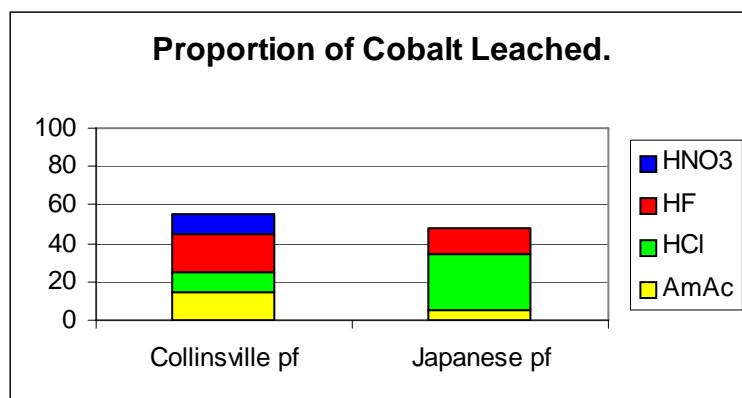


Figure 4.12., Proportions of Cobalt Leached.

Copper.

Figure 4.13. shows the proportions of copper mobilised by the leaching process. The leaching behaviour of copper is different for the Japanese and Collinsville pulverised fuel samples. The Collinsville sample shows sub-equal proportions of copper leached by nitric and hydrofluoric acids. The nitric acid soluble fraction is interpreted as being due to the dissolution of pyrite. The copper liberated by hydrofluoric acid is inferred to be associated with aluminosilicates. A sizeable proportion of the copper in the Collinsville sample was not liberated by the sequential leaching procedure, indicating a substantial organic mode of occurrence or shielding of inorganic mineral grains from dissolution by the organic matter.

Sequential leaching of the Japanese pulverised fuel sample liberated more copper than was originally measured by analysis of the raw coal. The poor mass balance achieved in the leaching procedure is attributed to analytical errors. A large proportion of the copper leached from the Japanese sample is liberated by hydrochloric acid. Palmer et al (1999) found that the hydrochloric acid soluble fraction of the copper was bound as chalcopyrite; a finding confirmed in their study by microprobe analysis. The proportion of copper leached by hydrofluoric acid was also substantial, and is attributed to copper associated with aluminosilicates. A subordinate proportion of copper was also leached by nitric acid, and is inferred as being liberated by dissolution of pyrite.

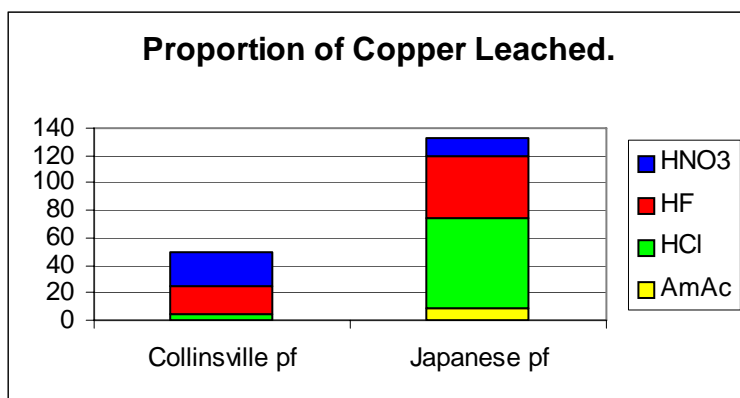


Figure 4.13., Proportions of Copper Leached.

Lead.

Figure 4.14. shows the proportions of lead mobilised by the reagents employed. The leaching behaviour of lead for the Japanese and Collinsville coal samples appears very similar, although the Japanese sample exceeds mass balance (attributed to analytical errors). Both samples show a large proportion of lead is leached by hydrochloric acid, indicating galena is the dominant mode of occurrence for lead in both coals (Palmer et al., 1999). A subordinate proportion of lead is also leached by nitric acid, indicating a lesser pyrite mode of occurrence. Both coals also show some lead is leached by hydrofluoric acid, but this is not considered significant. Not all the lead in the Collinsville sample was mobilised by the leaching procedure. Very few papers found in the literature indicate an organic mode of occurrence for lead (Appendix 2). Therefore, it is inferred that the unleached proportion of the lead in the Collinsville sample is present as galena (most likely given the above inferences), pyrite or lead selenide grains completely enclosed by the organic matrix of the coal, and thus isolated from the reagents.

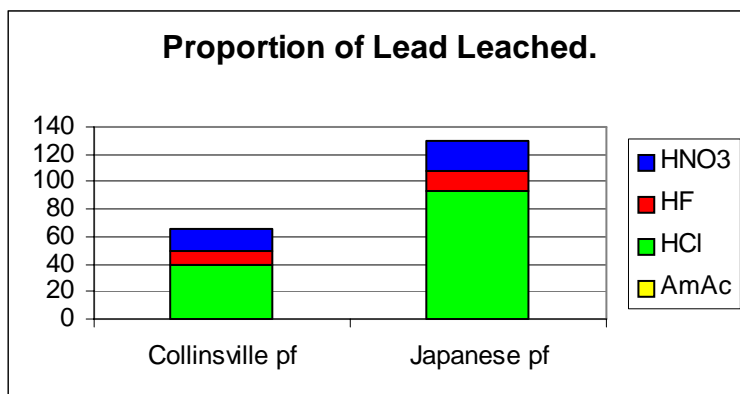


Figure 4.14., Proportions of Lead Leached.

Manganese.

Figure 4.15. shows the proportions of manganese mobilised by the reagents employed. Both the Collinsville and the Japanese power utility fuel samples show a high proportion of manganese is leached from the coal by hydrochloric acid, indicating the principle mode of occurrence of manganese is associated with carbonates. (NB, The sequential leach data provides some support of the use of manganese as the index element for the normative calculation of siderite in Section 3.2.3.) Some manganese is also leached from both coals by ammonium acetate. Previous work has ascribed ammonium acetate leached manganese as being organically bound or else due to ammonium acetate attacking carbonates (Palmer et al., 1999; Palmer et al., 1998). The Japanese pulverised fuel sample also shows some manganese is leached by hydrofluoric acid and nitric acid. Manganese leached by these two reagents is attributed to a minor silicate and pyrite mode of occurrence respectively (Palmer et al., 1999; Palmer et al., 1998). It should be noted that the mass balance for manganese in the Japanese fuel is poor, probably due to analytical errors.

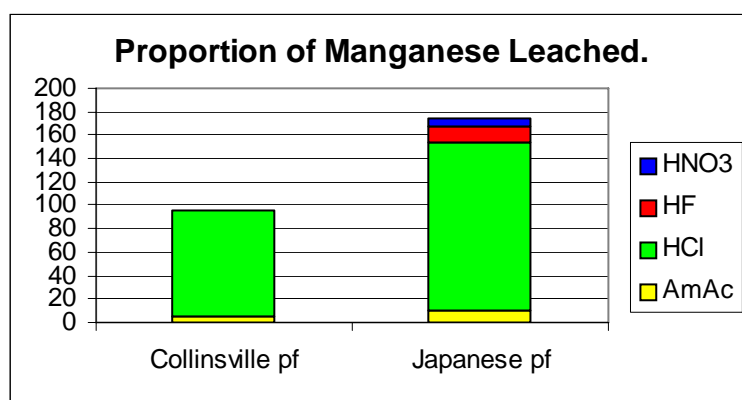


Figure 4.15., Proportions of Manganese Leached.

Nickel.

Figure 4.16. shows the proportions of nickel mobilised by the leaching process. The leaching behaviour of nickel is very different for the two coal samples tested. Leaching of the Collinsville sample found the highest proportion of nickel was leached by hydrofluoric acid indicating a dominant aluminosilicate association for this element. A silicate mode of occurrence has been noted in previous research (Palmer et al., 1998; Palmer et al., 1998); also Appendix 2. A lesser proportion of nickel was also leached by ammonium acetate, possibly indicating some organic association.

The relatively large proportion of nickel not mobilised by any reagent may indicate an organic association for some nickel in the coal (Willett et al., 2003). Subordinate proportions of nickel were also leached by hydrochloric acid and by nitric acid. The hydrochloric leachable nickel may be present associated with carbonates, nickel oxide or millerite (cf Palmer, Mroczkowski et al 1998). The most likely mode of occurrence for the nitric acid soluble nickel is pyrite, a mode of occurrence commonly noted in previous work (Appendix 2), although the proportion leached is below the level of significance.

In the case of the Japanese pulverised fuel sample, virtually all the mobilised nickel was leached by hydrochloric acid. Nickel mobilised by hydrochloric acid may be present associated with carbonates, nickel oxide, or millerite (see above). A large proportion of nickel was not mobilised by any reagent, indicating a large proportion of organically bound nickel in the Japanese pulverised fuel (Willett et al., 2003). A very minor proportion of nickel (below the level of significance) was leached by nitric acid indicating a minor sulphide association for some nickel.

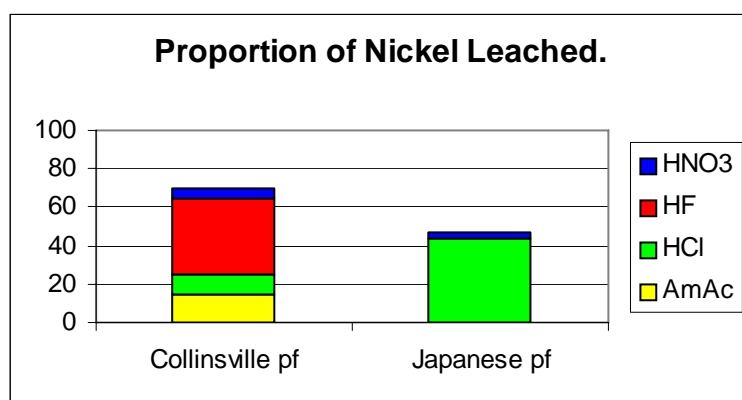


Figure 4.16., Proportions of Nickel Leached.

Selenium.

Figure 4.17. shows the proportions of selenium mobilised by the reagents employed. The sequential leaching results for the Collinsville coal suggests two modes of occurrence for selenium in this coal, namely associated with pyrite (the nitric acid soluble fraction) and organically bound (ie the fraction not mobilised by the leaching procedure). The selenium not mobilised by any reagent could also be the result of shielding of sulphide or selenide grains from dissolution by the organic matter (Willett et al., 2003).

The sequential leaching procedure failed to mobilise any selenium from the Japanese pulverised fuel sample, therefore it is inferred that all the selenium in this sample is organically bound. Both the organically bound and pyrite associated modes of occurrence were commonly noted in the literature search (Appendix 2).

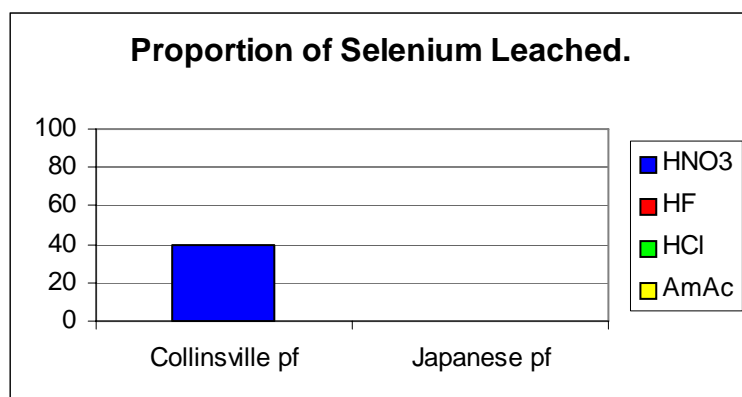


Figure 4.17., Proportions of Selenium Leached.

Tin.

Figure 4.18. shows the proportions of tin mobilised by the reagents employed. Very little definitive information on the mode of occurrence of tin has been found in the literature (Appendix 2). The result of sequential leaching of the Collinsville coal sample suggests most of the tin in this sample is associated with aluminosilicates. Finkelman (1980) noted low levels of tin associated with aluminosilicates. A graphically significant proportion of the tin in the Collinsville sample was also leached by ammonium acetate, but no guide to interpretation of this leachate could be found.

Tin was not leached from the Japanese power utility sample by any reagent. The failure of any reagent to mobilise tin from the coal is assumed to indicate an organic mode of occurrence for tin in this sample. An organic mode of occurrence for tin has been previously documented for some coals (Finkelman, 1980).

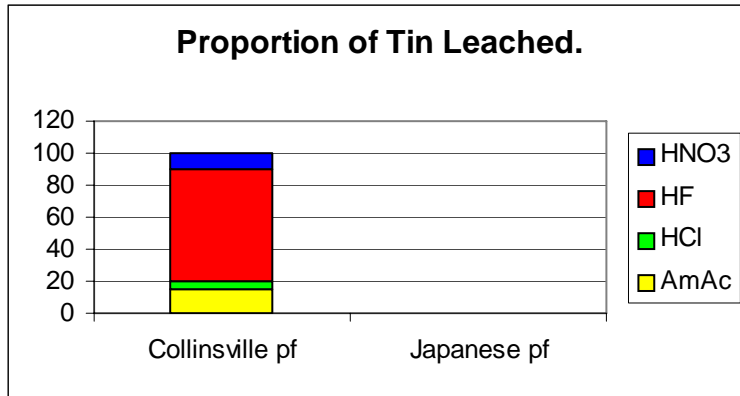


Figure 4.18., Proportions of Tin Leached.

Uranium.

Figure 4.19. shows the proportions of uranium mobilised by the leaching process. A large proportion of the leachable uranium in both the Collinsville and Japanese power utility samples was mobilised by hydrofluoric acid, indicating an association with aluminosilicates and/ or zircon (which is partially soluble in concentrated hydrofluoric acid) (Palmer et al., 1999; Palmer et al., 1998). A significant proportion of uranium in the parent coal is not mobilised by any reagent. An organic mode of occurrence is commonly cited in the literature (Appendix 2), therefore it is inferred that the unmobilised uranium is organically bound in both samples. In addition to the aluminosilicate/ zircon and organic modes of occurrence, a significant fraction of uranium in the Collinsville sample is mobilised by nitric acid, indicating a pyrite association for some of the uranium.

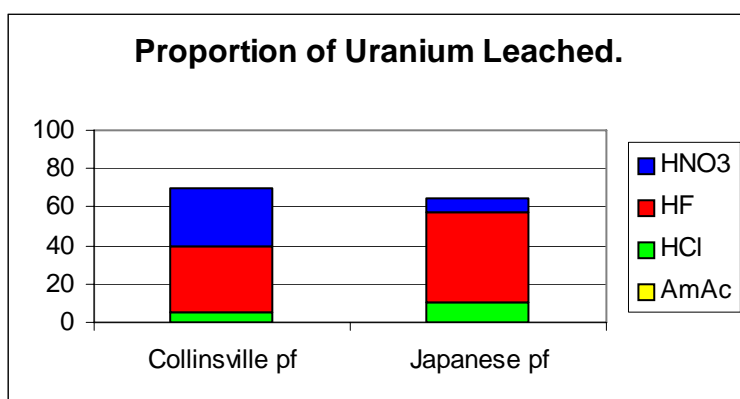


Figure 4.19., Proportions of Uranium Leached.

Vanadium.

Figure 4.20. shows the proportions of vanadium mobilised by the reagents employed. Both the Collinsville and the Japanese power utility fuel samples show a high

proportion of vanadium is leached from the coal by hydrofluoric acid indicating the principle mode of occurrence for vanadium is associated with aluminosilicates (clay minerals). A clay mineral association for vanadium is the dominant mode of occurrence found in the literature (Appendix 2). It is notable that the proportion of vanadium leached did not approach 100% for either of the two coals tested. The proportion of vanadium not leached may either be present associated with the organic fraction of the coal (another common mode of occurrence noted for vanadium; see Appendix 2), or else some aluminosilicate grains were sheltered from leaching by being completely enclosed by the organic matrix of the coal.

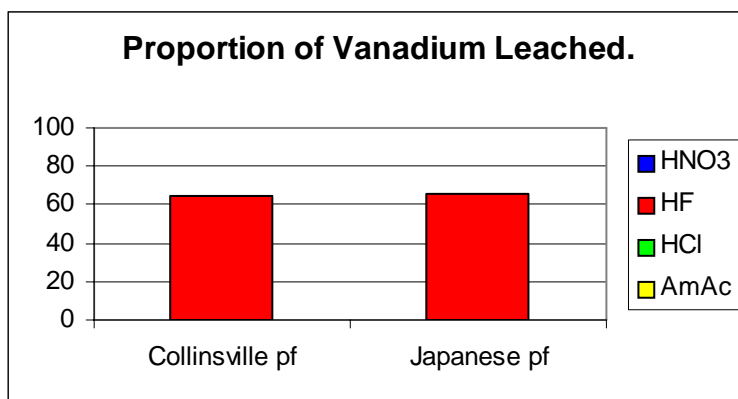


Figure 4.20., Proportions of Vanadium Leached.

Zinc.

Figure 4.21. shows the proportions of zinc mobilised by the reagents employed. Both the Collinsville and the Japanese pulverised fuel samples show a large proportion of the zinc in the coal is leached by hydrochloric acid. The hydrochloric acid soluble zinc fraction in the coals is inferred to be present as sphalerite, as previously found in other studies (Palmer et al., 1999; Palmer et al., 1998). The Japanese sample also shows a significant fraction of the zinc in the coal is leached by hydrofluoric acid. The HF leachable fraction is attributed to an association of some zinc with aluminosilicates.

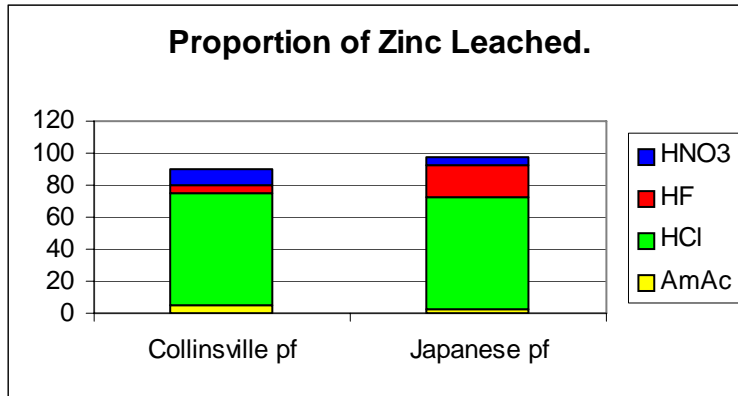


Figure 4.21., Proportions of Zinc Leached.

4.5. Mode of Occurrence of Other Elements Analysed for Individual Coals.

Some other elements were analysed for each of the individual coals. Modes of occurrence interpreted from the results of additional analyses from the sequential leaching experiments are outlined below.

Cadmium and Molybdenum – Japanese Pulverised Fuel Sample.

Figure 4.22. shows the proportions of cadmium and molybdenum mobilised by the reagents employed from the Japanese pulverised fuel sample. The major proportion of cadmium in the Japanese pulverised fuel sample is leached by hydrochloric acid. Previous research (Palmer et al., 1999; Palmer et al., 1998) has inferred the mode of occurrence of cadmium mobilised by hydrochloric acid is sphalerite. The sphalerite mode of occurrence has been noted in a number of other studies (Appendix 2). Another large proportion of cadmium was leached by hydrofluoric acid, implying an association with aluminosilicates. Very few examples of an aluminosilicate mode of occurrence have been found in the literature (Appendix 2). It is noted that the cadmium leach results for the Japanese pulverised fuel sample show a poor mass balance. The balance discrepancy is attributed to analytical errors.

Molybdenum has been previously found to have multiple modes of occurrence in some coals (Palmer et al., 1999). The Japanese pulverised fuel sample shows two distinct modes of occurrence. The proportion of molybdenum leached by ammonium acetate is inferred to be associated with the organic fraction of the coal. The proportion leached by hydrofluoric acid is inferred to be associated with

aluminosilicates. The proportion of molybdenum leached by hydrochloric acid is not considered significant.

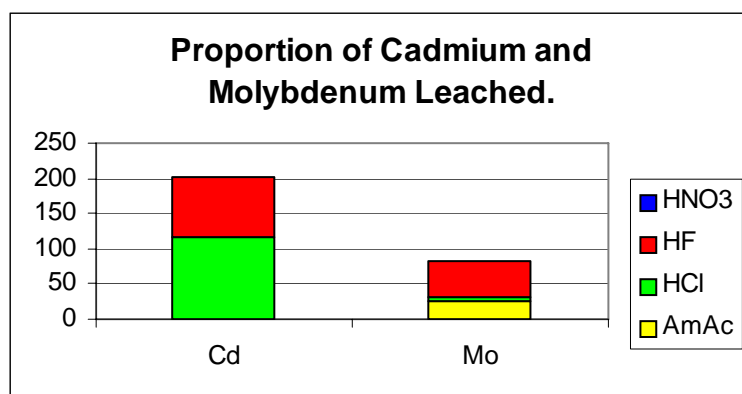


Figure 4.22., Proportions of Cadmium and Molybdenum Leached.

Rare-Earth Elements – Collinsville Pulverised Fuel Sample.

Figure 4.23. shows the proportions of rare earth elements mobilised by the reagents employed from the Collinsville pulverised fuel sample. Yttrium in the Collinsville pulverised fuel sample shows a complex leaching behaviour, also noted previously by Palmer, et al. (1999). Palmer, et al. (1999) attributed the hydrochloric and nitric acid leachable proportions as being present in the coal within the mineral xenotime. A further significant fraction of the yttrium in the Collinsville sample is mobilised by hydrofluoric acid, indicating some yttrium is associated with aluminosilicates. Yet another 20% of yttrium was not mobilised by any reagent, implying an organic association of a proportion of yttrium in the Collinsville coal, or sheltering of inorganic grains from dissolution by the organic matrix.

All the other rare earth element plus thorium (included here because of a similar behaviour) are predominantly leached by nitric acid. The nitric acid leached proportions of rare earth elements are inferred to be present in minerals such as monazite or xenotime. As noted by Palmer, et al. (1999), there is also some additional leaching of middle rare earth elements by hydrochloric acid, attributed to mobilisation of REE's from apatite. There is a reasonable trend showing that, with increasing atomic weight, an increasing proportion of the REE's are not mobilised by any reagent. Previous studies (Eskenazy, 1987; Kolker et al., 2000; Seredin, 1996) have found a tendency for heavy rare earth elements to be enriched in organic fractions of the coal. It is inferred that the poorly defined increase in the un-leached

REE fraction with increased atomic weight could be due to a progressive increase in the tendency of the heavy rare earth elements to be associated with the organic fraction of the coal.

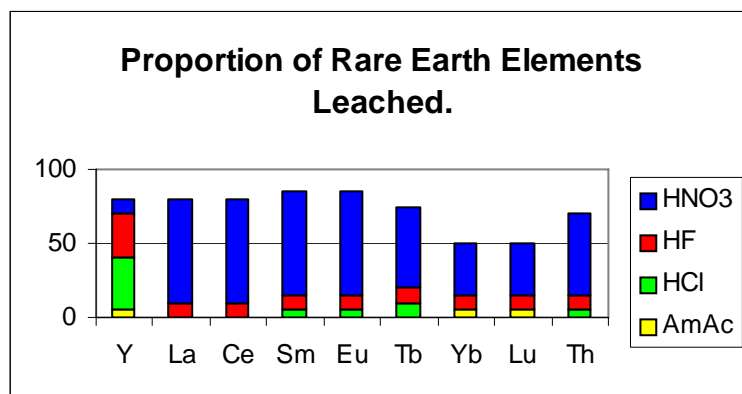


Figure 4.23., Proportions of Rare Earth Elements and Thorium Leached.

Aluminium, Bromine and Phosphorous – Collinsville Pulverised Fuel Sample.

Figure 4.24. shows the proportions of aluminium, bromine and phosphorous mobilised by the reagents employed from the Collinsville pulverised fuel sample.

Aluminium in the Collinsville pulverised fuel sample is almost entirely leached by hydrofluoric acid, indicating this element only occurs in aluminosilicates. The unleached fraction is not considered significant; one explanation could be small aluminosilicate grains isolated from reagent attack by organic matter.

It is generally agreed that bromine is organically associated in most coals (Finkelman, 1980; Swaine, 1990; Vassilev et al., 2000a). The large proportion of bromine not mobilised by any reagent is interpreted to indicate that most bromine is organically bound in the Collinsville pulverised fuel sample. However, a significant fraction of the bromine is mobilised by hydrofluoric acid. It is inferred that the proportion of the bromine mobilised by hydrofluoric acid is associated with aluminosilicates, a mode of occurrence previously noted by Swaine (1990) and Vassilev, et al. (2000a).

Most studies on the mode of occurrence of phosphorous in coal have concluded that the element is bound into various phosphate minerals (Appendix 2). No studies were found which show a silicate mode of occurrence for this element, so mobilisation of

phosphorous by hydrofluoric acid is puzzling. Assuming phosphorous is present as phosphates, the minor proportion of phosphorous mobilised by hydrochloric acid suggests the dominant phosphorous bearing mineral in the Collinsville Coal is different to the phosphate containing the bulk of the rare earth elements, possibly the minerals goyazite and gorceixite indicated by the graphical data in Section 3.2.3. A greatly subordinate fraction of the phosphorous in the Collinsville pulverised fuel sample also appears to be present in the same phosphates that are inferred to contain the rare earth elements, this fraction being mobilised by nitric and hydrochloric acids.

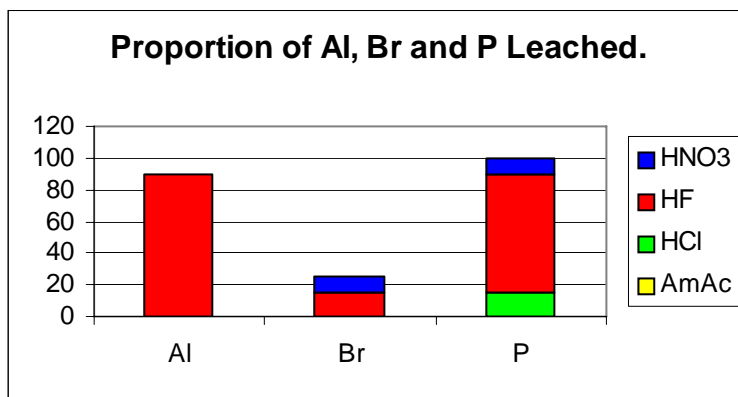


Figure 4.24., Proportions of Al, Br and P Leached.

Row 4 Transition Metals – Collinsville Pulverised Fuel Sample.

Figure 4.25. shows the proportions of Row 4 transition elements mobilised by the reagents employed from the Collinsville pulverised fuel sample.

The leaching profile of scandium for the Collinsville coals is very similar to profiles outlined by Palmer, Kolker et al (1999). Based on the interpretations of Kolker, Palmer et al (1999), the modes of occurrence are inferred to be aluminosilicate associated (the fraction mobilised by hydrofluoric acid) and organically associated (the fraction not mobilised by any reagent). However, it is also possible that the proportion of scandium not mobilised by any reagent could be due to sheltering of aluminosilicate grains from dissolution by the organic matter (Willett et al., 2003). The HCl mobilised mode is noted for the coals studied by Palmer, Kolker et al (1999), but is not explained.

The leaching profile of titanium for the Collinsville coals is also similar to profiles outlined by Palmer, Kolker et al (1999). Again, based on their interpretations, it is inferred that most of the titanium in the Collinsville coal is present as fine-grained titanium oxides and/ or associated with aluminosilicates. The un-leached titanium fraction is inferred to be the present as organically associated titanium, or is due to microscopic grains of Ti-oxides being isolated from reagents by organic matter (Willett et al., 2003).

The major fraction of the iron mobilised from the Collinsville pulverised fuel sample is leached by hydrochloric acid. Hydrochloric acid mobilised iron has been variously attributed to carbonates (probably siderite) (Palmer et al., 1999) or iron oxides (Palmer et al., 1998). A definitive inference of the HCl mobilised mode of occurrence cannot be provided on the basis of the present information, although graphical relationships presented in Section 3.2.3. would support a siderite mode of occurrence. An additional graphically significant proportion of iron is mobilised by HNO₃. The nitric acid mobilised iron fraction is inferred to occur as pyrite in the coal. A further 10% of iron in the pulverised fuel sample is mobilised by HF, and is attributed to an aluminosilicate association.

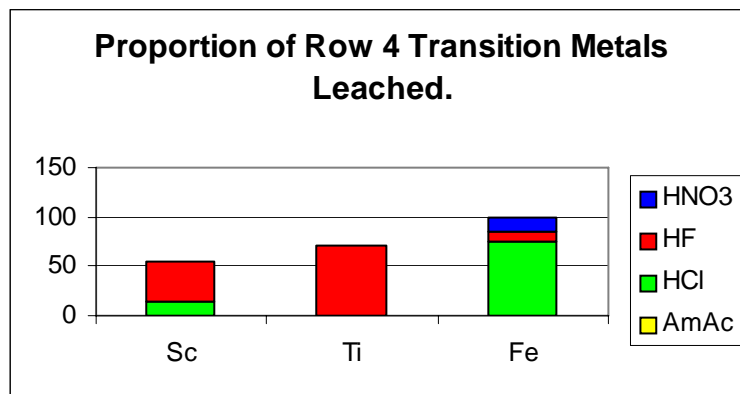


Figure 4.25., Proportions Row 4 Transition Metals Leached.

Heavy Metals – Collinsville Pulverised Fuel Sample.

Figure 4.26. shows the proportions of heavy metals mobilised by the reagents employed from the Collinsville pulverised fuel sample. No previous interpretations of leaching data for zirconium have been found. It is suggested that an aluminosilicate mode of occurrence can be inferred from the large proportion of this element mobilised by hydrofluoric acid. Finkelman (1980) suggested a dominantly inorganic

mode of occurrence for zirconium, but an aluminosilicate mode of occurrence was not noted. Zircon is generally insoluble to partially soluble in HF, possibly explaining the low leaching totals. Alternatively the un-leached proportion of zirconium in the Collinsville pulverised fuel sample could be inferred to be organically associated, a mode of occurrence noted previously by Finkelman (1980).

The leaching profile of tungsten for the Collinsville coals is similar to profiles outlined by Palmer et al (1999). Based on their interpretations, it is inferred that most of the tungsten in the Collinsville coal is present associated with aluminosilicates. The un-leached tungsten fraction is inferred to be the present as organically associated tungsten or as insoluble tungstates. The fractions leached by HNO₃ and HCl have also been noted by Palmer, Kolker et al (1999), but in the case of the Collinsville coal, these fractions only amount to 5% each and are not considered significant.

Hafnium was noted by Palmer et al (1999) to be predominantly leached by HF. Palmer, et al. imply this could be due to dissolution of zircons, which may have some Hf included in the crystal structure at an HfO₂/ZrO₂ ratio of 0.01. The ratio of hafnium (4.38ppm) to zirconium (144ppm) (calculated to include the weight of oxygen) in the Collinsville pulverised fuel sample is 0.02, which is of the right order of magnitude for crystal substitution in zircon. It is, therefore, inferred that hafnium is present as zircon in the pulverised fuel sample. The unleached fraction of the hafnium is ascribed to zircon that was not dissolved, either due to isolation by organic matter or insufficient reaction time.

A substantial proportion of mercury in the Collinsville pulverised fuel sample was leached by ammonium acetate (30%), while the overall proportion of mercury mobilised from the coal is low (55%). It is inferred that the ammonium acetate and unleached proportions of the mercury in the Collinsville pulverised fuel sample are organically bound. An additional significant proportion of mercury is leached from the Collinsville sample by nitric acid. The HNO₃ soluble fraction is ascribed to a pyrite mode of occurrence, also commonly noted in the literature (Appendix 2).

A statistically significant proportion of tantalum in the Collinsville pulverised fuel sample is leached by hydrofluoric acid, possibly indicating an association with

aluminosilicates. The low proportion of tantalum mobilised by the leaching process may indicate an organic association for the remainder of the tantalum in the coal, or that some aluminosilicate grains were isolated by organic matter from the leaching reagents.

The leaching results for thallium suggest two modes of occurrence for this element in the Collinsville pulverised fuel sample. The proportion leached by hydrofluoric acid indicates a dominant aluminosilicate association. However, a further proportion is mobilised by nitric acid indicating a lesser proportion is associated with pyrite. The un-leached proportion of thallium may be present in an organic association or could be in an inorganic phase isolated from the leaching process by surrounding organic matter.

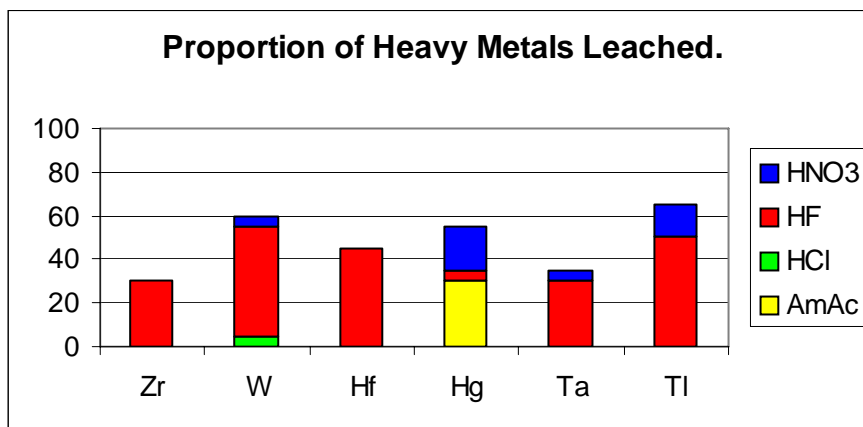


Figure 4.26., Proportions of Heavy Metals Leached.

Group I & II Elements – Collinsville Pulverised Fuel Sample.

Figure 4.27. shows the proportions of Group I and II elements mobilised by the reagents employed from the Collinsville pulverised fuel sample. The sequential leaching data for lithium strongly indicates an aluminosilicate mode of occurrence for this element. The minor un-leached proportion of lithium is probably present in aluminosilicate grains isolated from the leaching process by surrounding organic matter.

A substantial proportion of sodium was leached by hydrofluoric acid, indicating an aluminosilicate mode of occurrence. A lesser proportion was mobilised by ammonium acetate, possibly indicating sodium present in ionic form (Palmer et al.,

1999). A small but statistically significant proportion of sodium was also mobilised by hydrochloric acid. No explanation for the HCL-soluble fraction has been found in the literature, although leaching by HCl has been previously noted (Palmer et al., 1999).

Potassium is substantially leached from the Collinsville coal by hydrofluoric acid, indicating that this element is present in silicates. The proportions of potassium mobilised by hydrochloric acid and ammonium acetate are not considered significant.

The sequential leach data for rubidium is identical to the potassium results, again indicating this element is present in silicates. Again the proportions of rubidium mobilised by hydrochloric acid and ammonium acetate are not considered significant.

The sequential leach data for caesium suggest that a significant proportion of this element is associated with aluminosilicates. However, a statistically significant proportion of caesium is also mobilised by hydrochloric acid and ammonium acetate, similar to the findings of Palmer, et al. (1999). Palmer, et al. (1999) suggested an organic mode of occurrence appears unlikely given the high proportion of caesium mobilised by the sequential leaching, and concluded that the HCl and ammonium acetate-soluble caesium is present as exchangeable ions. It is assumed that the HCl and ammonium acetate soluble caesium in the Collinsville coal is also present as exchangeable ions based on the finding of Palmer et al. (1999). However, the high rank of the Collinsville coal would seem favour the ions being associated with a mineral rather than with the organic fraction of the coal.

Magnesium appears to be dominantly associated with carbonates, as evidenced by the high proportion of this element mobilised by hydrochloric acid. A lesser proportion of magnesium is also associated with aluminosilicates in the Collinsville pulverised fuel. A further proportion of magnesium is mobilised by ammonium acetate, possibly indicating some exchangeable organic mode of occurrence, although overall the total leached proportion is high.

Calcium shows a similar pattern of leaching to magnesium, suggesting this element is dominantly present as carbonates, with subordinate proportions associated with aluminosilicates and present as exchangeable ions.

Strontium is predominantly mobilised from the Collinsville pulverised fuel by hydrofluoric acid, indicating an aluminosilicate association. No other reagent mobilised a statistically significant proportion of strontium.

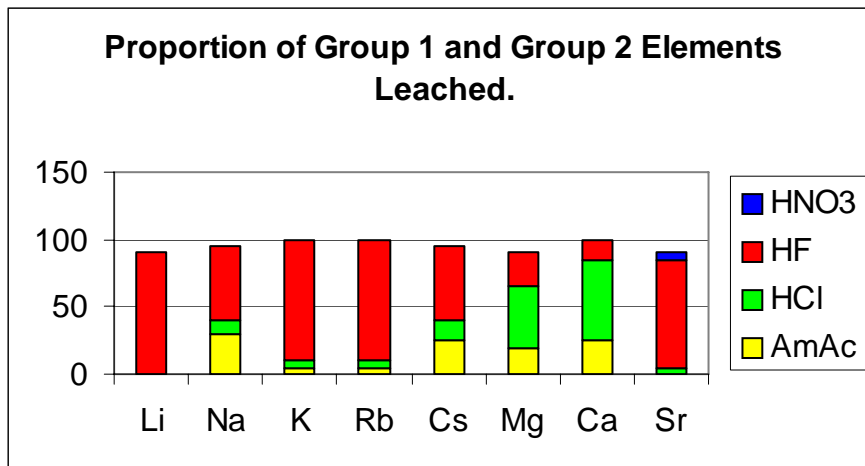


Figure 4.27., Proportions of Group I and II Elements Leached.

Table 4.3. tabulates the mode of occurrence inferred from sequential leach data for the elements discussed above.

Table 4.3. Tabulated Mode of Occurrence from Interpretation of Sequential Leach Data.

Element	Collinsville pf	Japanese pf
Aluminium	Aluminosilicates	
Iron	siderite/ FeO/ minor pyrite	
Calcium	carbonates	
Magnesium	carbonates/ minor aluminosilicates	
Sodium	aluminosilicates/ minor ionic (salt)	
Potassium	aluminosilicates	
Titanium	Ti oxides &/or aluminosilicates	
Manganese	carbonates	carbonates
Phosphorous	uncertain	
Arsenic	arsenates (oxidised pyr)/ pyrite/ organic	aluminosilicates/ subordinate organic
Boron	organic?	organic?
Barium	silicates/ minor barite	silicates/ barite
Beryllium	aluminosilicates/ organic	aluminosilicates/ organic
Bromine	organic	
Cadmium		sphalerite/ aluminosilicates
Cerium	monazite/ xenotime	
Cobalt	organic/ carbonate; monosulphide/ pyr	organic/ carbonate or monosulp/ silicates
Chromium	silicates/ organic/ minor pyrite	silicates/ org/ oxyhydroxides/ pyr
Caesium	aluminosilicates/ minor exchangeable ions	
Copper	pyrite/ aluminosilicate/ organic(?)	chalcopyrite/ aluminosilicates/ pyr
Europium	monazite/ xenotime/ minor apatite	
Hafnium	zircon	
Mercury	organic/ pyrite	
Lanthanum	monazite/ xenotime	
Lithium	aluminosilicates	
Lutetium	monazite/ xenotime	
Molybdenum		organic/ aluminosilicates
Nickel	aluminosilicate/ minor organic, pyrite	carbonates/ nickel oxide or millerite/ organic
Lead	galena	galena
Rubidium	aluminosilicates	
Antimony	organic/ minor pyrite-sulphides	organic/ aluminosilicates/ minor sulphides
Scandium	aluminosilicates/ organic	
Selenium	organic/ pyrite	organic
Samarium	monazite/ xenotime/ minor apatite	
Tin	aluminosilicates	organic
Strontium	aluminosilicates	
Tantalum	aluminosilicates/ organic	
Terbium	monazite/ xenotime/ minor apatite	
Thorium	monazite/ xenotime	
Thallium	aluminosilicates/ pyrite/ organic?	
Uranium	aluminosilicates &/or zircon/ organic/ pyr	aluminosilicates &/or zircon/ organic
Vanadium	aluminosilicates/ subordinate organic	aluminosilicates/ subordinate organic
Tungsten	aluminosilicates/ minor org/ tungstates	
Yttrium	monazite &/or xenotime/ organic	
Ytterbium	monazite/ xenotime/ organic	
Zinc	sphalerite	sphalerite/ aluminosilicates
Zirconium	zircon/ organic	

4.6. Significant Differences in the Modes of Occurrence between the Collinsville and Japanese Pulverised Fuel Samples.

The reproducibility of the sequential leaching technique is “about +/- 5 to 10 percent absolute” (Palmer et al., 1998). Therefore, for the purposes of the analysis undertaken in this section of the study, a difference in the proportion of a mode of occurrence between the two samples of 10% or more is taken as being significant. A number of elements analysed for leachates of the Japanese pulverised fuel sample have a poor mass balance and are not considered reliable for a difference analysis. The results of the sequential leaching study are reproduced in Table 4.4. with figures of absolute differences in modes of occurrence between the two samples.

Table 4.4. The Proportion of Each Trace Element Leached by Each Reagent and the Absolute Differences between Results for the Two Fuel Samples.

Sb	Collinsville pf	Japanese pf	Absolute Difference
AmAc	0	2	2
HCl	20	25	5
HF	10	17	7
HNO ₃	15	0	15
Organic	55	56	1
As	Collinsville pf	Japanese pf	Absolute Difference
AmAc	0	6	6
HCl	30	0	30
HF	40	64	24
HNO ₃	10	14	4
Organic	20	16	4
Ba	Collinsville pf	Japanese pf	Absolute Difference
AmAc	0	8	
HCl	10	61	Poor mass balance for Japanese pf
HF	65	72	
HNO ₃	20	12	
Be	Collinsville pf	Japanese pf	Absolute Difference
AmAc	10	5	
HCl	30	5	Poor mass balance for Japanese pf
HF	65	140	
HNO ₃	15	11	
B	Collinsville pf	Japanese pf	Absolute Difference
AmAc	10	20	
HCl	20	27	Poor mass balance for Japanese pf
HF		0	
HNO ₃	60	77	
Cr	Collinsville pf	Japanese pf	Absolute Difference
AmAc	0	0	0
HCl	5	16	11
HF	45	54	9
HNO ₃	5	3	2
Organic	45	27	18
Co	Collinsville pf	Japanese pf	Absolute Difference
AmAc	15	5	10
HCl	10	29	19
HF	20	14	6
HNO ₃	10	0	10
Organic	45	52	7
Cu	Collinsville pf	Japanese pf	Absolute Difference
AmAc	0	9	
HCl	5	66	Poor mass balance for Japanese pf
HF	20	45	
HNO ₃	25	13	
Organic	50		

Pb	Collinsville pf	Japanese pf	Absolute Difference
AmAc	0	0	
HCl	40	93	Poor mass balance
HF	10	15	for Japanese pf
HNO3	15	22	
Mn	Collinsville pf	Japanese pf	Absolute Difference
AmAc	5	10	
HCl	90	144	Poor mass balance
HF	0	14	for Japanese pf
HNO3	0	6	
Ni	Collinsville pf	Japanese pf	Absolute Difference
AmAc	15	0	15
HCl	10	44	34
HF	40	0	40
HNO3	5	3	2
Organic	30	53	23
Se	Collinsville pf	Japanese pf	Absolute Difference
AmAc	0	0	0
HCl	0	0	0
HF	0	0	0
HNO3	40	0	40
Organic	60	100	40
Sn	Collinsville pf	Japanese pf	Absolute Difference
AmAc	15	0	15
HCl	5	0	5
HF	70	0	70
HNO3	10	0	10
Organic	0	100	100
U	Collinsville pf	Japanese pf	Absolute Difference
AmAc	0	0	0
HCl	5	10	5
HF	35	47	12
HNO3	30	8	22
Organic	30	35	5
V	Collinsville pf	Japanese pf	Absolute Difference
AmAc	0	0	0
HCl	0	0	0
HF	65	66	1
HNO3	0	0	0
Organic	35	34	1
Zn	Collinsville pf	Japanese pf	Absolute Difference
AmAc	5	3	2
HCl	70	70	0
HF	5	20	15
HNO3	10	4	6
Organic	10	3	7

The only significant difference in the proportions of the antimony modes of occurrence between the two coals studied is the higher proportion of pyrite bound antimony in the Collinsville sample.

A significantly higher proportion of arsenic is leached from the Collinsville pulverised fuel sample by hydrochloric acid. It is inferred that the Collinsville sample contains a significantly higher proportion of arsenic associated with arsenates (AsO_4^{3-}), possibly resulting from oxidation of pyrite. In contrast, a significantly higher proportion of arsenic is leached from the Japanese pulverised fuel sample by hydrofluoric acid, indicating a higher proportion of aluminosilicate associated arsenic in the Japanese fuel sample.

There are significant differences in the proportion of chromium leached by hydrochloric acid and in the total proportion of chromium mobilised from the samples. The Japanese sample shows a higher proportion of chromium mobilised by hydrochloric acid, possibly indicating a higher proportion of oxyhydroxide bound chromium in this coal. The lower proportion of chromium mobilised from the Collinsville sample suggests this coal contains a higher proportion of organically-bound chromium compared to the Japanese pulverised-fuel sample.

The proportions of the cobalt modes of occurrence are very different between the two samples tested. Assuming the proportion of cobalt mobilised by ammonium acetate is bound to the organic matter of the coal and should be added to the unmobilised proportion, there is no significant difference in the proportion of organically-bound cobalt. However, the proportion of cobalt that is carbonate or monosulphide-bound is significantly higher in the Japanese sample, while the Collinsville sample contains a significantly higher proportion of cobalt associated with pyrite.

As for cobalt, the proportions of the nickel modes of occurrence are very different between the two samples tested. The organically-bound nickel appears to be very much higher for the Japanese sample, although if the nickel mobilised by ammonium acetate ascribed to the organic mode of occurrence the difference is minor. The Japanese sample also has a significantly larger proportion of nickel bound as millerite, nickel oxides, or carbonates. Conversely, the Collinsville sample has a significantly higher proportion of nickel associated with aluminosilicates.

Selenium in the Collinsville sample is associated with organic matter or with pyrite, whereas the Japanese sample has only organically-associated selenium. Therefore,

the Collinsville sample has a higher proportion of pyrite-associated selenium and a lower proportion of organically-bound selenium in comparison to the Japanese pulverised fuel sample.

The proportions of the tin modes of occurrence are very different for the two samples studied. The Collinsville sample has a higher proportion of tin associated with aluminosilicates and pyrite, whereas tin in the Japanese sample is entirely organically-associated. The Collinsville sample also shows a significantly higher proportion of tin mobilised by ammonium acetate, although the mode of occurrence releasing tin on treatment with ammonium acetate is uncertain.

There are two significant differences in the proportions of the uranium modes of occurrence between the two samples studied. The proportion of uranium associated with aluminosilicates is significantly higher for the Japanese sample, whereas the proportion of pyrite-associated uranium is significantly higher for the Collinsville sample.

There are no significant differences in mode of occurrence proportions for vanadium between the two pulverised fuel samples.

The only significant difference in the proportions of the zinc modes of occurrence between the two samples is the higher proportion of zinc associated with aluminosilicates in the Japanese sample.

4.7. Chapter Summary.

Pulverised fuel samples from the Collinsville coal-fired power station and from the Mitsui pulverised-fuel utility in Omutu City, Japan have been analysed for a range of major and trace elements. The elements gold, cerium, cobalt, europium, hafnium, lanthanum, lutetium, molybdenum, neodymium, scandium, selenium, samarium, strontium, tantalum, thorium, tungsten, and ytterbium are at the upper end or above the world average concentration range in the Collinsville pulverized fuel. The elements gold, hafnium, and thorium are at the upper end or above the world coal concentration range in the Japanese pulverized fuel. The concentration of the other analysed trace elements fit comfortably within world range of concentrations. The

mode of occurrence of the trace elements has been inferred using the USGS sequential-leaching procedure. Generally the mode of occurrence of elements examined in this study is similar to those found in previous studies. Significant differences in the mode of occurrence of antimony, arsenic, chromium, cobalt, nickel, selenium, tin, uranium, and zinc have been documented for the two pulverised fuels studied. Vanadium was found to have a virtually identical mode of occurrence in the two pulverised fuels studied.

Chapter 5.

Trace Element Partitioning Behaviour in Pulverised Fuel Combustion.

5.0. Chapter Resume.

Samples of bottom-ash and fly-ash were collected from several locations within two pulverised fuel combustion plants. The samples were deliberately gathered from two disparate power plants in order to maximise the chance of sampling two feed coals with some significant differences in trace element mode of occurrence. All samples were analysed for a range of trace and major elements by INAA and XRF, and for boron by microwave-digestion ICP-MS. Comparison is made of the partitioning behaviour of trace elements between two pulverised power stations (Chapter 5) in order to assess the influence that mode of occurrence (Chapter 4) exerts on the behaviour of trace elements in combustion (Section 8.2.).

5.1. Sample Description.

Samples of bottom-ash and fly-ash were gathered from two pulverised fuel combustion plants. The plants sampled were:

- The Collinsville Power Station, Collinsville, Northern Queensland, Australia. The Collinsville power station at the time of sampling burnt a blend comprising 70% Blake Seam coal and 30% Bowen Seam coal. The coal was mined from the Blake West, Blake Central and Bowen No2 pits at the Collinsville Opencast mine. Figure 5.1. shows the Collinsville power station. A schematic of the Collinsville power station noting the ash sampling points is shown in Figure 4.1.
- The Mitsui Coal Mining power plant, Omutu City, Kyushu, Japan. The Mitsui Coal Mining plant at the time of sampling burnt a blend of coal from Indonesia, China, and low-grade high-ash domestic coal, with some Russian coal from time to time. A schematic of the Mitsui power station, noting the ash sampling points, is shown in Figure 4.2.

Sampling of the bottom-ash and fly-ash at the Collinsville combustion plant was undertaken by Mr Ian Borthwick (plant manager), observed by the author. Samples

were taken over approximately 0.5 hours following sampling of the pulverised fuel as detailed in Chapter 4. Sampling at the Japanese Mitsui power station was undertaken by plant personnel and was not observed by the author. It was stressed to Mitsui management personnel that it was important to take the samples immediately following sampling of the pulverised fuel. It was considered important to sample the waste streams as soon as possible after sampling of the fuel stream in order to directly relate the mode of occurrence of trace elements being fed into the boiler with the partitioning behaviour of the elements found by analysis of the ash samples. However, the validity of the Mitsui samples is less assured.



Figure 5.1. The Collinsville coal fired power station.

All samples were analysed for a range of major and trace elements by commercial laboratories using INAA and XRF (as detailed in Section 4.2), apart from boron, which was measured by microwave ICP-MS. Analytical results are presented in Table 5.1. Because both the Mitsui and Collinsville fuel samples have been analysed by INAA using the same laboratory, the INAA figures (Table 5.1.) are used in the calculations detailed below. The USGS fuel analyses figures are not used in order to remove the potential for inter-laboratory differences between the fuel and ash samples. Note, it is assumed all errors involving the INAA analyses are systematic. The exception to the use of the Actlabs INAA comparison is iron in the Collinsville

pulverised-fuel sample. Generally an excellent relationship between the INAA and XRF figures for iron was found for all samples; the Collinsville pulverised fuel sample is one exception to this strong trend. However, the XRF result and the USGS result for iron in whole coal are the same (7400ppm) for the Collinsville pulverised fuel sample so the XRF figure for iron is used for partitioning behaviour calculations in Chapter 5.

It is important to note the author does not consider the samples gathered to be sufficient to characterise the mode of occurrence of trace elements in the feed coal or the partitioning behaviour of the trace elements in combustion for the electrical utilities concerned. Full characterisation of these factors would require sampling of pulverised fuel and waste streams over some longer time frame in order to capture variations in mode of occurrence and partitioning behaviour. The results of sample analysis outlined in this work are intended to provide a “snapshot” comparison of the partitioning behaviour of trace elements between two combustion plants using coal with trace elements present in different modes of occurrence.

Table 5.1. Elemental Concentrations of Major and Trace Elements in Combustion Plant Solid Waste Streams.

	Coll Pwr botm ash	Coll Pwr brnr level	Coll Pwr level 3	Coll Pwr supr htr	Coll Pwr U3 fly ash	Mitsui botm ash	Burner Outlet	Fly Ash Collector
	14/09/1999	14/09/1999	14/09/1999	14/09/1999	14/09/1999			
Ash % (air dried)	83.5		99.7	96.1	55.7	67.6	94.6	97.5
Major Elements								
Si (PPM)	192300	271200	314600	262900	131600	137300	192000	195900
Al (PPM)	164600	163800	129800	154300	109100	102400	146000	154400
Fe (PPM) (INAA)	49600	43700	34300	47800	25300	5980	49100	57700
Fe (PPM) (XRF)	51900	43700	33800	47100	23300	44800	54800	47600
Ca (PPM)	<0.03	<0.03	<0.03	<0.03	<0.03	1	6.8	8.9
Mg (PPM)	1000	500	<100	600	500	5700	7400	8000
Na (PPM)	739	876	744	817	807	337	2100	2940
K (PPM)	3000	8900	2400	1900	2500	600	1500	3600
Ti (PPM)	7200	9900	10100	10200	7800	6400	9300	11100
Mn (PPM)	1000	700	300	700	500	300	400	400
P (PPM)	1400	1500	1100	1500	2100	2500	3200	4200
S (%)	0.00	0.00	0.00	0.00	0.04	0.00	0.26	0.35
Trace Elements								
Au (PPB)	4.8	2	2	1.8	<2.1	5.5	64.8	70.7
Ag (PPM)	<0.3	<0.3	<0.3	<0.3	<0.3	<0.3	<0.3	<0.3
As (PPM)	1.1	3.8	3.7	4.5	5	1.8	2.5	6.6
B (PPM)	6	9	8	8	9	120	330	708
Ba (PPM)	1600	1600	720	1500	1900	160	740	1000
Br (PPM)	1.1	<0.21	<0.21	4.8	3.9	1.4	<0.2	<0.33
Ce (PPM)	110	150	150	150	180	17	100	140
Co (PPM)	18	23	27	26	20	4.6	22	31
Cr (PPM)	46	93	100	85	58	10	52	74
Cu (PPM)	66.8	80.51	68.79	81.69	54.03	67.6	98.38	123.83
Cs (PPM)	3	3	2.5	3.4	3	0.21	1.2	2.4
Eu (PPM)	1.67	2.51	2.42	2.51	2.81	0.34	2.47	3.22
Hf (PPM)	17	20	18	20	18	2	12	17
Hg (PPM)	<0.05	<0.05	<0.05	<0.05	<0.05	0.27	<0.05	1.1
Ir (PPM)	<0.1	<0.1	<0.1	<0.1	<0.1	<0.1	<0.1	<0.1
La (PPM)	60	92	84	87	100	8.5	60	78
Lu (PPM)	1.39	1.74	1.27	1.71	1.87	0.194	1.35	1.75
Mo (PPM)	1.7	4.5	3.2	<0.05	<0.05	1.6	2.8	5.2
Nd (PPM)	54	70	60	63	85	7.5	50	67
Ni (PPM)	95	92	110	98	<5	17	<5	<5
Pb (PPM)	33.4	49.7	45.86	61.5	74.64	12.17	32.16	50.7
Rb (PPM)	<1	<1	20	24	12	<1	21	22
Sb (PPM)	0.85	1.5	1.5	1.6	1.8	0.29	0.61	1.6
Sc (PPM)	22	29	29	30	27	4.9	27	39
Se (PPM)	0.7	2.8	1.2	<0.2	6.4	2.3	<0.2	3
Sm (PPM)	9.3	13	11	13	15	1.4	9	12
Sn (PPM)	2.5	3	4	6				
Sr (PPM)	430	610	310	530	860	160	870	1300
Ta (PPM)	2.3	2.4	2.2	2.4	2.1	0.21	1.1	1.4
Tb (PPM)	1.8	2.5	1.9	2.3	3	0.2	1.9	2.4
Th (PPM)	25	34	30	33	37	3	15	22
U (PPM) (INAA)	6.4	9	7.7	8	7.5	0.66	4.4	6.3
U (PPM) (XRF)	11.69	12.92	9.97	12.49	12.81	5.41	9.46	11.7
V (PPM)	66.8	99.4	100.7	96.1	85.22	173.06	262.04	335.4
W (PPM)	8.1	5.4	3.9	8.5	4.5	0.52	3	<1
Yb (PPM)	8.14	10.4	7.57	10	11.2	1.3	8.01	11.5
Zn (PPM)	70	130	160	160	210	18	68	110

NB – Figures in red are calculated using the INAA and XRF figures to adjust the Si, Al, Mg, Ti, Mn and P figures for losses on ignition. Insufficient sample remained to analyse for incombustible ash.

5.2. Factors Other than Mode of Occurrence Affecting Partitioning Behaviour.

Many factors other than elemental mode of occurrence can affect the partitioning behaviour of trace elements (see Section 1.4.4 for a detailed discussion), and the major factors are summarised as follows:

- a) Plant design and operating conditions. Both the Collinsville and Mitsui combustion plants are pulverised-fuel combustion systems operating at $\sim 1300^{\circ}\text{C}$ [(pers comm. Borthwick (1999) (Collinsville); pers comm. Nishioka (2000) (Mitsui plant)], suggesting operating temperature is not a factor. However, the Collinsville combustion plant uses a baghouse to collect fly-ash whereas the Mitsui plant captures fly-ash using an electrostatic precipitator (ESP) device. Significant retention of mercury and selenium in baghouse ash relative to ESP ash has been found by some workers (Mastalerz et al., 2004), and could be a factor controlling differences in partitioning behaviour of trace elements for the plants sampled for this study.
- b) Temperature variations within the combustion chamber. Mineral-rich regions in the combustion chamber may combust at a lower temperature than mineral-poor regions (Thompson and Argent, 1999). Therefore, a higher ash coal could cause more temperature anisotropy within the combustion chamber. The Collinsville pulverised-fuel sample was analysed as being 21.2% ash, whereas the Mitsui pulverised fuel was analysed as being 12.5% ash. If the research of Thompson & Argent (1999) is correct, there could be a higher potential for the Collinsville plant to suffer from temperature anisotropy within the boiler, potentially complicating the impact of trace element mode of occurrence on partitioning behaviour.
- c) The bulk chemistry of the coal and coal ash. Table 5.2. details the chemistry of the Collinsville and Mitsui pulverised-fuel samples, calculated to oxide percent in ash. For reasons outlined in Section 4.2., the USGS figure for calcium and the XRF/ USGS figure for iron in the Collinsville pulverised fuel sample is used in the calculation of figures in Table 5.2. Table 5.2. shows the major element ash chemistry of the Collinsville and Japanese pulverised fuels

is similar in most respects (based on the INAA and XRF figures for the two coals). Therefore, differences in the partitioning behaviour of trace elements between the Collinsville and Japanese combustion plants is unlikely to be due to major element differences. A correlation between the concentration of unburnt carbon and the concentration of mercury in ash has been noted by some authors (Hassett and Eylands, 1999; Mardon and Hower, 2004; Sakulpitakphon et al., 2000; Wu et al., 2000), with carbon form also having an influence (Hower and Masterlerz, 2001). The bottom-ash from both plants contains a lower proportion of incombustibles than the fly-ash samples. The exception to this trend is the hopper ash from Unit 3 of the Collinsville combustion plant, which has a very low (55.7%) incombustible content. therefore some capture of volatile elements in the bottom ash could be occurring.

Table 5.2. Major Element Oxides (% in Ash)

Element	Col Pwr pf	Col Pwr pf	Mitsui pf
	INAA	USGS	INAA
SiO ₂ (% in Ash)	49.99	58.36	49.39
Al ₂ O ₃ (% in Ash)	37.57	33.32	34.88
Fe ₂ O ₃ (% in Ash)	u/s	4.81	11.92
Fe ₂ O ₃ (% in Ash)	5.11		9.16
CaO (% in Ash)	0.32	0.30	0.00
MgO (% in Ash)	0.16	0.20	1.83
Na ₂ O (% in Ash)	2.55	0.12	0.29
K ₂ O (% in Ash)	<1.56	0.31	0.66
TiO ₂ (% in Ash)	2.02	1.90	2.21
Mn ₃ O ₄ (% in Ash)	0.07	0.09	0.06
P ₂ O ₅ (% in Ash)	0.66	0.59	1.52

5.3. Partitioning Behaviour.

It has long been known that trace elements partition differently between the bottom-ash, fly-ash, and flue gas waste streams from a pulverised-fuel combustion plant (see Section 1.4.3). The use of the relative enrichment factor was introduced to assess the partitioning behaviour of trace elements in combustion (Clarke and Sloss, 1992; Meij, 1995). Essentially the relative enrichment factor is the ratio of the expected concentration of a trace element in a sample if the element were concentrated entirely into the ash versus the measured concentration. The relative enrichment factor is calculated using Equation 5.1.

Equation 5.1. Calculation of Relative Enrichment.

$$RE = \frac{(\text{element concentration in ash})}{(\text{element concentration in coal})} \times \frac{(\% \text{ ash yield of coal})}{100}$$

Table 7.1 from Meij (1995) is reproduced below as Table 5.3. Table 5.3. is used as a guide to classify the trace elements according to their relative enrichment behaviour.

Table 5.3. Trace Element Classification into 3 Classes based on their behaviour during combustion in the boiler and ducts with their relative enrichment factors (RE).

THIS TABLE HAS BEEN REMOVED DUE TO
COPYRIGHT RESTRICTIONS

Source: Meij (1995), Table 7.1

Another factor called the enrichment factor was also assessed for use as an indicator of trace element partitioning behaviour. The enrichment factor normalises the concentration of trace elements against an element that is considered to be non-volatile and, therefore, does not concentrate or deplete across the waste streams. Usually a Class I lithophile element is chosen as the normalising element (eg Al or Si) (Clarke and Sloss, 1992). However, it seemed to the author that unless an element is proven to be non-volatile in all cases, the assumption that the normalising element partitions evenly across all waste streams could be flawed. The relative enrichment factor (Clarke and Sloss, 1992; Meij, 1995) rather than the enrichment factor is, therefore, used in this study to assess trace element partitioning behaviour.

To follow are graphs of the position of the sample within the combustion system versus the relative enrichment factor for that element. The positions of the samples are numbered, the numbers equating to the following locations within the boiler.

Collinsville Samples

- 1 = Bottom-ash
- 2 = Burner level
- 3 = Level 3
- 4 = Super heater
- 5 = Fly-ash bunker (composite of all fly-ash)

(See Figure 4.1.).

Mitsui Mining power plant

- 1 = Bottom-ash
- 2 = not sampled
- 3 = not sampled
- 4 = Outlet of burner
- 5 = Fly-ash bunker

(see Figure 4.2.).

Unfortunately calcium, an important major element in the sorption of trace elements, is not included in this part of the study due this element being present in many ash streams at concentrations below detection limit of INAA.

Silicon.

Silicon is classified as a Class I element for both the Collinsville and Mitsui combustion plants. Although the bottom-ash relative enrichment figures are both above 0.7 (Figure 5.2.), the relative enrichment figures for all the samples are ~1, suggesting little enrichment or depletion of this element between the combustion plant waste streams.

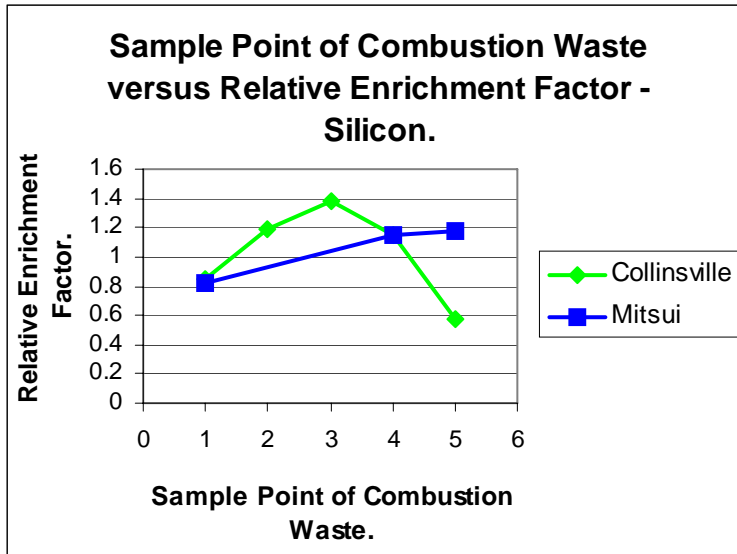


Figure 5.2. Relative Enrichment of Silicon.

Aluminium.

Aluminium is classified as a Class I element for both the Collinsville and Mitsui combustion plants. As with silicon, both the bottom-ash relative enrichment figures are above 0.7 (Figure 5.3.). The relative enrichment figures for the Collinsville samples are ~1, suggesting little enrichment or depletion of this element between the combustion plant waste streams. There is some evidence of enrichment of aluminium downstream in the Japanese pulverised-fuel utility, although it is considered insufficient to categorise the aluminium as a Class II element.

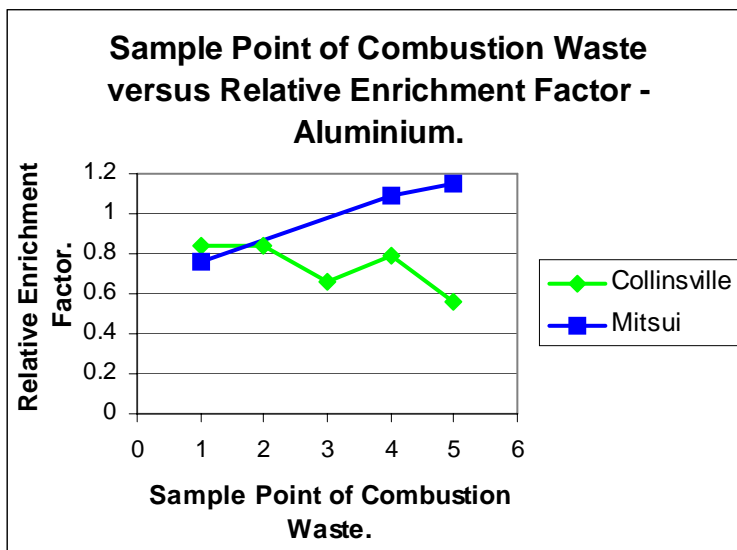


Figure 5.3. Relative Enrichment of Aluminium.

Iron.

Iron is classified as a Class I element for both the Collinsville and Mitsui combustion plants. As with silicon and aluminium, the bottom-ash relative enrichment figures are (well) above 0.7 (Figure 5.4.). However, the relative enrichment figures for all the samples are ~1 (with some enrichment in the bottom ash of the Collinsville plant), suggesting little enrichment or depletion of this element between the combustion plant waste streams.

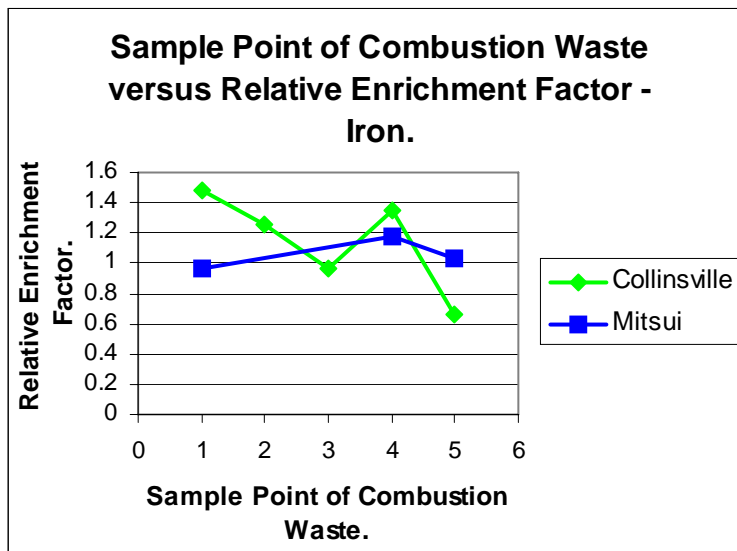


Figure 5.4. Relative Enrichment of Iron.

Magnesium.

Magnesium is classified as a Class I element for both the Collinsville and Mitsui combustion plants. As noted above for silicon, aluminium and iron, the bottom-ash relative enrichment figures exceed 0.7 (refer Figure 5.5.). However, the relative enrichment figures for all the samples are ~1, suggesting little enrichment or depletion of this element between the combustion plant waste streams.

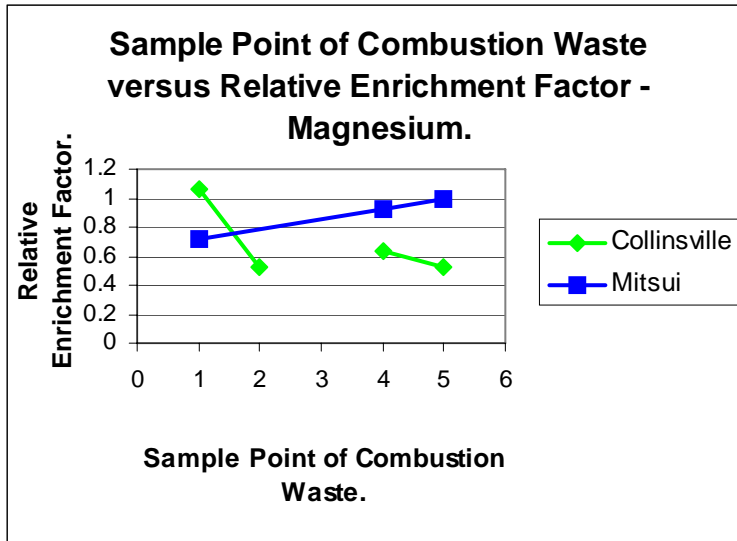


Figure 5.5. Relative Enrichment of Magnesium.

Sodium.

Sodium is classified as a Class III element for the Collinsville combustion plant because the relative enrichment factors are well below 1 across all samples suggesting the element is significantly depleted in all waste streams (Figure 5.6.). Sodium is classified as a Class IIc element for the Mitsui combustion plant because the bottom-ash relative enrichment figure is <0.7 , the PFA sample is ≈ 1 , and the fly-ash sample is ≤ 2 (Figure 5.6.). Thus sodium, shows significant enrichment in the fly-ash, probably due to condensation of this element downstream of the burner zone within the Mitsui combustion utility.

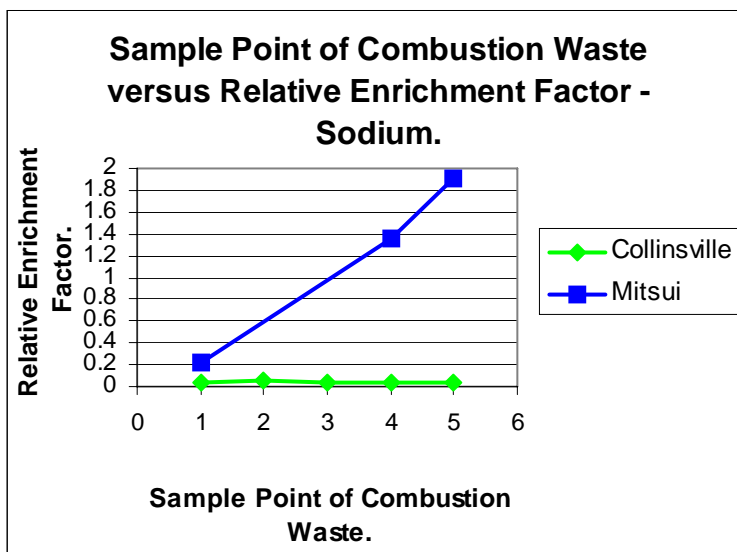


Figure 5.6. Relative Enrichment of Sodium.

Titanium.

Titanium is classified as a Class I element for both the Collinsville and Mitsui combustion plants. As with the other Class I elements listed above, both the bottom-ash relative enrichment figures exceed 0.7, and the fly-ash figures are ~1, suggesting little enrichment or depletion of this element between the combustion plant waste streams (Figure 5.7.).

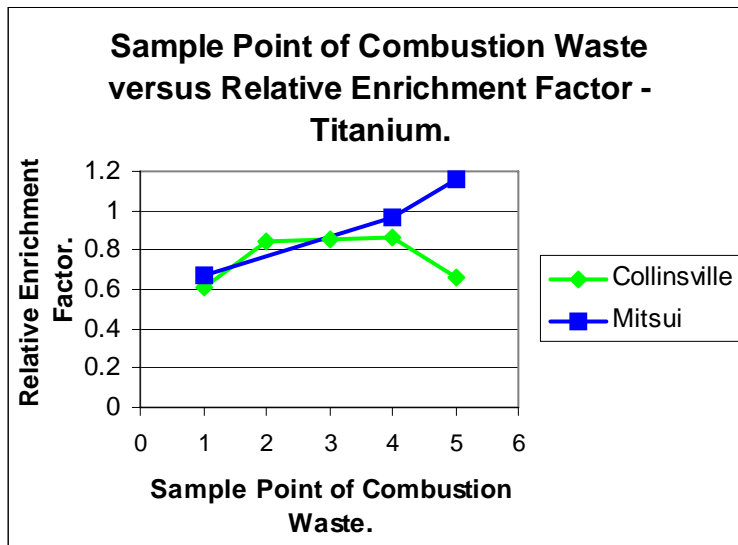


Figure 5.7. Relative Enrichment of Titanium.

Manganese.

Manganese is classified as a Class I element for the Mitsui combustion plant. The fly-ash figures are ~1, suggesting little enrichment or depletion of this element between the combustion plant waste streams (Figure 5.8.). Manganese is also classified as a Class I element in the Collinsville power station, however the bottom-ash appears significantly enriched in manganese. Possible explanations for this enrichment could be sample real enrichment in the bottom-ash, sample contamination or analytical error. Further sampling would be required to decide if this enrichment is real. The manganese and iron enrichment patterns are very similar, possibly indicating some underlying parallel control for these two elements.

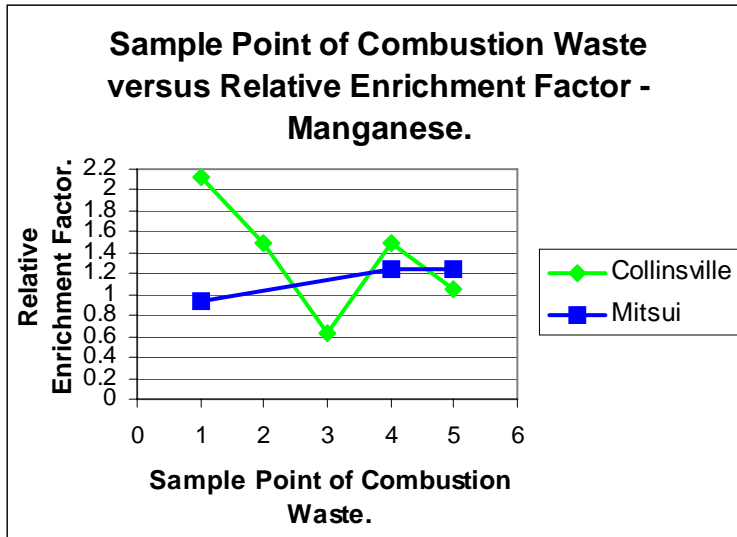


Figure 5.8. Relative Enrichment of Manganese.

Phosphorous.

Phosphorous is classified as a Class IIc element for both the Collinsville and Mitsui combustion plants. The bottom-ash figures are <0.7 for both combustion plants. Although the downstream wastes are not as enriched as would usually be expected for a Class IIc element, the fly-ash RE figures trend upward toward an RE of ~ 1 suggesting some downstream enrichment (Figure 5.9.). It also appears some phosphorous has been lost to the flue gas.

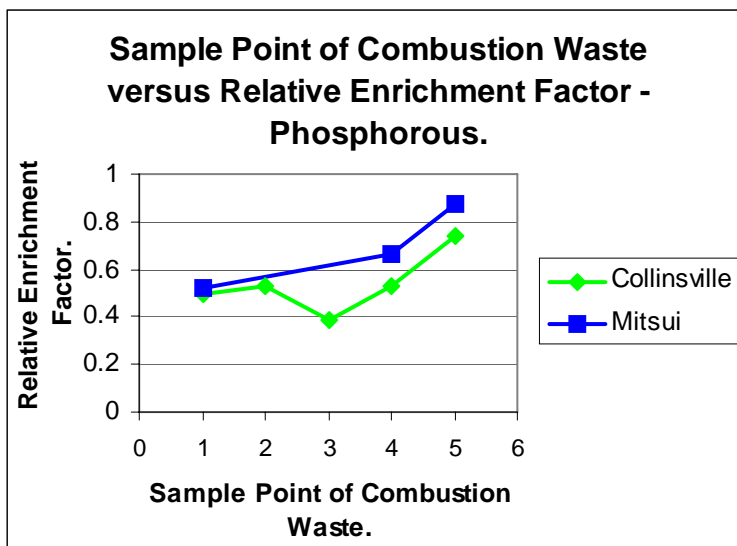


Figure 5.9. Relative Enrichment of Phosphorous.

Sulphur.

Both the Collinsville and Mitsui combustion plants show some minor enrichment of sulphur downstream in the solid waste (Figure 5.10.). However, sulphur is still substantially depleted in all solid waste streams and is, therefore, classified as a Class III element for both combustion plants.

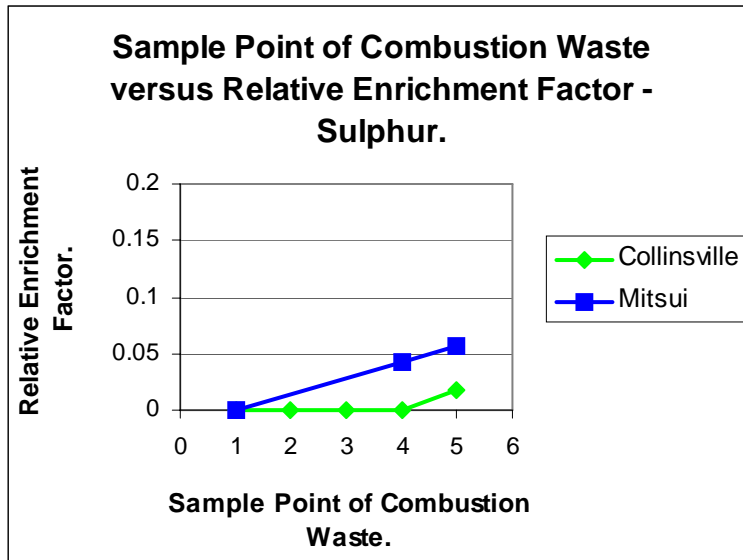


Figure 5.10. Relative Enrichment of Sulphur.

Gold.

A full suite of gold analyses is only available for the Mitsui combustion plant. Gold in the Mitsui combustion plant is classified as a Class IIa element because of the strong progressive enrichment of this element from the bottom-ash through to the fly-ash (Figure 5.11.), although the concentration of this element is very low and the classification should be considered provisional.

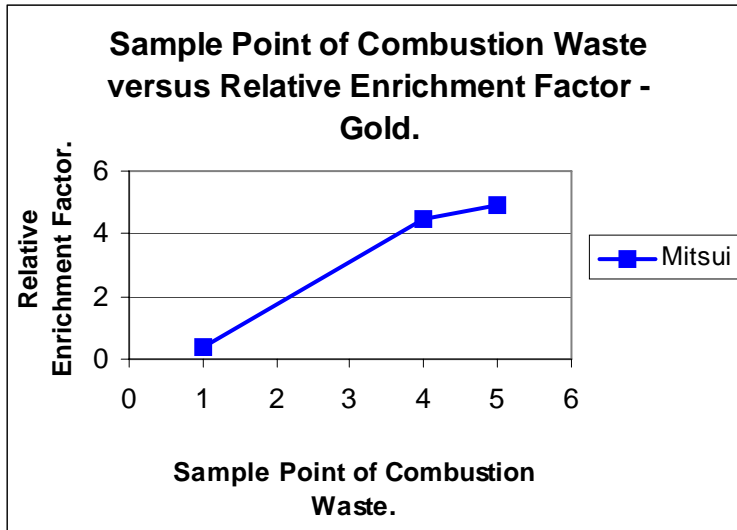


Figure 5.11. Relative Enrichment of Gold.

Arsenic.

Arsenic is very significantly depleted in all waste fractions of the Collinsville combustion plant, and is classified as a Class III element. Arsenic in the Mitsui combustion plant is also depleted in all waste fractions, however the fly-ash bunker waste is relatively more enriched than the other two waste stream samples (Figure 5.12.). Arsenic is classified as a Class III element, or possibly a Class II element if the enrichment in the fly-ash bunker waste is considered significant (Figure 5.12.), in the Mitsui combustion plant.

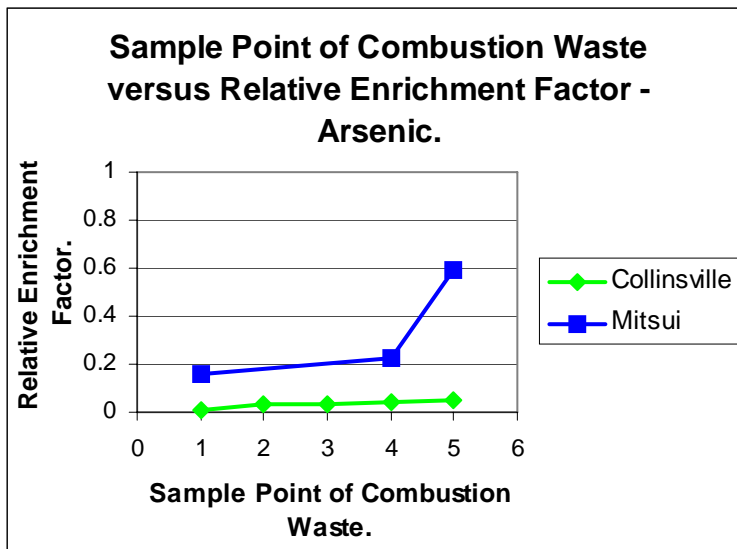


Figure 5.12. Relative Enrichment of Arsenic.

Boron.

Boron appears shows a similar behaviour to arsenic in the two combustion plants studied. Boron is depleted in all waste fractions of the Collinsville combustion plant, and is, therefore classified as a Class III element (Figure 5.13.). Boron in the Mitsui combustion plant is also depleted in all waste fractions, however the fly-ash bunker waste is considerably more enriched than the other two waste stream samples (Figure 5.13.). Boron is classified as a Class III element, or possibly a Class II element if the enrichment in the fly-ash bunker waste is considered significant, in the Mitsui combustion plant.

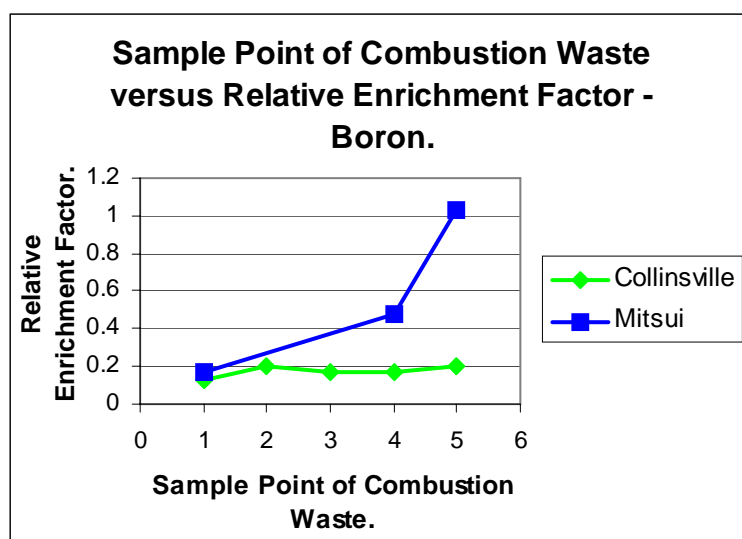


Figure 5.13. Relative Enrichment of Boron.

Barium.

Barium is classified as a Class I element in the Collinsville combustion plant because all RE figures are around 0.6 (ie close to 1) (Figure 5.14.), although barium is less enriched than would normally be expected for a Class I element. Barium is classified as a Class III element in the Mitsui combustion plant, at odds with the generally expected behaviour of this element. The Mitsui barium RE does show a slight relative enrichment trend from the bottom-ash the fly-ash, a Class II type feature (Figure 5.14.). However, all the RE values are well below the generally expected values for a Class II element, hence the classification of barium as a Class III element in the Mitsui plant.

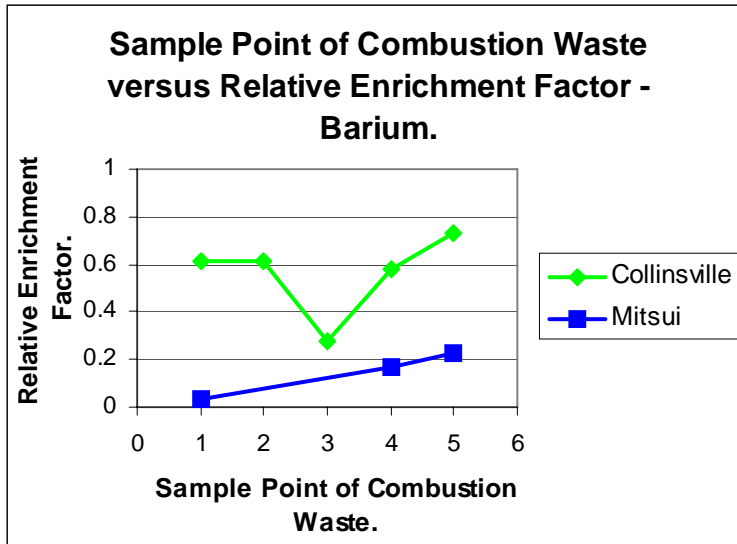


Figure 5.14. Relative Enrichment of Barium.

Cobalt.

Cobalt in the Collinsville combustion plant is depleted in all solid waste fractions (Figure 5.15.), and is classified as a Class III element. Although cobalt in the Mitsui plant is not as enriched in the bunker fly-ash as expected, the element is still classified as a Class II element because of the notable enrichment of this element from the bottom-ash to the fly-ash bunker, downstream in the combustion plant (Figure 5.15.).

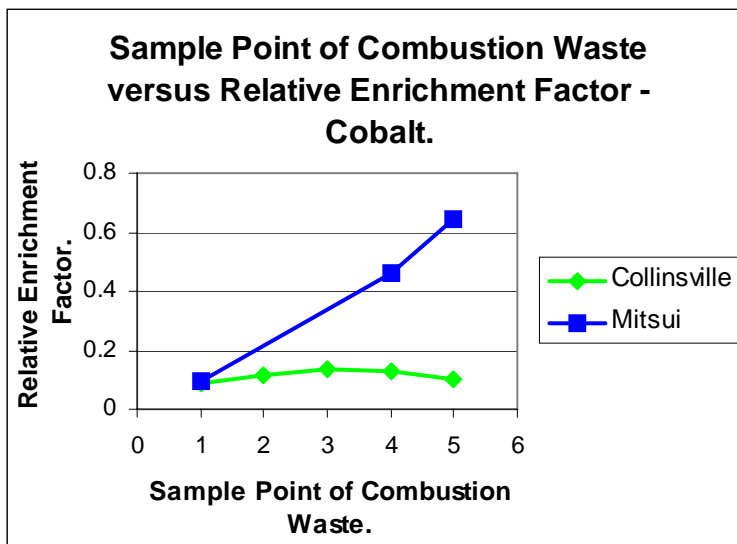


Figure 5.15. Relative Enrichment of Cobalt.

Chromium.

Figure 5.16. shows the behaviour of chromium in each of the two combustion plants studied. Chromium in the Collinsville combustion plant is depleted in all solid waste

fractions, and is classified as a Class III element. Although chromium in the Mitsui plant is not as enriched in the bunker fly-ash as expected, the element is still classified as a Class II element because of the notable enrichment of this element from the bottom-ash to the fly-ash bunker, downstream in the combustion plant.

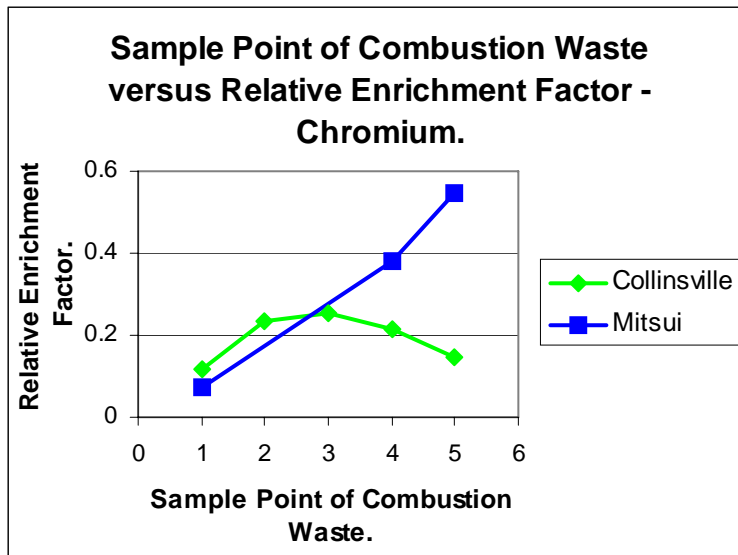


Figure 5.16. Relative Enrichment of Chromium.

Copper.

Copper in the Collinsville combustion plant is classified as a Class I element due to the consistent RE values of ~1 between the bottom-ash and the downstream fly-ash wastes (Figure 5.17.). Copper in the Mitsui combustion plant is classified as a Class II element because of the slight enrichment running downstream from the bottom-ash to the fly-ash (Figure 5.17.).

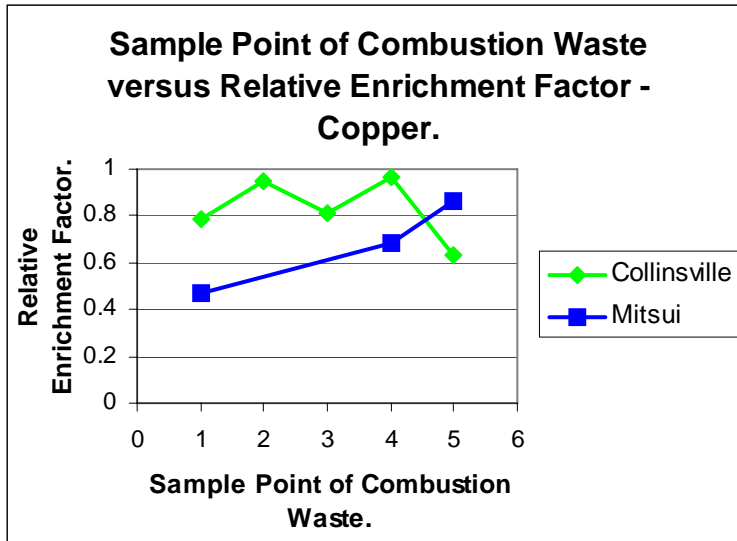


Figure 5.17. Relative Enrichment of Copper.

Caesium.

Caesium in the Collinsville combustion plant is classified as a Class III element due to the consistently low RE values ($\ll 1$) between the bottom-ash and the downstream fly-ash wastes (Figure 5.18.). Caesium in the Mitsui combustion plant, although consistently depleted in all waste streams (typical of a Class III element) is classified as a Class II element because of the slight enrichment running downstream from the bottom-ash to the fly-ash (Figure 5.18.).

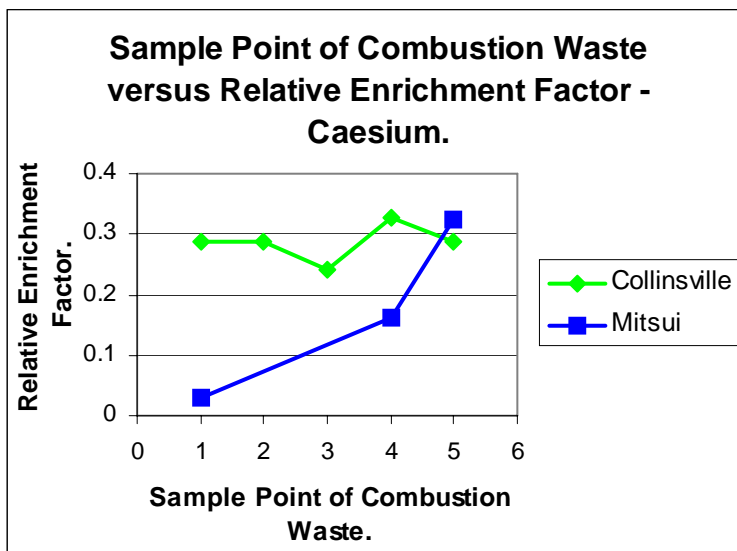


Figure 5.18. Relative Enrichment of Caesium.

Mercury.

Mercury in the Mitsui combustion plant is highly enriched in the fly-ash bunker sample, and depleted in the bottom-ash and burner outlet samples (Figure 5.19.). The enrichment of the bottom-ash relative to the burner outlet sample could be due to the high proportion of combustible (unburnt carbon?) in the bottom-ash (Table 5.1.). However, the mechanism for the significant enrichment of mercury in the fly-ash bunker waste is uncertain. Possibly the minor fraction of combustible (unburnt carbon?) material has captured mercury from the flue gas. The observed relative enrichment figures indicate that mercury in the Mitsui combustion plant should be classified as a Class IIb element.

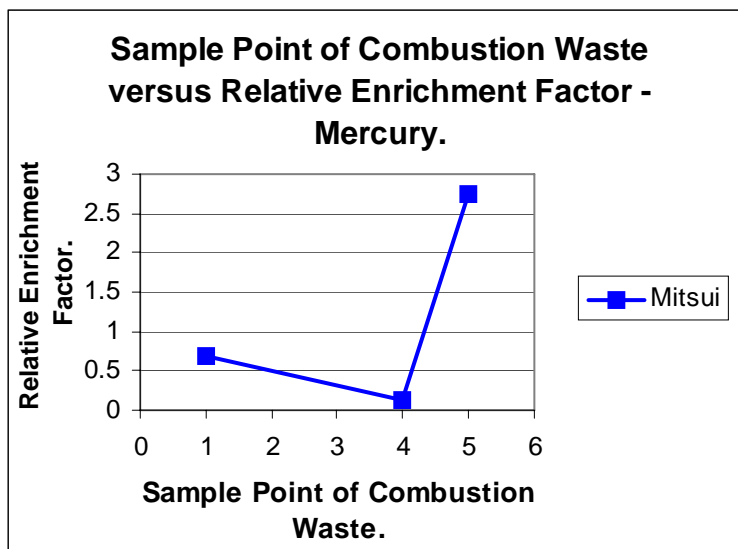


Figure 5.19. Relative Enrichment of Mercury.

Molybdenum.

Molybdenum is highly depleted in the Collinsville combustion plant waste streams, Mo concentrations being below detection limits for samples from the last two fly-ash sample points (Figure 5.20.). Molybdenum is classified as a Class III element in the Collinsville combustion plant. Molybdenum in the Mitsui combustion plant shows some downstream enrichment across the solid waste fractions, although Mo is still depleted in all solid waste (Figure 5.20.). Molybdenum is classified as Class III or Class II in the Mitsui combustion plant.

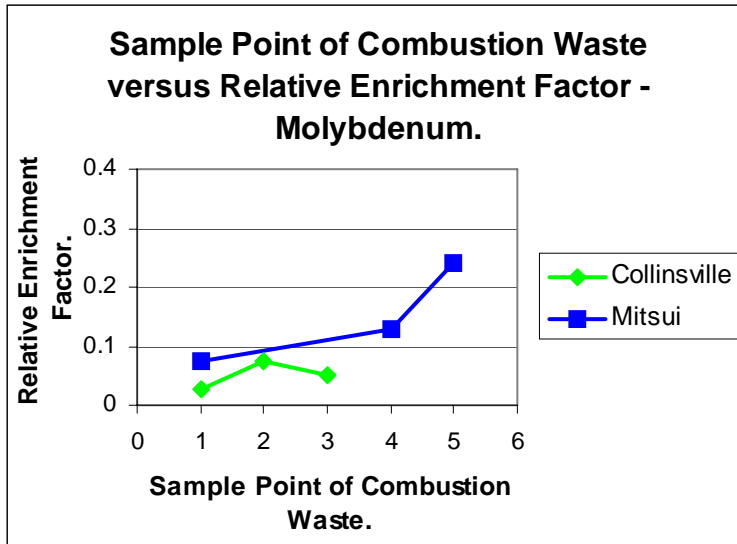


Figure 5.20. Relative Enrichment of Molybdenum.

Nickel.

Nickel is classified as a Class I element in the Collinsville combustion plant because of the lack of downstream enrichment exhibited by this element (Figure 5.21.). There is insufficient data to allow definitive classification of nickel in the Mitsui combustion plant. However, given the burnout outlet and fly-ash bunker samples contained nickel contents below the detection limits for INAA, it is likely all three samples points were depleted in nickel, similar to the bottom-ash RE data point shown in Figure 5.21. Such consistent depletion of nickel might suggest classification of nickel as a Class III element in the Mitsui combustion plant.

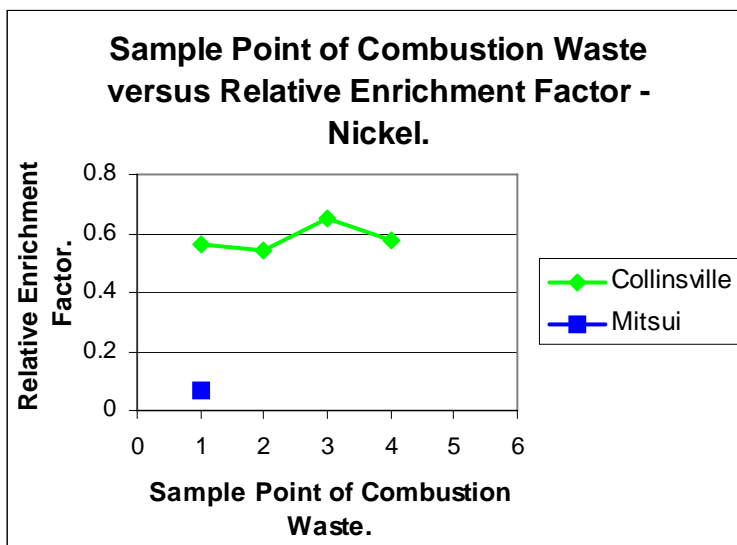


Figure 5.21. Relative Enrichment of Nickel.

Lead.

The trends of relative enrichment versus sample position for lead are strikingly similar for both the Mitsui and Collinsville combustion plants (Figure 5.22.). Although lead is depleted across all waste streams (<1), there is some relative enrichment in this element downstream in the combustion plant. Because of the notable enrichment of lead downstream, this element is classified as Class II for both combustion plants.

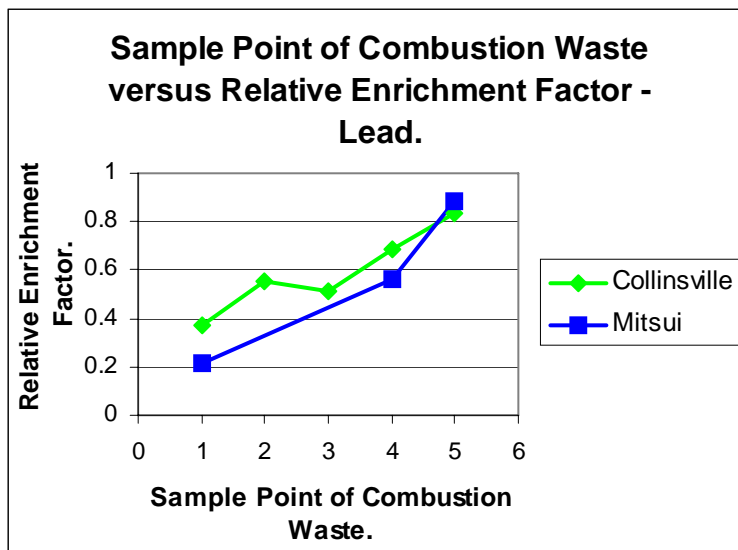


Figure 5.22. Relative Enrichment of Lead.

Rubidium.

Rubidium is present below the detection limits of INAA in samples of the bottom-ash and burner level in the Collinsville combustion plant. Further, the element appears to be depleted downstream, if the fly-ash bunker RE figure is believed (Figure 5.23.).

Given there is no apparent enrichment downstream, and all RE figures are close to or below 1, rubidium is classified as a Class I element in the Collinsville combustion plant. The available relative enrichment figures suggest rubidium is not enriched downstream in the Mitsui combustion plant, and should also be classified as a Class I element (Figure 5.23.).

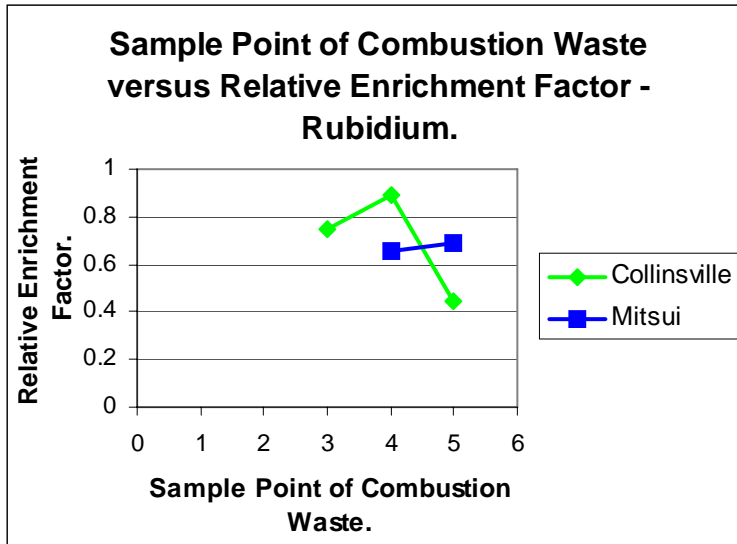


Figure 5.23. Relative Enrichment of Rubidium.

Antimony.

Antimony in the Collinsville combustion plant is classified as a Class III element due to the consistently low RE values ($\ll 1$) between the bottom-ash and the downstream fly-ash wastes (Figure 5.24.). Antimony in the Mitsui combustion plant, although consistently depleted in all waste streams (typical of a Class III element) is classified as a Class II element because of the notable enrichment running downstream from the bottom-ash to the fly-ash.

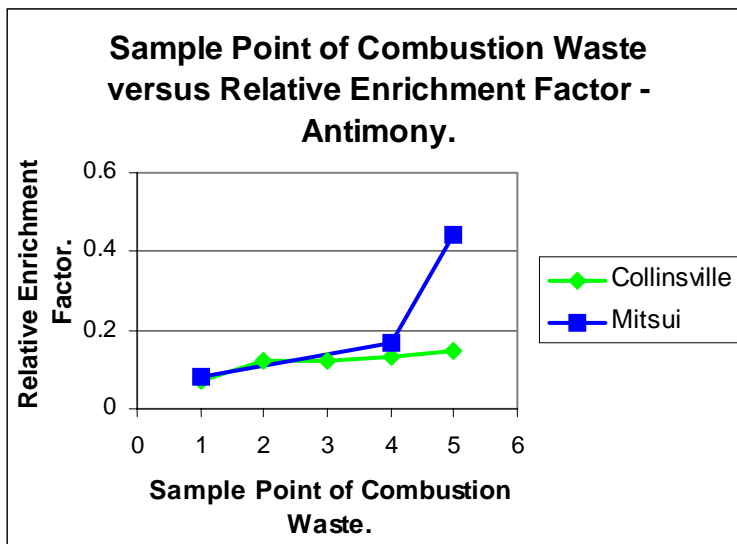


Figure 5.24. Relative Enrichment of Antimony.

Selenium.

Selenium appears to be consistently depleted in all waste fractions in both the Collinsville and Mitsui combustion plants (Figure 5.25.). Because of the consistently low relative enrichment values, selenium is classified as a Class III element for both combustion plants.

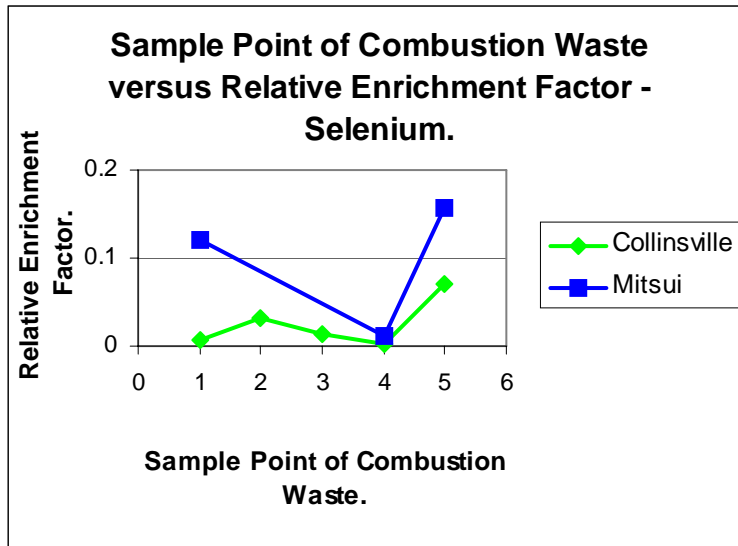


Figure 5.25. Relative Enrichment of Selenium.

Tin.

Tin in the Collinsville combustion plant, is consistently depleted in all waste streams (typical of a Class III element), but exhibits some Class II element type enrichment running downstream from the bottom-ash to the fly-ash (Figure 5.26.). Tin is classified as Class II or III in the Collinsville combustion plant.

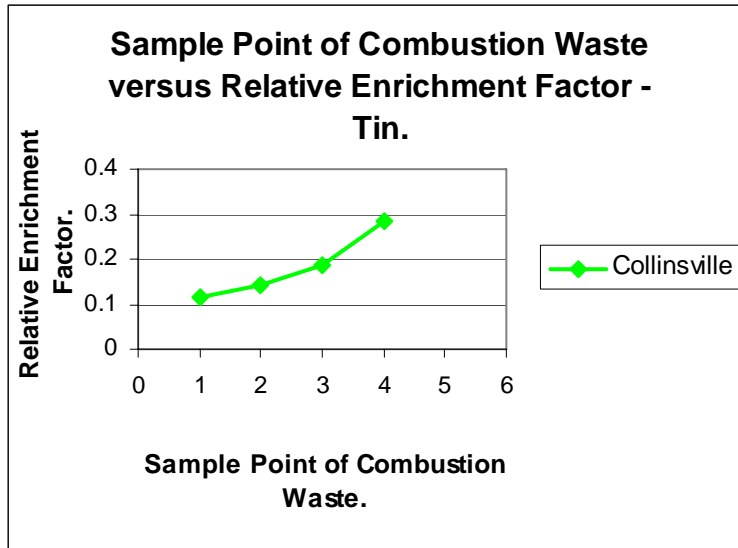


Figure 5.26. Relative Enrichment of Tin.

Thorium.

Thorium is mentioned separately from the rare earth elements because of the importance of this radionuclide element in environmental impact considerations of trace elements, although its' partitioning behaviour is very similar. However, as for the rare earth elements, thorium in the Collinsville combustion plant is classified as a Class III element due to the consistently low RE values ($\ll 1$) between the bottom-ash and the downstream fly-ash wastes (Figure 5.27.). Thorium in the Mitsui combustion plant, is consistently depleted in all waste streams (typical of a Class III element), but also exhibits some slight Class II element type enrichment running downstream from the bottom-ash to the fly-ash (Figure 5.27.). Thorium is classified as a Class II or III element in the Mitsui combustion plant.

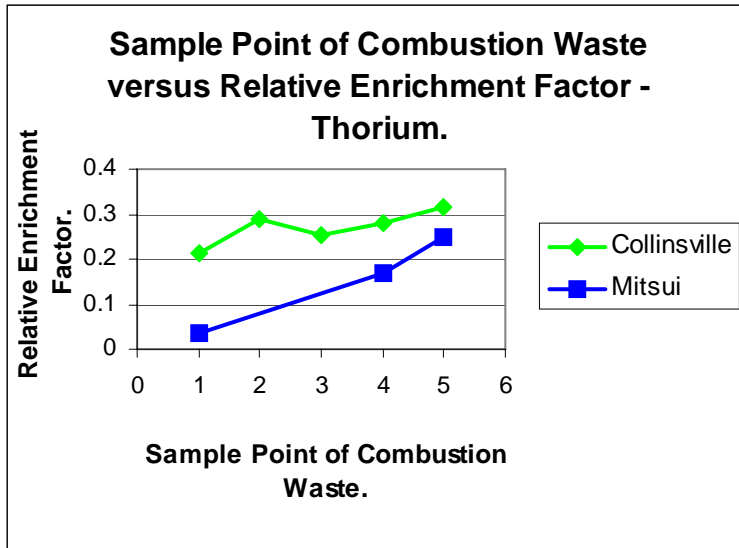


Figure 5.27. Relative Enrichment of Thorium.

Uranium.

The behaviour of uranium in the two combustion plans sampled appears similar to the behaviour of thorium and the rare earth elements. Uranium in the Collinsville combustion plant is classified as a Class III element due to the consistently low RE values ($\ll 1$) between the bottom-ash and the downstream fly-ash wastes (Figure 5.28.). Uranium in the Mitsui combustion plant, is consistently depleted in all waste streams (typical of a Class III element) (Figure 5.28.), but also exhibits some Class II type element enrichment running downstream from the bottom-ash to the fly-ash. Uranium is classified as Class II or III in the Mitsui combustion plant.

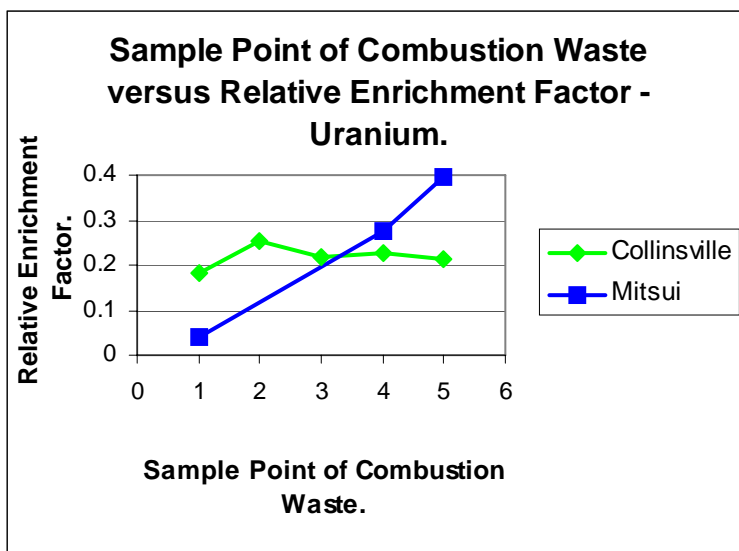


Figure 5.28. Relative Enrichment of Uranium.

Vanadium.

Vanadium in the Collinsville combustion plant remains consistently close to 1, and is classified as a Class I element (Figure 5.29.). Vanadium in the Mitsui combustion plant is also consistently close to 1 (characteristic of a Class I element), but may show some slight enrichment running downstream from the bottom-ash to the fly-ash (Figure 5.29.), and could, therefore, also be classified as a Class II element.

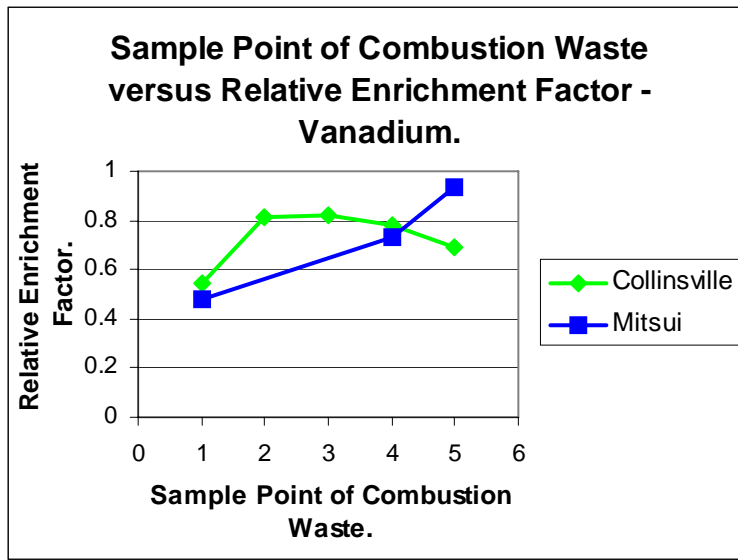


Figure 5.29. Relative Enrichment of Vanadium.

Tungsten.

The relative enrichment figures show tungsten is significantly depleted in all waste streams sampled and in both combustion plants (Figure 5.30.). Because of this depletion, tungsten is classified as a Class III element in both the Mitsui and Collinsville combustion plants.

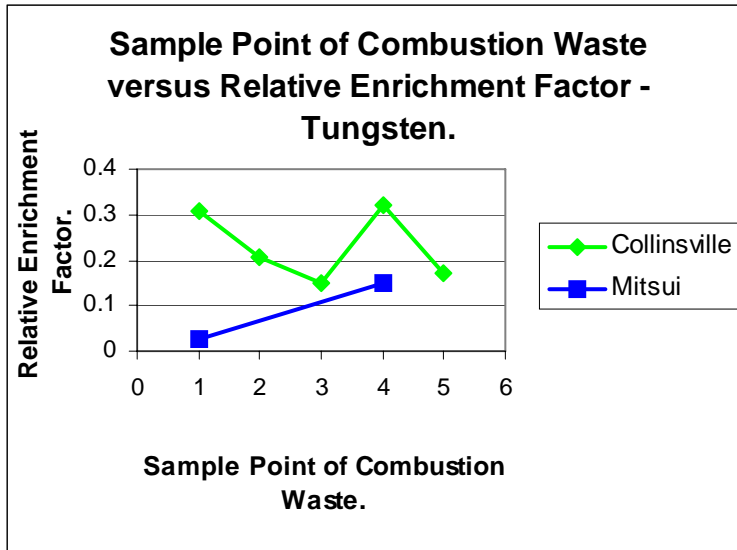


Figure 5.30. Relative Enrichment of Tungsten.

Zinc.

Zinc is significantly depleted in all waste streams sampled and in both combustion plants (Figure 5.31.). Because of this depletion, zinc is classified as a Class III element in both the Mitsui and Collinsville combustion plants. Both combustion plants show some slight enrichment of zinc running downstream from the bottom-ash to the fly-ash, a characteristic of Class II elements. The enrichment is particularly notable for the Mitsui plant, suggesting zinc could also be classified as a Class II element in that plant.

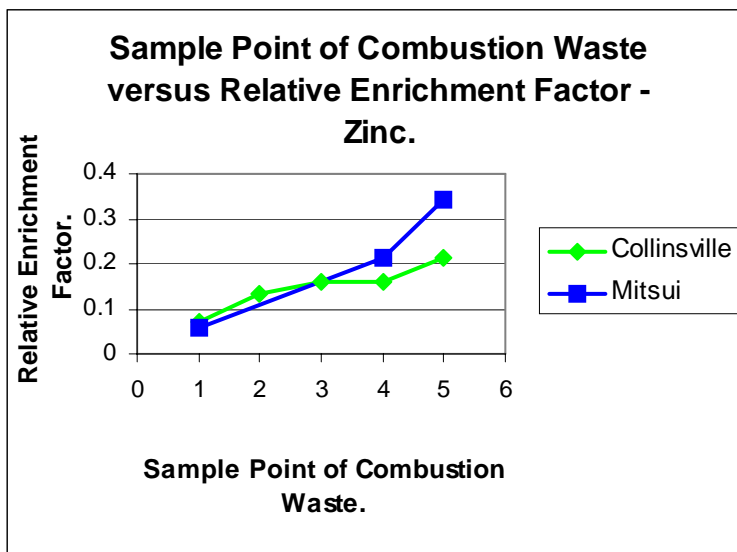


Figure 5.31. Relative Enrichment of Zinc.

Hafnium, Iridium, Strontium, Scandium, Tantalum and the Rare Earth Elements.

There is a notable similarity in the relative enrichment trends for the rare earth elements, hafnium, strontium, scandium, and tantalum between the Collinsville and Mitsui combustion plants. Because of this similarity, the rare earth elements, hafnium, iridium, strontium, scandium, and tantalum are considered as a group. The group of elements listed above are classified as Class III elements in the Collinsville combustion plant because of the consistently low RE values ($\ll 1$) between the bottom-ash and the downstream fly-ash wastes (see Figures 5.32., 5.33., 5.34., 5.36., 5.37., 5.38., 5.39., 5.40., 5.41., 5.42., 5.43., and 5.44.). The same group of elements listed above, although consistently depleted in all waste streams (characteristic of Class III element), are classified as Class II elements in the Mitsui combustion plants because of the slight enrichment running downstream from the bottom-ash to the fly-ash (see Figures 5.32., 5.33., 5.34., 5.36., 5.37., 5.38., 5.39., 5.40., 5.41., 5.42., 5.43., and 5.44.). All these elements usually classified as Class I in the literature (see Section 5.4.).

The exception to the notable similarities in the relative enrichment patterns for the two combustion plants is iridium. Iridium shows a startling consistency of depleted RE figures across all solid waste streams (Figure 5.35.). Iridium is classified as a Class III element in both the Collinsville and Mitsui combustion plants.

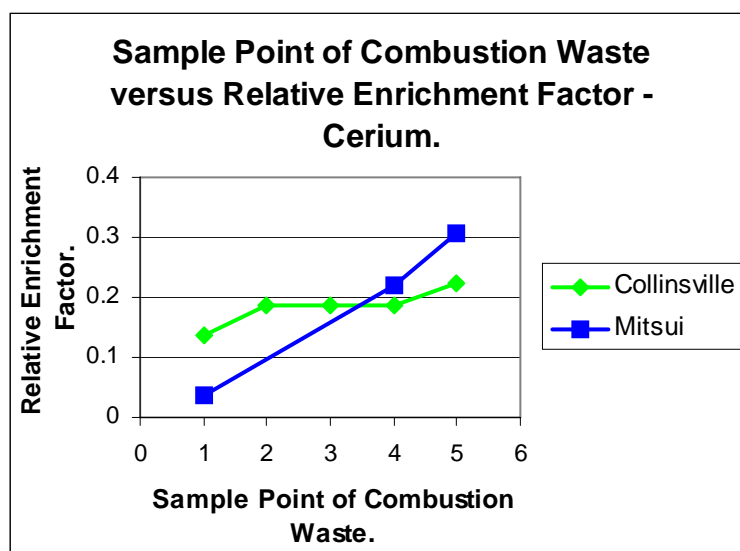


Figure 5.32. Relative Enrichment of Cerium.

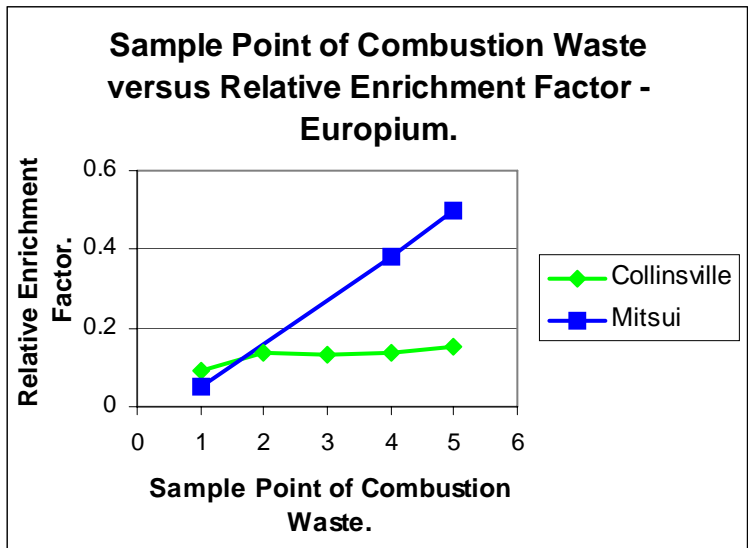


Figure 5.33. Relative Enrichment of Europium.

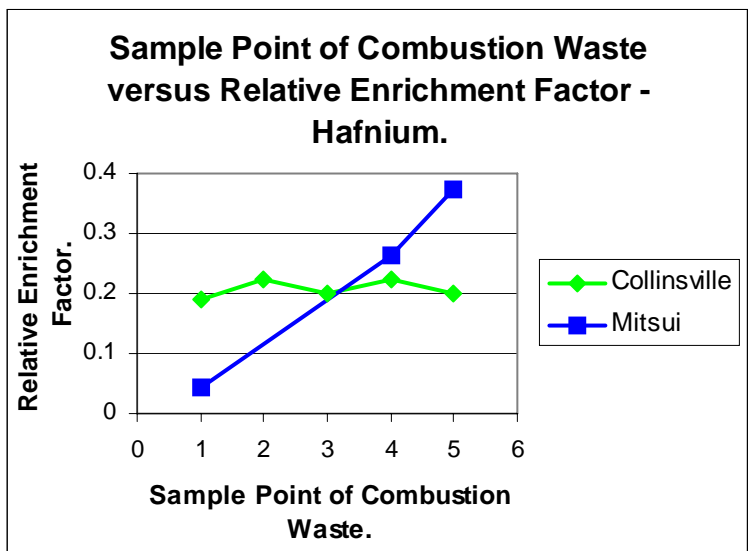


Figure 5.34. Relative Enrichment of Hafnium.

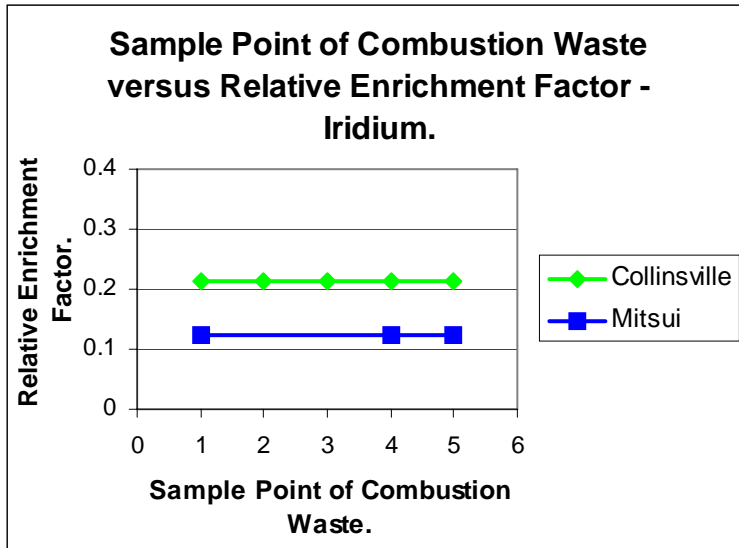


Figure 5.35. Relative Enrichment of Iridium.

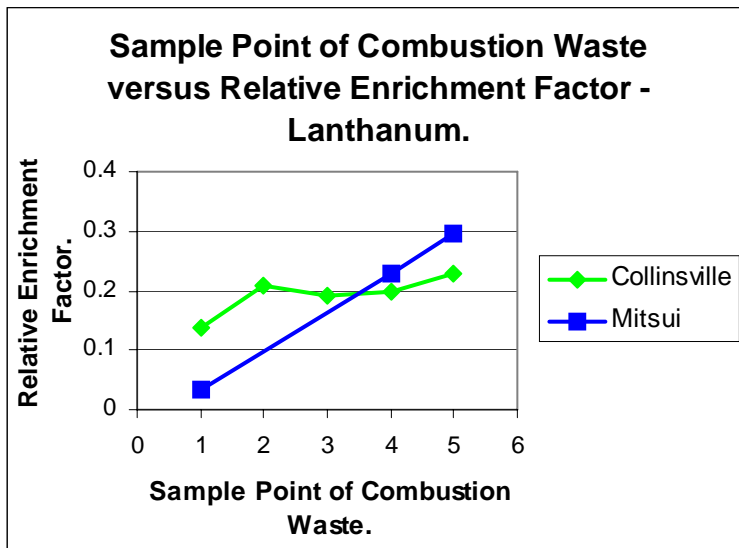


Figure 5.36. Relative Enrichment of Lanthanum.

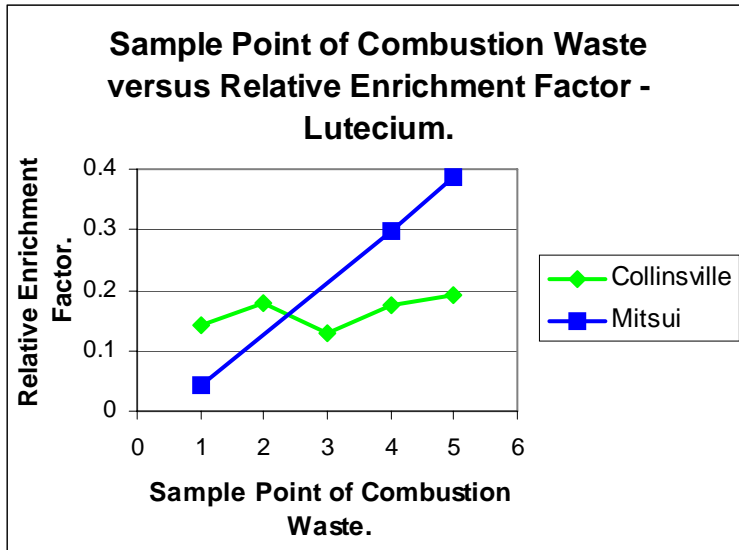


Figure 5.37. Relative Enrichment of Lutetium.

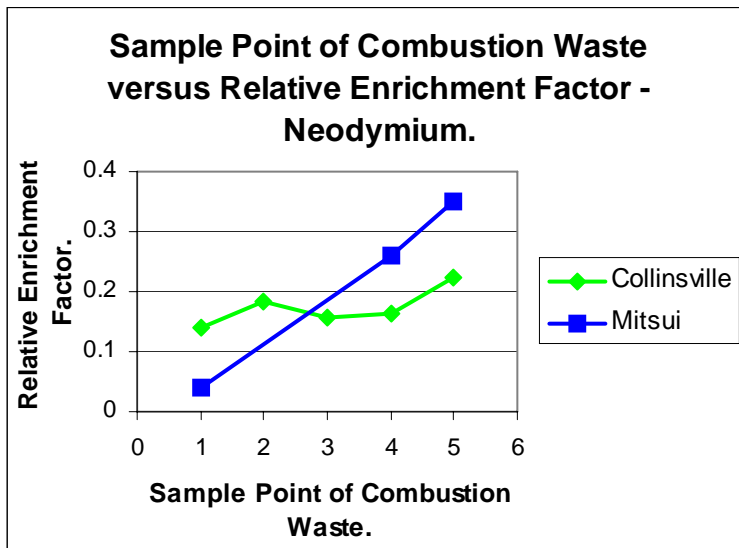


Figure 5.38. Relative Enrichment of Neodymium.

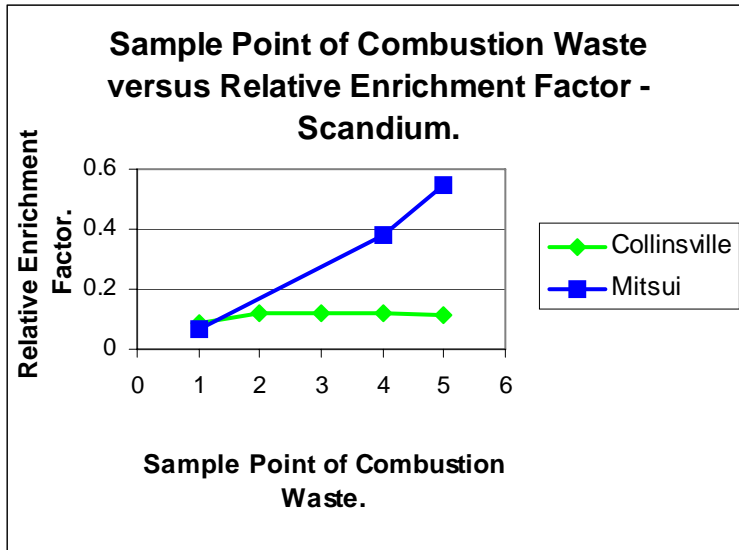


Figure 5.39. Relative Enrichment of Scandium.

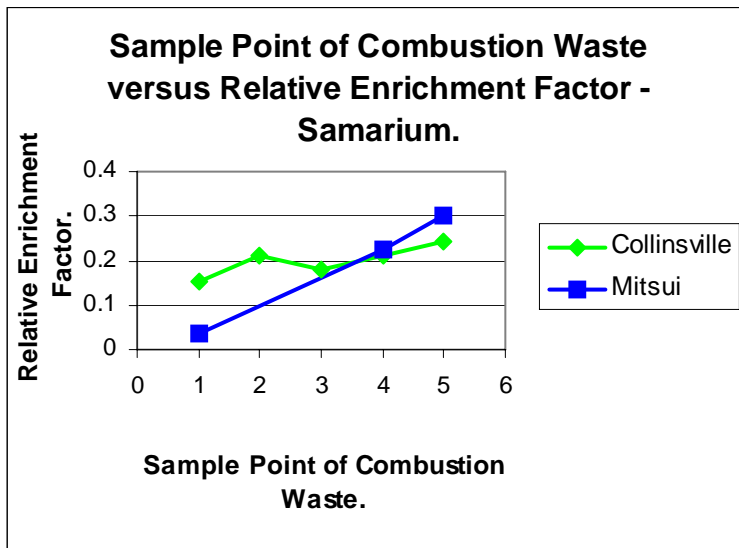


Figure 5.40. Relative Enrichment of Samarium.

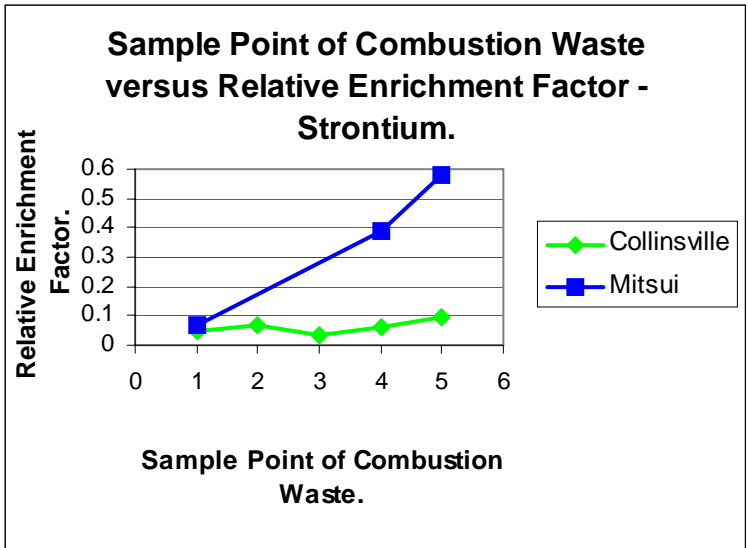


Figure 5.41. Relative Enrichment of Strontium.

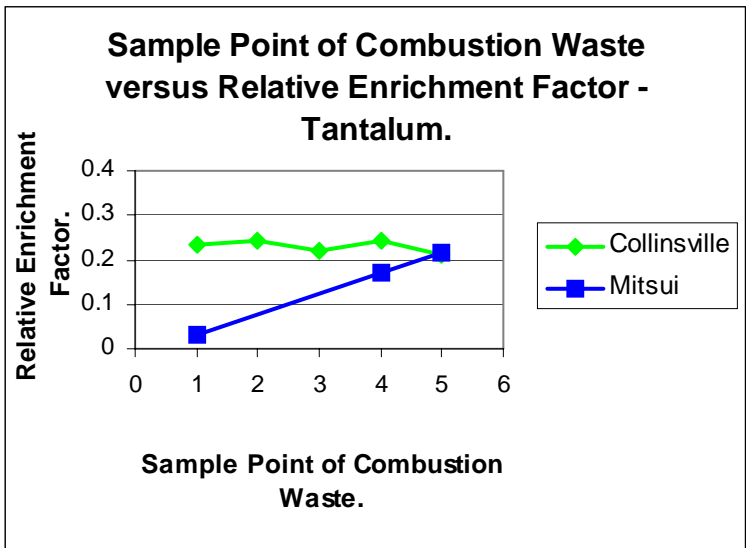


Figure 5.42. Relative Enrichment of Tantalum.

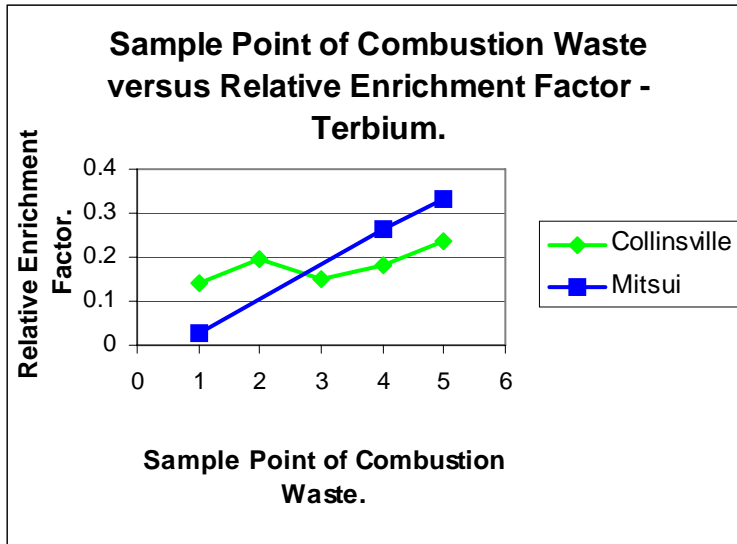


Figure 5.43. Relative Enrichment of Terbium.

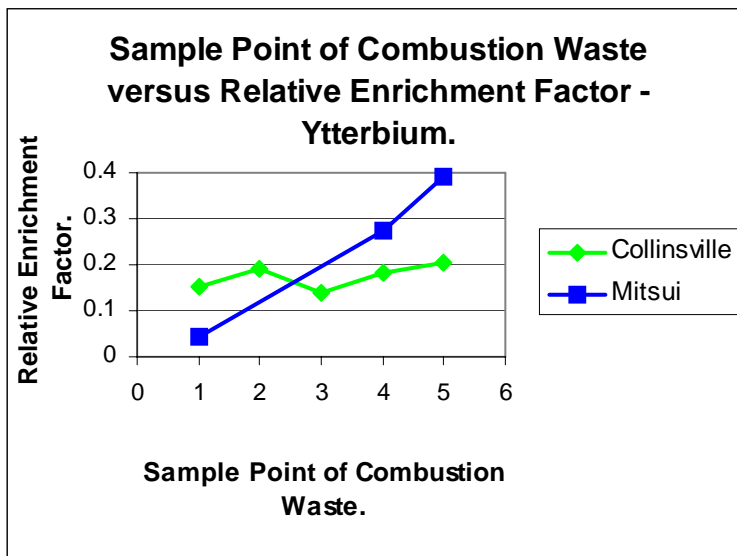


Figure 5.44. Relative Enrichment of Ytterbium.

5.4. Comparison of Partitioning Behaviour.

The most comprehensive recent publications on the partitioning behaviour of trace elements in combustion are Meij (1995) and Clarke (1995). Table 5.4. summarises the data of Meij and Clarke, along with results for combustion plants in this study.

The classification of the major elements silicon, aluminium, iron, magnesium, titanium, and sulphur, and the trace elements selenium and iridium are the same as found in the literature (Table 5.4.).

Sodium in the Collinsville combustion plant appears to be significantly more volatile than would be expected (Table 5.4.). The USGS figure for sodium in the fuel sample is considerably lower than the INAA figure, however the INAA figures for the fly-ash were used in calculating relative enrichment, so this should not be a source of error. Further, the Mitsui combustion plant classification agrees with the literature examples. Data presented in Section 4.4. of this work notes a high proportion of sodium is present in the Collinsville coal in ionic form (eg possibly NaCl). Potentially this ionic sodium is more volatile in the combustion plant and has been substantially lost during combustion.

Manganese is classified as a Class I element in both the Collinsville and Mitsui combustion plants, similar (slightly less volatile) to the IIC classification found in the literature (Table 5.4.). Phosphorous is also found to be less volatile in the Mitsui and Collinsville combustion plants compared to the published examples (Table 5.4.).

Gold was found to be moderately volatile, (IIA) but no literature classification of this element could be found.

Arsenic and boron were found to be highly volatile in the Collinsville combustion plant, and moderately to highly volatile in the Mitsui combustion plant. Generally arsenic and boron are classified as either Class II or Class III elements in the literature (Table 5.4.). However, the Collinsville and Mitsui solid wastes are significantly more depleted than would generally be expected.

Barium is classified as a Class I element in the Collinsville combustion plant, similar to the published Class IIC (relatively non-volatile) classification (Table 5.4.). However, barium in the Mitsui combustion plant is classified as a Class II/III (volatile) element, a classification at odds with the published literature (Table 5.4.).

Cobalt and chromium are classified as Class III elements in the Collinsville combustion plant, and Class II elements in the Mitsui combustion plant. Cobalt is classified as a Class IIB element, and chromium as a Class IIC element in the literature examples (Table 5.4.).

Copper in the Collinsville combustion plant is classified as a Class I element, ie non-volatile, and as a Class II element in the Mitsui combustion plant. Copper is classified as a Class IIB element in the literature (Table 5.4.), therefore the Collinsville copper appears to be less volatile than would be expected from the literature examples.

Caesium is classified as a Class III element in the Collinsville combustion plant, and as a Class II/III in the Mitsui combustion plant. Caesium is classified as Class I in the literature examples (Table 5.4.), so caesium in the Mitsui and Collinsville combustion plants appears to be more volatile than would be expected from the literature examples.

Mercury results are only available for the Mitsui combustion plant fly-ash, and the element is classified as a Class IIB element. The Mitsui classification of mercury is slightly less volatile than expected from the literature classification of mercury as a Class III element (Table 5.4.).

Molybdenum is classified as a Class III element in the Collinsville combustion plant, and as a Class II/III element in the Mitsui combustion plant, close to the expected literature classification of Class IIA (Table 5.4.).

Nickel is classified as a Class I element in the Collinsville combustion plant, and is less volatile than expected given the literature classification of the element is Class IIB (Table 5.4.). Conversely, nickel is classified as a Class III element in the Mitsui combustion plant, more volatile than expected from the literature classification (Table 5.4.).

Lead is classified as a Class III element in the Collinsville combustion plant, and as a Class II element in the Mitsui combustion plant. These results are in general agreement with the literature classification of lead as a Class IIA element (Table 5.4.).

Rubidium is classified as a Class I element in both the Collinsville and Mitsui combustion plants. Generally rubidium is classified as Class IIC (Table 5.4.),

suggesting this element is behaving in a less volatile manner in the Collinsville and Mitsui combustion plants.

Antimony is classified as a Class III element in the Collinsville combustion plant, and a Class II/III in the Mitsui combustion plant. Antimony is classified as a Class II element in the literature (Table 5.4.), suggesting antimony in the two combustion plants sampled in this study is more volatile than expected from published research.

Tin is classified as a Class II/III element in the Collinsville combustion plant. No partitioning classification for tin could be found in the literature.

Thorium and uranium are classified as Class III elements in the Collinsville combustion plant, and as Class II/III elements in the Mitsui combustion plant. Thorium is classified as a Class I element in the literature (Table 5.4.), indicating this element is significantly more volatile in both the Collinsville and Mitsui combustion plants than would be expected from published results. Uranium is classified as a Class IIB element in the literature (Table 5.4.), indicating this element is also behaving in a more volatile manner in the two studied combustion plants than would be expected from previous published results.

Vanadium is classified as a Class I element in the Collinsville combustion plant, and as a Class I/II element in the Mitsui combustion plant. Vanadium is classified as a IIB element in the published examples (Table 5.4.), therefore this element appears significantly less volatile in the Collinsville plant, and perhaps slightly less volatile than expected in the Mitsui plant.

Tungsten and zinc are both classified as a Class III elements in the Collinsville and Mitsui combustion plants. The classification of these elements as Class III makes tungsten more volatile in the studied combustion plants than expected from the literature classification of tungsten as a Class IIB element (Table 5.4.). Zinc is also slightly more volatile in the Collinsville and Mitsui combustion plants than expected from the Class IIA literature classification (Table 5.4.).

The rare earth elements and hafnium are classified as Class III elements in the Collinsville combustion plant, and Class II/III elements in the Mitsui combustion plant. Rare earth elements and hafnium are generally classified as Class I in the literature (Table 5.4.), indicating these elements are behaving in a significantly more volatile manner than would be expected from published classifications. A varying proportion of the rare earth elements in the Collinsville coal may be associated with the organic fraction of the coal, particularly the heavy rare earth elements. Possibly the organically bound rare earth elements are being volatilised. However, there appears to be no preferential volatilisation of the heavy REE's compared to the light REE's. Therefore, no conclusive reason for the significantly higher volatility of thorium, hafnium and the REE's in the Collinsville and Mitsui combustion plants compared to published examples can be given at this time.

Table 5.4. Partitioning Class of Elements in Collinsville, Mitsui and Literature Example Combustion Plants.

Element	Element Class		
	Collinsville	Mitsui	* Published
Silicon	I	I	I
Aluminium	I	I	I
Iron	I	I	I
Magnesium	I	I	I
Sodium	III	IIC	IIC
Titanium	I	I	I
Manganese	I	I	IIC
Phosphorous	IIC	IIC	IIB
Sulphur	III	III	III
Gold		IIA	
Arsenic	III	II/III	IIA
Boron	III	II/III	III
Barium	I	II/III	IIC
Cobalt	III	II	IIB
Chromium	III	II	IIC
Copper	I	II	IIB
Caesium	III	II/III	I
Mercury		IIB	III
Molybdenum	III	II/III	IIA
Nickel	I	III	IIB
Lead	III	II	IIA
Rubidium	I	I	IIC
Antimony	III	II/III	II
Selenium	III	III	III
Tin	II/III		
Thorium	III	II/III	I
Uranium	III	II/III	IIB
Vanadium	I	I/II	IIB
Tungsten	III	III	IIB
Zinc	III	II/III	IIA
Rare Earth Elements	III	II/III	I
Iridium	III	III	III

* Source Meij (1995); Clarke (1995)

5.5. Chapter Summary.

Samples of bottom-ash and fly-ash from various positions downstream of the combustion zone from the Collinsville and Mitsui power utilities have been analysed by INAA and XRF. Partitioning behaviour for major and trace elements has been

assessed using relative enrichment values. Some significant differences between the two plants and by comparison with other published classifications have been documented.

Chapter 6.

Trace Element Partitioning Behaviour in Carbonisation.

6.0. Chapter Resume.

Samples of feed coal, coke, and quench tower washings (breeze) were collected from the Bowen Coke works, Bowen, Northern Queensland, Australia. All samples were analysed for a range of trace and major elements by INAA and XRF. In addition some samples were analysed for boron by microwave digestion ICP-MS. The intention was to gather data on the partitioning behaviour of trace elements during carbonisation (no literature examples could be found).

6.1. Samples.

Splits of the train samples for the Bowen coke works trains over the period 25th August to 18th November 1999 were provided by Mr Ray Slater of Collinsville Coal. At the time of sampling, coal for the Bowen coke works was mined exclusively from the lower 2-3m of the Bowen Seam in the Bowen Central pit.

Coke and quench tower washings at the Bowen coke works, Bowen, Northern Queensland (Figure 6.1.) were sampled over the period 7th October to 2nd November 1999 by Mr John Laidlaw. The Bowen coke works uses beehive ovens for coke production (Figure 6.1.) Samples were bagged and labelled with the train number delivering the feed coal and the date of sampling.

Total moisture, proximate analysis, specific energy, crucible swelling number, and fluidity results for the Bowen coke works train samples were provided by Mount Isa Mines, who operated the Collinsville coal mine. All samples were analysed for a range of major and trace elements by commercial laboratories using INAA and XRF, apart from boron, which was measured by microwave ICP-MS. Analytical results are shown in Appendix 7. Boron was found to be present in very low concentrations (generally below the 3 ppm detection limit of ICP-MS) in the train samples and is not considered further in this study. A generally excellent relationship exists between the INAA and XRF figures for iron, suggesting the results of INAA and XRF analysis are comparable, at least for iron.



Figure 6.1. Bowen Coke Works.

6.2. Analysis Results.

Before assessing the partitioning behaviour of the trace elements in carbonisation, it was important to assess the consistency of delivered coal quality (total moisture, moisture (adb), ash yield (adb), volatile matter (adb), and crucible swelling), and trace element concentration in the feed coal, coke and breeze samples.

6.2.1. Coal Quality.

Figure 6.2. shows the results of the Bowen coke works train samples during the time period the Bowen coke works was sampled. It should be noted that a good consistent product quality in terms of ash yield, volatile matter, total moisture, moisture (adb), and crucible swelling number was delivered during the period of sampling. The consistency of quality delivered to the Bowen coke works is an important indicator of the validity of the partitioning behaviour assessment undertaken below.

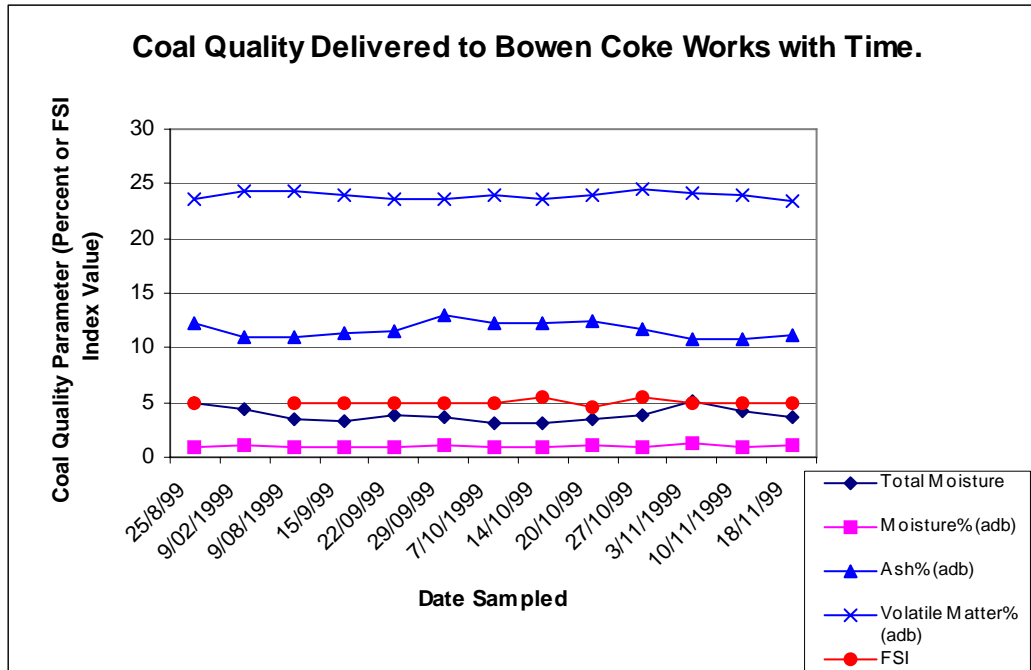


Figure 6.2. Quality Parameters of Coal Delivered to the Bowen Coke works During Time of Sampling.

6.2.2. Trace Element Partitioning Behaviour.

The partitioning behaviour of trace elements in carbonisation is examined individually by element. Each section includes graphs showing the analysed concentration of trace elements in the feed coal, coke, and breeze samples. Element partitioning behaviour is assessed using a modified version of the fly-ash relative enrichment calculation.

The original relative enrichment calculation is shown in Equation 6.1.

Equation 6.1.

$$RE = \frac{(\text{element concentration in ash})}{(\text{element concentration in coal})} \times \frac{(\% \text{ ash yield in coal})}{100}$$

However it is reasoned here that, since coke does not comprise 100% ash, the relative enrichment equation should be modified and the ash yield of the coke or breeze used as the divisor in the second part of the RE equation. NB, the assumption that solid wastes from pulverised fuel combustion comprise 100% ash or “incombustibles” could also be challenged. The modified coke relative enrichment equation (CRE) is presented in Equation 6.2..

Equation 6.2.

$$\text{CRE} = \frac{(\text{element concentration in coke or breeze})}{(\text{element concentration in coal})} \times \frac{(\% \text{ ash yield in coal})}{(\% \text{ ash yield, coke or breeze})}$$

Coke relative enrichment factors are calculated for each sample where elemental analyses for the feed coal and corresponding coke and/or breeze samples are available. Average concentrations for trace elements in feed coal, coke, and/or breeze are not used unless there is insufficient data available for corresponding samples. In many cases, insufficient data resulted from the removal of all “below detection limit” figures. In these cases coke relative enrichment factors are average figures calculated from the geometric average concentration of an element in the feed coal, coke and breeze (see Section 6.2.3. below).

The relative enrichment figures for breeze should be treated with caution. Only two breeze samples were collected from the quench tower wash settling pond due to the smaller volume of this waste relative to the product coke. Hence there is some uncertainty over the exact trains the breeze sample corresponds with, and samples are matched with feed coal based on the date of sampling only.

Average coke relative enrichment figures are calculated and detailed below. Average figures are geometric averages because, in many cases, one or two relative enrichment figures appeared radically different to the other CRE figures (eg sodium) and could be spurious. A geometric average allows the frequency distribution of the data to influence the average figure. Where average element concentration figures are used to calculate CRE, geometric average ash values for the coal, coke and breeze are used in the CRE equation.

Silicon.

Figure 6.3. shows the concentration of silicon in the feed coal and coke was relatively consistent during the period of sampling. The two samples of breeze from the quench tower pond show differing silicon concentrations.

Figure 6.4. presents the CRE figures over the period of sampling. As expected from the consistent concentration of silicon in both the feed coal and coke, the CRE figures

for coke are relatively consistent. Notably, the CRE figures for the breeze are similar once the influence for the different ash concentrations in the two breeze samples are normalised. The geometric average CRE figure is 0.96 for the coke samples and 1.04 for the breeze samples.

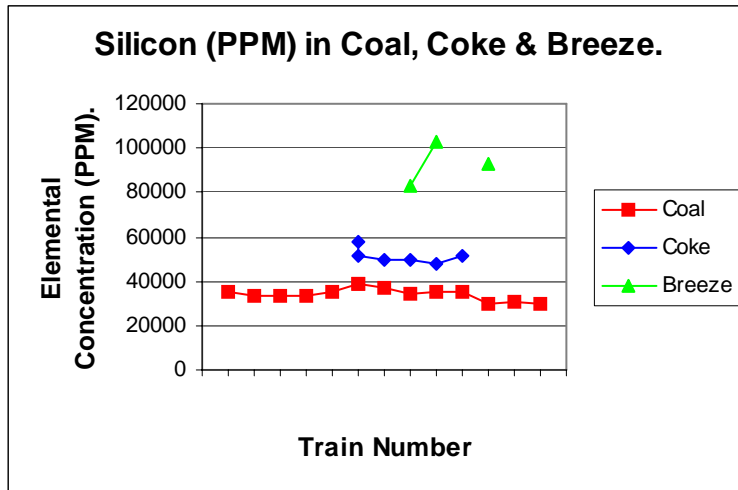


Figure 6.3. Concentration of silicon in feed coal and coke with time.

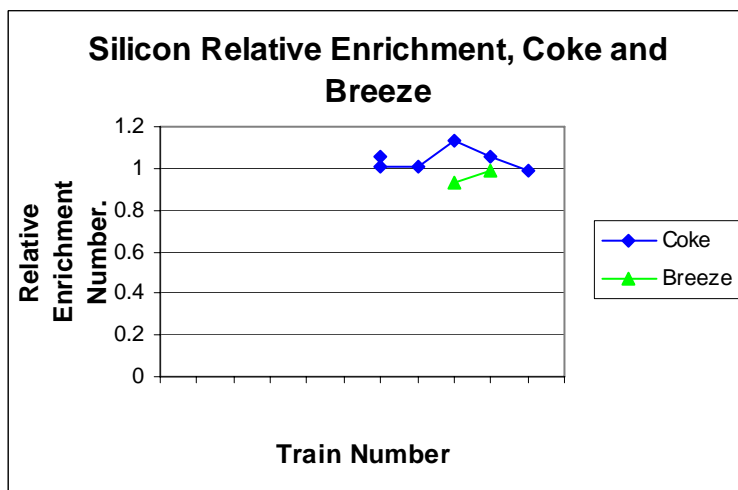


Figure 6.4. Silicon CRE for coke and breeze with time.

Aluminium.

The partitioning behaviour of aluminium in carbonisation is very similar to silicon. Figure 6.5. shows the concentration of aluminium in the feed coal and coke was relatively consistent during the period of sampling. The two samples of breeze from the quench tower pond show differing aluminium concentrations.

Figure 6.6. presents the CRE figures over the period of sampling. As expected from the consistent concentration of aluminium in both the feed coal and coke, the CRE

figures for coke are relatively consistent. As for silicon, CRE figures for the breeze are similar once the influence for the different ash concentrations in the two breeze samples are normalised. The geometric average CRE figure is 0.98 for the coke samples and 0.92 for the breeze samples.

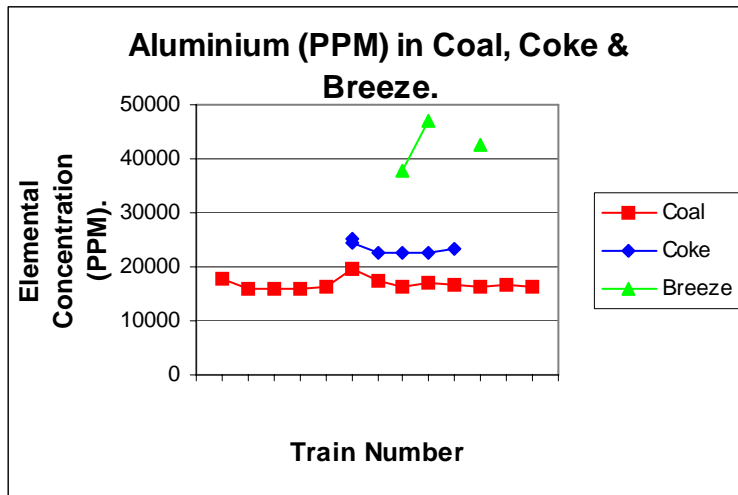


Figure 6.5. Concentration of aluminium in feed coal and coke with time.

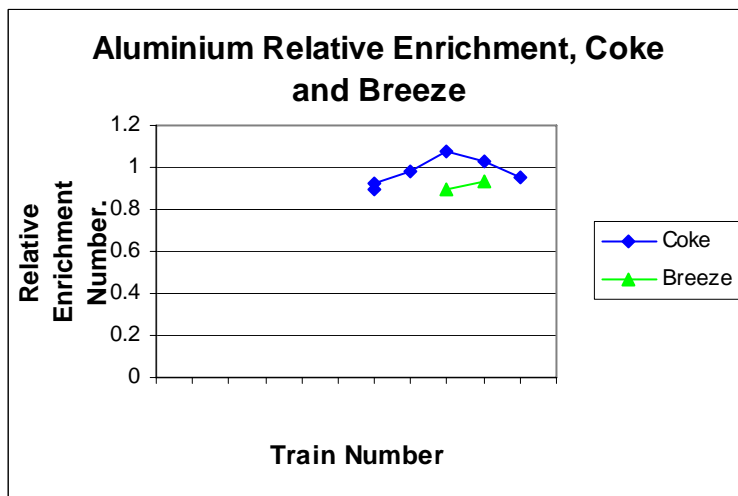


Figure 6.6. Aluminium CRE for coke and breeze with time.

Iron.

Figure 6.7. shows the concentration of iron in the feed coal, coke, and breeze was relatively consistent during the period of sampling.

Figure 6.8. presents the CRE figures over the period of sampling. As expected from the consistent concentration of iron in both the feed coal and coke, the CRE figures for coke are relatively consistent. However, the CRE figures for the breeze are

substantially different once the influence for the different ash concentrations in the two breeze samples are normalised. The geometric average CRE figure is 0.97 for the coke samples and 1.60 for the breeze samples.

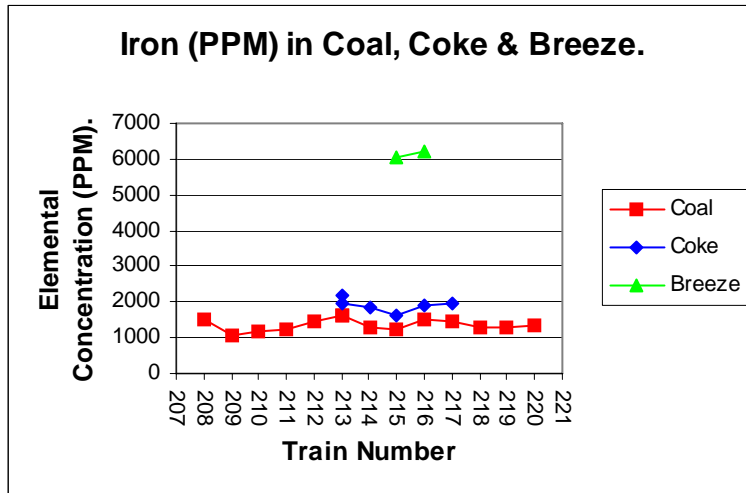


Figure 6.7. Concentration of iron in feed coal and coke with time.

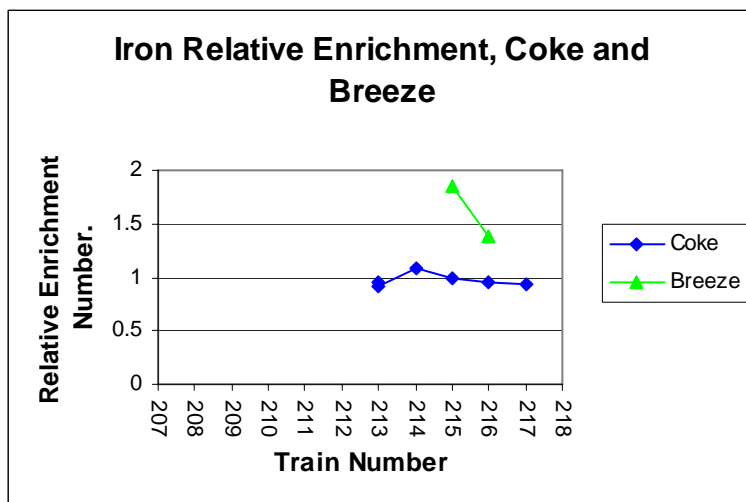


Figure 6.8. Iron CRE for coke and breeze with time.

Sodium.

Figure 6.9. shows the concentration of sodium in the feed coal, coke, and breeze was relatively consistent during the period of sampling apart from one coke sample that showed an unusually high sodium concentration.

Figure 6.10. presents the CRE figures over the period of sampling. As expected from the consistent concentration of sodium in both the feed coal and coke, the CRE figures for coke are relatively consistent (apart from the one high concentration coke

sample figure). The CRE figures for the breeze were also relatively consistent. The geometric average CRE figure is 1.54 for the coke samples and 2.33 for the breeze samples.

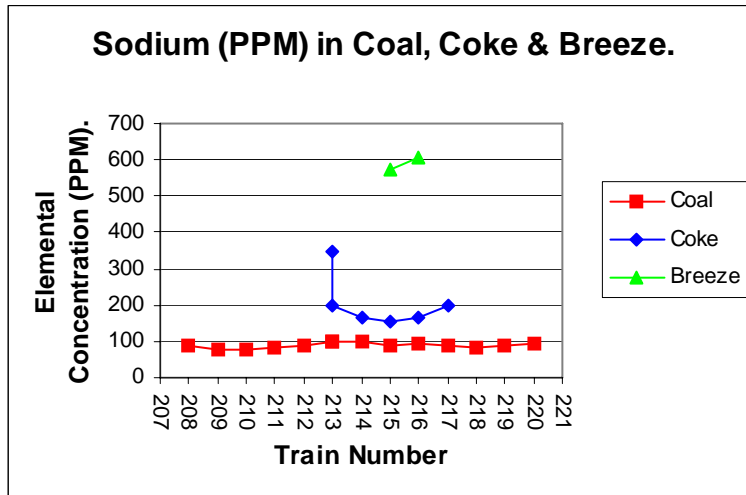


Figure 6.9. Concentration of sodium in feed coal and coke with time.

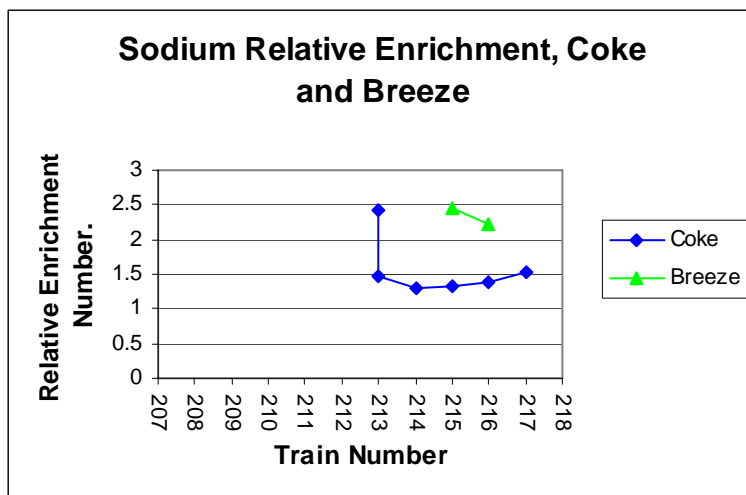


Figure 6.10. Sodium CRE for coke and breeze with time.

Titanium.

The partitioning behaviour of titanium in carbonisation is very similar to that of silicon and aluminium. Figure 6.11. shows the concentration of titanium in the feed coal and coke was relatively consistent during the period of sampling. The two samples of breeze from the quench tower pond show different concentrations of titanium.

Figure 6.12. presents the CRE figures over the period of sampling. As expected from the consistent concentration of titanium in both the feed coal and coke, the CRE figures for coke are relatively consistent. As for silicon and aluminium, the CRE figures for the breeze titanium are similar once the influence for the different ash concentrations in the two breeze samples are normalised. The geometric average CRE figure is 0.98 for the coke samples and 0.86 for the breeze samples.

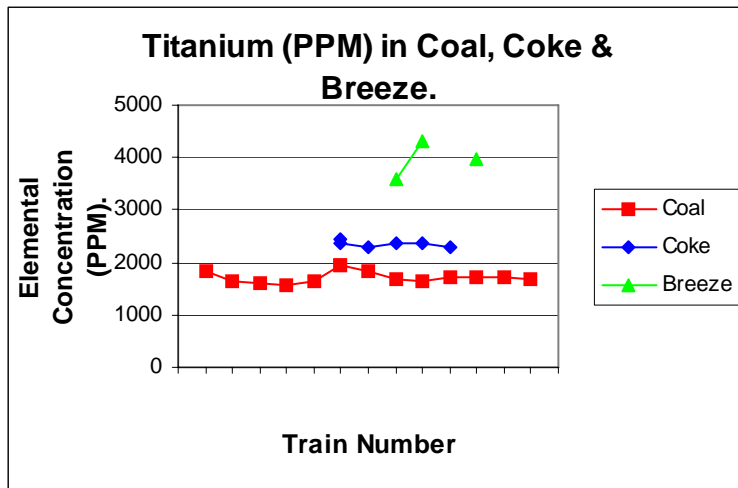


Figure 6.11. Concentration of titanium in feed coal and coke with time.

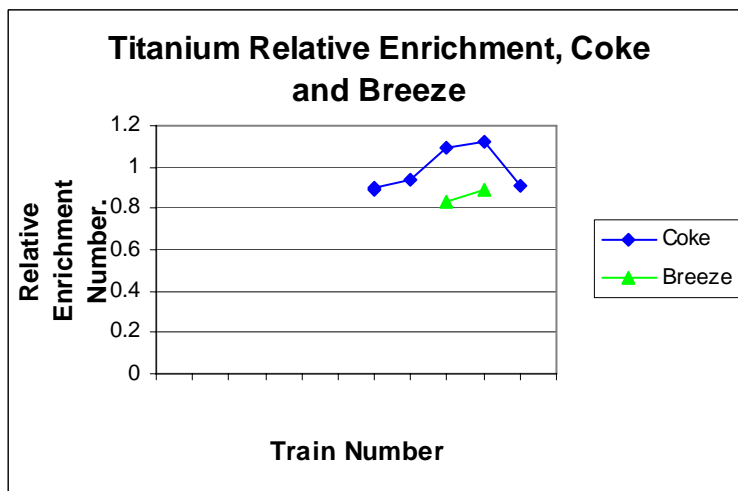


Figure 6.12. Titanium CRE for coke and breeze with time.

Manganese.

Figure 6.13. shows the concentration of manganese (where above the limit of detection) in the feed coal, coke, and breeze was consistent through out the period of sampling.

Figure 6.14. presents the CRE figures over the period of sampling. Because the concentrations in coke and breeze were found to be the same as for the feed coal, the coke is slightly depleted in manganese and the breeze is highly depleted in manganese suggesting progressive loss of this element during carbonisation. The geometric average CRE figure is 0.71 for the coke samples and 0.34 (only one breeze figure available) for the breeze samples.

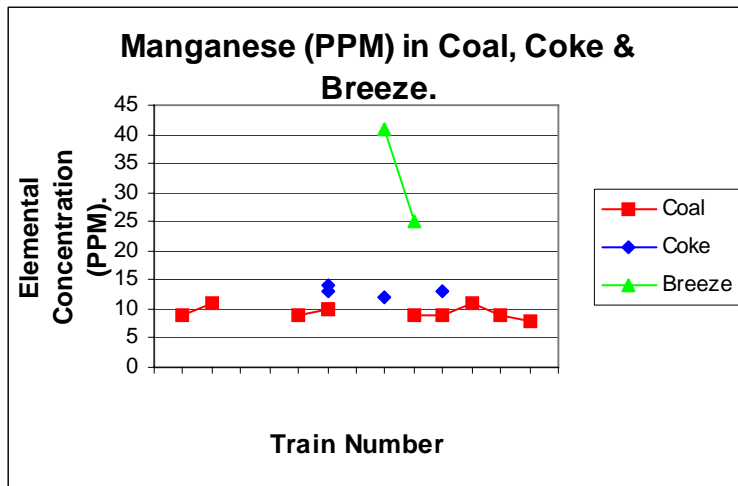


Figure 6.13. Concentration of manganese in feed coal and coke with time.

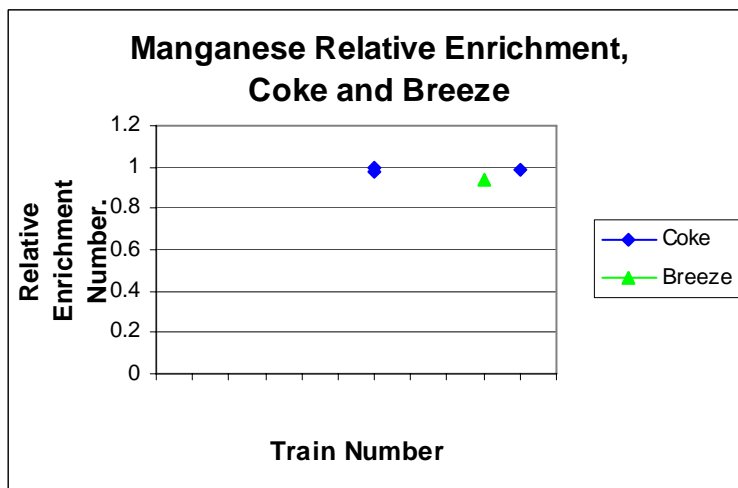


Figure 6.14. Manganese CRE for coke and breeze with time.

Phosphorous.

Figure 6.15. shows the concentration of phosphorous was consistent up until the time of Train 217. Following train 217, the phosphorous content of the coal jumped by 200ppm, and thereafter again remained static at the higher concentration level until the sampling period ended. The concentration of phosphorous in coke and breeze

appears to have been relatively consistent during the sampling period of these two product materials.

Figure 6.16. presents the CRE figures over the period of sampling. Both the coke and breeze figures appear to hover around a figure of 1, indicating phosphorous is not enriched or depleted in the coke and breeze products. The geometric average CRE figure is 0.91 for the coke samples and 0.99 for the breeze samples. The data proves that phosphorous is substantially retained in the coke and would report to the pig iron during reduction of the iron ore in the blast furnace if the coke was used in steel making.

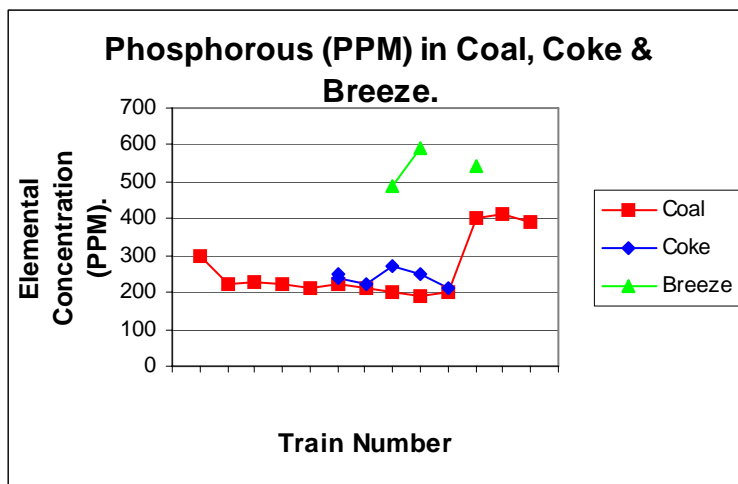


Figure 6.15. Concentration of phosphorous in feed coal and coke with time.

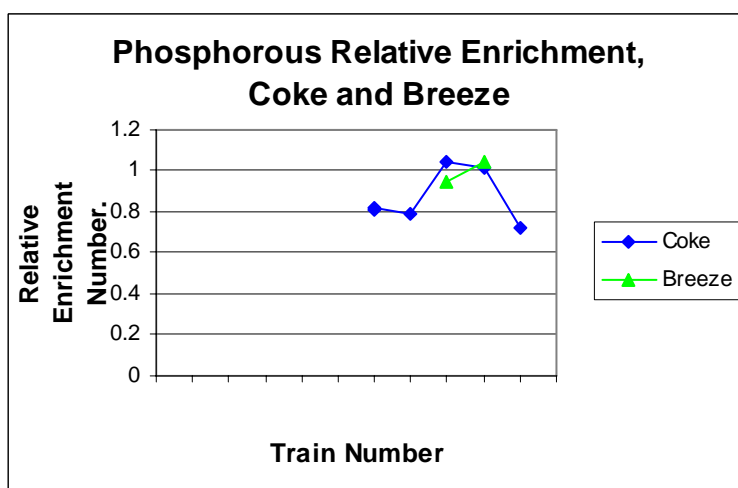


Figure 6.16. Phosphorous CRE for coke and breeze with time.

Sulphur.

Figure 6.17. shows the concentration of sulphur in the coal, coke, and breeze was relatively consistent over the period of sampling.

Figure 6.18. presents the CRE figures over the period of sampling. Sulphur in the coke appears to be moderately depleted, and sulphur appears to be highly depleted in the breeze. The geometric average CRE figure is 0.66 for the coke samples and 0.22 for the breeze samples. A 1% increase in the concentration of sulphur is thought to increase the coke consumption rate by as much as 32 kg per net ton of hot metal (Zimmerman, 1979) and greatly increase the production of slag. The data presented here shows that, although a high proportion of sulphur is volatilised, some is retained in the coke, therefore a low-sulphur coking coal would have an advantage over high-sulphur coking coals.

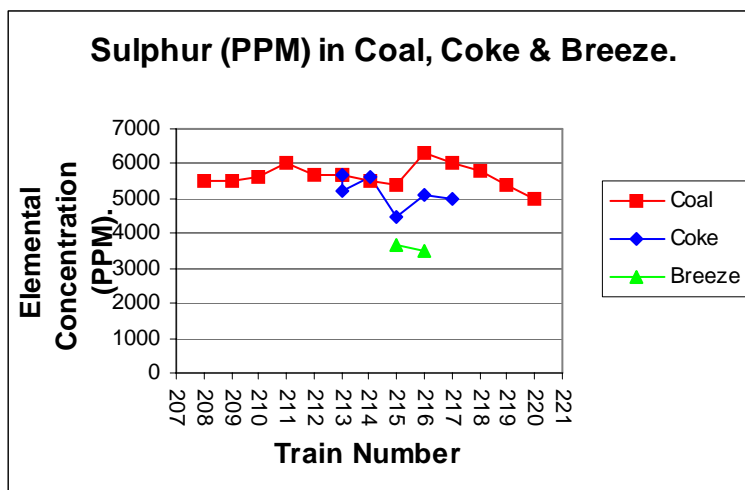


Figure 6.17. Concentration of sulphur in feed coal and coke with time.

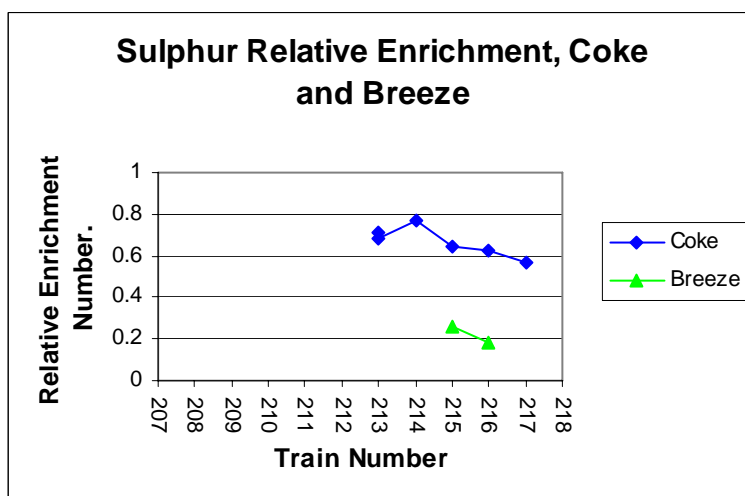


Figure 6.18. Sulphur CRE for coke and breeze with time.

Gold.

Figure 6.19. shows the concentration of gold in the coal, coke, and breeze was variable over the period of sampling.

Figure 6.20. presents the CRE figures over the period of sampling. Only three figures for CRE are available for the coke, and only one is available for breeze, so the CRE figures are indicative only. Gold in the coke appears to be moderately depleted, but is apparently highly enriched in the breeze. The geometric average CRE figure is 0.63 for the coke samples and 2.36 for the breeze samples. This assessment of the partitioning behaviour of gold should be treated as highly provisional due to the lack of data for this element.

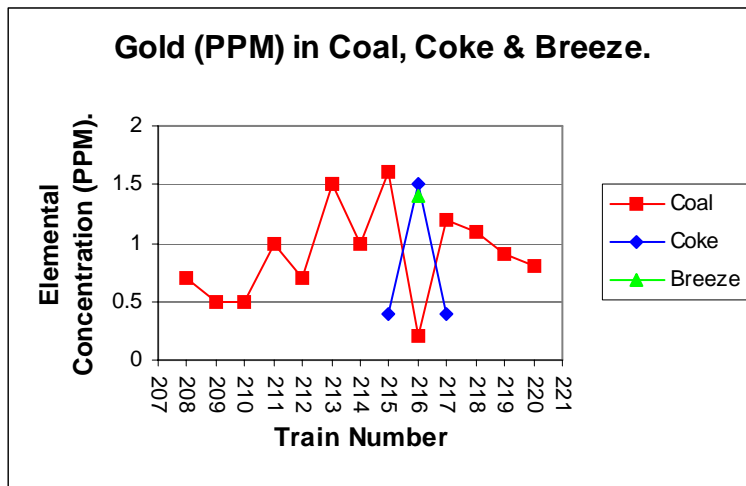


Figure 6.19. Concentration of gold in feed coal and coke with time.

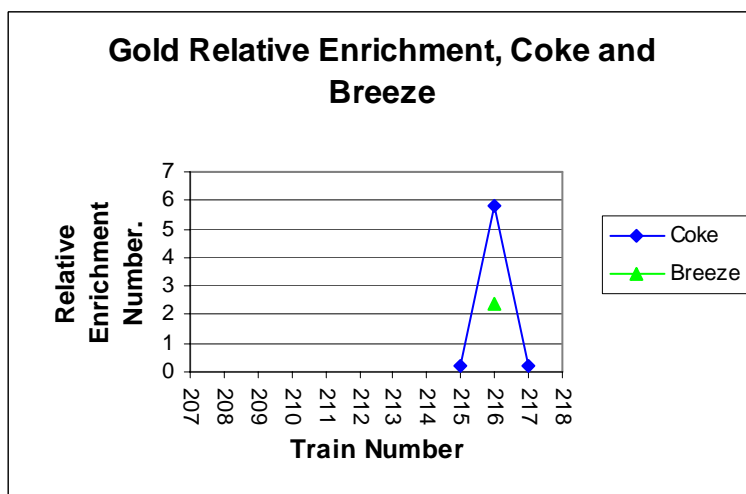


Figure 6.20. Gold CRE for coke and breeze with time.

Arsenic.

Figure 6.21. shows the concentration of arsenic in the coal and coke was reasonably consistent during the period of sampling, however arsenic concentration in the two breeze samples is radically different.

Figure 6.22. presents the CRE figures over the period of sampling. Arsenic in the coke appears to be moderately depleted, similar to sulphur. However, arsenic appears to be highly enriched in the breeze (although the two figures for arsenic are radically different). The geometric average CRE figure is 0.56 for the coke samples and 2.32 for the breeze samples (but note discussion on the latter in Section 8.3.).

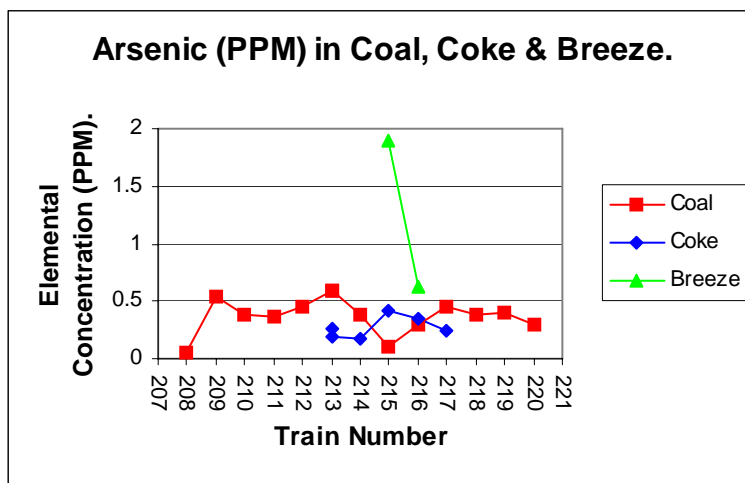


Figure 6.21. Concentration of arsenic in feed coal and coke with time.

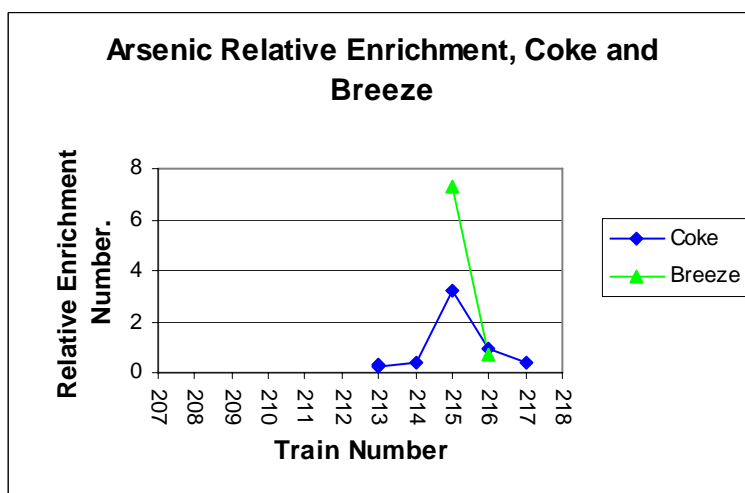


Figure 6.22. Arsenic CRE for coke and breeze with time.

Barium.

Figure 6.23. shows the concentration of barium in the coal, coke, and breeze was reasonably consistent during the period of sampling.

Figure 6.24. presents the CRE figures over the period of sampling. Barium in the coke appears to be neither enriched nor depleted, but is perhaps slightly depleted in the breeze. The geometric average CRE figure is 0.87 for the coke samples and 0.73 for the breeze samples.

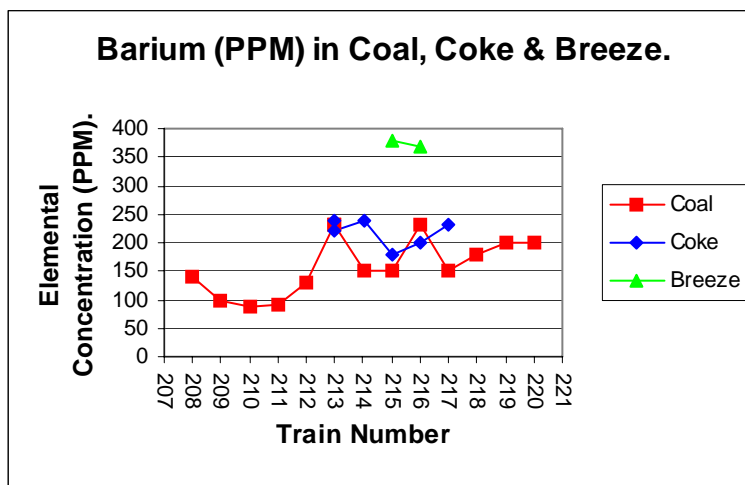


Figure 6.23. Concentration of barium in feed coal and coke with time.

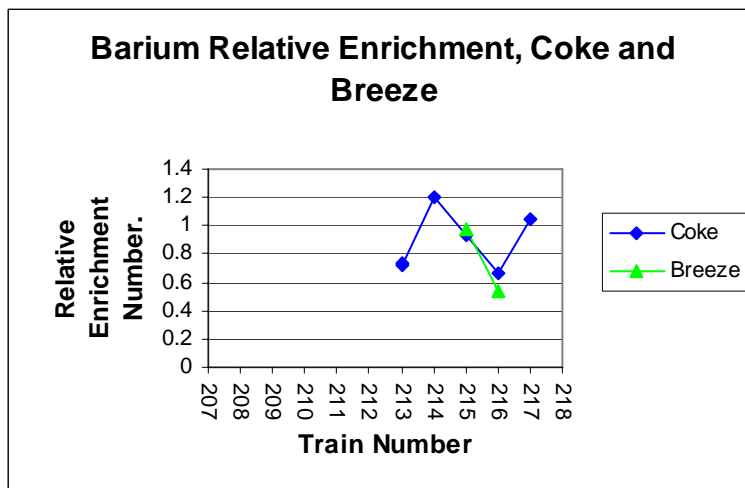


Figure 6.24. Barium CRE for coke and breeze with time.

Bromine.

Figure 6.25. shows the concentration of bromine in the coal, coke, and breeze was reasonably consistent during the period of sampling.

Figure 6.26. presents the CRE figures over the period of sampling. Bromine in both the coke and the breeze is highly depleted. The geometric average CRE figure is 0.22 for the coke samples and 0.18 for the breeze samples.

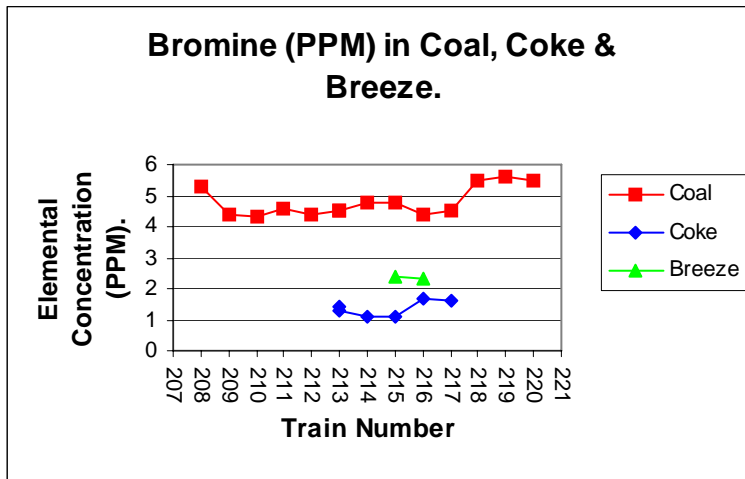


Figure 6.25. Concentration of bromine in feed coal and coke with time.

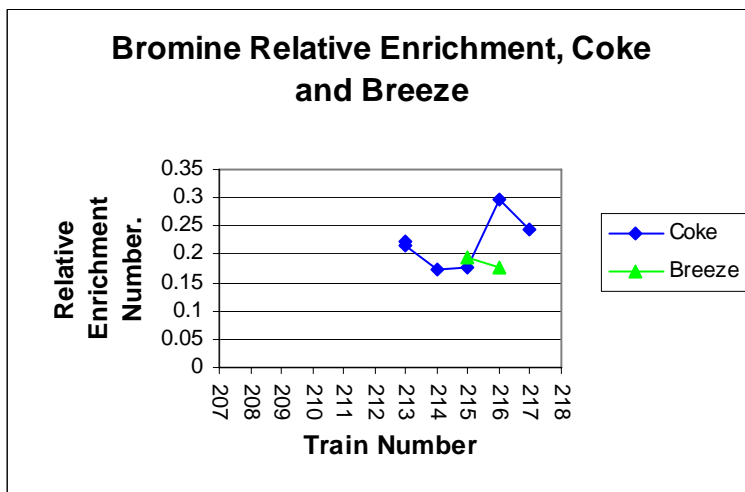


Figure 6.26. Bromine CRE for coke and breeze with time.

Cobalt.

Figure 6.27. shows the concentration of cobalt in the coal, coke, and breeze was reasonably consistent during the period of sampling.

Figure 6.28. presents the CRE figures over the period of sampling. Cobalt is neither enriched nor depleted in the coke, and is slightly enriched in the breeze. The

geometric average CRE figure is 0.95 for the coke samples and 1.28 for the breeze samples.

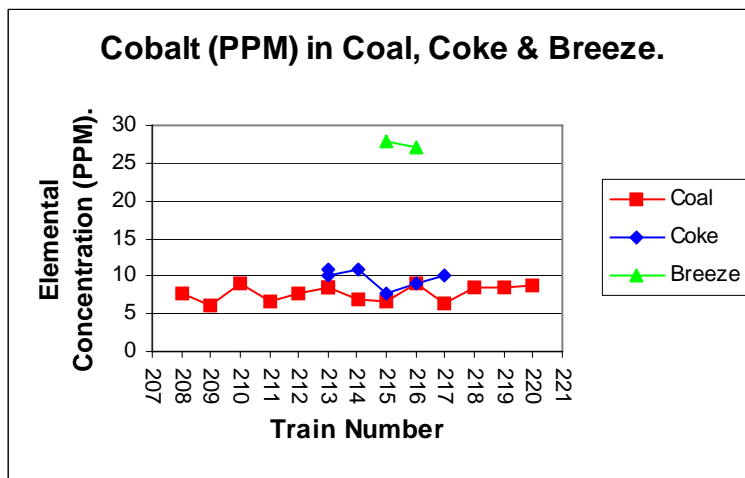


Figure 6.27. Concentration of cobalt in feed coal and coke with time.

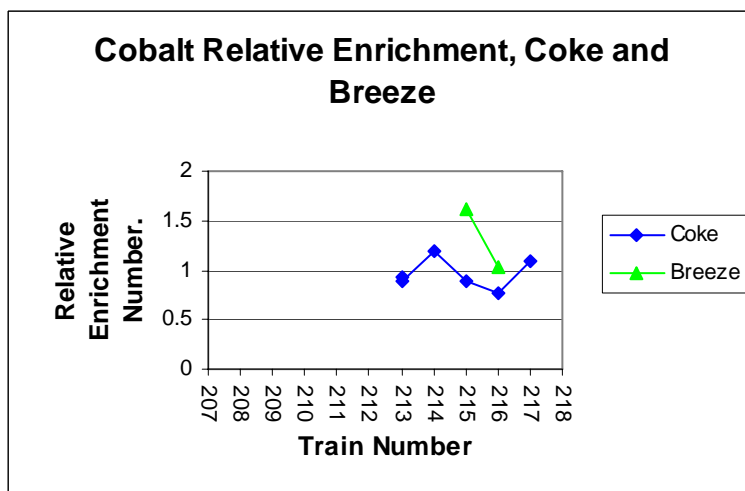


Figure 6.28. Cobalt CRE for coke and breeze with time.

Chromium.

Figure 6.29. shows the concentration of chromium in the coal, coke, and breeze was reasonably consistent during the period of sampling.

Figure 6.30. presents the CRE figures over the period of sampling. The CRE figures are quite variable for chromium in coke, with considerable enrichment of this element indicated by the CRE figure. Chromium is also enriched in the breeze, but apparently not to the same extent as the coke. Chromium is the only element to show a lesser

enrichment in the breeze compared to the coke. The geometric average CRE figure is 2.27 for the coke samples and 1.50 for the breeze samples.

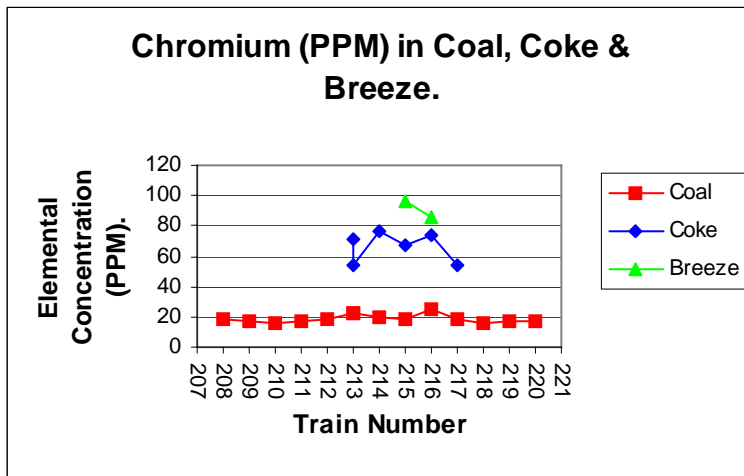


Figure 6.29. Concentration of chromium in feed coal and coke with time.

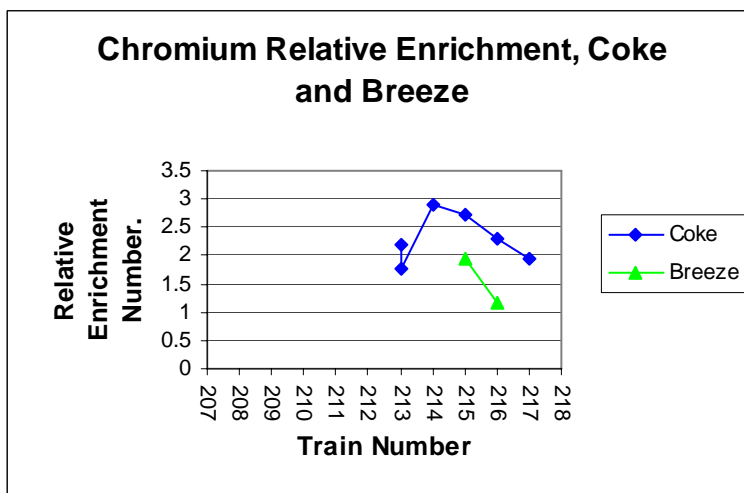


Figure 6.30. Chromium CRE for coke and breeze with time.

Caesium.

Figure 6.31. shows the concentration of caesium in the coal, coke, and breeze was moderately consistent during the period of sampling.

Figure 6.32. presents the CRE figures over the period of sampling. The CRE figures are quite variable for caesium in coke, but generally indicate a slight depletion of this element. Caesium apparently exhibits a moderate degree of depletion in the breeze. The geometric average CRE figure is 0.81 for the coke samples and 0.68 for the breeze samples.

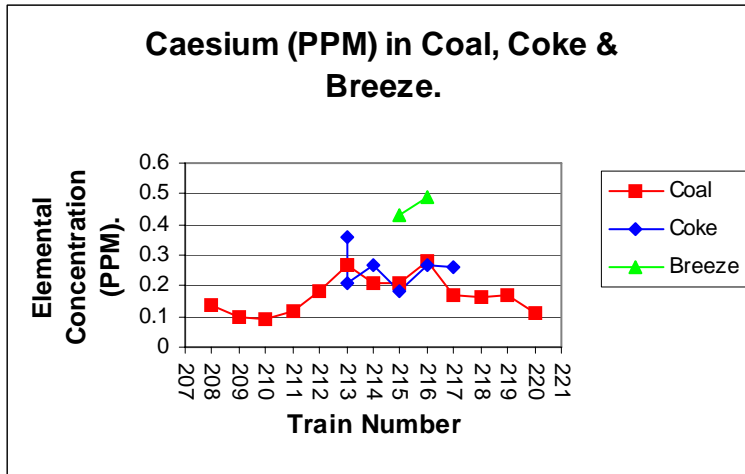


Figure 6.31. Concentration of caesium in feed coal and coke with time.

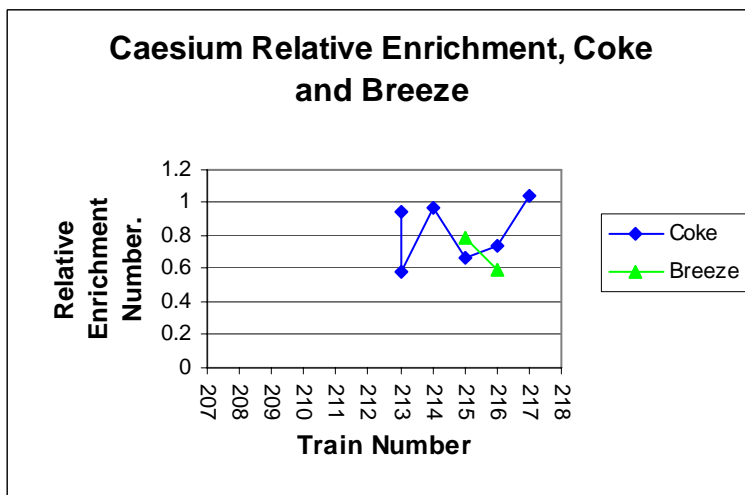


Figure 6.32. Caesium CRE for coke and breeze with time.

Hafnium.

Figure 6.33. shows the concentration of hafnium in the coal, coke, and breeze was moderately consistent during the period of sampling.

Figure 6.34. presents the CRE figures over the period of sampling. The CRE figures suggest the coke and breeze are neither enriched nor depleted in hafnium. The geometric average CRE figure is 0.88 for the coke samples and 1.00 for the breeze samples.

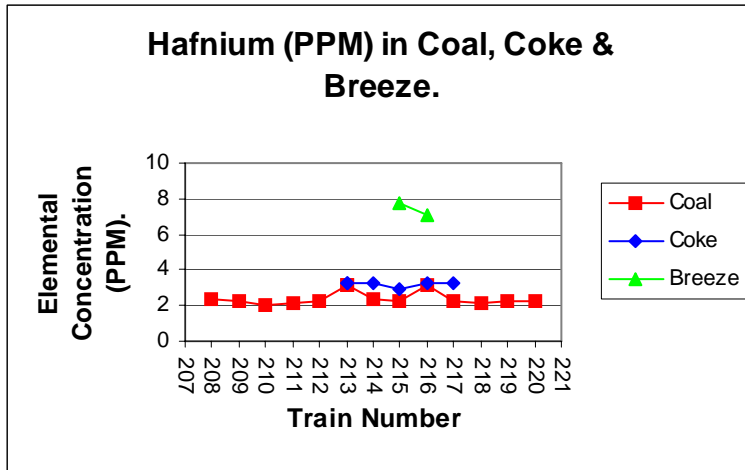


Figure 6.33. Concentration of hafnium in feed coal and coke with time.

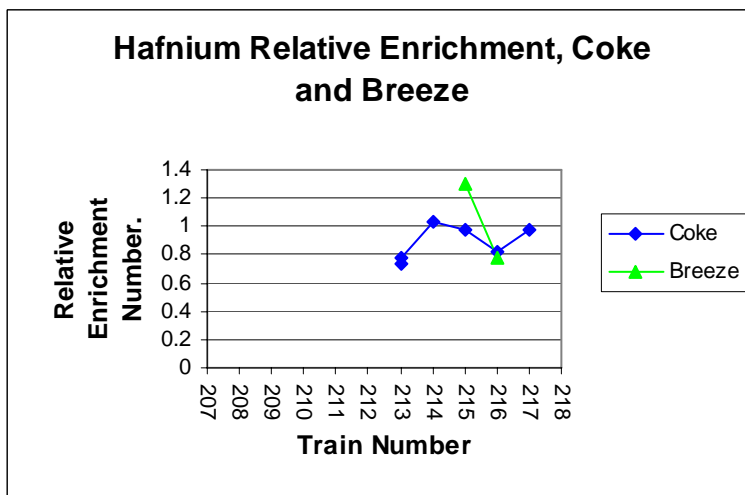


Figure 6.34. Hafnium CRE for coke and breeze with time.

Mercury.

Only two coal samples and three coke samples contained mercury at levels above the detection limit of INAA. Unfortunately the coke samples with detectable mercury did not correspond with the coal samples containing detectable mercury. Geometric average mercury concentrations were calculated for the coal and coke samples and for coal and coke ash percent values. CRE is calculated using the coal and coke average figures. A CRE of 1.11 is calculated for the coke, indicating moderate enrichment of mercury in the coke, a result at odds with expectations for such a volatile element. Possibly the coke has captured mercury in a similar fashion to the capture of mercury by unburnt carbon in fly-ash (Hassett and Eylands, 1999; Hower and Masterlerz, 2001; Mardon and Hower, 2004; Sakulpitakphon et al., 2000; Wu et al., 2000). However, few samples were above the detection limit of INAA so it is also possible

that the one high value for the first sample from train 213 could be biasing the average upward. The concentration of mercury in both breeze samples was below the detection limit of INAA, possibly indicating depletion of mercury in coke breeze.

Molybdenum.

A significant proportion of the coal and coke samples contained molybdenum at levels above the detection limit of INAA. Figure 6.35. suggests the concentration of molybdenum was reasonably consistent over the period of sampling. However, only two coke samples with detectable molybdenum corresponded to coal samples containing detectable molybdenum. Molybdenum was present at a concentration above the detection limit of INAA in both breeze samples, but neither breeze sample corresponded to a coal sample with detectable molybdenum. As for mercury, geometric-average molybdenum concentrations were calculated for the coal and coke samples and for coal and coke ash percent values. A CRE of 0.87 is calculated for the coke, indicating the coke is neither enriched nor depleted in molybdenum. A CRE of 1.28 is calculated for the breeze, indicating molybdenum is moderately enriched in the breeze.

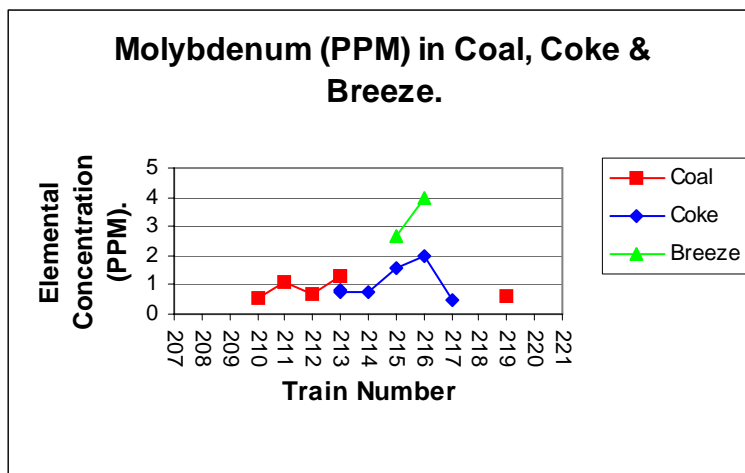


Figure 6.35. Concentration of molybdenum in feed coal and coke with time.

Nickel.

A number of coal and coke samples had nickel concentrations above the detection limit of INAA. Figure 6.36. suggests the concentration of nickel was reasonably consistent over the period of sampling. However, only three coke samples with detectable nickel corresponded to coal samples containing detectable nickel. Nickel

was not present in detectable concentrations in either of the two breeze samples. As for mercury and molybdenum, geometric average nickel concentrations were calculated for the coal and coke samples and for coal and coke ash percent values. A CRE of 1.00 is calculated for the coke, indicating the coke is neither enriched nor depleted in nickel. Because neither breeze sample contained nickel at a detectable concentration, it appears nickel is highly depleted in the breeze, however this inference cannot be quantified.

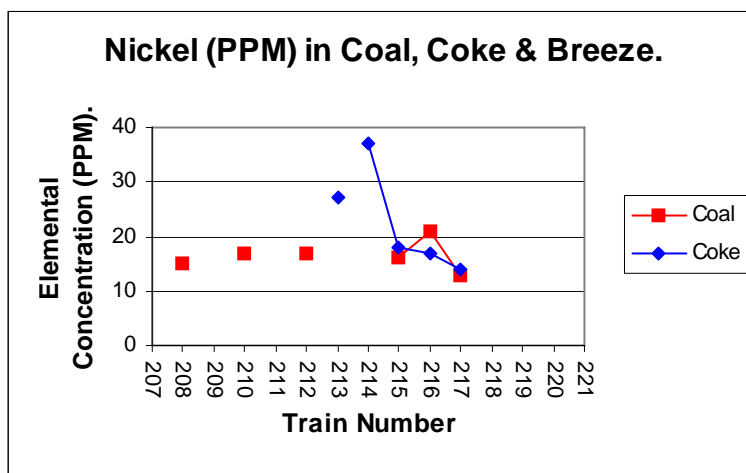


Figure 6.36. Concentration of nickel in feed coal and coke with time.

Rubidium.

A number of coal and coke samples and one breeze sample had rubidium concentrations above the detection limit of INAA. Figure 6.37. suggests the concentration of rubidium was reasonably consistent over the period of sampling. However, none of the coke samples or the breeze sample with detectable rubidium corresponded to coal samples containing detectable rubidium. As for mercury, molybdenum, and nickel, geometric-average rubidium concentrations were calculated for the coal and coke samples and for coal and coke ash percent values. A CRE of 1.15 is calculated for the coke, indicating the coke is neither enriched nor depleted in rubidium. A CRE of 0.78 is calculated for the breeze, perhaps indicating some slight depletion, although this CRE figure is only based on one breeze sample.

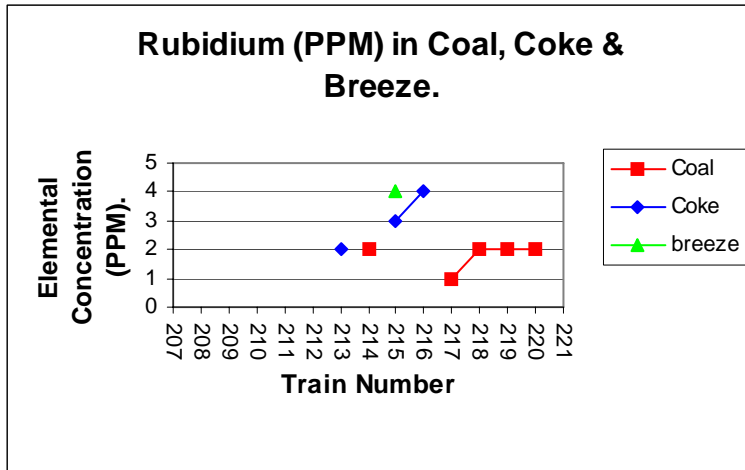


Figure 6.37. Concentration of rubidium in feed coal and coke with time.

Antimony.

Figure 6.38. shows the concentration of antimony in the coal, coke, and breeze was reasonably consistent during the period of sampling.

Figure 6.39. presents the CRE figures over the period of sampling. Antimony in the coke appears to be neither enriched nor depleted. However, antimony appears to be highly enriched in the breeze. The geometric average CRE figure is 0.97 for the coke samples and 2.46 for the breeze samples.

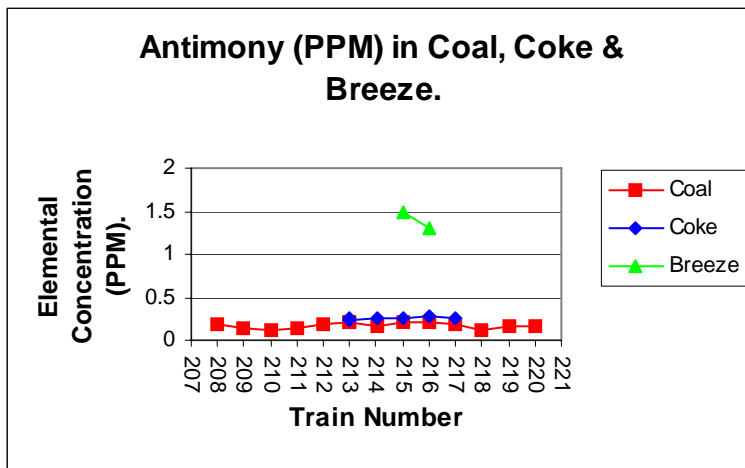


Figure 6.38. Concentration of antimony in feed coal and coke with time.

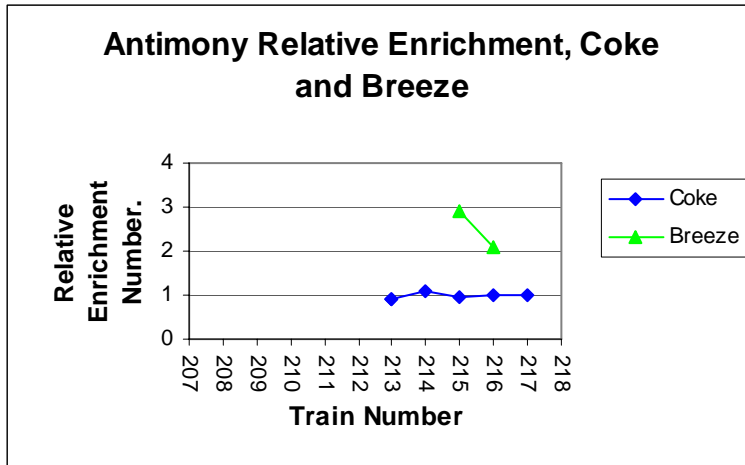


Figure 6.39. Antimony CRE for coke and breeze with time.

Selenium.

Figure 6.40. shows the concentration of selenium in the coal, coke, and breeze was reasonably consistent during the period of sampling.

Figure 6.41. presents the CRE figures over the period of sampling. Selenium in the coke appears moderately depleted. Selenium is apparently highly depleted in the breeze. The geometric average CRE figure is 0.67 for the coke samples and 0.32 for the breeze samples.

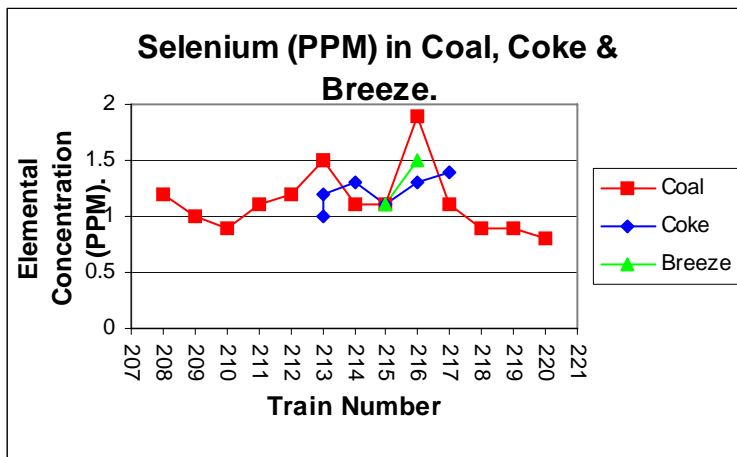


Figure 6.40. Concentration of selenium in feed coal and coke with time.

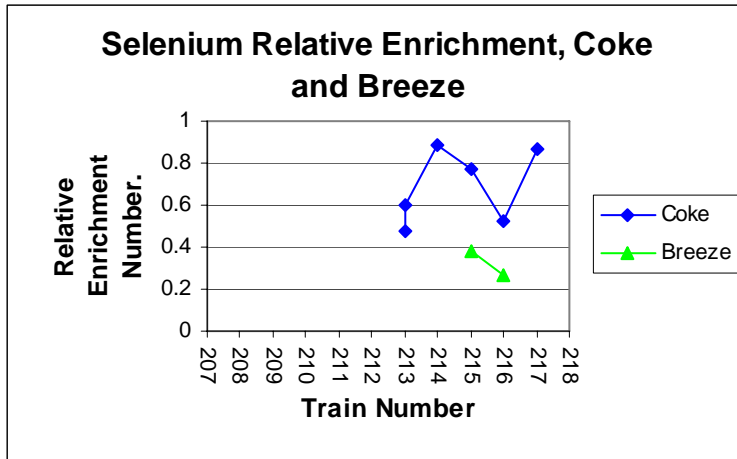


Figure 6.41. Selenium CRE for coke and breeze with time.

Strontium.

Figure 6.42. shows the concentration of strontium in the coal, coke, and breeze was relatively consistent during the period of sampling, although there is a marked jump in the strontium concentration in coal for the last three trains of the sampling period.

Figure 6.43. presents the CRE figures over the period of sampling. Strontium is neither enriched nor depleted in the coke, but is moderately enriched in the breeze. The geometric average CRE figure is 0.84 for the coke samples and 1.51 for the breeze samples.

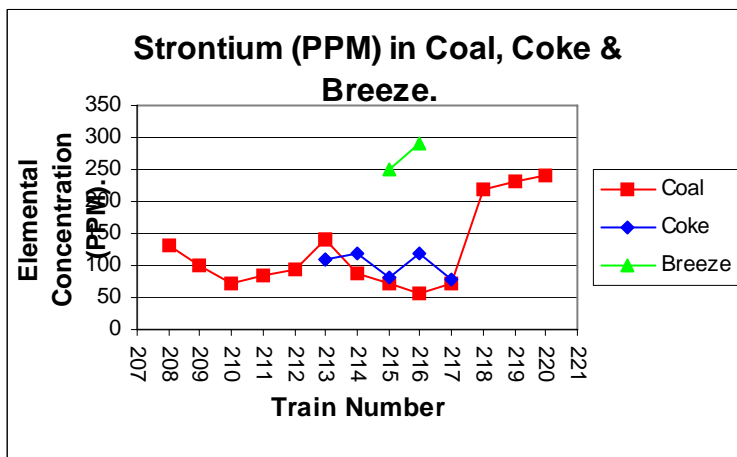


Figure 6.42. Concentration of strontium in feed coal and coke with time.

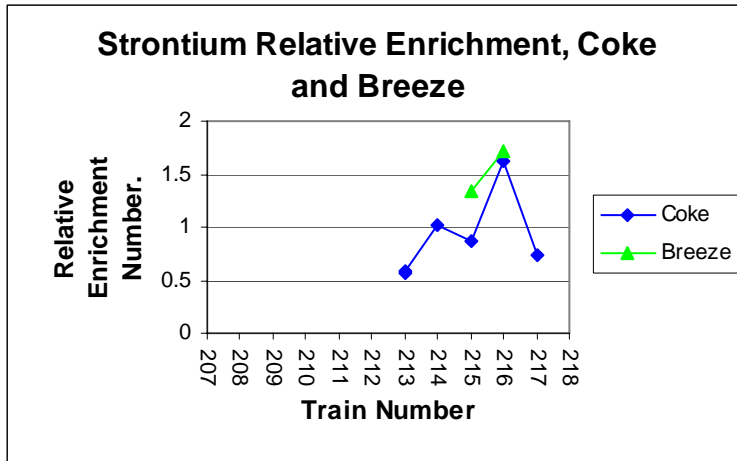


Figure 6.43. Strontium CRE for coke and breeze with time.

Thorium.

Figure 6.44. shows the concentration of thorium in the coal, coke, and breeze was consistent during the period of sampling.

Figure 6.45. presents the CRE figures over the period of sampling. The CRE figures suggest the coke and breeze are neither enriched nor depleted in thorium. The geometric average CRE figure is 0.93 for the coke samples and 0.88 for the breeze samples.

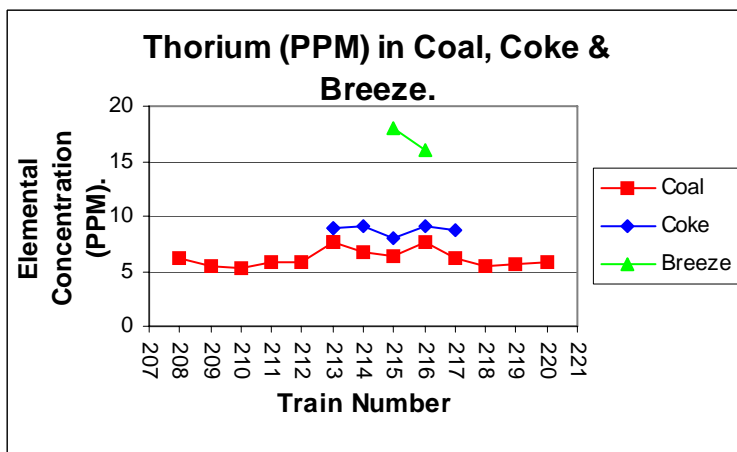


Figure 6.44. Concentration of thorium in feed coal and coke with time.

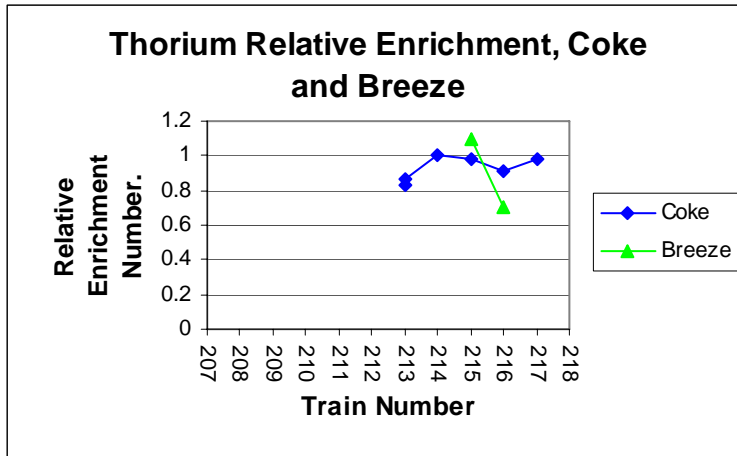


Figure 6.45. Thorium CRE for coke and breeze with time.

Uranium.

Figure 6.46. shows the concentration of uranium in the coal, coke, and breeze was consistent during the period of sampling.

Figure 6.47. presents the CRE figures over the period of sampling. The CRE figures suggest the coke and breeze are neither enriched nor depleted in uranium. The geometric average CRE figure is 1.07 for the coke samples and 0.94 for the breeze samples.

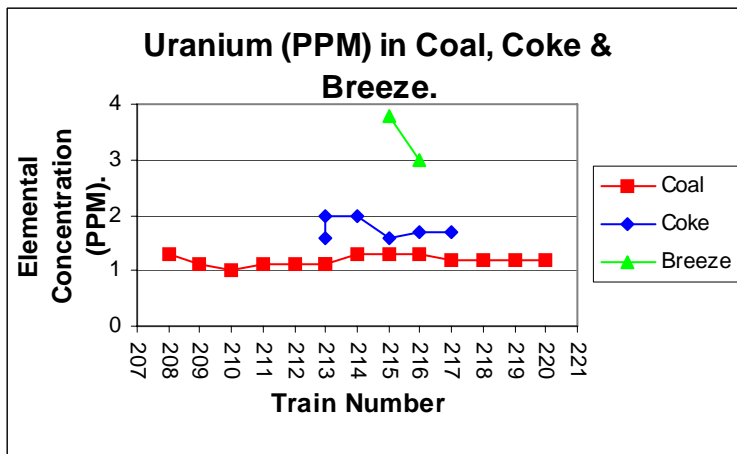


Figure 6.46. Concentration of uranium in feed coal and coke with time.

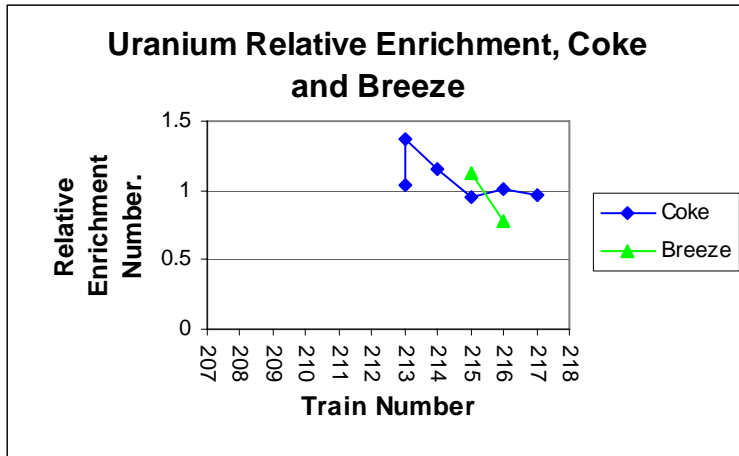


Figure 6.47. Uranium CRE for coke and breeze with time.

Tungsten.

Figure 6.48. shows the concentration of tungsten in the coal, coke, and breeze was moderately consistent during the period of sampling.

Figure 6.49. presents the CRE figures over the period of sampling. Tungsten in both the coke and the breeze is highly depleted. The geometric average CRE figure is 0.18 for the coke samples and 0.20 for the breeze samples.

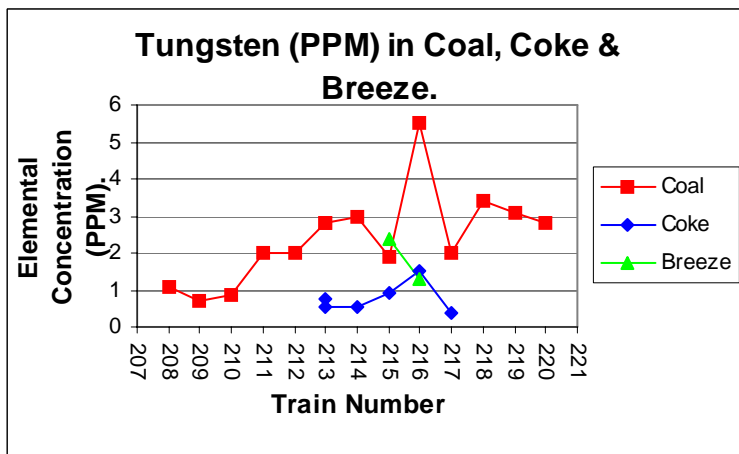


Figure 6.48. Concentration of tungsten in feed coal and coke with time.

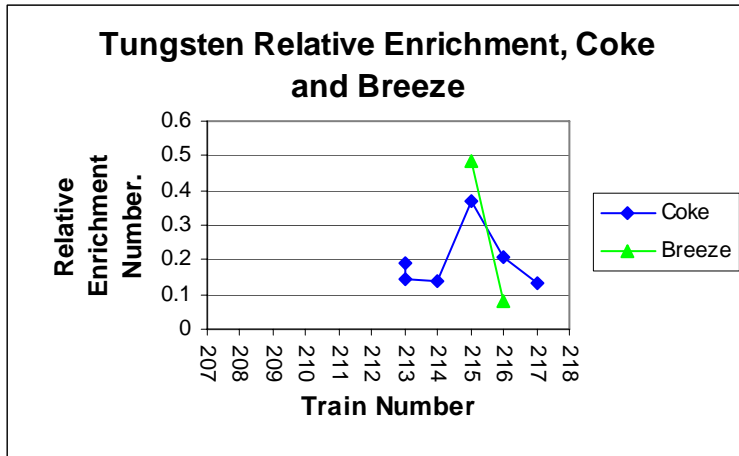


Figure 6.49. Tungsten CRE for coke and breeze with time.

Zinc.

Figure 6.50. shows the concentration of zinc in the coal, coke, and breeze was very consistent during the period of sampling.

Figure 6.51. presents the CRE figures over the period of sampling. Zinc is neither enriched nor depleted in the coke, but is moderately enriched in the breeze. The geometric average CRE figure is 0.88 for the coke samples and 1.57 for the breeze samples.

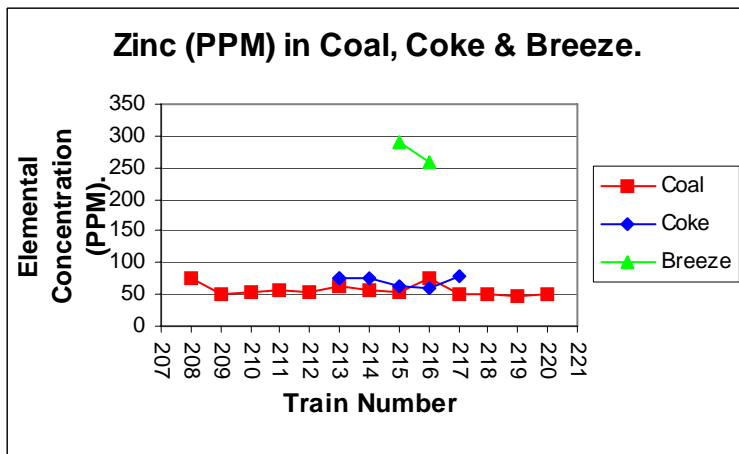


Figure 6.50. Concentration of zinc in feed coal and coke with time.

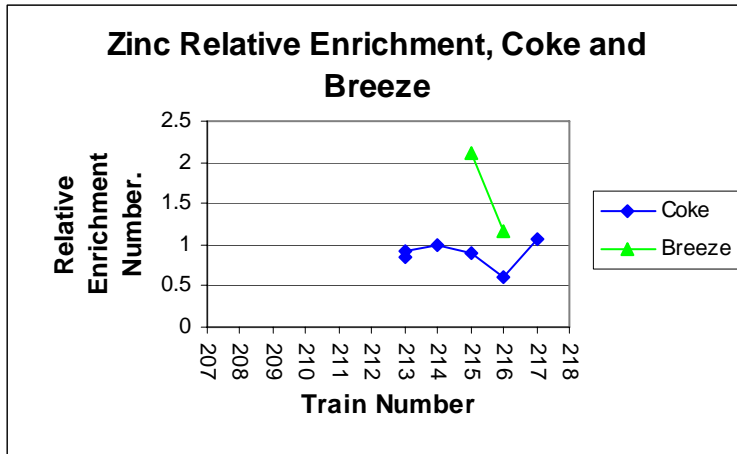


Figure 6.51. Zinc CRE for coke and breeze with time.

Scandium, tantalum and the Rare Earth Elements.

The partitioning behaviour of the scandium, tantalum, and the rare earth elements is generally very similar, so these elements are dealt with in one section. Figures 6.52., 6.53., 6.54., 6.55., 6.56., 6.57., 6.58., 6.59., 6.60., and 6.61. show the concentration of rare earth elements in the feed coal, coke, and breeze was consistent during the period of sampling, and the pattern of change element concentration were the same for scandium, tantalum, and the rare earth elements.

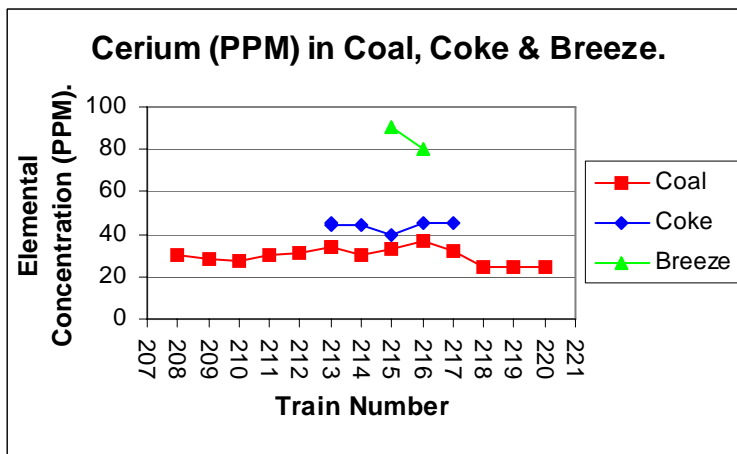


Figure 6.52. Concentration of cerium in feed coal and coke with time.

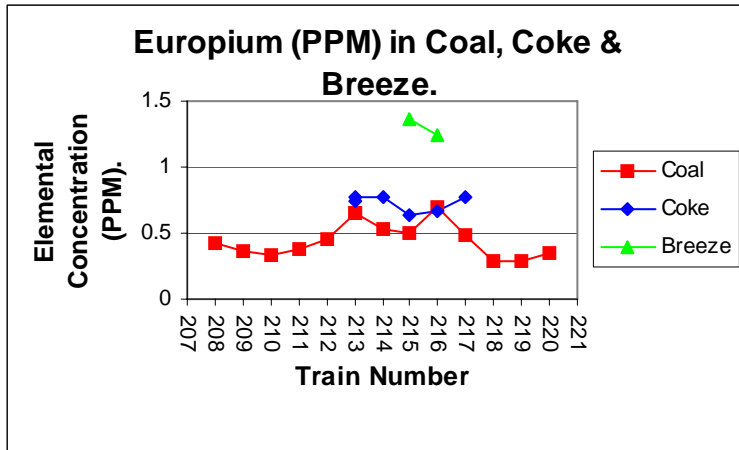


Figure 6.53. Concentration of europium in feed coal and coke with time.

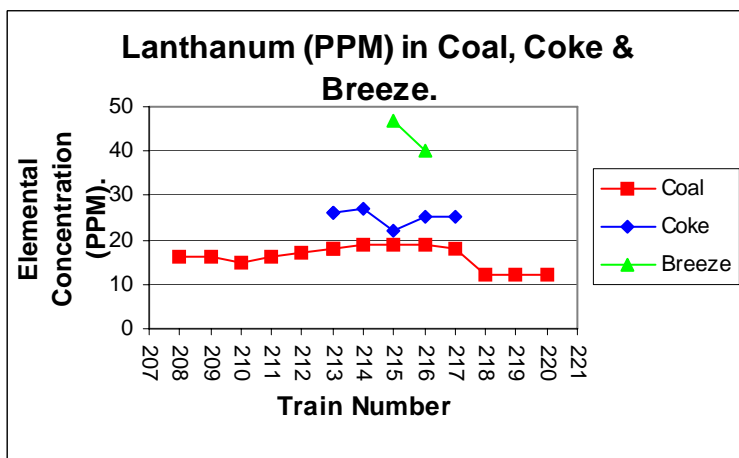


Figure 6.54. Concentration of lanthanum in feed coal and coke with time.

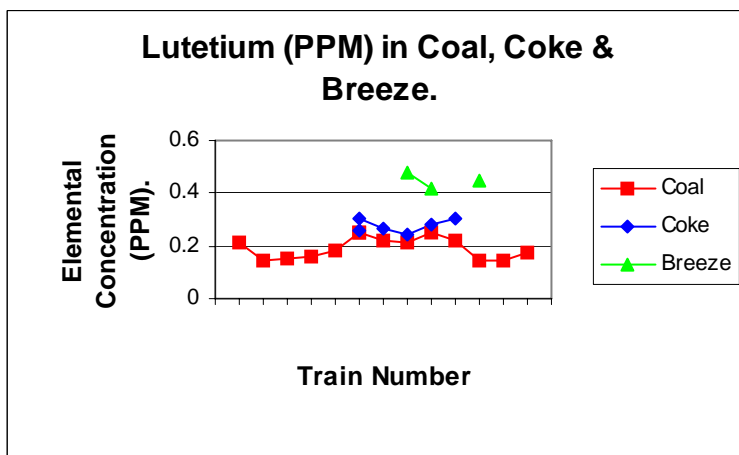


Figure 6.55. Concentration of lutetium in feed coal and coke with time.

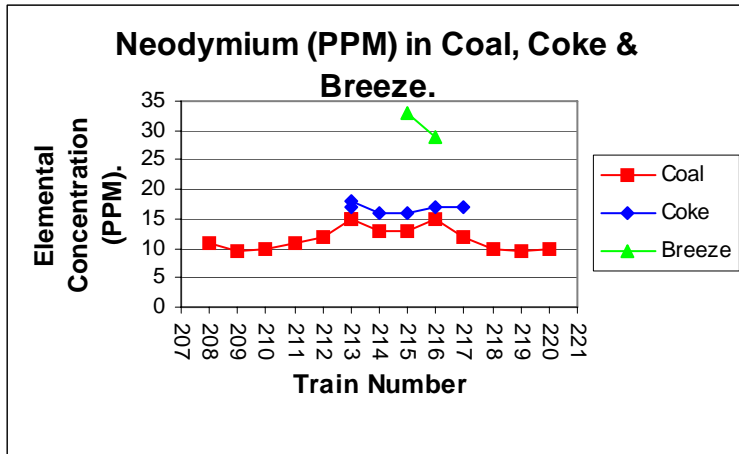


Figure 6.56. Concentration of neodymium in feed coal and coke with time.

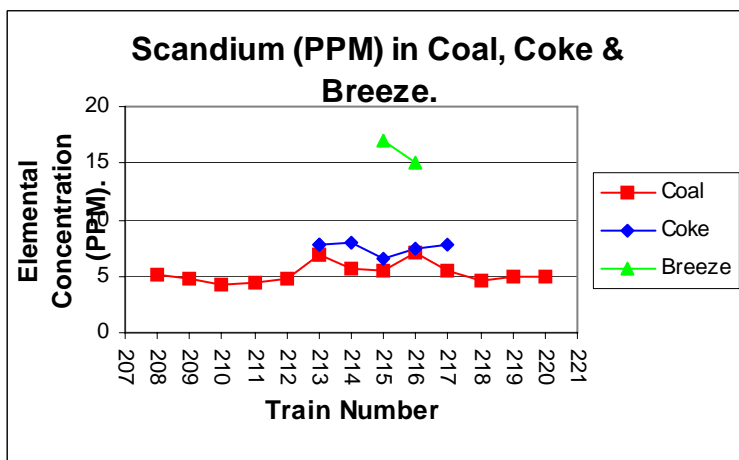


Figure 6.57. Concentration of scandium in feed coal and coke with time.

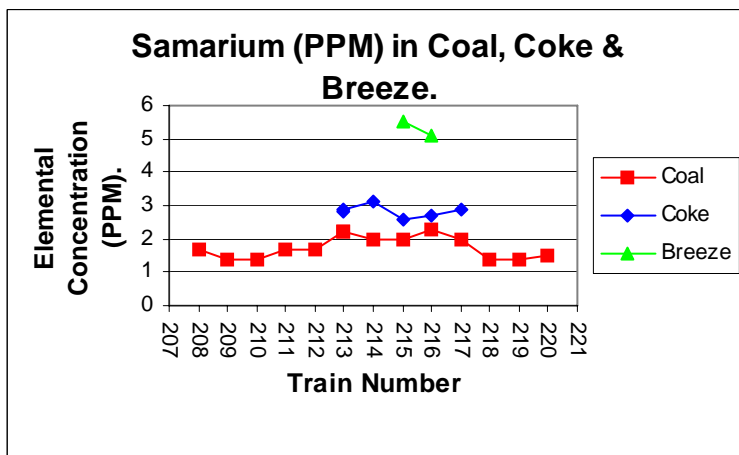


Figure 6.58. Concentration of samarium in feed coal and coke with time.

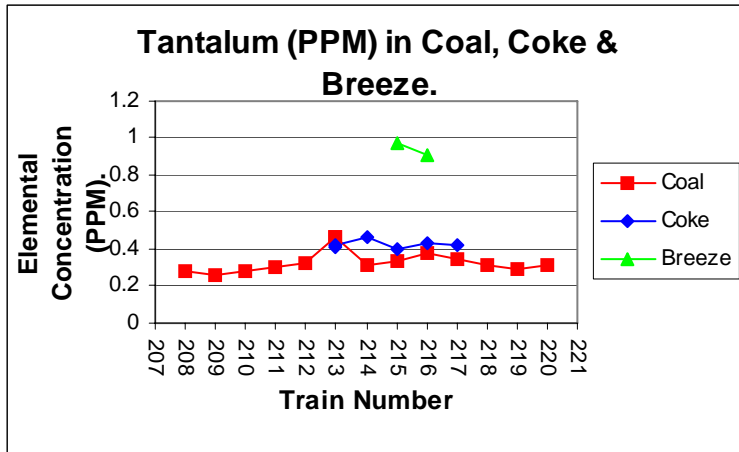


Figure 6.59. Concentration of tantalum in feed coal and coke with time.

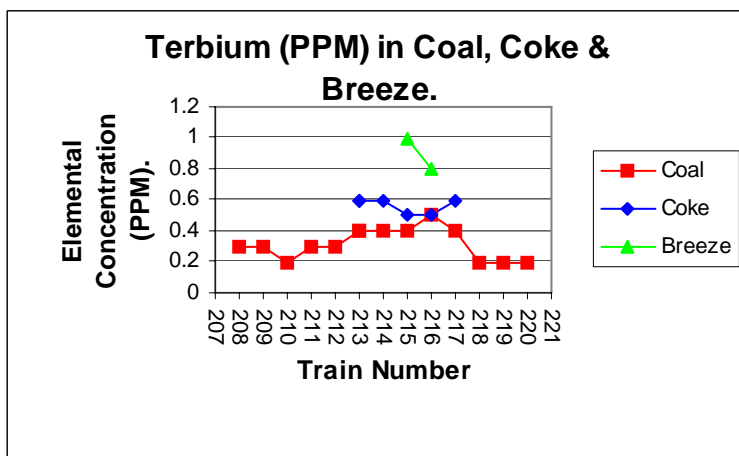


Figure 6.60. Concentration of terbium in feed coal and coke with time.

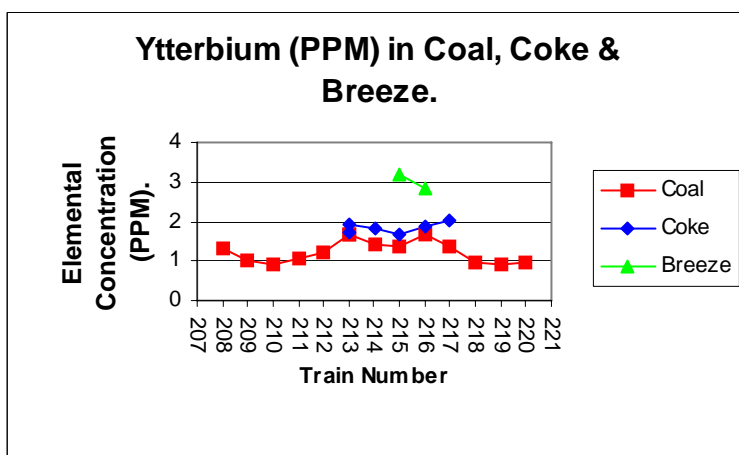


Figure 6.61. Concentration of ytterbium in feed coal and coke with time.

Figures 6.62., 6.63., 6.64., 6.65., 6.66., 6.67., 6.68., 6.69., 6.70., and 6.71. present the CRE figures over the period of sampling. As expected from the consistent concentration of scandium, tantalum, and the rare earth elements in both the feed coal

and coke, the CRE figures for coke are relatively consistent. The CRE figures for the breeze are also similar once the influence for the different ash concentrations in the two breeze samples are normalised. The geometric average CRE figures are as follows: cerium 0.97 for the coke and 0.88 for the breeze samples; europium 0.93 for the coke and 0.80 for the breeze; lanthanum 1.00 for the coke and 0.82 for the breeze; lutetium 0.88 for the coke and 0.70 for the breeze; neodymium 0.90 for the coke and 0.80 for the breeze; scandium 0.90 for the coke and 0.93 for the breeze; samarium 0.99 for the coke and 0.89 for the breeze; tantalum 0.83 for the coke and 0.96 for the breeze; terbium 1.01 for the coke and 0.72 for the breeze; and ytterbium 0.89 for the coke and 0.71 for the breeze. The CRE figures suggest that the light rare earth elements (La, Ce, Nd, Sm, and Eu) exhibit neither enrichment nor depletion in either the coke or the breeze. However, the heavy rare earth elements (Tb, Yb, and Lu), while also being neither enriched nor depleted in the coke, appear to be slightly depleted in the breeze.

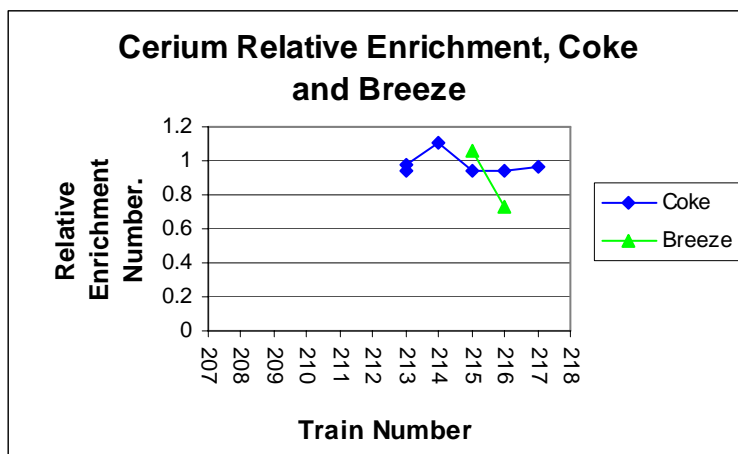


Figure 6.62. Cerium CRE for coke and breeze with time.

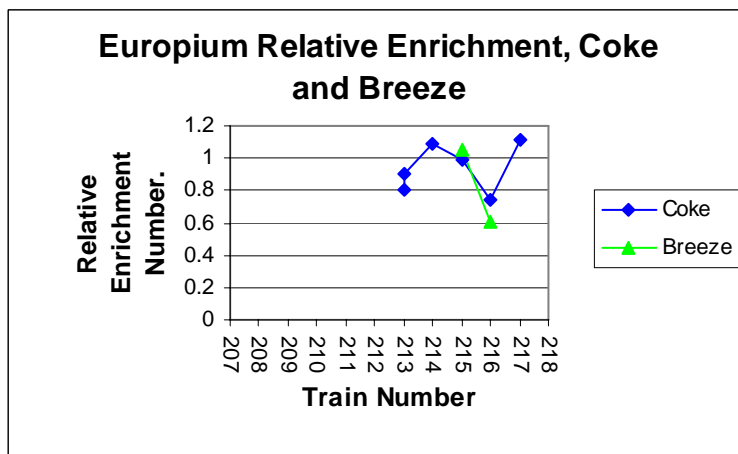


Figure 6.63. Europium CRE for coke and breeze with time.

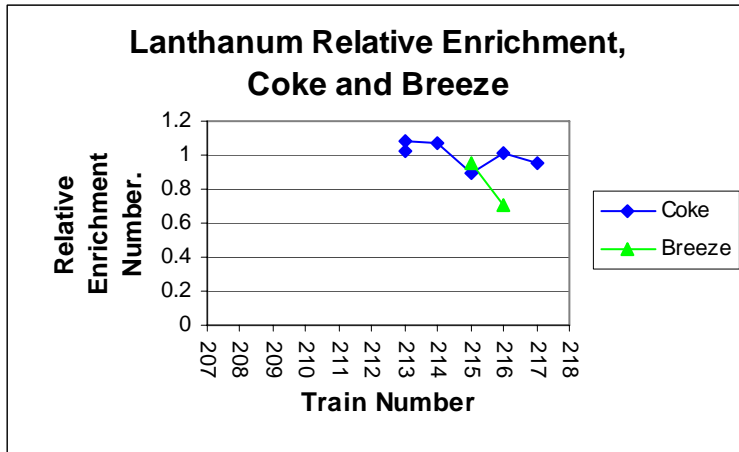


Figure 6.64. Lanthanum CRE for coke and breeze with time.

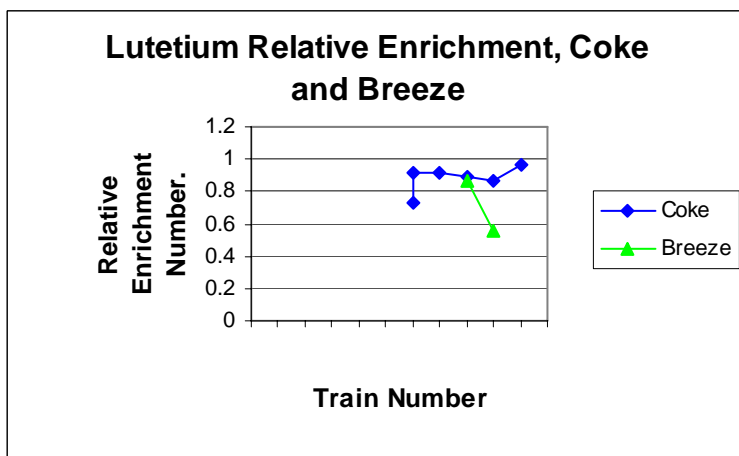


Figure 6.65. Lutetium CRE for coke and breeze with time.

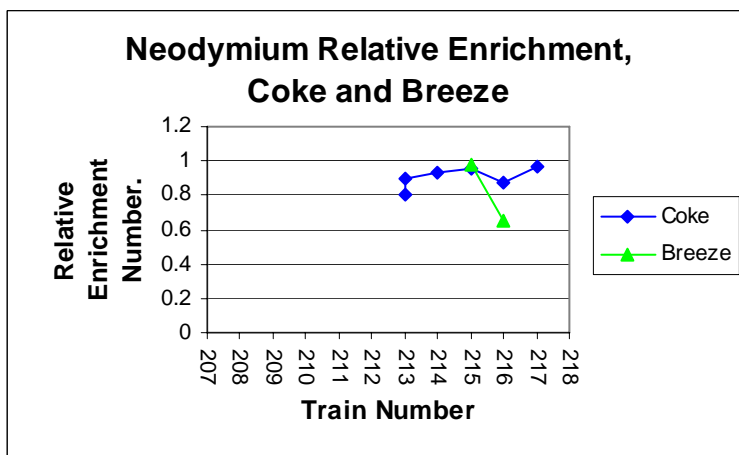


Figure 6.66. Neodymium CRE for coke and breeze with time.

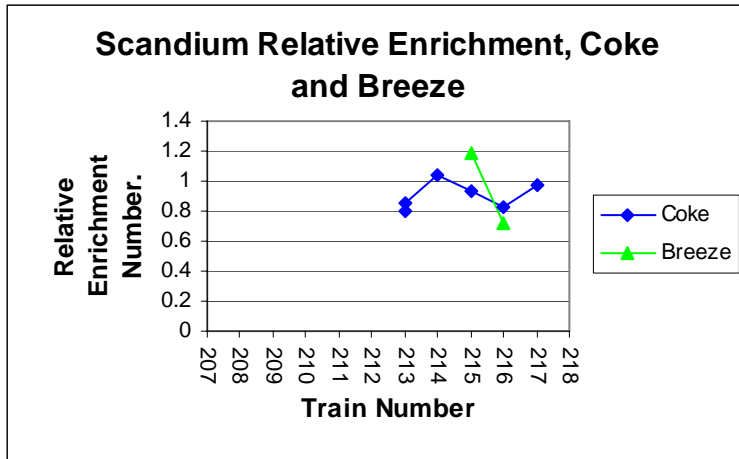


Figure 6.67. Scandium CRE for coke and breeze with time.

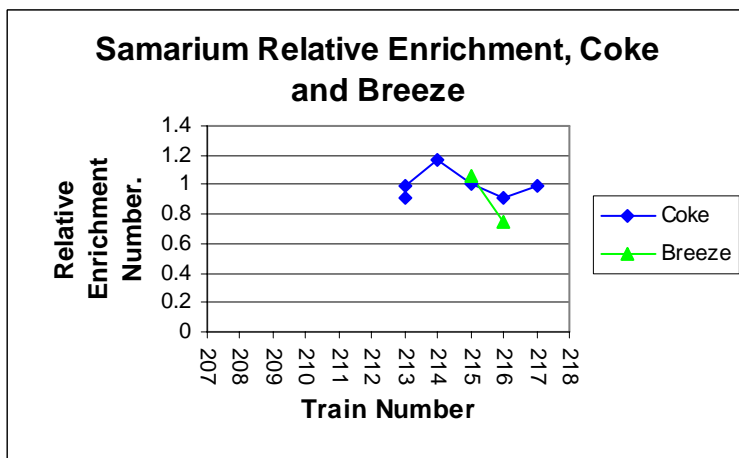


Figure 6.68. Samarium CRE for coke and breeze with time.

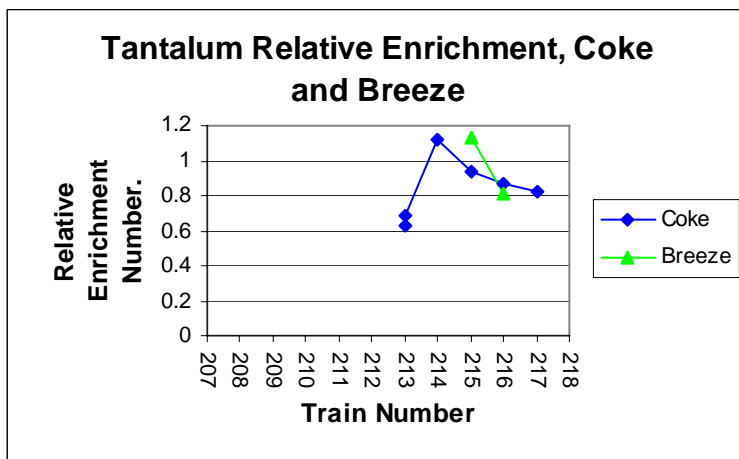


Figure 6.69. Tantalum CRE for coke and breeze with time.

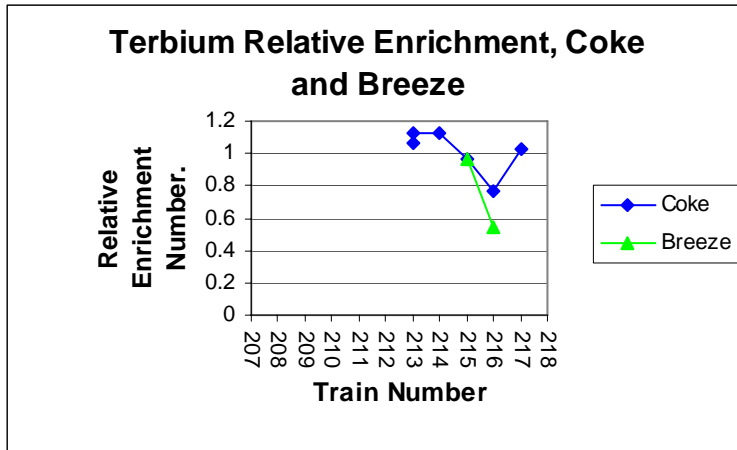


Figure 6.70. Terbium CRE for coke and breeze with time.

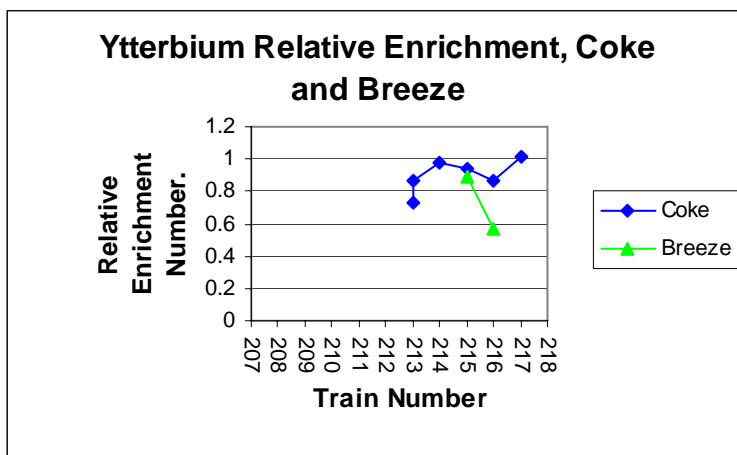


Figure 6.71. Ytterbium CRE for coke and breeze with time.

6.2.3. Grouping of Elements by Partitioning Behaviour in Carbonisation.

Major and trace elements have been classified according to their partitioning behaviour in carbonisation. No classification system was found in the literature so a new system is proposed here, and outlined in Table 6.1.

Table 6.1. Classification of Elements by Partitioning Behaviour in Carbonisation.

Coke	CRE	>1.2			0.8 - 1.2			0.6 - 0.8			<0.6		
	Class	1			2			3			4		
Breeze	CRE	<0.8	0.8 - 1.2	>1.2	<0.8	0.8 - 1.2	>1.2	<0.8	0.8 - 1.2	>1.2	<0.8	0.8 - 1.2	>1.2
	Class	1d	1a	1e	2d	2a	2e	3d	3a	3e	4d	4a	4e

Key. Breeze Class "D" = depleted, "A" = neither enriched or depleted, E = "enriched"

Some problems were encountered during development of the carbonisation-partitioning-behaviour classification system in that elements grouped together on the basis of their behaviour in coke could exhibit radically different behaviour in the breeze. It is likely that capture of some elements by the carbon fraction of the coke is

responsible, with some elements being better captured than others. A group of elements captured in coke may then exhibit different volatilities following complete “combustion” or loss of the volatile fraction of the coke and quenching of the coke mass. It is also recognised that this classification system has been developed for carbonisation in a beehive oven (a drying technology), and needs testing to determine the applicability of the system to carbonisation in a slot oven.

Classification according to the system outlined above for elements in the Bowen coke works is shown in Table 6.2. Coke Class 2 elements make up the bulk of the elements analysed in the Bowen coke works samples. Of the Coke Class 2 elements:

- Silicon, aluminium, titanium, manganese, phosphorous, hafnium, scandium, tantalum, thorium, uranium, lanthanum, cerium, neodymium, samarium, and europium are neither enriched nor depleted in the coke and breeze.
- Iron, cobalt, molybdenum, antimony, strontium, and zinc are neither enriched nor depleted in the coke, but are enriched in the breeze.
- Barium, caesium, mercury, nickel, rubidium, terbium, ytterbium and lutetium are neither enriched nor depleted in the coke but are depleted in the breeze.

Of the Coke Class 3 elements, manganese, sulphur, and selenium are depleted in the coke (as expected for their class) and also depleted in the breeze.

Of the Coke Class 4 elements:

- Bromine and tungsten are highly depleted in both the coke and the breeze, and are the most universally volatile elements in carbonisation.
- Gold and arsenic are highly depleted in the coke (as expected for the coke classification) but enriched in the breeze.

It is considered that the volatilised elements are substantially lost to the atmosphere, either directly, or via temporary adsorption to the wall of the beehive oven before re-volatilisation and final loss during carbonisation of the next coal charge.

Only two Coke Class 1 elements (sodium and chromium) are recognised. Both these elements are highly enriched in the coke and the breeze. The Coke Class 1

classification is curious since the only significant loss of mass in carbonisation is due to loss of volatile matter. Concentration of elements downstream as in combustion is not expected given complete volatilisation and condensation is unlikely in the beehive oven because the carbon is substantially retained in the coke and the carbonisation temperatures are lower. It is suggested that Coke Class 1 element behaviour could be caused by addition of sodium and chromium to the coke from sources other than the coal (oven bricks, metal surfaces at the coke works, contamination from the inside of the quench tower or from water used to quench the coke), or from contamination of samples following sample collection.

The classification of the partitioning behaviour of the analysed elements listed above will be compared to the classification of the same elements in combustion in Chapter 8.

Table 6.2. Classification of Element Partitioning Behaviour in Carbonisation.

Element	Coke Relative Enrichment	Breeze Relative Enrichment	Classification	Comments
Silicon	1.04	0.96	2a	
Aluminium	0.98	0.92	2a	
Iron (INAA)	0.97	1.60	2e	
Iron (XRF)	0.96	1.60	2e	
Magnesium	0.70	0.44	3d	many coke & coal analyses BDL
Sodium	1.50	2.33	1e	
Potassium		0.51	?	many coke & coal analyses BDL
Titanium	0.97	0.86	2a	
Manganese	0.99	0.94	2a	
Phosphorous	0.86	0.99	2a	
Sulphur	0.66	0.22	3d	
Gold	0.63	2.36	4e	many BDL; only 1 breeze figure
Arsenic	0.56	2.32	4e	
Barium	0.87	0.73	2d	
Bromine	0.22	0.18	4d	
Cobalt	0.95	1.28	2e	
Chromium	2.27	1.50	1e	
Caesium	0.81	0.68	2d	
Hafnium	0.88	1.00	2a	
Mercury	1.11		2d?	breeze analyses BDL
Molybdenum	0.87	1.28	2e	
Nickel	1.00		2d?	breeze analyses BDL
Rubidium	1.15	0.78	2d	many analyses BDL; only 1 breeze figure
Antimony	0.97	2.46	2e	
Scandium	0.90	0.93	2a	
Selenium	0.67	0.32	3d	
Strontium	0.84	1.51	2e	
Tantalum	0.83	0.96	2a	
Thorium	0.93	0.88	2a	
Uranium	1.07	0.94	2a	
Tungsten	0.18	0.20	4d	
Zinc	0.88	1.57	2e	
Lanthanum	1.00	0.82	2a	
Cerium	0.97	0.88	2a	
Neodymium	0.90	0.80	2a	
Samarium	0.99	0.89	2a	
Europium	0.93	0.80	2a	
Terbium	1.01	0.72	2d	
Ytterbium	0.89	0.71	2d	
Lutetium	0.88	0.70	2d	

6.3. Comparison of Coke Breeze and Soil Element Concentrations.

At the time of sampling, the breeze from the Bowen coke works was disposed of in a local landfill. Section 1.2 lists a number of trace elements that may be environmentally significant. The concentration of an element in a waste product has been shown to be a poor guide to the environmental impact of the waste materials (Dreher and Finkelman, 1992). However, the concentration of trace elements in the

breeze compared to the “average” concentration of trace elements in soils is shown in Table 6.2 as an indication of the trace elements of potential environmental interest that may be worthy of further investigation.

The concentration of the environmentally significant trace elements in the coke breeze is generally toward the middle or lower end of the corresponding soil concentration range. Only molybdenum, selenium, and zinc appear to lie toward the upper end of the range. Studies of fly-ash suggest zinc is soluble at pH 4 - 7, whereas molybdenum and selenium are soluble at pH 9 - 11 (Jones, 1995). Acidic leachate plumes from landfills have been identified in some situations (Greenhouse and Harris, 1983; Nobes, 1996), therefore mobilisation of zinc would appear to be the most likely possibility. A programme of leach testing to assess the mobility of a number of the more environmentally significant trace elements from the breeze is recommended, focussing on trace elements such as zinc that are readily mobilised in acidic environments.

Table 6.3. Trace Element Concentrations in Bowen Plant Coke Breeze and World Average Soils.

Element	Breeze Average Element Concentration (ppm)	Soil Average Element Ranges (ppm) *
Titanium	3950.00	1000 - 10000
Manganese	10.00	200 – 3000
Phosphorous	550.00	35 – 5300
Arsenic	1.27	1 – 50
Barium	375.00	100 – 3000
Cobalt	27.50	1 – 40
Chromium	91.00	5 – 1000
Mercury	BDL	0.01 - 0.5
Molybdenum	3.29	0.2 – 5
Nickel	BDL	5 – 500
Antimony	1.40	0.2 – 10
Scandium	16.00	<10 – 25
Selenium	1.30	0.1 – 2
Strontium	270.00	50 – 1000
Thorium	17.00	1 – 35
Uranium	3.40	0.7 – 9
Zinc	275.00	10 – 300

* Soil concentration figures from Swain, D.J. (1990) Trace Elements in Coal.

6.4. Chapter Summary.

Samples of feed coal, coke and breeze from the Bowen coke works have been analysed for a range of major and trace elements. The partitioning behaviour of most of the analysed elements has been inferred using a modified relative enrichment calculation called the Coke Relative Enrichment. Elements are classified into four classes based on their partitioning behaviour in coke, and further sub-divided based on their partitioning behaviour in breeze. A comparison of the concentration of trace elements of environmental significance in coke breeze (which is disposed of in a local landfill) and “average” soils has been made. The comparison found the concentration of trace elements in coke breeze is within the world average soil range, with only molybdenum, selenium, and zinc lying toward the upper end of the range.

Chapter 7.

Leachability of Trace Elements from Solid Waste from Pulverised Fuel Combustion.

7.0. Chapter Resume.

Samples of fly-ash and bottom-ash from the Collinsville and Mitsui pulverised fuel utilities were sampled and blended at a ratio of 80% fly-ash/ 20% bottom-ash. The composite sample was leached using the TCLP method. The aim of the work was to determine the concentration of several trace elements of environmental interest in the leachate, and to gain an indication of the proportion of analysed elements that are potentially mobilised following disposal of the solid waste.

7.1. Samples.

Samples of fly-ash and bottom-ash were gathered from the Collinsville and Mitsui coal fired power utilities as described in Section 5.1. Previous work suggests fly-ash comprises 75-80% of solid waste refuse from a power station (Murarka et al., 1993), with bottom-ash making up most of the remaining 20%. Therefore, a sample comprising 80% fly-ash and 20% bottom-ash was composited for each of the power utilities sampled. Four fly-ash samples from various locations downstream of the combustion zone were gathered from the Collinsville power utility. Equal weights of these four samples were obtained using a balance accurate to four decimal places to comprise 80% of the final sample (ie 20% each). Two fly-ash samples were gathered from the Mitsui power utility. Equal weights of the two samples were obtained using a balance accurate to four decimal places to comprise 80% of the final sample (ie 40% each). The remaining 20% of each composite sample was made up of the respective bottom-ashes.

The final leaching sample was composited to approximate the estimated makeup of the final waste stream from each utility. The concentration of the trace elements of interest in the composite sample was calculated from the weighted proportions of the respective fly-ash and bottom-ash results. The composite samples were leached using the TCLP protocol (United States Environmental Protection Agency, 1992) by Cawthron Laboratories, Nelson, New Zealand. The TCLP protocol was chosen to

provide a “worst case” scenario for leached element concentrations using a standard methodology, rather than to approximate and model the ash dump conditions at the site. The importance factor in the leach testing is that both samples were analysed by the same method (rather than a method appropriate to the individual sites) to provide comparable results for comparison in Section 8.2.2..

Leachate samples were analysed for trace elements of environmental interest for which comparative partitioning data (Chapter 5) was available. The concentration of antimony, arsenic, barium, boron, chromium, cobalt, copper, lead, manganese, nickel, selenium, vanadium, and zinc in the leachate was analysed using ICP-OES by Cawthron Laboratories, Nelson, New Zealand. The concentration of tin and uranium in the leachate was analysed using ICP-MS by Hill Laboratories, Hamilton, New Zealand. The aim of the experiment was to determine the concentration of trace elements in the leachate and provide an indication of the percentage of the trace element mobilised by the leaching procedure.

Some limited analysis of water from observational boreholes in the fly-ash dam and from a pond or “duck hole” in a stream adjacent to the Collinsville power ash dams was undertaken at the Advanced Analytical Centre, James Cook University, Townsville using ICP-MS. These results are discussed where available.

7.2. Results.

7.2.1. Concentration of Trace Elements in Combustion Wastes and Soils.

A restricted range of environmentally significant trace elements for which partitioning behaviour data is also available (Chapter 5) were analysed in the leachates. The concentration of these trace elements of interest in the various solid waste fractions for the Mitsui and Collinsville combustion plants is given in Table 7.1. along with the average concentration of the same trace elements in soils is also shown in Table 7.1.. Most of the trace elements are comfortably within the average concentration range of soils. Exceptions are selenium and, possibly, uranium in solid waste from the Collinsville utility, and boron, copper, selenium and, possibly, uranium in solid waste from the Mitsui utility. Because the average concentration of trace elements in the solid waste materials is generally well within the average soil concentration range, it

could be inferred that most of these elements have little potential for causing a negative environmental impact (although such an inference does not take account of the bioavailability of the element, dose rate, length of exposure and speciation of the element).

7.2.2. Concentration of Trace Elements in TCLP Leachates Compared to Water Quality Guidelines.

The TCLP method is used as an indicator of the water quality that might be expected following leaching of a particular material. Published guidelines are available for the concentration of a number of environmentally significant trace elements (plus other compounds and microbes) in recreational and drinking water. ANZAC Guidelines for Recreational water (Australia & New Zealand Environmental and Conservation Council. Agriculture & Resource Management Council of Australia & New Zealand., 2000) and the Drinking Water Standards of New Zealand (New Zealand Ministry of Health., 2000) were used to determine the preferred maximum concentration of the analysed trace elements in water for recreational and drinking purposes. Table 7.2. shows the TCLP data and the respective indicated maximum trace element concentration for the two classes of water quality.

Based on the comparison with the drinking and recreational water standards, the following conclusions are made:

- Arsenic concentration in both leachates is below the detection limit of the analysis method. Because the detection limit of the analytical method is above the drinkwater standard, no comment can be made about the suitability of the leachate arsenic in relation to the environmental standard. Table 7.3. details analysis results for arsenic in water from observation boreholes in the fly-ash dam and for a duck pond in an adjacent stream at the Collinsville power plant. Arsenic concentration is well below the drinkwater guideline value in the duck pond water.
- The concentration of boron in the Collinsville leachate is below the recommended guideline concentrations. Boron in the water from the observational bores and the adjacent duck pond at the Collinsville ash impoundment site confirms the inference that boron is below both

recommended guideline concentrations (Table 7.3.). Boron in the leachate from the Mitsui solid waste sample is well above both the recreational and drinkwater guideline values.

- Barium in the Collinsville leachate exceeds both the drinking and recreational guideline values. Barium in the Mitsui leachate exceeds the drinkwater guideline value.
- No guideline concentrations for cobalt were found.
- Chromium concentration in both leachate samples is below the concentration guideline values for both recreational and drinking water. It is important to note that the valence state of chromium is a critical factor in determining the toxicity of the element, hexavalent chromium being significantly more toxic than trivalent chromium (Appendix 1).
- Copper concentration in both leachate samples is below the concentration guideline values for both recreational and drinking water. Copper in the water from the observational bores and the adjacent duck pond at the Collinsville ash impoundment site confirms the inference that copper is below both recommended guideline concentrations (Table 7.3.).
- Manganese concentration in the Collinsville leachate exceeds both the recreational and drinkwater guideline concentrations. The concentration of manganese in the Mitsui leachate is below the recommended guideline concentrations.
- Nickel concentration in the Collinsville leachate exceeds the drinkwater standard but is below the recreational water guideline level. The concentration of nickel in the Mitsui leachate is below the recommended guideline concentrations.
- Lead concentration in both leachate samples is below the concentration guideline values for recreational and drinking water.
- The concentration of antimony in both leachate samples is below the detection limit of the analytical method, however, the detection limit is above the drinkwater guideline concentration. Because the detection limit of the analytical method is above the drinkwater standard, no comment can be made about the suitability of the leachate antimony in relation to the environmental standard

- Selenium concentration in the Collinsville leachate exceeds both the drinkwater and recreational water guidelines. However, the concentration of selenium in water from the observational bores and the adjacent duck pond at the Collinsville ash impoundment site (Table 7.3.) is well below the recommended guideline values. The concentration of selenium in the Mitsui leachate is substantially above both the recreational and drinking water guideline concentrations.
- Tin concentrations are below the limit of detection for both leachate samples and, therefore, below the guideline value for drinking water.
- Uranium is below the drinkwater guideline concentration value for both leachate samples.
- No guideline figures for vanadium concentrations for either recreational or drinkwater were found.
- Zinc concentrations are well below the threshold values for recreational water for both leachate samples.

It should be noted that this comparison is a worst-case situation, in that the comparison is made using undiluted TCLP leachate. In nature, some natural buffering by, particularly, clay minerals, reactions to produce secondary minerals, and dilution by surface and ground water would be expected in many instances.

Table 7.1. Trace Element Concentration in Ash and Bottom-ash.

	Coll Pwr botm ash 14/09/1999	Coll Pwr brnr level 14/09/1999	Coll Pwr level 3 14/09/1999	Coll Pwr Supr htr 14/09/1999	Coll Pwr U3 fly-ash 14/09/1999	Soil Average Element Range (ppm)
As (PPM)	1.1	3.8	3.7	4.5	5	1 – 50
B (PPM)	6	9	8	8	9	2 – 100
Ba (PPM)	1600	1600	720	1500	1900	100 – 3000
Co (PPM)	18	23	27	26	20	1 – 40
Cr (PPM)	46	93	100	85	58	5 – 1000
Cu (PPM)	66.8	80.51	68.79	81.69	54.03	2 – 100
Mn (PPM)	1000	700	300	700	500	200 – 3000
Ni (PPM)	95	92	110	98	<5	5 – 500
Pb (PPM)	33.4	49.7	45.86	61.5	74.64	2 – 100
Sb (PPM)	0.85	1.5	1.5	1.6	1.8	0.2 – 10
Se (PPM)	0.7	2.8	1.2	<0.2	6.4	0.1 – 2
Sn (PPM)	2.5	3	4	6		1 – 20
U (PPM) (INAA)	6.4	9	7.7	8	7.5	0.7 – 9
U (PPM) (XRF)	11.69	12.92	9.97	12.49	12.81	0.7 – 9
V (PPM)	66.8	99.4	100.7	96.1	85.22	20 – 500
Zn (PPM)	70	130	160	160	210	10 – 300
	Mitsui Botm ash	Burner Outlet	Fly-ash Collector			
As (PPM)	1.8	2.5	6.6			1 – 50
B (PPM)	120	330	708			2 – 100
Ba (PPM)	160	740	1000			100 - 3000
Co (PPM)	4.6	22	31			1 – 40
Cr (PPM)	10	52	74			5 – 1000
Cu (PPM)	67.6	98.38	123.83			2 – 100
Mn (PPM)	300	400	400			200 - 3000
Ni (PPM)	17	<5	<5			5 – 500
Pb (PPM)	12.17	32.16	50.7			2 – 100
Sb (PPM)	0.29	0.61	1.6			0.2 – 10
Se (PPM)	2.3	<0.2	3			0.1 – 2
U (PPM) (INAA)	0.66	4.4	6.3			0.7 – 9
U (PPM) (XRF)	5.41	9.46	11.7			0.7 – 9
V (PPM)	173.06	262.04	335.4			20 – 500
Zn (PPM)	18	68	110			10 – 300

Source of Soil Average Figures: Swaine (1995).

Table 7.2. Water Quality Guideline Values and TCLP Concentrations.

Element	Water Quality Guidelines		TCLP Leachate Concentration (ppm)	
	Recreational Water	Drink Water	Collinsville	Mitsui
As (PPM)	0.05	0.01	<0.060	<0.060
B (PPM)	1	1.4	0.44	12
Ba (PPM)	1	0.7	1.78	0.98
Co (PPM)			0.012	<0.010
Cr (PPM)	0.05	0.05	<0.010	0.173
Cu (PPM)	1	2	<0.010	<0.010
Mn (PPM)	0.1	0.5	0.684	<0.010
Ni (PPM)	0.1	0.02	0.053	<0.0050
Pb (PPM)	0.05	0.01	<0.030	<0.030
Sb (PPM)		0.003	<0.030	<0.030
Se (PPM)	0.01	0.01	0.061	0.144
Sn (PPM)		1	<0.01	<0.01
U (PPM) (INAA)		0.002	0.0004	<0.0004
U (PPM) (XRF)		0.002	0.0004	<0.0004
V (PPM)			0.187	0.529
Zn (PPM)	5		1.15	<0.050

Sources: ANZAC Guidelines for Recreational Water (2000); Drinking Water Standard of New Zealand (2000).

Table 7.3. Analysis of water from Observation Boreholes and Duck Pond in Stream Adjacent to Collinsville Power Plant Ash Dams.

Element	Duck Hole	Borehole 1	Borehole 2	Borehole 3
Arsenic (ppm)	<0.005	<0.005	<0.005	<0.005
Boron (ppm)	<0.100	0.139	0.283	0.182
Copper (ppm)	0.0083	0.045	0.036	0.061
Selenium (ppm)	<0.005	<0.005	<0.005	<0.005

7.2.3. Proportion of Trace Elements in Solid Waste Mobilised by the TCLP Protocol.

The TCLP protocol states that solid wastes are leached “with an amount of extraction fluid equal to 20 times the weight of the solid phase” (Section 2.3.7.). Therefore, to calculate the proportion of an element mobilised by the leaching protocol, the leachate concentration should be multiplied by twenty times to take account of the extraction fluid dilution factor. The twenty-fold concentration can then be calculated as a percentage of the calculated concentration of the element in the leached waste material. Table 7.4. shows the calculated concentration of trace elements in the composite solid waste sample and in the TCLP leachate along with the calculated percent of the element mobilised by the TCLP protocol.

The calculated concentration of arsenic in the Collinsville and Mitsui leaching samples is similar, and the concentration of arsenic in the leachate for both samples was below the detection limit of ICP-OES for this element. The leaching data suggests a low proportion of arsenic is mobilised from the solid wastes of both power stations (using the detection limit as an upper concentration cutoff, leaching must be less than 33% for the Collinsville plant and less than 30% for the Mitsui plant).

The calculated boron in the Collinsville leaching sample is considerably lower (8 ppm) than the concentration calculated for the Mitsui leaching sample (439.2 ppm). The proportion of boron mobilised from the Collinsville solid waste is very high (110% calculated, ie 100%). However, because of the low concentration of boron in the solid waste, the concentration of boron in the leachate is still below the threshold guidelines (Section 7.2.2.). The proportion of boron mobilised from the Mitsui solid waste is lower than that mobilised from the Collinsville waste (54.64%). However, because of the high concentration of boron in the solid waste, the concentration of boron in the leachate exceeds the threshold guidelines (Section 7.2.2.). These results suggest boron is more readily mobilised from the Collinsville solid waste sample. The high proportion of boron mobilised by the TCLP protocol suggests this element is one of most readily mobilised in this sample set (matched only by selenium), probably because it tends to be present as soluble borates adsorbed onto the surface of fine fly-ash particles (Clarke and Sloss, 1992) following combustion. Previous work has also found that boron is one of the trace elements most readily mobilised from fly-ash (Querol et al., 2001b).

The concentration of barium in the Collinsville solid combustion waste is approximately double the concentration of the same element in the Mitsui solid combustion waste. However, only very small proportions of barium are mobilised from the solid waste samples, the proportions mobilised being essentially equal for both power utility wastes. Because of the higher concentration of barium in the Collinsville solid waste, the concentration of this element in the leachate is double that of the Mitsui leachate.

The concentration of cobalt in the Collinsville and Mitsui solid waste samples is essentially the same. Cobalt in the Mitsui leachate is below the limit of detection, but

is marginally above the detection limit in the Collinsville leachate. It is inferred that the Mitsui cobalt is slightly less readily mobilised compared to the Collinsville cobalt.

The calculated concentration of chromium in the Collinsville solid combustion waste is ~24ppm higher than the concentration of chromium in the Mitsui combustion waste. In spite of this, the concentration of chromium in the Collinsville leachate is below the limit of detection. A minor fraction (6.6%) of the chromium was mobilised from the Mitsui solid waste sample. It is inferred chromium is more readily mobilised from the Mitsui waste sample.

The concentration of copper in the Mitsui combustion waste is ~32ppm higher than in the Collinsville combustion waste. However, the concentration of copper in both leachates is below the limit of detection suggesting copper is not readily mobilised from either solid waste sample.

The concentration of manganese in the Collinsville solid combustion waste is approximately double the concentration of the same element in the Mitsui solid combustion waste. A minor proportion of manganese in the Collinsville solid waste sample was mobilised by the TCLP protocol. The concentration of manganese is below the limit of detection in the Mitsui leachate. These results suggest manganese is not readily leached from either of the solid waste samples.

The concentration of nickel in the Collinsville solid combustion waste is 78ppm. Nickel concentration in the Mitsui combustion waste is indicative only because the fly-ash figures were below the limit of detection for INAA (5ppm). The Mitsui nickel figure is calculated assuming the concentration of nickel in the fly-ash is 5ppm as a “worst case” scenario. Only a small proportion of nickel is mobilised from the Collinsville solid waste. The concentration of nickel in the Mitsui leachate is below the limit of detection. These results suggest nickel is poorly mobilised by the TCLP protocol from either of the solid waste samples.

The concentration of lead in the Collinsville combustion waste is ~15ppm higher than in the Mitsui combustion waste. However, the concentration of lead in both leachates

is below the limit of detection suggesting lead is not readily mobilised from either solid waste sample.

The concentration of antimony in the Collinsville combustion waste is ~0.5ppm higher than in the Mitsui combustion waste. However, the concentration of antimony in both leachates is below the limit of detection suggesting antimony is not readily mobilised from either solid waste sample.

The concentration of selenium in the Collinsville combustion waste is ~0.6ppm higher than in the Mitsui combustion waste. However, 182.28% (ie 100%) of the selenium in the Mitsui solid waste is mobilised by the TCLP protocol whereas only ~56% of the selenium in the Collinsville solid waste is mobilised. These results suggest that selenium in the Collinsville solid waste is less readily mobilised in comparison to selenium in the Mitsui combustion waste. Selenium is one of the trace elements most readily mobilised by the TCLP protocol for the samples analysed, probably because the element tends to be present as soluble selenates adsorbed onto the surface of fly-ash particles (Gutenmann and Bache, 1976) following combustion. Previous work has also found that selenium is one of the trace elements most readily mobilised from fly-ash (Querol et al., 2001b).

No tin analyses are available for the Mitsui solid combustion waste so a comparison of the relative mobility of tin from the two solid combustion waste samples was not possible. The Collinsville results suggest tin is not readily mobilised from the solid waste by the TCLP protocol.

The concentration of uranium in the Collinsville solid combustion waste appears to be several parts per million higher than the concentration of uranium in the Mitsui solid waste sample (depending whether the INAA or XRF analyses are viewed as being the most reliable). The concentration of uranium in the Mitsui leachate is below the detection limit. Uranium appears to be very poorly mobilised from the Collinsville combustion waste by the TCLP protocol (<1%), the concentration of this trace element being barely above the detection limit in the leachate.

The concentration of vanadium in the Mitsui solid combustion waste is approximately double the concentration of the same element in the Collinsville solid combustion waste. Only a very small proportion of vanadium is mobilised from either of the solid waste samples, the proportions mobilised being similar for both samples (perhaps the Collinsville vanadium marginally more mobile).

As for vanadium, the concentration of zinc in the Collinsville solid combustion waste is approximately double the concentration of the same element in the Mitsui solid combustion waste. The concentration of zinc in the Mitsui leachate is below the limit of detection. A moderate proportion of zinc is mobilised from Collinsville solid waste sample.

Table 7.4. Calculated Proportions of Elements Mobilised by the TCLP Protocol.

Collinsville	Calculated Sample Concentration (ppm)	TCLP Leachate Concentration (ppm)	Percent Mobilised.
Element			
As (PPM)	3.62	<0.060	BDL
B (PPM)	8.00	0.44	110.00
Ba (PPM)	1464.00	1.78	2.43
Co (PPM)	22.80	0.012	1.05
Cr (PPM)	76.40	<0.010	BDL
Cu (PPM)	70.36	<0.010	BDL
Mn (PPM)	640.00	0.684	2.14
Ni (PPM)	78.00	0.053	1.36
Pb (PPM)	53.02	<0.030	BDL
Sb (PPM)	1.45	<0.030	BDL
Se (PPM)	2.18	0.061	55.96
Sn (PPM)	3.10	<0.01	BDL
U (PPM) (INAA)	7.72	0.0004	0.10
U (PPM) (XRF)	11.98	0.0004	0.07
V (PPM)	89.64	0.187	4.17
Zn (PPM)	146.00	1.15	15.75
Mitsui	Calculated Sample Concentration (ppm)	TCLP Leachate Concentration (ppm)	Percent Mobilised.
Element			
As (PPM)	4.00	<0.06	BDL
B (PPM)	439.20	12	54.64
Ba (PPM)	728.00	0.98	2.69
Co (PPM)	22.12	<0.010	BDL
Cr (PPM)	52.40	0.173	6.60
Cu (PPM)	102.40	<0.010	BDL
Mn (PPM)	380.00	<0.010	BDL
Ni (PPM)	7.40	<0.0050	BDL
Pb (PPM)	35.58	<0.030	BDL
Sb (PPM)	0.94	<0.030	BDL
Se (PPM)	1.58	0.144	182.28
U (PPM) (INAA)	4.41	<0.0004	BDL
U (PPM) (XRF)	9.55	<0.0004	BDL
V (PPM)	273.59	0.529	3.87
Zn (PPM)	74.80	<0.050	BDL

7.3. Discussion.

The concentration of the trace elements selenium and, possibly, uranium in Collinsville solid combustion wastes were noted to be above the published average concentration range for world soils. The TCLP protocol on the Collinsville composite sample found the trace elements barium, manganese, nickel, and selenium exceeded either one or both water quality guidelines. The concentration of the elements boron, copper, selenium and, possibly, uranium in Mitsui solid combustion wastes were

above the average concentration range for world soils. The TCLP protocol on the Mitsui composite sample found boron, barium, and selenium exceeded one or both of the water quality guidelines. These results show that, although high trace elements concentrations in solid combustion waste generally translate to high concentrations of that element in a leachate, some other elements may also be mobilised in sufficient quantities to exceed water quality guidelines even when present in relatively low concentrations. Therefore, analysis to determine elemental concentrations may not always be sufficient to determine environmental impact.

The above conclusion is further borne out by looking at percentages of trace elements mobilised. In general it was found most trace elements were poorly mobilised by the TCLP procedure. The exceptions to poor mobilisation were boron and selenium for both combustion waste samples. Boron from the Collinsville combustion waste was found to be highly mobile, with 100% extracted by leaching. However, because boron is present at a low concentration in the composite solid waste sample, boron concentration in the leachate was still below the water quality guideline values (apparently confirmed by the limited analysis of water samples from the site). Boron was also readily mobilised from the Mitsui composite waste sample (54.64%), a mobilisation proportion below that of the Collinsville sample. However, because of the very high concentration of boron in the Mitsui composite solid waste sample, the concentration of boron in the leachate was well above both water quality guideline concentration values.

Selenium was also readily mobilised from the Collinsville composite solid waste sample (~56%), and the concentration of selenium was above both water quality guideline values. However, limited analysis of water samples from the site found the concentration of selenium to be low. Possibly the low selenium concentration in the ash disposal site water samples is due to the practise of compacting the ash in “cells”, which are capped with soil to limit water percolation. Alternately, oxyanions such as arsenic, boron, molybdenum and selenium are most mobile at a pH of about 11 (Jones, 1995). Possibly the Collinsville leachate is not sufficiently alkaline to mobilise selenium, given the combustion plant ash is notably deficient in calcium (see Chapter 5). A more directed study to look at the leachability of selenium, the geochemistry of the fly-ash dam, and the pathways for water incursion would be

required to elucidate the reality and reasons for low selenium in the ash disposal site water at Collinsville.

Selenium was completely mobilised (100%) from the Mitsui composite solid waste sample, the concentration of this element being well above the water quality guideline values. It is notable that the concentration of selenium in the Collinsville composite solid waste sample was calculated to be 0.6ppm higher than that in the Mitsui sample.

The other trace elements analysed were generally very poorly mobilised, but a number of differences in the proportion of various elements extracted using the TCLP protocol were noted. These results again indicate that trace element concentration in solid wastes can be a poor indicator of elemental mobility and environmental impact.

7.4. Chapter Summary.

The analytical data suggests the concentration of a range of trace elements in solid combustion wastes from the Collinsville and Mitsui combustion utilities is within the world average range for soils. However, leaching of a composite solid waste sample made up of fly-ash and bottom-ash from each utility found that the concentration of some trace elements exceeded water quality guideline values. Further, it was found the proportion of individual trace elements mobilised by the TCLP protocol varied between the two composite samples. The results suggest elemental concentration is a poor indicator of environmental impact, and it could be difficult to predict given variations in the proportions of elements mobilised by leaching.

Chapter 8.

Synthesis.

8.0. Chapter Resume.

Chapter 8 synthesises analysis results and interpretation from preceding chapters. The mode of occurrence of trace elements determined from graphical and sequential leaching methods is compared. Inferences concerning the influence that trace element mode of occurrence exerts on element partitioning behaviour in combustion and leachability of solid combustion waste is discussed for several elements. A comparison between the partitioning behaviour of trace elements in combustion and carbonisation is presented.

8.1. Assessment of Trace Element Mode of Occurrence – Comparison of Graphical and Sequential Leaching Results.

The Collinsville pulverised-fuel utility at the time of sampling was supplied with a fuel blend comprising ~70% Blake seam coal (from the Blake Central and Blake West pits) and 30% Bowen seam coal (from the Bowen No.2 pit). Chapter 3 details the use of graphical relationships to determine the mode of occurrence of a number of trace elements in the Blake Central, Blake West and Bowen No.2 pits. Chapter 4 details the use of sequential leaching (undertaken according to the USGS protocol) to determine the mode of occurrence of trace elements in pulverised fuel being combusted in Unit 3 of the Collinsville combustion plant. This section discusses differences in the mode of occurrence of trace elements determined by graphical relationships and sequential leaching methods.

The mode of occurrence of trace elements in the Collinsville combustion plant pulverised fuel has been inferred from graphical relationships between normative mineral matter and trace element concentrations in channel ply samples from the in-ground coal, and the interpretation of the sequential leach results of the pulverised fuel. Table Table 8.1 shows the dominant mode of occurrence indicated by each of these two techniques.

Table 8.1. Comparison of Modes of Occurrence from Graphical and Sequential Leaching Methods.

Element	Graphical Mode		Sequential Leach Mode
	Blake Seam (70%)	Bowen Seam (30%)	
Aluminium	aluminosilicates	aluminosilicates	aluminosilicates
Iron	siderite	pyrite/ minor siderite	siderite/ FeO/ minor pyrite
Calcium	??carbonates	?	carbonates
Potassium	illite/ feldspar	illite	aluminosilicates
Manganese	siderite	siderite	carbonates
Magnesium	kaolinite	siderite	carbonates/ minor aluminosilicates
Sodium	feldspar	kaolinite	aluminosilicates/ minor ionic (salt)
Phosphorous	gorceixite/ goyazite	gorceixite/ goyazite	uncertain
Arsenic	pyrite	pyrite	arsenates (oxidised pyr)/ pyrite/ organic
Barium	gorceixite	gorceixite	silicates/ minor barite
Bromine	organic	illite	organic
Cerium	monazite/ minor illite	heavy minerals	monazite/ xenotime
Cobalt	organic	pyrite	organic/ carbonate; monosulphide/ pyr
Chromium	Pyrite (?)	Pyrite (?)	silicates/ organic/ minor pyrite
Caesium	illite	kaolinite	aluminosilicates/ minor exchangeable ions
Copper	pyrite	pyrite	pyrite/ aluminosilicate/ organic(?)
Europium	monazite/ minor illite	phosphates/ illite	monazite/ xenotime/ minor apatite
Hafnium	zircon/ heavy minerals	zircon	zircon
Mercury	pyrite	pyrite	organic/ pyrite
Lanthanum	monazite/ minor illite	illite	monazite/ xenotime
Lutetium	kaolinite/ monazite	kaolinite	monazite/ xenotime
Nickel	pyrite	pyrite	aluminosilicate/ minor organic, pyrite
Lead	pyrite	pyrite	galena
Rubidium	illite/ minor kaolinite	heavy minerals (?)	aluminosilicates
Antimony	kaolinite	pyrite	organic/ minor pyrite-sulphides
Scandium	gorceixite/ illite	kaolinite	aluminosilicates/ organic
Selenium	organic	pyrite	organic/ pyrite
Samarium	monazite/ minor kao	heavy minerals/ illite	monazite/ xenotime/ minor apatite
Strontium	goyazite	goyazite	aluminosilicates
Tantalum	kaolinite	heavy minerals/ illite	aluminosilicates/ organic
Terbium	monazite/ minor kao	illite	monazite/ xenotime/ minor apatite
Thorium	heavy mins/phos/ felds	heavy minerals/ illite	monazite/ xenotime
Titanium	rutile	rutile	Ti oxides &/or aluminosilicates
Uranium	phos/ zircon/ felds	zircon/ minor illite	aluminosilicates &/or zircon/ organic/ pyr
Vanadium	pyrite/ gorceixite	pyrite/ illite	aluminosilicates/ subordinate organic
Tungsten	heavy minerals	heavy minerals	aluminosilicates/ minor org/ tungstates
Ytterbium	kaolinite/ organic	kaolinite	monazite/ xenotime/ organic
Zinc	organic/ pyrite/ mixed	pyrite	sphalerite

In general the results appear comparable. The elements aluminium, iron, probably calcium, potassium, manganese, magnesium, sodium, phosphorous (?), cerium, cobalt, caesium, copper, europium, hafnium, selenium, tantalum, thorium, titanium, and uranium have the same dominant mode of occurrence indicated by both techniques. However, where the mode of occurrence is indicated to be

“aluminosilicate” or “carbonate” from the sequential leaching technique, the graphical relationship data provides more specific definition of the exact mineral type.

Examples of more specific mineral definition include the siderite mode of occurrence for iron, manganese and magnesium (cf carbonates), and illite in the Blake seam and kaolinite in the Bowen seam as the mode of occurrence for caesium (cf aluminosilicates). Further, the sequential leach results suggest selenium has two modes of occurrence (organic and associated with pyrite). The graphical relationships indicate the Blake seam is the source of the organically-bound selenium, and the Bowen seam is the source of the pyrite-bound selenium.

Trace elements inferred from graphical relationships to have a monazite/ xenotime/ zircon mode of occurrence (Ce, Eu, Hf, La, Lu, Sm, Ta, Tb, Th, U) required additional assumptions (as discussed in Sections 3.3.1.2. and 3.3.2.2.) that proved correct in this case. However, it should be recognised that the graphical deductions required an “extra leap” of inference, and greater confidence was achieved by having the inferences “checked” by the sequential leach results. Further, a number of these elements had several mode of occurrence, some of which were not indicated by the graphical method (eg some organic association for some fraction of the rare earth elements).

In some cases the mode of occurrence is comparable between the sequential leach data and the graphical data for one seam but not the other. Examples include bromine, lanthanum, lutetium, rubidium, scandium, and terbium. A further set of elements exhibit generally comparable modes of occurrence between the two techniques, although some modes do not match. Examples in this category include samarium, tungsten, and ytterbium.

Arsenic, barium, chromium, mercury, nickel, lead, antimony, vanadium and zinc have different modes of occurrence indicated by the two techniques, and are worthy of further discussion.

The mode of occurrence of arsenic indicated by the sequential-leach data is arsenates (AsO_4^{3-}), whereas the graphical analysis indicates a pyrite mode of occurrence for both Blake and Bowen seam channel samples. Palmer et al (1999) state “arsenate is

generally considered to form by oxidation of arsenic-bearing pyrite”. Therefore, the pyrite mode of occurrence inferred using the graphical method may be correct for the in-ground coal, however oxidation has changed the state of the host mineral in the pulverised fuel sample during the approximately two years storage prior to analysis. Further, the larger pyrite grains may have been rejected from the ball mill during pulverisation of the fuel, thereby preferentially removing some of the pyrite-associated arsenic.

The sequential leach data suggests barium is present in the pulverised fuel sample associated with aluminosilicates or as the mineral barite. The normative analysis inferred that barium is predominantly bound into the mineral gorceixite. An alternative to the USGS sequential leaching procedure was employed by Laban and Atkin (1999) to determine elemental modes of occurrence. These authors found 80% of barium was mobilised at Stage 1 of their leaching protocol by a mixture of 8ml of 5M HCl and 2ml of 40% (w/v) HF. It was stated that “the common Ba minerals such as barite (BaSO_4) and gorceixite ($\text{BaAl}_3(\text{PO}_4)_2(\text{OH})5\text{H}_2\text{O}$) will be dissolved in Stage 1” (Laban and Atkin, 1999). It is concluded that the USGS sequential-leaching data could be re-interpreted to support the gorceixite mode of occurrence for barium indicated by the normative analysis. Gorceixite is favoured as the mode of occurrence for barium over barite because the mineral was directly identified by XRD in sample BWB4.23-4.28 from the Blake West pit.

The sequential leach data for chromium indicates organic and silicate modes dominate with a minor pyrite mode also present. A pyrite mode of occurrence was indicated by the graphical relationship analysis of the channel samples, although this mode is does not appear likely from the literature. One possible explanation is that the pyrite mode of occurrence dominated in the raw coal, but removal of pyrite as heavy reject from the ball mill has reduced the significance of the pyrite bound chromium, or (more likely) the source of the element was the same for iron and chromium but the two elements have different associations (ie a physical relationship only). However, it is apparent the organic and silicate modes have not been indicated by the graphical analysis. Graphs of ash yield versus chromium all suggest an inorganic mode dominates. Possibly the enrichment of chromium in the silicates is too haphazard to

be inferred using graphical method. However, this difficulty is a clear indication of the shortcomings of relying only graphical relationships to infer mode of occurrence.

Graphical analysis of mercury suggests this element is associated with pyrite in the seams channel sampled at the Collinsville open cut. The sequential leach data indicates a significant organic mode of occurrence in addition to the pyrite mode. In general, the concentration of mercury in the channel ply sample used in the graphical analysis was low, often below the detection limit of INAA. It is possible, therefore, that only the major “concentration” mode (ie mercury-enriched pyrite) has been picked using graphical analysis. Further, as noted above, pyrite may have been removed by rejection from the pulverised fuel mill skewing the distribution of mercury toward the organic mode of occurrence in the sequential leach sample.

Nickel was another element that was found to be present at low concentrations, often below the INAA detection limit, in the channel ply samples used in the graphical analysis. As for mercury, it is possible that only the major “concentration” mode (ie nickel enriched pyrite) has been picked using graphical analysis.

The mode of occurrence of lead indicated by the sequential leach data is galena (PbS), whereas graphical analysis indicates pyrite as the mode of occurrence. Probably, the difference is caused by the normative analysis ascribing a pyrite mode of occurrence to all sulphur not organically bound, leading to a parallel graphical relationship. Further, lead analysis was only available for a few of the plys, reducing the confidence of the graphical analysis.

An organic-plus-minor-sulphide mode of occurrence for antimony was indicated by the sequential leach data. Graphical relationships suggested an association with kaolinite in the Blake seam samples, and an association with pyrite in the Bowen seam samples. The relationship between antimony and kaolinite noted for the Blake Seam samples is rated as fair (see Table 3.7.), while the relationship between antimony and pyrite for the Bowen seam samples was rated good (see Table 3.8.). It is suggested that source of the pyrite-bound antimony is the Bowen seam, implying the Blake seam was the source of the organically-bound antimony (although this was not indicated by the graphical relationships). Further, graphs of ash yield versus

antimony for the Blake seam samples found no relationships to indicate an organic association. Therefore, the conflict in the mode of occurrence results for the Blake seam samples remains a puzzle.

The sequential leach data suggests strontium is present in the pulverised-fuel sample associated with aluminosilicates. The normative analysis inferred that strontium is predominantly bound into the mineral goyazite. It is inferred from the leaching results of Laban and Atkin (1999) that, if gorceixite can be mobilised by the HCl/ HF reagent mix, gaoyazite may also be mobilised. Therefore, the USGS sequential-leaching data for strontium could (as for barium) be re-interpreted to support the goyazite mode of occurrence for strontium indicated by the normative analysis.

The sequential-leach data for vanadium indicates an association with aluminosilicates and a minor organic association. A graphical relationship with illite was noted for the Bowen seam samples, however the relationships with pyrite (noted for the Blake and Bowen seam samples) and gorceixite (noted for the Blake seam samples) are very puzzling (see Sections 3.3.1.2. and 3.3.2.2.). Possibly the conflict has arisen due to a lack of vanadium analyses. No other explanation can be suggested at this stage.

The mode of occurrence of zinc indicated by the sequential-leach data is sphalerite (ZnS), whereas graphical relationships indicate pyrite is the mode of occurrence for the Bowen seam samples, and mixed organic/ inorganic and pyrite modes of occurrence in the Blake seam samples. As noted above for lead, the difference is probably caused by the normative analysis ascribing a pyrite mode of occurrence to all sulphur not organically bound, leading to a parallel graphical relationship.

8.2. The Control of Mode of Occurrence on Trace Element Partitioning and Leachability.

8.2.1. The Control of Mode of Occurrence on Trace Element Partitioning.

A number workers have suggested trace element mode of occurrence in coal influences the element's partitioning behaviour in combustion (Finkelman, 1982). However, no studies were found by the author comparing the partitioning behaviour of trace elements with different modes of occurrence in combustion. Accordingly one

aim of this research was to gather samples to document differences in trace element partitioning behaviour and attempt to relate this behaviour to differences in the mode of occurrence of the element in the fuel.

Pulverised-fuel combustion, such as occurs at the Collinsville and Mitsui plants sampled for this study, involves milling the coal to ~70 to 80% <75 μ m (Berkowitz, 1993; Diessel, 1998) and then blowing the fuel into the combustion chamber.

Combustion is thought to proceed in three stages, namely 1) devolatilisation of the coal particles; 2) combustion of the volatile matter; and 3) combustion of the formed char particles (Tsai, 1982; Van Krevelen, 1993). Ignition of the coal particle is governed by competition between pyrolysis and oxidation (Berkowitz, 1993).

Devolatilisation on pyrolysis releases combustible gasses such as H₂, CO, CH₄, and higher hydrocarbons; and incombustible gases such as CO₂, H₂O, and tar vapours (Tsai, 1982). Moisture will evolve early as the temperature increases, with gases and heavy tarry substances emitted with further temperature increase (Smoot and Smith, 1985). Particle pyrolysis can vary from a few percent up to 70-80% of the total particle weight, and can take place in a few milliseconds or several minutes depending on size consist, coal type, and temperature conditions (Smoot and Smith, 1985). The combustion of volatiles is thought to be a very rapid process as long as excess oxygen is present (Van Krevelen, 1993). However, discharge and combustion of volatiles will impede oxidation of the char by blocking access of oxygen to the char surface (Berkowitz, 1993).

The residual char is oxidised or combusted by direct contact with oxygen at sufficiently high temperature (Smoot and Smith, 1985). Access of oxygen to reactive sites on the char particle is governed by char porosity and removal of reaction products from the vicinity of the particle (Chan et al., 1999). The oxidation of char is much slower than the devolatilisation process, and may take seconds for small particles up to several minutes for larger particles (Smoot and Smith, 1985). Reaction rates will vary with “coal type, temperature, pressure, char characteristics (size, surface area etc), and oxidiser concentration” (Smoot and Smith, 1985).

Mineral matter in the coal may either be released on pulverisation of the fuel (excluded minerals), or (if fine enough) remain within the coal particle (included minerals), and may coalesce as the char combusts (Seggiani et al., 2000; Yan et al., 2001a). Further, it has been found that char structure and burnout will govern the size of the ash released during combustion. Large ash particles ($>2\mu\text{m}$) are “formed by mechanisms such as coal or char fragmentation and the structural disintegration of char, coalescence of ash on the surface of a char particle, fragmentation of minerals due to inorganic reaction, shedding of ash particles from the surface of chars during combustion, and cenosphere formation” (Wu et al., 1999). Fine size ($<2\mu\text{m}$) ash particles result from “mechanisms such as ash species vaporisation, condensation and aggregation, chemical reaction of mineral grains to form fume particles, convective transport of organically bound and possibly small grained inorganic material away from the coal particle during coal devolatilisation, thermal shock of coal particles or excluded minerals, rapid evolution of gasses during mineral decomposition, char secondary fragmentation, and busting of cenospheres to produce fine particles” (Wu et al., 1999).

Mineral grains show varying tendencies to oxidise, with species such as pyrite being highly prone to oxidation and silica, rutile, kaolinite, and illite showing a low tendency to oxidise (Badin, 1984). However, as noted above, localised reducing conditions within the combustion chamber may exist and may have a profound effect on the behaviour of mineral matter. For example, pyrite thermally decomposes to FeS (partial melt) at 282°C under reducing conditions, and to Fe_2O_3 at 487°C under oxidising conditions. In general, the following mineral conversions are likely to take place in combustion: clay alters to mullite ($3\text{Al}_2\text{O}_3 \cdot 2\text{SiO}_2$); pyrite alters to iron (Fe^{3+}) oxides and SO_x ; calcite alters to calcium oxide (CaO) and CO_2 ; siderite alters to iron (Fe^{2+}) oxide and CO_2 ; and quartz softens (Swaine, 1995). Some unburnt carbon may also remain, depending on factors such maceral composition and the rank of the coal (Bailey et al., 1990; Su et al., 2001), the ash yield of the coal (Badin, 1984; Kurose et al., 2001), and plant operational factors (Tsai, 1982). Thus fly-ash consists of “glassy aluminosilicate phases with lesser amounts of mullite, quartz, magnetite, haematite and carbon” (Swaine, 1995).

In pulverised fuel combustion, trace elements partition between bottom-ash, fly-ash, and gaseous stack emissions. Trace elements have been classified according to their partitioning behaviour (Section 1.4.3), but variability for a particular element also exists. The partitioning behaviour of trace elements in combustion is influenced by the elemental volatility (Section 1.4.4.1.), mode of occurrence (Section 1.4.4.2.), major element chemistry of the ash (Section 1.4.4.3.), plant design and operating conditions (Section 1.4.4.4.), and temperature variations within the combustion chamber and between collection points (Section 5.2.).

One aim of this investigation is to examine the influence mode of occurrence has on the partitioning behaviour of trace elements in combustion. However, any significant influence due to factors other than mode of occurrence (plant design and operating conditions, temperature variations within the combustion chamber and the major element chemistry of the ash) (Section 5.2) must be discounted first.

The design and operating conditions are similar for the two plants studied, so this factor does not appear relevant (Section 5.2.).

Since the Mitsui feed-coal ash yield is ~10% less than the Collinsville feed-coal ash yield, a given element in the Collinsville combustion plant could behave in a less volatile manner than the same element in the Mitsui plant due to lower temperatures in mineral laden areas of the combustion chamber. However, the Mitsui trace elements are not consistently more volatile, an observation which appears to discount this factor as a major influence.

Ash chemistry could also exert a control. Section 5.2 noted a potential difference in the calcium content of the feed coal if the INAA results for Collinsville pulverised fuel are considered reliable. However, the very-low concentration of calcium in channel samples from the feed coal pits at the Collinsville open cut (Chapter 3; Appendix 4), the low calcium concentration in the fuel coal sample analysed by the USGS and the very low calcium concentration in the fly-ash samples suggest the INAA calcium analysis result for the coal is incorrect and the ash chemistry is, therefore, similar for the two plants studied (as outlined in Section 4.2.). Therefore,

ash chemistry does not appear to be a major factor controlling differences in partitioning behaviour.

The Collinsville combustion uses a baghouse to capture fly-ash, whereas the Mitsui plant uses an ESP to collect the fly-ash. Some differences in the concentration and, therefore, partitioning of trace elements can be caused by the lower temperature in a baghouse collection system compared to an ESP system, eg selenium (Mastalerz et al., 2004). If the type of collection system was a significant influence on the partitioning behaviour of selenium, the element should exhibit more volatility in the Mitsui plant; in fact the opposite is true.

It is concluded that the most significant variables controlling differences in trace element partitioning behaviour in the Collinsville and Mitsui pulverised-fuel combustion plants are mode of occurrence of the element in the feed coal and elemental volatility.

The following relationships exist between elemental state and volatility (Valkovic, 1983b).

For elements in oxides, sulphates, carbonates, silicates and phosphates:

$As \approx Hg > Cd > Pb \approx Bi \approx Tl > Ag \approx Zn > Cu \approx Ga > Sn > Li \approx Na \approx K \approx Rb \approx Cs$

For elements in the elemental state, the order is:

$Hg > As > Cd > Zn > Sb \geq Bi > Tl > Mn > Ag \approx Sn \approx Cu > Ga \approx Ge$

For sulphides the relative order of volatility is:

$As \approx Hg > Sn \approx Ge \geq Cd > Sb \approx Pb \geq Bi > Zn \approx Tl > Cu > Fe \approx Co \approx Ni \approx Mn \approx Ag$

The organic fraction of coal is well known to thermally decompose at very low temperatures, ie 150°C in a low-temperature oxygen-plasma ashing system (Finkelman et al., 1984), and may oxidise and self-heat at atmospheric temperatures (Clemens and Matheson, 1994; Jones, 2000). Oxidation of the organic fraction of coals is clearly highly exothermic and would readily release associated trace elements at an early stage of combustion. Ashing studies have found that organically-bound

elements are volatile at low temperatures (along with volatile elements such as mercury) (Finkelman et al., 1990; Richaud et al., 2004). Vassilev et al (2000) suggested “chlorine and bromine with a high volatile behaviour show a tendency for concentration in the easily decomposing phases in coal” (eg in particular, organics, chlorides, moisture, combined water and exchangeable cations). Further, trace elements associated with volatile matter (predominantly the non-aromatic fraction of the coal) (Teichmüller et al., 1998; Van Krevelen, 1993) will be released from the fuel particle and subjected to oxidation at a relatively early stage of combustion. Trace elements associated with the char (predominantly the aromatic fraction of the coal) will not be liberated until combustion of the volatile matter is complete and access of oxygen to the char surface enables oxidation of the carbon. It is possible that organically-associated elements may display different volatilities depending on whether they are bound to the aromatic or aliphatic fraction of the coal.

Pyrite decomposes at slightly higher temperatures than the organic matter, ie $\sim 520^{\circ}\text{C}$ in a nitrogen atmosphere (Chen et al., 2000), while ashing experiments found pyrite decays to haematite between 400°C and 500°C (Mitchell and Gluskoter, 1976). Demir et al. (2001) found pyrite thermally altered to pyrrhotite at temperatures of $250\text{-}850^{\circ}\text{C}$ (with subsequent further transformations to haematite and magnetite at $>850^{\circ}\text{C}$). Under reducing conditions, pyrite may form a partial melt at 282°C (Badin, 1984). Oxidation of pyrite is known to be highly exothermic (Moore and Moore, 1999). Further, experiments examining the effect of thermal shock on mineral matter found pyrite to be highly susceptible to breakage relative to calcite (Yan et al., 2001b). Querol et al (1995) suggested that elements with sulphide or organic affinities are oxidised during coal combustion and consequently show more volatile behaviour. If pyrite is present as large size grains, the mineral may be liberated from the coal during pulverisation of the fuel and be subject to thermal shock-induced size reduction, and oxidation and reduction reactions at an early stage of combustion.

Decomposition of carbonates is species dependant, siderite decaying at 480°C , magnesite at 620°C , calcite at 820°C , dolomite at 760°C and ankerite at 690°C (Dubrawski and Warne, 1987). Other experiments suggest siderite thermally decomposes at $370\text{-}530^{\circ}\text{C}$ (Maes et al., 2000). Further, decomposition of carbonates in air was found to be endothermic except for siderite, which was slightly exothermic

(Dubrawski and Warne, 1987; Maes et al., 2000). As for pyrite, if the carbonate minerals are present as large size grains, the mineral may be liberated from the coal during pulverisation of the fuel and be subject to oxidation and reduction reactions at an early stage of combustion. However, the interior of large mineral particles may not decompose during combustion if the residence time in the flame is very short (Fernandez-Turiel et al., 2004).

Finally, silicates melt at very high temperatures, so it is assumed that they would be the last minerals to release any associated trace elements. For example, kaolinite shows the following temperature controlled changes: kaolinite to meta-kaolinite (loss of H₂O) occurs at 498°C; meta-kaolinite to silicon spinel (involving loss of SiO₂) occurs at 926°C; silicon spinel to mullite type phase involving further loss of SiO₂ occurs at 1098°C; mullite type phase to mullite involving further loss of SiO₂ occurs at 1398°C; and complete melting does not occur until 1798°C (Badin, 1984). Other workers found the following sequence of alteration combustion plant furnaces: clay minerals dehydrate and dehydroxylate at 50 – 600°C; convert to glass at 850-1000°C; convert to glass, mullite and cristobalite at 1000-1100°C; and lose Na₂O₃ and K₂O from the glass, mullite and cristobalite mix at temperatures >1100°C (Demir et al., 2001) Clearly a number of the changes involving kaolinite occur at temperatures above those attained in pulverised fuel combustion or would not proceed to completion. Boron associated with tourmaline has been found to be less volatile than organically-associated boron (Boyd, 2002) and uranium present in coal as coffinite (U(SiO₄)_{1-x}(OH)_{4x}) has been found to be less volatile than uraninite (UO₂) (Clarke and Sloss, 1992).

It is suggested that the control mode of occurrence exerts on trace element partitioning behaviour reflects differences in the temperature at which major mode classes decay. Therefore, some modes may release trace elements completely at an early stage of combustion, while other modes will only partially release the element at a relatively late stage, or pass through the combustion system without attaining complete thermal decay or melting and thus substantially retain associated trace elements. The above data suggests the following order of mode of occurrence-controlled volatility (Hypothesis 1):

Hypothesis 1. Organic > Pyrite/ Sulphide > Carbonates >> Silicates

Sequential leach results provide semi-quantitative differences in mode of occurrence between the two pulverised fuel samples (Table 4.1.). This section attempts to relate the semi-quantitative differences in the mode of occurrence to differences in the volatility indicated by the relative enrichment calculations in Chapter 5.

Significant differences in mode of occurrence are observed between the two pulverised fuel samples (Table 8.2.). The predicted volatility column states the relative difference in volatility exhibited by the fly-ash relative enrichment as predicted from Hypothesis 1. The actual volatility column (Table 8.2.) lists the observed differences in element relative enrichments found in Chapter 5. Note the more volatile the element, the lower the relative enrichment values shown in the graphical data in Chapter 5 (ie the more the element is depleted in the solid waste due to loss of some proportion to the atmosphere in gaseous form).

Table 8.2. Significant Differences in Mode of Occurrence Related to Volatility and Leachability.

Element	Collinsville Power Modes	Japanese Power Modes	Predicted Volatility	Actual Volatility	Leaching Availability
Antimony	15% more pyrite	7% more silicates	Collinsville more volatile	Collinsville marginally more volatile	BDL
Arsenic	30% more arsenite	24% more aluminosilicate	Collinsville more volatile	Collinsville more volatile	BDL
Chromium	18% more organic	11% more oxyhydroxide	Collinsville more volatile	Collinsville more volatile	Japanese ash 6.60% higher
Cobalt	10% more organic, 10% more pyrite	19% more carbonate/monosulphide	Collinsville more volatile	Collinsville more volatile	Collinsville ash 1.05% higher
Nickel	15% more exchangeable (organic), 40% more silicate	34% more carb/ NiO/ millerite, 23% (or 8%) more organic	Japanese more volatile	Japanese more volatile	Collinsville ash 1.36% higher
Selenium	40% more pyrite	40% more organic	Japanese more volatile	Collinsville more volatile	Japanese ash 126.32% higher
Uranium	22% more pyrite	12% more silicate	Collinsville more volatile	Collinsville more volatile	Collinsville ash 0.07-0.10% higher
Vanadium	1% more organic	1% silicate	Equal volatility	Equal volatility	Collinsville 0.3% higher
Zinc	7% more organic, 6% more pyrite	15% more silicate	Collinsville more volatile	Collinsville more volatile	Collinsville ash 15.75% higher

In detail, 15% more antimony is bound into pyrite in the Collinsville pulverised fuel sample, while 7% more antimony is associated with silicates in the Japanese pulverised fuel sample. It is predicted in Hypothesis 1 that elements associated with pyrite are more volatile, and elements associated with silicates are less volatile. Therefore, antimony in the Collinsville combustion plant should exhibit greater volatility. Figure 5.24. shows the relative enrichment figures for antimony in the Collinsville coal are marginally lower than the Japanese relative enrichment figures for the same element, cautiously confirming the predicted relative volatility.

The Collinsville pulverised fuel sample contains 30% more arsenic bound as arsenite (from oxidation of pyrite?), whereas the Japanese pulverised fuel sample contains 24% more arsenic associated with silicates. It is predicted from Hypothesis 1 that

elements associated with arsenite (from pyrite) are more volatile, and elements associated with silicates are less volatile. Therefore, arsenic in the Collinsville combustion plant should exhibit greater volatility. Figure 5.12. shows the relative enrichment figures for arsenic in the Collinsville coal are significantly less than the Japanese relative enrichment figures for the same element, confirming the predicted relative volatility.

For the element chromium, the Collinsville pulverised fuel sample contains 18% more chromium associated with the organic fraction of the coal, whereas the Japanese pulverised fuel sample contains 11% more oxyhydroxide bound chromium. The behaviour of oxyhydroxides is uncertain, however it was predicted on the basis of the higher proportion of organically associated chromium in the Collinsville fuel sample that chromium would be more volatile in the Collinsville combustion plant. Figure 5.16. shows the relative enrichment figures for chromium in the two pulverised fuel combustion plants is initially similar, however chromium in the Collinsville combustion plant is more depleted in the downstream solid waste. It is considered that, overall, chromium is more volatile in the Collinsville combustion plant, and confirms the predicted relative volatility.

The Collinsville pulverised fuel sample contains 10% more organically associated and 10% more pyrite associated cobalt, whereas the Japanese pulverised fuel sample contains 19% more cobalt associated with carbonates or monosulphides. Hypothesis 1 indicates the relative volatility of the carbonate bound cobalt (in the Japanese combustion plant) will be less than the pyrite and organically associated cobalt (in the Collinsville combustion plant). Figure 5.15. shows the relative enrichment of cobalt in the Collinsville combustion plant solid waste is substantially lower than in the Japanese combustion plant, indicating cobalt is more volatile in the Collinsville combustion plant. The observed relative enrichment confirms the predicted relative volatility of cobalt.

In the case of nickel, the Collinsville pulverised fuel sample contains 15% more exchangeable nickel and 40% more nickel associated with silicates. The Japanese pulverised fuel sample contains 34% more nickel associated either with carbonates, nickel oxides or millerite, and either 23% or 8% (if the exchangeable nickel in the

Collinsville coal is considered organically associated) more organically associated nickel. The relative volatilities of exchangeable nickel, organically associated nickel, and carbonate/ nickel oxide/ millerite nickel is unclear. However, the Collinsville pulverised fuel sample contained substantially more silicate-associated nickel, so it was predicted that nickel would be substantially less volatile in the Collinsville combustion plant. Figure 5.21. shows the relative enrichment figures for nickel in the two pulverised fuel combustion plants. Unfortunately only one relative enrichment figure could be calculated for nickel in the Japanese combustion wastes because nickel was present at concentrations below the INAA detection limit in the two downstream waste samples. Given the low relative enrichment in the Japanese bottom-ash, and the fact nickel is below the detection limit in the other two combustion waste samples (suggesting total loss as gaseous nickel), it is considered that nickel is substantially more volatile in the Japanese combustion plant than in the Collinsville combustion plant. Again, the relative enrichment observations confirm the relative volatility predictions.

The Collinsville pulverised fuel sample contains 40% more pyrite associated selenium, whereas the Japanese pulverised fuel sample contains 40% more organically associated selenium. It was predicted from Hypothesis 1 that elements associated with pyrite are less volatile than organically associated elements. Therefore, selenium in the Japanese combustion plant should exhibit greater volatility. In fact Figure 5.25. shows that the selenium in the Collinsville combustion plant is generally more volatile than selenium in the Japanese combustion plant. The selenium observations do not confirm the predictions made from Hypothesis 1. Sampling of the Blake and Bowen seams (Sections 3.2.1. & 3.2.2.) noted visible pyrite in a number of plies. If the large sized pyrite were liberated from the coal by grinding (a reasonable assumption given coarse sized pyrite is commonly rejected from the mill at the Collinsville combustion plant; Slater pers. comm.. 1999), then at least some of the pyrite would be present in the combustion chamber as excluded mineral grains. Thermal shock may have resulted in rapid disintegration of the pyrite grains leading to exposure of a greater surface area to oxidation and reduction. Further, the early release of volatile matter from the coal particles may have resulted in localised reducing conditions within the combustion chamber allowing thermal decay of pyrite to occur at low temperatures (282°C). Potentially these factors may

explain why pyrite-associated selenium exhibits a greater volatility than organic associated selenium.

Table 8.2. shows the Collinsville pulverised fuel sample contains 22% more pyrite associated uranium, whereas the Japanese pulverised fuel sample contains 12% more silicate associated uranium. It is predicted from Hypothesis 1 that elements associated with pyrite are more volatile than elements associated with silicates. Therefore, uranium in the Collinsville combustion plant should exhibit greater volatility. Figure 5.28. shows, although the Japanese bottom-ash is more depleted in uranium than the Collinsville bottom-ash, overall the Collinsville solid wastes are more depleted in uranium. Therefore, Figure 5.28. appears to confirm the relative volatility prediction for uranium.

In the case of zinc, Table 8.2. shows the Japanese pulverised fuel sample contains 15% zinc associated with silicates. It is predicted zinc in the Collinsville combustion plant will exhibit greater volatility than zinc in the Japanese combustion plant. Figure 5.31. shows that, although relative enrichment figures are similar in the bottom-ash, the Collinsville downstream solid wastes are more depleted in zinc than the equivalent waste streams in the Japanese combustion plant. It is concluded that Figure 5.31. confirms the relative volatility prediction for zinc.

The mode of occurrence for vanadium is virtually identical for Collinsville and Japanese pulverised fuel samples, being mainly associated with silicates (1% difference) with a subordinate organic mode (1% difference) (Table 8.2.). It is predicted from Hypothesis 1 that the close similarity in mode of occurrence will result in close similarities in the partitioning behaviour of vanadium in the combustion plants studied. Figure 5.29. shows the vanadium relative enrichment figures for the Collinsville and Japanese combustion plants. Vanadium volatility appears to be higher in bottom-ash in the Japanese plant. However the relative enrichment figures are essentially identical at the super-heater/ outlet point. Collinsville fly-ash from the fly-ash bunker is more depleted in vanadium than the Japanese bunker fly-ash. Vanadium was considered a Class I (non volatile) element in the Collinsville combustion plant, and a Class I or II element (marginally volatile?) in the Mitsui combustion plant (Figure 5.29). Given the close similarity in the behaviour of

vanadium, the observed data appears consistent with Hypothesis 1, the marginal differences in partitioning behaviour possibly attributable to differences in the ash yield of the coal as outlined above and in Section 5.2.

It is apparent that there is a high degree of consistency between the observed relative volatility of a trace element and the relative volatility predicted from the temperature at which the mode of occurrence of that element thermally decays in combustion. It has long been considered that mode of occurrence of a trace element influences the partitioning behaviour of that element in combustion. However, to the author's knowledge, this study is the first time that the partitioning behaviour for two pulverised fuel plants has been related to mode of occurrence differences in the feed coal.

8.2.2. The Control of Mode of Occurrence on Trace Element Leachability.

A large proportion of the fly-ash produced around the world is disposed of in landfill sites. Landfills are now designed to avoid or minimise the leaching of pollutants including trace elements. In addition, leaching tests such as the TCLP protocol (Section 2.3.7.) are employed to assess the potential for pollutants to be released from a particular material.

The distribution of metals between silicate and non-silicate mineral phases has been found to influence the release of metals from fly-ash (Kim and Kazonich, 2004; Querol et al., 1995). Trace elements with an organic affinity (Mo, U, V, W) will be present in the ash as oxides that are very mobile at neutral pH (such as water leaching). Elements present in zircons or clays, are not released from the mineral structure and their chemical mobility is very low. Boron originally present in coal as tourmaline was not leached from the ash to the same degree as organically associated boron (Boyd, 2002). It is, therefore, suggested that (Hypothesis 2):

Hypothesis 2. Trace elements associated with silicate minerals will remain essentially unmobilised by the TCLP leaching. Elements associated with minerals that are readily thermally decomposed or with the organic fraction of the coal are volatilised and lost to varying degrees, with any residual element concentration being potentially available for mobilisation to varying degrees.

The percentage difference in TCLP mobility between the two plants studied is calculated for a particular element by subtracting the percentage of that element mobilised from the Collinsville composite ash sample from the percentage of that element mobilised from the Japanese composite sample (data in Table 7.4.). The percent differences are shown as absolute figures in Table 8.2.

The elements selenium and zinc exhibit a significant difference in the proportion of trace element remaining in the solid waste that is mobilised by the TCLP procedure (Table 8.2). The greatest difference in element mobilisation is exhibited by selenium, where a substantially higher (126%) proportion was leached from the Japanese combustion waste compared to the Collinsville solid waste (see Table 8.2.). A review of previous studies showed a high proportion of selenium is extracted from solid combustion wastes (Jones, 1995; Querol et al., 2001b). Organically bound selenium in the Japanese combustion plant was retained preferentially compared to selenium associated with pyrite in the Collinsville coal (Section 8.2.). The TCLP data suggests that the selenium retained by the Japanese combustion plant solid wastes is present in a form that is more readily mobilised compared to the selenium retained by the Collinsville solid combustion wastes. The leaching data supports Hypothesis 2 that, if a high proportion of a given trace element is volatilised, the residual proportion of that trace element remaining in the fly-ash is present in a form that can be mobilised by leaching, with selenium released from organic matter readily mobilised.

Zinc also shows a significant difference in the relative leachability between solid wastes from the two pulverised plants studied (a difference of 15.75%; Table 8.2.). Zinc in the Japanese combustion plant exhibited a lower volatility compared to zinc in the Collinsville combustion plant because of the higher proportion of silicate-associated zinc in the Japanese fuel coal (Section 8.2.). Although the Japanese solid wastes have retained a greater proportion of the fuel zinc, more zinc is leached from the Collinsville combustion wastes. It is concluded that the zinc in the Japanese combustion wastes is not liberated from the associated silicates and is, therefore, unavailable for mobilisation. The leaching results for zinc again support Hypothesis 2.

Vanadium shows an insignificant difference in the relative leachability between solid wastes from the two pulverised plants studied (a difference of 0.3%; Table 8.2.). The partitioning behaviour of vanadium in the two combustion plants studied was very similar due to the virtually identical mode of occurrence in the two feed coals (Section 8.2.). Vanadium is poorly mobilised from the composite ash samples subjected to the TCLP protocol, a behaviour considered to be due to retention of this element in the silicate mineral structure during combustion. The small percent difference in vanadium leachability suggests that where an element has the same mode of occurrence in two feed coals, the partitioning behaviour and leachability will be essentially identical, supporting Hypothesis 2.

Other trace elements for which comparative leaching figures are available have small, probably insignificant, relative differences in relative mobility. The small relative differences notwithstanding, the relative leaching behaviour of chromium (6.60% difference; Table 8.2.) and uranium (0.07 – 0.10% difference; Table 8.2.) appear to confirm Hypothesis 2, however the leaching behaviour of cobalt (difference 1.05%; Table 8.2.) and nickel (difference 1.36%; Table 8.2.) do not. Given the 40% higher proportion of silicate-associated nickel in the Collinsville sample, the observed marginally higher mobility of nickel from the Collinsville sample is in contradiction of Hypothesis 2.

The marginal differences in elemental mobility noted for the elements chromium, uranium, cobalt and nickel, considering the observed differences in relative enrichment, requires further consideration. One possible explanation is that the TCLP method has failed to mobilise some trace elements in significant quantities due to the pH of the extraction fluid. The extraction fluid pH employed in this work is stated as being 4.9. Jones (1995) notes that cations such as cadmium, copper, lead, nickel, and zinc are most mobile at pH 4 – 7. However, the mobility of these elements may be limited at this pH range by adsorption on an aluminosilicate, metal oxide, or hydroxide surface (Héquet et al., 2001; Jones, 1995). Jones (1995) notes the difficulty in predicting the extraction of elements from fly-ash wastes due to formation of secondary minerals. Another possibility is that the differences in the modes of occurrence in the coal responsible for the proportion of cobalt and nickel

retained in the solid waste are insufficient to cause significant differences in leachability.

The leaching results for elements where the differences in leachability are above the level of significance support Hypothesis 2. To the author's knowledge, this study is the first time differences in the relative leachability of trace elements from two pulverised combustion plants have been related to differences in the mode of occurrence of trace elements in the feed coal.

8.3. Comparison of the Partitioning Behaviour of Trace Elements in Combustion and Carbonisation.

The partitioning behaviour of trace elements in combustion has been extensively discussed and classified (Clarke and Sloss, 1992; Clemens et al., 1999; Clemens et al., 2000; Galbreath et al., 2000; Klika et al., 2001; Meij, 1995; Purchase, 1987; Seames and Wendt, 2000; Senior et al., 2000; Senior et al., 2000). However, no information on the partitioning behaviour of trace elements in carbonisation was found.

Carbonisation is a “destructive heating of coal in the absence of air with production of a solid, porous, carbonaceous residue, called coke or char, and evolution of volatile products” (Tsai, 1982). Coal carbonisation can be classified as high temperature carbonisation (final temperature $>900^{\circ}\text{C}$) and low temperature carbonisation (not $>700^{\circ}\text{C}$). Carbonisation in a beehive oven (such as the Bowen coke works) is classified as high temperature carbonisation (Berkowitz, 1993). High temperature carbonisation generally occurs at a maximum temperature of $900 - 1050^{\circ}\text{C}$ (Van Krevelen, 1993), the heat for the alteration of the coal being generated from combustion of the evolved volatiles in the beehive oven. Therefore, carbonisation in a beehive oven progresses from the top down (Berkowitz, 1993). The alteration of coal to coke occurs in two stages: melting of the coal at $350 - 380^{\circ}\text{C}$ accompanied by some swelling; and re-solidification at $450 - 515^{\circ}\text{C}$ into a “porous mass that shrinks and sets into semi-coke” (Diessel, 1998).

Coals that “melt” or develop thermoplastic behaviour are controlled by and restricted to a relatively narrow rank range (ACIRL, 1996; Diessel, 1998; Hower and Lloyd, 1999), depending also on coal type factors (Reifenstein, 1997; Rentel, 1987; Yoshida

et al., 2000) and the characteristics of any other coals in blend (Sakurovs, 2000). Coal within the coking rank range is a “macromolecular network of carbon-rich aromatic and hydroaromatic ring clusters” “arranged in well-ordered pre-graphitic layer planes and cross-linked by ether, thioether, methylene chains, carboxyl, and other oxygen based bridges” (Diessel, 1998). Further, trapped within the macromolecular network or loosely attached to it are small labile molecules of low molecular weight. Thermoplasticity is initiated by thermal cleaving of the cross-links and side chains producing free radicals and low molecular weight, hydrogen donating fluids (Clemens and Matheson, 1992; Clemens and Matheson, 1995; Clemens et al., 1989; Hayashi et al., 2000; Sakurovs, 2000; Tsai, 1982). These fluids stabilise the free radicals by donating hydrogen and provide a medium to allow molecular mobility of the aromatic compounds. Re-solidification occurs by direct covalent cross-linking of the aromatic clusters to form semi-coke once the intervening hydrogen rich fluids and gas has been expelled.

Today most coke is produced in slot ovens, which are 15.5 – 16.5m long, 6 – 6.7m high with widths varying between 30 – 55cm (depending on the carbonisation properties of the feed coal) (Berkowitz, 1993). Coal is charged into the slot oven and heated from the walls of the oven inward. Carbonisation in a slot oven produces a higher quality coke compared to a beehive oven because of the ability to control charge density, employ higher temperatures, and because oxygen is more effectively excluded. Carbonisation in a beehive oven will result in some combustion of the uppermost layers of coal and coke.

The intention of high temperature carbonisation is to produce a porous carbon mass to (in the case of steel making) act as a reductant for the iron oxides, to provide a source of heat from oxidation of the carbon, and to provide a thermal medium to allow hot gas to flow upward and liquid metal to drain down to the tap hole (ACIRL, 1996; Diez et al., 2002).

The obvious differences between the carbonisation process and combustion are the lower temperatures involved and the substantial retention of the aromatic carbon fraction of the parent coal as coke. No data was found outlining the partitioning behaviour of trace elements in carbonisation. The partitioning behaviour of trace

elements in carbonisation of Bowen seam coal at the Bowen coke works has led to the definition of “classes” of partitioning behaviour (Chapter 6). A comparison between the partitioning behaviour of elements in combustion of Blake and Bowen seam coal at the Collinsville combustion plant (Chapter 5) and carbonisation of the Bowen seam at the Bowen coke works (Chapter 6) is discussed below. The mode of occurrence of the elements (as inferred by graphical methods) and the partitioning classification of the element in combustion and carbonisation is presented in Table 8.3..

The elements silicon, aluminium, titanium, manganese and phosphorous are considered as Class I elements in combustion and Class 2a in carbonisation (Table 8.3.). These elements are neither enriched nor depleted in either the bottom or fly-ash in combustion, or in the coke or breeze in carbonisation, and are non-volatile in both processes. The partitioning behaviour of this group of elements is the same in both combustion and carbonisation.

Table 8.3. Trace Element Mode of Occurrence and Partitioning Behaviour in Combustion and Carbonisation.

Element	Blake Seam	Bowen Seam	Partitioning Class in Combustion	Partitioning Class in Carbonisation
Silicon	silicates	silicates	I	2a
Aluminium	aluminosilicates	aluminosilicates	I	2a
Iron	siderite	pyrite/ minor siderite	I	2e
Magnesium	kaolinite	Siderite	I	3d
Sodium	feldspar	kaolinite	III	1e
Titanium	rutile	Rutile	I	2a
Manganese	siderite	Siderite	I	2a
Phosphorous	gorceixite/ goyazite	gorceixite/ goyazite	I	2a
Sulphur	mainly organic	Mainly pyrite	III	3d
Arsenic	pyrite	Pyrite	III	4e
Barium	gorceixite	gorceixite	I	2d
Cobalt	organic	Pyrite	III	2e
Chromium	Pyrite (?)	Pyrite (?)	III	1e
Caesium	illite	kaolinite	III	2d
Molybdenum	mainly inorganic	Pyrite	III	2e
Nickel	pyrite	Pyrite	I	2d?
Antimony	kaolinite	Pyrite	III	2e
Selenium	organic	Pyrite	III	3d
Thorium	heavy mins/phos/ felds	heavy minerals/ illite	III	2a
Uranium	phos/ zircon/ felds	zircon/ minor illite	III	2a
Tungsten	heavy minerals	heavy minerals	III	4d
Zinc	organic/ pyrite/ mixed	Pyrite	III	2e

Iron is classified as a Class I element in combustion, but a Class 2e element in carbonisation Table 8.3.. Class 2e elements are neither enriched nor depleted in the coke, but enriched in the breeze. Iron is a non-volatile element, and it was expected that the partitioning behaviour in carbonisation would indicate a Class 2a element. Pyrite is the major iron-bearing mineral in the Bowen seam coal. Under reducing conditions, iron will thermally decompose at 282°C (Badin, 1984). Potentially this reduced iron oxide has been further reduced by reacting with the coke, causing localised zones of weakness in the coke structure and preferential washing out of iron enriched coke from these locations when the coke is quenched.

The elements magnesium, barium, and nickel were found to behave as Class I elements in combustion (Table 8.3.). The partitioning behaviour of barium and nickel in carbonisation was classified as Class 2d (Table 8.3.). Class 2d elements are neither enriched nor depleted in the coke, but depleted in the breeze. It appears that barium and nickel are exhibiting a more volatile behaviour in carbonisation than in combustion, as indicated by their depletion in the breeze. Magnesium is classified as a 3d element in carbonisation, indicating depletion in both coke and breeze. It appears magnesium is substantially more volatile in carbonisation than in combustion. The higher volatility of magnesium in carbonisation could be due to the carbonate mode of occurrence of magnesium in the coke works feed coal (Bowen seam). Magnesium in the feed coal for the Collinsville power station (70% Blake seam and 30% Bowen seam) would contain a mix of kaolinite associated (Blake seam) and carbonate associated (Bowen seam) magnesium. Section 8.2.1. has shown that trace elements associated with silicates are less volatile in combustion than carbonate associated trace elements. However, the behaviour of magnesium is not matched by the behaviour of manganese, which is non-volatile in carbonisation.

No elements with a Class II partitioning behaviour in combustion are available for comparison with carbonisation partitioning behaviour.

The elements cobalt, molybdenum, antimony, and zinc were found to behave as Class III elements in combustion (Table 8.3.) and classified as Class 2e elements in carbonisation (ie neither enriched nor depleted in the coke, but enriched in the breeze). These four elements are associated with pyrite in the Bowen seam, and the

partitioning behaviour mirrors that of iron (see discussion below). It is suggested that these elements are retained in the coke, with the partitioning behaviour in the breeze being similar to combustion once the coke has been combusted.

The element caesium is Classified as Class III in combustion and Class 2d in carbonisation. As noted for cobalt, antimony, molybdenum, and zinc, caesium appears to be substantially retained in coke, but is depleted in breeze, again suggesting the behaviour of the element is similar in combustion and carbonisation once the effect of retention in the coke is removed.

The elements sulphur and selenium are classified as Class III in combustion and Class 3d in carbonisation. The behaviour of these two elements appears similar in combustion and carbonisation.

The element tungsten is classified as a Class III element in combustion and as Class 4d in carbonisation. The behaviour of tungsten is similar in the two processes. Arsenic is classified as Class III in combustion and Class 4e in carbonisation. It appears that the behaviour of arsenic is similar in the two processes except the element is apparently enriched in the breeze (see below).

The elements thorium and uranium were classified as Class III elements in combustion (Table 8.3.). The behaviour of these elements in carbonisation classifies them as Class 2a, indicating substantially lower volatility in carbonisation (Table 8.3.). Thorium in the literature is generally considered as a non-volatile (Class I) element in combustion, so the classification of thorium as a Class III element in the Japanese and Collinsville combustion plants is somewhat surprising. Literature examples generally classify uranium as a semi-volatile element in combustion, possibly in part due to the commonly noted affinity of this element with the organic fraction of the coal. The classification of uranium as a Class III element in the Japanese and Collinsville combustion plants is also somewhat surprising.

Given both thorium and uranium in the Blake and Bowen seams appear to be dominantly associated with heavy minerals (monazite), the low elemental volatility in carbonisation is not surprising. However, the latter inference brings into question the

volatile behaviour noted in combustion. Either both uranium and thorium are released from monazite and promptly volatilised at the higher temperatures experienced in combustion, or else the combustion data is in error. If the Collinsville combustion results are in error, and noting the classification of these elements in the literature, it would perhaps be surprising that the Japanese combustion results are so similar. Therefore, it is suggested that monazite is rapidly destroyed at the high temperatures of the combustion plant (1300°C) and uranium and thorium are volatilised and lost up the stack. Possibly the threshold temperature at which monazite decomposes is not attained in carbonisation therefore thorium and uranium remain locked within the crystal lattice of the mineral.

The elements sodium and chromium are classified as Class III in combustion, but Class 1e (enriched in both coke and breeze) in carbonisation. As discussed in Chapter 6, some sort of contamination in the plant or post sampling is suspected for the coke works samples. Further analysis to understand the behaviour of these two elements in carbonisation is warranted.

Some parallels emerge from analysis of the partitioning behaviour of trace elements in carbonisation. All the elements enriched in the breeze regardless of the Coke Class (ie iron, arsenic, molybdenum, antimony and zinc) are associated with pyrite in the Bowen seam coal. It is suggested that these elements have mobilised from the coke during carbonisation (possibly due thermal decay of pyrite at low temperatures under reducing conditions, with further reduction of iron by carbon resulting in localised weakening of the coke structure), and become enriched on the outside surface or in locally weakened areas of the coke. When the coke is quenched, these elements wash out and are enriched in the breeze.

The behaviour of sulphur and selenium (also associated with pyrite in Bowen seam coal) are exceptions to the enrichment of pyrite bound elements in the breeze. Sulphur and selenium are known to behave in a chemically similar fashion, and both exhibit depletion in the coke (both Coke Class 3 elements). It is inferred that these two elements have been volatilised to such a degree that they have not been captured by the coke and have been substantially lost from the system during carbonisation.

Given the inferences regarding selenium and sulphur it is surprising that arsenic (a Coke Class 4 element) is not also depleted in the breeze. Table 8.4. presents figures of absolute difference between the two breeze CRE results for elements where two analytical results were available as a measure of CRE consistency. Indicatively, if the difference between the two CRE results is greater than the average CRE, then the consistency must be considered poor. Two elements show an absolute difference higher than the CRE average. In the case of tungsten, the difference amounts to double the CRE average, however both CRE figures still indicate depletion of the element in the breeze. In the case of arsenic the difference amounts to almost three times the CRE average, and varies from depletion (CRE 0.73) to considerable enrichment (CRE 7.33). Given the substantial difference in CRE figures and the fact the CRE figures vary from enriched to depleted, it is considered that the breeze CRE figure for arsenic is suspect. It is concluded that moderately volatile elements with a pyrite mode of occurrence in the coal (cobalt, antimony, molybdenum and zinc) are enriched in the breeze, whereas highly volatile elements associated with pyrite (selenium, sulphur, and, probably, arsenic) are volatilised from both coke and breeze.

In addition, it is notable that elements bound with silicates (silicon, aluminium, caesium and sodium) are non-volatile in carbonisation, although caesium is depleted in the breeze (as would be expected from a combustion Class III element). Elements associated with heavy minerals or illite also generally behaved in a non-volatile manner, the exception being tungsten that is highly volatile in both combustion and carbonisation.

It has long been known that phosphorous is substantially retained in the coke in carbonisation and will eventually report to the product steel (Ward et al., 1996) making it brittle (Dennis, 1963; Moore and Moore, 1999). This study shows that all but the most volatile trace elements examined are substantially retained in the coke due to capture or retention in the carbon structure and/ or because the lower temperatures involved in carbonisation do not liberate the element from the crystal structure of the host mineral. Loss of carbon by partial combustion in the beehive ovens or due to localised weakening of the coke mass by oxidation/ reduction reactions involving iron liberates the trace elements from the coke. All but the non-volatile elements then either volatilise or become concentrated in the breeze. In

particular, trace elements associated with pyrite in the coal are generally enriched in the breeze except for highly volatile elements that were lost from the coke during carbonisation. Silicate associated elements and elements associated with heavy minerals are generally retained in the breeze, again unless volatilised during carbonisation. The behaviour of trace elements liberated from the coke appears similar to the behaviour of the same element in combustion. It is suggested that, as for combustion, the partitioning behaviour of trace elements in carbonisation is related to both the volatility of the element and the mode of occurrence of the element in the feed coal.

Table 8.4. Absolute Difference Between Breeze CRE Figures.

Element	Breeze CRE	Absolute Difference
Silicon	0.96	0.06
Aluminium	0.92	0.04
Iron	1.60	0.47/ 0.17
Magnesium	0.44	N/A
Sodium	2.33	0.24
Titanium	0.86	0.06
Manganese	0.94	N/A
Phosphorous	0.99	0.1
Sulphur	0.22	0.08
Arsenic	2.32	6.59
Barium	0.73	0.43
Cobalt	1.28	0.59
Chromium	1.5	0.79
Caesium	0.68	0.2
Molybdenum	1.28	N/A
Nickel	N/A	N/A
Antimony	2.46	0.81
Selenium	0.32	0.12
Thorium	0.88	0.4
Uranium	0.94	0.35
Tungsten	0.20	0.41
Zinc	1.57	0.94

8.4. Chapter Summary.

A comparison of the mode of occurrence indicated for trace elements using graphical and sequential leaching methods found generally good agreement between the data sets. However, by using two methods to determine mode of occurrence, better definition of some modes inferred from sequential leaching, and support or improved confidence in some graphical inferences was possible. It is considered that the

application of two different methods provides a more robust determination of trace element mode of occurrence in the coals examined. Use of a direct analysis method such as SEM-EDX would provide further confidence in the determined mode of occurrence.

Assessment of the partitioning behaviour of trace elements in combustion found a strong relationship between semi-quantitative differences in mode of occurrence as determined by the USGS sequential leaching method and relative differences in element volatility. The general order of volatility appears to be organic and pyrite associated elements are more volatile than carbonate associated elements, which are more volatile than silicate/ aluminosilicate associated elements, reflecting differences in the temperature at which these major trace element modes break down in combustion. However the behaviour of selenium suggests that, under certain circumstances, pyrite associated trace elements may be more volatile than organically bound elements. Although these results should be considered provisional, the data consistently supports Hypothesis 1 across a range of trace elements. Therefore, it appears relative differences in trace element mode of occurrence as determined by the USGS sequential leaching method could provide a means of rating the relative volatilities of trace elements between two coals.

It is concluded that elemental mode of occurrence exerts some control on the proportion of an element that may be leached from ash. Elements retained in the ash are the unvolatilised residue remaining after coal combustion, and may be susceptible to leaching. However, trace elements associated with silicates are particularly immobile in fly-ash, probably because the element was never released from the silicate crystal matrix. The relative impact of the other modes of occurrence on trace element leachability is not clear from the present data set, and could be complicated by other factors such as formation of secondary minerals and controls exerted by hydro-geochemistry.

The behaviour of trace elements in combustion and carbonisation has been compared. In general it appears that all but the most volatile elements are retained in the coke. The behaviour of trace elements in the breeze is related to mode of occurrence in the

coal and elemental volatility. The partitioning behaviour of trace elements associated with pyrite show a particular consistency of partitioning behaviour in carbonisation.

Chapter 9

Conclusions and Further Work.

9.0. Pit Sample Data.

Figure 9.1. presents a flow diagram summarising the pit sample data.

9.0.1. Depositional Environment of the Blake and Bowen Seams.

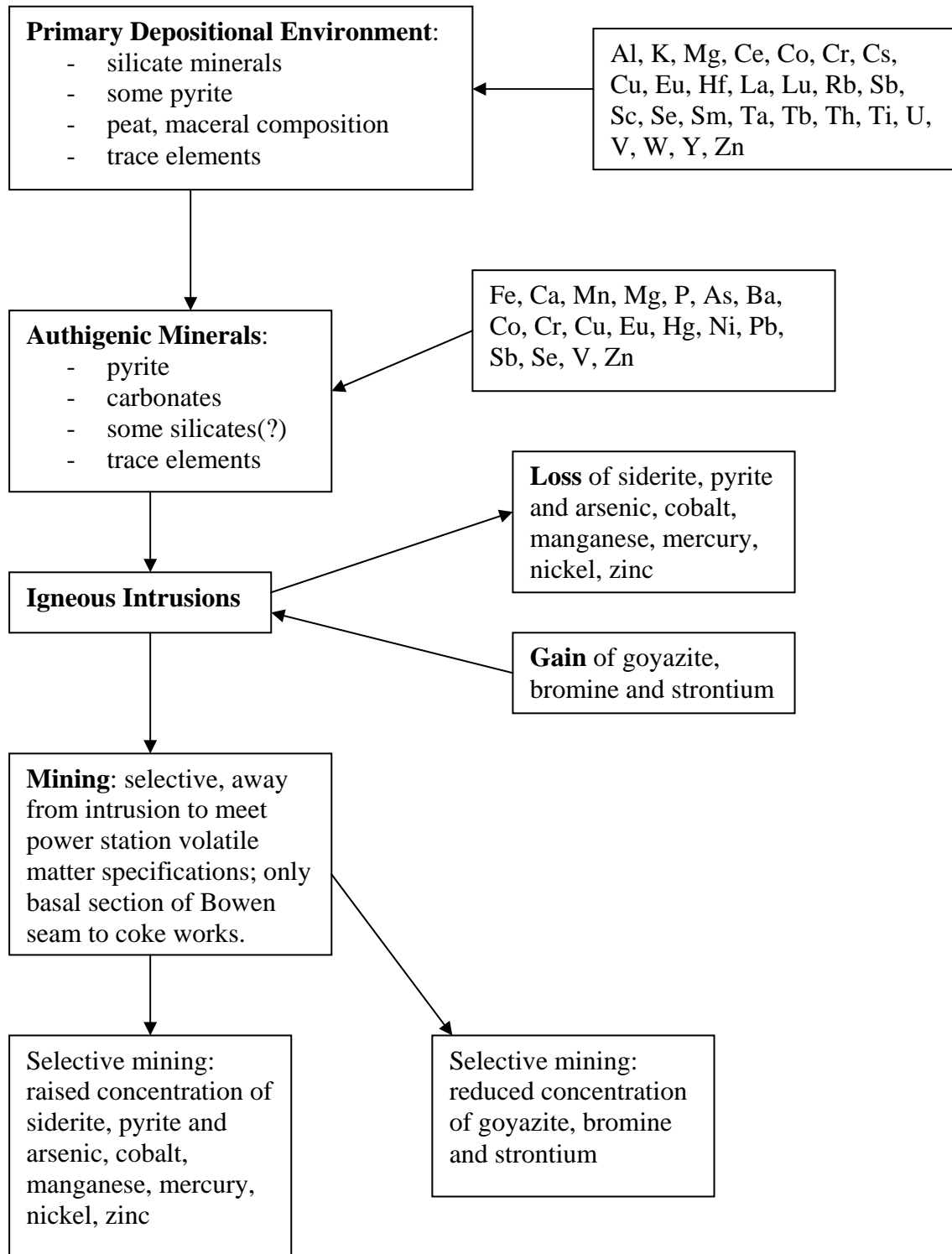
Both the Blake and the Bowen seam profiles examined contained a large proportion of dull coal lithotypes, and are high in inertinite, suggesting the peat was prone to periods of oxidation either due to drying or to influxes of oxygenated flood water. Deposition of the Blake seam was interrupted by numerous sediment incursions, as evidenced by the common stone bands in the coal. The stone partings, along with the generally high ash content of the coal, the low sulphur concentration and scarcity of pyrite are consistent with peat accumulation in a fluvial depositional environment, as previously proposed by other workers based on sedimentological evidence. In contrast, the moderate ash, absence of common stone bands, sulphur concentration of ~2% and the moderate pyrite content of the Bowen seam coal support previous sedimentological evidence that indicated peat accumulation in a raised mire in a fluvial paralic depositional environment (Woolfe et al., 1996).

9.0.2. Concentration and Mode of Occurrence of Trace Elements in the Blake and Bowen Seams.

The Blake seam channel samples contained higher than average concentrations of gold, hafnium, and thorium. The Bowen No.2 seam channel samples contained higher than average concentrations of gold and possibly copper. Compared to the earths crust, both the Blake and Bowen seam coal is enriched in the environmentally significant trace elements mercury and selenium, and (in one or more seams) molybdenum, antimony, lead, and uranium. The pulverised fuel sample from the Collinsville power utility contained higher than average concentrations of the elements gold, cerium, cobalt, europium, hafnium, lanthanum, lutetium, molybdenum, neodymium, scandium, selenium, samarium, strontium, tantalum, thorium, tungsten, and ytterbium.

A number of differences were found between the graphical and sequential leach indications of mode of occurrence, particularly for the elements arsenic, barium, chromium, mercury, nickel, lead, vanadium, and zinc. It is concluded that reliance on a single method of determining mode of occurrence would be unwise. In particular, determination of mode of occurrence using graphical methods requires considerable caution to avoid errors caused by multiple-mode trace elements and elements that are related physically but not chemically in the coal.

Figure 9.1. Collinsville Coalmine Pit Sample Summary.



The mode of occurrence of trace elements in the Collinsville combustion utility feed coal from combined interpretation of graphical relationships and sequential leaching data are as follows:

For the Blake Seam:

- Phosphorous, barium and strontium are associated with gorceixite and goyazite.
- Arsenic, copper, mercury, and nickel are associated with pyrite, although some mercury may also be organically associated.
- Chromium exhibits a physical relationship with pyrite, but is considered to be associated with silicates, plus chromites and/ or associated with the organic fraction of the coal.
- Bromine, cobalt, and selenium are associated with the organic fraction of the coal.
- Magnesium, antimony, and tantalum are associated with kaolinite.
- Caesium and rubidium are associated with illite.
- Lead is present as galena.
- Zinc is present as sphalerite.
- Most of the Rare Earth Elements and thorium are generally associated with monazite and/ or xenotime, with some minor affinity for illite or kaolinite.
- Hafnium and uranium are associated with zircon.
- Manganese is associated with siderite.
- Titanium is present as rutile or associated with aluminosilicates.
- Tungsten is present as tungstates.
- The mode of occurrence of vanadium is uncertain.

For the Bowen Seam:

- Phosphorous, barium, and strontium are associated with gorceixite and goyazite.
- Arsenic, cobalt, copper, mercury, molybdenum, nickel, antimony, and selenium are associated with pyrite, although some mercury may also be organically associated.
- Chromium exhibits a physical relationship with pyrite, but is considered to be associated with silicates, plus chromites and/ or associated with the organic fraction of the coal.

- Sodium, caesium, lutetium, scandium, and ytterbium are associated with kaolinite.
- Bromine, lanthanum, and terbium are associated with illite.
- Lead is present in galena.
- Zinc is present in sphalerite.
- Most of the Rare Earth Elements and thorium are generally associated with monazite and/ or xenotime, with some minor affinity for illite or kaolinite.
- Hafnium and uranium are associated with zircon.
- Magnesium and manganese are associated with siderite.
- Titanium is present as rutile or associated with aluminosilicates.
- Tungsten is present as tungstates.
- The mode of occurrence of rubidium and vanadium is uncertain.

9.0.3. The Effect of Igneous Intrusions on the Coal and on the Concentration of Trace Elements.

Igneous intrusions are located beneath the floor of the Bowen No.2 seam, above the roof of the Blake Central seam, and within the Blake West seam. In the Blake West seam, thermal alteration has coked the coal in a zone approximately 60cm thick adjacent to the intrusion, with a further surrounding zone of dull heat affected coal approximately 100cm thickness logged before “normal” variations in lithotype could be recognised. Vitrinite reflectance increased toward the intrusions from a background of $\sim R_o(\max)$ 1.20% for the Blake seam, and from a background of $\sim R_o(\max)$ 1.10% in the Bowen seam. Heat-affected samples were distinguished from relatively unaffected samples by the presence of semi-coke caused by the thermal alteration of vitrinite, or using an inferred alteration distance where petrographic samples were unavailable.

Depletion or enrichment of minerals and elements was inferred using ply-thickness weighted average concentration figures for altered and unaltered samples, and trends of concentration change toward the intrusion. The minerals siderite and pyrite are depleted in the heat-affected zone, probably due to the low temperature at which these minerals decompose. The mineral goyazite is enriched within the heat-affected zone, particularly toward the margin of the zone. The concentration of cobalt, mercury,

manganese (the index element for siderite), nickel, and possibly arsenic and zinc are consistently depleted in heat-affected samples from both the Blake seam and Bowen seam pits. These elements are associated with pyrite or siderite, and appear to have been liberated and expelled concurrent with the thermal decay of the host minerals. The behaviour of cobalt in the naturally coked coal is different to the partitioning behaviour of the element in carbonisation, coke from the Bowen coke works showing no depletion of cobalt. Bromine and strontium are enriched in heat-affected samples from both the Blake and Bowen seams. It is concluded the source of both bromine and strontium is the igneous intrusion. It is assumed that bromine is adsorbed to the heat-affected coal, and strontium is concentrated in areas sufficiently removed from the intrusion to allow the mineral goyazite to precipitate. Differing modes of occurrence between pits has resulted in inconsistent behaviour for the elements chromium, molybdenum, and possibly selenium, which are enriched in heat-affected zones in the Blake seam, but depleted in the heat-affected zone in the Bowen seam.

9.1. Combustion Sample Data

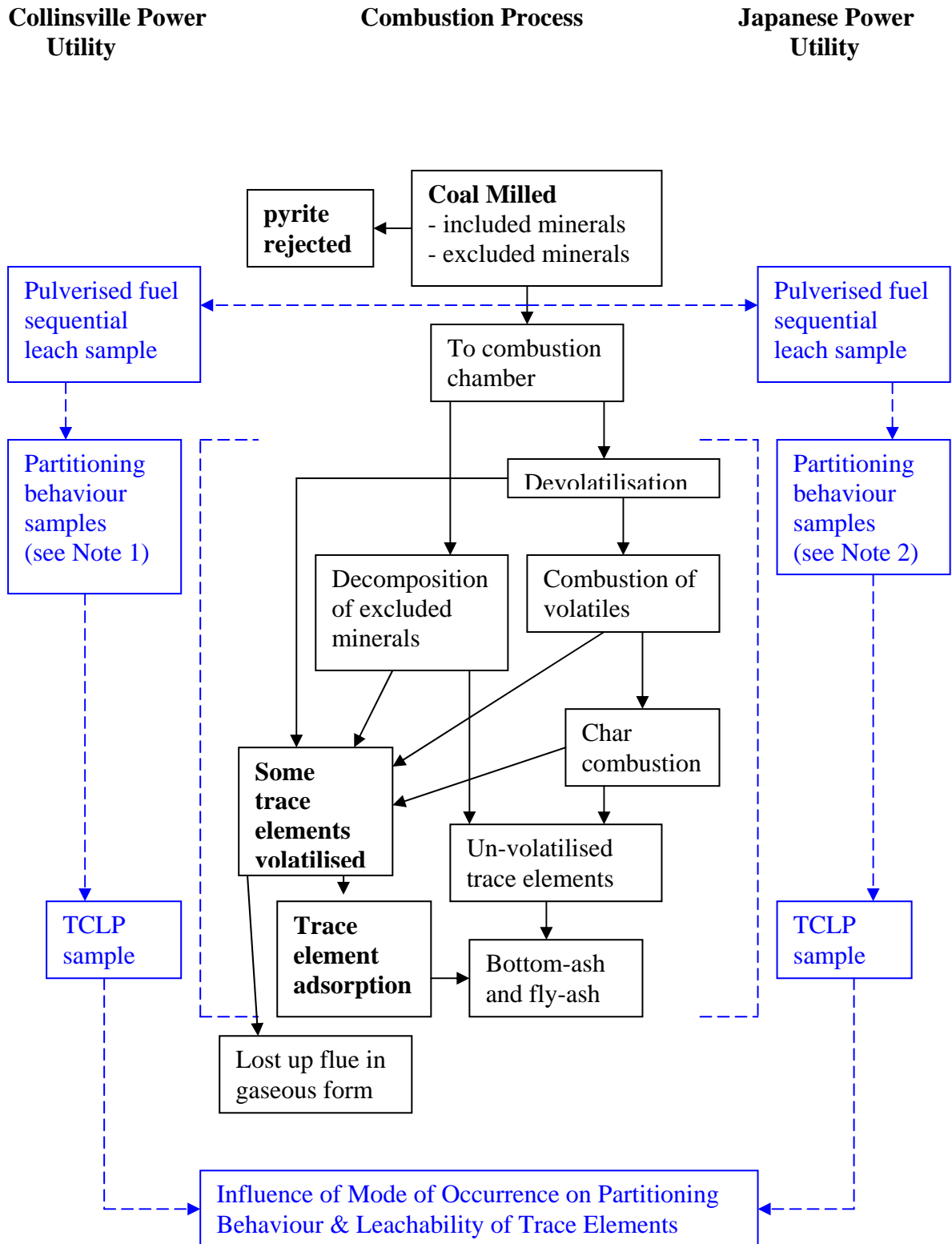
Figure 9.2. presents a flow diagram summarising the coal combustion data.

9.1.1. The Control of Mode of Occurrence on Trace Element Partitioning Behaviour in Combustion.

Mode of occurrence for pulverised fuel from the Collinsville and Japanese coal fired electricity utilities was inferred using sequential leach data. The elements antimony, arsenic, chromium, cobalt, nickel, selenium, uranium, and zinc were found to have significant differences in mode of occurrence between fuel samples from the two combustion plants studied. The element vanadium had almost identical modes of occurrence in fuel from both plants studied. Samples of fly-ash and bottom-ash were gathered from the Collinsville and Japanese combustion plants. The partitioning behaviour of trace elements in combustion was determined by calculating relative enrichment values for each element. A hypothesis that, for a given trace element, the organically-bound fraction is more volatile than the pyrite-bound fraction, which is more volatile than the carbonate-bound fraction, which is substantially more volatile than the silicate bound fraction, reflecting the temperature at which the host minerals thermally decompose, was tested. It was found that the hypothesis was supported by the data and that mode of occurrence exerts a clear control on the relative volatility of

a given element. It is concluded that relative differences in mode of occurrence inferred using the USGS sequential-leaching protocol could allow prediction of the relative volatilities of a trace element in different coals.

Figure 9.2. Coal Utilisation Summary Diagram - Combustion.



Note 1. In the Collinsville combustion plant, silicon, iron, magnesium, titanium, manganese, phosphorous, barium, copper, nickel, rubidium, and vanadium are neither enriched nor depleted in the bottom and fly-ash; tin exhibits depletion in the fly-ash; and sodium, sulphur, arsenic, boron, cobalt, chromium, caesium, molybdenum, lead, antimony, selenium, thorium, uranium, tungsten, zinc and the rare earth elements exhibit depletion in both bottom and fly-ash (ie the elements are substantially lost up the flue in gaseous form).

Note 2. In the Mitsui combustion plant silicon, iron, magnesium, titanium, manganese, phosphorous, rubidium, and vanadium are neither enriched nor depleted in the bottom and fly-ash; sodium, gold, arsenic, boron, barium, cobalt, chromium, copper, caesium, mercury, molybdenum, lead, antimony, thorium, uranium, vanadium, zinc, and the rare earth elements exhibit some enrichment in the fly-ash; and the elements sulphur, arsenic, boron, barium, caesium, molybdenum, nickel, antimony, selenium, thorium, uranium, tungsten, zinc, and the rare earth elements exhibit depletion in both bottom and fly-ash (ie the elements are substantially lost up the flue in gaseous form).

9.1.2. The Control of Mode of Occurrence on Trace Element Mobility from Combustion Waste Material.

The concentration of barium, manganese, and selenium in the Collinsville leachate exceeds both the recreational and drinkwater guideline concentrations. The concentration of nickel in the Collinsville leachate was found to exceed the recommended drinkwater concentration, but is below recreational water guideline value. The concentration of boron and selenium in the Mitsui leachate was found to exceed both the recreational and drinkwater guideline values. The concentration of barium in the Mitsui leachate was found to exceed the drinkwater standard. The concentration of a given trace element in ash was found to be a poor indicator of the proportion of the element leached from the composite ash samples.

A second hypothesis that trace elements associated with silicates in coal are substantially unavailable to leaching agents, whereas the residue left from volatilisation of an element associated with other modes in the coal is variably available for leaching was tested. The hypothesis was proven for elements where

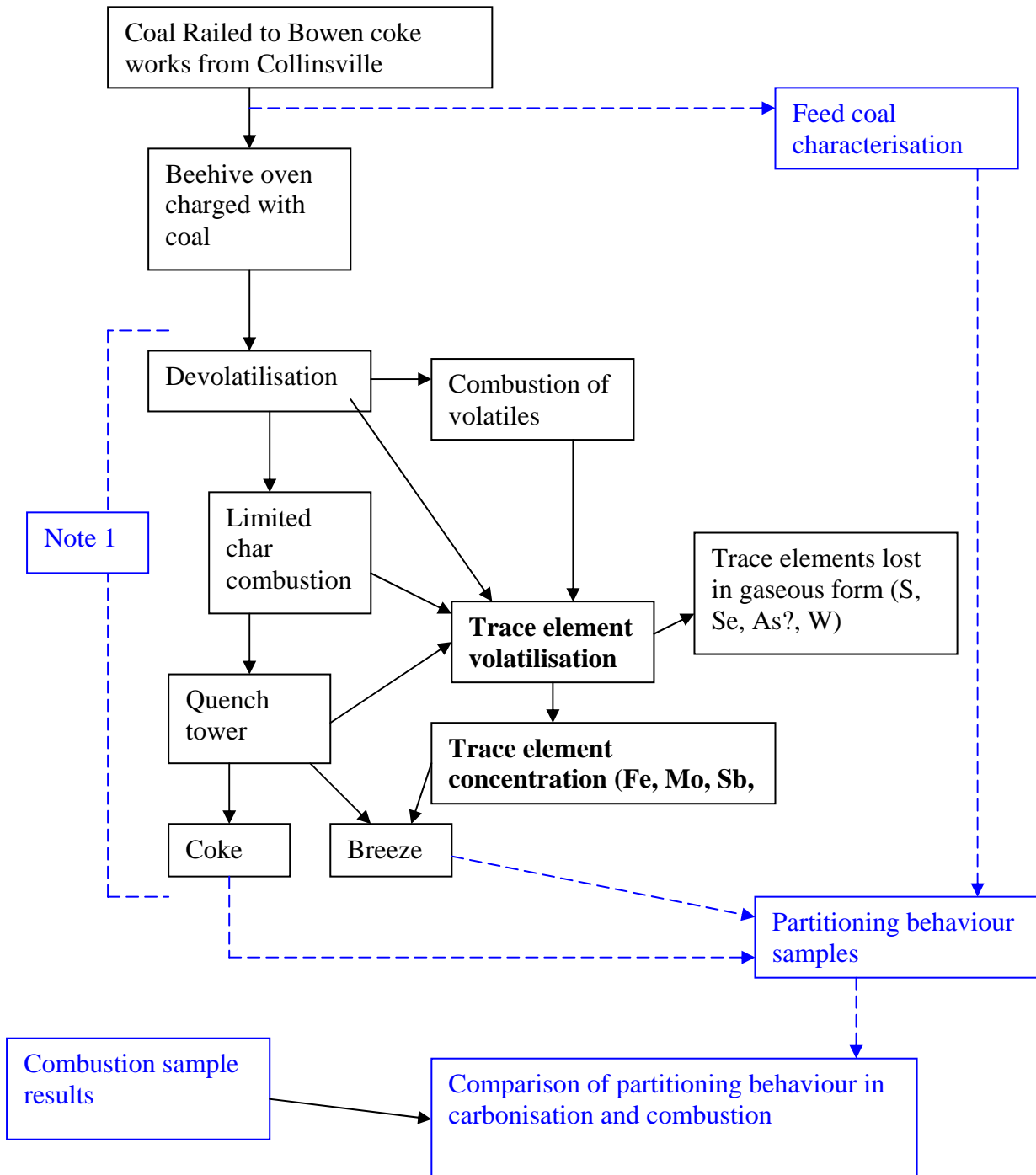
differences in mode of occurrence in the coal and absolute leachability were significant. It is concluded that the mode of occurrence of trace elements inferred from USGS sequential-leach data may have the potential to indicate the relative leachability of contained trace elements, although a number of other complex controls on element mobility exist and further directed work on the problem is required.

9.3. The Control of Mode of Occurrence on Trace Element Partitioning Behaviour in Carbonisation.

Figure 9.3 presents a summary flow diagram of the coal carbonisation data. A new index (the CRE index) was developed to categorise the partitioning behaviour of trace elements in the coke and breeze. Coke is classified as enriched (Class 1), neither enriched nor depleted (Class 2), depleted (Class 3), or highly depleted (Class 4). Breeze was classified as enriched (denoted “e”), neither enriched nor depleted (denoted “a”), and depleted (denoted “d”). It was found that all but the most volatile elements (sulphur, selenium, tungsten, and arsenic) are substantially retained in the coke. The quench tower washings (coke breeze plus ash from partial combustion in the beehive oven) were found to be enriched in pyrite-bound elements (iron, molybdenum, antimony, zinc) excepting the highly-volatile elements sulphur, selenium, and probably arsenic. Trace elements associated with silicates are neither enriched nor depleted in the breeze, excepting tungsten, which is highly volatile. The elements thorium and uranium are less volatile in the breeze compared to their behaviour in combustion, however the partitioning behaviour of these two elements in combustion is at odds with generally noted trends. It is concluded that the behaviour of trace elements in breeze from a beehive oven is generally similar to the behaviour of the element in combustion reflecting both the mode of occurrence of the element in the coal and the volatility of the element.

Figure 9.3. Coal Utilisation Summary Diagram – Combustion & Carbonisation.

Bowen Coke Works Carbonisation Process



Note 1. Silicon, aluminium, titanium, manganese, and phosphorous are neither enriched nor depleted in coke and breeze.

9.4. Further Work.

The following recommendations for possible future trace element investigations are made to assist the present Collinsville mine operator and Collinsville combustion utility operator.

One of the major reasons for analysing coal samples for trace elements is to infer the potential environment impact of using that coal from the concentration of environmentally significant trace elements. Analysis of the Blake Central and Blake West channel samples suggests a full seam product could contain higher than average concentrations of the environmentally sensitive element thorium. The Bowen No.2 pit channel sample analyses suggest a full seam product may contain a higher than average concentration of the environmentally significant element copper. The concentration figures for copper should be considered provisional because only a few samples had sufficient material to allow analysis for this element. Further, in comparison to crustal concentrations, both the Blake seam and Bowen seam coals are enriched in mercury and selenium. Analysis of Collinsville combustion plant feed coal suggests selenium and thorium are present at above average concentrations in the coal, although care should be taken in using one sample as an indicator of the overall trace element concentration of a feed coal over time. The TCLP data suggests the elements barium, manganese, and nickel may be mobilised at concentrations above recommended guidelines. Therefore, given the analysis results of the raw feed coals, the combustion plant fuel, and the leachate analysis data it is considered that at least barium, selenium, mercury, thorium, copper, manganese, and nickel warrant further investigation for the Collinsville coals. The following studies are recommended:

1. Undertake a further programme of channel sampling, possibly in larger plies, but from several locations along the current highwall to determine the concentration of the elements of interest and any vertical and lateral variations in concentration.
2. If the coal is being washed, examine the impact of coal washing on trace element concentration. It is notable that a large number of environmentally significant trace elements in the Bowen seam in particular are associated with pyrite, so coal washing may substantially reduce the concentration of some

elements in the final product. The concentration of trace elements in, and disposal of the washplant rejects should also be examined.

3. Monitoring of the Collinsville combustion utility feed coal over a period of several months should be undertaken to determine the long-term concentration of environmentally significant elements being delivered to the plant, and their partitioning behaviour in combustion. The concentration and mobility of trace elements from the solid wastes should also be examined as part of this work.
4. Further monitoring of trace element partitioning behaviour in the Bowen coke works should be contemplated given the time elapsed since samples were gathered for this study. Further, the environmentally significant trace elements cobalt, molybdenum, antimony, strontium, zinc, and possibly arsenic and chromium are enriched in the breeze samples analysed in this study. The breeze (at the time of sampling) was disposed of at a local landfill. It is recommended some breeze leaching tests be undertaken to assess the potential for environmentally deleterious trace elements to leach into the environment following disposal.

Analysis of a pulverised fuel sample from the Mitsui combustion utility found the coal was high in gold, hafnium, and thorium. The TCLP data suggests the elements boron, selenium, and barium may be mobilised at concentrations above recommended guidelines. The Mitsui combustion utility is fuelled with a blend of coals. It is recommended that each of the components of this blend be analysed for the environmentally significant elements thorium, boron, selenium, and barium to determine which coal has higher than average concentrations of these elements in the coal. Further, combustion testing with leaching of the resultant ash to determine which coal provides the more mobile trace elements should be considered, given that elemental concentration in the feed coal is a poor indicator of trace element mobility.

Apart from the above recommendations, which are specific to the Collinsville coals and Japanese combustion utility, the following recommendations for further work are made:

1. It appears that relative differences in mode of occurrence determined from USGS sequential leach method has the potential to infer relative differences in

trace element volatility. The conclusion is considered provisional because it relies on the analysis one set of samples from each of two power utilities. It is recommended that pilot scale combustion of several different coals with demonstrably different modes of occurrence for environmentally significant trace elements be undertaken under strictly controlled conditions to assess differences in the partitioning behaviour of the elements. Following on from this work, it is recommended that several power utilities being supplied with coals from unrelated coal basins be sampled over a period of at least one week and subjected to the same analysis undertaken in this work. If the results of a larger dataset validate the inferences presented here, strong support can be given to the use of the USGS sequential leach results for predicting the relative propensity of a coal to emit trace elements from the stack.

2. The relative volatility of trace elements bound to the organic fraction of the coal deserves further directed research. Given fuel particles combust in three stages (devolatilisation, combustion of volatile matter and char combustion), it is possible that the behaviour of organically-bound elements is different depending on whether the element is associated with aliphatic groups (\approx volatile matter) or aromatic groups (\approx char).
3. Attempts to link mode of occurrence with the propensity for trace elements to be leached suggests elements associated with silicates are relatively immobile compared to those associated with other modes of occurrence in coal. Further work to examine the link between mode of occurrence and the leachability of the element from pulverised fuel wastes is required.
4. Assessment of the behaviour of trace element during carbonisation in a slot oven should be examined.

In addition, the following analytical recommendations are made for future work:

1. All major elements should be determined using XRF analysis of fused discs. A number of key major elements (calcium, sodium, and potassium) were determined by INAA in this study. The difficulties in the high limit of detection of INAA for these elements was not discovered until too late. Further, the repeatability of INAA analysis of potassium appears to be poor.

2. Forms of sulphur analysis would have removed the need to determine pyrite by normative analysis. This test is expensive, particularly if undertaken on a ply-by-ply basis, and insufficient budget was available to undertake this work. However, future studies should budget on undertaking this test, particularly if graphical relationships are to be used to infer trace element mode of occurrence.
3. Ultimate analysis may have been useful in searching for determine graphical relationships between trace elements and the organic fraction of the coal, and for determining the influence on unburnt char on trace element retention in the fly-ash. Again, this test is expensive, but if possible future studies should budget for this work.
4. Some direct determination of trace element mode of occurrence using SEM-EDX or a similar technique would have aided graphical interpretations considerably.
5. Quantitative determination of mineralogical proportions from XRD using Rietveld-based procedures for all samples should be considered for future studies. Use of such a technique would greatly aid or could be used in place of the calculation of the concentration of mineral matter using normative analysis.

Reference List.

- ACIRL** (1996) *Coal Quality Course*.
- Agrawal, M., Singh, J., Jha, A. K., and Singh, J. S.** (1993) *Coal-Based Environmental Problems in a Low-Rainfall Tropical Region*. p27-57. in **Keefer, R. F. and Sajwan, K. S. eds** *Trace Elements in Coal and Coal Combustion Residues*. Lewis Publishers.
- Alastuey, A., Jiménez, A., Plana, F., Querol, X., and Suárez-Ruiz, I.** (2001) *Geochemistry, Mineralogy, and Technical Properties of the Main Stephanian (Carboniferous) Coal Seams from the Puertollano Basin, Spain*. *International Journal of Coal Geology* v45 p247-265.
- Anthony, E. J. and Jia, L.** (2000) *Agglomeration and Strength Development of Deposits in CFBC Boilers Firing High-Sulphur Fuels*. *Fuel* v79 p1933-1942.
- Armesto, L. and Merino, J. L.** (1999) *Characterization of Some Coal Combustion Solid Residues*. *Fuel* v78 p613-618.
- Asuen, G. O.** (1987) *Assessment of Major and Minor Elements in the Northumberland Coalfield, England*. *International Journal of Coal Geology*. v9 p171-186.
- Australia & New Zealand Environmental and Conservation Council. Agriculture & Resource Management Council of Australia & New Zealand.** (2000) *Australian & New Zealand Guidelines for Fresh and Marine Water Quality 2000*.
- Australian Standard 2916-1986** (1986) *Symbols for Graphical Representation of Coal Seams and Associated Strata*. Published by Standards Association of Australia.
- Ayala, J. M., Buergo, M. A., and Xiberta, J.** (1994) *The Use of Energy Dispersive X-Ray Fluorescence (EDXRF) as an Approximate Method of Analysing Ash and Sulphur Content in the Coals of the Asturias, Spain*. *Nuclear Geophysics* v8 p99-102.
- Badin, E. J.** (1984) *Coal Combustion Chemistry - Correlation Aspects*. *Coal Science and Technology* 6. Elsevier. 259pp
- Bailey, A.** (1981) *Chemical and Mineralogical Differences Between Kittaning Coals from Marine-Influenced Versus Fluvial Sequences*. *Journal of Sedimentary Petrology* v51 p383-395.
- Bailey, J. G., Tate, A., Diessel, C. F. K., and Wall, T. F.** (1990) *A Char Morphology System with Applications to Coal Combustion*. *Fuel* v69 p225-239.

- Baker, D. E., Pannebaker, F. G., Senft, J. P., and Coetzee, J. P.** (1993) *Baker Soil TestTM Applications for Land Reclamation, Animal Health and Food Chain Protection.* p119-133. in **Keefer, R. F. and Sajwan, K. S. eds** *Trace Elements in Coal and Coal Combustion Residues.* Lewis Publishers.
- Baker, J. C., Fielding, C. R., and De Caritat, P. Wilkinson M. M.** (1993) *Permian Evolution of Sandstone Composition in a Complex Back-Arc Extensional to Foreland Basin: The Bowen Basin, Eastern Australia.* Journal of Sedimentary Petrology v63 p6574-6585.
- Baruah, M. K., Kotoky, P., and Borah, G. C.** (2003) *Organic Affinity of Silver in Subbituminous Assam Coals.* Fuel v82 p1291-1293
- Beaton, A. P., Goodarzi, F., and Potter, J.** (1991) *The Petrography, Mineralogy and Geochemistry of a Paleocene Lignite from Southern Saskatchewan, Canada.* International Journal of Coal Geology v17 p117-148.
- Beaton, A. P., Kalkreuth, W., and MacNeil, D.** (1993) *The Geology, Petrology and Geochemistry of Coal Seams from the St. Rose and Chimney Corner Coalfields, Cape Breton, Nova Scotia, Canada.* International Journal of Coal Geology. v24 p47-73.
- Bencko, V. and Symon, K.** (1977a) *Health Aspects of Burning Coal with a High Arsenic Content: I Arsenic in Hair, Urine, and Blood of Children Residing in a Polluted Area.* Environmental Research v13 p378-385.
- Bencko, V. and Symon, K.** (1977b) *Health Aspects of Burning Coal with a High Arsenic Content: II Hearing Changes in Exposed Children.* Environmental Research v13 p386-395.
- Berkowitz, N.** (1993) *An Introduction to Coal Technology.* Academic Press, Inc. 398pp
- Billings, C. E. and Matson, W. R.** (1972) *Mercury Emissions from Coal Combustion.* Science v176 p1232-1233.
- Birk, D. and White, J. C.** (1991) *Rare Earth Elements in Bituminous Coals and Underclays of the Sydney Basin, Nova Scotia: Element Sites, Distribution, Mineralogy.* International Journal of Coal Geology v19 p219-251.
- Boggs, S. jr** (1987) *Principles of Sedimentology and Stratigraphy.* Merrill Publishing Company. 784pp.
- Bohor, B. F. and Gluskoter, H. J.** (1973) *Boron in Illite as an Indicator of Paleosalinity of Illinois Coals.* Journal of Sedimentary Petrology. v43 p945-956.
- Bonham, L. C.** (1980) *Migration of Hydrocarbons in Compacting Basins.* The American Association of Petroleum Geologists Bulletin v64 p549-567.
- Bouska, V.** (1981) *Geochemistry of Coal.* Elsevier. 284pp.

- Bouska, V. and Pesek, J.** (1999) *Quality Parameters of Lignite of the North Bohemian Basin in the Czech Republic in Comparison with the World Average Lignite*. International Journal of Coal Geology. v40 p211-235.
- Bowen, H. J. M.** (1966) *Trace Elements in Biochemistry*. Academic Press. 241pp.
- Boyd, R. J.** (2002) *The Partitioning Behaviour of Boron from Tourmaline during Ashing of Coal*. International Journal of Coal Geology. v53 p43-54.
- Bradley, W. C.** (1970) *Effect of Weathering on Abrasion of Granitic Gravel, Colorado River (Texas)*. Geological Society of America Bulletin v81 p61-80.
- Brockway, D. J., Ottrey, A. L., and Higgins, R. S.** (1991) *Inorganic Constituents*. Chpt 11, p597-650. in **Durie, R. A. ed** *The Science of Victorian Brown Coal*. Butterworth Heinemann.
- Brown, T. H.** (1990) *Solubility, Sorption, and Redox Relationships for Selenium in Reclaimed Environments - A Review*. p7-24. Proceedings of the 1990 Billings Land Reclamation Symposium on Selenium in Arid and Semi-Arid Environments, Western United States. 1990 US Geological Survey Circular 1064.
- Brownfield, M. E., Affolter, R. H., Stricker, G. D., and Hildebrand, R. T.** (1995) *High Chromium Contents in Tertiary Coal Deposits of Northwestern Washington - A Key to their Depositional History*. International Journal of Coal Geology v27 p153-169.
- Bustin, R. M. and Lowe, L. E.** (1987) *Sulphur, Low Temperature Ash and Minor Elements in Humid-Temperate Peat of the Fraser River Delta, British Columbia*. Journal of the Geological Society, London. v144 p435-450.
- Cameron, C. C., Esterle, J. S., and Palmer, C. A.** (1989) *The Geology, Botany and Chemistry of Selected Peat-Forming Environments from Temperate and Tropical Latitudes*. International Journal of Coal Geology. v12 p105-156.
- Carras, J. N.** (1995) *The Transport and Dispersion of Plumes from Tall Stacks*. Chpt 9, p146-177. in **Swaine, D. J. and Goodarzi, F. eds** *Environmental Aspects of Trace Elements in Coal*. Kluwer Academic Publishers.
- Casagrande, D. J. and Erchull, L. D.** (1976) *Metals in Okefenokee Peat-Forming Environments: Relation to Constituents Found in Coal*. Geochimica et Cosmochimica Acta. v40 p387-393.
- Casagrande, D. J. and Erchull, L. D.** (1977) *Metals in Plants and Waters in the Okefenokee Swamp and their Relationship to Constituents Found in Coal*. Geochimica et Cosmochimica Acta. v41 p1391-1394.
- Casagrande, D. J., Siefert, K., Berschinski, C., and Sutton, N.** (1977) *Sulphur in Peat-Forming Systems of the Okefenokee Swamp and Florida Everglades: Origins of Sulphur in Coal*. Geochimica et Cosmochimica Acta. v44 p161-167.

- Caswell, S. A., Holmes, I. F., and Spears, D. A.** (1984) *Water-Soluble Chlorine and Associated Major Cations from the Coals and Mudrocks of the Cannock and North Staffordshire Coalfields*. *Fuel* v63 p774-781.
- Centano, J. A., Martínez, L., Ladich, E. R., Page, N. P., Mullick, F. G., Ishak, K. G., Zheng, B., Gibb, H., Thompson, C., and Longfellow, D.** (2000) *Arsenic-Induced Lesions*. *Armed Forces Institute of Pathology and American Registry of Pathology*. 46pp
- Chan, M.-L., Jones, J. M., Pourkashanian, M., and Williams, A.** (1999) *The Oxidative Reactivity of Coal Chars in Relation to their Structure*. *Fuel* v78 p1539-1552.
- Chen, H., Li, B., and Zhang, B.** (2000) *Decomposition of Pyrite and the Interaction of Pyrite with Coal Organic Matrix in Pyrolysis and Hydrolysis*. *Fuel* v79 p1627-1631.
- Clark, R. B., Zeto, S. K., Ritchey, K. D., and Baligar, V. C.** (1999) *Boron Accumulation by Maize Grown in Acidic Soil Amended with Coal Combustion Products*. *Fuel* v78 p179-185.
- Clarke, L. B.** (1995) *The Fate of Trace Elements in Emissions Control Systems*. Chpt 8, p128-145. in **Swaine, D. J. and Goodarzi, F. eds** *Environmental Aspects of Trace Elements in Coal*. Kluwer Academic Publishers.
- Clarke, L. B. and Sloss, L. L.** (1992) *Trace Elements - Emissions from Coal Combustion and Gasification*. IEA Coal Research, London. 111pp.
- Clemens, A. H., Damiano, L. F., Gong, D., and Matheson, T. W.** (1999) *Partitioning Behaviour of Some Toxic Volatile Elements During Stoker and Fluidised Bed Combustion of Alkaline Sub-Bituminous Coal*. *Fuel* v78 p1379-1385.
- Clemens, A. H., Deely, J. M., Gong, D., Moore, T. A., and Shearer, J. C.** (2000) *Partitioning Behaviour of Some Toxic Trace Elements During Coal Combustion - the Influence of Events Occurring During the Deposition Stage*. *Fuel* v79 p1781-1784.
- Clemens, A. H. and Matheson, T. W.** (1992) *Further Studies of Gieseler Fluidity Development in New Zealand Coals*. *Fuel*. v71 p193-197.
- Clemens, A. H. and Matheson, T. W.** (1994) *Low Temperature Oxidation of New Zealand Coals*. *Chemistry in New Zealand*. ? p7-10.
- Clemens, A. H. and Matheson, T. W.** (1995) *The Effect of Selected Additives and Treatments on Gieseler Fluidity in Coals*. *Fuel*. v74 p57-62.
- Clemens, A. H., Matheson, T. W., Lynch, L. J., and Sakurovs, R.** (1989) *Oxidation Studies of High Fluidity Coals*. *Fuel*. v68 p1162-1167.

- Cohen, D. and Ward, C. R.** (1991) *Sednorm - A Program to Calculate a Normative Mineralogy for Sedimentary Rocks Based on Chemical Analyses*. Computers & Geosciences. v17 p1235-1253.
- Coin, C. D. A.,** (1995) *Statistical Analysis of Industrial Plant Data of Coke Production*. ACARP Project C1605. pp106.
- Couch, E. L.** (1971) *Calculation of Paleosalinities from Boron and Clay Mineral Data*. The American Association of Petroleum Geologists Bulletin. v55 p1829-1837.
- Couch, G.** (1994) *Understanding Slagging and Fouling in PF Combustion*. IEACR/72 118pp.
- Crosdale, P. J.** (1995) *Lithotype Sequences in the Early Miocene Maryville Coal Measures, New Zealand*. International Journal of Coal Geology. v28 p37-50.
- Crowley, S. S., Warwick, P. D., Ruppert, L. F., and Pontolillo, J.** (1997) *The Origin and Distribution of HAPs Elements in Relation to Maceral Composition of the A1 Lignite Bed (Paleocene, Calvert Bluff Formation, Wilcox Group), Calvert Mine Area, East-Central Texas*. International Journal of Coal Geology. v34 p327-343.
- Cullers, R. L.** (1994) *The Controls on the Major and Trace Element Variation of Shales, Siltstones, and Sandstones of Pennsylvania-Permian Age from Uplifted Continental Blocks in Colorado to Platform Sediment in Kansas, USA*. Geochimica et Cosmochimica Acta. v58 p4955-4972.
- Curtis, C. D.** (1964) *Studies on the use of Boron as a Palaeoenvironmental Indicator*. Geochimica et Cosmochimica Acta v28 p1125-1135.
- Curtis, C. D., Coleman, M. L., and Love, L. G.** (1986) *Pore Water Evolution During Sediment Burial from Isotopic and Mineral Chemistry of Calcite, Dolomite and Siderite Concretions*. Geochimica et Cosmochimica Acta v50 p2321-2334.
- Dai, S., Ren, D., and Ma, S.** (2004) *The Cause of Endemic Fluorosis in Western Guizhou Province, Southwest China*. Fuel v83 p2095-2098.
- Daniels, E. J. and Altaner, S. P.** (1993) *Inorganic Nitrogen in Anthracite from Eastern Pennsylvania, USA*. International Journal of Coal Geology. v22 p21-35.
- Deer, W. A., Howie, R. A., and Zussman, J.** (1989) *An Introduction to the Rock-Forming Minerals*. Longman Scientific and Technical. 528pp.
- Degens, E. T., Williams, E. G., and Keith, M. L.** (1958) *Environmental Studies of Carboniferous Sediments. Part II: Application of Geochemical Criteria*. American Association of Petroleum Geologists Bulletin v42 p981-997.

- Demir, I., Hughes, R. E., and DeMaris, P. J.** (2001) *Formation and Use of Coal Combustion Residues from Three Types of Power Plants Burning Illinois Coals.* Fuel v80 p1659-1673.
- Dennis, W. H.** (1963) *Metallurgy of the Ferrous Metals.* Sir Isaac Pitman & Sons Ltd. 393pp
- Dewison, M. G.** (1989) *Dispersed Kaolinite in the Barnsley Seam Coal (U.K.): Evidence for a Volcanic Origin.* International Journal of Coal Geology v11 p291-304.
- Dewison, M. G. and Kanaris-Sotiriou, R.** (1986) *The Determination of Trace Elements in Whole Coal by Rhodium Tube X-Ray Fluorescence Spectrometry: a Rock Based Synthetic Coal Calibration.* International Journal of Coal Geology. v6 p327-341.
- Diessel, C. F. K.** (1992) *Coal-Bearing Depositional Systems.* Springer-Verlag. 721pp.
- Diessel, C. F. K.** (1998) *Technological Applications.* Chpt 9, p519-614. in **Taylor, G. H., Teichmüller, M., Davis, A., Diessel, C. F. K., Littke, R., and Robert, P.** *Organic Petrology.* Gebrüder Borntraeger.
- Diez, M. A., Alvarez, R., and Barriocanal, C.** (2002) *Coal for Metallurgical Coke Production: Predictions of Coke Quality and Future Requirements for Coke Making.* International Journal of Coal Geology. v50 p389-412.
- Dilles, S. J. and Hill, P. A.** (1984) *Vertical Distribution of Copper and Zinc in Coal Zones A, B, C, D, Hat Creek, British Columbia.* Economic Geology. v79 p1936-1940.
- Dominik, J. and Stanley, D. J.** (1993) *Boron, Beryllium and Sulphur in Holocene Sediments and Peats of the Nile Delta, Egypt: Their use as Indicators of Salinity and Climate.* Chemical Geology. v104 p203-216.
- Doolan, K. J., Turner, K. E., Mills, J. C., Knott, A. C., and Ruch, R. R.,** (1985) *Volatilities of Inorganic Elements in Coals During Ashing.* BHP Central Laboratories. 13pp.
- Dreher, G. B. and Finkelman, R. B.** (1992) *Selenium Mobilization in a Surface Coal Mine, Powder River Basin, Wyoming, U.S.A.* Environmental Geology and Water Science v19 p155-167.
- Dubrawski, J. V. and Warne, S. StJ.** (1987) *Use of Differential Scanning Calorimetry in Measuring the Thermal Decomposition of Mineral Carbonates Occurring in Coal.* Fuel v66 p1733-1736.
- Duke, W. L.** (1985) *Hummocky Cross-Stratification, Tropical Hurricanes, and Intense Winter Storms.* Sedimentology v32 p167-194.
- Eagar, R. M.** (1962) *Boron Content in Relation to Organic Carbon in Certain Sediments of the British Coal Measures.* Nature. v196 p428-431.

- Elms, R. G., Matthews, R. D., and Chapman, D. G.** (1987) *Notes on the Geology of the Lignite Resources - Esperance, Western Australia.* Australian Journal of Coal Geology. v4, p1. p101-110.
- Eskenazy, G. M.** (1982) *The Geochemistry of Tungsten in Bulgarian Coals.* International Journal of Coal Geology. v2 p99-111.
- Eskenazy, G. M.** (1987) *Rare Earth Elements in a Sampled Coal from the Pirin Deposit, Bulgaria.* International Journal of Coal Geology. v7 p301-314.
- Eskenazy, G. M.** (1999) *Aspects of the Geochemistry of Rare Earth Elements in Coal: An Experimental Approach.* International Journal of Coal Geology v38 p285-295.
- Eskenazy, G., Delibaltova, D., and Mincheva, E.** (1994) *Geochemistry of Boron in Bulgarian Coals.* International Journal of Coal Geology. v25 p93-110.
- Evans, J. R., Sellers, G. A., Johnson, R. G., Vivit, D. V., and Kent, J.,** (2001) *The Chemical Analysis of Argonne Premium Coal Samples. United States Geological Survey Bulletin 2144.*
- Faure, G.** (1991) *Principles and Applications in Geochemistry.* Prentice Hall. 600pp
- Feng, X. and Hong, Y.** (1999) *Modes of Occurrence of Mercury in Coals from Guizhou, People's Republic of China.* Fuel v78 p1181-1188.
- Fernández-Turiel, J. L., de Carvalho, W., Cabañas, M., Querol, X., and López-Soler, A.** (1994) *Mobility of Heavy Metals from Coal Fly-ash.* Environmental Geology v23 p264-270.
- Fernandez-Turiel, J-L., Georgakopoulos, A., Gimeno, D., Papastergios, G., and Kolovos, N.** (2004) *Ash Deposition in a Pulverised Coal-Fired Power Plant after High-Calcium Lignite Combustion.* Energy & Fuels v18 p1512-1518.
- Finkelman, R. B.** (1978) *Determination of Trace Element Sites in the Waynesburg Coal by SEM Analysis of Accessory Minerals.* Scanning Electron Microscopy. v1 p143-148.
- Finkelman, R. B.** (1979) *Mode of Occurrence of Accessory Sulfide and Selenide Minerals in Coal.* p407-412. Neuvième Congrès International de Stratigraphie et de Géologie du Carbonifère. 1979 Washington and Champaign-Urbana.
- Finkelman, R. B.** (1980) *Modes of Occurrence of Trace Elements in Coal.* PhD Thesis, University of Maryland. Also USGS Open File Report No. OFR-81-99 (1981). 301pp.
- Finkelman, R. B.** (1982) *Modes of Occurrence of Trace Elements and Minerals in Coal.* p141-149. in **Filby, R. H., Carpenter, B. S., and Ragaini, R. C.** eds *Atomic and Nuclear Methods in Fossil Energy Research.* Plenum Publishing.

- Finkelman, R. B.** (1993) *Trace and Minor Elements in Coal*. Chpt 28, p593-607. in **Engel, M. H. and Macko, S. A. eds** *Organic Geochemistry*. Plenum Press.
- Finkelman, R. B.** (1994) *Modes of Occurrence of Potentially Hazardous Elements in Coal: Levels of Confidence*. *Fuel Processing Technology*. v39 p21-34.
- Finkelman, R. B.** (1995) *Modes of Occurrence of Environmentally - Sensitive Trace Elements in Coal*. Chpt 3, p24-50. in **Swaine, D. J. and Goodarzi, F. eds** *Environmental Aspects of Trace Elements in Coal*. Kluwer Academic Publishers.
- Finkelman, R. B.** (2000) *Current Topics on Trace Elements and Toxic Metal Ion Studies: Environmental Legislation, Management and Use of Some Waste Products Containing Toxic Metals*. Conference Proceedings - Metals, Health and the Environment. 2000 University of Canterbury, New Zealand.
- Finkelman, R. B., Bostick, N. H., Dulong, F. T., Senftle, F. E., and Thorpe, A. N.** (1998) *Influence of an Igneous Intrusion on the Inorganic Geochemistry of a Bituminous Coal from Pitkin County, Colorado*. *International Journal of Coal Geology*. v36 p223-241.
- Finkelman, R. B., Fiene, F. L., Miller, R. N., and Simon, F. O. eds**, (1984) *Interlaboratory Comparison of Mineral Constituents in a Sample from the Herrin (No. 6) Coal Bed from Illinois*. *U.S. Geological Survey Circular 932*. USGS. 42pp.
- Finkelman, R. B., Palmer, C. A., Krasnow, M. R., Aruscavage, P. J., Sellers, G. A., and Dulong, F. T.** (1990) *Combustion and Leaching Behaviour of Elements in the Argonne Premium Coal Samples*. *Energy & Fuels*. v4 p755-766.
- Finkelman, R. B., Simons, D. S., Dulong, F. T., and Steel, E. B.** (1984) *Semi-Quantitative Ion Microprobe Mass Analyses of Mineral-Rich Particles from the Upper Freeport Coal*. *International Journal of Coal Geology*. v3 p279-289.
- Finkelman, R. B. and Stanton, R. W.** (1978) *Identification and Significance of Accessory Minerals from a Bituminous Coal*. *Fuel* v57 p763-768.
- Fishman, N. S., Rice, C. A., Breit, G. N., and Johnson, R. D.** (1999) *Sulphur-Bearing Coatings on Fly-ash from a Coal-Fired Power Plant: Composition, Origin, and Influence on Ash Alteration*. *Fuel* v78 p187-196.
- Foner, H. A., Robl, T.L., Hower, J. C., and Graham, U. M.** (1999) *Characterization of Fly-ash from Isreal with Reference to its Possible Utilization*. *Fuel* v78 p215-223.
- Fyfe, W. S.** (1999) *Clean Energy for 10 Billion Humans in the 21st Century: Is It Possible?* *International Journal of Coal Geology* v40 p85-90.

- Galbreath, K. C., Toman, D. L., Zygarlicke, C. J., and Pavlish, J. H.** (2000) *Trace Element Partitioning and Transformations During Combustion of Bituminous and Subbituminous U.S. Coals in a 7-kW Combustion System.* Energy & Fuels. v14. p1265-1279.
- Gayer, R. A., Rose, M., Dehmer, J., and Shao, L.-Y.** (1999) *Impacts of Sulphur and Trace Element Geochemistry on the Utilization of a Marine-Influenced Coal - Case Study from the South Wales Variscan Foreland Basin.* International Journal of Coal Geology. v40 p151-174.
- Ghosh, R., Majumder, T., and Ghosh, D. N.** (1987) *A Study of Trace Elements in Lithotypes of some Selected Indian Coals.* International Journal of Coal Geology v8 p269-278.
- Gluskoter, H. J. and Lindahl, P. C.** (1973) *Cadmium: Mode of Occurrence in Illinois Coals.* Science v181 p264-266.
- Gluskoter, H. J. and Ruch, R. R.** (1971) *Chlorine and Sodium in Illinois Coals as Determined by Neutron Activation Analyses.* Fuel v50 p65-76.
- Godbeer, W. C. and Swaine, D. J.** (1995) *The Deposition of Trace Elements in the Environs of a Power Station.* Chpt 10, p178-203. in **Swaine, D. J. and Goodarzi, F. eds** *Environmental Aspects of Trace Elements in Coal.* Kluwer Academic Publishers.
- Goodarzi, F.** (1987a) *Comparison of Elemental Distribution in Fresh and Weathered Samples of Selected Coals in the Jurassic-Cretaceous Kootenay Group, British Columbia, Canada.* Chemical Geology. v63 p21-28.
- Goodarzi, F.** (1987b) *Concentration of Elements in Lacustrine Coals from Zone A Hat Creek Deposit No. 1, British Columbia, Canada.* International Journal of Coal Geology. v8 p247-268.
- Goodarzi, F.** (1987c) *Elemental Concentrations in Canadian Coals 2. Byron Creek Collieries, British Columbia.* Fuel v66 p250-254.
- Goodarzi, F.** (1988) *Elemental Distribution in Coal Seams at the Fording Coal Mine, British Columbia, Canada.* Chemical Geology v68 p129-154.
- Goodarzi, F.** (1995a) *Geology of Trace Elements in Coal.* Chpt 4, p51-75. in **Swaine, D. J. and Goodarzi, F. eds** *Environmental Aspects of Trace Elements in Coal.* Kluwer Academic Publishers.
- Goodarzi, F.** (1995b) *The Effects of Weathering and Natural Heating on Trace Elements of Coal.* Chpt 5, p76-92. in **Swaine, D. J. and Goodarzi, F. eds** *Environmental Aspects of Trace Elements in Coal.* Kluwer Academic Publishers.
- Goodarzi, F., Foscolos, A. E., and Cameron, A. R.** (1985) *Mineral Matter and Elemental Concentrations in Selected Western Canadian Coals.* Fuel v64 p1599-1605.

- Goodarzi, F. and Swaine, D. J.** (1993) *Chalcophile Elements in Western Canadian Coals*. International Journal of Coal Geology. v24 p281-292.
- Goodarzi, F. and Swaine, D. J.,** (1994) *Paleoenvironmental and Environmental Implications of the Boron Content of Coals*. Geological Survey of Canada Bulletin 471. Geological Survey of Canada 76pp.
- Goodarzi, F. and Van Der Flier-Keller, E.** (1988) *Distribution of Major, Minor and Trace Elements in Hat Creek Deposit No. 2, British Columbia, Canada*. Chemical Geology v70 p313-333.
- Goodarzi, F. and Van Der Flier-Keller, E.** (1989) *Organic Petrology and Geochemistry of Intermontane Coals from British Columbia 3. The Blakeburn Opencast mine near Tulameen, British Columbia, Canada*. Chemical Geology. v75 p227-247.
- Gray, V. R.** (1987) *Prediction of Ash Fusion Temperature from Ash Composition for Some New Zealand Coals*. Fuel. v66 p1230-1239.
- Greenhouse, J. P. and Harris, R. D.** (1983) *Migration of Contaminants in Groundwater at a Landfill: A Case Study*. Journal of Hydrology v63 p177-197.
- Grieve, D. A. and Goodarzi, F.** (1993) *Trace Elements in Coal Samples from Active Mines in the Foreland Belt, British Columbia, Canada*. International Journal of Coal Geology v24 p259-280.
- Gunn, P. R.** (1988) *Naturally Coked Coal of the Collinsville - Newlands Area, North Queensland*. University of Newcastle unpublished MSc thesis. 230pp.
- Gupta, D. C.** (1999) *Environmental Aspects of Selected Trace Elements Associated with Coal and Natural Waters of Pench Valley Coalfield of India and their Impact on Human Health*. International Journal of Coal Geology v40 p133-149.
- Gutenmann, W. H. and Bache, C. A.** (1976) *Selenium in Fly-ash*. Science. v191 p966-967.
- Hassett, D. J. and Eylands, K. E.** (1999) *Mercury Capture on Coal Combustion Fly-ash*. Fuel v78 p243-248.
- Hatch, J. R., Gluskoter, H. J., and Lindahl, P. C.** (1976) *Sphalerite in Coals from the Illinois Basin* Economic Geology v71 p613-624.
- Hayashi, J.-i., Denma, D., Takahashi, H., Kumagai, H., and Chiba, T.** (2000) *Experimental Examination of Existing Slurry Models for Coal Softening and Resolidification*. Fuel. v79 p391-397.
- Helble, J. J.** (2000) *A Model for the Air Emissions of Trace Metallic Elements from Coal Combustors Equipped with Electrostatic Precipitators*. Fuel Processing Technology v63 p125-147.

- Helle, S., Alfaro, G., Kelm, U., and Tascón, J. M. D.** (2000) *Mineralogical and Chemical Characterisation of Coals from Southern Chile*. International Journal of Coal Geology. v44 p85-94.
- Héquet, V., Ricou, P., Lecuyer, I., and Le Cloirec, P.** (2001) *Removal of Cu^{2+} and Zn^{2+} in Aqueous Solutions by Sorption onto Mixed Fly-ash*. Fuel v80. p851-856.
- Herring, J. R.** (1990) *Selenium Geochemistry - A Conspectus*. p25-33. Proceedings of the 1990 Billings Land Reclamation Symposium on Selenium in Arid and Semi-Arid Environments, Western United States. 1990 US Geological Survey Circular 1064.
- Hower, J. C. and Bland, A. E.** (1989) *Geochemistry of the Pond Creek Coal Bed, Eastern Kentucky Coalfield*. International Journal of Coal Geology v11 p205-226.
- Hower, J. C. and Lloyd, W. G.** (1999) *Petrographic Observations of Gieseler Semi-Cokes from High Volatile Bituminous Coals*. Fuel v78 p445-451.
- Hower, J. C. and Masterlerz, M.** (2001) *An Approach Toward a Combined Scheme for the Petrographic Classification of Fly-ash*. Energy & Fuels v15 p1319-1321.
- Hower, J. C. and Parekh, B. K.** (1991) *Chemical/Physical Properties and Marketing*. Chpt 1, p3-94. in **Leonard, J. W. III ed and Hardinge, B. C. assoc ed** *Coal Preparation*. Society for Mining, Metallurgy, and Exploration, Inc.
- Hower, J. C., Robl, T. L., and Thomas, G. A.** (1999) *Changes in the Quality of Coal Combustion By-Products Produced by Kentucky Power Plants, 1978 to 1997: Consequences of Clean Air Act Directives*. Fuel v78 p701-712.
- Hower, J. C., Ruppert, L. F., Eble, C. F., and Graham, U. M.** (1996) *Geochemical and Palynological Indicators of the Paleoecology of the River Gem Coal bed, Whitley County, Kentucky*. International Journal of Coal Geology. v31 p135-149.
- Huggins, F. E. and Huffman, G. P.** (1996) *Modes of Occurrence of Trace Elements in Coal from XAFS Spectroscopy*. International Journal of Coal Geology. v32 p31-53.
- Huggins, F. E., Najih, M., and Huffman, G. P.** (1999) *Direct Speciation of Chromium in Coal Combustion By-Products by X-ray Absorption Fine Structure Spectroscopy*. Fuel v78 p233-242.
- Huggins, F. E., Shah, N., Huffman, G. P., Kolker, A., Crowley, S., Palmer, C. A., and Finkelman, R. B.** (2000) *Mode of Occurrence of Chromium in Four US Coals*. Fuel Processing Technology. v63 p79-92.

- Hulett, L. D. Jr, Weinberger, A. J., Northcutt, K. J., and Ferguson, M.** (1980) *Chemical Species in Fly-ash from Coal-Burning Power Plants*. Science. v210 p1356-1358.
- International Committee for Coal and Organic Petrology** (1998) *The New Vitrinite Classification (ICCP System 1994)*. Fuel v77 p349-358.
- International Committee for Coal and Organic Petrology (ICCP)** (2001) *The New Inertinite Classification (ICCP System 1994)*. Fuel v80 p459-471.
- ISO – International Standard ISO 7404-3.** (1994a) *Methods for the Petrographic Analysis of Bituminous Coal and Anthracite - Part 3: Method of Determining Maceral Group Composition*. Second Edition International Organisation for Standardization.
- ISO – International Standard ISO 7404-5.** (1994b) *Methods for the Petrographic Analysis of Bituminous Coal and Anthracite - Part 5: Method of Determining Microscopically the Reflectance of Vitrinite*. Second Edition International Organisation for Standardization.
- Jiménez, A., Martínez-Tarazona, M. R., and Suárez-Ruiz, I.** (1999) *The Mode of Occurrence and Origin of Chlorine in Puertollano Coals (Spain)*. Fuel v78 p1559-1565.
- Johnson, R. G., Sellers, G. A., and Fleming, S. L.** (1989) *The Determination of Major and Minor Elements in Coal Ash and Chlorine and Phosphorous in Whole Coal by X-Ray Fluorescence Spectrometry*. Geological Survey Bulletin (Washington). Report No B 1823 p35-38.
- Jones, D. R.** (1995) *The Leaching of Major and Trace Elements from Coal Ash*. Chpt 12, p221-262. in **Swaine, D. J. and Goodarzi, F. eds** *Environmental Aspects of Trace Elements in Coal*. Kluwer Academic Publishers.
- Jones, J. C.** (2000) *On the Role of Times to Ignition in the Thermal Safety of Transportation of Bituminous Coals*. Fuel v79 p1561-1562.
- Karayigit, A. I., Gayer, R. A., Ortac, F. E., and Goldsmith, S.** (2001) *Trace Elements in the Lower Pliocene Fossiliferous Kangal Lignites, Sivas, Turkey*. International Journal of Coal Geology v47 p73-89.
- Karayigit, A. I., Gayer, R. A., Querol, X., and Onacak, T.** (2000) *Contents of Major and Trace Elements in Feed Coals from Turkish Coal-Fired Power Plants*. International Journal of Coal Geology v44 p169-184.
- Keefer, R. F.** (1993) *Coal Ashes - Industrial Wastes or Beneficial By-Products?* p3-9. in **Keefer, R. F. and Sajwan, K. S. eds** *Trace Elements in Coal and Coal Combustion Residues*. Lewis Publishers.
- Keefer, R. F., Bhumbla, D. K., and Singh, R. N.** (1993) *Accumulation of Mo in Wheat and Alfalfa Grown on Fly-ash-Amended Acid Mine Spoils*. p239-258. in **Keefer, R. F. and Sajwan, K. S. eds** *Trace Elements in Coal and Coal Combustion Residues*. Lewis Publishers.

- Keller, E. A.** (1992) *Environmental Geology*. Prentice Hall 560pp
- Khorasani, G. K., Murchison, D. G., and Raymond, A. C.** (1990) *Molecular Disordering in Natural Cokes Approaching Dyke and Sill Contacts*. *Fuel* v69 p1037-1046.
- Kim, A. G. and Kazonich, G.** (2004) *The Silicate/ Non-Silicate Distribution of Metals in Fly-ash and its Effect on Solubility*. *Fuel* v83 p2285-2292.
- Kizilshtein, L. Ya. and Kholodkov, Yu. I.** (1999) *Ecologically Hazardous Elements in Coals of the Donets Basin*. *International Journal of Coal Geology* v40 p189-197.
- Klika, Z., Bartonová, L., and Spears, D. A.** (2001) *Effect of Boiler Output on Trace Element Partitioning During Coal Combustion in Two Fluidised-Bed Power Stations*. *Fuel* v80 p907-917.
- Klusek, C. S., Heit, M., and Hodgkiss, S.** (1993) *Trace Element Concentrations in the Soft Tissues of Transplanted Freshwater Mussels Near a Coal-Fired Power Plant*. p59-95. in **Keefer, R. F. and Sajwan, K. S. eds** *Trace Elements in Coal and Coal Combustion Residues*. Lewis Publishers.
- Knapp, J.** (1999) *The Outlook for Coal*. Developing World Energy 1999 Special Edition to Mark the 25th Anniversary of the International Energy Agency. p77-78.
- Knott, A. C., Thompson, S. C., and Lee, J. B.**, (1985) *Characterization, Treatment, Disposal of Coal Wastes in an Environmentally Acceptable Manner*. BHP Central Laboratories. 76pp.
- Kolker, A. and Finkelman, R. B.** (1998) *Potentially Hazardous Elements in Coal: Mode of Occurrence and Summary of Concentration Data for Coal Components*. *Coal Preparation*. v19 p133-157.
- Kolker, A., Huggins, F. E., Palmer, C. A., Shah, N., Crowley, S. S., Huffman, G. P., and Finkelman, R. B.** (2000) *Modes of Occurrence of Arsenic in Four US Coals*. *Fuel Processing Technology* v63 p167-178.
- Kortenski, J. and Bakardjiev, S.** (1993) *Rare Earth and Radioactive Elements in Some Coals from the Sofia, Svoge and Pernik Basins, Bulgaria*. *International Journal of Coal Geology*. p237-246.
- Krishna De, A.** (1996) *Trace Elements in Health and Diseases*. Books for All. 93pp
- Kurose, R., Ikeda, M., and Makino, H.** (2001) *Combustion Characteristics of High Ash Coal in a Pulverised Coal Combustion*. *Fuel* v80 p1447-1455.
- Laban, K. L. and Atkin, B. P.** (1999) *The Determination of Minor and Trace Element Associations in Coal using a Sequential Microwave Digestion Procedure*. *International Journal of Coal Geology*. v41 p351-369.

- Lewis, D. W. and McConchie, D.** (1994) *Analytical Sedimentology*. Chapman & Hall. 197pp.
- Li, Z.** (2002) *Mineralogy and Trace Elements of the Cretaceous Greymouth Coals and their Combustion Products*. Canterbury University unpublished PhD thesis. 179pp
- Li, Z., Moore, T. A., Weaver, S. D., and Finkelman, R. B.** (2001) *Crocoite: An Unusual Mode of Occurrence for Lead in Coal*. v45 p289-293.
- Lindahl, P. C. and Finkelman, R. B.** (1986) *Factors Influencing Major, Minor, and Trace Element Variations in U.S. Coals*. p61-69. in **Vorres, K. S. ed** *Mineral Matter and Ash in Coal*. ACS Symposium Series No. 301, American Chemical Society, Washington D.C.
- Linton, R. W., Loh, A., Evans, C. A. Jr, and Williams, P.** (1976) *Surface Predominance of Trace Elements in Airborne Particles*. Science v191 p852-854.
- Liu, K., Gao, Y., Riley, J. T., Pan, W-P., Mehta, A. K., Ho, K. K., and Smith, S. R.** (2001) *An Investigation of Mercury Emission from FBC Systems Fired with High-Chlorine Coals*. Energy & Fuels v15 p1173-1180.
- Liu, K., Xie, W., Li, D., Pan, W-P., Riley, J. T., and Riga, A.** (2000) *The Effect of Chlorine and Sulphur on the Composition of Ash Deposits in a Fluidised Bed Combustion System*. Fuel v79 p963-972.
- Lyons, P. C., Palmer, C. A., Bostick, N. H., Fletcher, J. D., Dulong, F. T., Brown, F. W., Brown, Z. A., Krasnow, M. R., and Romankiw, L. A.** (1989) *Chemistry and Origin of Minor and Trace Elements in Vitrinite Concentrates from a Rank Series from the Eastern United States, England, and Australia*. International Journal of Coal Geology v13 p481-527.
- Maes, I. I., Gryglewicz, G., Yperman, J., Franco, D. V., D'Haes, J. D'Olieslaeger M., and Van Poucke, L. C.** (2000) *Effect of Siderite in Coal on Reductive Pyrolytic Analyses*. Fuel v79 p1873-1881.
- Mann, W. R. and Cavaroc, V. V.** (1973) *Composition of Sand Released from Three Source Areas Under Humid, Low Relief Weathering in the North Carolina Piedmont*. Journal of Sedimentary Petrology. v43 p870-881.
- Mardon, S. M. and Hower, J. C.** (2004) *Impact of Coal Properties on Coal Combustion By-Product Quality: Examples from a Kentucky Power Plant*. International Journal of Coal Geology v59 p153-169.
- Maroto-Valer, M. M., Taulbee, D. N., and Hower, J. C.** (2001) *Characterization of Differing Forms of Unburnt Carbon Present in Fly-ash Separated by Density Gradient Centrifugation*. Fuel v80 p795-800.
- Martini, I. P. and Johnson, D. P.** (1987) *Cold-climate, Fluvial to Paralic Coal-Forming Environments in the Permian Collinsville Coal Measures, Bowne Basin, Australia*. International Journal of Coal Geology. v7 p365-388.

- Mastalerz, M., Hower, J. C., Drobnik, A., Mardon, S. M., and Lis, G.** (2004) *From In-Situ Coal to Fly-ash: A Study of Coal Mines and Power Plants from Indiana*. International Journal of Coal Geology v59 p171-192
- McCarthy, T. S., McIver, J. R., Cairncross, B., Ellery, W. N., and Ellery, K.** (1989) *The Inorganic Chemistry of Peat from the Maunachira Channel-Swamp System, Okevango Delta, Botswana*. Geochimica et Cosmochimica Acta. v53 p1077-1089.
- Meij, R.** (1995) *The Distribution of Trace Elements During the Combustion of Coal*. Chpt 7, p111-127. in **Swaine, D. J. and Goodarzi, F. eds** *Environmental Aspects of Trace Elements in Coal*. Kluwer Academic Publishers.
- Menon, M. P., Sajwan, K. S., Ghuman, G. S., James, J., and Chandra, K.** (1993) *Elements in Coal and Coal Ash Residues and Their Potential for Agricultural Crops*. p259-287. in **Keefer, R. F. and Sajwan, K. S. eds** *Trace Elements in Coal and Coal Combustion Residues*. Lewis Publishers.
- Miller, B. B., Dugwell, D. R., and Kandiyoti, R.** (2002) *Partitioning of Trace Elements During the Combustion of Coal and Biomass in a Suspension-Firing Reactor*. Fuel v81 p159-171.
- Miller, R. N. and Given, P. H.** (1986) *The Association of Major, Minor and Trace Inorganic Elements with Lignites. I. Experimental Approach and Study of a North Dakota Lignite*. Geochimica et Cosmochimica Acta. v50 p2033-2043.
- Miller, R. N. and Given, P. H.** (1987) *The Association of Major, Minor and Trace Inorganic Elements with Lignites. II. Minerals, and Major and Minor Element Profiles, in Four Seams*. Geochimica et Cosmochimica Acta. v51 p1311-1322.
- Mills, J. C. and Turner, K. E.,** (1980) *Direct Determination of Trace Elements in Coal and Coal Products. Part I Wavelength Dispersive X-Ray Fluorescence Spectrometry*. BHP Central Laboratories. 42pp.
- Mitchell, R. S. and Gluskoter, H. J.** (1976) *Mineralogy of Ash of Some American Coals: Variations with Temperature and Source*. Fuel v55 p90-96.
- Moore, N. A. and Moore, T. A.** (1999) *A Review of Current Coal Research in New Zealand*. New Zealand Mining. p24-29.
- Moore, T. A. and Fergusson, D. A.** (1997) *Coal and Combustion in the Waikato: Predicting Ash Clinkering Potential for In-Ground Resources*. Author preprint 7th New Zealand Coal Conference. 1997
- Mukhopadhyay, P. K., Goodarzi, F., Crandlemire, A. L., Gillis, K. S., MacNeil, D. J., and Smith, W. D.** (1998) *Comparison of Coal Composition and Elemental Distribution in Selected Seams of the Sydney and Stellarton Basins, Nova Scotia, Eastern Canada*. International Journal of Coal Geology. v37 p113-141.

- Mukhopadhyay, P. K., Lajeunesse, G., and Crandlemire, A. L.** (1996) *Mineralogical Speciation of Elements in an Eastern Canadian coal and their Combustion Residues from a Canadian Power Plant*. International Journal of Coal Geology. v32 p279-312.
- Mukhopadhyay, P. K., Lajeunesse, G., Crandlemire, A. L., and Finkelman, R. B.** (1999) *Mineralogy and Geochemistry of Selected Coal Seams and their Combustion Residues from the Sydney Area, Nova Scotia, Canada*. International Journal of Coal Geology v40 p253-254.
- Murarka, I. P., Mattigod, S. V., and Keefer, R. F.** (1993) *An Overview of Electric Power Institute (EPRI) Research Related to Effective Management of Coal Combustion Residues*. p11-24. in **Keefer, R. F. and Sajwan, K. S. eds** *Trace Elements in Coal and Coal Combustion Residues*. Lewis Publishers.
- Nadkarni, R. A.** (1980) *Multitechnique Multielemental Analysis of Coal and Fly-ash*. Analytical Chemistry v52 p929-935.
- Ness, S.** (1998) *X-Ray Analytical Techniques. X-Ray Fluorescence (XRF) and X-Ray Diffraction (XRD)*. Analytical Testing Technology. p6-12.
- New Zealand Ministry of Health.** (2000) *Drinking-Water Standards for New Zealand 2000* NZ Government Publication
- Newman, J.** (1985) *Palaeoenvironments, Coal Properties and their Inter-Relationship in Paparoa and Selected Brunner Coal Measures on the West Coast of the South Island*. Canterbury University unpublished PhD Thesis. 269pp
- Newman, J.** (1991) *Isorank Variation in Vitrinite Chemistry 1: Vitrinite Reflectance*. Oil Conference 1991, Christchurch, New Zealand. 1991 Christchurch, NZ.
- Newman, J., Johnson, J., and Lake, P.** (1991) *Isorank Variation in Vitrinite Chemistry 2: Sterane and Triterpane Maturity Indicators*. Oil Conference 1991, Christchurch, New Zealand. 1991 Christchurch, NZ.
- Newman, N. A.** (1988) *Mineral Matter in Coals of the West Coast, South Island, New Zealand*. Canterbury University unpublished PhD Thesis. 293pp.
- Newman, N. A., Moore, T. A., and Esterle, J. S.** (1997) *Geochemistry and Petrography of the Taupiri and Kupakupa Coal Seams, Waikato Coal Measures (Eocene), New Zealand*. Fuel v33 p103-133.
- Nobes, D. C.** (1996) *Troubled Waters: Environmental Applications of Electrical and Electromagnetic Methods*. Surveys in Geophysics v17 p393-454.
- O'Gorman, J. V. and Walker, P. L. Jr** (1971) *Mineral Matter Characteristics of Some American Coals*. Fuel v50 p135-151.

- Odom, I. E., Doe, T. W., and Dott, R. H. Jr** (1976) *Nature of Feldspar-Grain Size Relations in some Quartz-Rich Sandstones*. *Journal of Sedimentary Petrology* v46 p862-870.
- Palmer, C. A. and Filby, R. A.** (1984) *Distribution of Trace Elements in Coal from the Powhatan No. 6 Mine, Ohio*. *Fuel* v63 p318-328.
- Palmer, C. A. and Klizas, S. A.,** (2001) *Compilation of Multitechnique Determinations of 51 Elements in 8 Argonne Premium Coal Samples. The Chemical Analysis of Argonne Premium Coal Samples. United States Geological Survey Bulletin 2144*.
- Palmer, C. A., Kolker, A., Willett, J. C., Mroczkowski, S. J., Finkelman, R. B., Taylor, K. C., Dulong, F. T., and Bullock, J. H. Jr,** (1999) *Preliminary Report on the International Energy Agency Mode of Occurrence Inter-Laboratory Comparison: Phase I; USGS Results. Open-File Report 99-160. U.S. Department of the Interior. U.S. Geological Survey. 26pp*.
- Palmer, C. A. and Lyons, P. C.** (1996) *Selected Elements in Major Minerals from Bituminous Coal as Determined by INAA: Implications for Removing Environmentally Sensitive Elements from Coal*. *International Journal of Coal Geology* v32 p151-166.
- Palmer, C. A., Mroczkowski, J., Finkelman, R. B., Crowley, S. S., and Bullock, J. H.** (1998) *The Use of Sequential Leaching to Quantify the Modes of Occurrence of Elements in Coal*. 28pp. Proceedings, Fifteenth Pittsburgh Coal Conference, Pittsburgh, PA. 1998
- Panov, B. S., Dudik, A. M., Shevchenko, O. A., and Matlak, E. S.** (1999) *On Pollution of the Biosphere in Industrial Areas: the Example of the Donets Coal Basin*. *International Journal of Coal Geology* v40 p199-210.
- Patterson, J. H., Ramsden, A. R., Dale, L. S., and Fardy, J. J.** (1986) *Geochemistry and Mineralogical Residences of Trace Elements in Oil Shales from Julia Creek, Queensland, Australia*. *Chemical Geology* v55 p1-16.
- Pierce, B. S. and Stanton, R. W.** (1990) *Pyritic Sulphur and Trace-Element Affinities of the Upper Freeport Coal Bed, Allegheny Formation, West-Central Pennsylvania*. p64-65. USGS USGS Research on Energy and Resources - 1990. Program and Abstracts. 1990 US Geological Survey Circular 1060.
- Pollock, S. M., Goodarzi, F., and Riediger, C. L.** (2000) *Mineralogical and Elemental Variation of Coal from Alberta, Canada: An Example from the No.2 Seam, Genesee Mine*. *International Journal of Coal Geology*. v43 p259-286.
- Potter, P. E., Shimp, N. F., and Witters, J.** (1963) *Trace Elements in Marine and Fresh-Water Argillaceous Sediments*. *Geochimica et Cosmochimica Acta*. v27 p669-694.
- Potts, P. J.** (1987) *A Handbook of Silicate Rock Analysis*. Blackie 621pp.

- Purchase, N. G.** (1987) *Major and Trace Element Variations in Huntly Power Station Ash Streams*. p1-12. 1987 Coal Research Conference, Wellington, New Zealand
- Querol, X., Alastuey, A., Lopez-Soler, A., Plana, F., Fernandez-Turiel, J. L., Zeng, R., Xu, W., Zhuang, X., and Spiro, B.** (1997a) *Geological Controls on the Mineral Matter and Trace Elements of Coals from the Fuxin Basin, Liaoning Province, Northeast China*. *International Journal of Coal Geology*. v34 p89-109.
- Querol, X., Alastuey, A., Lopez-Soler, A., Plana, F., Mantilla, E., Juan, R., Ruiz, C. R., and La Orden, A.** (1999a) *Characterization of Atmospheric Particulates around a Coal-Fired Power Station*. *International Journal of Coal Geology* v40 p175-188.
- Querol, X., Alastuey, A., Lopez-Soler, A., Plana, F., Zeng, R., Zhao, J., and Zhuang, X.** (1999b) *Geological Controls on the Quality of Coals from the West Shandong Mining District, Eastern China*. *International Journal of Coal Geology*. v42 p63-88.
- Querol, X., Fernández-Turiel, J. L., and López-Soler, A.** (1995) *Trace Elements in Coal and their Behaviour During Combustion in a Large Power Station*. *Fuel* v74 p331-343.
- Querol, X., Finkelman, R. B., Alastuey, A., Huerta, A., Palmer, C. A., Mroczkowski, S., Kolker, A., Chenery, S. N. R., Robinson, J. J., Juan, R., and López-Soler, A.** (1998) *Quantitative Determination of Modes of Occurrence of Major, Minor, and Trace Elements in Coal: A Comparison of Results from Different Methods*. p51-56. AIE 8th Australian Coal Science Conference. 1998
- Querol, X., Klika, Z., Weiss, Z., Finkelman, R. B., Alastuey, A., Juan, R., López-Soler, A., Plana, F., Kolker, A., and Chenery, S. R. N.** (2001a) *Determination of Element Affinities by Density Fractionation of Bulk Coal Samples*. *Fuel* v80 p83-96.
- Querol, X., Umaña, J. C., Alastuey, A., Ayora, C., Lopez-Soler, A., and Plana, F.** (2001b) *Extraction of Soluble Major and Trace Elements from Fly-ash in Open and Closed Leaching Systems*. *Fuel* v80 p801-813.
- Querol, X., Whateley, M. K. G., Fernández-Turiel, J. L., and Tuncali, E.** (1997b) *Geological Controls on the Mineralogy and Geochemistry of the Beypazari Lignite, Central Anatolia, Turkey*. *International Journal of Coal Geology*. v33 p255-271.
- Quick, J. C.** (1992) *Fundamental Characterization of New Zealand Bituminous Coal for Prediction of Carbonization Behaviour - with Special Emphasis on Fluorometric Analysis*. University Canterbury 282pp.

- Ramesh, A. and Kozinski, J. A.** (2001) *^{29}Si , ^{27}Al and ^{23}Na Solid-State Nuclear Magnetic Resonance Studies of Combustion-Generated Ash.* Fuel v80 p1603-1610.
- Rao, P. D. and Walsh, D. E.** (1997) *Nature and Distribution of Phosphorous Minerals in Cook Inlet Coals, Alaska.* International Journal of Coal Geology. v33 p19-42.
- Reifenstein, A. P.** (1997) *Transformation of Coal Grains to Coke Microstructure.* Coke Making International. v9 p45-49.
- Ren, D., Zhao, F., Wang, Y., and Yang, S.** (1999) *Distributions of Minor and Trace Elements in Chinese Coals.* International Journal of Coal Geology. v40 p109-118.
- Rentel, K.** (1987) *The Combined Maceral-Microlithotype Analysis for the Characterization of Reactive Inertinites.* International Journal of Coal Geology. v9 p77-86.
- Richaud, R., Herod, AA., and Kandiyoti, R.** (2004) *Comparison of Trace Element Contents in Low-Temperature and High-Temperature Ash from Coals and Biomass.* Fuel v83 p2001-2012.
- Riley, K. W. and Saxby, J. D.** (1986) *Organic Matter and Vanadium in Toolebuc Formation, Northern Eromanga Basin and Southern Carpentaria Basin.* Geological Society of Australia Special Publication. v12 p267-272.
- Riley, K. and Dale, L.** (2000) *Trace Elements in the Coals of the Bowen Basin: Good for Business?* Bowen Basin Symposium 2000 2000
- Rivoldini, A. and Cara, S.** (1992) *Boron Determination in Sulcis Coal Ash by Inductively Coupled Plasma-Optic Emission Spectrometry.* Chemical Geology v98 p317-322.
- Robbins, E. I., D'Agostino, J. P., Carter, V., Fanning, D. S., Gamble, C. J., Ostwald, J., Van Hoven, R. L., and Young, G. K.** (1990) *Manganese Nodules and Microbial Fixation of Oxidised Manganese in the Huntley Meadows Wetland, Fairfax County, Virginia.* p69-70. USGS Research on Energy and Resources - 1990. Program and Abstracts. 1990 US Geological Survey Circular 1060.
- Robbins, E. I., Zielinski, R. A., Otton, J. K., Owen, D. E., Schumann, R. R., and McKee, J. P.** (1990) *Microbially Mediated Fixation of Uranium, Sulphur, and Iron in a Peat-Forming Montane Wetland, Larimer County, Colorado.* p70-71. USGS Research on Energy and Resources - 1990. Program and Abstracts. 1990 US Geological Survey Circular 1060.

- Sakulpitakphon, T., Hower, J. C., Schram, W. H., and Ward, C. R.** (2004) *Tracking Mercury from the Mine to the Power Plant: Geochemistry of the Manchester Coal Bed, Clay County, Kentucky*. *International Journal of Coal Geology* v57 p127-141.
- Sakulpitakphon, T., Hower, J. C., Trimble, A. S., Schram, W. H., and Thomas, G. A.** (2000) *Mercury Capture by Fly-ash: Study of the Combustion of a High-Mercury Coal at a Utility Boiler*. *Energy & Fuels* v14 p727-733.
- Sakurovs, R.** (2000) *Some Factors Controlling the Thermoplastic Behaviour of Coals*. *Fuel*. v79 p379-389.
- Sandhu, S. S., Mills, G. L., and Sajwan, K. S.** (1993) *Leachability of Ni, Cd, Cr, and As from Coal Ash Impoundments of Different Ages on the Savannah River Site*. p165-182. in **Keefer, R. F. and Sajwan, K. S.** eds *Trace Elements in Coal and Coal Combustion Residues*. Lewis Publishers.
- Schwab, A. P.** (1993) *Extractable and Plant Concentrations of Metals in Amended Coal Ash*. p185-211. in **Keefer, R. F. and Sajwan, K. S.** eds *Trace Elements in Coal and Coal Combustion Residues*. Lewis Publishers.
- Seames, W. S. and Wendt, J. O. L.** (2000) *Partitioning of Arsenic, Selenium, and Cadmium during the Combustion of Pittsburgh and Illinois #6 Coals in a Self-Contained Combustor*. *Fuel Processing Technology*. v63 p179-196.
- Seggiani, M., Bardi, A., and Vitolo, S.** (2000) *Prediction of Fly-Ash Size Distribution: A Correlation between the Char Transition Radius and Coal Properties*. *Fuel* v79 p999-1002.
- Senior, C. L., Bool, L. E. III, and Morency, J. R.** (2000) *Laboratory Study of Trace Element Vaporization from Combustion of Pulverised Coal*. *Fuel Processing Technology*. v63 p109-124.
- Senior, C. L., Bool, L. E. III, Srinivasachar, S., Pease, B. R., and Porle, K.** (2000) *Pilot Scale Study of Trace Element Vaporization and Condensation during Combustion of a Pulverised Sub-Bituminous Coal*. *Fuel Process Technology* 63 p149-165.
- Senior, C. L., Sarofim, A. F., Zeng, T., Helble, J. J., and Mamani-Paco, R.** (2000) *Gas-Phase Transformations of Mercury in Coal-Fired Power Plants*. *Fuel Processing Technology*. v63 p197-213.
- Senior, C. L., Zeng, T., Che, J., Ames, M. R., Sarofim, A. F., Olmez, I., Huggins, F. E., Shah, N., Huffman, G. P., Kolker, A., Mroczkowski, S., Palmer, C., and Finkelman, R.** (2000) *Distribution of Trace Elements in Selected Pulverised Coal as a Function of Particle Size and Density*. *Fuel Processing Technology*. v63 p215-241.
- Seredin, V. V.** (1996) *Rare Earth Element-Bearing Coals from the Russian Far East Deposits*. *International Journal of Coal Geology*. v30 p101-129.

- Shearer, J. C., Moore, T. A., Vickridge, I. C., and Deely, J. M.** (1997) *Tephra as a Control on Trace Element Distribution in Waikato Coals*. Author preprint 7th New Zealand Coal Conference. 1997
- Sheng, J., Huang, B. Zhang J., Zhang, H., Sheng, J., Yu, S., and Zhang, M.** (2003) *Production of Glass from Coal Fly-ash*. Fuel v82 p181-185.
- Shi, L. and Xu, X.** (2001) *Study of the Effect of Fly-ash on Desulphurisation by Lime*. Fuel v80 p1969-1973.
- Singh, R. M., Singh, M. P., and Chandra, D.** (1983) *Occurrence, Distribution and Probable Source of the Trace Elements in Ghugus Coals, Warda Valley, Districts Chandrapur and Yeotmal, Maharashtra, India*. International Journal of Coal Geology. v2 p371-381.
- Skinner, B. J. and Porter, S. C.** (1987) *Physical Geology*. John Wiley and Sons. 750pp.
- Sloss, L. L. and Gardner, C. A.** (1995) *Sampling and Analysis of Trace Emissions from Coal-Fired Power Stations*. I.E.A. Coal Research, London. 74pp
- Smith, L.** (1999) *XRD and XRF Analyses of Coal*. James Cook University, Unpublished BSc(hons) Thesis. 66pp
- Smoot, L. D. and Smith, P. J.** (1985) *Coal Combustion and Gasification*. Plenum Press. 443pp.
- Sokol, E. V., Kalugin, V. M., Nigmatulina, E. N., Volkova, N. I., Frenkel, A. E., and Maksimova, N. V.** (2002) *Ferrospheres from Fly-ashes of Chelyabinsk Coals: Chemical Composition, Morphology and Formation Conditions*. Fuel v81 p867-876.
- Spears, D. A.** (1964) *The Major Element Geochemistry of the Mansfield Marine Band in the Westphalian of Yorkshire*. Geochimica et Cosmochimica Acta. v28 p1679-1696.
- Spears, D. A.** (1965) *Boron in Some British Carboniferous Sedimentary Rocks*. Geochimica et Cosmochimica Acta v29 p315-328.
- Spears, D. A., Manzanares-Papayanopoulos, L. I., and Booth, C. A.** (1999) *The Distribution and Origin of Trace Elements in a UK Coal; the Importance of Pyrite*. Fuel. v78 p1671-1677.
- Spears, D. A. and Martinez-Tarazona, M. R.** (1993) *Geochemical and Mineralogical Characteristics of a Power Station Feed-Coal, Eggsborough, England*. International Journal of Coal Geology. v22 p1-20.
- Spears, D. A., Rippon, J. H., and Cavender, P. F.** (1999) *Geological Controls on the Sulphur Distribution in British Carboniferous Coals: a Review and Reappraisal*. International Journal of Coal Geology. v40 p59-81.

- Spears, D. A. and Zheng, Y.** (1999) *Geochemistry and Origin of Elements in some UK Coals*. International Journal of Coal Geology. v38 p161-179.
- Staub, J. R. and Cohen, A. D.** (1978) *Kaolinite-Enrichment Beneath Coals; A Modern Analog, Snuggedy Swamp, South Carolina*. Journal of Sedimentary Petrology. v48 p203-210.
- Steel, K. M. and Patrick, J. W.** (2001) *The Production of Ultra Clean Coal by Chemical Demineralisation*. Fuel v80 p2019-2023.
- Steenari, B.-M., Schelander, S., and Lindqvist, O.** (1999) *Chemical and Leaching Characteristics of Ash from Combustion of Coal, Peat and Wood in a 12MW CFB - a Comparative Study*. Fuel v78 p249-258.
- Su, S., Pohl, J. H., Holcombe, D., and Hart, J. A.** (2001) *A Proposed Maceral Index to Predict Combustion Behavior of Coal*. Fuel v80 p699-706.
- Suggate, R. P.** (1998) *Analytical Variation in Australian Coals Related to Coal Type and Rank*. International Journal of Coal Geology. v37 p179-206.
- Swaine, D. J.** (1989) *Environmental Aspects of Trace Elements in Coal*. Journal of Coal Quality. v8 p67-71.
- Swaine, D. J.** (1990) *Trace Elements in Coal*. Butterworths. 278pp.
- Swaine, D. J.** (1995) *The Contents and some Related Aspects of Trace Elements in Coals*. Chpt 2, p5-23. in **Swaine, D. J. and Goodarzi, F. eds** *Environmental Aspects of Trace Elements in Coal*. Kluwer Academic Publishers.
- Swaine, D. J.** (1995) *The Formation, Composition and Utilisation of Flyash*. Chpt 11, p204-220. in **Swaine, D. J. and Goodarzi, F. eds** *Environmental Aspects of Trace Elements in Coal*. Kluwer Academic Publishers.
- Swaine, D. J. and Goodarzi, F.** (1995) *General Introduction*. Chpt 1, p1-4. in **Swaine, D. J. and Goodarzi, F. eds** *Environmental Aspects of Trace Elements in Coal*. Kluwer Academic Publishers.
- Szalay, A.** (1964) *Cation Exchange Properties of Humic Acids and their Importance in the Geochemical Enrichment of UO_2^{++} and Other Cations*. Geochimica et Cosmochimica Acta. v28 p1605-1614.
- Szalay, A. and Szilágyi, M.** (1967) *The Association of Vanadium with Humic Acids*. Geochimica et Cosmochimica Acta v31 p1-6.
- Szilágyi, M.** (1971) *The Role of Organic Material in the Distribution of Mo, V and Cr in Coal Fields*. Economic Geology v66 p1075-1078.
- Taylor, S. R.** (1964) *Abundance of Chemical Elements in the Continental Crust: A New Table*. Geochimica et Cosmochimica Acta. v28 p1273-1285.

- Teichmüller, M., Littke, R., and Robert, P.** (1998) *Coalification and Maturation*. Chpt 3, p86-174. in **Taylor, G. H., Teichmüller, M., Davis, A., Diessel, C. F. K., Littke, R., and Robert, P.** *Organic Petrology*. Gebrüder Borntraeger.
- Teichmüller, M., Taylor, G. H., Littke, R., and Swaine, D. J.** (1998) *The Nature of Organic Material - Macerals and Associated Minerals*. Chpt 4, p175-274. in **Taylor, G. H., Teichmüller, M., Davis, A., Diessel, C. F. K., Littke, R., and Robert, P.** *Organic Petrology*. Gebrüder Borntraeger.
- Teixeira, E. C., Binotto, R. B., Sanchez, J. D., Migliavacca, D., and Fachel, J. M. G.** (1999) *Environmental Assessment and Characterization of Residues from Coal Processing and Steel Industry Activities*. *Fuel* v78 p1161-1169.
- Thompson, D. and Argent, B. B.** (1999) *Coal Ash Composition as a Function of Feedstock Composition*. *Fuel* v78 p539-548.
- Toole-O'Neil, B., Tewalt, S. J., Finkelman, R. B., and Akers, D. J.** (1999) *Mercury Concentration in Coal - Unraveling the Puzzle*. *Fuel* v78 p47-54.
- Tsai, S. C.** (1982) *Fundamentals of Coal Beneficiation and Utilization*. Elsevier 375pp
- Underwood, E. J.** (1977) *Trace Elements in Human and Animal Nutrition*. Academic Press. 545pp.
- United States Environmental Protection Agency** (1992) *Toxicity Characteristic Leaching Procedure*. Method 1311 35pp
- Urban, N. R., Eisenreich, S. J., Grigal, D. F., and Schurr, K. T.** (1990) *Mobility and Diagenesis of Pb and ²⁴⁰Pb in Peat*. *Geochimica et Cosmochimica Acta*. v54 p3329-3346.
- Valkovic, V.** (1983a) *Trace Elements in Coal. Volume I*. CRC Press. pp210.
- Valkovic, V.** (1983b) *Trace Elements in Coal. Volume II*. CRC Press. pp281.
- Van Der Flier-Keller, E. and Bartier, P.** (1993) *Application of Geographic Information Systems to Interpretation of Coal Geochemistry Data*. *International Journal of Coal Geology*. v24 p293-308.
- Van Der Flier-Keller, E. and Fyfe, W. S.** (1986) *Geochemistry of Two Cretaceous Coal-Bearing Sequences: James Bay Lowlands, Northern Ontario, and Peace River Basin, Northeast British Columbia*. *Canadian Journal of Earth Sciences*. v24 p1038-1052.
- Van Krevelen, D. W.** (1993) *Coal. Typology - Physics - Chemistry - Constitution*. Elsevier pp979
- Various** (1974) *The Book of Popular Science*. Grolier International Inc.

- Vassilev, S. V., Braekman-Danheux, C., Laurent, Ph., Thiemann, T., and Fontana, A.** (1999) *Behaviour, Capture and Inertization of Some Trace Elements During Combustion of Refuse-Derived Char from Municipal Solid Waste*. *Fuel* v78 p1131-1145.
- Vassilev, S. V., Eskenazy, G. M., and Vassileva, C. G.** (2000a) *Contents, Modes of Occurrence and Origin of Chlorine and Bromine in Coal*. *Fuel* v79 p903-921.
- Vassilev, S. V., Eskenazy, G. M., and Vassileva, C. G.** (2000b) *Contents, Modes of Occurrence and Behaviour of Chlorine and Bromine in Combustion Wastes from Coal-Fired Power Stations*. *Fuel* v79 p923-937.
- Vickridge, I. C., Sparks, R. J., and Bibby, D. M.** (1990) *Nuclear Microprobe Studies of Boron and Calcium Distributions in Waikato Coals, New Zealand*. *Fuel* v69 p660-662.
- Vuthaluru, H. B.** (1999) *Remediation of Ash Problems in Pulverised Coal-Fired Boilers*. *Fuel*. v78 p1789-1803.
- Wadge, A. and Hutton, M.** (1986) *The Uptake of Cadmium, Lead and Selenium by Barley and Cabbage Grown in Soils Ammended with Refuse Incinerator Fly-ash*. *Plant and Soil* v96 p407-412.
- Wang, J. and Tomita, A.** (2003) *A Chemistry on the Volatility of Some Trace Elements during Coal Combustion and Pyrolysis*. *Energy & Fuels* v17 p954-960.
- Ward, C.** (1980) *Mode of Occurrence of Trace Elements in some Australian Coals*. *Coal Geology* v2 p77-98.
- Ward, C. R.** (2002) *Analysis and Significance of Mineral Matter in Coal Seams*. *International Journal of Coal Geology* v50 p135-168.
- Ward, C. R., Corcoran, J. F., Saxby, J. D., and Read, H. W.** (1996) *Occurrence of Phosphorous Minerals in Australian Coal Seams*. *International Journal of Coal Geology*. v30 p185-210.
- Ward, C. R., Spears, D. A., Booth, C. A., Staton, I., and Gurba, L. W.** (1999) *Mineral Matter and Trace Elements in Coals of the Gunnedah Basin, New South Wales, Australia*. *International Journal of Coal Geology*. v40 p281-308.
- Ward, C. R. and Taylor, J. C.** (1996) *Quantitative Mineralogical Analysis of Coals from the Callide Basin, Queensland, Australia using X-Ray Diffractometry and Normative Interpretation*. *International Journal of Coal Geology*. v30 p211-229.
- Weinstein, L. H., Arthur, M. A., Schneider, R. E., Woodbury, P. B., Laurence, J. A., Beers, A. O., and Rubin, G.** (1993) *Uptake of Chemical Elements by Terrestrial Plants Growing on Coal Fly-ash Landfill*. p213-237. in **Keefer, R. F. and Sajwan, K. S. eds** *Trace Elements in Coal and Coal Combustion Residues*. Lewis Publishers.

- White, R. N., Smith, J. V., Spears, D. A., Rivers, M. L., and Sutton, S. R.** (1989) *Analysis of Iron Sulphides from UK Coal by Synchrotron Radiation X-Ray Fluorescence*. Fuel v68 p1480-1486.
- Willett, J. C., Finkelman, R. B., Palmer, C. A., Kolker, A., and Belkin, H. E.** (2003) *Analysis of Selective Leaching Residues of Four U.S. Coals*. CD-ROM 20th Annual International Pittsburgh Coal Conference. Sept 15th - 19th. Pittsburgh, Pennsylvania, U.S.A.
- Wood, J. M.** (1974) *Biological Cycles for Toxic Elements in the Environment*. Science. v183 p1049-1052.
- Woolfe, K. J., Crosdale, P. J., and Slater, R.** (1996) *Mire Death in the Bowen to Scott-Dennison Interval, Collinsville Coal Measures, Queensland*. Australian Journal of Earth Sciences. v43 p91-96.
- Wu, B., Peterson, T. W., Shadman, F., Senior, C. L., Morency, J. R., Huggins, F. E., and Huffman, G. P.** (2000) *Interactions between Vapor-Phase Mercury Compounds and Coal Char in Synthetic Flue Gas*. Fuel Processing Technology v63 p93-107.
- Wu, H., Wall, T., Guisu, L., and Bryant, G.** (1999) *Ash Liberation from Included Minerals during Combustion of Pulverised Coal: the Relationship with Char Structure and Burnout*. Energy & Fuels - an American Chemical Society Journal. v13 p1197-1202.
- Yan, L., Gupta, R. P., and Wall, T. F.** (2001a) *The Implication of Mineral Coalescence Behaviour on Ash Formation and Ash Composition During Pulverised Coal Combustion*. Fuel v80 p1333-1340.
- Yan, L., Gupta, R., and Wall, T.** (2001b) *Fragmentation Behavior of Pyrite and Calcite during High-Temperature Processing and Mathematical Simulation*. Energy & Fuels v15 p389-394.
- Yan, R., Gauthier, D., Flamant, G., and Badie, J. M.** (1999) *Thermodynamic Study of the Behaviour of Minor Coal Elements and their Affinities to Sulphur During Coal Combustion*. Fuel. v78. p1817-1829.
- Yee, H. S., Measures, C. I., and Edmond, J. M.** (1987) *Selenium in the Tributaries of the Orinoco in Venezuela*. Nature v326 p686-689.
- Yoshida, T., Iino, M., Takanohashi, T., and Katoh, K.** (2000) *Study on Thermoplasticity of Coals by Dynamic Viscoelastic Measurement: Effect of Coal Rank and Comparison with Gieseler Fluidity*. Fuel. v79. p399-404.
- Zeng, H., Jin, F., and Guo, J.** (2004) *Removal of Elemental Mercury from Coal Combustion Flue Gas by Chloride-Impregnated Activated Carbon*. Fuel v83 p143-146.
- Zhang, J. Y., Zheng, C. G., Ren, D. Y., Chou, C.-L., Liu, J., Zeng, R. S., Wang, Z. P., Zhao, F. H., and Ge, Y. T.** (2004) *Distribution of Potentially Hazardous Trace Elements in Coals from Shanxi Province, China*. Fuel v83 p129-135.

Zheng, B., Ding, Z., Huang, R., Zhu, J., Yu, X., Wang, A., Zhou, D., Mao, D., and Su, H. (1999) *Issues of Health and Disease Relating to Coal Use in Southwestern China*. International Journal of Coal Geology. v40 p119-132.

Zhuang, X., Querol, X., Zeng, R., Xu, W., Alastuey, A., Lopez-Soler, A., and Plana, F. (2000) *Mineralogy and Geochemistry of Coal from the Liupanshui Mining District, Guizhou, South China*. International Journal of Coal Geology v45 p21-37.

Zimmerman, R. E. (1979) *Evaluating and Testing the Coking Properties of Coal*. Miller Freeman Publications Inc. 144pp.

Zodrow, E. I., Banerjee, S. K., and Jessome, D. R. (1987) *Uranium Content and Distribution in Whole-Coal Samples, Sydney Coalfield (Upper Carboniferous), Nova Scotia, Canada*. International Journal of Coal Geology. v8 p299-303.

Zubovic, P., Stadnichenko, T., and Sheffey, N. B. (1961) *Chemical Basis of Minor-Element Associations in Coal and Other Carbonaceous Sediments*. United States Geological Society Professional Paper 424D D345-D348.

Appendix 1

Health Effects of Trace Elements

Introduction.

Appendix 1 presents some data on the health impacts of the four groups of environmentally significant elements set out in Table 1.2. (Swaine and Goodarzi, 1995; Zhang et al., 2004). It should be noted that “health impact” is not anthropocentric in nature, and any negative impact on any part of the biosphere is generally viewed as undesirable by local, regional and national authorities as well as by the public. Any emphasis on human health impacts in this document are, therefore, merely a reflection of the literature reviewed.

Many of the trace elements listed as potentially environmentally deleterious if they are concentrated to toxic levels by coal utilisation are essential in low concentrations for the growth and well being of plants and animals. There is potential for trace elements from coal combustion waste to provide environmentally useful by-products if managed properly. However, predicting the toxicity of an element in the biosphere is not a simple matter of presence, or indeed of elemental concentration. An organism’s diet, source of exposure, synergistic and antagonistic element interactions, elemental speciation and tolerance variations between species all play an important role in determining any adverse effects caused by element absorption. Further, some poisons such as lead are cumulative so environmental and health impacts may not be immediately apparent.

The source of much of Appendix 1 is Underwood (1977), with other references cited in-text.

Antimony.Comments.

Antimony has no known function in living organisms and is not considered by Underwood (1977) as being among the more toxic elements.

Toxic effects.

Bowen (1966) suggests insoluble sulphides such as antimony sulphide are toxic by virtue of their reactivity with proteins and enzymes. Toxicity may lead to a slight decrease in lifespan or some suppression of growth.

Arsenic.

Comments.

Arsenic is distributed through out tissues and fluids of the body in very low concentrations (hair often has higher contents). Deficiency may cause impairment of growth and development. Arsenic may be beneficial in that the action of the element resembles that of antibiotics. The form of the arsenic is important. For example organically-bound arsenic is rapidly absorbed and rapidly eliminated; AsO_3 is also easily absorbed but more is retained.

Toxic Effects.

Arsenic is thought to inhibit the activity of a wide range of enzyme systems, but variability in the susceptibility of individuals is high. Gupta (1999) suggests that the toxicity of trivalent arsenic is higher than that of pentavalent arsenic. The general toxicity effects of arsenic are; direct inhibition of cellular respiration, mutagenic effects, and haemolysis (Krishna De, 1996). Arsine gas causes rapid haemolysis and potentially long term renal damage. Arsenite (As^{3+}) is absorbed from the digestive tract and may accumulate to high levels in tissues. Organoarsenils can cause toxicity to the liver and kidney (Krishna De, 1996). Symptoms of arsenic poisoning include nausea, vomiting, diarrhoea, burning of the mouth and throat, and severe abdominal pains. Recent reports show ingestion of high concentrations of arsenic is responsible for skin lesions, skin and liver cancers, and probably bladder and kidney cancers (Centano et al., 2000). Smaller toxic doses result in weakness, prostration, and muscular aching with few gastrointestinal changes. Skin and mucosal changes often develop with peripheral neuropathy and linear pigmentations in the fingernails. Headache, drowsiness, confusion, and convulsions are seen in both acute and chronic As intoxication. Studies found arsenic poisoning led to loss of hearing in children (Bencko and Symon, 1977b) and that burning of high arsenic coal had reduced or entirely excluded bee populations over affected areas (Bencko and Symon, 1977a).

Synergism/ Antagonism.

Arsenic has been reported to have antagonistic interactions with selenium, decreasing retention and increasing secretion of Se from the liver into the bile.

Barium.Comments.

While there is no evidence of an essential function in living organisms, a deficiency may cause growth suppression. Barium is poorly absorbed from food.

Toxic Effects.

Barium is thought to have a low toxicity by the oral route [also (Bowen, 1966)] with no observable effects on longevity, body weight, or the incidence of tumours. Bowen (1966) suggests a possible mode of toxic action of barium might be by forming a stable precipitate or chelate with essential metabolates. It was also suggested by Bowen (1966) that barium may replace structurally- or electrochemically-important elements in the cell, leading to loss of function.

Beryllium.

Bowen (1966) lists the cation Be^{2+} as very toxic; Swaine (1990) states “beryllium is potentially a toxic element”. It was suggested by Bowen (1966) that beryllium may replace structurally- or electrochemically-important elements in the cell, causing a loss of function. Inhalation of insoluble BeO may also lead to lung damage.

Boron.Comments.

Boron is known to be essential in higher land plants but no evidence was found for any requirement by animals. Boron is rapidly and almost completely absorbed from food and excreted. Very high intakes may cause temporary retention in tissues producing serious toxic effects.

Toxic Effects.

The most probable toxic environmental impact is on the health of plants [also (Clark et al., 1999; Valkovic, 1983b)]. Swaine (1990) suggested, “relatively small excesses may cause harm in some situations”, with susceptibility being species specific.

Cadmium.Comments.

Cadmium is virtually absent in humans at birth and accumulates up to the age of about 50 years old, the levels reflecting dietary intake. Ash enriched in cadmium from coal combustion may fall on plants and be incorporated into plant tissues at a concentration factor of three to seven (Keller, 1992). Cadmium may be further concentrated up the food chain (biomagnification). Cadmium is characterised by a lack of a homeostatic control mechanism and is tenaciously retained in the body. The element has powerful interactions with other divalent metals both during absorption and in tissues, particularly the liver and kidneys. Cadmium is poorly absorbed from most diets, but may be better absorbed from the lungs following inhalation depending on its physical state.

Synergism/ Antagonism.

There is competition between cadmium and the elements zinc and mercury. Cadmium may also depress the absorption of copper, iron, cobalt, and calcium. Cadmium may promote loss of calcium from the body, with bone losses noted in studies of rats. High intakes of zinc and selenium may give some protection against cadmium poisoning.

Toxic Effects.

Cadmium is toxic to virtually every system in animal's bodies, whether ingested, injected, or inhaled. Changes to the kidneys, liver, gastrointestinal tract, heart, reproductive system, pancreas, and blood system have been observed. Hepatic protein bound cadmium has been associated with emphysema and other chronic pulmonary diseases without unusual contact with cadmium. Cadmium has also been found to induce hypertension in rats, rabbits, and dogs. Bowen (1966) suggests cadmium may combine with the membrane of a cell, affecting its permeability.

Chlorine.

Chlorine is well known as a toxic gas, having been used by the Germans during World War I. Bowen (1966) listed chlorine as one of the elements that may combine with the cell membrane affecting its permeability, or replace structurally or electrochemically important elements in the cell thus destroying their function. Much

of the interest in chlorine is due to the corrosion of the combustion plant caused by its combining with hydrogen to form corrosive HCl.

Chromium.

Comments.

Chromium is widely distributed in humans, concentration declining with age except in the lungs. The concentration variations found in human liver and kidneys were presumed to reflect differences in Cr intake. Inorganic chromium is poorly absorbed in animals and man regardless of dose. Hexavalent Cr is better absorbed (by a factor of two) than trivalent Cr. Deficiency is characterised by impaired growth and longevity, and by disturbances in glucose, lipid, and protein metabolism. Corneal defects may also result from deficiency.

Synergism/ Antagonism.

Zinc deficiency in rats was found to cause increased absorption of chromium.

Metabolic antagonism between chromium and vanadium has been noted.

Toxic Effects.

Hexavalent Cr is 100 times more toxic than trivalent Cr (Gupta, 1999). Other authors note that Cr^(VI) is both toxic and carcinogenic, and is also more soluble than Cr^(III) (Huggins et al., 1999). Exposure to chromite dust has been correlated with a greater incidence of lung cancer. Chromite taken orally in doses of 50ppm has been associated with growth depression and liver and kidney damage in experimental animals. Gupta (1999) lists symptoms of chromium poisoning as allergic skin irritations, dermatitis, irritation to mucus membranes, conjunctiva, gastrointestinal ulcers, and chrome holes (penetrating ulcers around the fingernails, eyelids, and occasionally forearms).

Cobalt.

Comments.

Cobalt appears to be required for the synthesis of Vitamin B12. Deficiency causes emaciation, listlessness, and decreased metabolic efficiency. Vitamin B12 contains about 4% cobalt (Krishna De, 1996). Excessive of cobalt causes coronary failure and disfunction of the thyroid (Krishna De, 1996).

Synergism/ Antagonism.

Cobalt absorption is significantly increased in rats and man when the diet is deficient in iron due to the mutual antagonism between Fe and Co absorption.

Toxic Effects.

Excessive accumulation mainly occurs in the liver, kidneys, and bones. Bowen (1966) lists Co^{2+} as a very toxic element, and suggests it might form very stable chelates with amino, imino, and sulphhydryl groups, thereby blocking the activity of these compounds. Chronic exposure to cobalt at high concentrations has been found to cause goitre (Gupta, 1999).

Copper.

Comments.

Copper is an element essential for good health, being involved in many vital functions in the body, eg assists in formation of haemoglobin, regulating oxidation-reduction enzymes, etc (Krishna De, 1996). Concentration in tissues is variable. Deficiency causes anaemia, impaired absorption of iron, skeletal abnormalities, nervous disorders, lack of pigmentation in hair and wool, infertility, cardiovascular disorders, and diarrhoea. Newborn and very young animals are often rich in copper compared to adults.

Synergism/ Antagonism.

Copper interacts with zinc, iron, cadmium, and molybdenum. Molybdenum and manganese combine to severely limit copper retention.

Toxic Effects.

Excess consumption leads to some accumulation of copper, especially in the liver; decreased food intake and growth rate; anaemia; jaundice; liver disease; and brain disease. As noted for cobalt, Bowen (1966) suggests copper may form very stable chelates with amino, imino, and sulphhydryl groups, thereby blocking the activity of these compounds. In this regard, copper's toxicity is second only to mercury. Inhalation of airborne copper may cause irritation of the respiratory tract and metal

fume fever (Gupta, 1999). Copper is also lethal to green algae at 0.01ppm (Bowen, 1966).

Fluorine.

Comments.

Fluorine concentration in tissues is low, with the element tending to concentrate in bones and teeth. Soluble fluorides are rapidly and almost completely absorbed from the gastrointestinal tract, even at high intakes. Small quantities of insoluble fluoride can be almost as well absorbed as the soluble fluorides. The absorbed fluorine is rapidly distributed through the body and rapidly lost from the blood due to uptake by the skeleton and excretion. Fluorine is important for growth and reproduction, and may help prevent dental decay and increase the strength of bones.

Toxic Effects.

Fluorosis may be exhibited by dental deformation or mottling of teeth, skeletal fluorosis (changes in bone structure), mineralisation of tendons, limited movement of joints, bow legs, knock-knees, spinal curvature (Dai et al., 2004), inhibition of lipase activity so fatty acid utilization is blocked, and lack of appetite. Fluorine may also form highly acidic HF in combustion processes.

Lead.

Comments.

Underwood (1977) suggested there was some evidence for an essential role for lead in the diet but more data was required.

Synergism/ Antagonism.

Absorption and retention of lead is greatly affected by the dietary intake of calcium, phosphorous, iron, copper, and zinc. Subnormal intakes of calcium and phosphorous increase lead retention in body tissues; retention decreases as calcium is increased from below to above requirements. Lowering of phosphorous intake similarly increased lead retention. The effects of calcium and phosphorous on lead retention are additive. The symptoms of lead toxicity are exacerbated in rats with an iron deficiency. Absorption of lead is greater than Co or Mn absorption induced by the same iron deficiency. High concentrations of lead appear to reduce copper levels in

the body. It is possible that increased levels of zinc and lead together enhance the toxicity of lead compared to the same concentration of lead alone.

Toxic Effects.

Lead is a cumulative poison so it may take a protracted period of exposure at lower concentrations for toxicity to become apparent. Lead poisoning is characterised by neurological affects (encephalopathy and neuropathy), particularly in children with low tolerance to lead. Symptoms of brain damage are reduced brain growth, hyperactivity, and behavioural disturbance. Lead poisoning may also cause renal tubular dysfunction and anaemia. According to Gupta (1999) symptoms may begin with anorexia, muscle discomfort, malaise, and headache, as well as gastrointestinal effects. Chronic CNS effects (lead encephalopathy) may include symptoms such as clumsiness, vertigo, headache, insomnia, restlessness, and irritability. As the condition progresses, the patient may become confused and lethargic followed by coma. Other symptoms include an ashen colour to the face, stooped posture, poor muscle tone, and emaciation. Lead poisoning affects pregnancy, lactation and menopause and lead is hazardous to the foetus. Historians have suggested that lead poisoning may have led to the demise of the Roman Empire. Lead was used by the Romans in pots for processing grape juice into syrup, in cups for drinking, in cosmetics, in medicines, and to pipe water to houses. High lead contents in the bones of ancient Romans supports this hypothesis (Keller, 1992).

Mercury.

Comments.

Mercury is distributed widely in all tissues (particularly in kidneys), and occurs widely in the biosphere. The metabolic behaviour of mercury varies depending on the chemical form of the element presented to the animal, interactions with other elements, and the genetic make up of the animal.

Synergism/ Antagonism.

There is metabolic antagonism between mercury and selenium.

Toxic Effects.

Mercury is highly toxic and poisoning has been found among goldsmiths, mirror makers, and furriers (the term 'mad as a hatter' derives from the neurological effects on furriers using mercuric nitrate to treat furs). Subacute poisoning causes neurological changes manifested as tremors with vertigo, moodiness and depression along with salivation, stomatitis, and diarrhoea. Alkyl derivatives such as methyl mercury are even more toxic, and result in progressive loss of coordination, loss of vision and hearing, and mental deterioration arising from toxic neuroencephalopathy in which the nerve cells of the cerebral and cerebellar cortex are selectively involved. Methyl mercury can also be transferred via the placenta to the foetus, resulting in congenital defects (Minamata disease). Minamata disease takes its name from the widespread congenital defects caused by consuming fish from Minamata Bay, Japan, which had been polluted by the dumping of mercury-laden industrial wastes.

Manganese.

Comments.

A manganese deficiency causes impaired growth, skeletal abnormalities, disturbed or impaired reproductive function, atonia of the newborn, and defects in lipid and carbohydrate metabolism. The degree and expression of deficiency symptoms is species dependant.

Synergism/ Antagonism.

Manganese competes with iron and cobalt for uptake, so manganese absorption is increased or decreased with deficiency or excesses of these two elements. Manganese deficiency may be aggravated by excessive dietary intake of calcium. High intake of manganese may interfere with retention of phosphorous.

Toxic Effects.

A high intake of manganese may retard growth and depress appetite in growing pigs and calves. Anaemia may result from the antagonism of manganese with iron. In humans, manganese may enter the body as an oxide dust or via the gastrointestinal tract from contaminated environments. The lungs may act as a point from which manganese is continuously absorbed. Manganese poisoning in humans is characterised by severe psychiatric disorder (locura manganis), which resembles

schizophrenia, followed by permanently crippling neurological disorder clinically similar to Parkinson's disease. The manganese psychosis is characterised by "uncontrollable laughter, euphoria, impulsiveness, sexual excitement followed by impotency and speech disability" (Gupta, 1999).

Molybdenum.

Comments.

Molybdenum is present in low concentrations in all tissues and fluids of the body. Molybdenum is essential for growth and may assist fluoride in preventing tooth decay. The toxicity of the element depends on the species, age of individual, chemical form, and element interactions of the molybdenum.

Synergism/ Antagonism.

High levels of sulphate and tungstate reduce the retention of molybdenum. Copper interferes with molybdenum uptake and visa versa. A ratio of copper to molybdenum of 2:1 in plants is thought to cause molybdenosis (toxic excesses) in grazing animals (Keefer et al., 1993; Schwab, 1993). Manganese can also block or antagonise the limiting affect of Mo on copper retention. Calcium and phosphorous may enhance the uptake of molybdenum by plants in some circumstances (Keefer et al., 1993).

Toxic Effects.

Bowen (1966) suggests insoluble sulphides such as molybdenum sulphide are toxic by virtue of their reactivity with proteins and enzymes. Excess molybdenum causes growth retardation, loss of body weight, diarrhoea, alopecia, dermatosis, anaemia, limb deformity, deficient lactation, male sterility, degradation of connective tissues, and interference with some enzyme and thyroxine activities. Molybdenosis due to high Mo causes depletion of Cu in the liver and blood of sheep and cattle (Baker et al., 1993).

Nickel.

Comments.

Nickel is present in low concentrations in all animal tissues and fluids. Dietary nickel is poorly absorbed. Deficiency causes pigmentation changes, dermatitis, friable liver, excessive accumulation of the element in the liver, bones and aorta, impaired growth

and reproductive performance, liver changes, decreased cholesterol, delayed sexual maturity, and anaemia.

Synergism/ Antagonism.

Decreased nickel causes anaemia due to decreased retention of iron. Rhenium may interact with nickel.

Toxic Effects.

Krishna De (1996) suggests that “abnormally high levels of dietary nickel are required to cause toxicity in humans” and is, therefore, not a “practical consideration for man”. Ingestion may cause eczema. Dermatitis caused by nickel in jewellery and other items is relatively common, and dermatitis among workers has been blamed on exposure to nickel in refineries. Nickel may affect the respiratory tract (causing neoplasia). Nickel has also been implicated as a pulmonary carcinogen in tobacco smoke and nickel dust may also be carcinogenic. Gupta (1999) lists the symptoms of nickel poisoning as “asthma, CNS effects, gastrointestinal effects, headache, neoplasia of lung and respiratory tract”. The most serious type of poisoning is caused by inhalation of nickel carbonyl (Krishna De, 1996). Nickel carbonyl is an airborne industrial effluent that can cause nausea, dizziness, headache, and chest pains in 1-5 days, and severe pulmonary symptoms, tachycardia and extreme weakness; death may follow in 4-13 days.

Phosphorous.

Phosphorous is vital to all living things, is found in brain and nerve tissue, and is important in bone formation and muscle action. The amount of phosphorous present in the body must be in proper proportion to calcium for normal bone formation to occur. Phosphorous also plays an essential role in plant development (Various, 1974). Bowen (1966) notes that P absorbed via the lungs is highly toxic; a fact historically substantiated by the bone diseases of the match girls in London in the 1800's. However, Swaine (1990) suggests that ‘environmental problems from P in coal are not to be expected, but levels of P in coke are of prime importance in steel making’.

Selenium.

Comments.

Selenium occurs in all the cells and tissues of the animal body in concentrations that vary with the tissue and the level and form of Se in the diet. The liver and kidneys contain the most Se. Interaction with other elements also influences the retention of Se. Toxicity studies suggest that Se is most readily absorbed via seleniferous grains, with low absorption of selenites and selenates and very low absorption from selenides and elemental Se. Selenium is essential for growth and prevention of various diseases conditions including muscular dystrophy (degenerative muscle diseases), exudative diathesis (haemorrhages arising from abnormal permeability of capillary walls), pancreatic atrophy, poor immune system response, and reproductive disorders. Research suggests Se may protect against cancer, with studies of 10 cities with populations of 40,000-70,000 showing a high inverse relationship ($R = 0.96$) between blood Se levels and human cancer death rates. Krishna De (1996) notes “the action of selenium may be related vitamin E as the two substances appear to act synergistically in curing the hepatic disease, breast cancer, hypertension and certain muscle disorders induced in animals”. It has also been reported that a proper combination of vitamin E and selenium prevents ageing.

Synergism/ Antagonism.

Selenium has a strong tendency to complex with heavy metals, therefore Se metabolism is influenced by the dietary intake of several such elements. There is metabolic antagonism between Se and both Hg and Ag. The dietary levels of arsenic, silver, mercury, copper, and cadmium may modify the toxicity of Se, with each element apparently exerting protection action by its own mechanism. Sulphur and selenium are antagonistic in plant nutrition (Weinstein et al., 1993).

Toxic Effects.

There is a very narrow range between selenium deficiency and toxicity (Herring, 1990). Selenosis in grazing animals results in “alkali disease” and “blind staggers”, which are expressions of chronic and acute Se toxicity, respectively. Se poisoning in stock animals is characterised by dullness, lack of vitality, emaciation and roughness of coat, loss of hair, soreness and sloughing hoofs, stiffness and lameness due to the erosion of the joints of long bones, atrophy of the heart, cirrhosis of the liver, and

anaemia. Acute Se poisoning may also lead to blindness, abdominal pain, salivation, grating of the teeth, and some degree of paralysis. Respiration is disturbed and death results from respiration failure, starvation, and thirst. Toxicity varies according to species and diet. Some plants concentrate Se; others mirror the Se content of the soil but alter the form of the element making it more available for absorption.

Silver.

Comments.

Silver is present in very low concentrations in soil, plants, and animal tissues. Underwood (1977) states that there is no evidence for an essential role for silver in living organisms, and that it is not ranked among the more toxic elements.

Synergism/ Antagonism.

Silver interacts with selenium and copper. Silver is the strongest copper antagonist (followed by Cd, Mo, Zn, and sulphate in decreasing order), so a high Ag diet will accentuate a Cu deficiency.

Toxic Effects.

Bowen (1966) suggests insoluble sulphides such as silver sulphide are toxic by virtue of their reactivity with proteins and enzymes. Bowen also states that silver is notably poisonous to fungal spores. Underwood (1977) suggests cardiac enlargement is produced by a high silver diet.

Thallium.

Swaine (1990) notes the interest in thallium in coal is “probably because of the known toxic properties of Tl compounds”. He further notes, “there used to be a rat poison containing Tl, which was administered once to remove a recalcitrant husband”. Bowen (1966) suggests insoluble sulphides such as thallium sulphide are toxic by virtue of their reactivity with proteins and enzymes.

Thorium.

Thorium is of interest biologically and environmentally because of its radioactivity (Swaine, 1990).

Tin.Comments.

Tin is an essential nutrient for growth and is present in low concentrations in human and animal tissues. Tin may accumulate in high concentrations where food is in contact with tin plate unless the container is resin coated. Tin is poorly absorbed and retained by humans.

Toxic Effects.

Consumption of food with a high concentration of tin may cause some gastrointestinal disturbance. Subacute tin poisoning resulted in reduced growth, feed efficiency, and haemoglobin levels when the dietary intake of Fe and Cu were low. Bowen (1966) states that tin is lethal to green algae at concentrations of 0.02ppm. Bowen also notes that inhalation of insoluble particles of SnO₂ and volatile forms of Sn may cause lung damage and allow absorption of tin to toxic levels.

Uranium.

Uranium is of interest biologically and environmentally because of its radioactivity (Swaine, 1990).

Vanadium.Comments.

Vanadium is widely distributed in animal tissues, but little is known of its role in the metabolism of organisms. Deficiency causes impaired growth, reproduction, and disturbed lipid metabolism. Vanadium may also be required for mineralization of bones, teeth and in reducing tooth decay.

Synergism/ Antagonism.

Vanadate inhibits uptake of chromate by respiring mitochondria and visa versa (mutual antagonism).

Toxic Effects.

Vanadium is relatively toxic (Underwood, 1977; Valkovic, 1983b), and may induce growth depression. Toxicity may be completely prevented by EDTA, which apparently inhibits V absorption from the gastrointestinal tract. Diet composition is also important in the uptake of V.

Zinc.

Comments.

Zinc is an essential nutrient (Swaine, 1990), and is distributed throughout human tissues, with 20% of zinc found in the skin. Deficiency causes growth retardation (caused by impaired DNA synthesis and cell division), nutritional dwarfism, hypogonadism, loss of taste acuity and disordered taste, alopecia, skin lesions, facial eczema, skeletal abnormalities, limb deformities, and stiffness. A deficiency of Zn during brain development permanently affects brain function. Zinc deficiencies may also cause a “variety of plant diseases causing low yields, poor seed development and even total crop loss” (Keller, 1992).

Synergism/ Antagonism.

High calcium intake protects sheep from the toxic effects of a high zinc diet (see below). Zinc may antagonise copper and iron metabolism (particularly if the dietary contents of these two elements are low), and may also antagonise Cd.

Toxic Effects.

Anaemia may result from a high Zn diet with subnormal contents of iron, copper, cytochrome oxidase, and catalase in the diet. Sheep and cattle are less tolerant than some other species and may exhibit excessive salt consumption, wood chewing and mild anaemia. Toxicity is species dependant, with some plants adapted to grow in areas of high zinc concentration (Bowen, 1966). Bowen (1966) suggests zinc may form very stable chelates with amino, imino, and sulphhydryl groups, thereby blocking the activity of these compounds.

Appendix 2

Mode of Occurrence of Trace Elements in Coal

Introduction.

The modes of occurrence for elements of environmental significance is reviewed. In an attempt to provide a more visual indication of the relative dominance or likelihood of the various modes of occurrence found for each element, the modes of occurrence have been “scored” as follows: a) for a paper with one mode of occurrence noted for an individual element, a score of 1 is given for that mode; b) for a paper where several modes of occurrence are listed, the scores are divided equally among the modes to sum to 1, eg for a paper where three modes of occurrence are noted, each mode gets a score of 1/3 unless, c) for paper which uses a qualifier such as “mainly” or “mostly” a higher score is given to the main mode of occurrence, eg if a paper lists two modes of occurrence for an element, the “main” mode gets a score of 2/3, the other mode a score of 1/3. Following scoring, all the scores for each mode were summed and calculated to a percentage of the total score for all modes for the element in question. The score percentages are then represented as bar charts following each literature list.

Antimony.

Organically bound - (Goodarzi and Swaine, 1993) (and in sulphides), (Lyons et al., 1989) (or inorganically bound), (Palmer et al., 1998) (also sulphides and silicates), (Palmer et al., 1999) (also pyrite and silicates), (Swaine, 1990) (or in various sulphides).

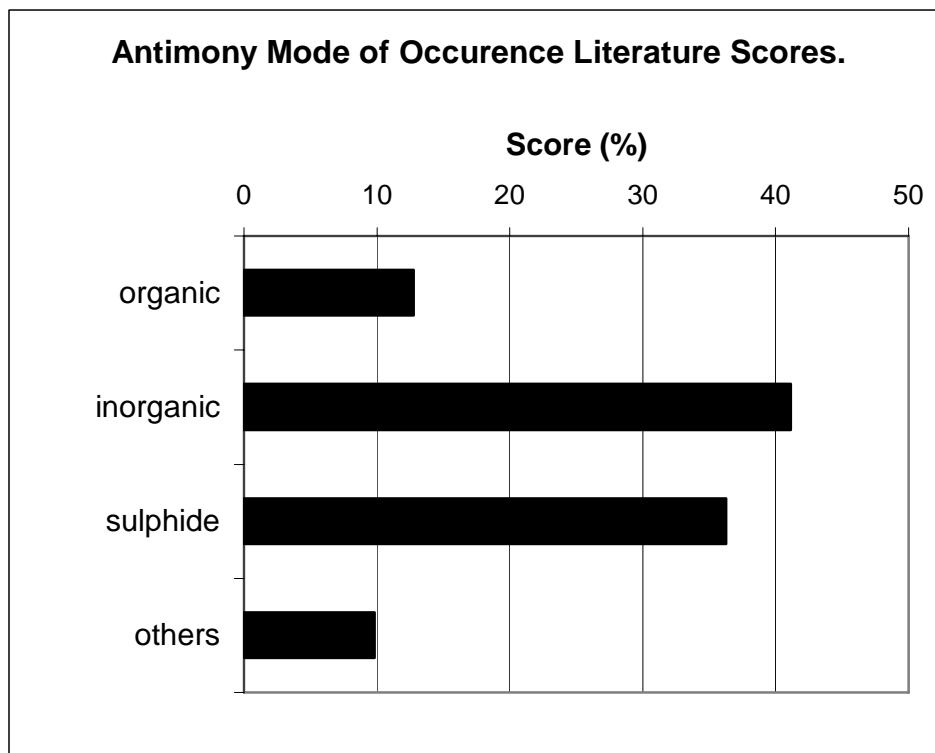
Inorganically bound - (Beaton et al., 1991), (Crowley et al., 1997), (Goodarzi, 1988), (Goodarzi, 1987b), (Grieve and Goodarzi, 1993) (and inorganic, probably sulphides), (Lyons et al., 1989) (and organic), (Shearer et al., 1997) (??).

Sulphide bound - (Alastuey et al., 2001), (Finkelman, 1995), (Palmer et al., 1998) (also organic and silicates), (Palmer et al., 1999) (pyrite) (also organics and silicates), (Querol et al., 1995), (Spears and Zheng, 1999), (Spears et al., 1999), (Swaine, 1990).

Others - (Palmer et al., 1998) (silicates) (also sulphides and organic), (Palmer et al., 1999) (silicates) (also organics and pyrite), (Querol et al., 1997b) (zeolites).

Finkelman (1995) suggests that antimony may be bound into pyrite or accessory sulphides, but gives this indication a low (4/10) level of confidence. A number of published studies find that antimony is bound into sulphides, particularly if the inorganic indications are included as a sulphide mode of occurrence. Some authors

suggest that antimony may also be organically bound. A number of researchers analyse for antimony but do not indicate a mode of occurrence, perhaps due to the low concentration of this element in many coals. The scoring of the modes of occurrence indicates inorganic (unspecified) and sulphides modes dominate.



Arsenic.

Organically bound - (Goodarzi, 1988), (Goodarzi, 1987b) (low rank coal) (NB the graphs for the two Goodarzi papers appear to conflict with stated results, ie they appear to indicate an inorganic mode of occurrence), (Goodarzi and Van Der Flier-Keller, 1988), (Huggins and Huffman, 1996) (at low ranks), (Karayigit et al., 2001), (Kolker et al., 2000) (dominantly pyrite, some arsenate), (Lyons et al., 1989) (or sulphate), (Palmer et al., 1999) (also pyrite), (Senior et al., 2000) (also pyrite).

Inorganically bound - (Beaton et al., 1991), (Crowley et al., 1997), (Goodarzi, 1987c), (Helle et al., 2000), (Shearer et al., 1997).

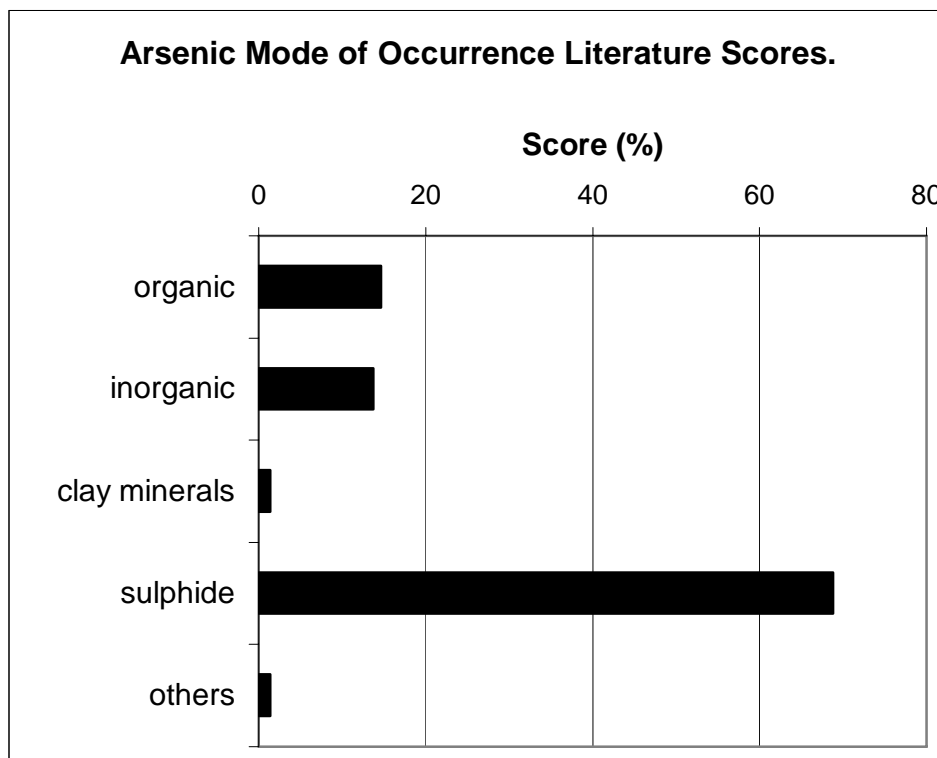
Clay bound - (Van Der Flier-Keller and Fyfe, 1986) (and sulphides)

Sulphide (pyrite) bound - (Alastuey et al., 2001), (Beaton et al., 1993), (Bouska, 1981), (Finkelman, 1995), (Gayer et al., 1999), (Goodarzi and Swaine, 1993), (Goodarzi and Van Der Flier-Keller, 1988) (arsenopyrite), (Grieve and Goodarzi,

1993), (Hower et al., 1996), (Huggins and Huffman, 1996) (or organically bound at low rank), (Kolker et al., 2000) (also organic & some arsenate), (Lyons et al., 1989) (or organically bound), (Mukhopadhyay et al., 1996), (Mukhopadhyay et al., 1998), (Palmer and Filby, 1984), (Palmer and Lyons, 1996), (Palmer et al., 1998) (some arsenates?), (Palmer et al., 1999) (also organic), (Pierce and Stanton, 1990), (Querol et al., 1995), (Querol et al., 1997b) (?) (also zeolites?), (Querol et al., 1999b), (Senior et al., 2000) (also organic), (Spears and Zheng, 1999), (Swaine, 1990) (but notes others possible), (Spears et al., 1999), (Van Der Flier-Keller and Fyfe, 1986) (or clay bound), (Ward et al., 1999), (White et al., 1989).

Others - (Querol et al., 1997b) (zeolites?) (also pyrite?).

Finkelman (1995) gives a level of confidence of 8/10 that arsenic will be present as sulphides; recent research has apparently increased confidence in this inference (Kolker and Finkelman, 1998). The literature search appears to support Finkelman's view, particularly if the inorganically bound elements are assumed to be sulphide bound. It also appears possible that arsenic may be organically bound at low ranks, although the graphs and conclusions of the two Goodarzi papers noted above require clarification.



Barium.

Organically bound - (Beaton et al., 1991) (? Intermediate affinity), (Bouska, 1981) (also barite and clays), (Casagrande and Erchull, 1977) (in peats), (Lyons et al., 1989) (& inorganic, local controls), (Miller and Given, 1986) (partly) (lignites), (Miller and Given, 1987) (dominantly) (lignites), (Mukhopadhyay et al., 1998) (and inorganic), (Spears and Martinez-Tarazona, 1993), (Van Der Flier-Keller and Fyfe, 1986).

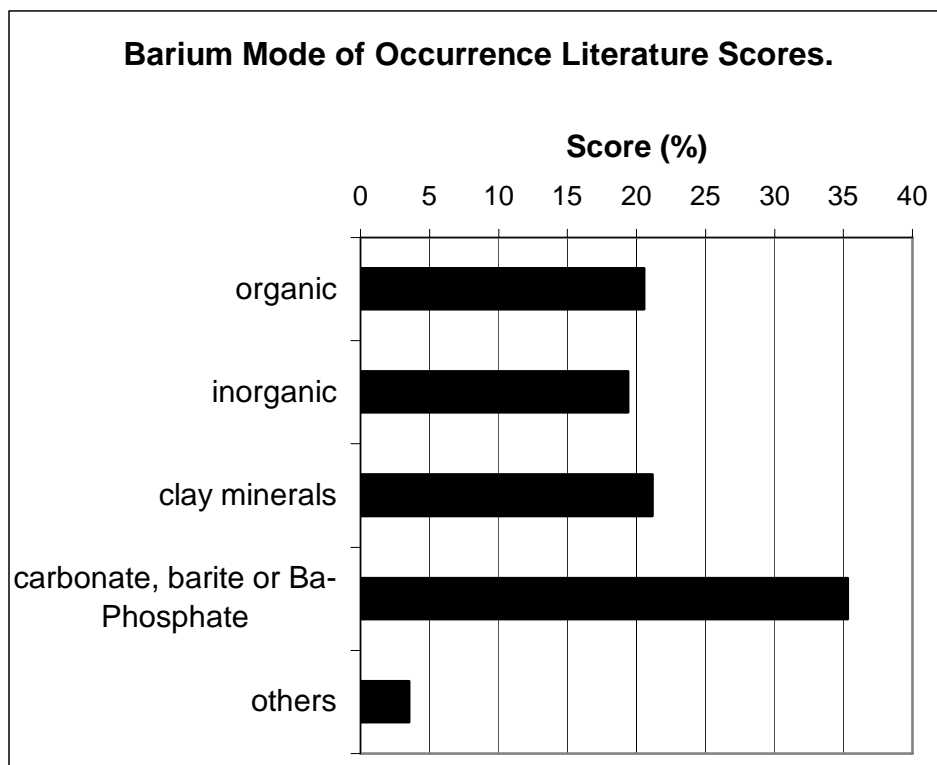
Inorganically bound - (Beaton et al., 1991), (Ghosh et al., 1987) (authigenic), (Ghosh et al., 1987) (detrital or authigenic?), (Goodarzi and Van Der Flier-Keller, 1989) (volcanoclastics), (Karayigit et al., 2001), (Lyons et al., 1989) (& organic), (Mukhopadhyay et al., 1998) (mixed organic).

Clay bound - (Bouska, 1981), (Palmer and Filby, 1984) (mainly), (Querol et al., 1995) (& feldspars?), (Querol et al., 1997a) (aluminosilicates), (Querol et al., 1999b) (aluminosilicates), (Singh et al., 1983) (silicate minerals).

Carbonate, Barite or Ba- Phosphate bound - (Bouska, 1981) (barite), (Finkelman, 1995) (barite & other accessory minerals), (Hower and Bland, 1989) (carbonates), (Laban and Atkin, 1999) (barite or gorceixite) (some in carbonates and organically bound), (Miller and Given, 1986) (sulphate, carbonate), (Palmer and Lyons, 1996) (barite or barium phosphates), (Palmer et al., 1999), (Hower et al., 1996) (carbonates), (Seredin, 1996) (crandallite minerals), (Ward et al., 1999) (goyazite – gorceixite - crandallite).

Others - (Querol et al., 1997b) (zeolites).

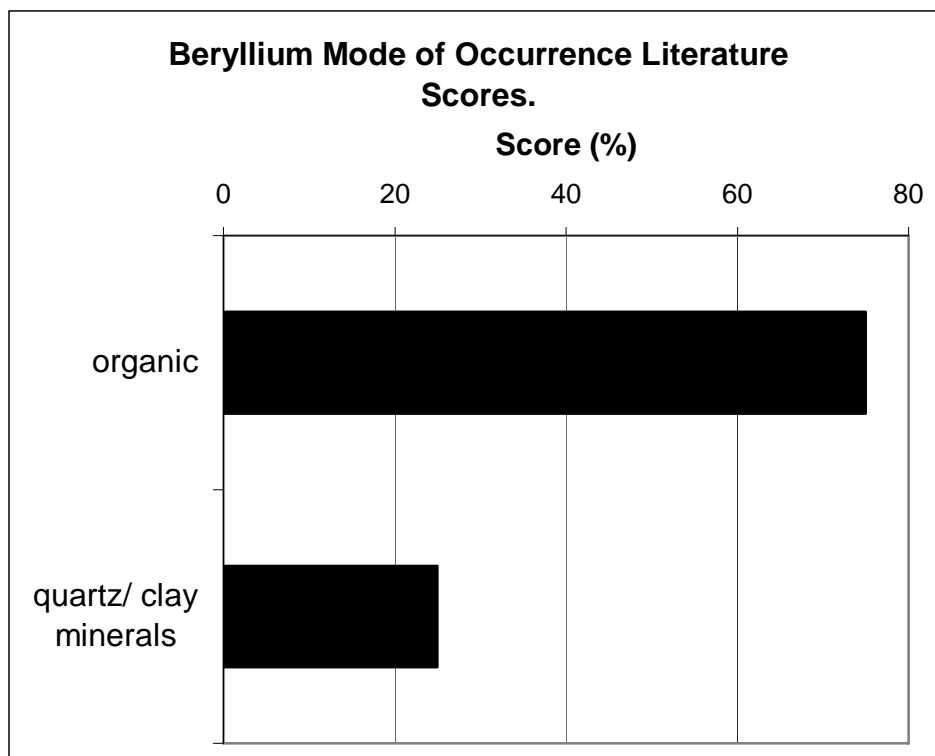
Barium has been inferred or found to occur in a variety of modes of occurrence. Definitive indications as to the type of inorganic association would be more useful in determining a general trend, but the carbonate/ barite or Ba phosphate category appears to dominate. Finkelman (1995) suggested that barium occurs as barite or other Ba bearing minerals, giving the mode of occurrence a confidence of 6/10.



Beryllium.

Organically bound - (Asuen, 1987), (Bouska, 1981), (Crowley et al., 1997), (Finkelman, 1995), (Miller and Given, 1986) (lignites), (Mukhopadhyay et al., 1998), (Palmer et al., 1999) (also organics), (Querol et al., 1995), (Querol et al., 1997b), (Swaine, 1990) (some quartz & clay associations possible), (Valkovic, 1983a).
Quartz/ clay minerals - (Singh et al., 1983), (Palmer et al., 1998) (silicates?), (Palmer et al., 1999) (also organics), (Querol et al., 1997a) (aluminosilicates).

Zubovic et al (Zubovic et al., 1961) found that Be^{2+} forms very stable organic compounds. It is, therefore, not surprising that beryllium has been generally interpreted as bound to the organic fraction of the coal. Finkelman (1995) rates the confidence in the mode of occurrence as only 4/10 because of the lack of direct evidence (the low atomic number of the element makes it undetectable by XRF and like methods).



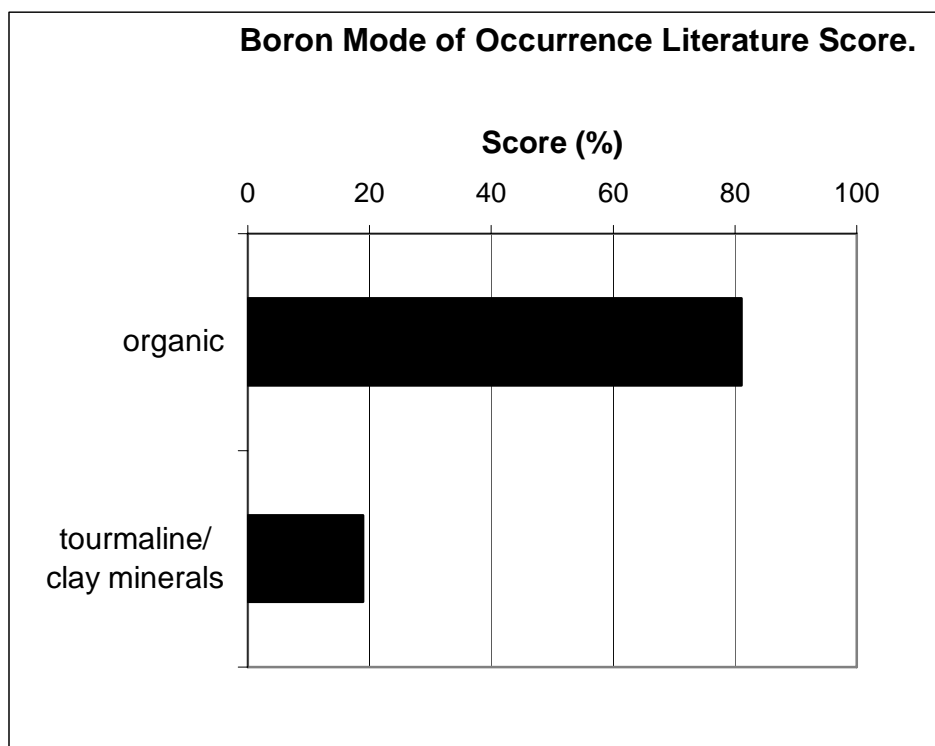
Boron.

Organically bound - (Alastuey et al., 2001), (Beaton et al., 1991), (Bouska, 1981) (becoming inorganic with increase in rank), (Eskenazy et al., 1994) (some in illite/muscovite), (Finkelman, 1995), (Goodarzi, 1987b), (Goodarzi, 1987c), (Goodarzi, 1988), (Goodarzi and Van Der Flier-Keller, 1988), (Grieve and Goodarzi, 1993) (?), (Helle et al., 2000), (Lyons et al., 1989) (mainly), (Newman et al., 1997), (Querol et al., 1995) (and tourmaline), (Querol et al., 1997b), (Querol et al., 1997a), (Querol et al., 1999b) (also aluminosilicates), (Shearer et al., 1997), (Swaine, 1990) (sometimes clay or tourmaline), (Valkovic, 1983a), (Vickridge et al., 1990), (Ward, 1980) (sometimes in clay).

Tourmaline/Clay bound - (Bohor and Gluskoter, 1973) (illites + others?), (Eskenazy et al., 1994) (but mainly organically bound), (Mukhopadhyay et al., 1998) (tourmaline or illite), (Querol et al., 1995) (tourmaline) (and organic), (Querol et al., 1999b) (also organically bound), (Zhuang et al., 2000).

Finkelman (1995) gave the organic mode of occurrence for boron a confidence level of 6/10, and most of the authors listed have indicated that boron is bound into the organic fraction of the coal. However boron does have a strong affinity for illite

(Spears, 1964) and the use of graphing methods could misinterpret the mode of occurrence if the clay minerals were disseminated throughout the organic fraction.



Cadmium.

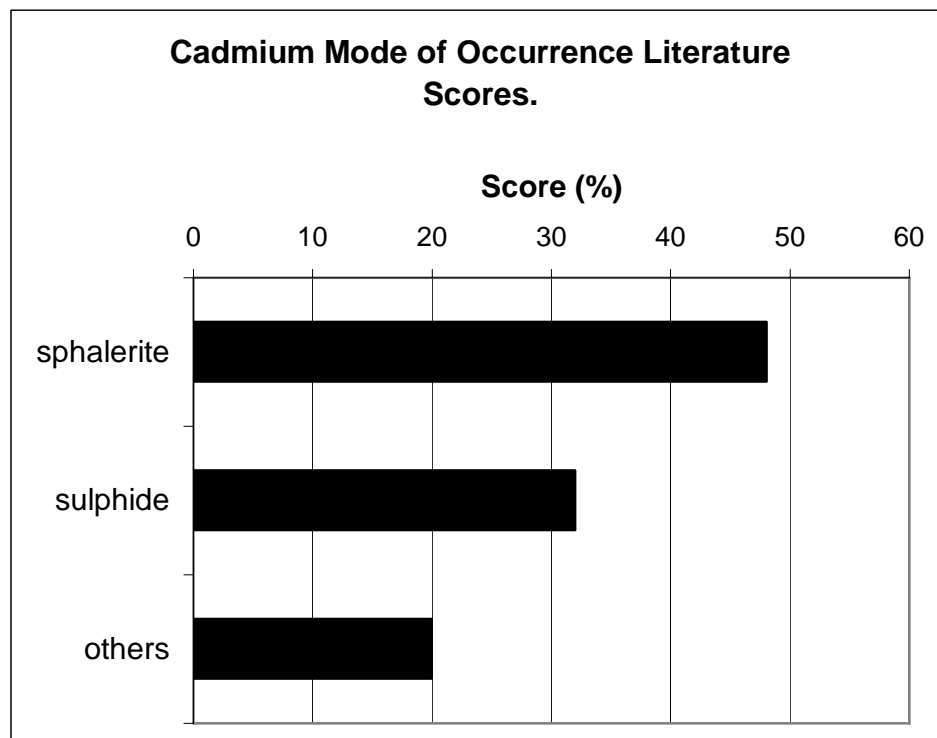
Sphalerite bound - (Bouska, 1981), (Finkelman, 1995), (Gluskoter and Lindahl, 1973), (Grieve and Goodarzi, 1993) (?), (Hatch et al., 1976), (Mukhopadhyay et al., 1998) (mixed), (Palmer et al., 1998) (some in pyrite), (Palmer et al., 1999) (some in organics), (Swaine, 1990) (but also notes some clay, carbonate, pyrite and organic associations).

Sulphide bound - (Alastuey et al., 2001), (Pierce and Stanton, 1990), (Palmer et al., 1998) (mostly in sphalerite), (Querol et al., 1995), (Querol et al., 1999b), (Van Der Flier-Keller and Fyfe, 1986).

Others - (Crowley et al., 1997) (inorganic), (Karayigit et al., 2001) (inorganically bound), (Palmer et al., 1999) (organic) (mostly sphalerite), (Querol et al., 1997b) (zeolites).

Finkelman (1995) gives a confidence level of 8/10 for a sphalerite mode of occurrence for cadmium, the Cd substituting for Zn in the mineral lattice. This

literature review supports Finkelman's confidence level, but notes the potential for a number of other minor modes of occurrence.



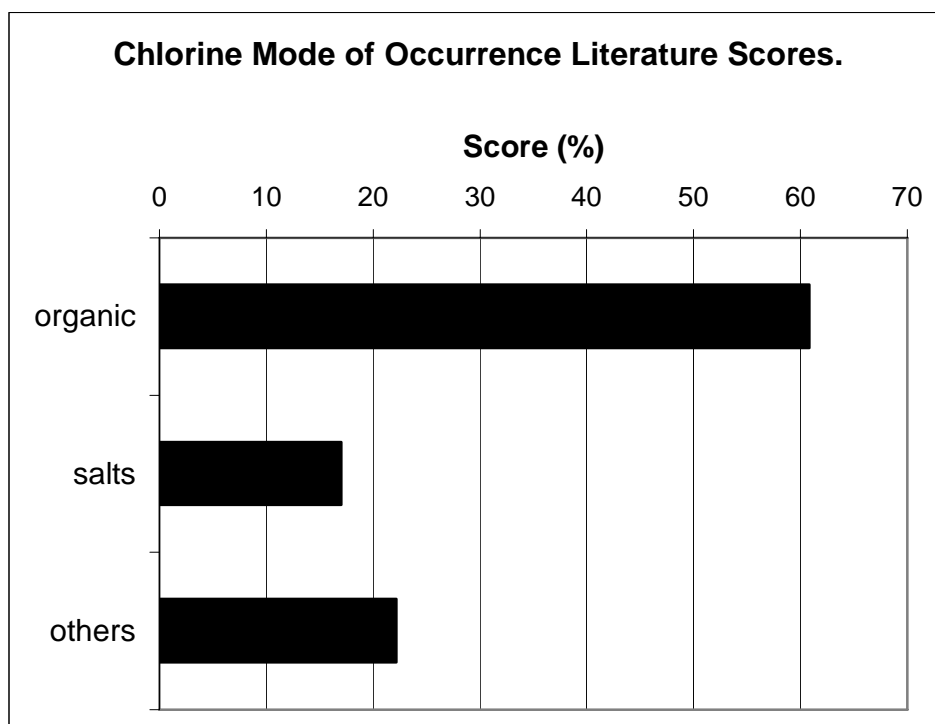
Chlorine.

Organically bound - (Beaton et al., 1991) (intermediate affinity, some correlation with carbonates?), (Caswell et al., 1984) (or as salt), (Finkelman, 1995) (adsorbed to macerals or as chloride ions), (Gluskoter and Ruch, 1971) (or as salt), (Goodarzi, 1987b), (Goodarzi, 1987a), (Goodarzi, 1988), (Grieve and Goodarzi, 1993), (Mukhopadhyay et al., 1998), (Jiménez et al., 1999), (Shearer et al., 1997), (Swaine, 1990) (or as chloride ions), (Van Der Flier-Keller and Fyfe, 1986), (Vassilev et al., 2000a), (Ward, 1980).

Salt bound - (Bouska, 1981), (Caswell et al., 1984) (or organically bound), (Elms et al., 1987), (Gluskoter and Ruch, 1971), (Jiménez et al., 1999) (?) (mostly organic).

Others - (Finkelman, 1995) (chloride ions), (Huggins and Huffman, 1996) (chloride ions), (Seredin, 1996) (F/Cl carbonates), rare earth element phosphates, (Spears and Zheng, 1999) (Na & Cl in pore waters, no speciation specified), (Vassilev et al., 2000a) (impurity components in crystalline & amorphous inorganic constituents, in the fluid constituents and as discrete minerals).

In the past the accepted modes of occurrence of chlorine have been inorganic chlorides, most commonly sodium, potassium, and calcium chlorides, but possibly also magnesium and iron chlorides, and adsorbed to macerals (Finkelman, 1995; Gluskoter and Ruch, 1971). More recently, Huggins and Huffman (1996), using XAFS spectroscopy, have suggested that chlorine is present as “chloride anions in the moisture associated with the macerals and not as specific mineral chlorides nor as organochlorine compounds”. They suggest chloride ions are the one major mode of occurrence in virtually all coals regardless of rank and geographic location! Finkelman (1995) gave a confidence level of 6/10 that chlorine is present as chloride ions in pore water or adsorbed onto macerals. If Huggins and Huffman (1996) are correct, this analysis may need to be reviewed.



Chromium.

Organically bound - (Bouska, 1981), (Casagrande and Erchull, 1976) (in peats), (Casagrande and Erchull, 1977) (in peats), (Finkelman, 1995) (also inorganic/chromites), (Ghosh et al., 1987) (mixed), (Huggins and Huffman, 1996) (and bound to clays), (Laban and Atkin, 1999) (also silicates), (Lyons et al., 1989) (and inorganic), (Miller and Given, 1986) (lignites), (Palmer et al., 1998) (mostly in clays), (Palmer et

al., 1999) (some in clays, rare in chromites), (Senior et al., 2000) (also silicates), (Swaine, 1990) (also in clays/ chromites), (Szilágyi, 1971) (late stage enrichment).
Inorganically bound - (Beaton et al., 1991)(?), (Crowley et al., 1997), (Finkelman, 1995) (also organic and chromite), (Ghosh et al., 1987) (mixed), (Goodarzi, 1987b), (Goodarzi, 1988), (Goodarzi and Van Der Flier-Keller, 1988), (Goodarzi and Van Der Flier-Keller, 1989), (Grieve and Goodarzi, 1993), (Helle et al., 2000), (Laban and Atkin, 1999) (silicates) (also organically bound), (Lyons et al., 1989) (or organically bound), (Mukhopadhyay et al., 1998) (clays?), (Shearer et al., 1997), (Ward, 1980) (some organic).

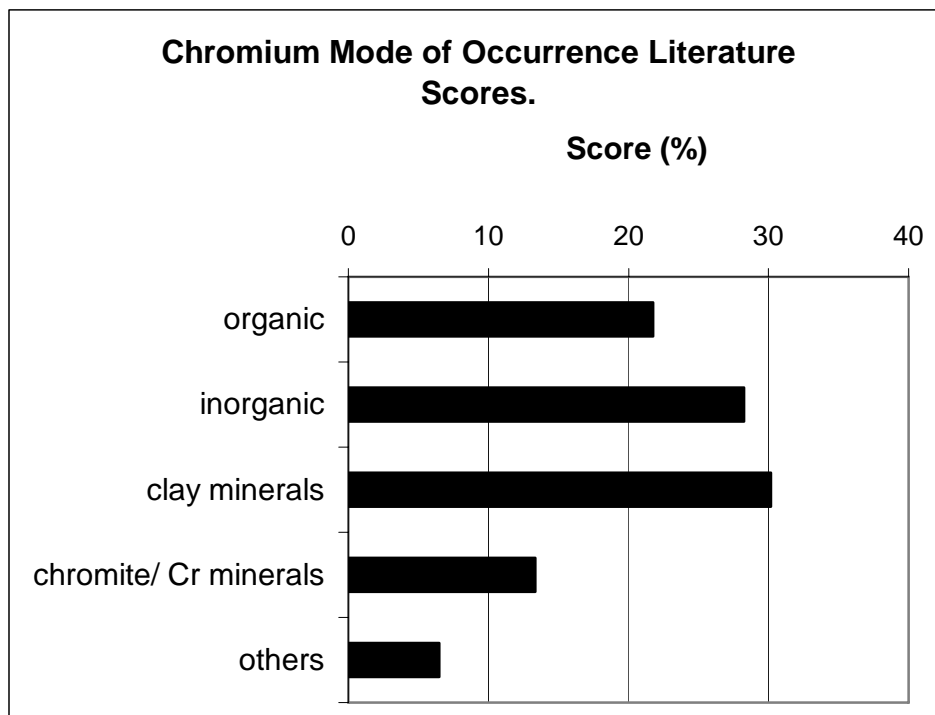
Clay bound - (Alastuey et al., 2001), (Asuen, 1987), (Hower and Bland, 1989), (Hower et al., 1996) (or chromite), (Huggins and Huffman, 1996) (and in chromites or organically bound), (Kolker and Finkelman, 1998) (also in amorphous CrO(OH) and Cr bearing spinels), (Palmer and Filby, 1984), (Palmer and Lyons, 1996), (Palmer et al., 1998) (some in organics), (Palmer et al., 1999) (much in organics, some in chromites), (Querol et al., 1995) (and feldspars), (Querol et al., 1997a) (aluminosilicates), (Querol et al., 1999b) (aluminosilicates), (Singh et al., 1983) (terrigenous ash material, clay qtz etc), (Spears and Zheng, 1999), (Swaine, 1990) (or organically bound), (Van Der Flier-Keller and Fyfe, 1986) (or chromite?).

Chromite/ Cr bearing minerals - (Brownfield et al., 1995), (Finkelman, 1995) (or organically/ inorganically bound), (Hower et al., 1996) (or clays), (Huggins and Huffman, 1996) (or clays/ organically bound), (Kolker and Finkelman, 1998) (also in amorphous CrO(OH) and Cr bearing spinels) (also in illite), (Palmer et al., 1999) (also organics and clays), (Pollock et al., 2000) (chromite/ magnetite), (Swaine, 1990) (or with clays or organically bound), (Van Der Flier-Keller and Fyfe, 1986) (or with clays), (Ward et al., 1999) (Cr bearing minerals??).

Others - (Senior et al., 2000) (silicates) (also organically bound), (Kolker and Finkelman, 1998) (amorphous CrO(OH) (also Cr spinels and illite), (Li et al., 2001) (croicoite), (Querol et al., 1997b) (zeolites).

Finkelman (1995) gives a very poor 2/10 level of confidence in an organic or clay mode of occurrence of chromium. However, it has been suggested that recent work has increased confidence that chromium occurs in illite, or as Cr spinels or as an amorphous CrO(OH) (Kolker and Finkelman, 1998). The indication of organic or inorganic affinity described in many papers does not assist in solving the problem.

For example could the apparent organic affinity be due to finely dispersed chromites; is the inorganic affinity due to chromium in chromites or clay minerals? Finkelman (1995) [see also (Finkelman, 1980)] noted that the mode of occurrence for chromium was poorly understood at that time. Although recent work (Kolker and Finkelman, 1998) has perhaps given some greater confidence, this literature search suggests there is no clear dominant mode of occurrence for chromium.



Cobalt.

Organically bound - (Beaton et al., 1991) (intermediate affinity), (Casagrande and Erchull, 1976) (in peats), (Crowley et al., 1997), (Finkelman, 1995) (at low ranks), (Ghosh et al., 1987) (woody parts), (Laban and Atkin, 1999) (also some present in clays, sulphides and carbonates), (Lyons et al., 1989) (mainly inorganically bound), (Palmer et al., 1999), (Singh et al., 1983), (Swaine, 1990) (also linnaeite, clays & sulphides), (Ward, 1980).

Inorganically bound - (Grieve and Goodarzi, 1993), (Helle et al., 2000), (Hower and Bland, 1989), (Karayigit et al., 2001), (Lyons et al., 1989) (some organically bound), (Shearer et al., 1997).

Sulphide bound - (Bouska, 1981) (also clays), (Finkelman, 1995) (some in clays and organics), (Goodarzi, 1987b) (?) (or carbonates?), (Laban and Atkin, 1999) (also

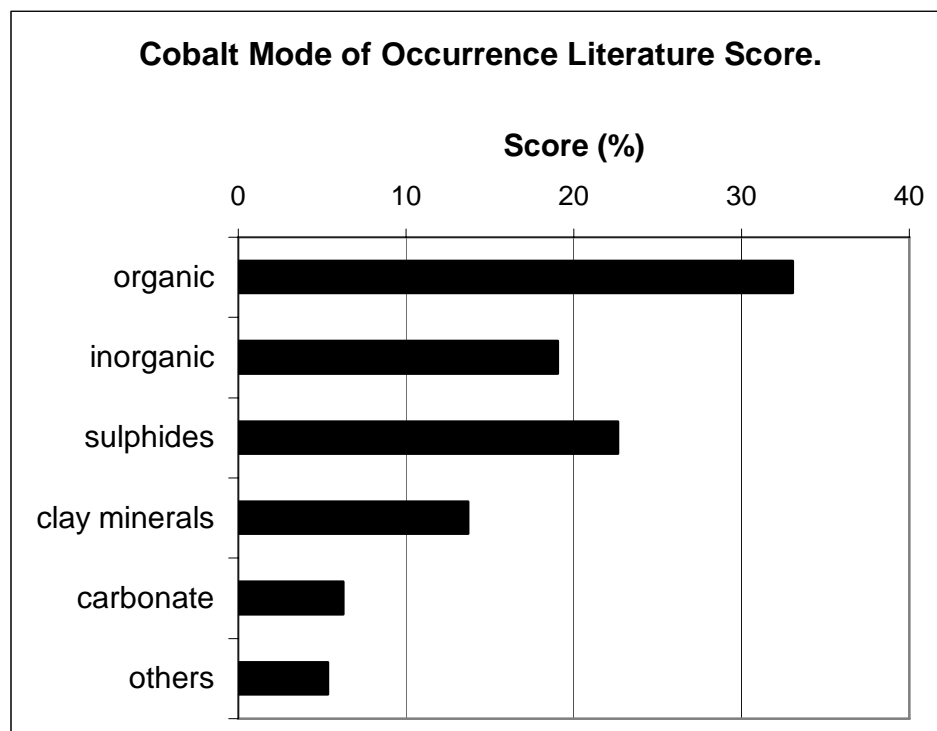
organically bound and in clay minerals and carbonates), (Palmer and Lyons, 1996) (pyrite) (or clays), (Palmer et al., 1998) (pyrite?), (Palmer et al., 1999), (Querol et al., 1995), (Querol et al., 1999b), (Swaine, 1990) (also linnaeite, clays and organically bound).

Clay bound - (Alastuey et al., 2001), (Bouska, 1981), (Finkelman, 1995) (also sulphides and organically bound), (Hower et al., 1996) (also chromites), (Laban and Atkin, 1999) (also organically bound, and in sulphides and carbonates) (Palmer and Lyons, 1996) (illite) (also pyrite), (Swaine, 1990) (also linnaeite, sulphides, organically bound).

Carbonate bound - (Goodarzi, 1987b) (?) (or sulphides?), (Laban and Atkin, 1999) (also organically bound & in sulphides and clay minerals), (Ward et al., 1999)(siderite).

Others - (Hower et al., 1996) (chromites) (or clays), (Querol et al., 1997b) (zeolites).

Finkelman (1995) gives a low confidence level of only 4/10 for the modes of occurrence of cobalt. This low confidence is reflected in the broad range of occurrence modes found in the published literature reviewed here.



Copper.

Organically bound - (Asuen, 1987), (Bouska, 1981) (some in pyrite), (Casagrande and Erchull, 1977) (in peats), (Ghosh et al., 1987) (or chalcopyrite), (Hower and Bland, 1989) (mixed organic/ inorganic?), (Miller and Given, 1986) (lignites), (Palmer et al., 1999) (also silicates in pyrite/ chalcopyrite), (Querol et al., 1997a) (also aluminosilicates), (Swaine, 1990) (and chalcopyrite), (Van Der Flier-Keller and Fyfe, 1986) (and clay minerals/ sulphides).

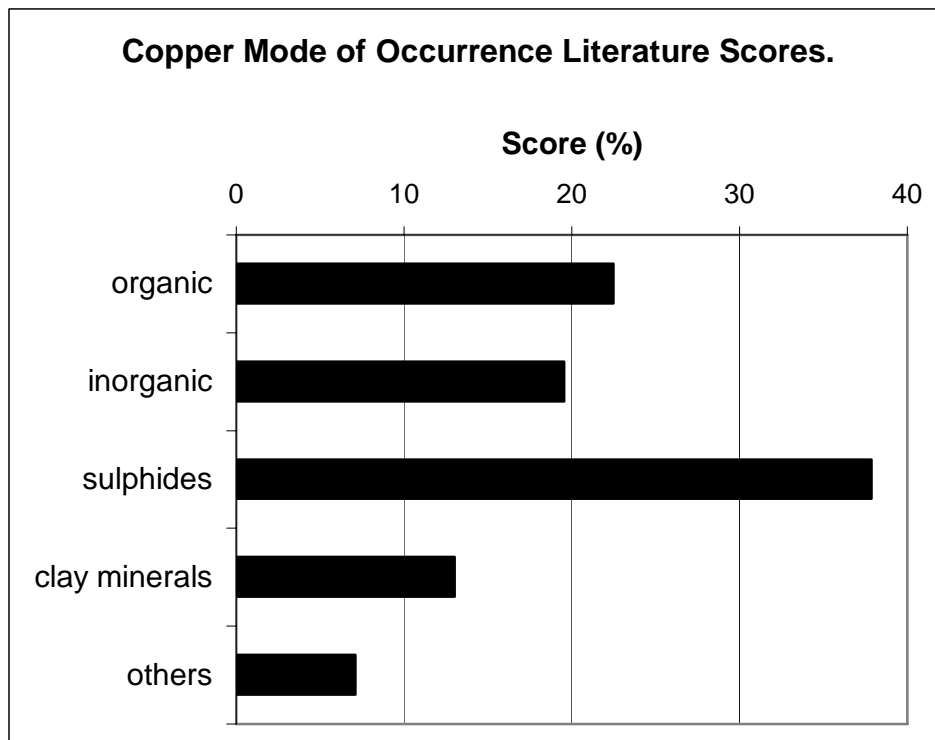
Inorganically bound - (Dilles and Hill, 1984), (Grieve and Goodarzi, 1993), (Helle et al., 2000), (Hower and Bland, 1989) (mixed organic/ inorganic?), (Karayigit et al., 2001), (Lyons et al., 1989).

Sulphide bound - (Bouska, 1981) (pyrite) (and organically bound), (Beaton et al., 1993), (Finkelman, 1995) (chalcopyrite), (Gayer et al., 1999) (solid solution in pyrite), (Ghosh et al., 1987) (chalcopyrite) (or organically bound), (Laban and Atkin, 1999) (and in clay minerals), (Mukhopadhyay et al., 1998) (sulphides), (Palmer et al., 1999) (pyrite/ chalcopyrite) (also organic and silicates), (Singh et al., 1983) (pyrites), (Spears and Martinez-Tarazona, 1993) (pyrite), (Swaine, 1990) (chalcopyrite) (or organically bound), (Spears et al., 1999), (Van Der Flier-Keller and Fyfe, 1986) (sulphides) (also in clay minerals or organically bound), (Ward, 1980) (sulphides), (White et al., 1989) (sulphides).

Clay mineral bound - (Alastuey et al., 2001), (Laban and Atkin, 1999) (and in sulphides), (Palmer et al., 1999) (silicates) (also pyrite/ chalcopyrite and organics), (Querol et al., 1995) (clay minerals and feldspars), (Querol et al., 1997a) (also organic), (Van Der Flier-Keller and Fyfe, 1986) (also sulphides/ organically bound).

Others - (Karayigit et al., 2000) (copper chlorides), (Querol et al., 1997b) (zeolites).

Finkelman (1995) gave a high 8/10 confidence level in a chalcopyrite mode of occurrence for copper. The literature research supports this confidence, particularly if some of the inorganically bound copper, and some of the copper in pyrite, is present as chalcopyrite.



Fluorine.

The mode of occurrence of fluorine is not well understood at present. The following authors suggest fluorine mode of occurrence may be: apatite (Bouska, 1981); apatites, fluorites, amphiboles, clays & micas (Finkelman, 1995); fluorapatite (Grieve and Goodarzi, 1993); F/Cl carbonates (Seredin, 1996); inorganic (concentrated in tephra layers) (Shearer et al., 1997); fluorapatite, fluorite, clays, micas, minor organically bound (Swaine, 1990).

Finkelman (1995) states the mode of occurrence for fluorine is various minerals, and gives a confidence level of 5/10, the mode of occurrence apparently highly specific to the deposit concerned.

Lead.

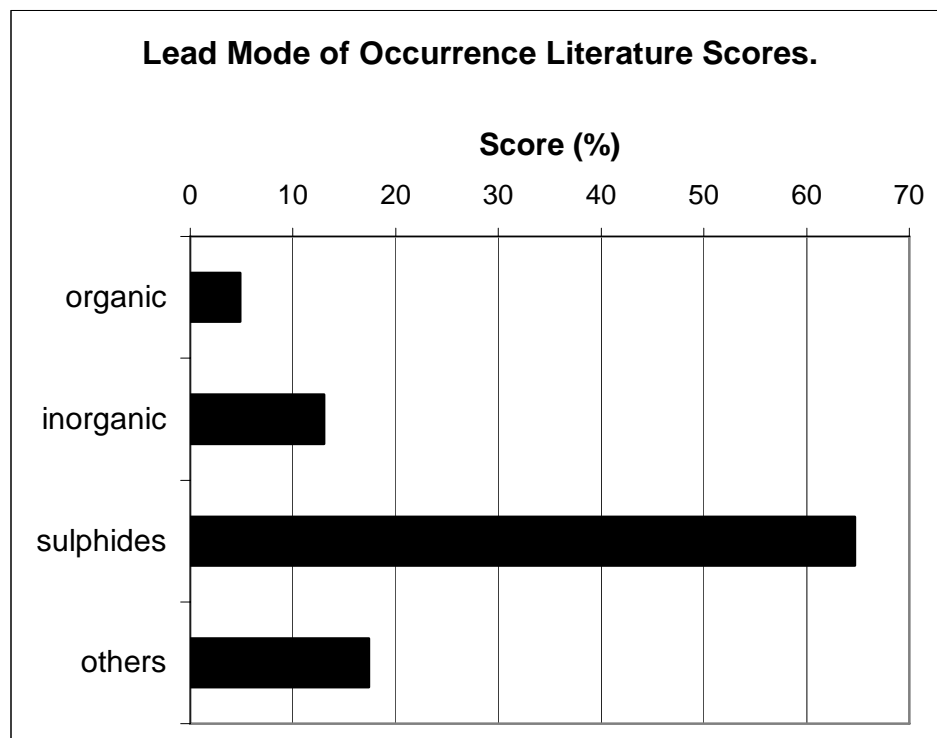
Organically bound - (Ghosh et al., 1987) (logic may be questionable), (Van Der Flier-Keller and Fyfe, 1986) (or in clay minerals).

Inorganically bound - (Crowley et al., 1997), (Grieve and Goodarzi, 1993), (Karayigit et al., 2001), (Shearer et al., 1997).

Sulphide bound - (Alastuey et al., 2001) (probably galena), (Asuen, 1987), (Beaton et al., 1993), (Bouska, 1981) (pyrite or galena), (Finkelman, 1995) (galena and others) (also selenides), (Gayer et al., 1999) (solid solution in pyrite), (Hower et al., 1996), (Mukhopadhyay et al., 1998) (galena or pyrite), (O'Gorman and Walker, 1971) (pyrite), (Palmer et al., 1998) (pyrite or galena), (Palmer et al., 1999) (galena or pyrite), (Pierce and Stanton, 1990) (pyrite), (Querol et al., 1995), (Querol et al., 1997b), (Singh et al., 1983) (pyrite, sulphides), (Spears and Martinez-Tarazona, 1993) (pyrite), (Spears and Zheng, 1999) (pyrite), (Spears et al., 1999), (Swaine, 1990)(galena) (also selenides and exchanging for Ba in Ba minerals), (Ward, 1980), (White et al., 1989).

Others - (Finkelman, 1995) (selenides), (Karayigit et al., 2000) (BiPb sulphides), (Li et al., 2001) (crocoite), (Querol et al., 1997a) (aluminosilicates), (Swaine, 1990) (selenides or exchanging for Ba in Ba minerals), (Van Der Flier-Keller and Fyfe, 1986) (clay minerals).

The above list shows that the most common mode of occurrence found for lead is sulphides. This information supports Finkelman (1995), who gives a high 8/10 level of confidence in a sulphide/ galena mode of occurrence for lead.



Manganese.

Organically bound - (Crowley et al., 1997), (Finkelman, 1995) (minor, carbonate mode dominant), (Hower and Bland, 1989) (mixed affinity), (Huggins and Huffman, 1996) (also in carbonates & illite), (Lyons et al., 1989) (also inorganic), (Miller and Given, 1986) (also in minerals) (lignites), (Miller and Given, 1987) (mixed affinity) (lignites), (Mukhopadhyay et al., 1998) (also carbonates), (Querol et al., 1997b), (Swaine, 1990) (The organic is thought to dominate at low ranks, carbonates and others at high ranks).

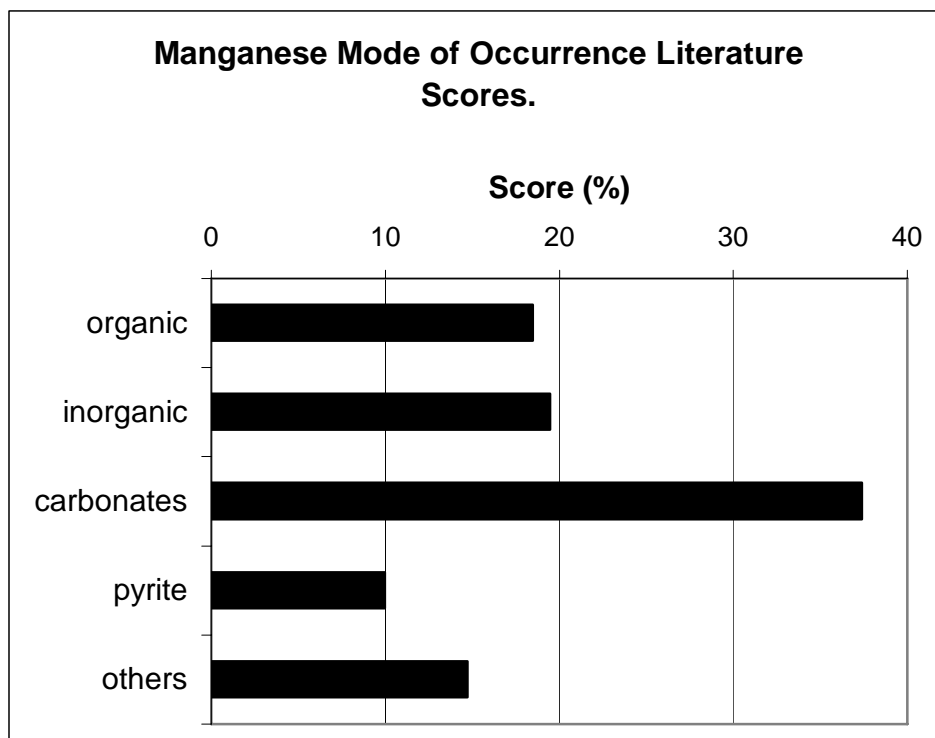
Inorganically bound - (Ghosh et al., 1987) (detritals), (Goodarzi and Van Der Flier-Keller, 1988), (Hower and Bland, 1989) (mixed affinity), (Karayigit et al., 2001), (Lyons et al., 1989) (also organic), (Miller and Given, 1986) (also organic), (Miller and Given, 1987) (also organic), (Shearer et al., 1997).

Carbonate bound - (Alastuey et al., 2001), (Asuen, 1987), (Bouska, 1981), (Finkelman, 1995) (ankerite/ siderite), (Goodarzi, 1987b) (siderite), (Laban and Atkin, 1999) (also some in sulphides), (Mukhopadhyay et al., 1998) (siderite), (Newman et al., 1997), (Palmer et al., 1998) (some in pyrite or silicates), (Palmer et al., 1999), (Querol et al., 1995), (Querol et al., 1997a) (also phosphates), (Swaine, 1990) (particularly at higher ranks), (Ward et al., 1999) (?).

Pyrite bound - (Finkelman, 1995) (minor compared to carbonates?), (Laban and Atkin, 1999) (mainly in carbonates), (Palmer and Filby, 1984), (Palmer et al., 1998) (mainly carbonates, silicates), (Spears and Martinez-Tarazona, 1993) (?), (Swaine, 1990) (minor).

Others - (Bouska, 1981) (silicates, oxides), (Finkelman, 1995) (some clays), (Huggins and Huffman, 1996) (illite) (also organic and carbonates), (Palmer and Filby, 1984) (clay minerals) (with pyrite), (Palmer et al., 1998) (silicates) (also (mainly) carbonates, some pyrite), (Querol et al., 1997a) (phosphates) (also carbonates), (Robbins et al., 1990) (in peat), (Swaine, 1990) (minor amongst other modes).

Finkelman (1995) gives a high 8/10 level of confidence that the mode of occurrence of manganese is in carbonates. The published literature indicates that a number of other modes are possible, and some change with increasing rank may also occur.



Mercury.

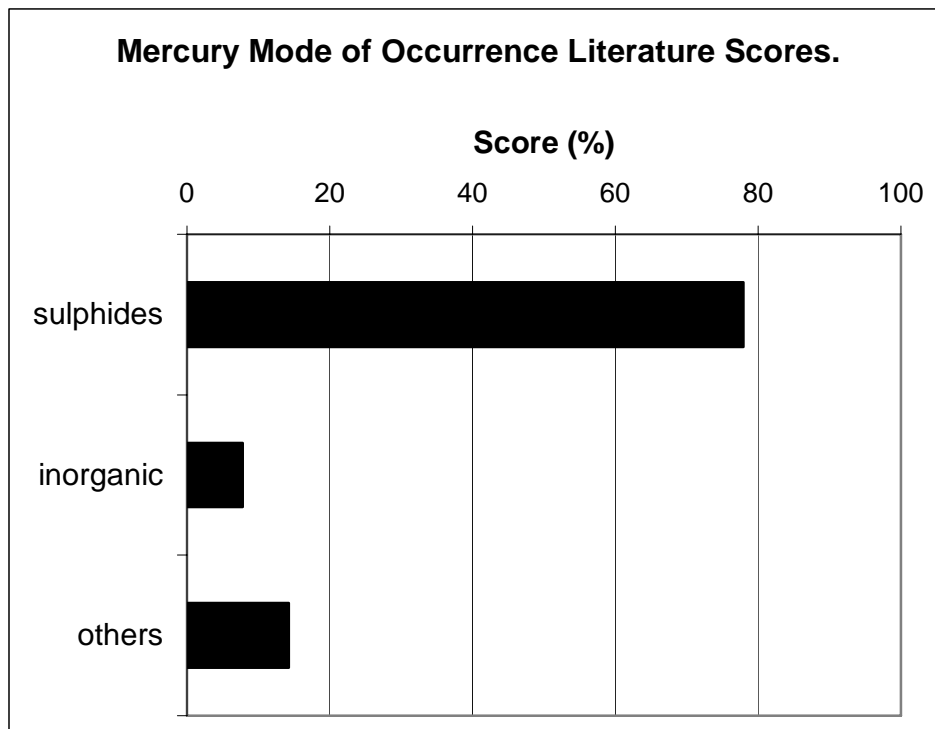
Sulphide bound - (Bouska, 1981), (Crowley et al., 1997), (Finkelman, 1995), (Palmer and Filby, 1984), (Pierce and Stanton, 1990), (Palmer et al., 1998) (some organically bound), (Palmer et al., 1999) (some organically bound), (Querol et al., 1995), (Senior et al., 2000) (also monosulphides/ oxidised pyrite), (Swaine, 1990) (and others, see below), (Toole-O'Neil et al., 1999).

Inorganically bound - (Grieve and Goodarzi, 1993)

Others - (Finkelman, 1995) (occasionally sphalerite), (Palmer et al., 1998)

(organically bound) (mainly pyrite), (Palmer et al., 1999) (organics) (also pyrite), (Senior et al., 2000) (monosulphides/ oxidised pyrite) (mainly pyrite), (Swaine, 1990) (metallic mercury, cinnabar, sphalerite, organically bound) (last mode uncertain).

Finkelman (1995) gives a confidence level of 6/10 for mercury being present in pyrite. Although the literature reviewed suggests this level of confidence is justified, analysis of mercury is plagued by analysis difficulties. Generally mercury is present in low concentrations in coal, and is easily volatilised (therefore ash cannot be analysed).



Molybdenum.

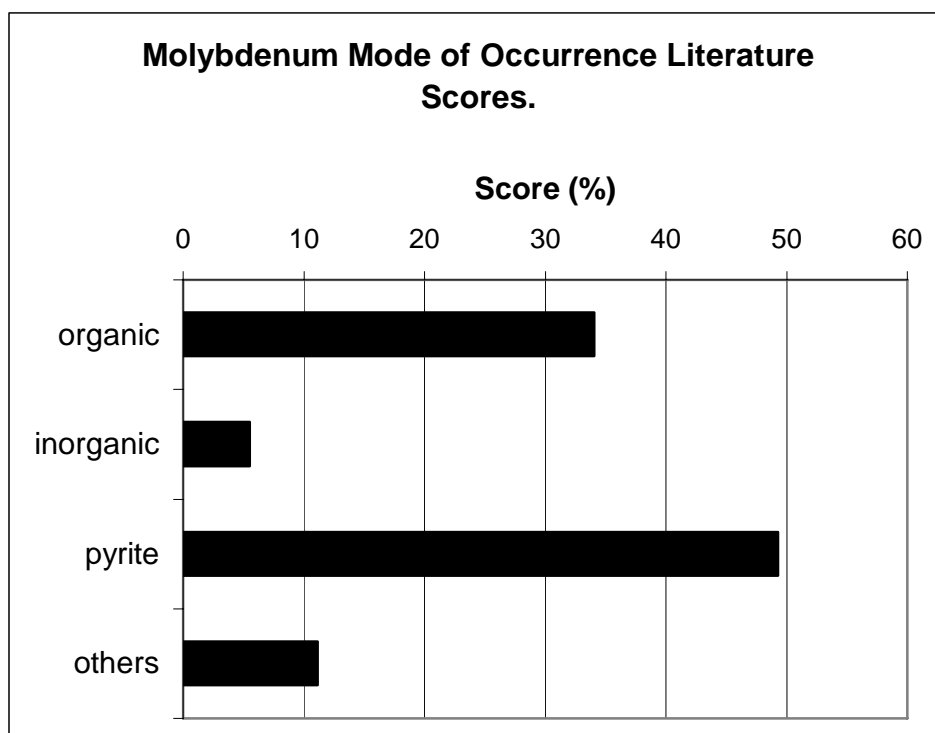
Organically bound - (Asuen, 1987), (Beaton et al., 1991) (intermediate affinity), (Bouska, 1981) (some pyrite, clay), (Finkelman, 1995) (subordinate to pyrite modes?), (Ghosh et al., 1987) (mixed affinity), (Goodarzi and Swaine, 1993) (also pyrite), (Karayigit et al., 2001), (Mukhopadhyay et al., 1998) (also organic and inorganic detrital), (Palmer et al., 1999) (also silicates, some in pyrite), (Querol et al., 1997a), (Swaine, 1990) (also pyrite), (Szilágyi, 1971), (Van Der Flier-Keller and Fyfe, 1986) (also clays).

Inorganically bound - (Beaton et al., 1991) (intermediate affinity), (Ghosh et al., 1987) (mixed affinity), (Mukhopadhyay et al., 1998) (clastics) (also organic and pyrite).

Pyrite bound - (Alastuey et al., 2001), (Beaton et al., 1993), (Bouska, 1981) (also organic and clays), (Finkelman, 1995) (also some organically bound), (Gayer et al., 1999), (Goodarzi and Swaine, 1993) (also organically bound), (Mukhopadhyay et al., 1998) (also organically bound and inorganic clastics), (Palmer et al., 1999) (mostly organics or silicates), (Querol et al., 1995), (Querol et al., 1997b) (sulphides?), (Querol et al., 1999b), (Spears and Zheng, 1999), (Spears et al., 1999), (Ward, 1980) (also some phosphate minerals), (White et al., 1989).

Others - (Bouska, 1981) (some clay bound), (Palmer et al., 1999) (clay) (also organics, some in pyrite), (Van Der Flier-Keller and Fyfe, 1986) (clays), (Ward, 1980) (some phosphate minerals).

The literature search suggests the most common modes of occurrence for molybdenum are in pyrite or organically bound (especially if some of the inorganically bound molybdenum is actually present as pyrite). Finkelman (1995) gives a low level of confidence (2/10) in pyrite as the dominant mode of occurrence due to a lack of direct evidence. The inclusion of more recent literature in this study suggests some minor upgrading of the confidence level may be possible.



Nickel.

Organically bound - (Finkelman, 1995) (plus other modes, see below), (Ghosh et al., 1987) (non woody portions of proto coal (clarain), (Kolker and Finkelman, 1998) (also pyrite and marcasite), (Laban and Atkin, 1999) (mainly clay and sulphide bound), (Lyons et al., 1989) (dominantly inorganic), (Miller and Given, 1986), (Newman, 1988), (Palmer et al., 1998) (also silicates, pyrite, millerite, nickel oxides), (Palmer et al., 1999) (also pyrite, carbonates, silicates), (Singh et al., 1983) (also in terrigenous ash and sulphides), (Shearer et al., 1997) (?), (Swaine, 1990) (also pyrite

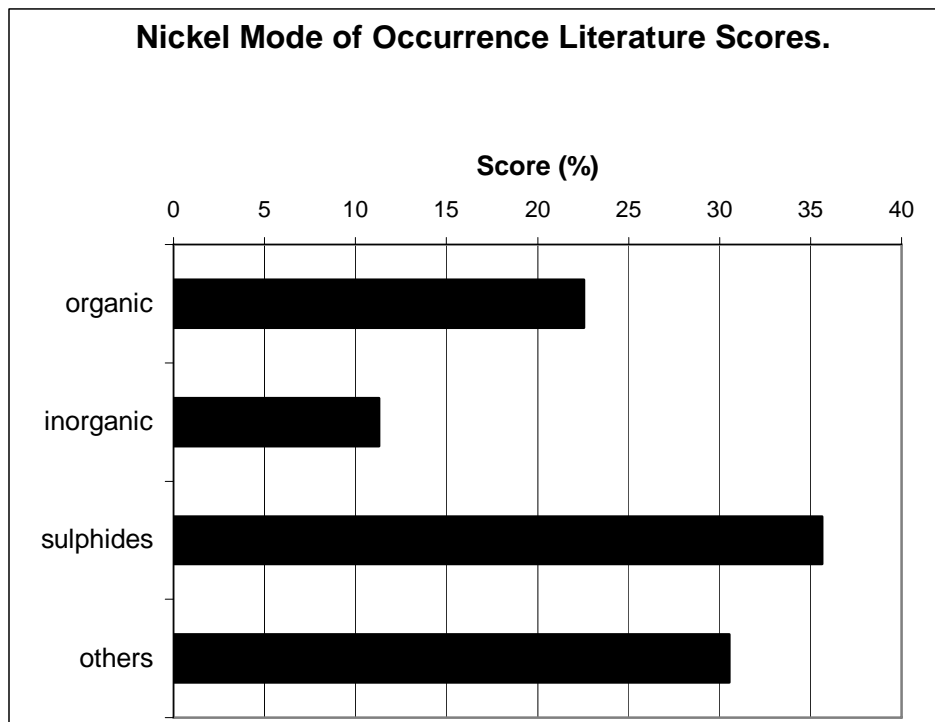
and clays), (Van Der Flier-Keller and Fyfe, 1986) (also clays/ pyrite bound), (Ward, 1980) (dominant mode).

Inorganically bound - (Beaton et al., 1991), (Crowley et al., 1997), (Helle et al., 2000), (Lyons et al., 1989) (some organic).

Sulphide bound - (Alastuey et al., 2001), (Asuen, 1987), (Beaton et al., 1993), (Bouska, 1981) (millerite), (Finkelman, 1995) (millerite, linnaeite, ullmanite, some in pyrite), (Gayer et al., 1999) (solid solution in pyrite), (Huggins and Huffman, 1996) (pyrite?), (Kolker and Finkelman, 1998) (pyrite and marcasite) (also organically bound), (Laban and Atkin, 1999) (also clay bound, some organically bound), (Palmer et al., 1998) (also organics, silicates, nickel oxides), (Palmer et al., 1999) (also organics, carbonates, silicates), (Singh et al., 1983) (also organic, some in terrigenous ash), (Spears and Martinez-Tarazona, 1993) (pyrite), (Swaine, 1990) (plus others), (Van Der Flier-Keller and Fyfe, 1986) (and organic/ clay bound), (White et al., 1989).

Others - (Bouska, 1981) (bravoite, siegenite?), (Finkelman, 1995) (traces in galena, sphalerite, clausthalite, spinels etc), (Hower et al., 1996) (clays or chromites), (Laban and Atkin, 1999) (clay minerals) (also sulphides, some organically bound), (Mukhopadhyay et al., 1998) (mixed layer clays), (Palmer and Lyons, 1996) (calcite), (Palmer et al., 1998) (nickel oxides, silicates) (also organics, sulphides), (Palmer et al., 1999) (silicates, carbonates) (also pyrite and organics), (Querol et al., 1995) (clay minerals and feldspars), (Querol et al., 1997b) (zeolites), (Querol et al., 1997a) (aluminosilicates), (Swaine, 1990) (clays, also sulphides and organics), (Spears et al., 1999), (Van Der Flier-Keller and Fyfe, 1986) (clays) (also sulphides and organics).

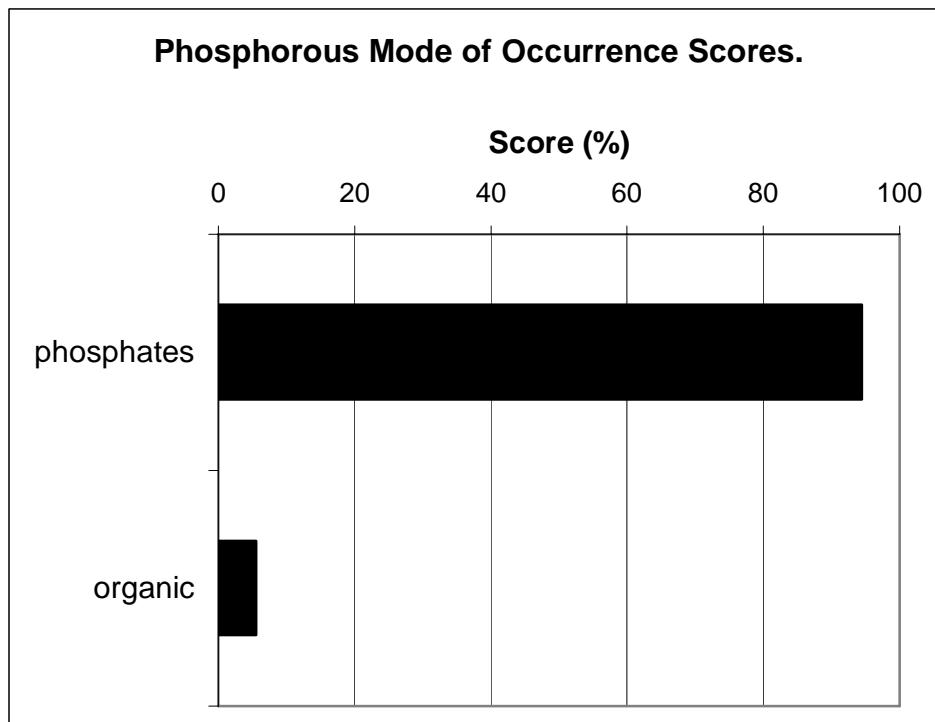
Finkelman (1995) gives a low 2/10 level of confidence in the mode of occurrence for nickel, and this literature review has found a wide variety of reported nickel modes. However, recent work has increased the level of confidence in a sulphide or organic mode of occurrence for nickel (Kolker and Finkelman, 1998).



Phosphorous.

Phosphate bound - (Birk and White, 1991) (apatite), (Finkelman, 1995) (rare earth phosphates, apatite, crandallite group) (notes also possible organic mode), (Karayigit et al., 2001) (apatite, monazite, fossil shells), (Laban and Atkin, 1999) (apatite, gorceixite & goyazite), (Newman, 1988) (crandallite, some apatite), (Newman et al., 1997) (some sort of poorly crystallized authigenic phosphate?), (Querol et al., 1997b) (hydroxylapatite), (Rao and Walsh, 1997) (crandallite), (Swaine, 1990) (phosphates) (also notes a possible organic mode), (Ward et al., 1996) (apatite, goyazite, gorceixite, crandallite, collophane?), (Ward et al., 1999) (zircon apatite or remobilised).

Finkelman (1995) notes some float/sink data that suggests an organic mode of occurrence may be in error due to the finely disseminated nature of some phosphate minerals in coal. He gives a level of confidence of 6/10 that phosphorous is present as phosphates, but notes the possibility of an organic mode of occurrence. The phosphate mode dominates literature examples of phosphorous modes of occurrence.



Selenium.

Organically bound - (Crowley et al., 1997), (Finkelman, 1995) (plus other modes), (Huggins and Huffman, 1996) (also selenite), (Lyons et al., 1989) (also inorganically bound), (Mukhopadhyay et al., 1998) (also inorganically bound), (Palmer et al., 1998) (also pyrite, some clausthalite), (Palmer et al., 1999) (also pyrite), (Senior et al., 2000) (also pyrite), (Swaine, 1990) (as ferroselite adsorbed to coal), (Valkovic, 1983a) (also inorganically bound).

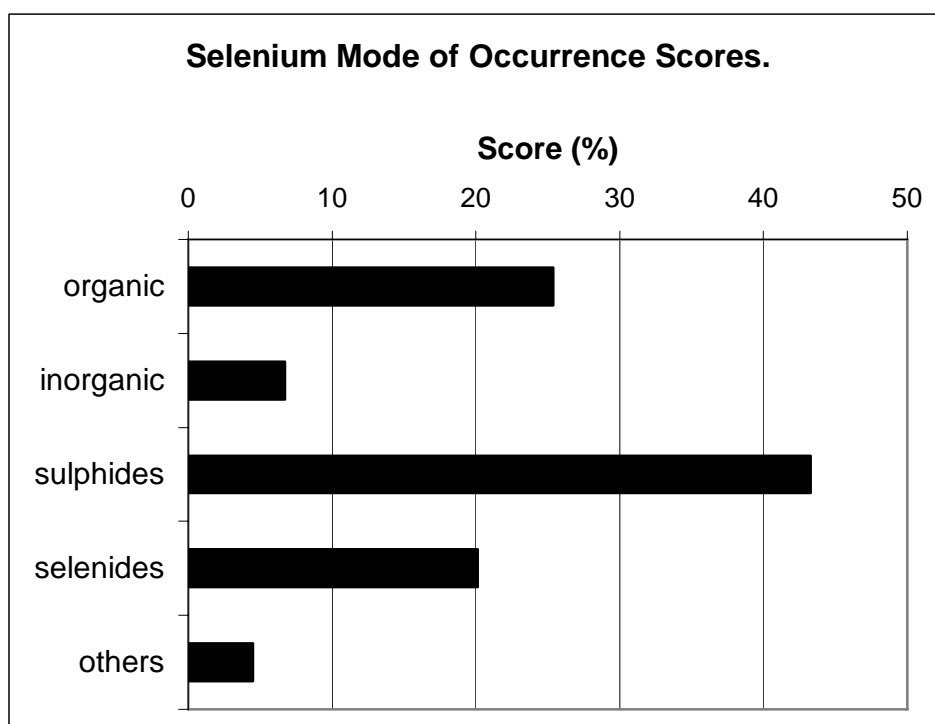
Inorganically bound- (Lyons et al., 1989) (also organically bound), (Mukhopadhyay et al., 1998) (also organically bound), (Valkovic, 1983a) (also organically bound).

Sulphides - (Finkelman, 1995) (pyrite & other accessory sulphides), (Goodarzi and Swaine, 1993) (galena), (Palmer and Filby, 1984) (pyrite), (Palmer and Lyons, 1996) (pyrite), (Palmer et al., 1998) (also organics and some clausthalite), (Palmer et al., 1999) (also organics), (Pierce and Stanton, 1990) (pyrite), (Senior et al., 2000) (also organic bound), (Spears and Zheng, 1999) (pyrite), (Swaine, 1990) (pyrite), (Spears et al., 1999) (pyrite), (White et al., 1989) (pyrite).

Selenide bound - (Finkelman, 1995), (Goodarzi and Swaine, 1993) (clausthalite, also native selenium), (Huggins and Huffman, 1996) (selenate oxidation state), (Miller and Given, 1986) (selenite form of gypsum), (Swaine, 1990) (clausthalite, also native selenium).

Others - (Goodarzi and Van Der Flier-Keller, 1989) (clays?).

This literature search suggests some organic adsorption may be possible for selenium, but the sulphide or selenide mode of occurrence in coal will dominate in most cases. Finkelman (1995) gives a high 8/10 level of confidence that selenium will be bound into pyrite, accessory sulphides or selenides, a conclusion supported by this literature search.



Silver.

Both Finkelman (1995) and Swaine (1990) state that silver is found in various sulphides, including silver sulphide (argentite), or as a trace in sphalerite, galena, pyrite or as native silver. Other possible modes noted include organically bound (Baruah et al., 2003), adsorbed onto the coal, in calcite, siderite, barite or hematite.

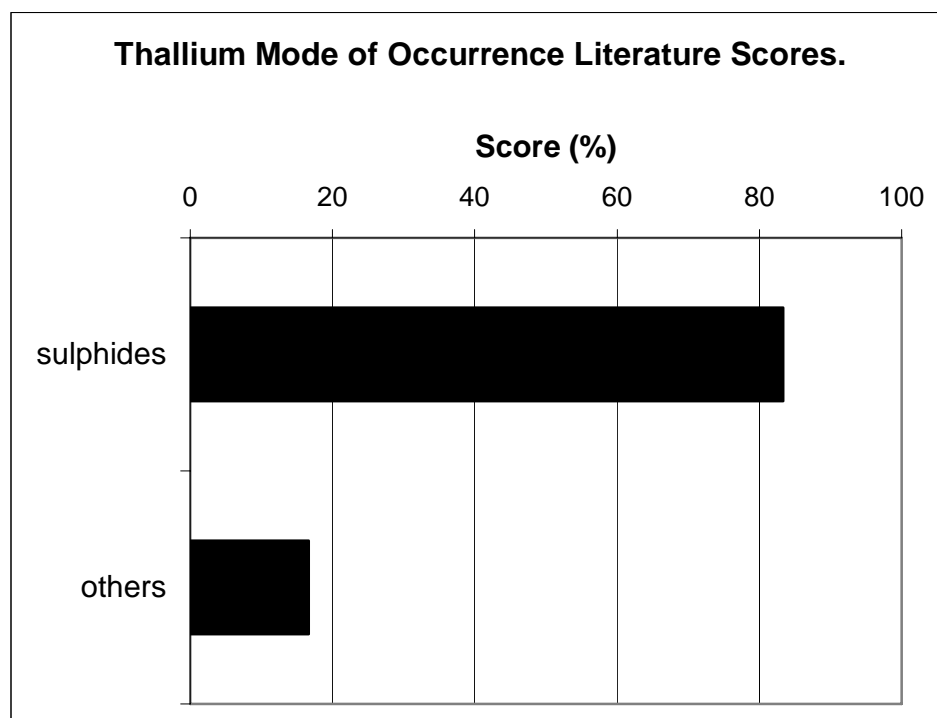
Finkelman (1995) gives a confidence level of 4/10 that the mode of occurrence of silver is sulphides. No further comments can be added on the basis of this literature review.

Thallium.

Sulphides - (Bouska, 1981) (pyrite), (Finkelman, 1995) (pyrite), (Querol et al., 1995) (iron sulphides), (Ward et al., 1999) (pyrite), (White et al., 1989) (pyrite).

Others - (Querol et al., 1997b) (zeolites).

The literature suggests that in the majority of coals, thallium will be present in pyrite. Finkelman (1995) gives a level of confidence of 4/10 for a pyrite mode of occurrence because of the lack of direct evidence.



Thorium.

Organically bound - (Palmer et al., 1999) (also monazite, carbonates(?), silicates).

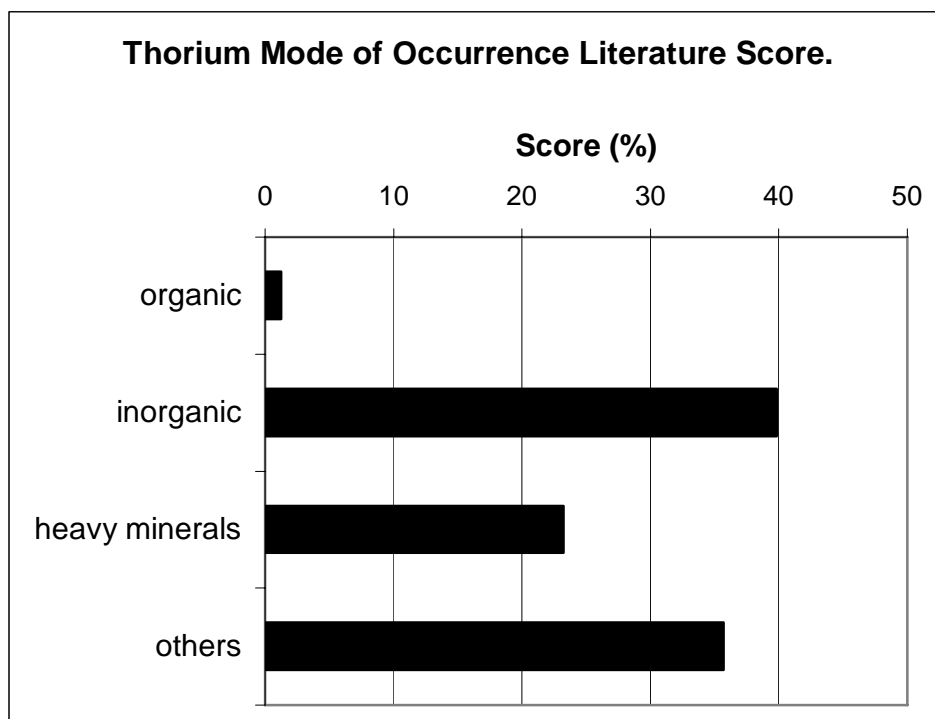
Inorganically bound - (Beaton et al., 1991) (?), (Goodarzi, 1987b), (Goodarzi, 1988), (Grieve and Goodarzi, 1993), (Karayigit et al., 2001), (Kortenski and Bakardjiev, 1993), (Lyons et al., 1989), (Querol et al., 1999b) (aluminosilicates).

Heavy minerals - (Finkelman, 1995) (monazite, xenotime, zircon), (Palmer and Filby, 1984) (rutile, zircon, monazite), (Palmer et al., 1998) (monazite and xenotime) (some from silicates, zircon), (Palmer et al., 1999) (also organics and carbonates?), (Swaine,

1990) (monazite, zircon, xenotime), (Van Der Flier-Keller and Fyfe, 1986) (also clays, organics).

Others - (Alastuey et al., 2001) (aluminium-silicate group), (Palmer and Lyons, 1996) (quartz, illite, kaolinite), (Palmer et al., 1998) (silicates), (also monazite, xenotime), (Palmer et al., 1999) (carbonates, silicates) (also organics?, heavy minerals), (Querol et al., 1995) (clay minerals, feldspars), (Querol et al., 1997b) (phosphate), (Querol et al., 1997a) (aluminosilicates), (Spears and Zheng, 1999) (clay minerals), (Van Der Flier-Keller and Fyfe, 1986) (clays/ organics) (also heavy minerals).

Finkelman (1995) gives a high (8/10) confidence level in thorium is primarily associated with monazite (which is a common accessory mineral in coal), and to a lesser degree with xenotime and zircon. The literature search appears to support this confidence, particularly if the inorganically bound mode is taken to be heavy minerals, however a number of possible modes have also been found.



Tin.

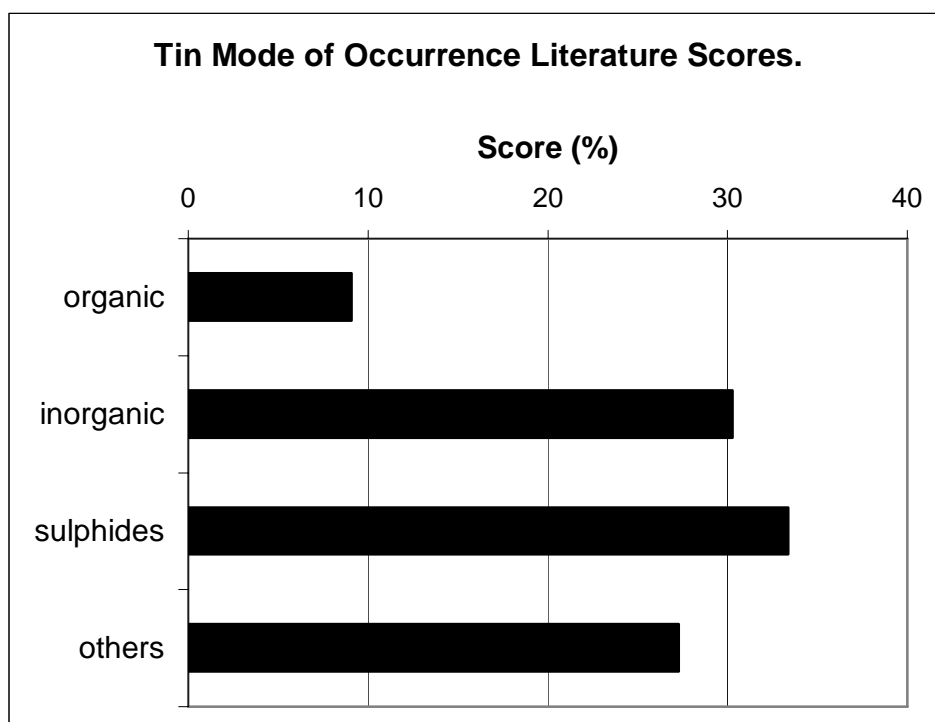
Organically bound - (Bouska, 1981) (also inorganically bound), (Swaine, 1990) (?) (plus other modes).

Inorganically bound - (Bouska, 1981), (Finkelman, 1995) (some modes listed, see below), (Karayigit et al., 2001), (Ward et al., 1999).

Sulphide/ oxide bound - (Finkelman, 1995) (oxides such as cassiterite, Sn sulphides), (O'Gorman and Walker, 1971) (cassiterite), (Querol et al., 1999b), (Swaine, 1990).

Others - (Alastuey et al., 2001) (aluminium-silicate group), (Querol et al., 1997b) (zeolites) (Querol et al., 1997a) (aluminosilicates).

There is a general consensus that most tin is inorganically bound in coal, probably as either oxides or sulphides, hence Finkelman (1995) states a moderate 6/10 confidence level for this element. Some papers mention a possible organic association (perhaps a misinterpretation due to the finely disseminated nature of tin minerals?), but there appears to be little confidence in this mode.



Uranium.

Organically bound - (Beaton et al., 1991) (intermediate affinity), (Bouska, 1981), (Finkelman, 1995) (also some mineral modes), (Karayigit et al., 2001), (Kortenski and Bakardjiev, 1993), (Lyons et al., 1989), (Palmer et al., 1998) (chelates) (also silicates, carbonates), (Palmer et al., 1999) (also zircons, U-oxides, silicates), (Querol et al., 1997b), (Robbins et al., 1990), (Swaine, 1990) (also some mineral modes and with

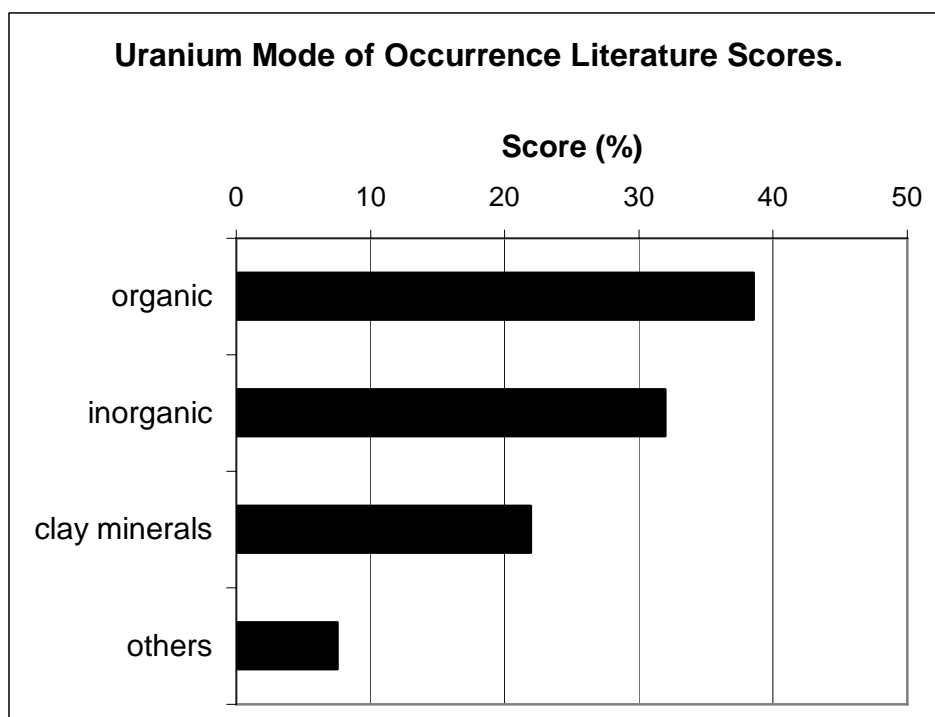
clays), (Szalay and Szilágyi, 1967), (Van Der Flier-Keller and Fyfe, 1986) (but mainly clays).

Inorganically bound - (Beaton et al., 1991) (intermediate affinity), (Crowley et al., 1997), (Gayer et al., 1999) (?), (Goodarzi, 1987b), (Goodarzi, 1987c), (Goodarzi, 1988), (Goodarzi and Van Der Flier-Keller, 1989), (Grieve and Goodarzi, 1993), (Mukhopadhyay et al., 1998).

Clay association - (Palmer and Lyons, 1996) (mainly kaolinite, some in illite), (Querol et al., 1995) (clays and feldspars), (Palmer et al., 1998) (including zircons) (also carbonates or chelates), (Palmer et al., 1999) (silicates) (also organics, zircon, U-oxides), (Querol et al., 1997a) (aluminosilicates), (Swaine, 1990) (also organics and mineral modes), (Van Der Flier-Keller and Fyfe, 1986), (Zodrow et al., 1987).

Others (mineral modes) - (Finkelman, 1995) (zircon, uraninite, monazites, apatites), (Palmer et al., 1998) (carbonates) (also chelates, silicates), (Palmer et al., 1999) (U-oxides, zircons) (also organics, silicates), (Swaine, 1990) (uraninite, coffinite, antunite, torbernite, carnotite, carbonates).

Finkelman (1995) gives a high 7/10 level of confidence that uranium will occur in organic association and with some accessory minerals (as listed above). However, a number of papers read during this literature search find an inorganic association for uranium. Many of these papers investigate Canadian coals so regional geological controls could be responsible. However, Swaine (1990) suggests that uranium could enter the mire in carbonate complexes, which then release uranyl ions to form uranyl-organic complexes. This mechanism would leave open the possibility of misinterpreting a graph of ash vs uranium (the approach used in most of the papers finding an inorganic affinity); ie, although the ash and uranium are genetically related, the mode of occurrence association is no longer valid due to the syndepositional mobility of uranium. (See (Finkelman, 1980) for discussion on misinterpretation of graphical methods).



Vanadium.

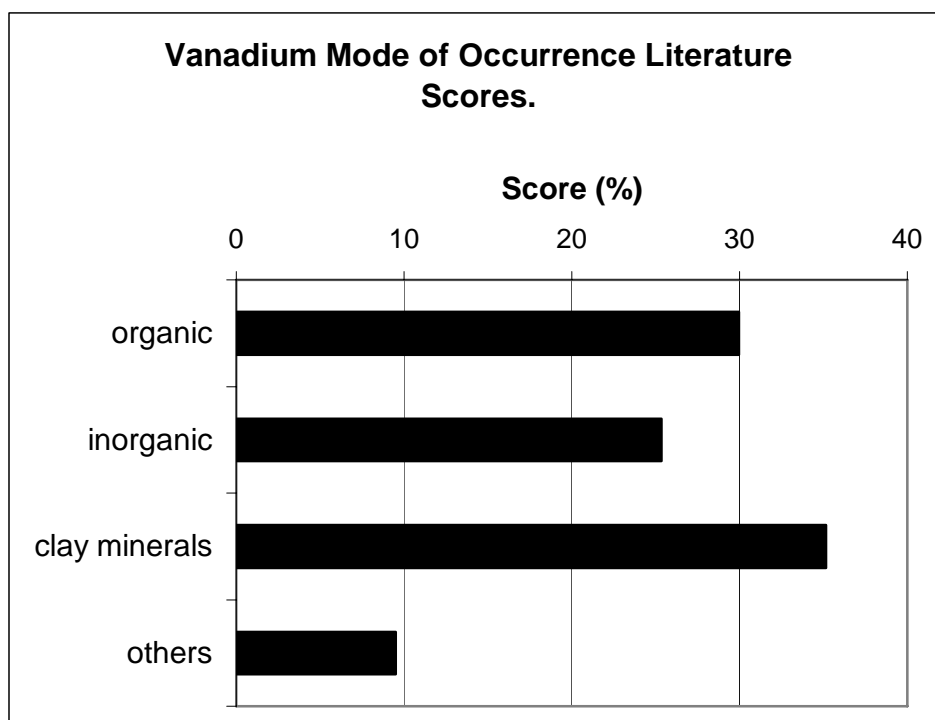
Organically bound - (Finkelman, 1995) (also clays), (Lyons et al., 1989) (some inorganic), (Miller and Given, 1986), (Palmer et al., 1999) (also silicates), (Querol et al., 1995) (also clays and feldspars), (Querol et al., 1997b) (also zeolites?), (Singh et al., 1983), (Spears and Martinez-Tarazona, 1993), (Swaine, 1990) (minor) (mainly clays and specific minerals), (Szalay, 1964) (experimental association), (Szilágyi, 1971), (Ward, 1980) (also V minerals?).

Inorganically bound - (Beaton et al., 1991), (Ghosh et al., 1987), (Goodarzi, 1987b), (Goodarzi, 1988), (Helle et al., 2000), (Lyons et al., 1989) (minor) (mainly organic), (Shearer et al., 1997) (tephra falls), (Ward et al., 1999) (?).

Clay minerals - (Alastuey et al., 2001), (Asuen, 1987), (Finkelman, 1995) (also organics), (Huggins and Huffman, 1996) (illite), (Mukhopadhyay et al., 1998), (Palmer and Filby, 1984) (and others?), (Palmer et al., 1999) (silicates) (also organics), (Querol et al., 1995) (also organics), (Querol et al., 1997a) (aluminosilicates), (Spears and Zheng, 1999), (Swaine, 1990) (some organics) (also specific minerals), (Van Der Flier-Keller and Fyfe, 1986).

Others - (O'Gorman and Walker, 1971) (pyrite), (Querol et al., 1997b) (zeolites), (Swaine, 1990) (minerals such as roscoelite), (Ward, 1980) (unspecified minerals) (also organics).

Finkelman (1995) gives the clay and organic modes of occurrence for vanadium a poor 3/10 level of confidence due to a high degree of uncertainty and the lack of a clear dominance of any one mode. This literature search found that the organic and clay bound modes of occurrence were found most often for vanadium, however there is a broad range of alternatives so no improvement on Finkelman's estimate can be made.



Zinc.

Organically bound - (Bouska, 1981) (also pyrite, sphalerite), (Huggins and Huffman, 1996) (also sphalerite), (Miller and Given, 1986), (Querol et al., 1997a) (also aluminosilicates), (Swaine, 1990) (also sphalerite), (Van Der Flier-Keller and Fyfe, 1986) (also clays and sphalerite).

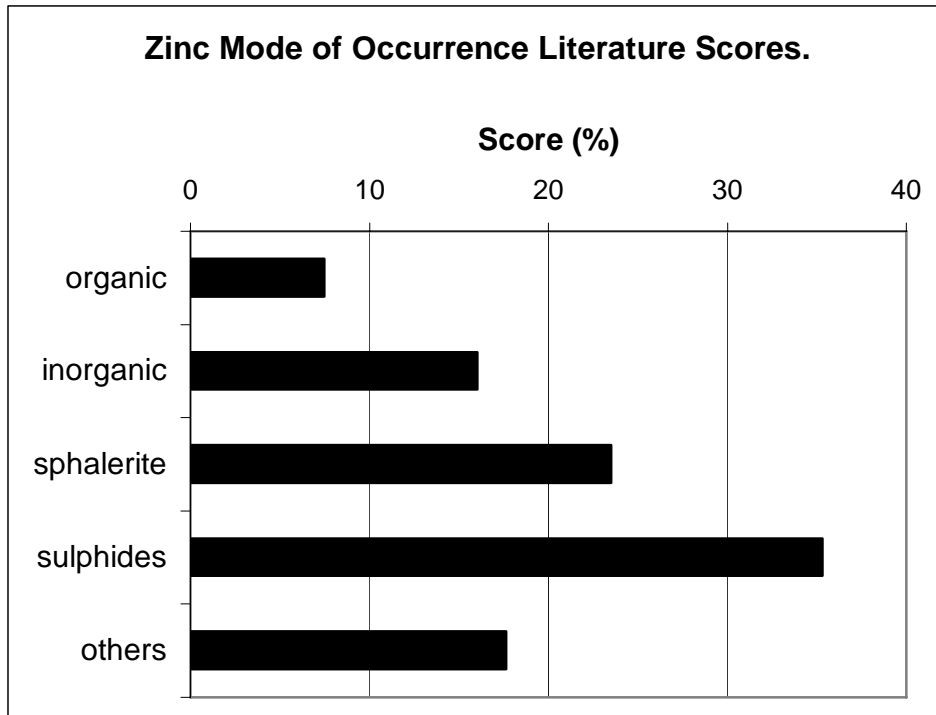
Inorganically bound - (Beaton et al., 1991), (Goodarzi, 1988), (Grieve and Goodarzi, 1993), (Helle et al., 2000), (Shearer et al., 1997).

Sphalerite - (Bouska, 1981) (also organic and pyrite), (Finkelman, 1995) (minor in sulphides), (Gluskoter and Lindahl, 1973), (Hatch et al., 1976), (Karayigit et al., 2001), (Laban and Atkin, 1999) (pyrites, some carbonates) (Mukhopadhyay et al., 1998) (also pyrite), (Palmer et al., 1998) (also pyrite), (Palmer et al., 1999) (also some pyrite, illite), (Senior et al., 2000) (also pyrite?), (Swaine, 1990) (also organics), (Van Der Flier-Keller and Fyfe, 1986) (also clays and organics).

Sulphides - (Alastuey et al., 2001), (Asuen, 1987), (Beaton et al., 1993), (Bouska, 1981) (also organics, sphalerite), (Finkelman, 1995) (minor compared to sphalerite), (Laban and Atkin, 1999) (pyrite) (also sphalerite, some carbonates), (Mukhopadhyay et al., 1998) (pyrite) (also sphalerite), (Palmer et al., 1998) (also sphalerite), (Palmer et al., 1999) (also sphalerite, some illite), (Pierce and Stanton, 1990) (pyrite), (Querol et al., 1995), (Senior et al., 2000) (mainly sphalerite), (Spears and Martinez-Tarazona, 1993) (pyrite), (Ward, 1980) (pyrite), (White et al., 1989) (only in some pyrites studied).

Others - (Hower et al., 1996) (clays and chromites), (Laban and Atkin, 1999) (carbonates) (also sphalerite and pyrite), (Palmer and Lyons, 1996) (calcite), (Palmer et al., 1999) (illite) (also sphalerite, some pyrite), (Querol et al., 1997b) (zeolites), (Querol et al., 1997a) (also organic), (Spears et al., 1999), (Van Der Flier-Keller and Fyfe, 1986) (clays) (also organics and sphalerite).

Finkelman (1995) gives a high 8/10 confidence level in a sphalerite or minor sulphide mode of occurrence for zinc. This literature search supports Finkelman's confidence assessment.



Appendix 3

Maceral and Ro(max) Analysis Results

Blake Central Pit							
Two Block Average	BC 0 - 50	BC 50 - 1.00	BC 1.00 - 1.50	BC 1.50 - 2.00	BC 2.00 - 2.50	BC 2.50 - 3.00	BC 3.00 - 3.50
Total Vitrinite	0.0	0.0	0.0	0.0	0.0	0.0	0.0
Total Inertinite	41.4	50.2	67.2	55.7	75.4	70.0	65.0
Total Liptinite	0.0	0.0	0.0	0.0	0.0	0.0	0.0
Total Minerals	13.8	3.4	2.4	4.8	3.6	1.8	3.6
Total Rock Fragments	0.0	0.0	0.0	0.2	0.0	0.0	0.0
Total Semi-Coke	44.8	46.4	30.4	39.4	21.0	28.2	31.4
Ro(max)	N/A	N/A	N/A	N/A	N/A	N/A	N/A
Comments	<p>Carbonates infilling inertinite lumina; some apparantly zoned. Clays infilling telinite or Authigenic euohedral crystals noted within semi-coke. Some pyrite present as fracture infills.</p> <p>Pyrite present as infill. No variation in reflectance within inertinite group.</p> <p>Pyrite generally massive; disaggregated infill(?)</p> <p>Some intertinities altered to semi-coke. Pyrite present as a fracture infill.</p> <p>Reduced variation in reflectance within inertinite group. Some development of semi-coke in inertinite. Rare pyrite infilling fractures.</p>						

Blake Central Pit (cont)

Two Block Average	BC 3.50 - 4.00	BC 4.00 - 4.13	BC 4.13 - 4.18	BC 4.18 - 4.22	BC 4.22 - 4.55	BC 4.55 - 5.00	BC 5.00 - 5.11	BC 5.11 - 5.39
Total Vitrinite	7.4	15.1	70.0	0.0	0.0	38.2	0.0	16.2
Total Inertinite	69.8	81.5	25.4	0.0	91.6	51.0	0.0	72.2
Total Liptinite	0.0	0.8	0.0	0.0	0.0	0.0	0.0	0.0
Total Minerals	5.2	2.6	4.6	0.0	5.2	10.8	0.0	11.6
Total Rock Fragments	0.0	0.0	0.0	High Ash	0.0	0.0	High Ash	0.0
Total Semi-Coke	17.6	0.0	0.0	0.0	3.2	0.0	0.0	0.0
Ro(max)	N/A	1.39	1.36	N/A	N/A	1.30	N/A	1.28
Comments	Reduced variation in reflectance within inertinite group; other grains differences apparent. Vitrinite varies from unaltered to coked.		Some ultra-fine incipient semi-coke in vitrinite. Some clay infilling of cell lumina.	Virtually 100% rock fragments. Clays and crystalline minerals (carbonates?), sometime within telinite/ fusinite lumina.	Reduced variation in reflectance within inertinite group. No vitrinite, virtually all inertinite with some ultra-fine semi-coke or re-grown mineral matter between inertinite. V fine pyrite veinlets in places.	Clay and carbonate(?) infilling telinite lumina.	Virtually 100% rock fragments. Clays and crystalline minerals (carbonates?), sometime within telinite/ fusinite lumina.	Some ultra-fine semi-coke in vitrinite. Clay infilling fusinite/ semifusinite lumens. Pyrite infilling fractures.

Blake Central Pit (cont)

Two Block Average	BC 5.39 - 5.49	BC 5.49 - 6.11	BC 6.11 - 6.13	BC 6.13 - 6.23	BC 6.23 - 6.35	BC 6.35 - 6.37	BC 6.37 - 6.55	BC 6.55 - 6.63	BC 6.63 - 6.88
Total Vitrinite	0.0	41.2	0.0	47.2	11.0	0.0	31.2	7.4	9.2
Total Inertinite	90.8	54.8	0.0	39.2	75.8	0.0	62.0	35.6	41.2
Total Liptinite	0.0	0.1	0.0	0.0	0.0	0.0	0.4	0.0	0.0
Total Minerals	7.4	3.9	0.0	12.2	10.2	0.0	6.4	3.2	10.6
Total Rock Fragments	0.0	0.0	High Ash	1.4	3.0	High Ash	0.0	53.8	39.0
Total Semi-Coke	1.8	0.0	0.0	0.0	0.0	0.0	0.0	0.0	0.0
Ro(max)	N/A	1.22	N/A	1.25	1.29	N/A	1.25	1.25	1.28

Comments	Appears baked; reduced variation in reflectance within inertinite group. Clays re-ordering (?) between inert grains.	Carbonate or silica infilling telinite. Some clay infilling fusinite/ semifusinite. Few good specimens for point counting or Ro(max) measurement.	100% rock fragments, not worth point counting.	Clay sometime infilling telinite/ semifusinite cell lumina or as large masses. Some rock fragments.	Pyrite sometimes associated with carbonates.	100% rock fragments with some clay-infilled telinite; not worth point counting.	Very ashy sample; only 30 Ro(max) measurements possible. Clays/ carbonates infilling telinite.	Vitrinite very rare; where present signs of incipient semi-coke development in relic cell lumina. Carbonate and clays infilling fusinite/ semifusinite. Numerous rock fragments & detrital macerals. Rare green reflecting acicular crystals.
-----------------	--	---	--	---	--	---	--	---

Blake West Pit

Two Block Average	BWB 3.25 - 3.56	BWB 3.56 - 3.71	BWB 3.71 - 3.91	BWB 3.93 - 4.23	BWB 4.23 - 4.28	BWB 4.28 - 4.40	BWB 4.40 - 4.43	BWB 4.43 - 4.67	BWB 4.67 - 5.13
Total Vitrinite	21.5	36.0	20.8	10.1	48.2	56.2	0.0	49.8	23.6
Total Inertinite	75.1	33.2	70.3	84.3	49.4	40.0	0.0	47.2	62.4
Total Liptinite	1.8	0.8	1.7	1.4	0.4	1.0	0.0	0.8	0.4
Total Minerals	1.6	30.0	7.2	3.6	2.0	2.8	0.0	2.2	13.6
Total Rock Fragments	0.0	0.0	0.0	0.6	0.0	0.0	High Ash	0.0	0.0
Total Semi-Coke	0.0	0.0	0.0	0.0	0.0	0.0	0.0	0.0	0.0
Ro(max)	1.28	1.23	1.23	1.12	1.29	1.23	N/A	1.24	1.32

Comments	Some incipient development of semi-coke in telocollinite bands.	Rare incipient semi-coke development. Pyrite present as veinlet infills.	Clay infilling of lumens in fusinite/ semifusinite common. Rare bituminite/ exudatinitite noted.	Sample low in vitrinite with some incipient to moderate development of semi-coke in some vitrinite. Carbonate infilling of some semi-fusinite. Only 30 measurements of Ro(max) possible due to lack of sites.	Incipient development of semi-coke in vitrinite.	Very fine incipient semi-coke development in some vitrinite. Pyrite infilling some very fine fractures.	100% rock fragments. Some mineralised telinite. Rare telocollinite and fusinite/ semifusinite could be contamination.	Telinite lumina infilled by clays or carbonates.
-----------------	---	--	--	---	--	---	---	--

Bowen No.2 Pit							
Two Block Average	BO 0 - 10	BO 10 - 15	BO 37 - 72	BO 1.15 - 1.85	BO 2.45 - 2.60	BO 2.90 - 3.01	BO 3.61 - 4.21
Total Vitrinite	25.6	41.2	16.2	38.0	0.0	0.0	0.0
Total Inertinite	57.2	51.4	80.2	58.2	19.4	54.8	63.4
Total Liptinite	0.3	0.0	0.2	0.0	0.0	0.0	0.0
Total Minerals	16.9	7.4	3.4	3.8	8.3	0.4	2.6
Total Rock Fragments	0.0	0.0	0.0	0.0	0.0	0.0	0.0
Total Semi-Coke	0.0	0.0	0.0	0.0	72.3	44.8	34.0
Ro(max)	1.05	1.07	N/A	1.18	N/A	N/A	N/A
Comments	Rare evidence for coalescing pyrite framboids, or pseudomorphing xylem. Rare clay infilling of telinite.		Too few telocollinite grains to allow measurement of Ro(max).		Some clays(?) infilling relic cells in telinite/fusinite. Rare showing semi-fus morphology.	Reduced variation in reflectance within inertinite group.	High proportion of coarse fibrous mozaic. Reduced variation in reflectance within inertinite group.

Appendix 4

Proximate and Elemental Analysis Results for Collinsville Channel Samples.

Blake Central Pit - Channel Samples									
	BC 0.00-0.50	BC 0.50-1.00	BC 1.00-1.50	BC 1.50-2.00	BC 2.00-2.50	BC 2.50-3.00	BC 3.00-3.50	BC 3.50-4.00	BC 4.00-4.13
From	0.00	0.50	1.00	1.50	2.00	2.50	3.00	3.50	4.00
To	0.50	1.00	1.50	2.00	2.50	3.00	3.50	4.00	4.13
IM	0.9	1.0	0.9	0.7	0.7	1.1	1.0	0.8	0.9
ASH	37.5	22.8	20.0	15.8	14.8	14.6	15.2	14.2	13.7
VM	9.0	10.3	11.3	13.4	14.5	15.5	16.7	18.4	19.4
VM (daf)	14.6	13.5	14.3	16.0	17.2	18.4	19.9	21.6	22.7
FC	52.6	65.9	67.8	70.1	70.0	68.8	67.1	66.6	66.6
Major Elements (% in whole coal)									
Si (PPM)	126438	71818	63895	50506	45701	41692	42007	32740	31372
Al (PPM)	34591	26945	22698	18914	18332	20724	22724	21376	27697
Fe (PPM)	10300	4840	4260	4040	3830	3990	5510	9280	3630
Fe (PPM)	9015	4711	4040	3719	3563	3780	5122	9101	3029
Ca (PPM)	<300	<300	<300	<300	<300	<300	<300	<300	<300
Mg (PPM)	571	425	338	255	<14.80	341	394	585	282
Na (PPM)	587	654	306	258	485	463	618	372	181
K (PPM)	4600	<500	<500	<500	<500	1700	<500	<500	<500
Ti (PPM)	6877	3477	2658	1982	1985	1845	2309	1679	1132
Mn (PPM)	68	29	27	18	11	22	41	112	21
P (PPM)	96	62	45	46	330	621	197	1439	1179
S (PPM)	10100	7400	5800	6400	6400	6300	6800	5900	4900
Au (PPB)	1.3	<0.2	<0.2	<0.2	<0.2	0.6	0.4	0.8	0.6
Ag (PPM)	<0.3	<0.3	<0.3	<0.3	<0.3	<0.3	<0.3	<0.3	<0.3
As (PPM)	2.40	0.04	0.05	0.35	0.34	0.43	0.12	0.40	0.54
Ba (PPM)	200	110	92	45	51	60	66	69	100
Br (PPM)	7.5	7.8	8.1	8.3	8.5	7.7	7.0	6.0	5.0
Ce (PPM)	87	51	38	23	37	50	25	38	74
Co (PPM)	2.8	1.7	1.4	2.5	2.4	2.7	3.6	3.9	5.1
Cr (PPM)	87	40	33	26	23	21	25	18	12
Cs (PPM)	1.50	1.00	1.20	0.82	0.71	0.57	0.69	0.25	0.4
Cu (PPM)	44.25								
Eu (PPM)	1.37	0.64	0.50	0.37	0.44	0.54	0.42	0.41	0.62
Hf (PPM)	9.1	5.0	4.0	3.0	3.0	3.2	3.5	2.3	4.6
Hg (PPM)	<0.05	<0.05	0.19	0.18	<0.05	<0.05	<0.05	0.13	0.18
Ir (PPM)	<0.2	<0.2	<0.2	<0.2	<0.2	<0.2	<0.2	<0.2	<0.2
La (PPM)	53	31	21	12	21	32	13	19	53
Lu (PPM)	0.82	0.24	0.20	0.15	0.17	0.18	0.21	0.19	0.34
Mo (PPM)	2.60	1.40	1.90	0.86	2.50	2.20	1.60	1.10	<0.05
Nd (PPM)	27.0	15.0	12.0	7.8	12.0	14.0	8.6	13.0	22.0
Ni (PPM)	20	<2	<2	<2	<2	<2	<2	<2	<2
Pb (PPM)	27.38								
Rb (PPM)	10	8	9	<1	<1	<1	<1	<1	<1
Sb (PPM)	0.43	0.27	0.27	0.21	0.2	0.21	0.22	0.18	0.68
Sc (PPM)	14.0	8.2	5.6	4.9	5.3	5.3	5.6	5.2	5
Se (PPM)	2.0	2.3	2.3	2.4	2.2	1.7	2.6	1.6	1.9
Sm (PPM)	5.4	2.6	2.2	1.6	2	2.3	1.8	1.9	3.7
Sr (PPM)	<10	<10	<10	<10	87	130	54	160	400
Ta (PPM)	1.00	0.65	0.48	0.36	0.34	0.35	0.52	0.31	0.37
Tb (PPM)	1.1	0.6	0.3	0.3	0.3	0.4	0.4	0.3	0.9
Th (PPM)	22.0	11.0	8.5	6.7	7.1	7.9	9.4	6.3	12.0
U (PPM)	5.1	2.3	1.7	1.5	1.4	1.7	2.0	1.3	1.6
U (PPM)	7.50								
V (PPM)	55.88								
W (PPM)	9.2	4.7	2.7	2.2	2.1	1.9	2.2	1.3	1.6
Yb (PPM)	5.58	1.62	1.48	1.11	1.21	1.31	1.27	1.21	2.32
Zn (PPM)	3	16	19	27	-2	27	25	37	22

Blake Central Pit - Channel Samples (cont)									
	BC 4.13-4.18	BC 4.18-4.22	BC 4.22-4.55	BC 4.55-5.00	BC 5.00-5.11	BC 5.11-5.39	BC 5.39-5.49	BC 5.49-6.11	BC 6.11-6.13
From	4.13	4.18	4.22	4.55	5.00	5.11	5.39	5.49	5.98
To	4.18	4.22	4.55	5.00	5.11	5.39	5.49	5.98	6.13
IM	0.8	0.7	0.6	0.6	0.5	0.9	0.7	0.9	0.8
ASH	10.5	67.2	29.2	19.2	60.8	29.1	34.3	14.1	70.4
VM	23.2	16.4	16.1	20.5	16.3	18.7	16.7	14.1	15.9
VM (daf)	26.2	51.1	22.9	25.6	42.1	26.7	25.7	16.6	55.2
FC	65.5	15.7	54.1	59.7	22.4	51.3	48.3	70.9	12.9
Major Elements (% in whole coal)									
Si (PPM)	24899	161898	75979	46351	150709	72554	95963	37196	170124
Al (PPM)	23376	155258	56320	41195	135169	54026	55308	26368	158502
Fe (PPM)	660	1360	4090	2540	2550	12900	9460	2820	2220
Fe (PPM)	549	1125	3750	2423	2535	11549	8985	2391	1750
Ca (PPM)	<300	<300	<300	<300	<300	2700	<300	<300	<300
Mg (PPM)	208	974	506	329	1106	860	240	201	1011
Na (PPM)	182	358	201	219	390	426	170	134	425
K (PPM)	<500	<500	<500	<500	800	2200	<500	<500	1800
Ti (PPM)	1455	3260	4186	1720	5722	2087	3920	1699	4066
Mn (PPM)	<10.50	<67.20	29	16	<60.80	104	103	19	<70.40
P (PPM)	118	130	183	606	203	170	159	105	77
S (PPM)	4700	1500	4400	5700	2400	5300	3700	6200	2000
Au (PPB)	0.5	<0.2	2.5	1.9	<0.2	0.9	3.2	0.6	0.3
Ag (PPM)	<0.3	<0.3	<0.3	<0.3	<0.3	<0.3	<0.3	<0.3	<0.3
As (PPM)	<0.05	0.41	1.10	0.68	0.92	0.18	1.10	0.85	1.50
Ba (PPM)	120	100	180	150	140	150	170	71	110
Br (PPM)	4.3	1.2	4.6	5.3	2.0	5.2	4.7	5.0	1.4
Ce (PPM)	45	50	150	120	67	77	140	70	45
Co (PPM)	7.8	2.9	3.7	5.9	4.1	6.0	3.3	11	5.4
Cr (PPM)	12	15	33	13	15	20	30	12	10
Cs (PPM)	0.32	1.10	0.79	0.35	1.10	0.54	0.51	0.24	1.5
Cu (PPM)		38.98			52.29		42.53		35.20
Eu (PPM)	0.60	0.52	1.48	1.04	1.17	0.59	2.22	1.05	0.64
Hf (PPM)	11.0	16.0	11.0	9.2	16.0	13.0	7.9	4.9	12.0
Hg (PPM)	<0.05	<0.05	0.44	<0.05	0.07	<0.05	<0.05	0.19	<0.05
Ir (PPM)	<0.2	<0.2	<0.2	<0.2	<0.2	<0.2	<0.2	<0.2	<0.2
La (PPM)	18	23	71	72	25	24	63	33	25
Lu (PPM)	0.49	0.45	0.93	0.77	0.80	1.10	1.58	0.92	0.41
Mo (PPM)	<0.05	<0.05	<0.05	<0.05	<0.05	<0.05	2.00	<0.05	3.10
Nd (PPM)	22.0	22.0	66.0	49.0	45.0	37.0	77.0	36.0	22.0
Ni (PPM)	33	<2	<2	<2	<2	<2	31	32	<2
Pb (PPM)		14.78			17.02		17.84		5.63
Rb (PPM)	<1	5	8	<1	7	5	<1	<1	12
Sb (PPM)	2.00	0.88	1.20	1.50	1.50	0.99	1.00	1.00	0.89
Sc (PPM)	6.2	6.4	15.0	8.4	12.0	19.0	12.0	6.5	5.3
Se (PPM)	4.1	1.2	2.7	3.6	2.7	3.6	2.9	2.9	0.6
Sm (PPM)	4.2	3.8	12.0	7.3	7.2	8.4	14.0	5.7	3.1
Sr (PPM)	110	<10	<10	480	140	<10	<10	<10	<10
Ta (PPM)	0.75	3.60	1.00	0.82	3.60	1.10	1.50	0.40	3.70
Tb (PPM)	1.0	0.8	2.2	1.4	1.3	2.0	2.3	1.1	0.7
Th (PPM)	19.0	42.0	34.0	16.0	35.0	22.0	24.0	8.7	20.0
U (PPM)	6.4	6.3	5.5	3.4	5.6	3.5	2.9	1.5	3.3
U (PPM) (XRF)		10.08			7.90		6.52		5.63
V (PPM)		20.83			10.34		29.41		<0.7
W (PPM)	1.3	4.1	7.5	1.7	7.5	4.2	6.2	1.9	5.1
Yb (PPM)	3.32	3.00	6.09	4.69	5.08	7.80	9.12	6.04	2.73
Zn (PPM)	47	76	37	17	43	33	45	26	36

Blake Central Pit - Channel Samples (cont)							
	BC 6.13-6.23	BC 6.23-6.35	BC 6.35-6.37	BC 6.37-6.55	Repeat 1	BC 6.55-6.63	BC 6.63-6.88
From	6.13	6.23	6.35	6.37	6.55	6.55	6.63
To	6.23	6.35	6.37	6.55	6.55	6.63	6.88
IM	1.0	0.7	0.4	1.0		0.9	0.8
ASH	16.7	28.9	69.7	24.7		58.8	54.5
VM	23.2	18.8	16.2	19.4		14.7	15.5
VM (daf)	28.2	26.7	54.2	26.1		36.5	34.7
FC	59.1	51.6	13.7	54.9		25.6	29.1
Major Elements (% in whole coal)							
Si (PPM)	43715	73773	178572	65536		160023	150969
Al (PPM)	32006	45121	149823	39706		109426	91725
Fe (PPM)	830	20500	1480	11900	12400	3120	8930
Fe (PPM)	937	19329	1692	10953		2820	8331
Ca (PPM)	<300	<300	<300	<300	<300	<300	<300
Mg (PPM)	329	487	1331	700		923	1219
Na (PPM)	300	318	607	523	479	451	488
K (PPM)	<500	2500	3000	2500	<500	3600	8000
Ti (PPM)	1813	1553	1079	1766		6270	5643
Mn (PPM)	18	259	42	157		<58.80	112
P (PPM)	94	73	150	84		146	143
S (PPM)	5100	8200	1600	6200	0	2500	2500
Au (PPB)	0.6	0.2	0.5	<0.2	3	0.3	<0.2
Ag (PPM)	<0.3	<0.3	<0.3	<0.3	<0.3	<0.3	<0.3
As (PPM)	0.82	<0.05	1.00	0.65	0.52	<0.05	<0.05
Ba (PPM)	110	95	80	140	93	180	210
Br (PPM)	4.8	5.2	1.6	6.1	5.6	2.9	2.9
Ce (PPM)	69	92	130	81	72	120	120
Co (PPM)	14.0	9.4	5.0	10.0	12.0	5.2	7.1
Cr (PPM)	12	18	19	23	24	46	50
Cs (PPM)	0.44	0.64	1.3	0.72	0.85	2.70	6.30
Cu (PPM)		30.06	53.67			56.45	49.60
Eu (PPM)	0.96	1.29	1.52	1.20	1.13	2.01	2.02
Hf (PPM)	16.0	6.0	6.5	5.4	5.7	9.0	10.0
Hg (PPM)	<0.05	0.06	0.24	0.42	<0.05	0.50	<0.05
Ir (PPM)	<0.2	<0.2	<0.2	<0.2	<0.2	<0.2	<0.2
La (PPM)	42	53	72	43	39	67	60
Lu (PPM)	0.64	0.75	1.04	0.75	0.75	0.89	0.86
Mo (PPM)	<0.05	1.20	3.60	<0.05	9.70	<0.05	<0.05
Nd (PPM)	32.0	44.0	62.0	37.0	23.0	57.0	54.0
Ni (PPM)	32	34	38	64	<2	57	<2
Pb (PPM)		26.30	16.03			22.34	33.25
Rb (PPM)	<1	9	11	9	11	26	37
Sb (PPM)	1.00	0.55	0.68	0.54	0.51	0.62	0.67
Sc (PPM)	7.8	11.0	6.9	12.0	14.0	17.0	22.0
Se (PPM)	3.8	3.3	2.2	3.2	3.1	1.4	4.3
Sm (PPM)	4.9	7.2	11.0	6.3	5.7	9.5	9.0
Sr (PPM)	<10	<10	<10	<10	<10	<10	<10
Ta (PPM)	1.00	0.77	3.20	0.67	0.63	1.40	1.20
Tb (PPM)	1.0	1.5	2.5	1.4	1.4	1.8	1.6
Th (PPM)	28.0	18.0	15.0	12.0	12.0	21.0	25.0
U (PPM)	4.7	3.6	5.9	3.3	2.8	3.9	3.9
U (PPM) (XRF)		6.94	6.27			4.70	5.45
V (PPM)		15.61	7.67			60.56	101.37
W (PPM)	2.7	3.6	5.8	3.0	3.3	4	5.3
Yb (PPM)	4.01	4.92	6.61	4.82	4.96	5.54	5.63
Zn (PPM)	30	34	51	40	53	56	76

Blake West Pit - Channel Samples									
	BW 0.00-0.11	BW 0.11-0.20	BW 0.20-0.48	BW 0.48-0.93	BW 1.20-1.60	BW 1.60-2.05	BW 2.05-2.65	BW 2.65-3.15	BW 3.15-3.75
From	0.00	0.11	0.2	0.48	0.93	1.33	1.78	2.38	2.88
To	0.11	0.2	0.48	0.93	1.33	1.78	2.38	2.88	3.48
IM	0.8	0.8	0.8	0.7	0.6	0.6	1.2	1.7	1.8
ASH	27.6	22.9	18.5	17.3	38.9	14.2	13.8	15.6	16.7
VM	18.4	19.5	19.8	20.4	14.2	20.7	10.4	7.9	3.7
VM (daf)	25.7	25.6	24.5	24.9	23.5	24.3	12.2	9.6	4.5
FC	53.2	56.8	60.9	61.6	46.3	64.5	74.6	74.8	77.8
Major Elements (whole coal)									
Si (PPM)	83630	69754	61418	58237	152548	43417	39474	37567	21519
Al (PPM)	35231	30729	20557	19146	23549	21226	21010	26335	17242
Fe (PPM)	10100	5810	3750	2560	2370	1690	1920	9590	9820
Fe (PPM)	10062	5872	3792	2636	2405	1445	1958	9574	5825
Ca (PPM)	<300	<300	<300	<300	<300	<300	<300	<300	<300
Mg (PPM)	366	307	201	255	386	150	259	316	343
Na (PPM)	170	148	136	177	200	152	238	299	376
K (PPM)	2800	<500	1000	1100	700	<500	<500	<500	<500
Ti (PPM)	3374	2651	2019	1762	4669	2045	1856	1999	1343
Mn (PPM)	26	16	13	<17.3	<38.9	<14.2	10	22	14
P (PPM)	66	82	56	42	57	79	489	189	316
S (PPM)	S.O.A.	10900	8500	7500	S.O.A.	6100	S.O.A.	S.O.A.	S.O.A.
Au (PPB)	1.2	0.6	0.2	-0.2	1.1	0.7	1.5	1.6	<0.2
Ag (PPM)	<0.3	<0.3	<0.3	<0.3	<0.3	<0.3	<0.3	<0.3	<0.3
As (PPM)	3.50	3.20	1.50	1.60	0.67	0.75	1.80	3.00	1.80
Ba (PPM)	70	89	30	39	70	49	71	92	300
Br (PPM)	9.4	9.9	11.0	10.0	5.8	5.1	18.0	23.0	16.0
Ce (PPM)	22	48	45	32	42	23	43	38	65
Co (PPM)	3.4	2.5	2.2	4.7	5.2	12.0	2.1	2.2	5.6
Cr (PPM)	82	36	30	22	56	24	22	31	61
Cs (PPM)	0.50	0.37	0.18	0.20	0.39	0.18	0.33	0.48	1.30
Cu (PPM)					59.52				119.74
Eu (PPM)	0.66	1.29	0.78	0.40	0.57	0.30	0.46	0.55	0.82
Hf (PPM)	5.8	4.2	3.2	2.6	6.5	2.8	3.1	3.8	4.2
Hg (PPM)	0.33	0.16	<0.05	<0.05	<0.05	<0.05	<0.05	0.08	<0.05
Ir (PPM)	<0.2	<0.2	<0.2	<0.2	<0.2	<0.2	<0.2	<0.2	<0.2
La (PPM)	11	23	23	18	23	13	26	20	40
Lu (PPM)	0.70	0.86	0.35	0.15	0.26	0.14	0.15	0.21	0.26
Mo (PPM)	1.10	0.77	3.00	1.90	<0.05	1.10	0.65	2.00	1.80
Nd (PPM)	8.1	22.0	17.0	10.0	13.0	7.2	12.0	12.0	21.0
Ni (PPM)	<2	24	<2	10	18	32	<2	13	<2
Pb (PPM)					16.73				15.03
Rb (PPM)	10	11	4	4	4	<1	<1	<1	6
Sb (PPM)	0.18	0.18	0.18	0.14	0.20	0.17	0.16	0.24	0.44
Sc (PPM)	22.0	12.0	6.0	4.6	8.6	4.5	5.4	6.6	8.2
Se (PPM)	0.3	1.0	2.1	2.0	2.7	2.3	2.2	2.2	2.7
Sm (PPM)	2.2	4.7	3.2	1.8	2.4	1.4	2.1	2.2	3.5
Sr (PPM)	<10	<10	<10	<10	<10	<10	160.00	130.00	380.00
Ta (PPM)	0.51	0.37	0.31	0.21	0.87	0.33	0.34	0.40	0.45
Tb (PPM)	0.6	1.0	0.6	0.3	0.4	0.2	0.3	0.4	0.5
Th (PPM)	9.5	6.4	6.0	5.1	13.0	5.8	5.8	9.0	9.3
U (PPM)	1.6	1.5	1.3	1.1	2.6	1.3	1.1	1.7	1.7
U (PPM) (XRF)					3.50				1.34
V (PPM)					26.45				12.08
W (PPM)	3.5	2.8	2.1	1.8	6.5	1.6	1.5	2.8	8.2
Yb (PPM)	4.73	5.70	2.52	1.05	1.89	0.95	1.05	1.51	1.86
Zn (PPM)	34	26	29	19	63	110	16	25	33

Blake West Pit - Channel Samples (cont)									
	BWB 0.00-0.65	BWB 0.65-1.25	BWB 1.25-1.90	BWB 1.90-1.98	BWB 1.98-2.05	BWB 2.05-2.72	BWB 2.72-2.78	BWB 2.78-3.04	BWB 3.04-3.15
From	5.48	6.13	6.73	7.38	7.46	7.53	8.2	8.26	8.52
To	6.13	6.73	7.38	7.46	7.53	8.2	8.26	8.52	8.63
IM	2.0	1.1	1.9	0.8	1.0	1.0	0.7	1.1	1.0
ASH	36.6	24.3	19.9	62.2	6.6	14.9	64.1	19.6	14.9
VM	6.2	8.5	14.1	14.1	17.4	21.1	16.5	21.9	21.2
VM (daf)	10.1	11.4	18.0	38.1	18.8	25.1	46.9	27.6	25.2
FC	55.2	66.1	64.1	22.9	75.0	63.0	18.7	57.4	62.9
Major Elements (whole coal)									
Si (PPM)	84273	53904	45329	143131	13215	32388	146352	35366	33220
Al (PPM)	72304	55187	44386	143317	12776	32149	140638	34772	31972
Fe (PPM)	6480	2640	1070	1710	1280	2510	1320	21300	2870
Fe (PPM)	6473	3038	1148	1868	1228	2327	1251	22108	2834
Ca (PPM)	<300	<300	<300	<300	<300	<300	<300	<300	<300
Mg (PPM)	1150	473	368	1122	201	332	1023	943	297
Na (PPM)	932	511	287	581	221	228	442	1550	187
K (PPM)	8100	<500	<500	<500	2400	1400	1500	<500	800
Ti (PPM)	4459	2583	2156	5018	2016	2303	4589	1150	1395
Mn (PPM)	32	24	16	37	5	28	<64.1	298	42
P (PPM)	2089	981	760	272	804	749	155	480	768
S (PPM)	S.O.A.	S.O.A.	S.O.A.	S.O.A.	S.O.A.	S.O.A.	S.O.A.	S.O.A.	S.O.A.
Au (PPB)	1.1	1.4	<0.2	<0.2	2.2	0.3	0.6	<0.2	0.5
Ag (PPM)	<0.3	<0.3	<0.3	<0.3	<0.3	<0.3	<0.3	<0.3	<0.3
As (PPM)	1.10	0.70	0.60	1.30	0.82	0.14	0.61	1.10	0.61
Ba (PPM)	1400	530	530	300	340	590	190	380	660
Br (PPM)	28.0	24.0	11.0	3.6	10.0	6.8	2.2	11.0	5.2
Ce (PPM)	100	57	95	28	110	90	7	48	76
Co (PPM)	1.9	1.8	3.8	3.3	3.6	3.2	2.2	3.7	5.4
Cr (PPM)	24	17	16	18	20	17	12	10	11
Cs (PPM)	5.10	1.20	1.00	3.10	0.41	0.91	1.70	0.45	0.73
Cu (PPM)	68.44			53.49			32.69		
Eu (PPM)	1.28	0.74	1.04	0.54	1.42	1.13	0.20	0.57	0.81
Hf (PPM)	19.0	12.0	9.3	15.0	14.0	8.0	13.0	9.8	6.4
Hg (PPM)	<0.05	<0.05	<0.05	<0.05	<0.05	<0.05	<0.05	0.14	0.14
Ir (PPM)	<0.2	<0.2	<0.2	<0.2	<0.2	<0.2	<0.2	<0.2	<0.2
La (PPM)	60	33	56	17	70	54	4	27	42
Lu (PPM)	0.60	0.50	0.68	0.50	0.77	0.80	0.28	0.37	0.48
Mo (PPM)	2.70	<0.05	<0.05	6.50	1.00	1.50	4.50	<0.05	2.40
Nd (PPM)	43.0	21.0	38.0	9.2	36.0	38.0	2.0	18.0	31.0
Ni (PPM)	15	<2	15	<2	15	<2	<2	<2	<2
Pb (PPM)	30.38			15.55			7.05		
Rb (PPM)	13	4	3	5	<1	<1	7	<1	<1
Sb (PPM)	1.10	0.78	1.40	2.00	0.94	1.10	1.10	0.44	0.51
Sc (PPM)	8.2	7.2	8.1	6.0	9.0	8.6	3.1	7.4	7.1
Se (PPM)	1.9	3.5	3.0	1.9	2.3	3.2	2.3	2.4	3.3
Sm (PPM)	8.8	4.7	7.0	3.0	9.3	7.6	1.0	3.7	5.3
Sr (PPM)	1000.00	430.00	320.00	150.00	290.00	330.00	64.00	270.00	380.00
Ta (PPM)	4.50	1.70	0.75	3.00	0.63	0.62	3.80	0.36	0.67
Tb (PPM)	1.5	1.1	1.4	0.6	1.6	1.4	0.4	0.7	1.1
Th (PPM)	62.0	27.0	15.0	25.0	27.0	11.0	24.0	16.0	10.0
U (PPM)	7.1	4.6	3.3	4.2	3.2	2.8	3.5	3.3	3.1
U (PPM)	12.08			5.60			5.13		
V (PPM)	17.57			2.49			3.85		
W (PPM)	6.1	3.3	1.5	5.2	2.9	1.4	5.8	1.6	2.1
Yb (PPM)	4.27	3.55	4.72	3.59	5.62	5.62	1.91	2.70	3.52
Zn (PPM)	20	21	70	110	55	32	22	58	61

Blake West Pit - Channel Samples (cont)									
	BWB 3.15-3.25	BWB 3.25-3.56	BWB 3.56-3.71	BWB 3.71-3.93	BWB 3.93-4.23	BWB 4.23-4.28	BWB 4.28-4.40	BWB 4.40-4.43	BWB 4.43-4.67
From	8.63	8.73	9.04	9.19	9.41	9.71	9.76	9.88	9.91
To	8.73	9.04	9.19	9.41	9.71	9.76	9.88	9.91	10.15
IM	0.7	1.0	0.7	0.9	1.0	1.0	0.9	0.8	1.0
ASH	55.8	11.8	42.4	17.7	14.2	8.5	12.1	75.2	10.3
VM	24.9	20.6	19.7	19.8	19.7	23.6	23.7	15.0	23.9
VM (daf)	57.2	23.6	34.6	24.3	23.2	26.1	27.2	62.5	26.9
FC	18.6	66.6	37.2	61.6	65.1	66.9	63.3	9.0	64.8
Major Elements (whole coal)									
Si (PPM)	80427	34828	100846	40882	29186	8870	25374	172298	21977
Al (PPM)	81394	15733	96469	39085	27539	10835	23708	164970	20670
Fe (PPM)	144000	1600	2300	1500	8080	17100	5700	7480	3010
Fe (PPM)	136663	1126	2208	1421	7804	18500	5907	6958	3175
Ca (PPM)	<300	<300	<300	<300	3800	3200	<300	<300	<300
Mg (PPM)	3373	210	660	271	428	417	281	1554	228
Na (PPM)	1200	172	291	163	196	489	280	583	372
K (PPM)	<500	<500	1000	<500	<500	<500	2200	2400	<500
Ti (PPM)	527	1064	4078	2988	2524	855	3090	7004	2157
Mn (PPM)	5061	15	<42.4	12	93	255	83	102	40
P (PPM)	131	889	349	492	582	1898	403	121	426
S (PPM)	2300	4100	2800	4300	3500	6300	4000	1400	5000
Au (PPB)	0.5	0.4	<0.2	0.8	0.5	0.3	2.3	<0.2	0.5
Ag (PPM)	<0.3	<0.3	<0.3	<0.3	<0.3	<0.3	<0.3	<0.3	<0.3
As (PPM)	0.20	0.51	0.68	0.94	1.50	0.43	0.73	1.40	0.72
Ba (PPM)	160	1500	380	460	360	1100	250	130	260
Br (PPM)	5.0	6.6	2.7	5.5	5.4	6.9	4.3	1.0	4.2
Ce (PPM)	10	85	26	58	49	27	39	17	35
Co (PPM)	8.5	4.8	7.6	5.0	5.4	6.8	9.8	3.7	13.0
Cr (PPM)	13	19	19	24	28	12	32	21	26
Cs (PPM)	0.60	0.67	1.10	0.65	0.88	0.18	1.20	4.10	0.78
Cu (PPM)	30.69		20.78					35.34	
Eu (PPM)	0.38	1.35	0.38	0.68	0.72	0.56	0.48	0.25	0.48
Hf (PPM)	3.5	4.8	6.7	6.9	4.2	1.8	4.6	7.0	4.1
Hg (PPM)	<0.05	<0.05	0.24	0.1	0.09	<0.05	<0.05	<0.05	<0.05
Ir (PPM)	<0.2	<0.2	<0.2	<0.2	<0.2	<0.2	<0.2	<0.2	<0.2
La (PPM)	5	47	14	33	26	15	22	14	20
Lu (PPM)	0.76	0.81	0.48	0.59	0.46	0.16	0.23	0.26	0.19
Mo (PPM)	3.20	0.50	2.40	1.30	0.42	0.39	0.10	9.90	1.30
Nd (PPM)	4.5	42.0	8.2	20.0	20.0	11.0	13.0	4.1	12.0
Ni (PPM)	22	<2	<2	<2	24	<2	43	<2	16
Pb (PPM)	6.70		13.14					5.26	
Rb (PPM)	9	<1	8	<1	<1	<1	<1	21	<1
Sb (PPM)	0.46	0.36	0.65	0.40	0.24	0.34	0.24	0.40	0.22
Sc (PPM)	21.0	8.7	7.9	9.6	7.7	3.8	6.7	11.0	8.3
Se (PPM)	0.3	2.0	1.3	2.5	1.8	1.5	2.9	0.5	2.2
Sm (PPM)	2.3	9.7	2.1	4.0	4.2	2.7	2.2	1.1	2.1
Sr (PPM)	<10	650.00	180.00	290.00	330.00	910.00	270.00	<10	320.00
Ta (PPM)	1.30	0.35	1.50	0.59	0.45	0.16	0.41	1.20	0.41
Tb (PPM)	1.0	2.0	0.5	0.9	0.8	0.5	0.4	0.4	0.4
Th (PPM)	7.0	8.2	9.6	14.0	8.3	2.8	7.7	8.5	6.5
U (PPM)	3.1	2.1	2.6	2.7	1.2	0.8	1.6	2.6	1.4
U (PPM)	6.70		2.97					2.26	
V (PPM)	16.18		32.22					30.83	
W (PPM)	<0.2	<0.2	2.7	<0.2	2.1	<0.2	1.5	3.3	<0.2
Yb (PPM)	5.49	6.06	3.50	4.02	3.22	1.21	1.61	1.81	1.41
Zn (PPM)	150	49	50	52	30	21	25	30	23

Blake West Pit - Channel Samples (cont)									
	BWB 4.67-5.13	BWB 5.13-5.51	BWB 5.51-6.25	BWB 6.25-6.75	BWB 6.75-7.25	BWB 7.25-7.75	BWB 7.75-8.25	BWB 8.25-8.75	BWB 8.75-9.25
From	10.15	10.61	10.99	11.73	12.23	12.73	13.23	13.73	14.23
To	10.61	10.99	11.73	12.23	12.73	13.23	13.73	14.23	14.73
IM	1.0	1.3	1.4	1.0	1.0	1.1	1.2	1.0	0.9
ASH	20.9	34.5	74.1	18.5	17.8	17.0	13.3	12.8	9.1
VM	20.3	18.0	14.8	20.1	21.1	21.0	20.9	21.3	22.2
VM (daf)	26.0	28.0	60.4	25.0	26.0	25.6	24.4	24.7	24.7
FC	57.8	46.2	9.7	60.4	60.1	60.9	64.6	64.9	67.8
Major Elements (whole coal)									
Si (PPM)	46654	74483	162028	38575	33973	35186	29126	27949	21838
Al (PPM)	44138	67158	146471	32830	31553	31934	24431	23297	14120
Fe (PPM)	3400	12900	17400	14900	12600	8480	4590	6720	4850
Fe (PPM)	3506	11981	14361	12919	12203	8044	4254	6340	4440
Ca (PPM)	<300	<300	<300	<300	2500	2200	<300	<300	<300
Mg (PPM)	417	1152	1764	822	883	778	606	500	233
Na (PPM)	433	525	1330	347	1480	1980	1830	797	313
K (PPM)	3000	2500	4700	<500	1100	<500	<500	<500	<500
Ti (PPM)	3282	9721	11863	3872	2130	2125	1859	1643	1281
Mn (PPM)	35	209	135	211	174	113	48	83	27
P (PPM)	1094	808	383	938	2077	975	797	714	454
S (PPM)	4000	4200	S.O.A.	3600	5300	5700	5300	4400	S.O.A.
Au (PPB)	1.3	3.0	<0.2	<0.2	<0.2	<0.2	1.0	0.5	0.4
Ag (PPM)	<0.3	<0.3	<0.3	<0.3	<0.3	<0.3	<0.3	<0.3	<0.3
As (PPM)	2.30	1.40	2.30	1.70	0.88	1.20	0.77	0.53	0.56
Ba (PPM)	430	350	200	200	190	140	130	76	66
Br (PPM)	4.9	7.4	3.7	7.4	8.9	11.0	10.0	6.9	7.2
Ce (PPM)	49	87	57	120	37	27	33	30	33
Co (PPM)	9.3	7.2	5.3	8.3	8.4	11.0	10.0	10.0	9.3
Cr (PPM)	32	120	170	70	23	24	21	19	17
Cs (PPM)	1.20	4.50	4.30	1.40	1.10	0.99	0.75	0.73	0.25
Cu (PPM)		33.81	38.53						
Eu (PPM)	0.90	1.27	1.01	2.00	0.76	0.51	0.52	0.43	0.36
Hf (PPM)	4.3	10.0	11.0	7.3	3.5	3.3	3.0	3.0	2.2
Hg (PPM)	0.18	<0.05	<0.05	<0.05	0.1	<0.05	0.13	0.15	0.14
Ir (PPM)	<0.2	<0.2	<0.2	<0.2	<0.2	<0.2	<0.2	<0.2	<0.2
La (PPM)	32	50	38	69	19	15	18	16	16
Lu (PPM)	0.25	0.46	0.36	0.62	0.31	0.24	0.18	0.17	0.10
Mo (PPM)	2.10	0.15	1.00	1.40	0.99	1.00	0.86	1.10	1.40
Nd (PPM)	17.0	27.0	20.0	48.0	15.0	9.2	12.0	9.7	12.0
Ni (PPM)	<2	<2	34	35	20	<2	23	14	20
Pb (PPM)		25.88	21.49						
Rb (PPM)	4	9	14	3	3	6	3	3	2
Sb (PPM)	0.27	0.42	0.40	0.39	0.24	0.23	0.20	0.15	0.18
Sc (PPM)	8.2	21.0	25.0	19.0	8.3	5.8	5.1	4.7	1.9
Se (PPM)	2.0	0.9	0.2	2.1	2.0	2.2	2.6	2.0	2.0
Sm (PPM)	3.5	4.4	4.1	8.4	3.2	1.8	2.0	1.8	1.7
Sr (PPM)	550.00	310.00	280.00	350.00	190.00	110.00	98.00	110.00	110.00
Ta (PPM)	0.84	2.00	1.40	0.97	0.36	0.33	0.35	0.30	0.20
Tb (PPM)	0.7	1.0	0.8	1.4	0.7	0.5	0.4	0.3	0.2
Th (PPM)	7.6	16.0	14.0	10.0	5.3	6.0	6.2	5.0	3.8
U (PPM)	2.1	4.0	3.2	2.2	1.1	1.6	1.2	1.1	0.8
U (PPM) (XRF)		5.52	5.19						
V (PPM)		179.75	157.83						
W (PPM)	1.6	3.5	3.3	2.4	1.2	1.3	1.6	1.1	1.0
Yb (PPM)	1.88	3.55	2.52	4.53	2.13	1.54	1.23	1.26	0.71
Zn (PPM)	41	78	80	40	39	35	24	20	22

Bowen No.2. Pit - Channel Samples									
	BO 0.00-0.10	BO 0.10-0.15	BO 0.15-0.34	BO 0.34-0.37	BO 0.37-0.72	BO 0.72-1.07	BO 1.07-1.09	BO 1.09-1.15	BO 1.15-1.85
From	0	0.1	0.15	0.34	0.37	0.72	1.07	1.09	1.15
To	0.1	0.15	0.34	0.37	0.72	1.07	1.09	1.15	1.85
IM	1.1	0.9	0.7	0.7	0.7	0.9	1.0	0.8	0.9
ASH	33.4	22.5	19.5	31.8	14.4	11.7	25.9	6.2	12.9
VM	20.5	22.5	19.1	19.2	20.6	24.6	24.1	25.5	22.4
VM (daf)	31.3	29.4	23.9	28.4	24.3	28.1	33.0	27.4	26.0
FC	45.0	54.1	60.7	48.3	64.3	62.8	49.0	67.5	63.8
Major Elements (whole coal)									
Si (PPM)	57539	45486	54959	54378	45434	29081	52619	17052	37937
Al (PPM)	35195	30388	24493	19271	16893	13940	30386	7370	16674
Fe (PPM)	106000	41100	15000	109000	5160	16800	52900	52300	6670
Fe (PPM)	86545	40108	14435	104876	4956	15409	53924	5189	6418
Ca (PPM)	<300	<300	<300	<300	<300	<300	<300	<300	<300
Mg (PPM)	461	380	278	127	239	<11.7	306	107	189
Na (PPM)	172	102	108	95	91	135	109	77	105
K (PPM)	3700	1000	3200	26000	3100	500	500	1100	<500
Ti (PPM)	1970	1239	1679	2226	1576	1468	2163	1068	1541
Mn (PPM)	70	37	22	32	23	62	56	7	22
P (PPM)	52	89	43	32	44	20	40	20	47
S (PPM)	86200	48200	19600	92900	10900	24300	60900	15000	13200
Au (PPB)	2.3	0.4	<0.2	<0.2	<0.2	0.4	<0.2	<0.2	0.8
Ag (PPM)	<0.3	<0.3	<0.3	<0.3	<0.3	<0.3	<0.3	<0.3	<0.3
As (PPM)	4.30	2.00	0.74	30.00	0.44	3.30	17.00	0.38	1.10
Ba (PPM)	900	110	150	83	55	47	140	57	58
Br (PPM)	5.3	4.8	6.2	4.3	5.2	3.9	4.2	3.4	3.5
Ce (PPM)	26	27	41	41	33	21	26	15	23
Co (PPM)	3.4	3.4	2.1	2.0	1.1	3.1	2.9	1.0	2.3
Cr (PPM)	140	47	37	51	26	20	35	13	22
Cs (PPM)	0.59	0.34	0.18	0.40	0.16	0.17	0.95	0.08	0.24
Cu (PPM)	59.12	40.50					43.77		
Eu (PPM)	0.64	0.66	0.75	0.59	0.40	0.27	0.32	0.18	0.31
Hf (PPM)	4.4	2.3	2.8	2.9	2.8	2.1	2.8	1.6	2.2
Hg (PPM)	1.3	0.56	0.45	1.9	0.2	0.36	1.3	<0.05	<0.05
Ir (PPM)	<0.2	<0.2	<0.2	<0.2	<0.2	<0.2	<0.2	<0.2	<0.2
La (PPM)	12	14	23	27	19	11	13	9	11
Lu (PPM)	0.91	0.65	0.53	0.35	0.17	0.10	0.08	0.15	0.13
Mo (PPM)	1.80	1.00	1.40	5.20	1.50	1.70	2.60	1.00	0.56
Nd (PPM)	7.8	9.2	15.0	12.0	9.6	6.3	6.5	4.9	7.4
Ni (PPM)	<2	<2	30	<2	<2	<2	<2	<2	<2
Pb (PPM)	13.69	10.58					12.95		
Rb (PPM)	8	8	6	10	<1	<1	8	<1	<1
Sb (PPM)	0.29	0.13	0.13	0.44	0.15	0.16	0.30	0.14	0.14
Sc (PPM)	13.0	6.5	5.5	4.8	4.8	3.6	4.2	2.3	4.5
Se (PPM)	0.3	1.8	0.5	8.0	1.1	3.5	5.4	2.3	1.7
Sm (PPM)	2.3	2.3	2.7	2.3	1.8	1.1	1.3	0.8	1.3
Sr (PPM)	<10	<10	<10	<10	<10	<10	<10	<10	<10
Ta (PPM)	0.35	0.26	0.40	0.36	0.31	0.22	0.29	0.23	0.28
Tb (PPM)	0.7	0.7	0.7	0.5	0.3	0.2	0.3	0.2	0.2
Th (PPM)	7.0	4.3	7.6	6.3	6.5	4.5	4.3	3.1	5.5
U (PPM)	1.5	0.8	1.4	1.6	1.3	1.1	1.3	0.8	1.0
U (PPM)	4.68	2.93					2.59		
V (PPM)	115.56	25.20					22.27		
W (PPM)	5.8	3.0	3.8	4.4	1.8	1.7	3.9	1.2	1.4
Yb (PPM)	6.05	4.28	3.54	2.39	1.17	0.73	0.55	0.98	0.85
Zn (PPM)	40	43	38	25	15	19	28	10	18

Bowen No.2. Pit - Channel Samples (cont)							
	BO 1.85-2.45	BO 2.45-2.60	BO 2.60-2.90	Repeat 2	BO 2.90-3.01	BO 3.01-3.61	BO 3.61-4.21
From	1.85	2.45	2.6	2.6	2.91	3.01	3.61
To	2.45	2.6	2.91	2.91	3.01	3.61	4.21
IM	1.0	0.9	0.9		1.3	0.8	0.9
ASH	9.9	8.6	16.0		11.9	9.7	11.5
VM	21.2	23.3	16.5		17.4	15.3	13.1
VM (daf)	23.8	25.7	19.9		20.0	17.1	15.0
FC	67.9	69.2	66.6		69.4	74.2	74.5
Major Elements (whole coal)							
Si (PPM)	28479	15583	47513		29417	25680	26201
Al (PPM)	12539	11380	19749		16351	14776	14620
Fe (PPM)	4570	7330	7720	7950	6970	4060	15000
Fe (PPM)	4359	6523	6632		8997	3823	14575
Ca (PPM)	<300	6900	<300	<300	2000	<300	<300
Mg (PPM)	<9.9	218	346		402	180	310
Na (PPM)	105	114	157	136	132	137	480
K (PPM)	<500	<500	900	<500	<500	<500	2100
Ti (PPM)	1441	862	2911		1216	1658	1475
Mn (PPM)	22	10	43		16	18	29
P (PPM)	600	2603	86		395	567	448
S (PPM)	10700	14700	12900	0	15900	11700	21800
Au (PPB)	0.5	0.5	0.5	<0.2	0.4	<0.2	0.5
Ag (PPM)	<0.3	<0.3	<0.3	<0.3	<0.3	<0.3	<0.3
As (PPM)	0.54	1.60	0.62	0.59	0.41	1.00	1.90
Ba (PPM)	36	150	130	150	120	70	90
Br (PPM)	4.9	5.7	7.2	7.9	6.7	7.6	10.0
Ce (PPM)	27	33	26	24	24	28	25
Co (PPM)	1.4	2.2	1.8	2.2	2.0	1.8	2.5
Cr (PPM)	19	12	33	34	34	19	27
Cs (PPM)	0.11	0.29	0.40	0.58	0.47	0.20	0.20
Cu (PPM)							
Eu (PPM)	0.31	0.36	0.40	0.40	0.37	0.36	0.30
Hf (PPM)	1.7	1.3	4.0	4.4	3.8	2.5	2.5
Hg (PPM)	<0.05	<0.05	<0.05	<0.05	0.12	0.11	0.32
Ir (PPM)	<0.2	<0.2	<0.2	<0.2	<0.2	<0.2	<0.2
La (PPM)	15	21	10	9	10	14	13
Lu (PPM)	0.12	0.08	0.21	0.21	0.20	0.15	0.13
Mo (PPM)	0.49	0.88	0.98	3.20	1.30	1.00	1.50
Nd (PPM)	7.4	10.0	8.4	7.0	7.5	8.5	7.1
Ni (PPM)	13	<2	24	<2	<2	<2	<2
Pb (PPM)							
Rb (PPM)	<1	<1	<1	4	<1	<1	<1
Sb (PPM)	0.09	0.50	0.16	0.15	0.13	0.12	0.23
Sc (PPM)	3.9	3.9	8.9	9.1	7.8	4.4	4.4
Se (PPM)	1.1	3.1	1.5	1.5	1.4	1.4	2.8
Sm (PPM)	1.3	1.5	1.8	1.4	1.6	1.5	1.3
Sr (PPM)	100.00	330.00	79.00	<10	<10	260.00	170.00
Ta (PPM)	0.26	0.17	0.49	0.45	0.46	0.27	0.27
Tb (PPM)	0.2	0.3	0.3	0.3	0.3	0.3	0.2
Th (PPM)	4.7	3.1	9.2	9.2	8.7	5.4	5.6
U (PPM)	1.1	1.0	1.8	1.9	1.9	1.1	0.9
U (PPM) (XRF)							
V (PPM)							
W (PPM)	1.4	0.8	3.5	3.6	3.5	1.1	2.5
Yb (PPM)	0.81	0.50	1.41	1.44	1.32	0.94	0.86
Zn (PPM)	11	9	18	18	16	3	16

Appendix 5

XRD Analysis of Low Temperature Ash.

XRD Analysis of Low Temperature Ash.						
	BC 0 - 50	BC 3.50 - 4.00	BC 4.00 - 4.13	BC 4.18 - 4.22	BC 6.55 - 6.63	BC 6.63 - 6.88
Mineral						
Quartz%	90	65			70	80 - 50
Kaolinite%	10	35	85	100	30	20
Illite%	tr	tr	15			tr?
Pyrite%	tr	tr?	tr?			
Marcasite%						
Feldspar%		tr?			tr?	
Siderite%		tr?	tr?			tr?
Gorciexite%						
Anatase%			tr?			
Apatite%			tr?			
	BWB 3.56 - 3.71	BWB 4.23 - 4.28	BWB 4.43 - 4.67			
Mineral						
Quartz%			tr?			
Kaolinite%	90	10	75			
Illite%	10	10	25			
Pyrite%			tr?			
Marcasite%		15				
Feldspar%						
Siderite%		55				
Gorciexite%		10				
Anatase%						
Apatite%						

XRD Analysis of Low Temperature Ash (cont).				
	BO 0 - 10	BO 37 - 72	BO 1.15 - 1.85	BO 3.61 - 4.21
Mineral				
Quartz%	80	85	85	75 - 40
Kaolinite%	20	15	15	15 - ++
Illite%				tr?
Pyrite%	unassigned			10
Marcasite%				
Feldspar%				
Siderite%				
Gorciexite%				
Anatase%				
Apatite%				

Appendix 6

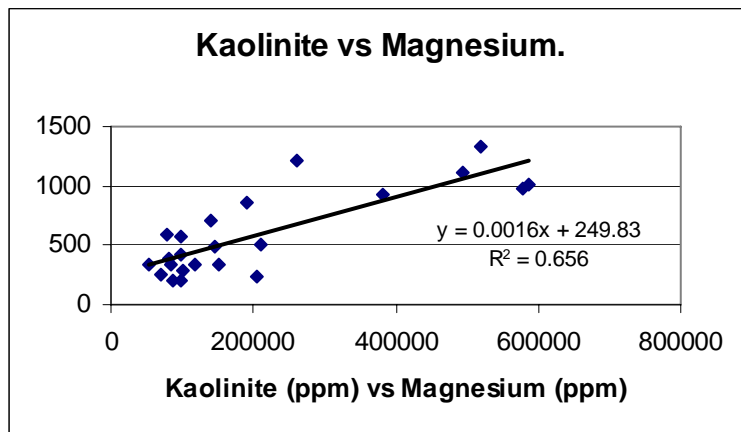
**Graphs to Determine Mode of Occurrence of Trace Elements
in Blake Central, Blake West and Bowen No.2 Pits.**

Appendix 6, Part 1 – Blake Seam Mode of Occurrence Cross Plots.

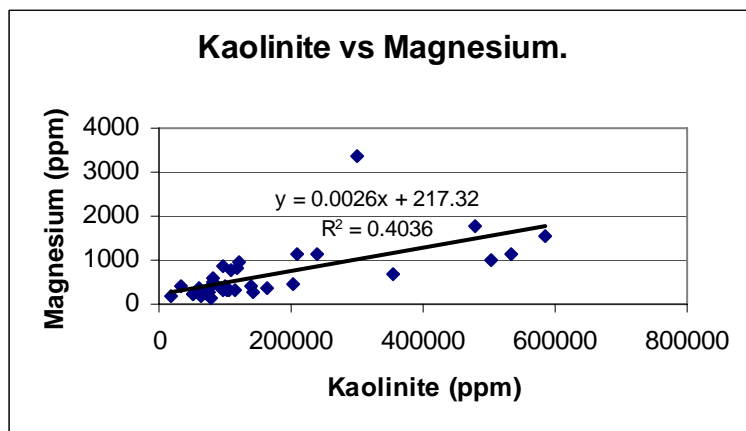
NB Points shown in red (where differentiated) are considered heat affected.

A61A Magnesium.

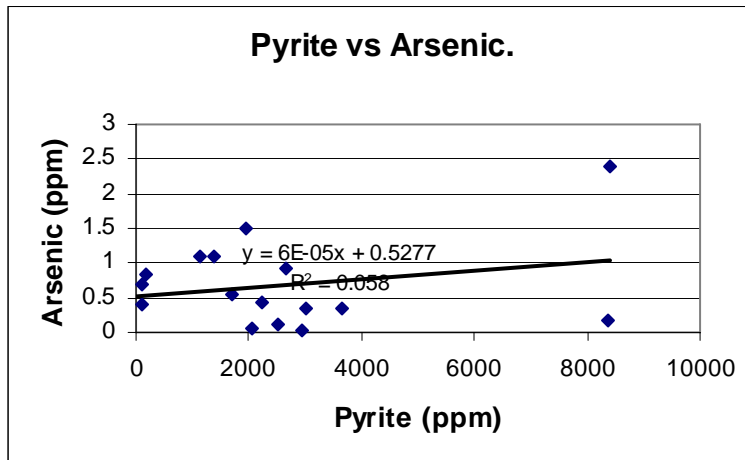
Blake Central.



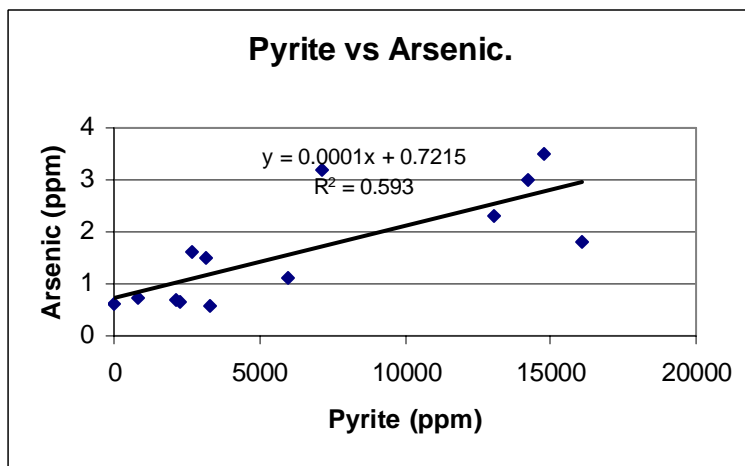
Blake West.

**A61B Arsenic.**

Blake Central

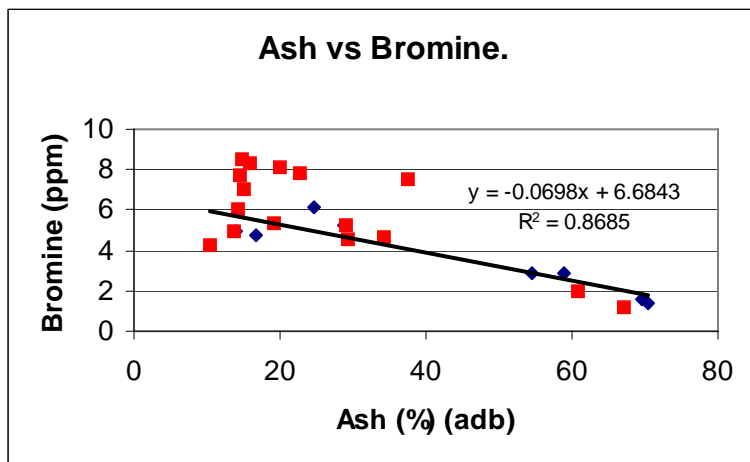


Blake West.

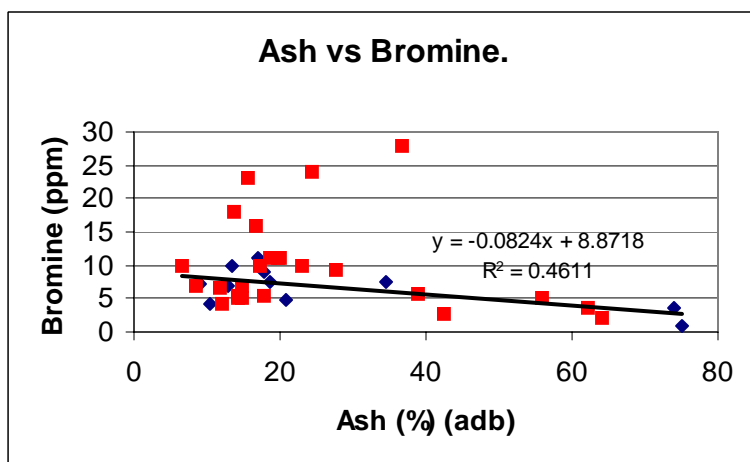


A61C Bromine.

Blake Central

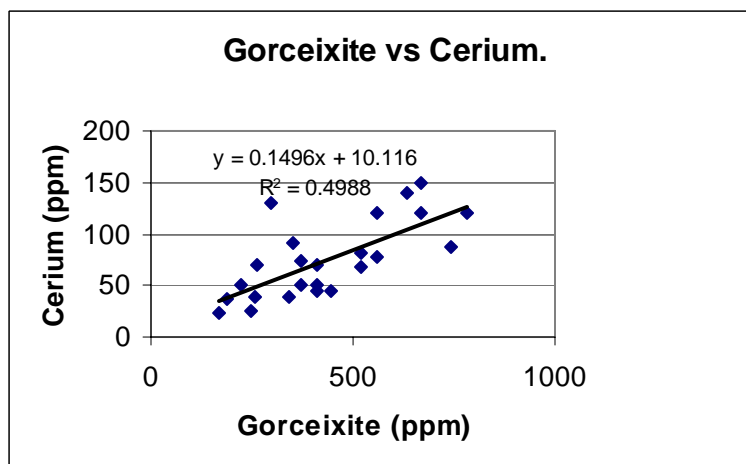
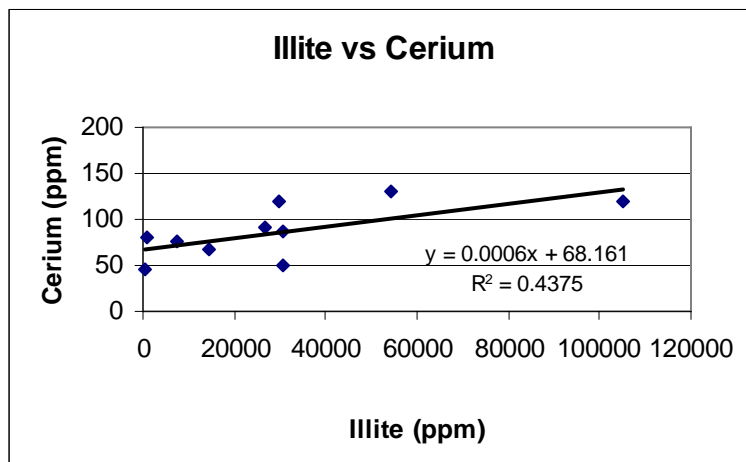


Blake West

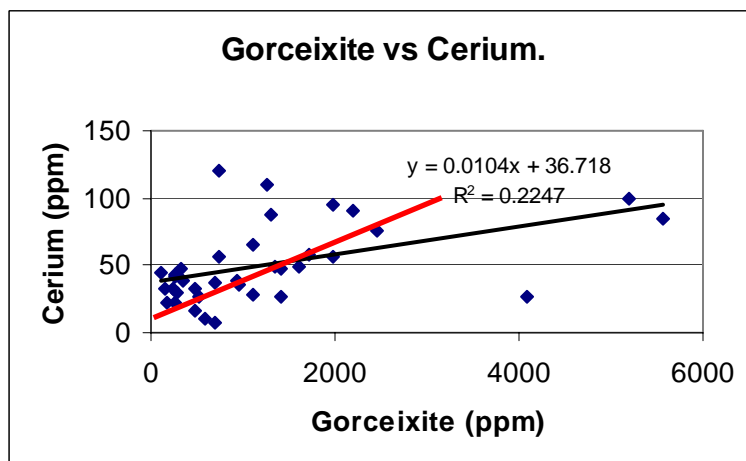


A61D Cerium.

Blake Central

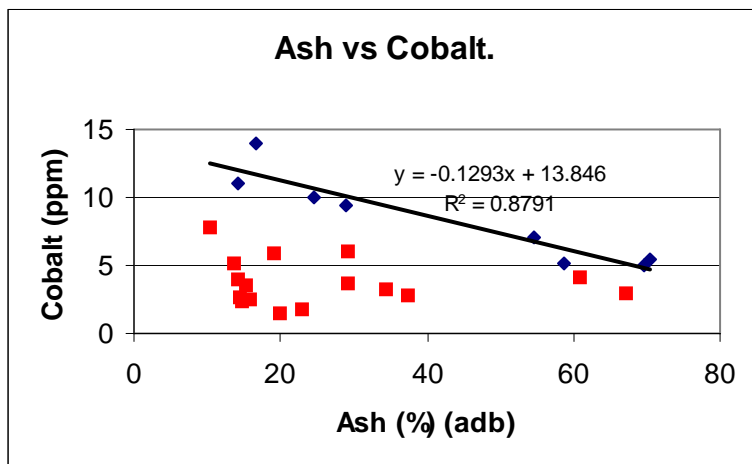


Blake West

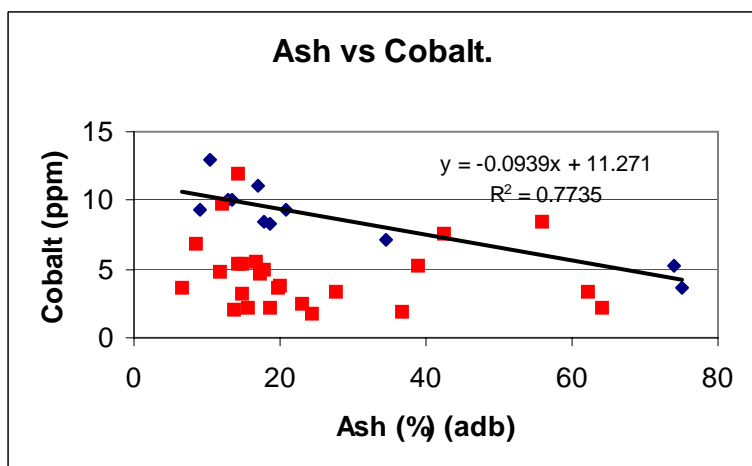


A61E Cobalt.

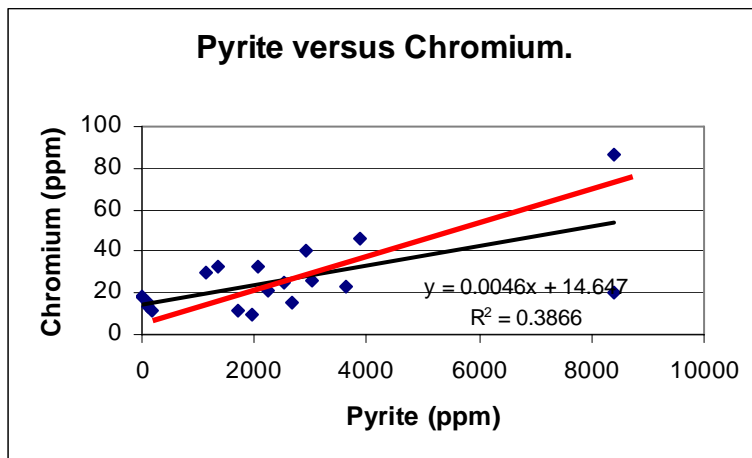
Blake Central



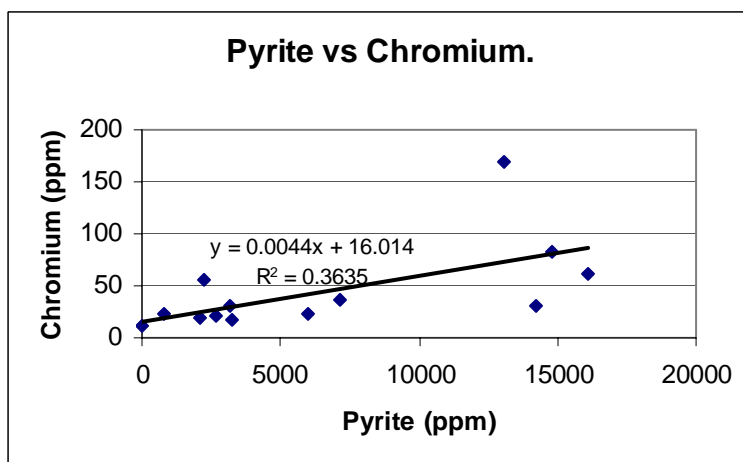
Blake West

**A61F Chromium.**

Blake Central

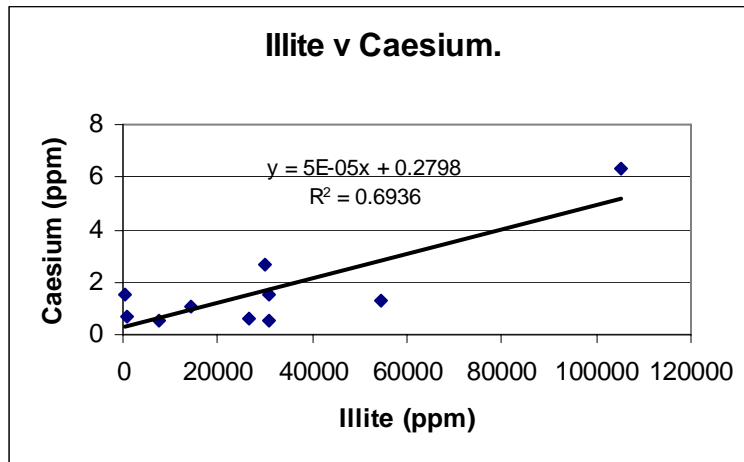


Blake West

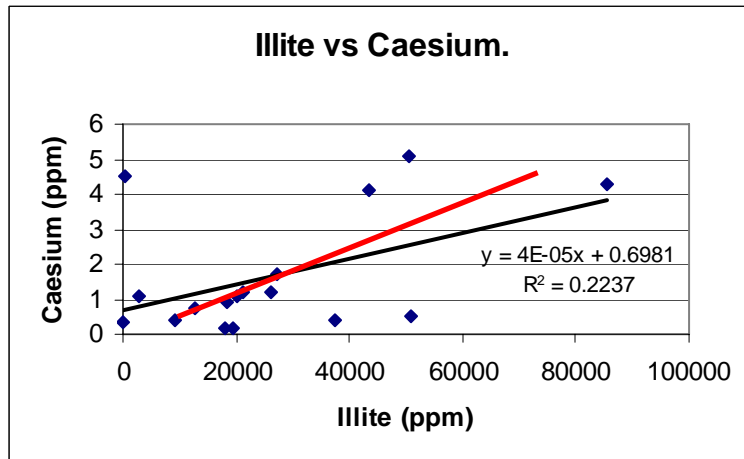


A61G Caesium.

Blake Central

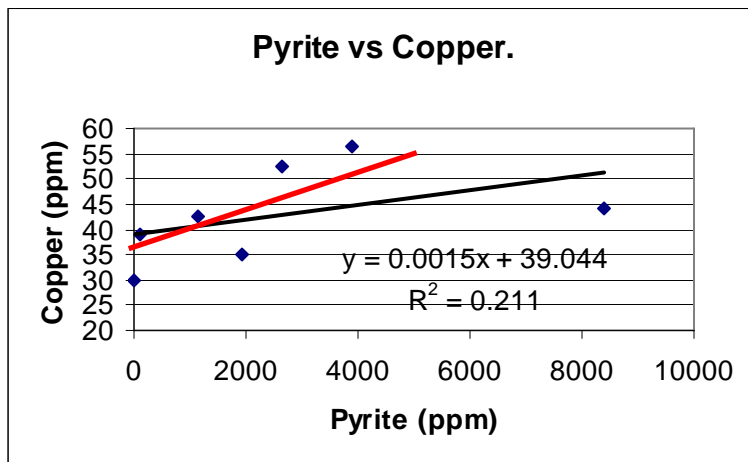


Blake West

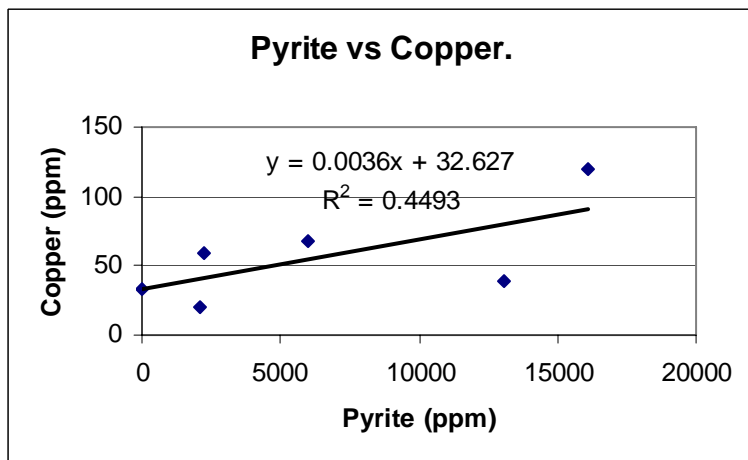


A61H Copper.

Blake Central

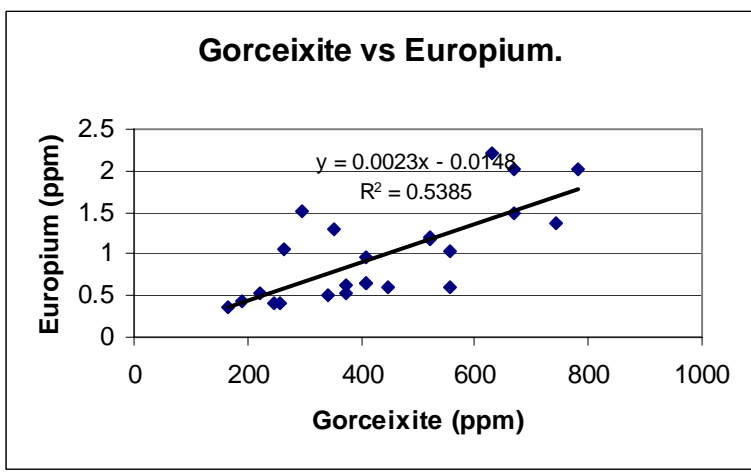
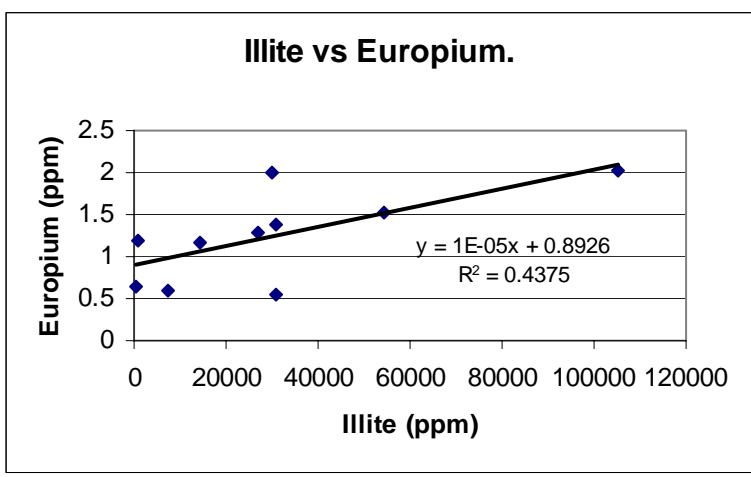


Blake West

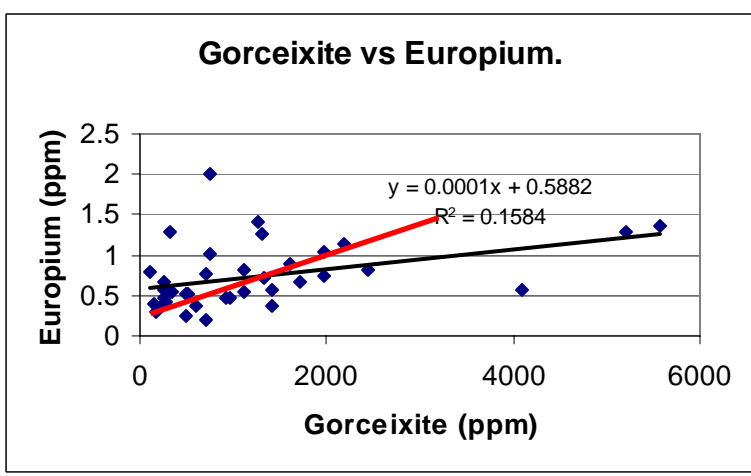


A61I Europium.

Blake Central

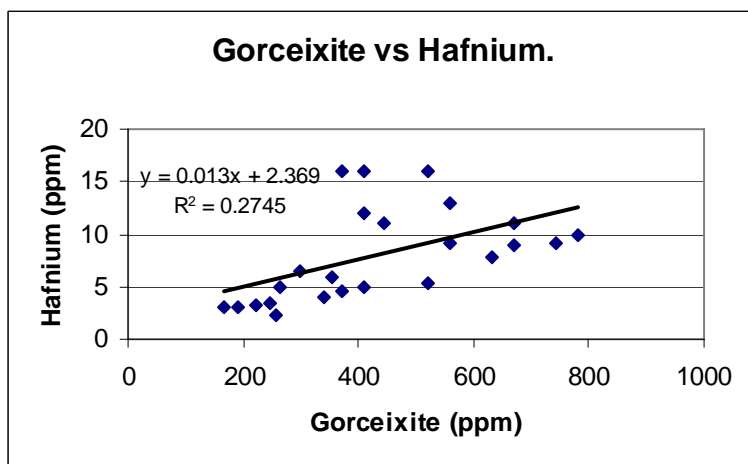
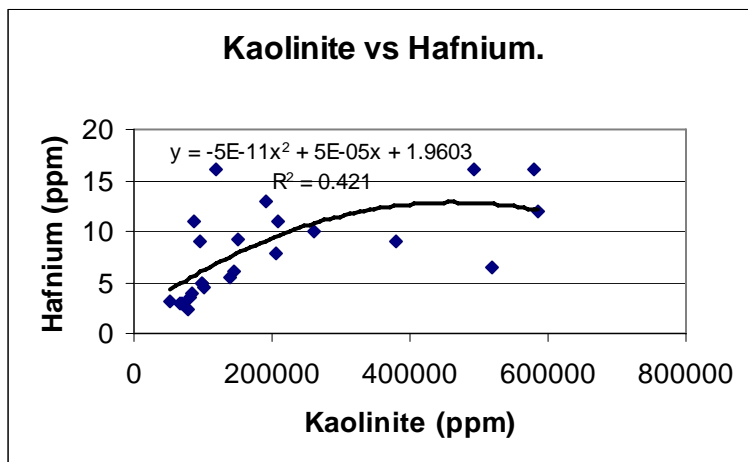


Blake West

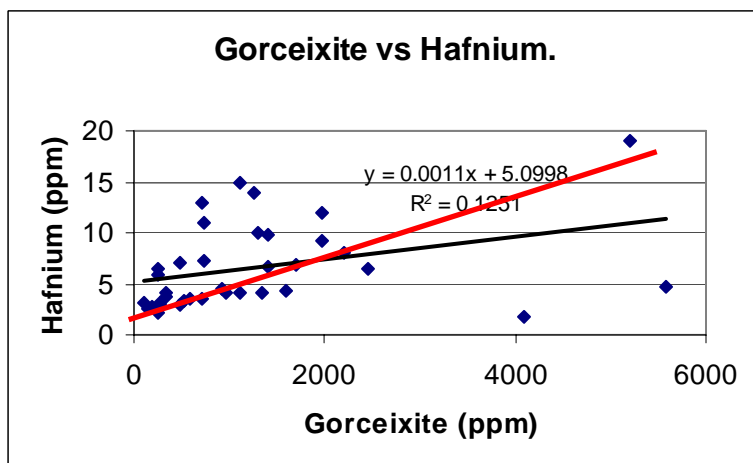


A61J Hafnium.

Blake Central

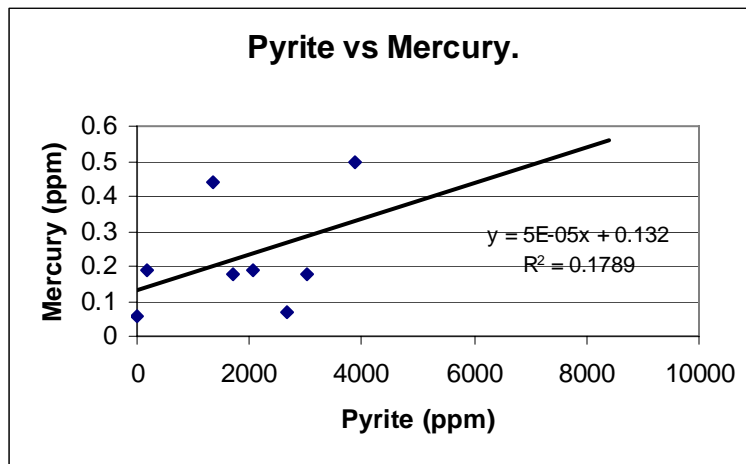


Blake West

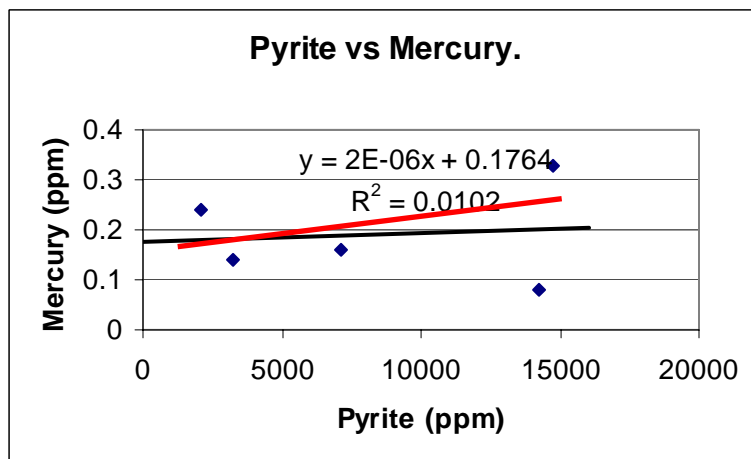


A61K Mercury.

Blake Central

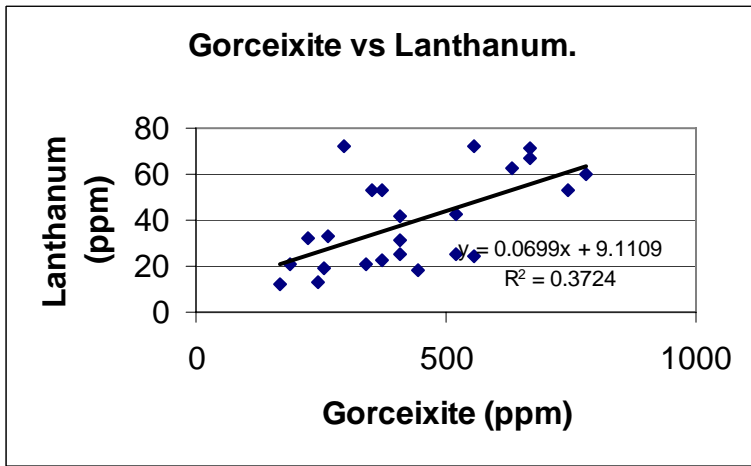
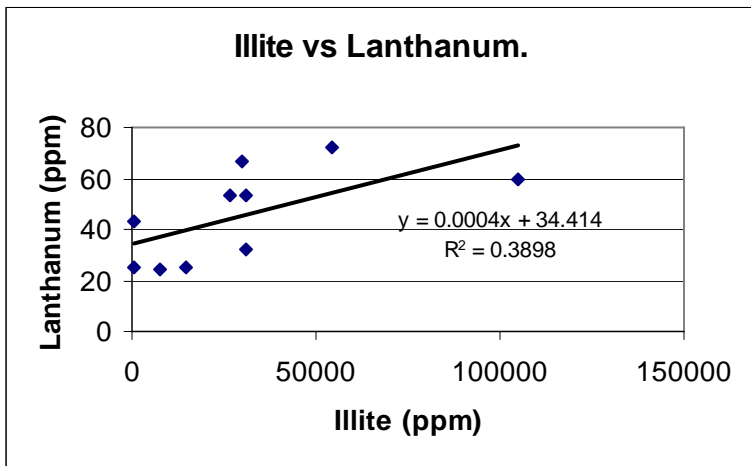


Blake West

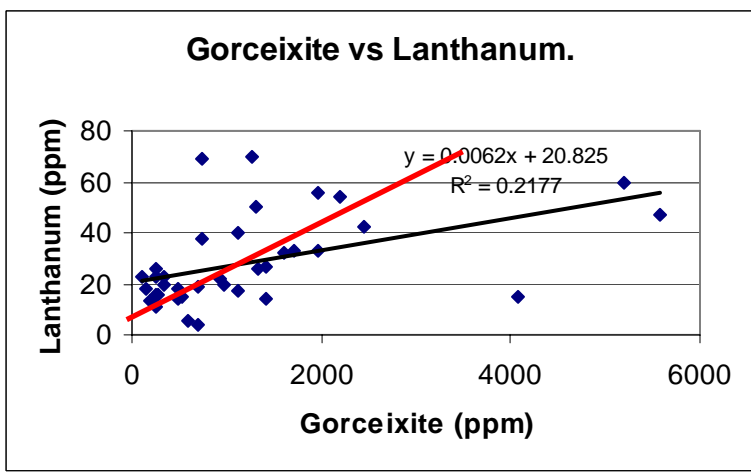


A61L Lanthanum.

Blake Central

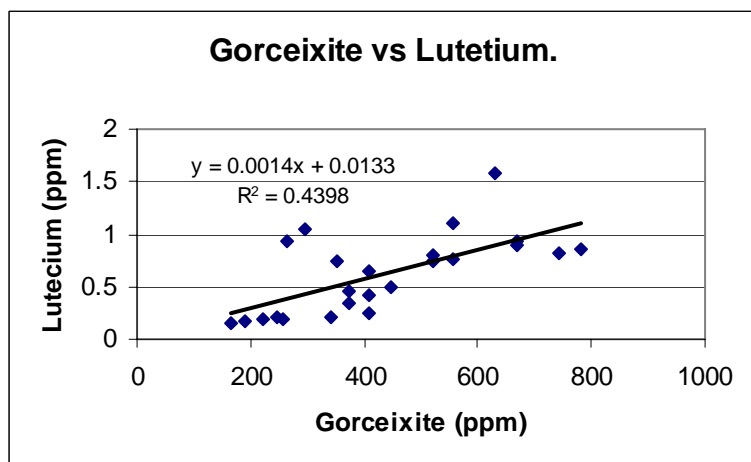
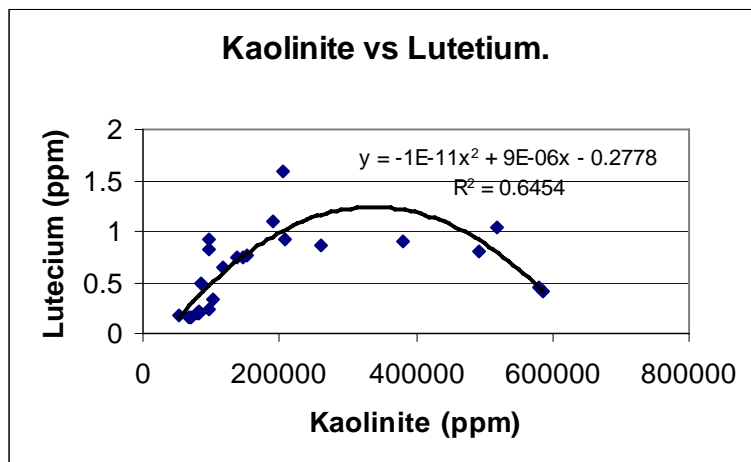


Blake West

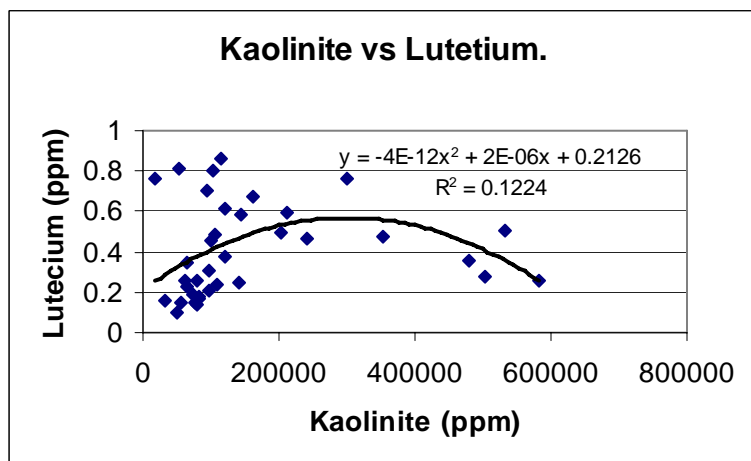


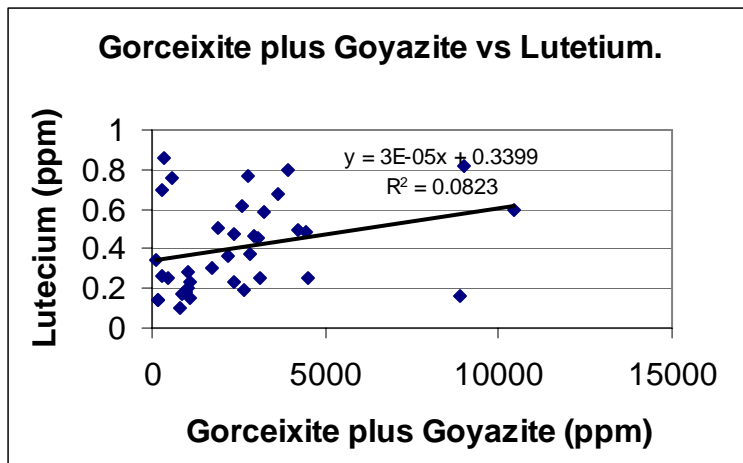
A61M Lutetium.

Blake Central



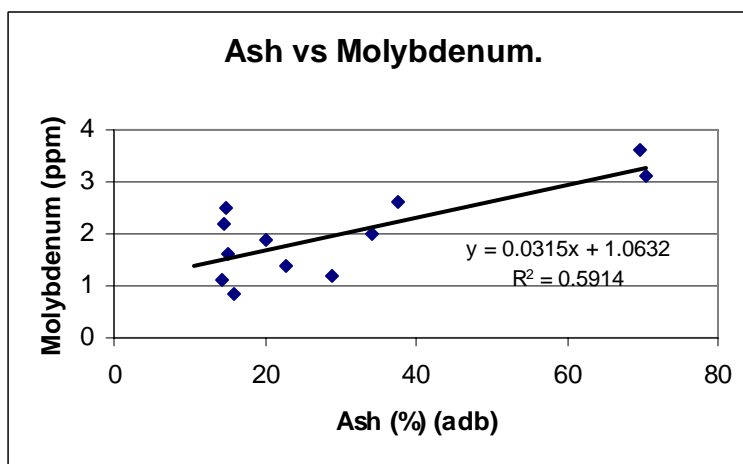
Blake West



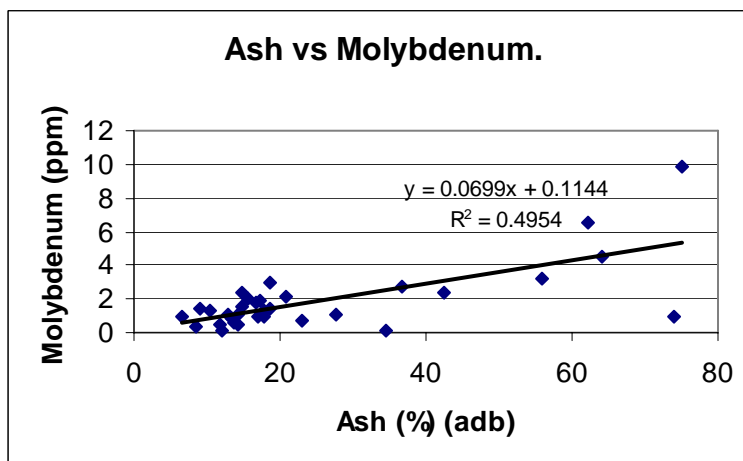


A61N Molybdenum.

Blake Central

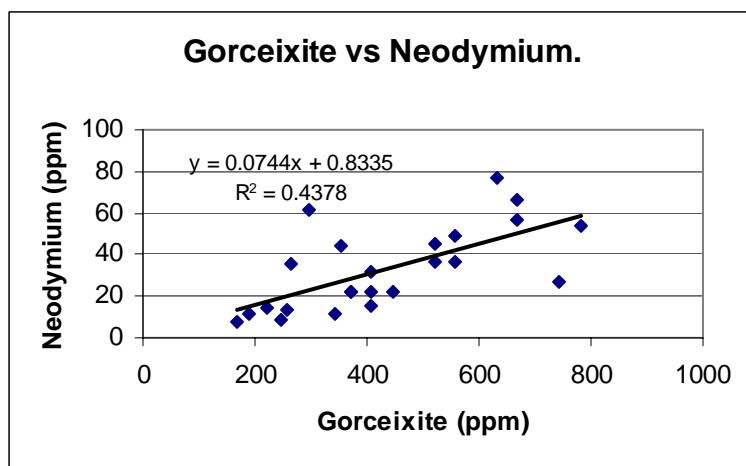
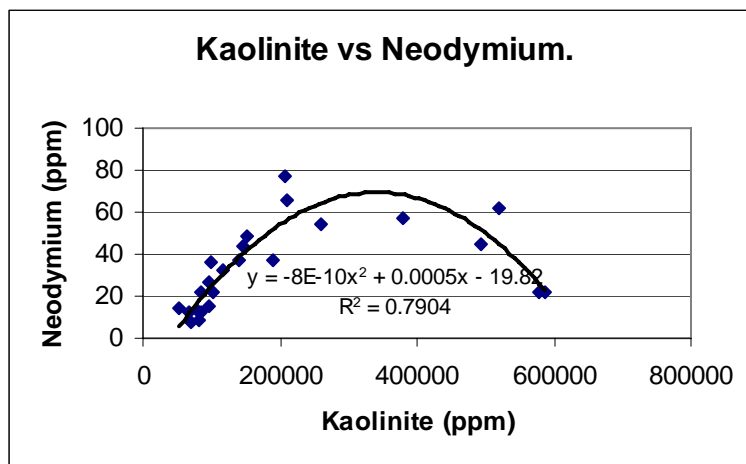


Blake West

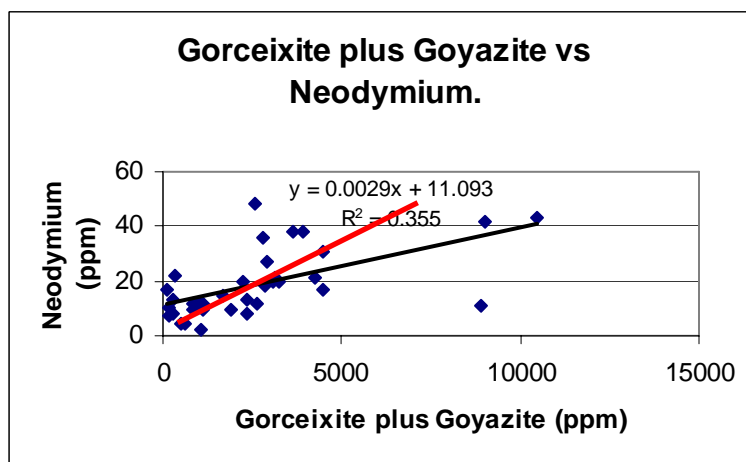


A61O Neodymium.

Blake Central

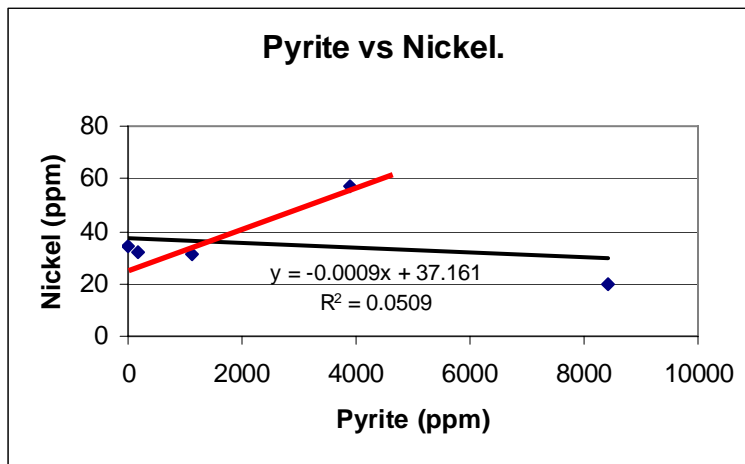


Blake West

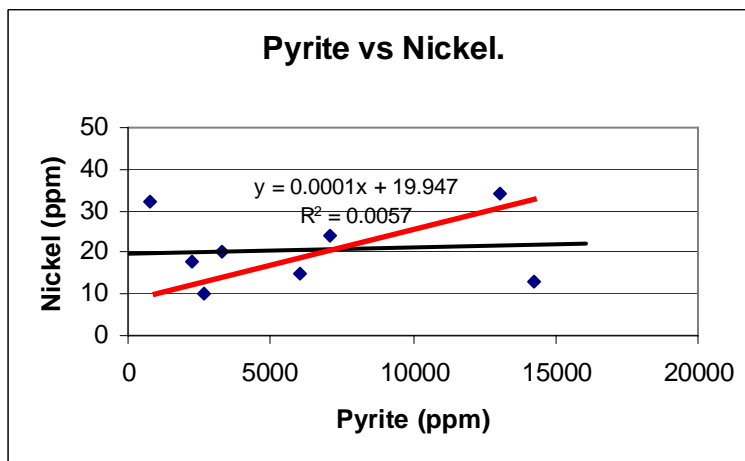


A61P Nickel.

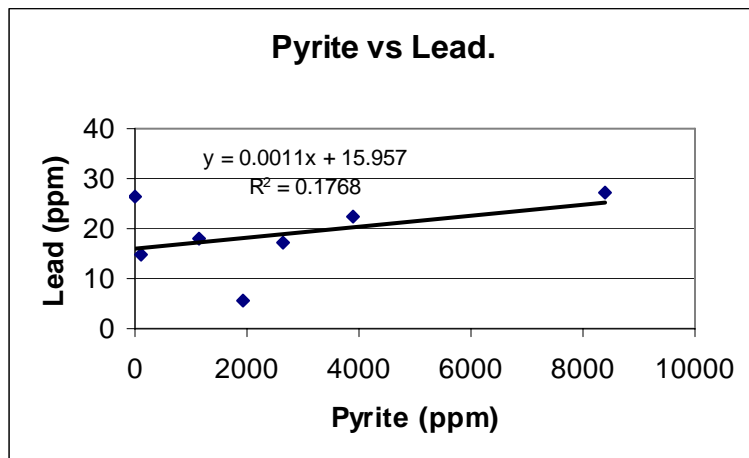
Blake Central



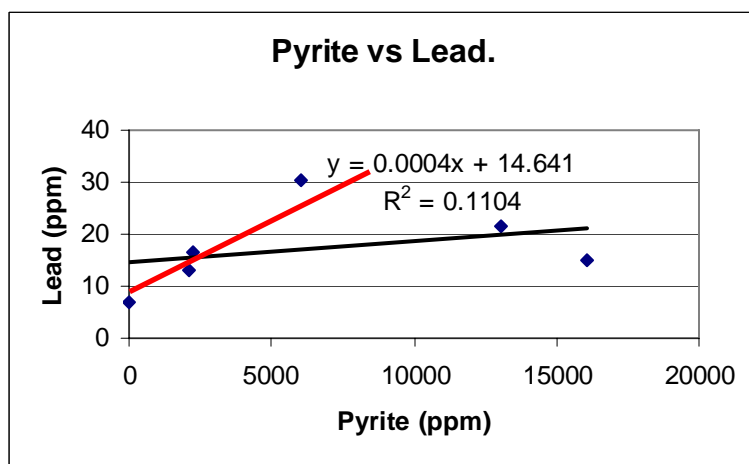
Blake West

**A61Q Lead.**

Blake Central

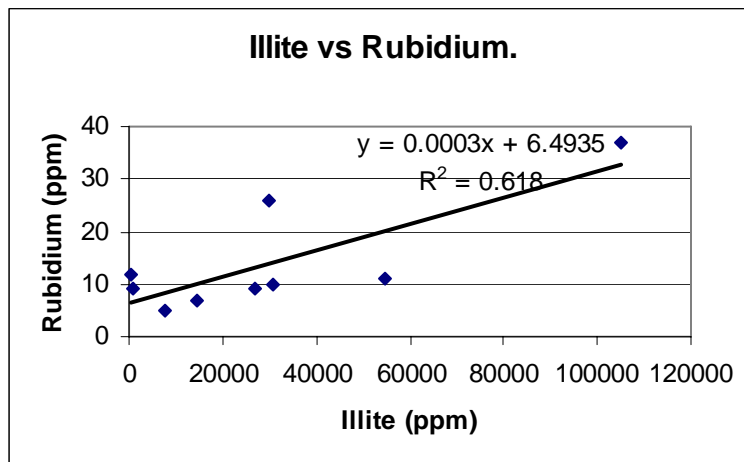


Blake West

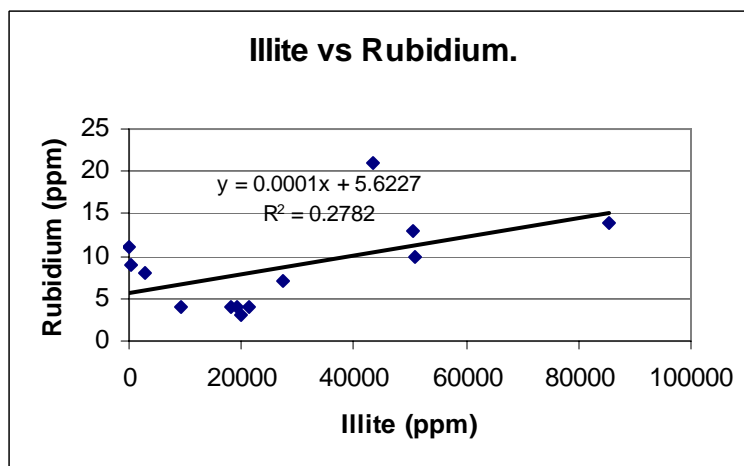
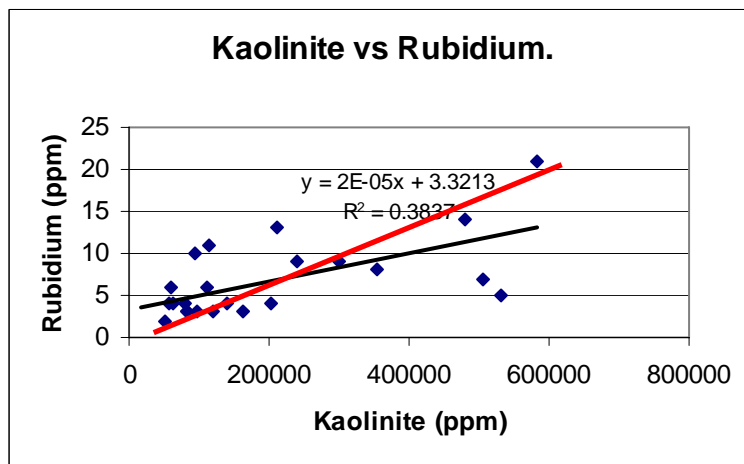


A61R Rubidium.

Blake Central

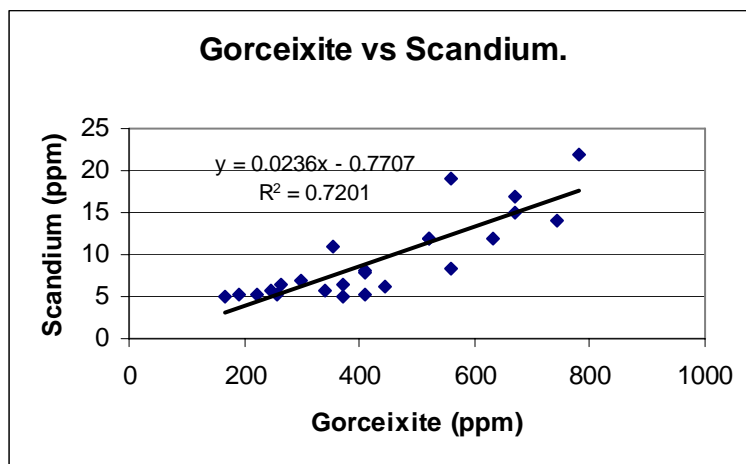


Blake West

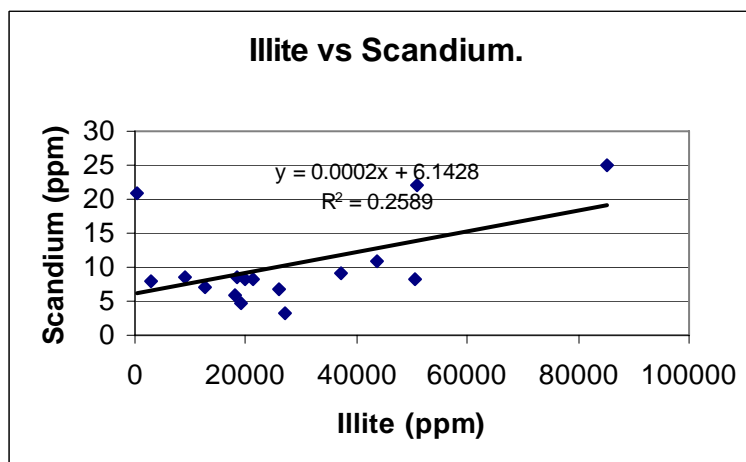


A61S Antimony.

Blake Central

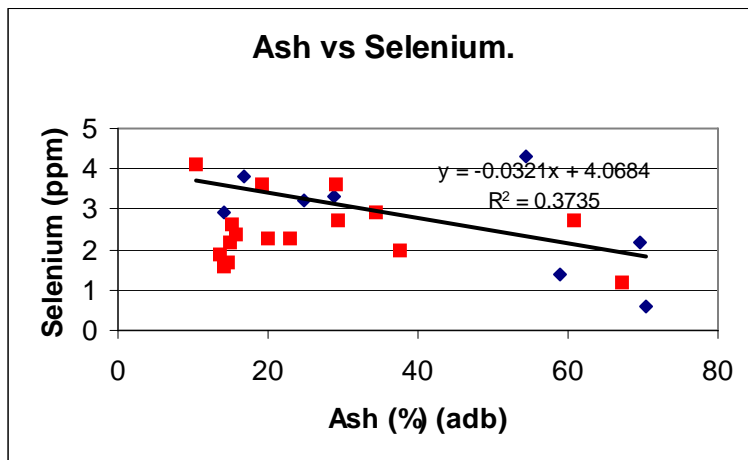


Blake West

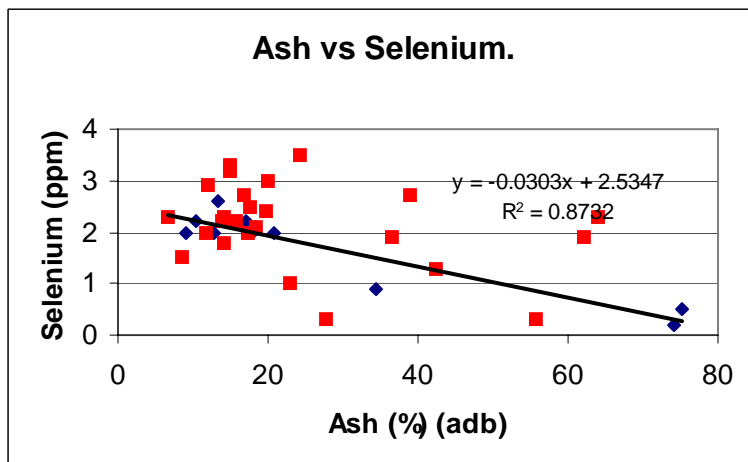


A61U Selenium.

Blake Central

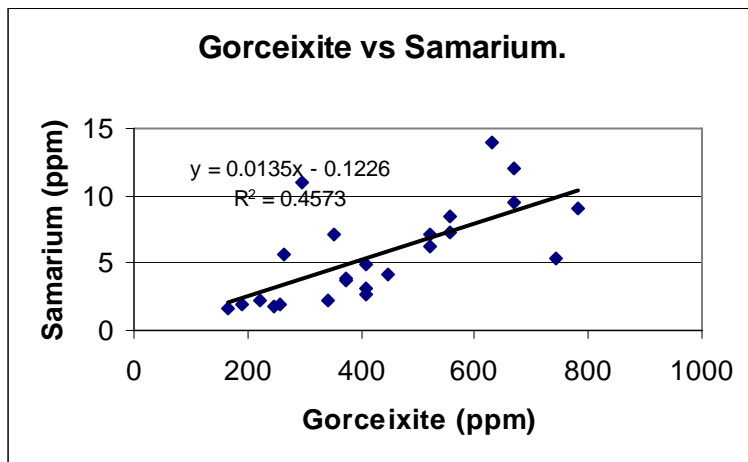


Blake West

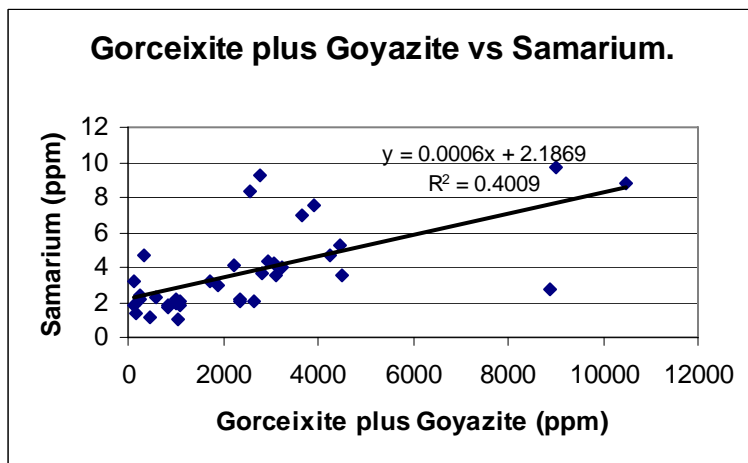


A61V Samarium.

Blake Central

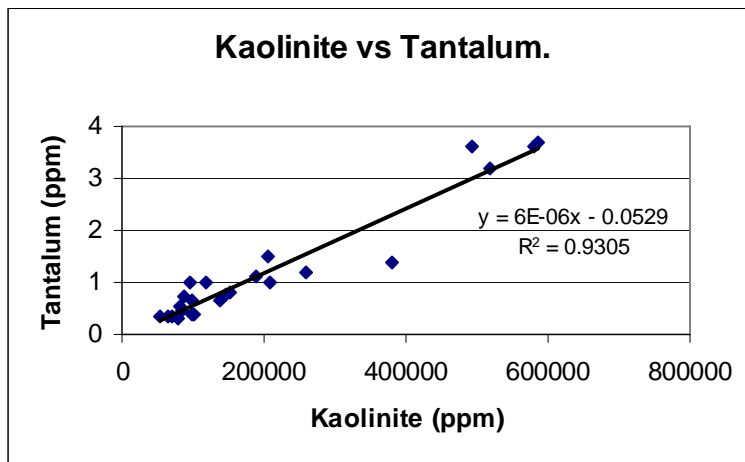


Blake West

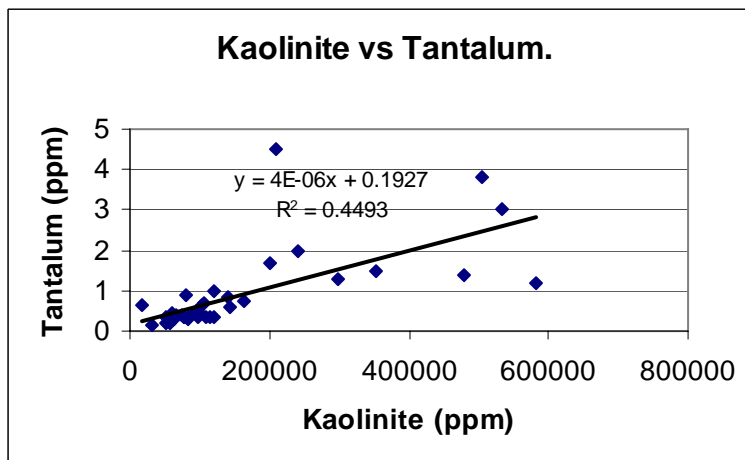


A61W Tantalum.

Blake Central

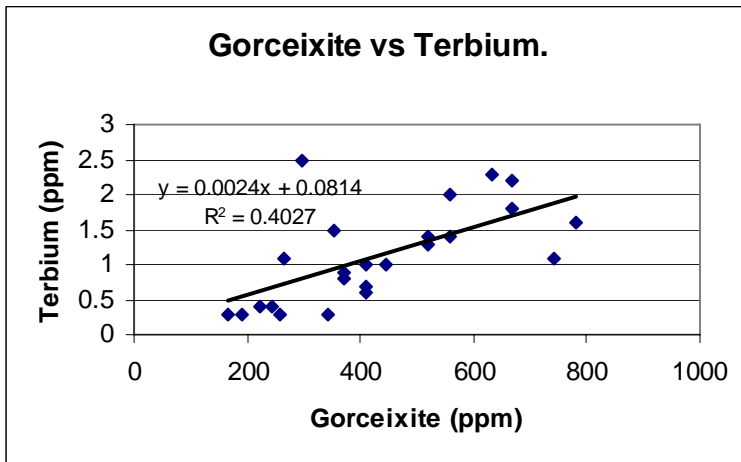


Blake West

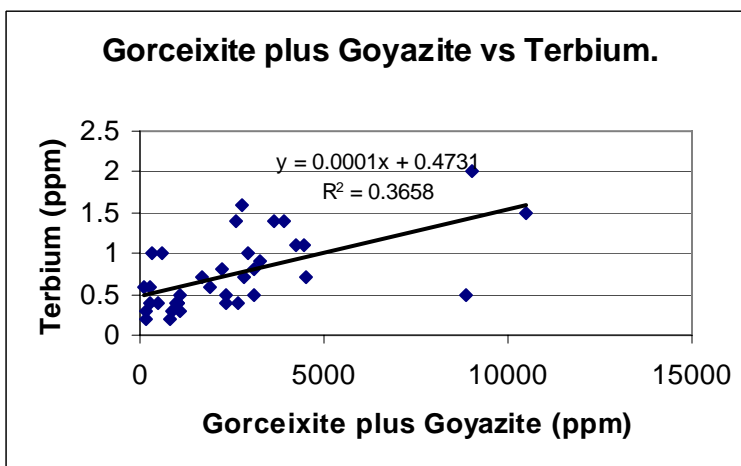
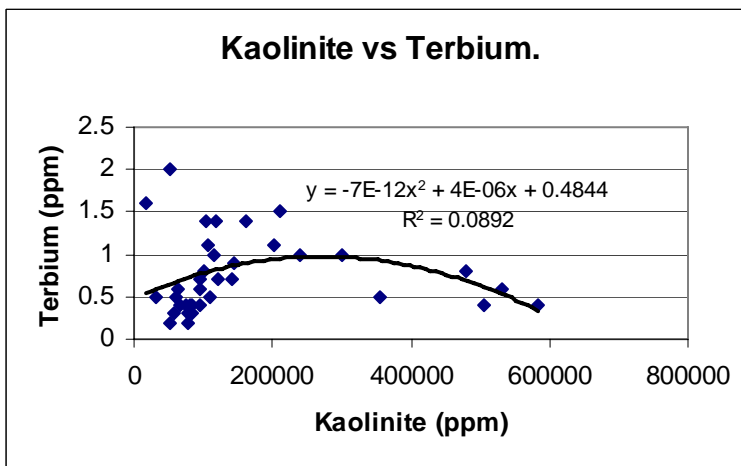


A61X Terbium.

Blake Central

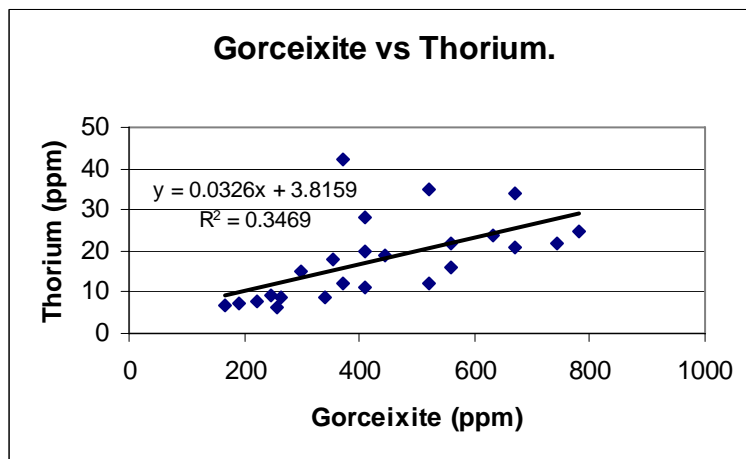
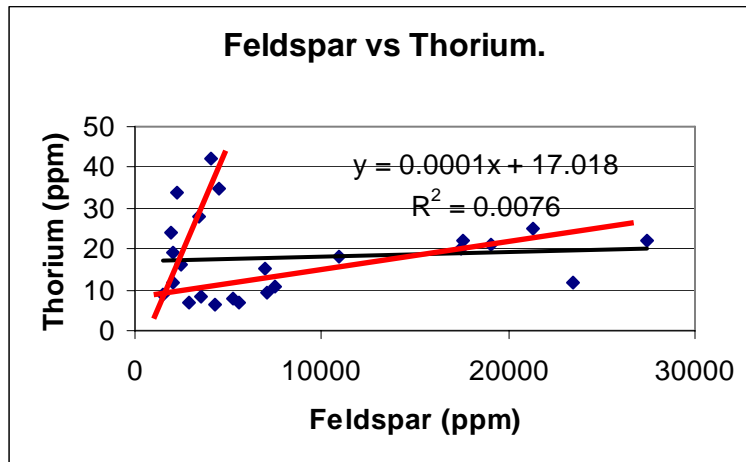


Blake West

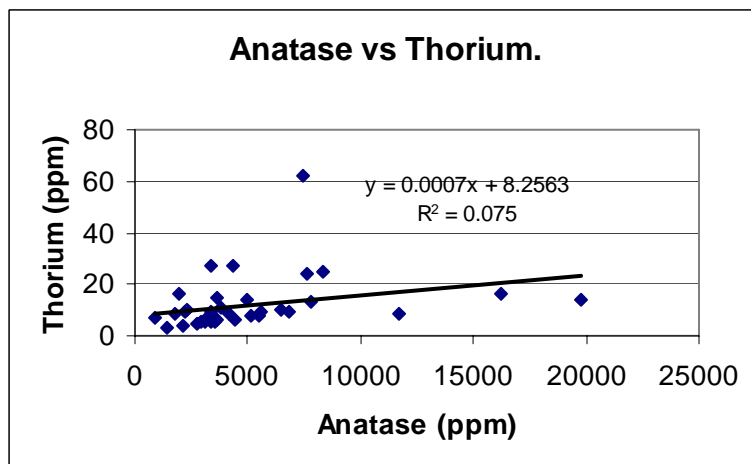


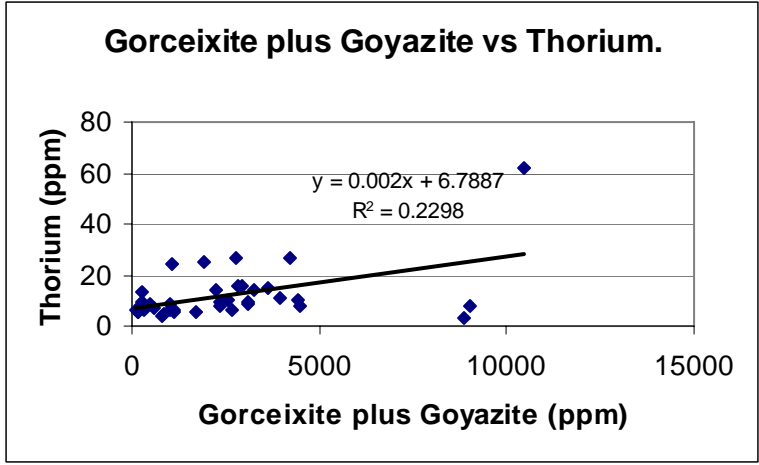
A61Y Thorium.

Blake Central



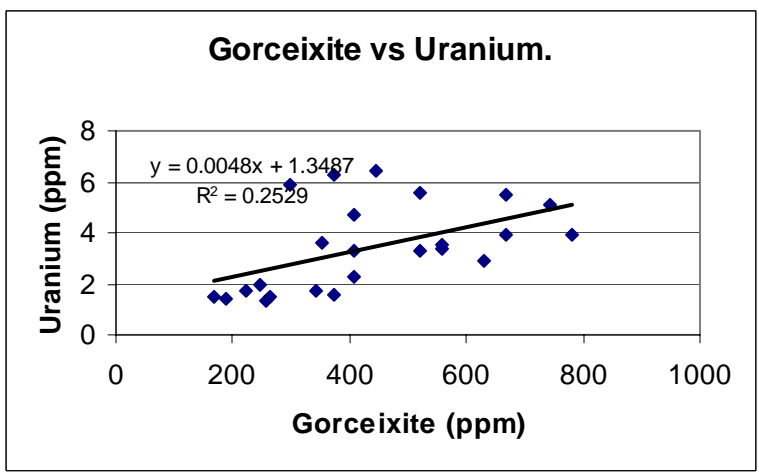
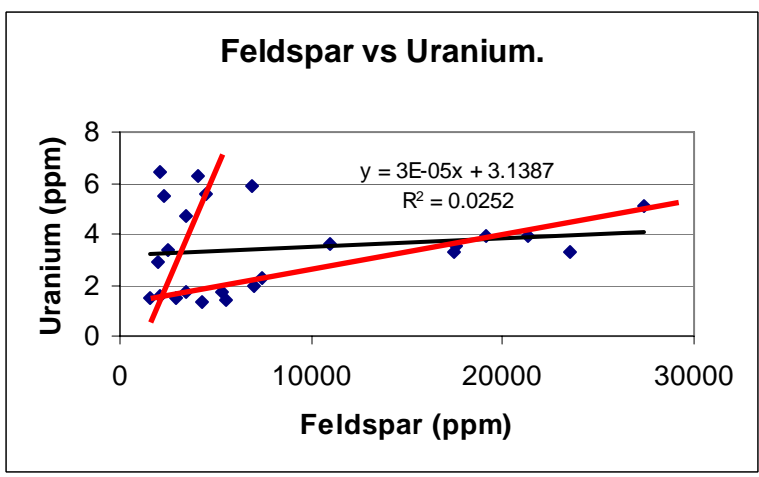
Blake West



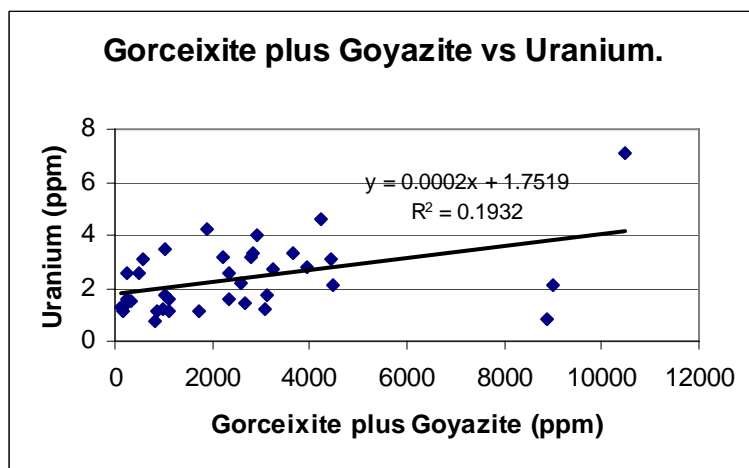
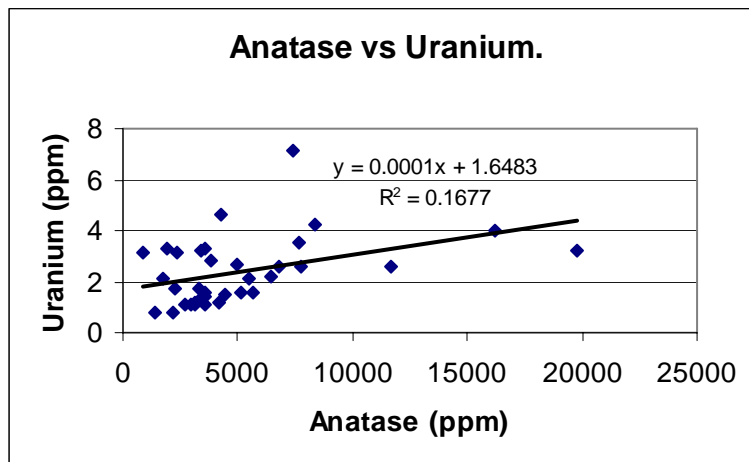


A61Z Uranium.

Blake Central

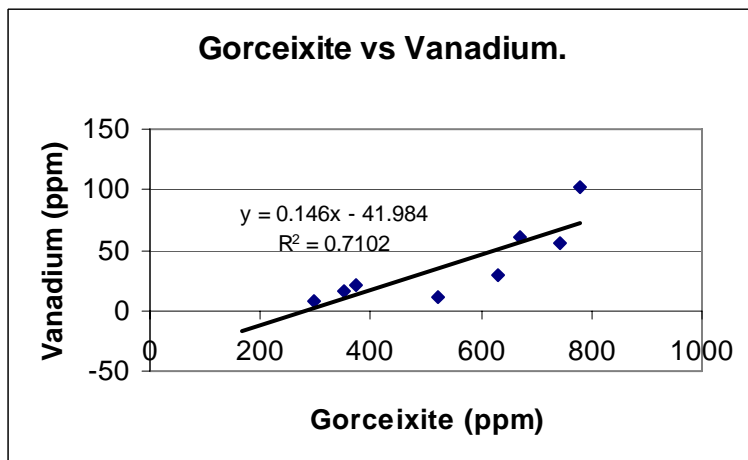
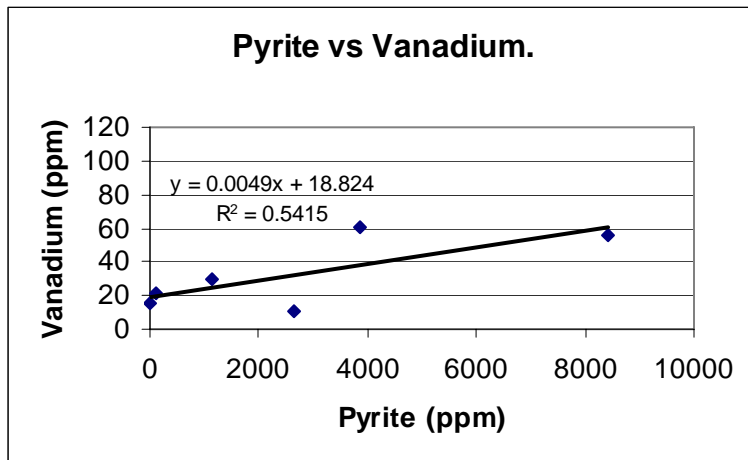


Blake West

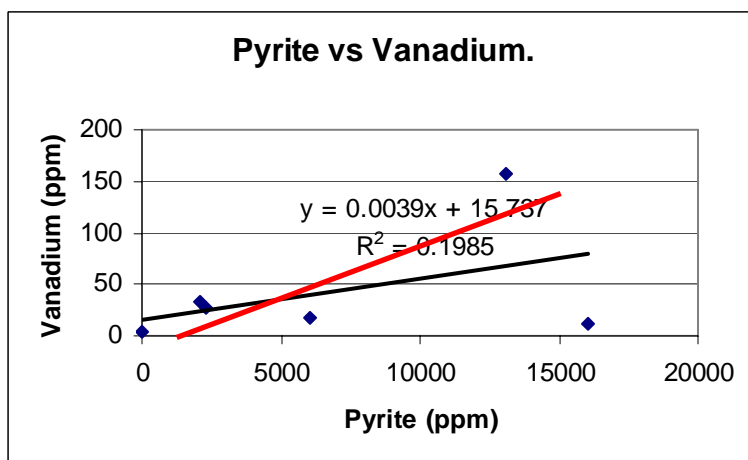


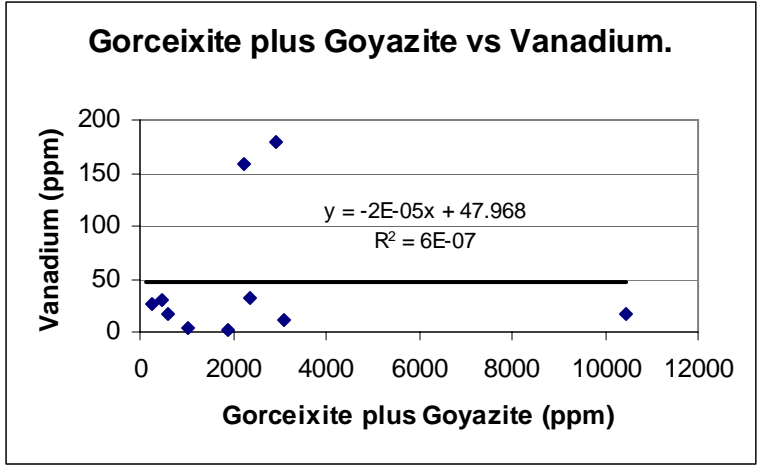
A61AA Vanadium.

Blake Central



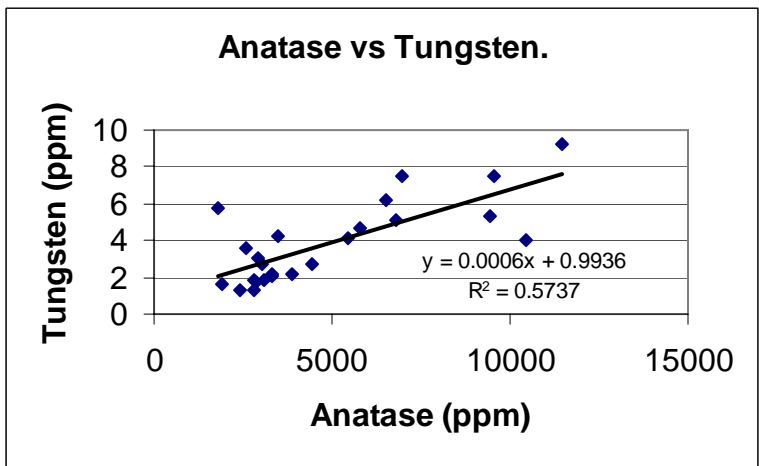
Blake West



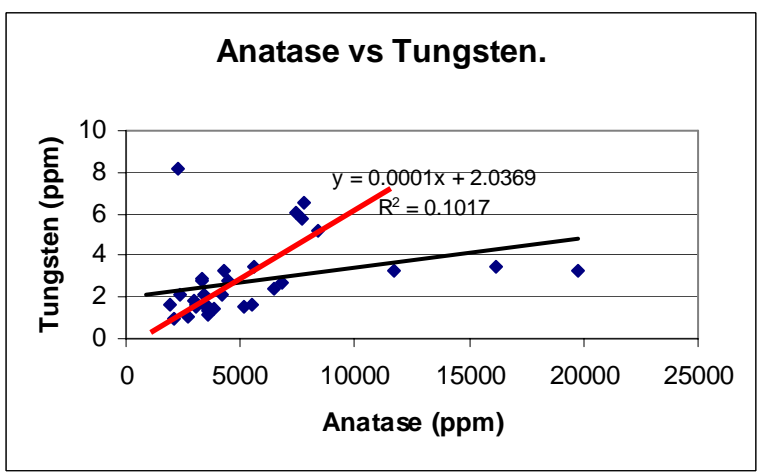


A61AB Tungsten.

Blake Central

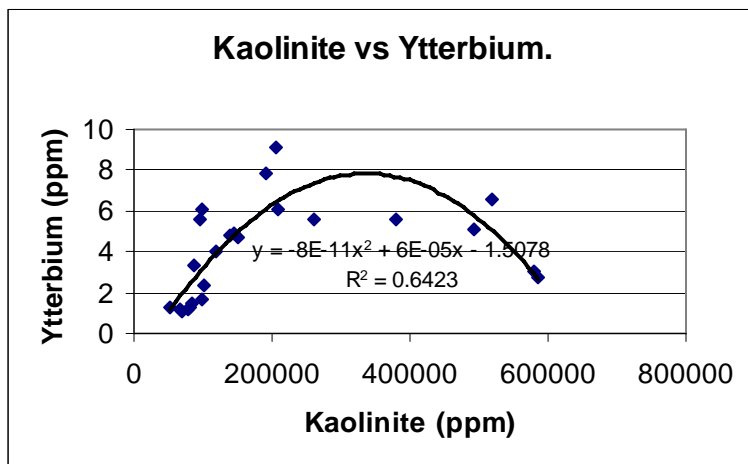


Blake West

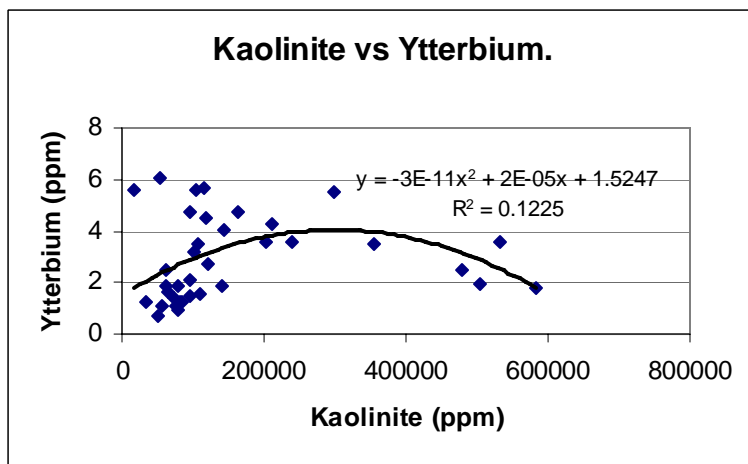


A61AC Ytterbium.

Blake Central

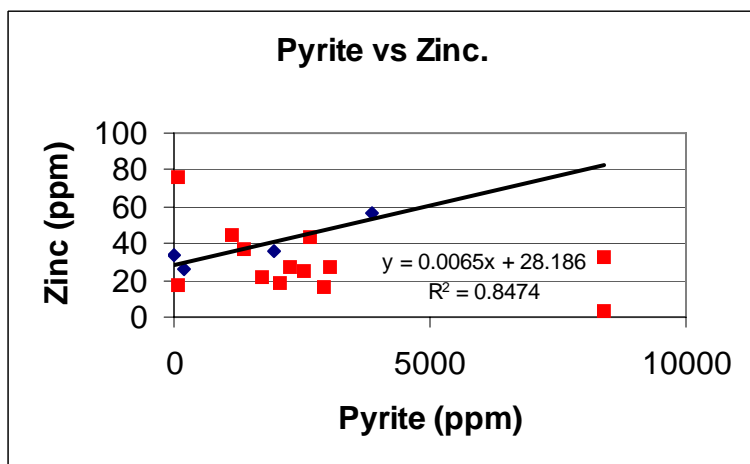
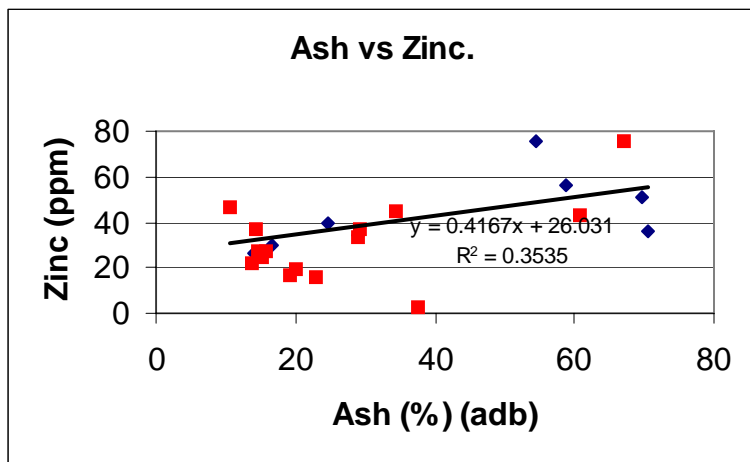


Blake West

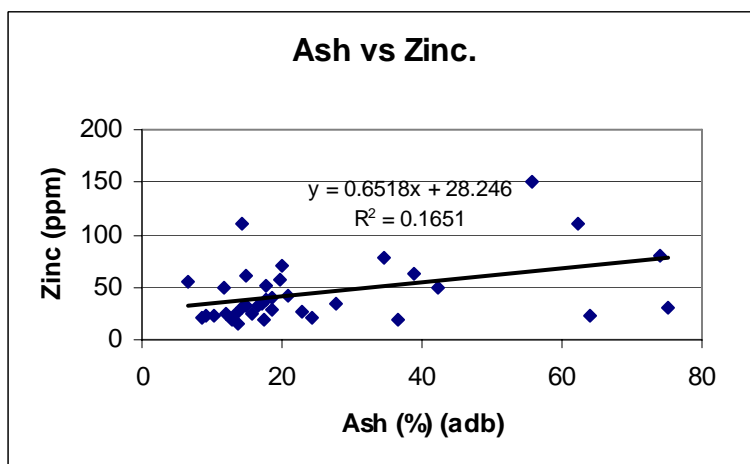


A61AD Zinc.

Blake Central

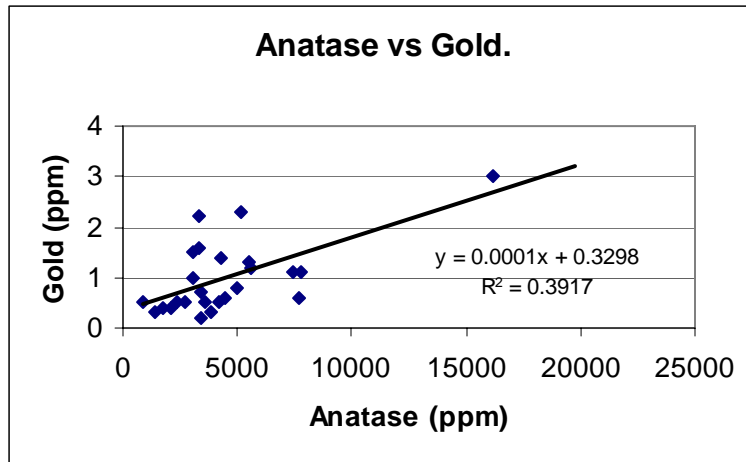


Blake West



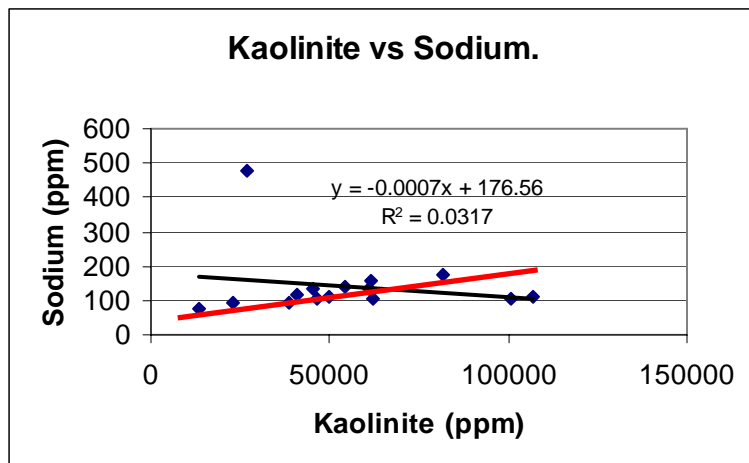
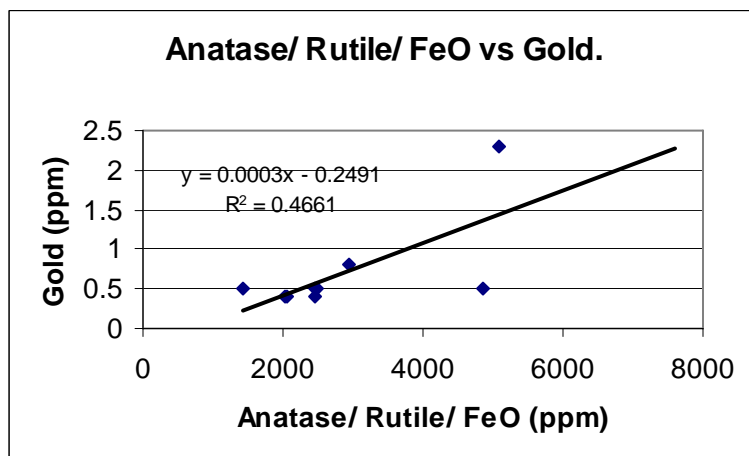
A61AE Gold (Blake West only).

Blake West

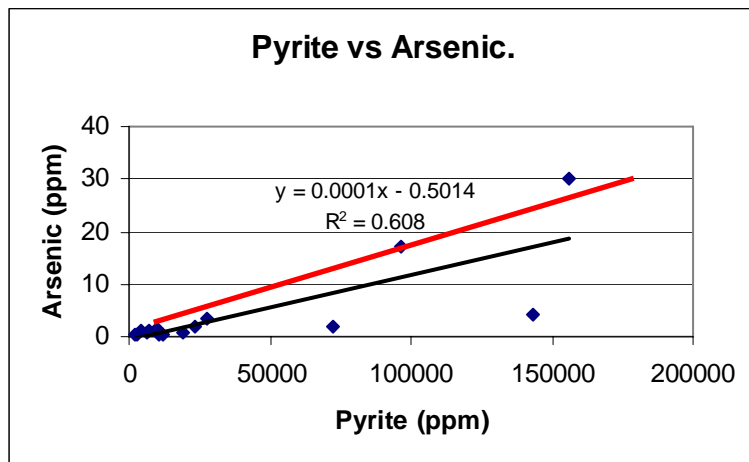


Appendix 6, Part 2 – Bowen No.2 Seam Mode of Occurrence Cross Plots.

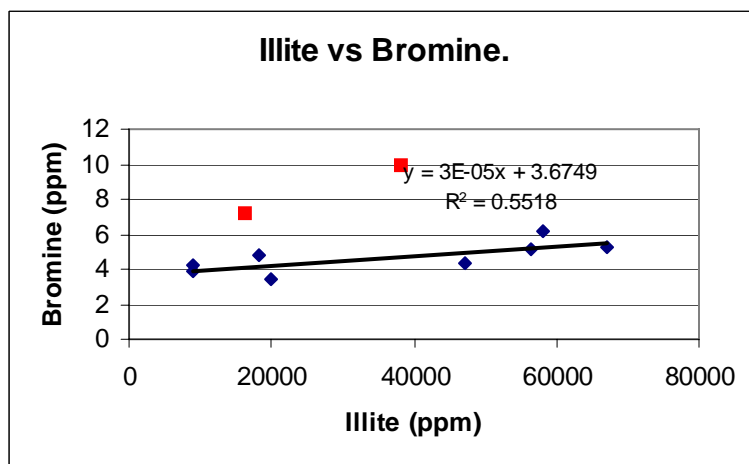
NB Points shown in red (where samples are differentiated) are considered heat affected.

A62A Sodium.**A62B Gold.**

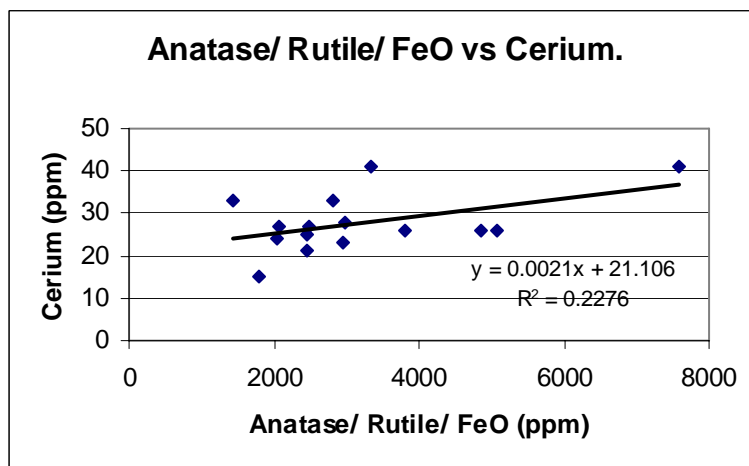
A62C Arsenic.



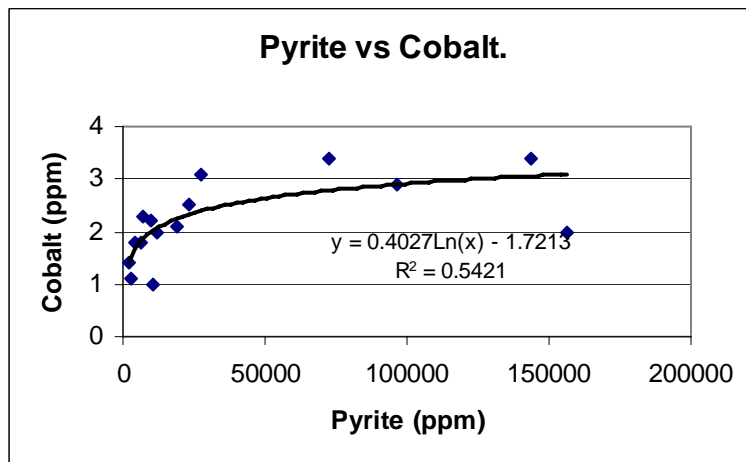
A62D Bromine.



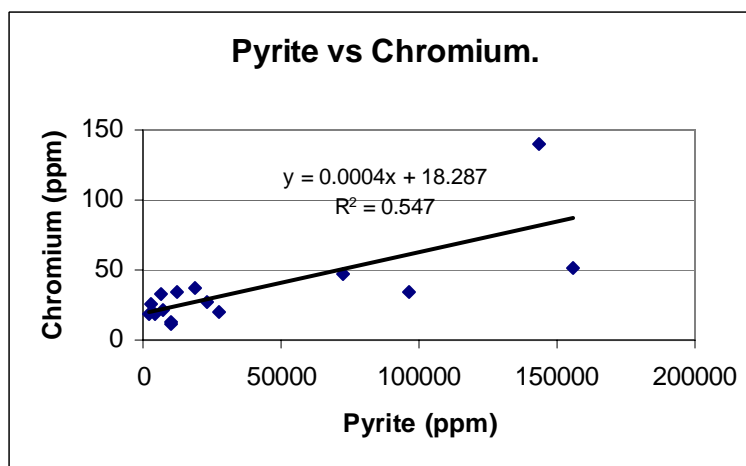
A62E Cerium.



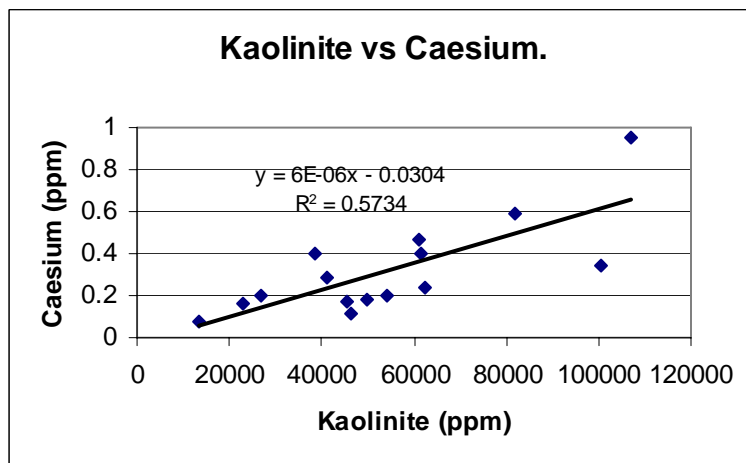
A62F Cobalt.



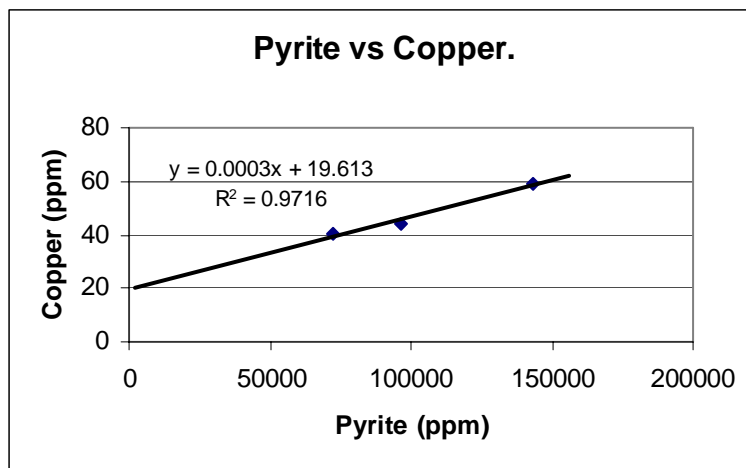
A62G Chromium.



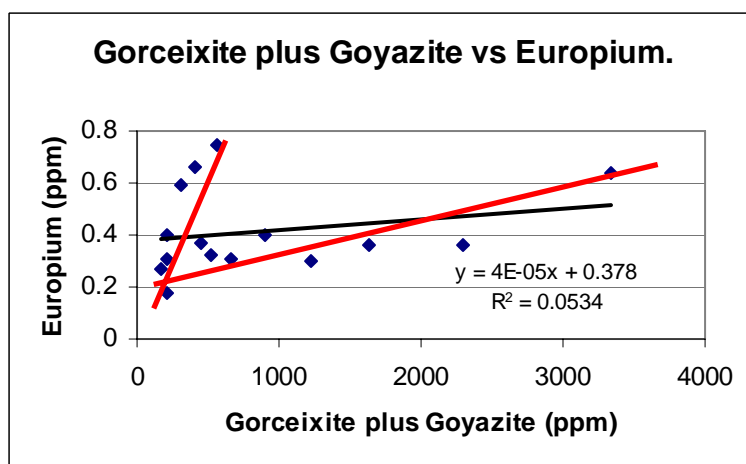
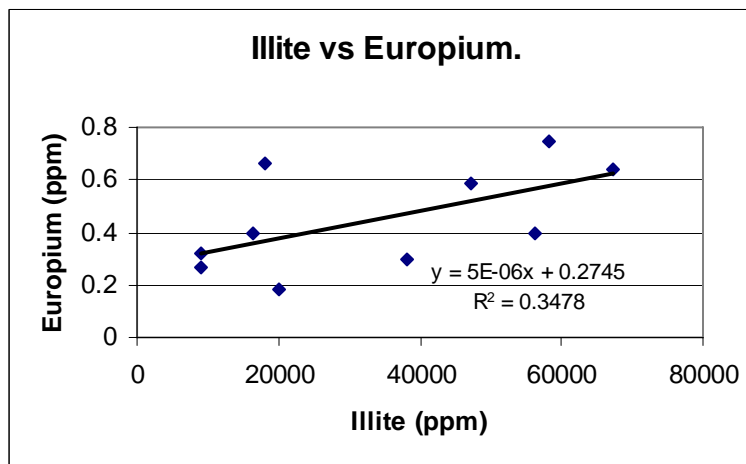
A62H Caesium.



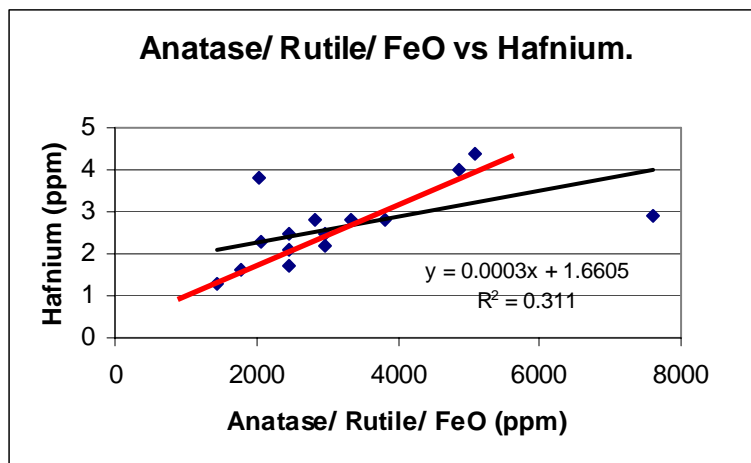
A62I Copper.



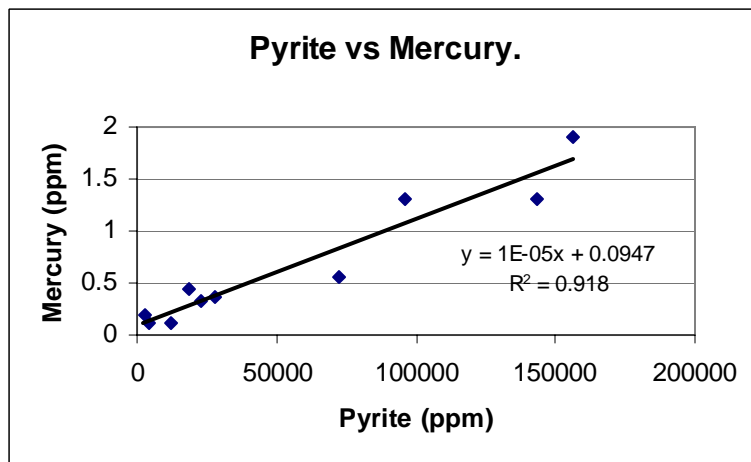
A62J Europium.



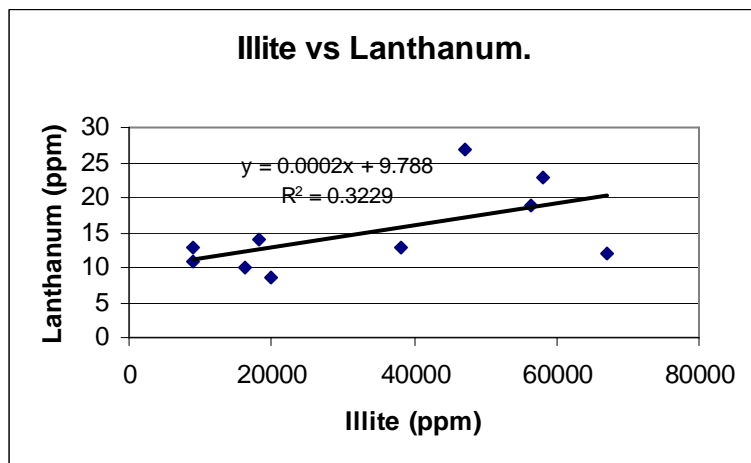
A62K Hafnium.



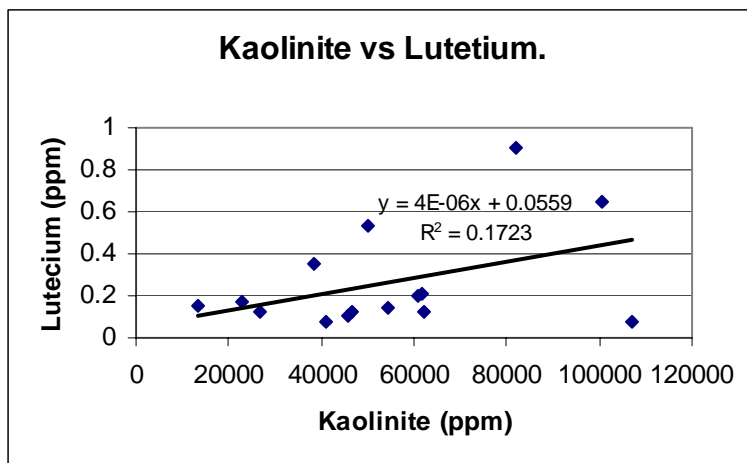
A62L Mercury.



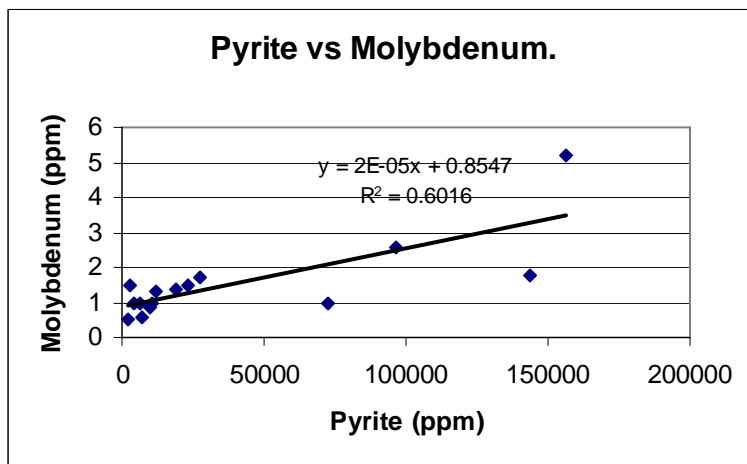
A62M Lanthanum.



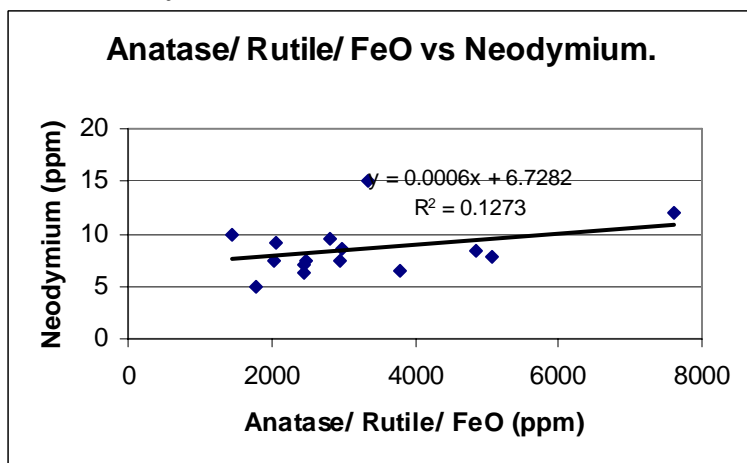
A62N Lutetium.



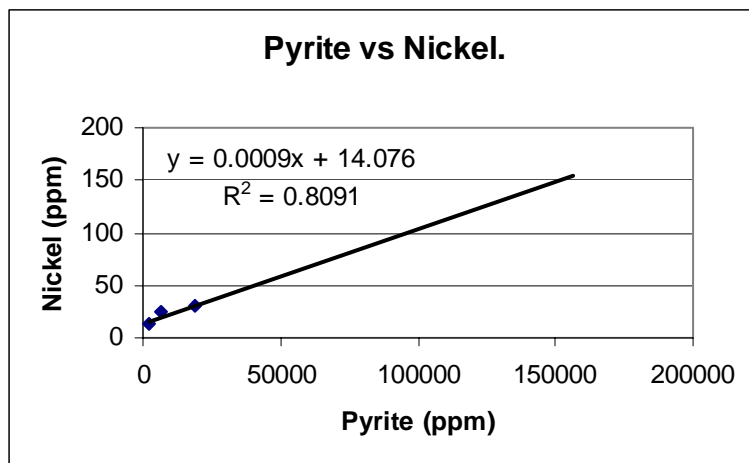
A62O Molybdenum.



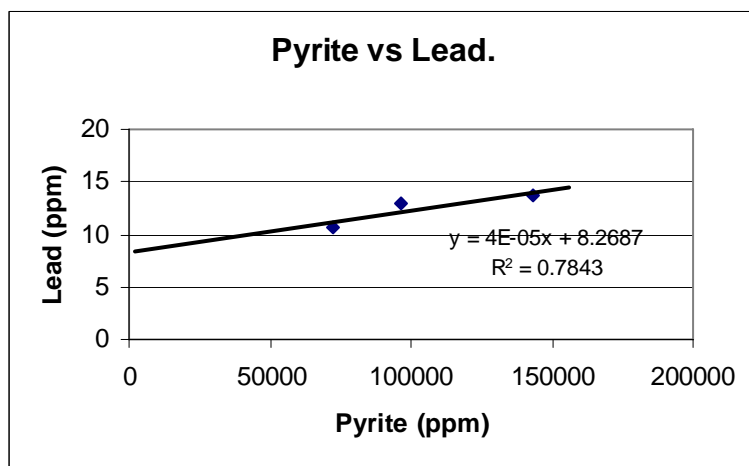
A62P Neodymium.



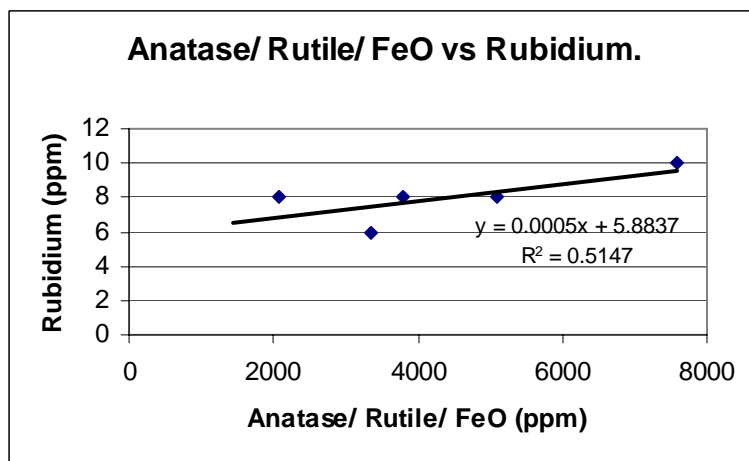
A62Q Nickel.

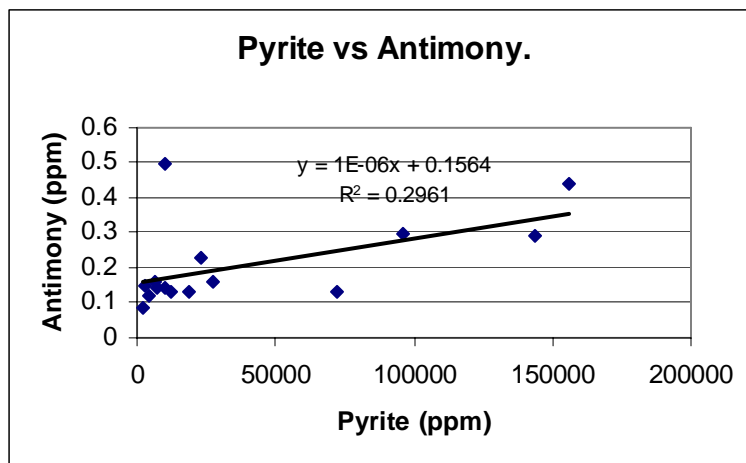
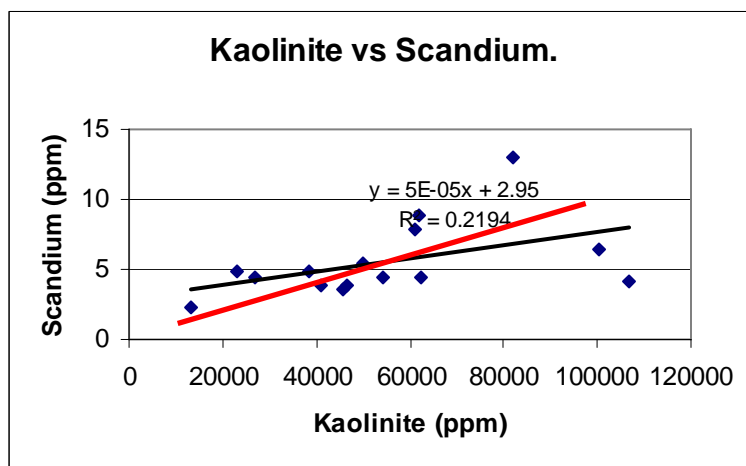
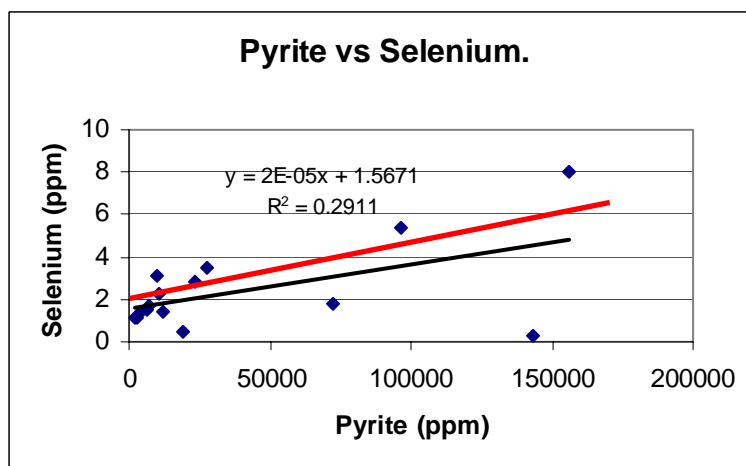


A62R Lead.

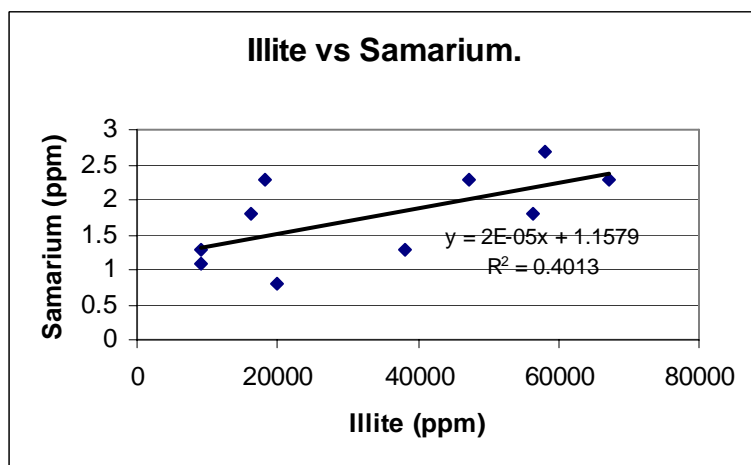
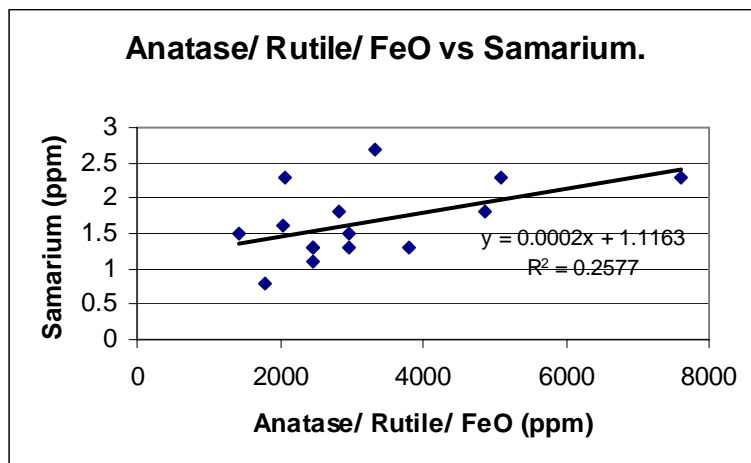


A62S Rubidium.

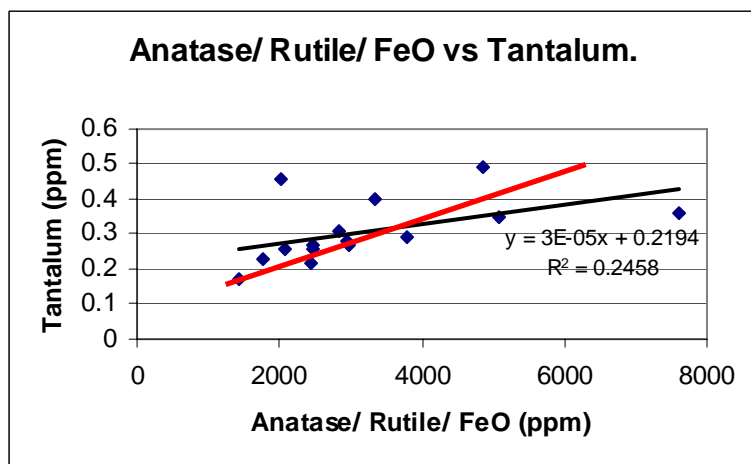


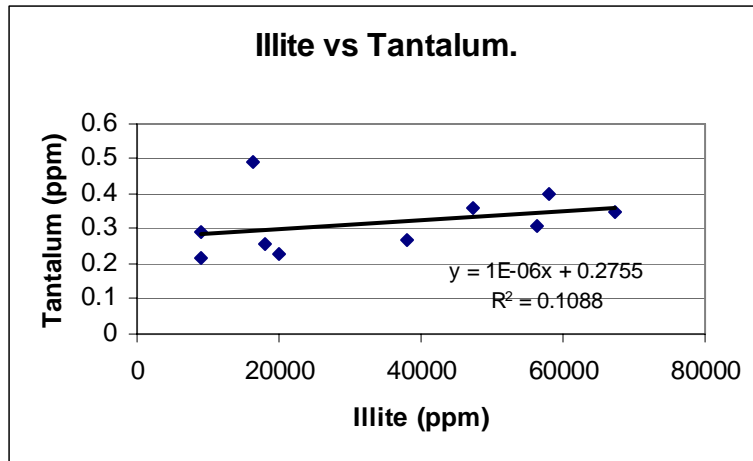
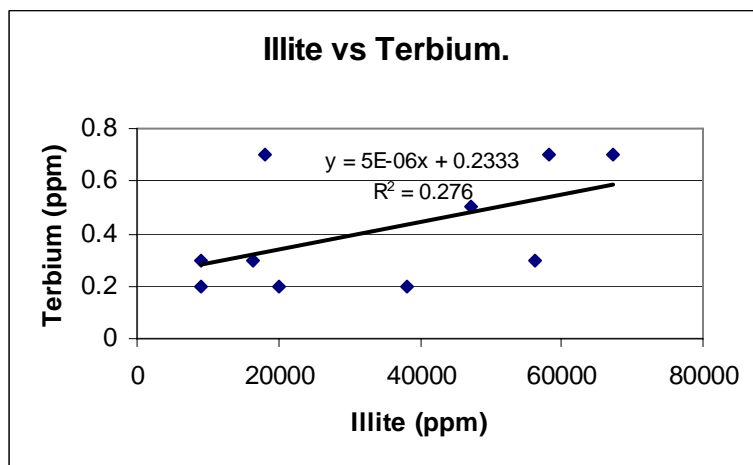
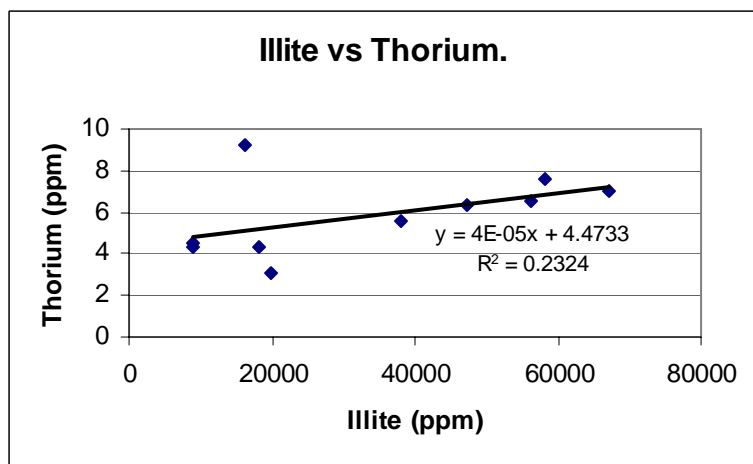
A62T Antimony.**A62U Scandium.****A62V Selenium.**

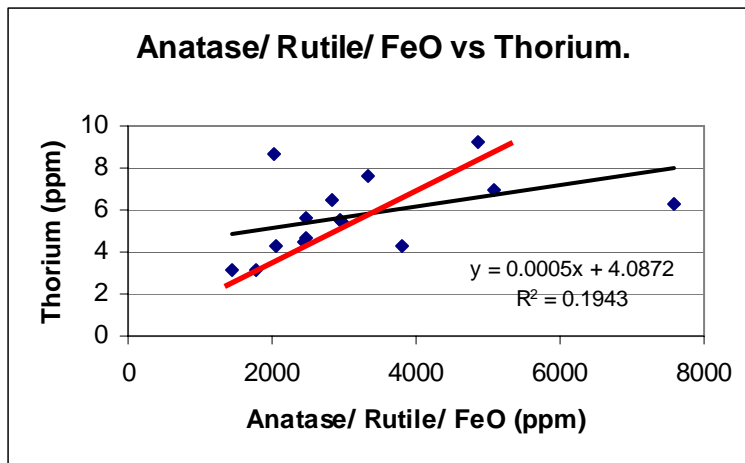
A62W Samarium.



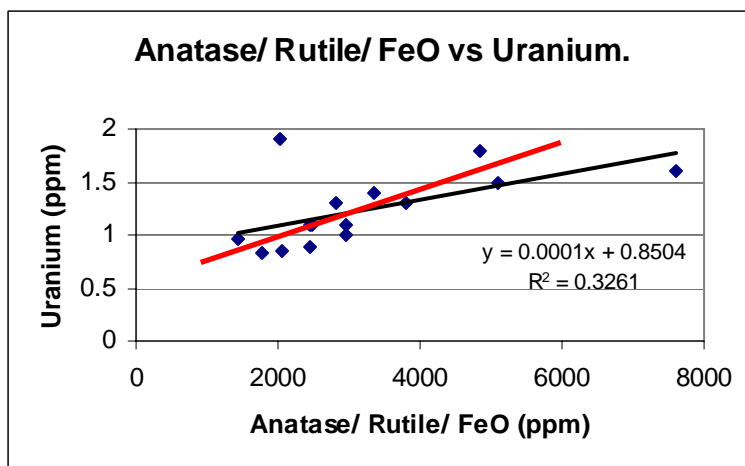
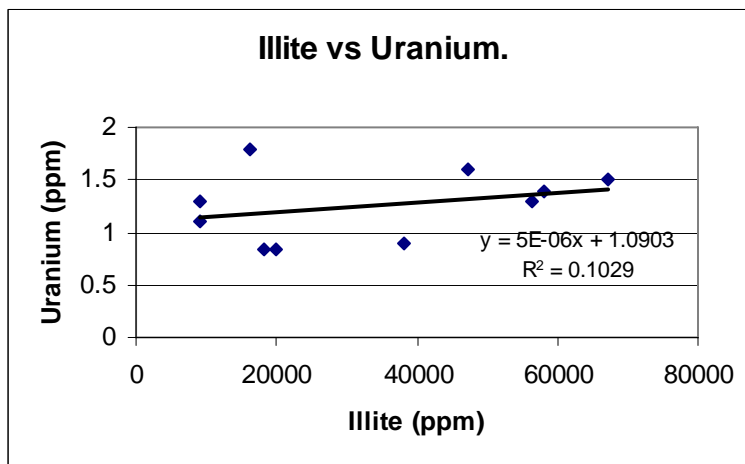
A62X Tantalum.

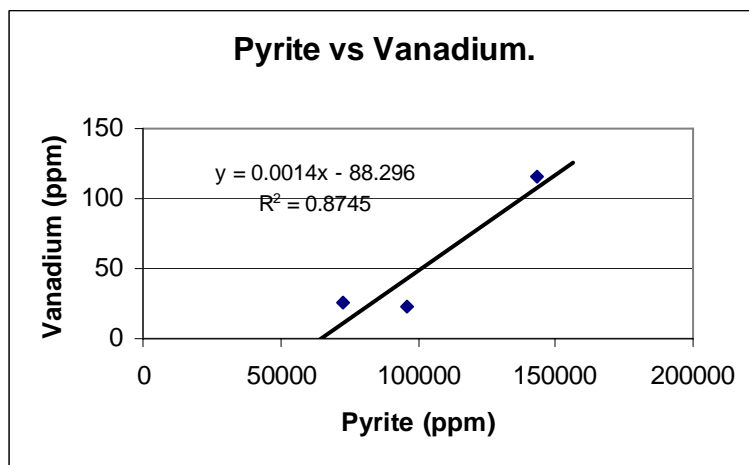
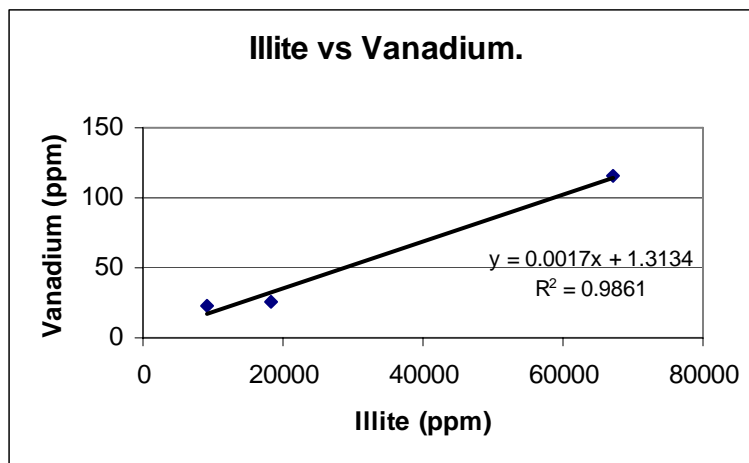
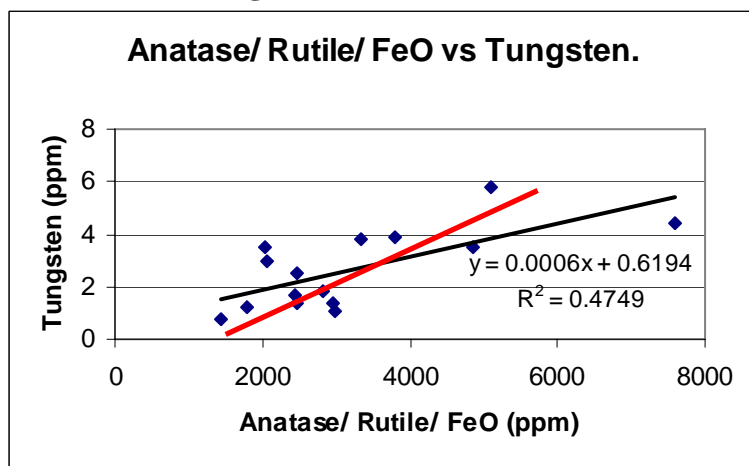


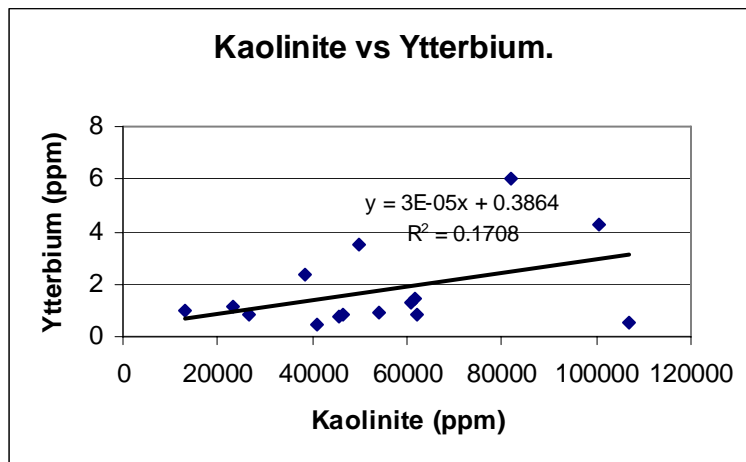
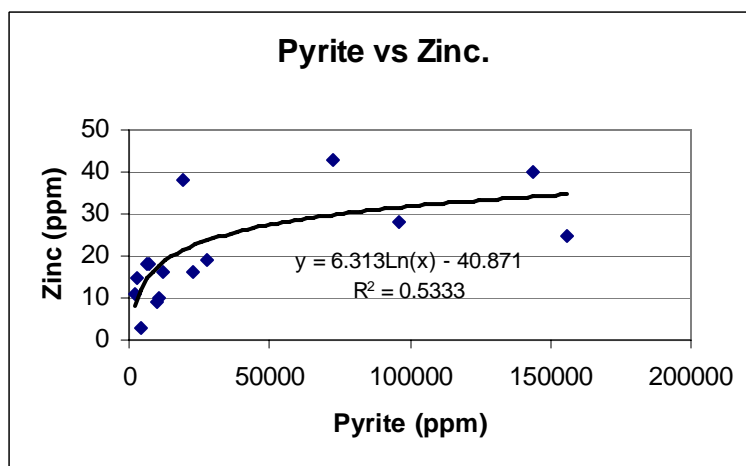
**A62Y Terbium.****A62Z Thorium.**



A62AA Uranium.



A62AB Vanadium.

A62AC Tungsten.


A62AD Ytterbium.**A62AE Zinc.**

Appendix 7

Proximate and Elemental Analysis Results for Bowen Coke Works Samples.

Coke Works Samples.									
	Coal Train No.	Coal Train No.	Coal Train No.	Coal Train No.	Coal Train No.	Coal Train No.	Repeat 3	Coal Train No.	Coal Train No.
	208	209	210	211	212	213	213	214	215
Date Sampled	25/8/99	9/02/1999	9/08/1999	15/9/99	22/09/99	29/09/99		7/10/1999	14/10/99
Analysis - Air Dried Basis									
Total Moisture	4.90	4.30	3.50	3.30	3.80	3.70		3.10	3.10
Moisture% ISO 5068-1983	1.00	1.10	0.90	1.00	1.00	1.10		1.00	0.90
Ash% ISO 1171-1981	12.20	10.90	11.00	11.30	11.60	13.00		12.20	12.30
Volatile Matter% ISO 562-1981	23.60	24.30	24.30	24.00	23.60	23.60		23.90	23.60
Fixed Carbon %	63.20	63.70	63.80	63.70	63.80	62.30		62.90	63.20
SE Mj/kg	30.38	30.80	30.84	30.70	30.59	30.07		30.38	30.38
FSI	5.00	-	5.00	5.00	5.00	5.00		5.00	5.50
Fluidity (ddpm)					1532.00	2271.00		1250.00	700.00
Major Elements									
Si (PPM)	35601	33369	33514	33445	35555	38512		37433	34157
Al (PPM)	17682	15842	16075	15787	16417	19779		17344	16238
Fe (PPM) (INAA)	1510	1090	1170	1210	1430	1620	1680	1280	1260
Fe (PPM) (XRF)	1501	1075	1198	1115	1429	1386		1175	1083
Ca (PPM)	<300	<300	<300	<300	<300	<300	<300	<300	<300
Mg (PPM)	<10	<10	<10	<10	<10	<10		<10	<10
Na (PPM)	88	79	79	80	91	101	74	97	90
K (PPM)	<500	<500	<500	<500	700	<500	<500	<500	<500
Ti (PPM)	1820	1630	1620	1580	1660	1960		1830	1670
Mn (PPM)	9	11	<10	<10	9	10		<10	<10
P (PPM)	300	220	230	220	210	220		210	200
S (PPM)	5500	5500	5600	6000	5700	5700		5500	5400
Au (PPB)	0.7	0.5	0.5	1	0.7	1.5	1.2	1	1.6
Ag (PPM)	<0.3	<0.3	<0.3	<0.3	<0.3	<0.3	<0.3	<0.3	<0.3
As (PPM)	0.05	0.54	0.39	0.37	0.45	0.59	0.75	0.38	0.1
B (PPM)		<3	<3		<3		<3		
Ba (PPM)	140	100	89	91	130	230	250	150	150
Be (ppm)									
Br (PPM)	5.3	4.4	4.3	4.6	4.4	4.5	5.5	4.8	4.8
Cd (PPM)									
Co (PPM)	7.7	6.2	9.1	6.7	7.7	8.5	9.1	6.9	6.7
Cr (PPM)	19	17	16	17	18	23	26	20	19
Cu (PPM)									
Cs (PPM)	0.14	0.1	0.09	0.12	0.18	0.27	0.33	0.21	0.21
Hf (PPM)	2.4	2.2	2	2.1	2.2	3.2	3.6	2.4	2.3
Hg (PPM)	0.08	<0.05	<0.05	<0.05	<0.05	<0.05	0.16	<0.05	<0.05
Ir (PPM)	<0.1	<0.1	<0.1	<0.1	<0.1	<0.1	<0.1	<0.1	<0.1
Mo (PPM)	<0.05	<0.05	0.58	1.1	0.68	1.3	1.2	<0.05	<0.05
Ni (PPM)	15	<2	17	<2	17	<2	27	<2	16
Pb (PPM)									
Rb (PPM)	<1	<1	<1	<1	<1	<1	3	2	<1
Sb (PPM)	0.19	0.15	0.12	0.14	0.18	0.2	0.25	0.17	0.2
Sc (PPM)	5.1	4.8	4.2	4.5	4.8	6.9	7.8	5.7	5.5
Se (PPM)	1.2	1	0.9	1.1	1.2	1.5	2	1.1	1.1
Sn (PPM)									
Sr (PPM)	130	100	72	85	95	140	120	89	72
Ta (PPM)	0.28	0.26	0.28	0.3	0.32	0.46	0.45	0.31	0.33
Th (PPM)	6.2	5.4	5.2	5.8	5.8	7.7	7.4	6.8	6.3
U (PPM) (INAA)	1.3	1.1	1	1.1	1.1	1.1	1.2	1.3	1.3
U (PPM) (XRF)									
V (PPM)									
W (PPM)	1.1	0.71	0.85	2	2	2.8	2.8	3	1.9
Zn (PPM)	76	50	53	58	54	62	78	58	53
La (PPM)	16	16	15	16	17	18	19	19	19
Ce (PPM)	30	28	27	30	31	34	37	30	33
Nd (PPM)	11	9.6	10	11	12	15	12	13	13
Sm (PPM)	1.7	1.4	1.4	1.7	1.7	2.2	2.1	2	2
Eu (PPM)	0.43	0.36	0.34	0.38	0.46	0.65	0.63	0.53	0.5
Tb (PPM)	0.3	0.3	0.2	0.3	0.3	0.4	0.5	0.4	0.4
Yb (PPM)	1.31	1.03	0.928	1.07	1.21	1.66	1.69	1.42	1.38
Lu (PPM)	0.213	0.147	0.152	0.163	0.181	0.251	0.254	0.22	0.214

Coke Works Samples.								
	<u>Coal</u> <u>Train No.</u>	<u>Coal</u> <u>Train No.</u>	<u>Coal</u> <u>Train No.</u>	<u>Coal</u> <u>Train No.</u>	<u>Coal</u> <u>Train No.</u>	<u>Coke</u> <u>Train No.</u>	<u>Coke</u> <u>Train No.</u>	<u>Coke</u> <u>Train No.</u>
	216	217	218	219	220	213	213	214
Date Sampled	20/10/99	27/10/99	3/11/1999	10/11/1999	18/11/99	7/10/1999	8/10/1999	10/10/1999
Analysis - Air Dried Basis								
Total Moisture	3.40	3.90	5.10	4.20	3.60			
Moisture% ISO 5068-1983	1.10	0.90	1.20	1.00	1.10			
Ash% ISO 1171-1981	12.50	11.70	10.80	10.80	11.10	18.30	17.30	16.20
Volatile Matter% ISO 562-1981	24.00	24.60	24.10	23.90	23.40			
Fixed Carbon %	62.40	62.80	63.90	64.30	64.40			
SE Mj/kg	30.24	30.59	30.80	30.87	30.72			
FSI	4.50	5.50	5.00	5.00	5.00			
Fluidity (ddpm)	905.00	549.00	1485.00	758.00				
Major Elements								
Si (PPM)	35027	35419	29647	30800	29817	57432	51865	50014
Al (PPM)	16952	16751	16227	16709	16394	25001	24319	22668
Fe (PPM) (INAA)	1520	1460	1300	1270	1360	2190	1960	1830
Fe (PPM) (XRF)	1181	1460	1265	1265	1280	2292	1565	1429
Ca (PPM)	<300	<300	<300	<300	<300	<300	<300	<300
Mg (PPM)	<10	300	40	200	10	70	<20	<20
Na (PPM)	93	88	84	87	96	346	199	167
K (PPM)	900	<500	<500	<500	<500	<500	<500	<500
Ti (PPM)	1640	1720	1700	1710	1680	2460	2360	2280
Mn (PPM)	9	9	11	9	8	14	13	<10
P (PPM)	190	200	400	410	390	250	240	220
S (PPM)	6300	6000	5800	5400	5000	5700	5200	5600
Au (PPB)	0.2	1.2	1.1	0.9	0.8	<0.2	<0.2	<0.2
Ag (PPM)	<0.3	<0.3	<0.3	<0.3	<0.3	0.4	<0.3	<0.3
As (PPM)	0.29	0.45	0.39	0.4	0.3	0.26	0.19	0.18
B (PPM)					4			
Ba (PPM)	230	150	180	200	200	240	220	240
Be (ppm)								
Br (PPM)	4.4	4.5	5.5	5.6	5.5	1.4	1.3	1.1
Cd (PPM)								
Co (PPM)	8.9	6.3	8.4	8.5	8.8	11	10	11
Cr (PPM)	25	19	16	17	17	71	54	77
Cu (PPM)								
Cs (PPM)	0.28	0.17	0.16	0.17	0.11	0.36	0.21	0.27
Hf (PPM)	3.1	2.3	2.1	2.2	2.2	3.3	3.3	3.3
Hg (PPM)	<0.05	<0.05	<0.05	0.13	<0.05	0.26	<0.05	0.11
Ir (PPM)	<0.1	<0.1	<0.1	<0.1	<0.1	<0.1	<0.1	<0.1
Mo (PPM)	<0.05	<0.05	<0.05	0.61	<0.05	0.85	0.72	0.78
Ni (PPM)	21	13	<2	<2	<2	27	<2	37
Pb (PPM)								
Rb (PPM)	<1	1	2	2	2	<1	2	<1
Sb (PPM)	0.21	0.18	0.12	0.16	0.16	0.25	0.24	0.25
Sc (PPM)	7	5.4	4.6	5	4.9	7.8	7.8	7.9
Se (PPM)	1.9	1.1	0.9	0.9	0.8	1	1.2	1.3
Sn (PPM)								
Sr (PPM)	57	73	220	230	240	110	110	120
Ta (PPM)	0.38	0.35	0.31	0.29	0.31	0.41	0.42	0.46
Th (PPM)	7.7	6.1	5.4	5.7	5.8	9	8.9	9.1
U (PPM) (INAA)	1.3	1.2	1.2	1.2	1.2	1.6	2	2
U (PPM) (XRF)								
V (PPM)								
W (PPM)	5.5	2	3.4	3.1	2.8	0.75	0.54	0.56
Zn (PPM)	75	51	50	48	50	75	76	76
La (PPM)	19	18	12	12	12	26	26	27
Ce (PPM)	37	32	25	25	25	45	44	44
Nd (PPM)	15	12	10	9.6	10	17	18	16
Sm (PPM)	2.3	2	1.4	1.4	1.5	2.8	2.9	3.1
Eu (PPM)	0.69	0.48	0.29	0.29	0.35	0.74	0.78	0.77
Tb (PPM)	0.5	0.4	0.2	0.2	0.2	0.6	0.6	0.6
Yb (PPM)	1.68	1.36	0.957	0.917	0.976	1.72	1.9	1.84
Lu (PPM)	0.252	0.217	0.147	0.148	0.173	0.26	0.306	0.269

Coke Works Samples.					
	Coke Train No.	Coke Train No.	Coke Train No.	POND ASH	POND ASH
	215	216	217		
Date Sampled	18/10/1999	26/10/1999	2/11/1999	13/10/99	26/10/99
Analysis - Air Dried Basis					
Total Moisture					
Moisture% ISO 5068-1983					
Ash% ISO 1171-1981	15.90	16.20	17.10	31.90	37.10
Volatile Matter% ISO 562-1981					
Fixed Carbon %					
SE Mj/kg					
FSI					
Fluidity (ddpm)					
Major Elements					
Si (PPM)	49895	47973	51237	82701	102785
Al (PPM)	22678	22559	23358	37761	47141
Fe (PPM) (INAA)	1610	1890	1980	6040	6230
Fe (PPM) (XRF)	1477	1569	1735	4732	5304
Ca (PPM)	<300	<300	<300	<300	<300
Mg (PPM)	<20	<20	<20	80	100
Na (PPM)	155	167	197	574	608
K (PPM)	<500	<500	<500	1000	1400
Ti (PPM)	2370	2380	2280	3590	4330
Mn (PPM)	12	<10	13	41	25
P (PPM)	270	250	210	490	590
S (PPM)	4500	5100	5000	3700	3500
Au (PPB)	0.4	1.5	0.4	<0.2	1.4
Ag (PPM)	<0.3	<0.3	<0.3	<0.3	<0.3
As (PPM)	0.42	0.35	0.24	1.9	0.63
B (PPM)					
Ba (PPM)	180	200	230	380	370
Be (ppm)					
Br (PPM)	1.1	1.7	1.6	2.4	2.3
Cd (PPM)					
Co (PPM)	7.7	8.9	10	28	27
Cr (PPM)	67	74	54	96	86
Cu (PPM)				59.65	83.1
Cs (PPM)	0.18	0.27	0.26	0.43	0.49
Hf (PPM)	2.9	3.3	3.3	7.8	7.1
Hg (PPM)	<0.05	0.15	<0.05	<0.05	<0.05
Ir (PPM)	<0.1	<0.1	<0.1	<0.1	<0.1
Mo (PPM)	1.6	2	0.47	2.7	4
Ni (PPM)	18	17	14	<2	<2
Pb (PPM)				25.52	30.05
Rb (PPM)	<1	3	4	4	<1
Sb (PPM)	0.25	0.27	0.26	1.5	1.3
Sc (PPM)	6.6	7.5	7.7	17	15
Se (PPM)	1.1	1.3	1.4	1.1	1.5
Sn (PPM)					
Sr (PPM)	80	120	79	250	290
Ta (PPM)	0.4	0.43	0.42	0.97	0.91
Th (PPM)	8	9.1	8.7	18	16
U (PPM) (INAA)	1.6	1.7	1.7	3.8	3
U (PPM) (XRF)				2.87	3.34
V (PPM)				43.07	53.8
W (PPM)	0.91	1.5	0.38	2.4	1.3
Zn (PPM)	62	60	79	290	260
La (PPM)	22	25	25	47	40
Ce (PPM)	40	45	45	91	80
Nd (PPM)	16	17	17	33	29
Sm (PPM)	2.6	2.7	2.9	5.5	5.1
Eu (PPM)	0.64	0.66	0.78	1.36	1.24
Tb (PPM)	0.5	0.5	0.6	1	0.8
Yb (PPM)	1.68	1.89	2.01	3.21	2.82
Lu (PPM)	0.245	0.282	0.306	0.478	0.42